PNNL-11860
UC-400

Laboratory Directed Research and Development Annual Report

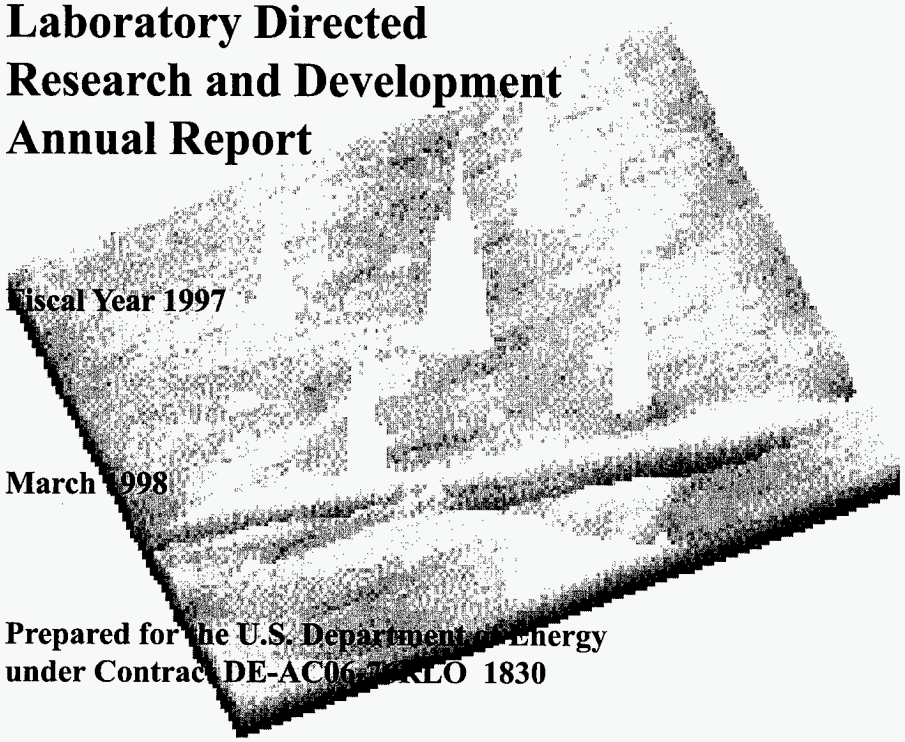

Fiscal Year 1997

March 1998

Prepared for the U.S. Department of Energy
under Contract DE-AC06-76RLO 1830

Pacific Northwest National Laboratory
Operated for the U.S. Department of Energy
by Battelle

DISCLAIMER

PACIFIC NORTHWEST LABORATORY
operated by
BATTELLE MEMORIAL INSTITUTE
for the
UNITED STATES DEPARTMENT OF ENERGY
under Contract DE-AC06-76RLO 1830

PNNL-11860

Laboratory Directed Research and Development Annual Report

Fiscal Year 1997

March 1998

Prepared for
the U.S. Department of Energy
under Contract DE-AC06-76RLO 1830

Pacific Northwest National Laboratory
Richland, Washington 99352

Contents

Introduction x

Overview and Management Process xi

Atmospheric Sciences

A New Tool for Complex Tropospheric Air Quality Systems 1

Biotechnology

750 MHz NMR Determination of the Three-Dimensional Structure of a Unique Reductive Dehalogenase 7

A Rapid and Efficient Automated Nucleic Acid Extraction/Purification/Concentration System for Environmental Samples 9

Adaptation of Mycofiltration Phenomena for Wide-Area and Point-Source Decontamination of CW/BW Agents 10

Automated, Integrated Mesoscale Continuous Flow Multichannel PCR Thermocycler for Rapid Nucleic Acid Diagnostics 14

Bioremediation: Mycofiltration Mesocosm Study for the Cleanup of Oil-Contaminated Soil 16

Electron Paramagnetic Resonance of Environmental Enzymes 20

Evaluation of Cellular Response to Insult 22

Mechanism of Biotransformation of Environmental Contaminants 24

Microbial Gene Expression and Genetic Engineering 26

Microbial Informatics 28

Microbiosystems Development 30

Molecular and Functional Analyses for Evaluating Microbial Treatment Process Performance 31

Molecular Biology Infrastructure 33

Novel Foreign Protein Production from Waste Starch 35

Phylogenetic Analysis of Anaerobic Dechlorinators 36

Production of Foreign Protein Pharmaceuticals Using Transgenic Whole Plant and Cell Culture 37

Radium Complexation and Linkage to Monoclonal Antibodies for Cancer Therapy 40

Sequencing and Functional Analysis of *Thermus* Strain IRB-SA 42

Use of Extremophillic Microorganisms for Use in Targeted Industrial Applications 44

Chemical Instrumentation and Analysis

A Flow Injection/Electrochemical System for Detection of DNA Damage 49

Aerosol Analysis by Laser Desorption in an Ion Trap Mass Spectrometer—Determination of Design Specifications for On-Line Instrumentation 51

Chemical Speciation of Radionuclides and Tritium in Nuclear Process Effluents 52

Component Interface 54

Development of a Field Portable Matrix-Assisted Laser Desorption/Ionization Mass Spectrometer for Pathogen Detection 56

Development of High Performance Field-Portable Electrospray Ionization Fourier Transform Ion Cyclotron Resonance Mass Spectrometer 57

Flow Injection Analysis 58

Immunochromatographic Sorbents for the Selective Collection of Chemical and Biological Warfare Agents 60

Micromachined Aerosol Collection System for Pathogen Detection 63

Multispectral Imaging for the Detection of Leaking Explosives from UXO 65

Rapid Detection of Bacterial Fingerprints by Matrix-Assisted Laser Desorption/Ionization Mass Spectrometry (MALDI-MS) 68

Versatile Synthesis Method for Sensing Materials 71

Computer and Information Science

A Metadata-Based Approach for Retrieval of Heterogeneous Data 75

Applied Intelligence Systems 77

Applied Mathemetics and Computer Science 78

Automated Document and Text Processing 80

Feature Extraction and Signature Tracking (FEAST) 83

Heterogeneous Information Systems Linkages 85

Individual Document Analysis and Comparison 88

Internet Platform Technology 91

On-Line Collaborative Instruments 93

PNNL-LBNL Virtual Research Facility 96

Design and Manufacturing Engineering

A Multicontinuum Approach to Composite Material Characterization and Predictive Analysis for Composite Structures 101

BW System Integration: Mesofluidics Motherboard 102

Freeform Fabrication of Structural Metal Components 103

Power Line Robot Conceptual Design 104

Ecological Science

Ecological Modeling of Regional Responses to Global Change 107

Integration of Acoustic Doppler Current Profiler Subsurface Sensing and Global Positioning Systems Technology 109

Integration of Unmanaged Ecosystems into the Global Change Assessment Model 111

Electronics and Sensors

Automated Electrooptical Identification of Pathogenic Microorganisms 115

Enhanced RF Tags 117

Fiber Optic Sensor Platform 118

Gas Composition Instrument 120

Genetically Engineered Sensors 122

Imaging the Neurological Mental Processing of the Human Brain 123

Investigation of OSL Materials for IR/UV IFF Tags 126

Low Cost Demodulator - Novel Fiber Grating Sensor 128

Low Cost Endoscope for Viewing Inaccessible Areas 130

Portable Ultrasensitive Biological Sensor 131

Position Sensing for Hand-Held Wand 134

Sensors and Controls for Advanced Manufacturing 135

Ultrasound Vector Velocity 136

Experimental Toxicology

Determination of Estrogenic Effects of Environmental Contaminants 141

Health Protection and Dosimetry

Detection of the *Helicobacter Pylori* Infection Using Infrared Laser Breath Analysis 145

Development of PBPK Modeling for Mixed Waste Applications 147

Development of Specific Absorption Rate (SAR) Measurement 149

Performance Testing of Non-Radiological Instrumentation 150

Radium-223 Immunoconjugates for Cancer Therapy 152

Hydrologic and Geologic Sciences

Determining Reactive-Well Design Parameters 157

Immobilizing DNAPL's Using Clathrate Hydrates 158

In Situ Redox Manipulation Permeable Barrier Research 160

Microbiologic Controls on Contaminant Behavior 162

Speciation of Uranyl Aqueous and Surface Complexes by Cryogenic Spectroscopic Methods 165

Stochastic Methods for Bioremediation and Geochemical Modeling 167

Subsurface Reactive Transport 169

Marine Sciences

An Integrated Capability for Remote Sensing of Bottom Conditions in Near Shore Coastal Systems 173

Materials Science and Engineering

A Smart Molecular Membrane System for Wastewater Treatment and Recycle 177

Advanced Multilayer Panels for Construction Applications 179

Antimicrobial Coatings 181

Biocatalyst for Remediation 183

Biological Interactions/Materials Biocompatibility 186

Development of Improved Oxygen Electrolyzer Membranes 188

Dissolvable Stents 190

Gas Selective Thin Film Barrier Materials 191

High Functionality Surfaces and Structures in Microchannels 192

High Precision Rapid Prototyping 194

Interfacial Interactions of Biomolecules 196

Light Emitting Polymers 198

Mechanisms of Radiolytic Decomposition of Complex Nuclear Waste Forms 202

Near Net Shape Forming of Resorbable and Implantable Devices 205

Thermoreversible Polymeric Gels 207

Molecular Science

Application of Mass Spectrometry to Life Science and Bioremediation Research 211

Catalytic Chemistry of Metal Oxides 213

Colloid-Colloid Interactions: Forces and Dynamics 215

Computational Boron Chemistry 217

Development of a Whole Organ Perfusion System for Use in PBPK Modeling 220

Development of Dynamic Nuclear Polarization-Enhanced Capabilities for Applications in Environmental and Health-Related Research 222

DNA Replication and Repair 224

Eicosanoid Synthesis Following Exposure to Environmental Chemicals 226

Experimental and Theoretical Study of Oxyanion Chemistry on Mineral Surfaces 227

Glass Structure, Chemistry and Stability 230

Glutathione Transferase Molecular Dynamics Simulation 231

Magnetic Resonance Spectroscopy Studies of Glasses, Minerals and Catalysts 233

Mechanisms of Heterogeneous Electron-Transfer Reactions at Fe-Bearing Mineral Surfaces 236

Molecular Modeling of Bacterial Lipopolysaccharide/Amino Acid Binding in Solution and to Mineral Surfaces 238

Near Field Optical Microscopy of Dehalogenase Electron Transport 239

Near Field Spectrographic Mapping and Manipulation of Enzymatic Reactions in Biological Membranes 241

NMR Studies of Proteins 242

Protein-DNA Complexes: Dynamics and Design 244

Rational Redesign of Warfare Nerve Agent Degrading Enzyme: Phosphotriesterase 246

Spectroelectrochemistry 249

X-Ray Adsorption Fine Structure 251

Nuclear Science and Engineering

Silicon-Based Beta Sensor for Onsite Inspection 255

Process Science and Engineering

Advanced Biotreatment for Industrial and Municipal Wastewater 259

Advanced Technologies for Selective Anion Separation 260

Biological Catalysis and Processes for Chemical Synthesis 262

Catalytic Hydrothermal Reductions 264

Catalytic Upgrading of C_5 Feedstocks to Ethylene and Propylene Glycols 266

Characterization of Rapid Dechlorinators: Remediation of DNAPL 267

Chemical Process and Reactor Modeling for Innovative Conversion 269

Controlled Oxidation Reactions of Organics by a Unique Gas Phase Corona Heterogencous Reactor System 270

Cost Indexed Process Design Heuristics 272

Development and Testing of Microchemical Separations 274

Enhanced Mixing for Supercritical Fluid Oxidation–Phase Separations 276

Extension of Acid Hydrolysis for the Minimization of Biosludge 279

Feasibility of Membrane-Plasma Reactor for Partial Oxidation 281

"Glow Discharge Plasma" Process 286

Hydrocarbon Processing with Microsystems 289

Integration of Advanced Technologies for Selective Anion Separation 291

Isolation and Use of Extremophilic Bacteria for the Treatment of High Nitrate and Sulfate Containing Wastes 292

Lattice-Boltzmann Simulation of Microfluid Systems 294

Ligand Design and Testing in Support of Metal Ion Separations 295

Micromachined Electrokinetic Converter for the Treatment of Tank Wastes 296

Micromachined Fuel Cell Systems 298

Mixed Waste Treatment with Iron Reducing Bacteria 300

Molecular Design of Agents for Selective Anion Separation 301

Novel Photocatalytic Reactor Technology 303

Novel Small-Scale Membrane Reactor Fuel Processor Technology 305

Plasma Spray Coating of Small Diameter Tubes with Aluminum 306

Production of Medical Isotopes Using Microtechnology 307

Real-Time Tomographic Ultrasonic Velocimetry and Densitometry 308

Recycling Heavy Metal Process Streams: Biogenic Sulfide Precipitation 310

Separation via "Enhanced Diffusion" 311

Spray Coating Supercritical Carbon Dioxide to Eliminate or Reduce VOC Emissions 313

Stabilized Native Enzymes and Chemical Treatment for Conversion of Organic Chemicals from Biomass 314

Superstructural Assembly of Materials for Selective Anion Separation 316

Risk and Safety Analysis

Cell and Tumor Growth Kinetics 319

Cell Signaling Mechanisms 323

Comparative Metabolism and Pharmacokinetics 326

Development of Risk Modules for the RT3D Bioremediation Code 329

Direct and Indirect Genotoxic Mechanisms 331

Enhanced Windows Version of MEPAS 333

Integrated Contaminant-Based Ecological Risk Assessment Methodology 334

Integrated Environmental Decision Support Tool 336

Technical Analysis and Integration of Health Effects Data 338

Toxicodynamic Modeling 340

Socio-Technical Systems Analysis

Life Cycle Assessment Design Tools 345

Management of International Environmental Treaties in Support of Environmental Security 347

Navigating Obstacles to Environmental Technology Deployment Using Environmental Management Systems (EMS) 350

Statistics and Applied Mathematics

Use of Wavelet Methods for the Homogenization of Dynamics 355

Thermal and Energy Systems

Flat Residential Commercial Light Architecture 359

High Performance Micro Heat Engine Development 360

Integrated Mesoscopic Fuel Cell and Fuel Processor 363

Mesoscopic Heat Actuated Heat Pump 365

Microscale Air-Side Heat Transfer Enhancement 367

Molecular Dynamics Simulation 368

Acronyms and Abbreviations 373

Introduction

The Department of Energy Order 413.2[a] establishes DOE's policy and guidelines regarding Laboratory Directed Research and Development (LDRD) at its multiprogram laboratories. As described in 413.2, LDRD is "research and development of a creative and innovative nature which is selected by the Laboratory Director or his or her designee, for the purpose of maintaining the scientific and technological vitality of the Laboratory and to respond to scientific and technological opportunities in conformance with the guidelines in this Order."

DOE Order 413.2 requires that each laboratory submit an annual report on its LDRD activities to the cognizant Secretarial Officer through the appropriate Operations Office Manager. The report provided in this document represents Pacific Northwest National Laboratory's LDRD report for FY 1997.

During FY 1997, 165 LDRD projects were selected for support through Pacific Northwest National Laboratory's LDRD project selection process. Total funding allocated to these projects was $12.9 million. This amount represents 3 percent of the Laboratory's operating budget, which is half of the 6 percent maximum allowed by DOE Order 413.2.

In recognition that the Laboratory must focus on a defined set of research that reflects our missions and unique assets, LDRD investments are focused on developing new and innovative approaches in research which support our "core technical capabilities." Currently, the Laboratory's core technical capabilities have been identified as

- Atmospheric Sciences
- Biotechnology
- Chemical Instrumentation and Analysis
- Computer and Information Science
- Design and Manufacturing Engineering
- Ecological Science
- Electronics and Sensors
- Experimental Toxicology
- Health Protection and Dosimetry
- Hydrologic and Geologic Sciences
- Marine Sciences
- Materials Science and Engineering
- Molecular Science
- Nuclear Science and Engineering
- Process Science and Engineering
- Risk and Safety Analysis
- Socio-Technical Systems Analysis
- Statistics and Applied Mathematics
- Thermal and Energy Systems

In this report, the individual summaries of LDRD projects are organized according to these core technical capabilities. The largest proportion of Laboratory-level LDRD funds is allocated to our capability in molecular science and the second largest allocation is in process science and engineering. A significant proportion of the Laboratory's LDRD funds were allocated to projects proposed by individual researchers or small research teams within the various technical research organizations. Funding allocated to each of these projects is typically $50K or less.

The projects described in this report represent the Laboratory's investment in its future and are vital to maintaining the ability to develop creative solutions for the scientific and technical challenges faced by DOE and the nation. In accordance with DOE guidelines, the report provides

- an overview of the Laboratory's LDRD program and the management process used for the program
- a 5-year project funding table
- project summaries for each LDRD project
- brief descriptions and funding profiles for each new project started in FY 1998 (Attachment).

(a) U.S. Department of Energy Order DOE 413.2, Laboratory Directed Research and Development, 04-09-92.

Overview and Management Process

The relevance and value of a Department of Energy (DOE) multiprogram laboratory lies in its ability to apply science and technology to national needs that fall within the missions of the DOE. The increasing complexity of these needs and the inadequacy of using conventional approaches demand that creativity and innovation underlie scientific and technological efforts so that new and novel solutions are discovered and applied. In addition, new ideas and opportunities frequently occur at a faster pace than can be anticipated or adopted in the federal budget process.

A national laboratory must establish and maintain an environment in which creativity and innovation is encouraged and supported if it is to fulfill its missions and remain viable in the long term. For these reasons, external reviews of the DOE multiprogram laboratories have consistently recommended that laboratory directors be given discretion to select research and development projects for support and to allocate a percentage of their operating budgets to provide this support.

The Laboratory Directed Research and Development (LDRD) program allows the Pacific Northwest National Laboratory to assist DOE in fulfilling its missions and contributes to other priority needs of the nation. Pacific Northwest National Laboratory's program supports creative endeavors in areas of strategic national importance that utilize the core technical capabilities of the Laboratory. The Laboratory seeks to continually replenish its inventory of ideas that have the potential to address major national needs. The principal goals of the LDRD program are to 1) encourage the advancement of basic science and fundamental research at the Laboratory, and 2) develop major new research and development approaches and capabilities. Specific objectives are to:

- foster an environment that encourages creativity and innovation
- fund new and novel ideas that have scientific/technical merit but that cannot be funded promptly through programmatic channels
- investigate new ideas/concepts to the proof-of-principle stage.

The LDRD program serves to enhance the morale and vitality of the Laboratory's scientific and technical staff and to recognize their importance to the future of the Laboratory. This program has a major impact on our staff by providing a mechanism to promptly pursue new ideas and concepts and to enrich the Laboratory's capabilities.

Program Benefits

Pacific Northwest National Laboratory's LDRD program has provided a number of benefits relative to the generic goals of fostering creativity and innovation within the Laboratory. The program has also provided specific benefits to the Laboratory that have allowed it to assume a major role in the development of science and technology to address significant national needs, such as the environmental restoration of DOE sites and global climate change.

When Pacific Northwest National Laboratory became an Energy Research laboratory in 1985, one of the major DOE directives was strengthening its fundamental research capabilities. A strengthened fundamental research component would establish a sound scientific basis for the Laboratory's applied research and development programs that would provide a complete capability for the integrated management of scientific and technical programs of national importance.

LDRD has been the principal vehicle by which the Laboratory has made substantial progress in improving its fundamental research base. The new capabilities developed at PNNL in molecular science, high-performance computing, biotechnology, and the environmental sciences have enhanced its ability to serve DOE missions. These new capabilities have changed and renewed the institutional vitality of the Laboratory during a time when the Hanford Site was undergoing significant changes that appeared likely to undermine this vitality.

The national goal of restoring DOE sites, the total cost of which is now estimated to exceed $100 billion, will never be accomplished in a reliable and cost-effective manner without significant contributions from science and technology. These contributions will range from developing a fundamental understanding of the effects of contaminants on molecular structure and function, to developing innovative new technologies for processing wastes. Bioremediation is an example of where advances in both fundamental science and applied engineering will be necessary if it is to be successfully implemented.

Similarly, a rational and defensible approach to addressing global environmental change will not be developed until the nature of possible changes are more fully understood and the impacts of alternative mitigating strategies are analyzed. Investments in advanced computing underlie the Laboratory's approach to these and other major scientific areas.

The LDRD program has allowed PNNL to initiate the process of bringing the capabilities of the national scientific and technical community to bear on these environmental problems. These efforts are still evolving and significant challenges remain. However, many of the Laboratory's ideas and concepts related to these areas were originally developed with LDRD funds and are now receiving programmatic support from DOE. Examples include previous LDRD-supported work in the atmospheric sciences that is now being applied through Pacific Northwest National Laboratory's participation in the Atmospheric Research Measurement (ARM) program, and studies in chemical dynamics that are now being supported by the Office of Basic Energy Sciences. Another example is PNNL's success in the Environmental Management Science Program (EMSP) where many of the Laboratory's winning proposals were based on concepts initially explored through LDRD. It is believed that current LDRD projects in process science and engineering, bioremediation, and health effects research will produce similar scientific and technical benefits as national efforts in these areas more fully emerge.

Pacific Northwest National Laboratory has traditionally made a portion of its LDRD funding available to small, interdisciplinary teams of researchers with new ideas or concepts that require only a small amount of funding (typically less than $50K) for initial testing. This practice is planned to be continued because of the significant scientific and technical benefits that have resulted.

In summary, LDRD has enabled Pacific Northwest National Laboratory to enhance its research vitality as a DOE multiprogram laboratory during a period of significant change. LDRD has facilitated the Laboratory's ability to make significant contributions to addressing national problems, particularly in the environmental research area which represents the primary distinctive signature of the Laboratory. It is essential that PNNL and the other DOE laboratories retain the capability provided by LDRD if their full capacity to assist DOE and the nation is to be realized.

Laboratory Directed Research and Development Management Process at Pacific Northwest National Laboratory

At Pacific Northwest National Laboratory, LDRD is funded through a Laboratory overhead account applied to the value added base on all PNNL 1830 Contract accounts. The PNNL Director of Finance is responsible for ensuring that these funds are accumulated and accounted for in the appropriate manner. Formal proposals in an authorized format are required for each LDRD project.

Decisions regarding funding levels for the LDRD accounts are made by the Laboratory Director, with assistance from the Laboratory Strategy Council (composed of the Associate Laboratory Directors). Primary responsibility for allocations to individual LDRD projects within these accounts also rests with the Director and the Strategy Council. The Laboratory Technical Council (composed of the leaders of the core technical capabilities) and the Laboratory Business Council (composed of major DOE program managers) play key roles in developing recommendations for the Director on these allocations. The Laboratory Technical Council has primary responsibility for ensuring the technical soundness of the LDRD investments, through peer reviews conducted by both internal and external scientific reviewers. The Associate Laboratory Director for Strategic Planning has responsibility for the general oversight and conduct of PNNL's LDRD program.

All projects are reviewed for technical merit by line managers and/or scientific staff, and in some cases by external peer reviewers. Written guidance pertaining to the criteria and guidelines for LDRD projects provided in DOE Order 413.2 is widely distributed to Laboratory staff. Adherence to these criteria is further ensured through reviews by the LDRD Office. Individual projects are usually limited to $1M in total funding and $500K in a single fiscal year. The Director of Finance is responsible for financial oversight of the LDRD program. Accountability for individual LDRD projects rests with the principal investigators conducting the projects and their cognizant line manager.

The major sequential steps of Pacific Northwest National Laboratory's LDRD process are as follows:

- Ongoing LDRD projects are reviewed for technical progress in achieving their intended goals.
- Initial concepts for new LDRD investments are solicited through the Laboratory's business planning process managed by the Associate Laboratory Director for Strategic Planning.

- Based on the approval of Pacific Northwest National Laboratory's LDRD Plan by DOE, initial funding allocations for the LDRD accounts are approved by the Laboratory Director and a request for proposals is issued.

- Line managers solicit proposals for specific LDRD projects from research staff and select projects as candidates for funding. Each manager selecting an LDRD project must certify in writing that the project has been peer-reviewed and meets the requirements of DOE 413.2.

- All LDRD project proposals and the electronic files must be submitted to the Laboratory's LDRD Office for review for compliance with DOE requirements after the principal investigator and the cognizant manager have signed them. All documentation required to meet National Environmental Policy Act (NEPA) and other environmental, safety, and health compliance requirements for the projects must also be submitted.

- The emphasis of the proposals is on the technical objectives and approaches that will be incorporated in the project.

- The Budget and Analysis Office has established six-digit alpha codes that are used to represent the work breakdown structure (WBS) code for each of the LDRD accounts. After a project receives final approval, a project-level work breakdown structure code is assigned by the LDRD Office for each LDRD project.

Primary responsibility for ensuring adequate technical review of LDRD projects rests with line managers. In addition, regular peer reviews of selected activities are performed by the Laboratory Technical Council and the Strategic Planning Directorate. Additional oversight of the progress of the LDRD investments is provided by the Laboratory Strategy Council. Some of the major LDRD investment areas, such as molecular science and process science and engineering, also have designated advisory councils that include external advisors in their peer reviews of the status and progress of the research. The various technical reviews constitute the most important means of ensuring that LDRD funds are used for their intended purpose.

Principal investigators and management are also required to develop input to meet all DOE LDRD reporting requirements. These requirements include the LDRD annual reports and the quantitative survey of LDRD project results. Selected principal investigators may also be asked to participate in periodic DOE LDRD program reviews, which are organized by the LDRD Office. The LDRD Office has primary responsibility for developing the annual LDRD Plan.

Atmospheric Sciences

A New Tool for Complex Tropospheric Air Quality Systems

Carl M. Berkowitz, Xindi Bian, Jerome Fast, Shiyuan Zhong (Earth Systems)

Study Control Number: PN97003/1144

Project Description

The goal of this project was to synthesize existing capabilities in atmospheric chemistry and dynamic modeling through development of an in-core, interactive multiphase chemistry/regional-scale atmospheric modeling system. This modeling system will enable PNNL scientists to study important feedback processes between clouds, aerosols, and gas-phase chemistry. Although the feedback processes are acknowledged in the scientific literature to be of importance, they have not been explicitly studied in detail because of computational complexities, uncertainties associated with atmospheric heterogeneous chemical processes, and the interdisciplinary expertise required.

The tool we proposed to develop for studying complex tropospheric air quality applications included a coupled version of the Regional Atmospheric Modeling System (RAMS) and the Global Chemistry Model (GChM). These models have been coupled in a one-way approach in that wind, temperature, and moisture fields computed by RAMS are passed into GChM; however, there are no mechanisms to permit the simulation of feedback processes. A fully coupled modeling system, consisting of two distinct but closely linked parts, could significantly extend our fundamental knowledge of radiation-cloud-aerosol-gas-phase interactions. Although a fully coupled version of RAMS and GChM could not be completed by the end of the fiscal year, progress on that coupling was achieved with meaningful improvements to the current one-way approach.

Technical Accomplishments

The following summary of technical accomplishments is presented in the same order in which the work was proposed.

1. *Coupling of RAMS and GChM*

- Development of the in-core coupling of RAMS and GChM

  Coupling of the two codes was accomplished on a Sun Ultra workstation. The basic philosophy in coupling the codes was to limit the number of modifications for each model. We originally planned to create a new main program that would make separate calls to RAMS and GChM at certain time steps within a loop. However, we found it simpler to execute the GChM modules within the RAMS framework.

  A common block of variables (horizontal and vertical wind components, temperature, humidity, eddy diffusivity, pressure, and zenith angle) used by both models was established. At the end of the RAMS time integration loop, a subroutine was added that updates the meteorological variables so that the most recent values can be used by the chemistry calculations. Immediately following the call to this subroutine, a statement was added to call the GChM modules. Since the time step for the meteorological variables is much smaller (e.g., 30 seconds) than is needed by the chemistry integration (e.g., 5 minutes), a constant has been added to control how frequently the GChM modules are executed. Although GChM computes the zenith angle needed to evaluate diurnally varying photolysis rates, the zenith angle from RAMS is now used so that this variable is consistent between the two codes. Other minor aspects of the codes were also changed, including duplicative subroutine names and calls to IEEE routines.

  One advantage of in-core, one-way coupling is that RAMS can efficiently feed the meteorological quantities to GChM at frequent intervals. Air quality modeling studies have traditionally employed an out-of-core approach in which the chemistry model reads meteorological quantities from a file at relatively coarse time intervals, typically on the order of an hour. The chemistry model then either linearly interpolates the meteorological quantities in time or assumes that meteorology is constant over the coarse time interval. Previous studies have shown that this approach can produce significant errors for long-range transport applications. Boundary layer quantities, such as the mixed-layer depth, can also change significantly over a short period of time so that an adequate description of vertical diffusion may not be obtained when assuming constant meteorology over a 1-hour period. With in-core coupling, the most recent values are used at small time steps so that these problems are eliminated.

- Development of a consistent horizontal coordinate system

  A latitude/longitude coordinate system had previously been used in GChM to describe the horizontal transport, whereas RAMS had used an orthogonal polar

stereographic system. Before any coupling could proceed, a common coordinate system had to be selected, and one of the two models recast into this system. Because GChM is largely an in-house system designed in a highly modularized framework, the latitude/longitude system was reformulated to that of RAMS. This involved rewriting the governing equation from a simple latitude (λ), longitude (ϕ) coordinate, to one defined as

$$x = \left(\frac{2a \cos(\phi)}{1 + \sin(\phi)} \right) \cos(\lambda - \lambda^*) + X_0$$

$$y = \left(\frac{2a \cos(\phi)}{1 + \sin(\phi)} \right) \sin(\lambda - \lambda^*) + Y_0$$

where a, X_0, and Y_0 are the earth's radius, and X-Y origin of the RAMS polar stereographic system. A corresponding map factor algorithm for this coordinate system also was developed using existing code from the RAMS model.

- Initial step toward including aerosol-radiation feedback processes in the integrated modeling system

  Work was initiated on improving the existing radiation and cloud physics schemes in RAMS as a first step toward incorporating the aerosol-radiation feedback processes in the integrated modeling system. There are two types of radiation schemes in the current version of RAMS. One scheme (Mahrer and Pielke 1977) requires relatively little computational expense, but does not include the radiative effects of clouds. Another scheme (Chen and Cotton 1983) is computational expensive, but accounts for the radiative effects of clouds. Because one of the important impacts of atmospheric aerosols on radiation is through indirect effect on clouds, the Chen-Cotton scheme in RAMS which accounts for radiative effect of clouds is a natural choice as the radiation scheme for the integrated modeling system. Unfortunately, we have found, through previous simulations and comparisons with surface radiative flux measurements, this scheme tends to produce an underestimation of shortwave radiative fluxes by 10% to 15% under most conditions. To improve the calculated shortwave radiative fluxes, we have replaced the existing Chen-Cotton scheme in RAMS with a new version. The new version of the scheme has been tested with a case study which has shown considerable improvement in the simulated shortwave radiative fluxes over the old version. We have also sped up the computation of longwave radiation by eliminating the calculations of fractional cloud cover that was never used in practice but consumed much computation time because it involves an iterative process.

2. *Development of Emission Inventories Compatible with the Integrated Modeling System*

   The U.S. Environmental Protection Agency (EPA) supplied regional-scale emissions employed in this version of GChM. This inventory is known as the "RADM AP-45" case, and is based on EPA's 1990 Interim Emissions Inventory. It contains hourly emissions of 22 species in eight vertical atmospheric layers over a 5-day summertime period characterized by warm temperatures for eastern North America. The 121 hours (5 days plus 1 hour) of emissions data were temporally averaged to produce a mean hourly value at each of the 35 x 38 x 8 grid cells of the emissions domain. This reduction had the benefit of reducing the size of emission files by one-fifth thus reducing the time required for model input/output.

3. *Development of Post-Processing Graphics*

   A new graphical tool was developed to display the results of the coupled modeling system. Both meteorological and chemical values were combined in the graphics to facilitate interpretation of the relationship between meteorological processes on chemical production, transport, diffusion, and final removal via deposition and reaction. Interactive Display Language (IDL), a commercial software, was used for this purpose (IDL is a flexible graphics language that permits the user to create a wide variety of plots using script files that contains programming commands similar to FORTRAN).

4. *Verification of the Integrated Modeling System*

   Our preliminary verification study was done using data collected during the 1995 Southern Oxidants Study (SOS). SOS was a large regional-scale field measurement program centered in Nashville, Tennessee, involving scientists from public, private, and academic institutions. One of its goals was to determine the relative importance of volatile organic compounds and NO_x in ozone production. Both airborne and surface measurements were readily available to us and used to verify the performance of the model.

   The evolution of the ozone in the vicinity of Nashville was predicted by the coupled modeling system for July 12 during the 1995 SOS field campaign. Two versions of the modeling system were created. For the first version (out-of-core), GChM read in meteorological quantities from RAMS at 1-hour intervals from external files. This is the traditional approach used by chemistry models. The second version was the in-core RAMS and

GchM code with the frequency of the meteorological variables updated in GChM temporarily set to 1 hour. The results from the second version were compared to those from the first version to verify that the new in-core code was working properly. Two simulations were performed by both versions of the code. One simulation was initialized with a constant ozone concentration of 30 ppb and the other simulation was initialized with a vertical ozone profile that contained a maximum concentration of 85 ppb at 1 km AGL, consistent with early morning aircraft observations on July 12.

5. *Scoping Study*

The technical accomplishments described above provide evidence that our team has achieved our stated goal of producing a fully coupled RAMS and GChM modeling system in 2.5 months with a $25K budget. The primary benefit of the effort to date is a reduction in modeling uncertainties associated with time interpolation of meteorological fields used in GChM with an off-line coupled system. We have also made significant progress in developing an emission inventory compatible with the fully integrated modeling system and in improving radiative budget calculations in RAMS in order to account for the important feedback processes between meteorology and chemistry.

References

C. Chen and W.R. Cotton. 1983. A one-dimensional simulation of the stratocumulus-capped mixed layer. *Boundary-Layer Meteor.*, 25, 289-321.

Y. Mahrer and R.A. Pielke. 1977. A numerical study of the airflow over irregular terrain. *Beitrage zur Physik der Atmosphare,* 50, 98-113.

Biotechnology

750 MHZ NMR Determination of the Three-Dimensional Structure of a Unique Reductive Dehalogenase

Michael A. Kennedy (Macromolecular Structure and Dynamics)

Study Control Number: PN95001/977

Project Description

Tetrahydroquinone reductive dehalogenase (TeCH-RD) is a bacterial enzyme that has been isolated from *Flavobacterium* sp. strain ATCC 39723. It has been shown to be involved in the degradative pathway of pentachlorophenol. Specifically, TeCH-RD carries out the reductive dechlorination of tetrachlorhydroquinone to dichlorohydroquinone. TeCH-RD is 247 amino acids in length with a corresponding molecular weight of 28.1 kD. The goal of this project is to use nuclear magnetic resonance spectroscopy to determine the three-dimensional solution-state structure of the enzyme. An integrated biophysical, biochemical, analytical, and modeling approach is being used to identify the three-dimensional structure of TeCH-RD.

Technical Accomplishments

Tetrachloro-*p*-hydroquinone reductive dehalogenase (TeCH-RD) was recently purified from a pentachlorophenol-degrading *Flavobacterium* sp. strain ATCC 39723. The enzyme is thought to first catalyze the formation of a hydroquinone-glutathione adduct between a tetrachloro-*p*-hydroquinone (TeCH) and a glutathione and then to split the adduct at the expense of another glutathione to produce 2,3,6-trichloro-*p*-hydroquinone and the oxidized form of glutathione (GS-SG). The deduced amino acid sequence shows strong similarity with two previously reported plant glutathione transferases (GSTs). TeCH-RD is the only reductive dehalogenase that has been characterized to date. The enzyme's ability in splitting hydroquinone-glutathione adducts may represent a new type of activity catalyzed by GSTs, which is very important to prevent building up multiple substituted hydroquinone-glutathione adducts. Hydroquinones, metabolites of many xenobiotics, react with glutathione to form multiple substituted (more than one glutathione per quinone hydroquinone glutathione) adducts. The conjugates recently have been shown to be more toxic than the original quinone metabolites in animal studies.

Nuclear magnetic resonance spectroscopy is the leading method for determination of solution-state protein structure. Secondary structure of proteins up to 31.4 kD have been determined at 600 MHZ with 0.7 mM solutions of uniformly ^{15}N and ^{13}C-labeled materials. The current estimate of the molecular weight range for complete three-dimensional NMR structure determination of proteins, employing the latest innovations in fractional deuteration of protein sidechains and using up to 750 MHZ field strengths, is between 30 and 60 kD. We have been able to show that under buffer conditions being used for NMR studies, TeCH-RD exists as a monomer in solution. Therefore, the TeCH-RD subunit is well within the molecular weight range for structural studies.

Strain JD01, an *E. coli* JM105 harboring the TeCH-RD expression vector, pJD01 has been used to produce large quantities of TeCH-RD. Overproduction of TeCH-RD is induced by the addition of isopropylthio-β-D-galactoside. For ^{15}N-labeled and ^{15}N, ^{13}C-TeCH-RD production, JD01 is cultured in Isogro (Isotec, Inc.) labeled protein hydrolysate. Triply labeled protein including ^{2}H, ^{13}C, and ^{15}N, has been prepared from cultures grown in media based on deuterated algae grown in heavy water and with labeled carbon and nitrogen sources.

Preliminary NMR studies initiated indicated that TeCH-RD was a good candidate for NMR investigation. ^{1}H-^{15}N-heteronuclear multiple quantum coherence spectra collected at 750 MHZ shows excellent resolution. We found aggregation to be a problem over time and have taken steps to solve this problem. While we optimize conditions for studying the native protein, we have explored subcloning the protein into its distinct domains and site directed mutagenesis to eliminate unnecessary cysteine residues that could be susceptible to oxidation over time. Figure 1 shows a detailed homology model of TeCH-RD. The protein appears to be divided into two distinct domains, the N-terminal domain that includes a two-strand beta sheet and an alpha helix in the substrate binding region of the protein and the C-terminal domain that is composed of a bundle of alpha helices. The two

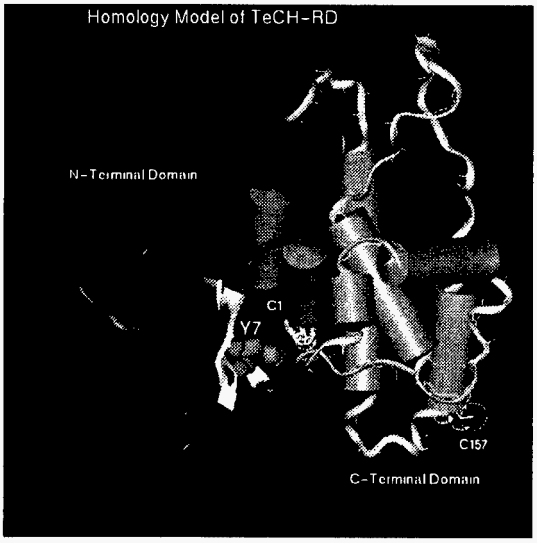

Figure 1. Homology model of TeCH-RD indicating two distinct structural domains and the position of the two cysteine residues.

cysteine residues are indicated with a space-filling surface. C157 is positioned on the surface of the protein. We are preparing a site-directed mutant C157S to minimize oxidation induced aggregation. We have also pcr cloned out the cDNA coding for each of the domains. Figure 2 shows an agarose gel of the pcr product for the N-terminal

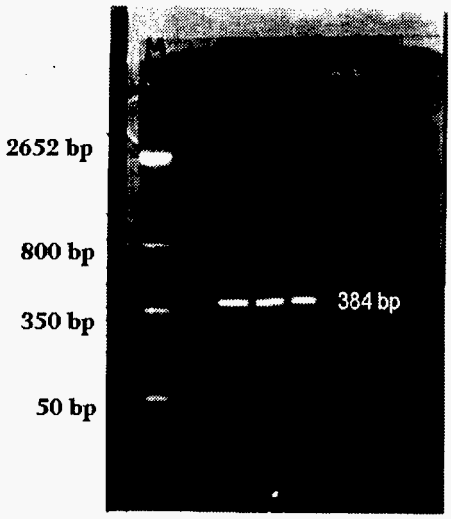

Figure 2. Agarose gel showing the 384 base pair pcr product that encodes for the N-terminal domain of TeCH-RD.

domain of TeCH RD. The 384 bp DNA fragment is clearly indicated. Figure 3 shows the pcr fragment corresponding to the C-terminal domain of TeCH-RD. The pcr fragments have been cloned into appropriate expression vectors and are being screened for successful insertion. These approaches are continuing to be pursued in our structural investigations of TeCH-RD by NMR spectroscopy.

Figure 3. Agarose gel showing the 434 base pair pcr product that encodes for the C-terminal domain of TeCH-RD.

Publication

D.W. Hoyt, J. Zhao, J. Trewhella, and M.A. Kennedy. "Comparison of Small Angle -x-ray Scattering and Gradient Encoded NMR diffusion Experiments for Assaying the Aggregation State of Proteins in Solution." (in preparation).

A Rapid and Efficient Automated Nucleic Acid Extraction/ Purification/Concentration System for Environmental Samples

Fred J. Brockman, Darrell P. Chandler, Jay W. Grate, Cynthia Bruckner-Lea (Biogeochemistry)

Study Control Number: PN97004/1145

Project Description

The objective of this project is to develop approaches for the rapid, specific, sensitive, and simultaneous detection and identification of microorganisms based upon their specific nucleic acid content. The expected results of this research include an understanding of nucleic acid hybridization conditions required for successful and efficient hybridization of an environmental nucleic acid sample; a demonstration of automated nucleic acid purification from environmental samples; and integration of a sample processing module into a rapid, automated, mesoscale, compact detection system for microorganisms in environmental samples.

Technical Accomplishments

Initial research into DNA array and state-of-the-art gene detection technology consistently showed that the commercial sector has advanced high-speed thermocyclers for the polymerase chain reaction and miniaturized genosensor array elements, but that sample preparation, processing, and delivery to the detector is the limiting technology for fully integrated gene-based detection systems. This conclusion was consistently and universally supported by several visits and discussions with genosensor companies, potential clients (NASA, DARPA, DoD, USDA), collaborators (University of Alabama, Birmingham; Perkin-Elmer, Genometrix, Nanogen, Clinical Microsensors, Life Technologies) and other LDRD focus areas (Food Safety and Agricultural Pathogens, Medical Technologies). Therefore, development of the nucleic acid extraction and purification component of this project was emphasized in 1997 and will continue during FY 1998. A separate proposal focusing on purely electronic detection of nucleic acids on a genosensor microarray has been submitted as a new start proposal for FY 1998.

Based upon our prior experience extracting nucleic acids from environmental samples, we developed a cadre of nucleic acid purification techniques. Affinity resins can be sequence-specific (as in oligo-dT sepharose for purification of eukaryotic mRNA) or use a more general physical property of nucleic acids (e.g., electrostatic interactions), but they all use a solid support in a column or spin-filter format. With the affinity purification concepts in hand, we identified, pursued, and developed a collaboration with Cindy Bruckner-Lea and Jay Grate of the Environmental and Molecular Sciences Laboratory (EMSL), experts in flow injection and microfluidics technology.

The flow injection system developed in FY 1997 is operated under computer control and results in 10 µL to 10 mL of fluid handling capability. The second-generation flow cell developed under this project retains microparticles (>3 µm). We performed basic research to identify the flow regimes and programming steps necessary to manipulate microparticles ranging from 3 to 80 µm in size and from sepharose to silica in plasticity. Fundamental issues were addressed and dominated experimental work during FY 1997.

A significant body of literature exists for solution- and mixed-phase nucleic acid hybridizations, but affinity capture of large (> 1 Kbp) nucleic acids with surface-bound probes has not been thoroughly addressed. Further, very little information exists for the affinity capture and purification of dilute nucleic acids, in solution- or mixed-phase experiments. An experimental plan for assessing nucleic acid capture and purification efficiency at low DNA and RNA concentrations (< 10^6 copies) was therefore implemented for comparative analysis of benchmark affinity purification procedures versus comparable flow system performance.

Initial results showed that affinity purification of 1 ng genomic DNA (ca. 10^6 target sequences) is equally efficient in different butters with an absolute capture and detection limit ca. 1 to 10 pg (10^3 to 10^4 targets). Additional comparisons of benchmark and flow system capture of 1 ng genomic DNA suggest that the flow system offers a 10^3-fold increase in capture efficiency with a twofold reduction in sample processing time relative to the benchmark procedures. More impressive gains in purification/detection sensitivity and processing times are expected under a continuation of this project in FY 1998.

Adaptation of Mycofiltration Phenomena for Wide-Area and Point-Source Decontamination of CW/BW Agents

Jack Q. Word, Susan A. Thomas, Ann S. Drum, Peter Becker, Margaret R. Pinza, Ted Divine (Marine Sciences Laboratory)

Study Control Number: PN97006/1147

Project Description

The objective of our laboratory bench study was to test the effectiveness of a new biotechnology for decontamination/ remediation of chemical warfare (CW) and biological warfare (BW) agent contamination: *mycofiltration*[1], the application of living fungal mycelium[2] to remove/degrade contaminants. Based on the known capabilities of wood-degrading higher fungi, and using relevant surrogates to represent the CW and BW agents of interest, we developed methods, identified candidate proprietary fungal strains[3], measured the effectiveness of degradation, and determined as a proof of concept the efficiency and applicability of this approach to the treatment of CW/BW contaminants that are typically difficult and costly to address.

We also made progress toward meeting our longer-range objectives to identify and isolate active fungal enzymes that can facilitate capture or destruction of contaminants apart from the living fungal system. Our focus is on the development of a fungal enzyme-based CW/BW decontamination system that could be applied to equipment, personnel, and structures, and that in combination with application of the living mycelial systems could address wider-area decontamination, remediation, and detection.

Sixteen proprietary fungal strains were screened for their ability to grow in the presence of the sarin surrogate, dimethyl methylphosphonate (DMMP), and to effectively degrade the contaminant. Our experiments compared mycelial activity on three types of agar medium representing the range of environments that could be encountered in actual field situations. The range of sarin surrogate concentrations applied in the experiments reflect a realistic contaminant exposure that would likely be encountered in the field. Our screening resulted in the identification of 12 strains that are good candidates for effective application to CW decontamination, and among these, at least 5 that possibly could be deployed in very low- or non-nutrient conditions. We found that the addition of nutrient enrichment results in a decline in contaminant degradation by the mycelium. The effective fungal strains we identified are proposed for further evaluation under mesocosm and field conditions.

Using a species of fecal coliform bacteria, *Escherichia coli,* as a simulant pathogenic bacterial BW agent, we carried out experiments by which we identified at least one proprietary mycelial strain that inhibits/delays the bacteria's log-phase growth, one that completely inhibits its growth, and several that appear to actively attack or destroy the bacteria. Our observations and photodocumentation of liquid and crystal forms of the suite of enzymes or other exudates produced by each fungal strain in the presence of the contaminants contributes new basic scientific information. We are testing the isolated crystals for their specific enzyme activity and characteristics.

Technical Accomplishments

Team members received intensive training at Fungi Perfecti to establish fungal culture/expansion techniques, which we subsequently modified and adapted to our experimental design at the Marine Sciences Laboratory.

DMMP Experiments. We conducted preliminary laboratory bench-scale DMMP experiments using one proprietary fungal strain to test our method and analytical techniques. This strain achieved about 40% removal of DMMP over a 4-week period. In further preliminary steps, we tested toxicity/tolerance of five fungal strains to the sarin surrogate, established that there is robust growth in a range from 0.9 μg/g to 900 μg/g DMMP, which reflects a realistic set of values from low to high that would be likely to be encountered at a field site exposed to CW agents, and that there is no decline in growth with exposure to 100% DMMP. It was necessary to eliminate bacterial contaminants from the commercial reagent DMMP, and to demonstrate that these bacteria were not capable of remediation of the compound.

After we had developed appropriate growth medium, established the appropriate time-scale for experiments, and adapted chemical analytical procedures specific to this study, we conducted lab-scale DMMP tests. In approximately 500 test plates, 16 naive[4] fungal strains were exposed to 0.9, 9, 90, and 900 μg/g DMMP mixed into three different agar media—one enriched-nutrient,

one low-nutrient, and one non-nutrient (water-agar) medium—for a period of approximately 16 weeks. The experiment was terminated and chemical analyses were conducted to determine removal of DMMP by the different mycelial strains.

Results are summarized in Figure 1. Mycelia grown in the non-nutrient and low-nutrient agars achieved from 10% to >50% removal of DMMP, and variation in their effectiveness was related to differences among the fungal strains. However, fewer fungal strains were able to grow successfully on the non-nutrient medium. The enriched medium did not enhance the effectiveness of fungal degradation of DMMP; rather, removal of DMMP was close to zero for all 16 species.

The use of low-nutrient agar appears to be a useful technique for screening fungal strains both for tolerance of and for ability to remove CW contaminants. The effectiveness of certain strains in a non-nutrient medium is an indication that mycelial systems or their enzymes could be conditioned for decontamination of synthetic equipment and structures, for example, when a nutrient substrate (i.e., cellulose) is not present.

Escherichia coli Experiments. We selected and screened proprietary fungal strains by their characteristic growth, enzyme exudates, natural predation on bacteria, and other features. We also selected, based on literature search and personal communications, and acquired an appropriate *E. coli* strain for the purpose of these experiments. Initially, we established culture techniques, media, and analytical methods, whereby both fungus and bacteria can be grown together during exponential expansion periods on the same medium and under the same temperature regime, with tight analytical precision.

The experiment was carried out using Costar Transwell cell culture chambers, which are small cups with a central well insert that has a 12-μ pore-size membrane across the bottom, and sampling ports to allow access to the well and the outer chamber. Five mycelial strains were selected and cultured in nutrient broth in Transwell cell culture chambers either as a central plug under the membrane or as a ring around the insert well. At the start date of the experiment, three fungal strains were adequately grown for use. One hundred individual *E. coli* bacteria were introduced into each chamber, which was then incubated at room temperature in a humidity chamber in the dark, and sampled at 4 hours, 12 hours, 1 day, 2 days, and 3 days after bacterial inoculation. The broth culture in the Transwell insert and in the outer well surrounding the insert was sampled at each appointed hour through the ports, and the colony-forming units were analyzed by plating and counting. One of the three tested species is a probable candidate and another is extremely promising for this application.

Supplementary Experiments. During FY 1997, we performed a number of supplementary experiments. To enhance our capability to work in a variety of environments and conditions, and in anticipation of addressing a broader spectrum of CW/BW agents, we expanded our working-set of fungal strains to 26, including strains suited to arid, tropical, and other varied climatic or habitat conditions.

Enzymes - Several experiments were devoted to the photomicrographic documentation of mycelial development and growth on various agar media with and without CW/BW contaminants. These experiments allowed us to observe distinctive liquid enzyme exudates concentrated on the aerial portions of the mycelia (Figure 2), and further, to discover crystalline forms of exudates, which we believe to

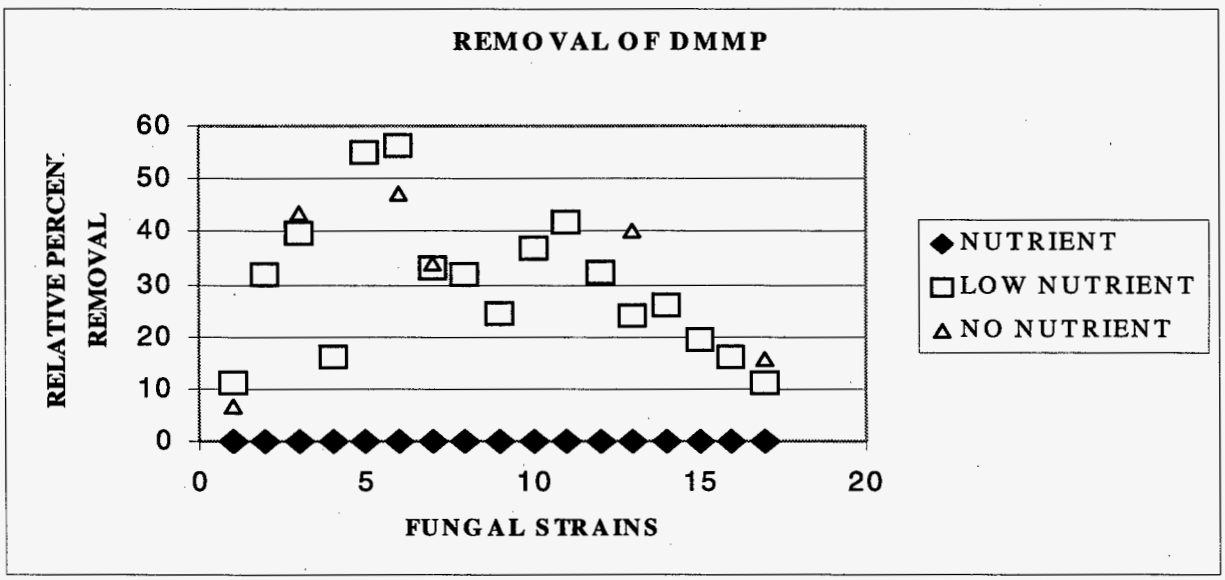

Figure 1. Relative percentage of removal of DMMP by proprietary fungal strains in non-nutrient and low-nutrient agar compared with that in nutrient-enriched agar.

Figure 2. Liquid enzyme exudate released by aerial portion of mycelium.

be enzymes, released by the growing mycelia into the agar, broth, or water-agar substrate under various conditions (Figure 3). We have found the crystals to be stable, and insoluble in saline, ethanol, methanol, and isopropyl alcohol. We began testing the crystals to determine their activity with regard to facilitating contaminant breakdown and to study their general characteristics, and we developed methods to harvest and isolate (separate from all traces of agar) sufficient quantities for further experiments. We are presently conducting protein assay of the compounds.

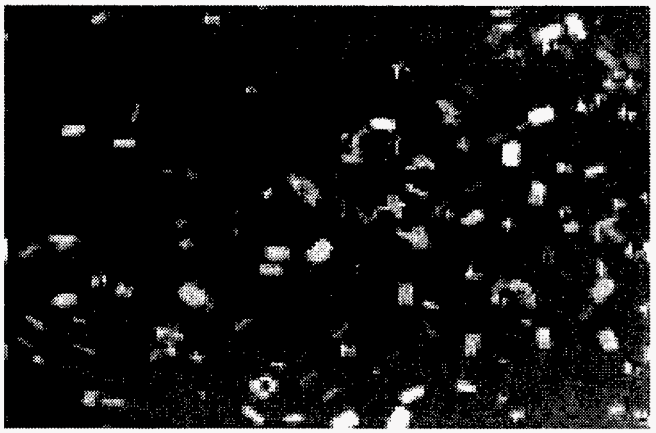

Figure 3. Crystalline forms of fungal exudate released in agar.

Our observations have advanced the basic scientific understanding of fungal degradation processes; crystal forms such as these are previously unreported in the literature. It appears that the fungal mycelia produce or mobilize different crystals, which we believe to be different enzymes, under exposure to different contaminants. We documented relatively dense production of crystals by mycelia in water-agar, in which DMMP was likely the only available nutrient source, despite nonrobust fungal growth.

Antibiotic - In our supplementary experiments with *E. coli*, we identified one mycelial strain that appears to completely inhibit growth of the bacteria (Figure 4). We documented the attraction of *E. coli* to an octahedral crystal type produced by Strain H, and the subsequent immobilization and apparent death of the bacteria (Figure 5).

Strain E (white) beginning to surround and engulf three *E. coli* colonies (gray)

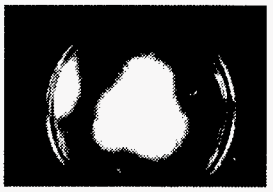

Strain F fungus (white) surrounded by three *E. coli* colonies (gray); no aggressive interaction

Strain H (white) completely inhibiting the growth of *E. coli* colonies that had been introduced into the three wells visible around the mycelium

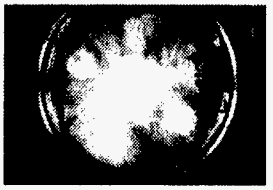

Strain P (white) aggressively attacking and reducing three *E. coli* colonies (gray)

Figure 4. *E. coli* was introduced into three wells in each agar plate surrounding a "plug" of fungal mycelium. The interaction with four different fungal strains is described; note complete inhibition of bacterial growth by Strain H.

IMPA - In the final weeks of FY 1997, we established an experiment analogous to the prior DMMP screening, but using 26 fungal strains on low-nutrient agar contaminated with isopropyl methylphosphonic acid (IMPA), another sarin surrogate. We observe strong growth of a large subset of the strains, and production of a suite of liquid and crystallized fungal exudates in the presence of IMPA. Chemical analysis is planned for early FY 1998.

Conclusion

Our objective was to test the effectiveness of mycelial systems for decontamination and remediation of CW/BW-affected materials. We accomplished the following:

- identified candidate fungal strains capable of degrading CW surrogates
- identified candidate fungal strains capable at least of demobilizing, and apparently of destroying (digesting) bacteria, under experimental conditions
- documented various liquid and crystal fungal exudates produced in response to various substrata and contaminants

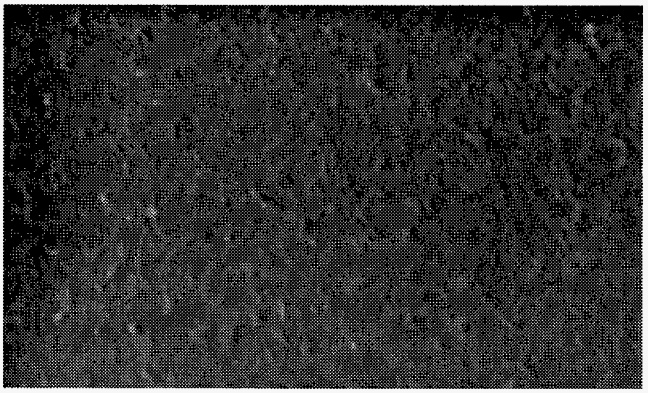

A

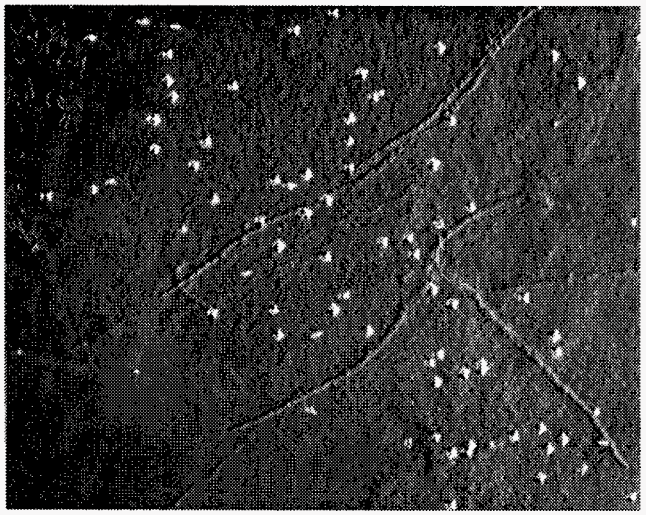

B

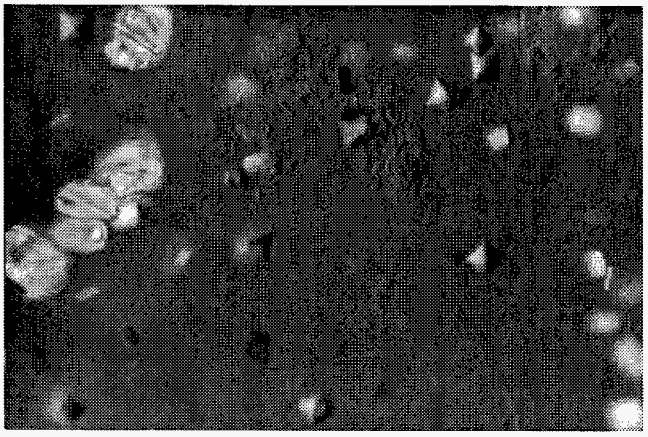

C

Figure 5. *E. coli* interaction with Strain H crystal exudates: a) *E. coli* dispersal outside crystal field in agar; b) motile *E. coli* approaching crystal field in agar (note mycelium); and c) *E. coli* clustered around octahedral crystals, and second polygon crystal type released by Strain H in presence of bacteria.

- developed laboratory testing procedures that permit evaluation of the effectiveness of mycelial systems in removing/destroying BW/CW surrogates
- determined that nutrient enrichment of substrate is detrimental to the effectiveness of mycelial systems in CW surrogate removal
- cultured 26 proprietary fungal strains with widely varying growth characteristics and environmental tolerances
- demonstrated that fungal strains modify the substrate, such as altering its pH
- tested combinations of strains for remediation/ decontamination.

Reference

P. Stamets. 1993. *Growing Gourmet & Medicinal Mushrooms*. Ten Speed Press, Berkeley, California.

---

1. The term *micofiltration* was coined by Paul Stamets, first published in Stamets 1993, p.15.
2. *Mycelium* is the perennial body of a fungus, which takes the form of a loosely organized mass of threadlike cells that permeate the substrate at a density of 1 mile of mycelium per cubic inch. The strands are invisible to the naked eye, except when they bundle together to form a thicker mat.
3. Proprietary fungal strains are cultured from wild species; selected, propagated, and supplied to us by our colleague Paul Stamets; and are identified only by code name (e.g., A,B,C).
4. Not preconditioned by previous exposure to DMMP.

Automated, Integrated Mesoscale Continuous Flow Multichannel PCR Thermocycler for Rapid Nucleic Acid Diagnostics

Mark T. Kingsley (Environmental Characterization and Risk Assessment)

Study Control Number: PN97016/1157

Project Description

A combination of novel materials selection, microfabrication technologies, mesoscale integration, microprocessor control for flexible system architecture (i.e., readily operator customizable for any desired application), combined with microchannel capillary electrophoresis and fiber optic detection will provide a rapid, robust, rugged nucleic acid amplification, detection and identification device—AIM-PCR. The multichamber thermocycler device will be micromachined into various plastic polymers including polycarbonate. The chambers/wells will be disposable, the micromachined heater system will be reused. Each of the chambers/wells will be set up as an independently addressable grid system, therefore the channels can be reprogrammed as needed to alter the cycle timing parameters. Each well will be independent of the other wells for programming/cycling purposes; therefore a series of different primer/probe combinations can be cycled simultaneously. By employing a "TaqMan" approach, amplification/detection can occur in real time. If a fingerprint modality is the desired output, the PCR products can be loaded onto a microchannel capillary electrophoresis system, or micro-capillary HPLC for product separation and sizing. The products can be detected either via ultraviolet absorbance or fluorescence. The product sizes can be compared to the on-board data library and an answer to identify provided. Additional product detection options are mass spectrometry and DNA hybridization arrays.

Technical Accomplishments

At the second annual Microfabrication Technology for Biomedical Applications symposium (October 1996), it was learned that at least two firms (Affymatrix and Perkin Elmer) were developing prototype micromachined PCR systems. Discussions were held with Perkin-Elmer in FY 1997 and we concluded that our approach, with independent heating for each well, was a potentially novel approach and design work was begun. A relatively large (sample volume) device (for ease of sample addition/removal) was initially planned. Thermal modeling of this design, conducted by Hank Reid, ruled out this design as too power hungry and also indicated problems in heat transfer laterally between sample chambers. Subsequently, a smaller chamber design was implemented along with a different design for the heat sink and other layers. This initial four-well design is static (i.e., not flow-through). This will allow us to concentrate on issues of the heating and control functions, stability, and the overall operation of the control program. Fabrication of the initial four-chamber prototype has been completed; initial programming of the control software for cycler operation has been implemented. The current sample chamber wells are constructed of thermal conducting plastic from a mold created for their fabrication. Other moldable plastic polymers will be tested to determine their usefulness with this design. The sample well/chamber is independent of the heating pads, therefore the relatively inexpensive sample wells can be replaced with clean sample chambers for subsequent amplifications. (See Figure 1.)

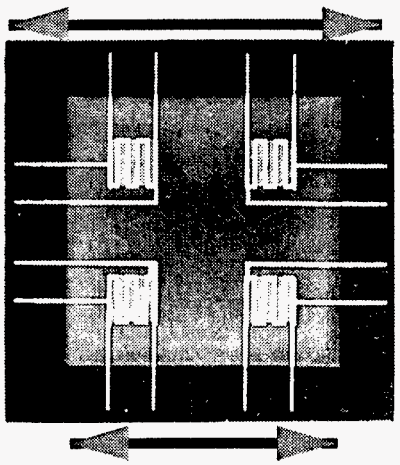

Figure 1. Prototype four-position, independently addressable thermocycler heater module. The four sample well chambers, molded from 25% carbon filled polyamide plastic polymer, and Pyrex glass lid and integral seals (not shown) are clamped on top of the heater system. The sample wells, containing DNA solution and chemistries sit directly above the individual heater modules.

The thermal modeling of the initial design proved extremely useful and indicates that we will have to pay great attention to thermal bleed between the individual heaters/sample chambers. The commercial firms pursuing PCR-chips are employing one heating element for all

sample wells; one reason may be ease of design to avoid the issues of thermal bleed in a multiheater system. We think the ability to independently control the thermal characteristics of the amplification provides us with an additional level of control of amplifications in addition to modifying the sample chemistries (approach taken by Perkin Elmer).

Bioremediation: Mycofiltration Mesocosm Study for the Cleanup of Oil-Contaminated Soil

Meg Pinza, Peter Becker, Susan Thomas (Environmental Technologies)

Study Control Number: PN97020/1161

Project Description

The objective of this laboratory study was to test the bioremediation effectiveness of living fungal mycelium on the petroleum hydrocarbons of Bunker C oil in both alder chip and soil substrate. Comparisons were made based on quantification of the standardized oil components (aromatics and alkanes) at the start, middle, and end points of the experiment. We addressed the effectiveness of mycelium and microbial populations separately as well as in combination, with appropriate controls and baseline information. A secondary objective was to compare the rate at which such degradation occurs. A proprietary strain of the fungus *Pleurotus ostreatus* was selected, cultured, and evaluated for the transformation or removal of the petroleum products. We developed methods for the bench-scale tests and evaluated the end products of the transformation. In addition, we conducted supplementary experiments to help elucidate the mechanism of fungal breakdown of oil and to explore the associated enzyme activity; to screen several species for their effectiveness; and to test the system at the mesocosm scale under field conditions.

We found that the most effective treatment among those tested was an application orchestrated to let our selected, mycelium dominate, but to act in combination with the native microbiota present in alder chips and soil. Based on results from other studies, we expected that the oil-contamination in soils treated with *Pleurotus ostreatus* mycelium would be transformed and reduced by at least 80%. In our 8-week experiment, the polynuclear aromatic hydrocarbons (PAHs) were reduced by 97% by the most effective treatment; the higher-molecular-weight PAHs (4- to 6-ring) by 62%; and lower-molecular-weight PAHs (2- to 3-ring) by 99%. Total alkanes (C_8 to C_{29}) were diminished by 82% during the same time period; the longer-chain alkanes (C_{15} to C_{29}) by 80%; and the shorter-chain alkanes (C_8 to C_{14}) by 89%. In our mesocosm test, we attained 92.3% removal of PAHs in 12 weeks under outdoor, field conditions, using a combination of two proprietary fungal strains and a mycelial mat deployment system.

Technical Accomplishments

The experiment was carried out at laboratory bench scale, in 4-L glass test chambers containing 1 kg substrate. We used a 2% by weight application of a standard oil mix (500 g Bunker C oil diluted with 3 L Number 2 diesel) in substrate consisting of either soil, alder chips, or a combination of the two. Ten treatments were applied with three replicates, and appropriate controls and quality controls were run concurrently (Table 1). The results are shown in Tables 2 and 3. The most effective treatment (H), namely a community consisting of our proprietary strain of fungal mycelium in the dominant role, with the native fungal/bacterial populations from the alder chip and soil substrate, accomplished a 97% removal of PAHs and 82% removal of alkanes in a period of 8 weeks (see highlighted column H in Tables 2 and 3). We developed methods that can be applied to any number of parallel studies and commercial applications.

Table 1. Summary of treatments.

A.	Oil, mycelium, autoclaved alder
B.	Oil, mycelium, nonautoclaved alder
C.	Oil, nonautoclaved alder
D.	Oil, soil
E.	Oil, soil, autoclaved alder
F.	Oil, soil, nonautoclaved alder
G.	Oil, soil, mycelium, autoclaved alder
H.	Oil, soil, mycelium, nonautoclaved alder
I.	Oil, autoclaved soil
J.	Oil, autoclaved alder

Supplementary Experiments. During FY 1997, we performed a number of supplementary experiments to broaden the number and variety of mycelial strains in culture to around 20, to further our understanding of the mechanisms of fungal degradation of contaminants and of the enzymes that mediate the reactions; to expand our capability to deploy mycelial systems in the field; and to challenge the

Table 2. Percentage of each PAH removed from the test chambers after 8 weeks.

TEST CHAMBER CODE	A	B	C	E	F	G	H	J
COMPOUND								
naphthalene	83%	95%	68%	98%	99%	99%	100%	36%
biphenyl	44%	72%	42%	99%	99%	99%	99%	-6%
acenaphthylene	78%	58%	29%	89%	92%	86%	88%	34%
acenaphthene	89%	73%	37%	94%	95%	96%	97%	11%
fluorene	90%	71%	34%	99%	100%	97%	100%	9%
dibenzothiophene	78%	51%	34%	89%	87%	91%	97%	14%
2-RINGS	68%	76%	44%	98%	98%	98%	99%	9%
phenanthrene	60%	39%	26%	94%	97%	94%	99%	18%
anthracene	79%	1%	10%	71%	86%	87%	93%	18%
fluoranthene	40%	-38%	9%	73%	79%	82%	89%	-3%
3-RINGS	60%	37%	25%	93%	96%	94%	98%	18%
pyrene	73%	25%	5%	28%	19%	70%	62%	8%
benzo(a)anthracene	74%	39%	13%	71%	80%	84%	90%	8%
chrysene	45%	19%	9%	40%	47%	60%	65%	12%
benzo(b)fluoranthene	30%	23%	10%	25%	30%	43%	61%	12%
benzo(k)fluoanthene	11%	12%	21%	45%	53%	44%	78%	9%
4-RINGS	62%	25%	8%	37%	38%	68%	66%	9%
benzo(e)pyrene	31%	21%	9%	21%	21%	45%	36%	9%
benzo(a)pyrene	91%	43%	13%	21%	25%	79%	58%	12%
perylene	17%	21%	57%	29%	26%	44%	59%	26%
indeno(1,2,3-c,d)pyrene	25%	24%	-16%	29%	30%	59%	46%	-13%
dibenzo(a,h,)anthracene	45%	32%	10%	18%	13%	51%	40%	19%
5-RINGS	50%	29%	25%	23%	23%	57%	48%	14%
benzo(g,h,I)perylene	56%	24%	13%	17%	14%	59%	51%	16%
TOTAL PAH	65%	64%	38%	94%	94%	95%	97%	12%

cultured mycelial strains with a variety of contaminants, with extreme concentrations of contaminants, and with a range of environmental conditions.

Expand Strains in Culture - We expanded our culture strains from the original single strain of *Pleurotus ostreatus* to about 20 strains selected for potential application to a range of chemical and biological targets, and a range of environmental tolerance. We tested most of these strains with petroleum hydrocarbon contaminants, and identified those with the greatest natural affinity to attack this class of compounds—that is, to grow robustly in medium containing oil, and to rapidly degrade the petroleum product. We have found no strains in our screening that do not grow on or use petroleum hydrocarbons at least of 2%, and up to 100% concentration by weight of oil to substrate.

Enzymes - Several experiments have been devoted to the photomicrographic examination of the development and growth of mycelial cultures on various agar media. These experiments have led to the observation of distinctive liquid enzymes exuded by the aerial portions of the mycelia, and further, to discovery of crystalline forms of enzyme exudates released by the growing mycelia and pushed ahead through the substrate. Some of these crystals are produced, we believe, as broad spectrum, low-specificity enzymes, and others are released in response to particular contaminants/food sources in the environment. We feel that these stable crystal forms may have important implications for chemotaxis and enzyme degradation processes. This phenomenon has not yet been reported by other researchers in the mycological literature. We have isolated some of the crystals, and we are currently beginning to test their properties and activity.

Mesocosm Experiment - In this important step toward broad-scale field application, we used a combination of two selected, mycelial strains to address 2% contamination by weight of oil (Bunker C/diesel) in a 50-lb soil substrate, outdoors in Pacific Northwest weather conditions for 12 weeks. Our treatment attained 92.5% removal of total PAHs, with particularly high rates of removal of the larger, 5- and 6-ring compounds. At the halfway-point of the experiment (sampled at 6 weeks), the removal of PAHs was

Table 3. Percentage of each alkane removed from the test chambers after 8 weeks.

TEST CHAMBER CODE	A	B	C	E	F	G	H	J
COMPOUND								
c8								
c9	97%	95%	94%	95%	98%	97%	97%	94%
c10	90%	93%	91%	94%	98%	96%	96%	85%
c11	71%	85%	67%	89%	96%	93%	94%	59%
c12	48%	67%	30%	77%	86%	83%	90%	28%
c13	43%	63%	19%	74%	79%	78%	89%	16%
c14	27%	47%	9%	58%	63%	65%	84%	7%
Low Alkanes	48%	66%	33%	74%	81%	79%	89%	30%
c15	22%	52%	5%	59%	56%	66%	81%	-5%
c16	21%	45%	0%	50%	54%	56%	77%	-5%
c17	13%	56%	6%	62%	74%	66%	84%	0%
pristane	6%	21%	7%	26%	37%	31%	40%	2%
c18	14%	48%	10%	63%	58%	59%	82%	3%
phytane	2%	15%	3%	17%	26%	15%	29%	-1%
c19	13%	41%	9%	50%	60%	50%	74%	4%
c20	7%	37%	8%	47%	62%	47%	79%	-1%
c21	14%	33%	4%	43%	62%	48%	76%	-3%
c22	14%	36%	7%	45%	65%	50%	78%	-1%
c23	15%	32%	6%	44%	63%	48%	78%	0%
c24	10%	31%	6%	45%	64%	48%	79%	2%
c25	10%	28%	-1%	48%	62%	47%	76%	5%
c26	5%	22%	-16%	53%	61%	46%	77%	7%
c27	-9%	9%	-19%	53%	60%	46%	70%	6%
c28	0%	-1%	-21%	44%	56%	-39%	65%	-2%
c29	-23%	14%	23%	-20%	19%	35%	43%	-47%
c30	-14%	-16%	-11%	34%	38%	25%		-12%
c32	-29%	-35%	-20%	24%				-40%
High Alkanes	14%	42%	14%	50%	57%	52%	73%	-1%
Total Alkanes	22%	47%	18%	55%	63%	59%	76%	7%

already 77.1%. These results are comparable to those attained in the laboratory bench-scale tests. In comparison with published results of bioremediation (using bacterial systems, with periodic fertilization and tilling) and phytoremediation (using plants, with periodic fertilization and initial tilling), this degradation of the aromatic components in oil is significantly faster (weeks instead of years), more efficient (close to 100%, instead of 50%), and will be ultimately more economical because there is no need for fertilization or tilling of mycelial applications (see Drake 1997; Glass 1997).

Field Deployment - In the mesocosm (above) and other experiments, we also tested and had excellent success with a unique field deployment technique for both terrestrial and aquatic application using coca-fiber mats on which to grow and transfer the living mycelium (Figure 1). We can dehydrate the mats, fully grown with mycelium, for storage and subsequent rehydration for field deployment. We deployed mats in various settings, including both terrestrial and (floating) aquatic, combining plants with the mycelium on some of the mats. We successfully tested the ability of the mycelial mats to persist and grow robustly in the field, in spite of mycovores (animals that eat fungus) and extremes of weather. Other field deployment techniques that we tested included culturing mycelium on bamboo stakes that can be driven into the ground, on rice grass mats, and on corn stalk materials, among others.

Challenge Tests - Some examples of the challenge studies we conducted are as follows: we freeze-dried mycelial mats for long-term storage, and rehydrated them for deployment. We cultured several selected strains exposed to or directly in medium containing Bunker-C/diesel oil mix, and found that in successive steps of culture, we could *precondition* the mycelium to prefer oil to nutrient agar medium. We cultured several selected strains exposed to 100% pure Bunker-C/diesel oil either by direct pipetting of oil onto an existing culture, or by surrounding a plug of mycelium with disks soaked in oil, or by incorporating the

Figure 1. Field deployment: mycelial mat floating in freshwater catchment pond.

oil into agar. The mycelium grew successfully, and nearly completely degraded the oil within a few weeks. The initial effect of the fungal enzymes on the Bunker C oil was to decrease its viscosity. Subsequently, the oil was transported cell-to-cell within the mycelium, and was gradually broken down (the disappearance is readily observed, day by day). We observed particular liquid/crystal forms of enzyme exudate produced in response to the presence of oil.

Conclusion

In our objective analysis of the remedial treatment of oil contaminated soil using various combinations of a selected cultured mycelial strain, autoclaved and nonautoclaved soil, and autoclaved and nonautoclaved alder chips, we demonstrated that a combination of the selected, cultured mycelial strain of *Pleurotus ostreatus* as the dominant entity, acting with resident bacteria and fungi native to alder chips and soil, was most effective of all the treatments that we compared in reducing levels of PAHs and alkanes during the 4- and 8-week intervals after inoculation. We were able to demonstrate in a supplementary, mesocosm-scale experiment that the results we attained at laboratory bench-scale are valid for outdoor, field conditions as well.

Only slightly less effective in all cases and somewhat more effective in removal of some high-molecular-weight PAHs in our bench-scale experiments was the application of our selected strain of *Pleurotus ostreatus* alone, without any microbial community. However, because the native microbiota in both soil and alder is at least 50% fungal mycelium, and because native *Pleurotus ostreatus* was very likely among the dominant fungal species in the nonautoclaved alder chip micro-community, we cannot in our present analysis account for the potential overlap of fungal, and specifically of *Pleurotus* activity in the degradation process. This does not detract from the strength of applying selected, cultured mycelial strains to remediation, but rather lends support to our community approach to the application. The presence of specific fungal strains in any given sample of soil at a site that requires remediation is fortuitous at best, determined by a complex set of opportunities and environmental conditions. For remediation, control of the dominant, active species is important if the treatment is to be both successful and repeatable.

References

E.N. Drake. 1997. "Phytoremediation of aged petroleum hydrocarbons in soil." In *Proceedings, IBC Second Annual Conference on Phytoremediation*, June 18-19, 1997, Seattle, Washington.

D.J. Glass. 1997. "Evaluating phytoremediation's potential share of the remediation market." In *Proceedings, IBC Second Annual Conference on Phytoremediation*, June 18-19, 1997, Seattle, Washington.

Publication

S.A. Thomas, M.R. Pinza, P. Becker, J.Q. Word, and P. Stamets. 1997. Draft Report: Bioremediation: Mycofiltration Study for the Cleanup of Oil-Contaminated Soil. Battelle Marine Sciences Laboratory, Sequim, Washington. (To be adapted for submittal to *Environmental Health Perspectives.*)

Electron Paramagnetic Resonance of Environmental Enzymes

Michael K. Bowman (Macromolecular Structure and Dynamics)

Study Control Number: PN96021/1088

Project Description

The long-term goal of this effort is to isolate and to understand the structure and functional details of enzymes with metal reduction activities. These activities are important for bioremediation and for understanding radionuclide and toxic metal fate and transport. We will apply the advanced instrumentation of EMSL to characterize key structural details such as the location and structure of the heme site and the reduction site in the putative metal reducing enzyme from *Shewanella alga*. We will also investigate the action of inhibitors of its activity. We hope to eventually develop a sufficient understanding of the mechanism of these enzymes to predict their behavior in the subsurface and to make directed alterations to their metal substrate specificity.

Technical Accomplishments

We are studying *S. alga* because of its ability to reduce iron and other metals, particularly Co, U, Cr, and other potentially important environmental contaminants. Although it remains to be confirmed, current indications are that 1) the terminal iron reductase (TIR) is a membrane-associated cytochrome with an apparent molecular weight derived from gel mobility of 37 kDa, and 2) the TIR has reductase activity for several metal and radionuclide contaminants.

Terminal Iron Reductase Identity

We have purified nine heme proteins from *S. alga* Strain BrY grown under anaerobic conditions to test some of their biochemical and spectroscopic properties. Heme proteins in fractions from ion exchange columns were checked by optical absorption spectroscopy and gel electrophoresis (SDS-PAGE), Figure 1, using heme stain and Coomassie Blue stain and purified as needed using additional ion exchange columns to obtain a purity of >90% with high yields.

The 37 kDa protein seems to have all the properties expected of the TIR. The 37 kDa protein is predominantly membrane bound, as is the metal reductase activity in

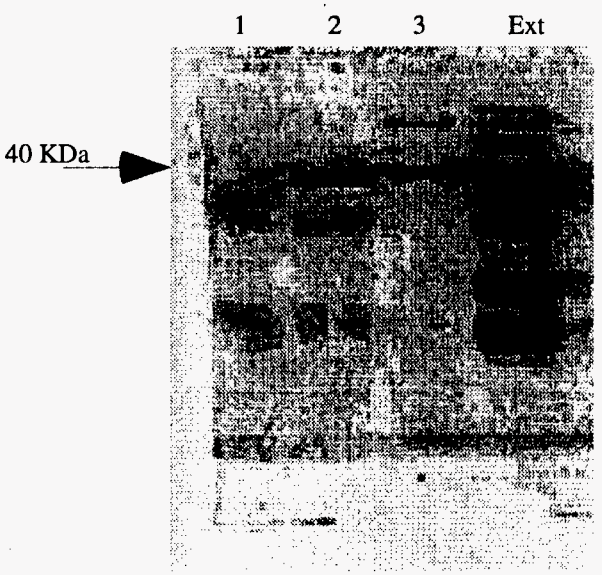

Figure 1. SDS-PAGE of membrane fractions from *S. alga* purified on a DE52 ion exchange column. Lane 2 - the pure 37 kDa band; Lane 3 - 37 kDa band with a high molecular weight heme protein; Lane 4 - the crude membrane extract with six different heme proteins.

Ten different heme proteins were seen in different cell compartments:

Periplasmic location	95	85	45	37	33	6
Cytoplasmic location	95	85	37	33	14	
Membrane bound	90	50	45	37	30	

S. alga. The optical absorption spectrum of the native and the reduced protein, Figure 2, clearly shows characteristic spectra of a c_3 type cytochrome. The spectrum of the

oxidized sample has the main Soret band at 408.0 nm; upon reduction the Soret band shifts to 418.5 nm and an additional sharp band appears at 553.0 nm. These characteristics are similar to the cytochrome c_3 in *D. vulgaris* and *D. desulfuricans* reported to have metal reductase activity.

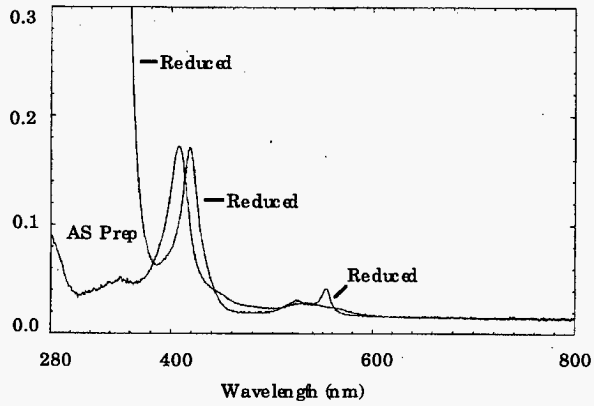

Figure 2. Optical absorption spectrum of oxidized and reduced forms of the purified 37 kDa cytochrome from *S. alga*.

The low temperature (~10 K) electron paramagnetic resonance (EPR) spectra of the 37 kDa fraction (Figures 3 and 4) clearly show resonances due to a rhombic, high-spin ferric heme (S=5/2); a rhombic, low-spin ferric heme (S=1/2); and a copper center. The pulsed EPR spectroscopy known as HYSCORE indicates that the copper center in the 37 kDa protein has a histidine ligand.

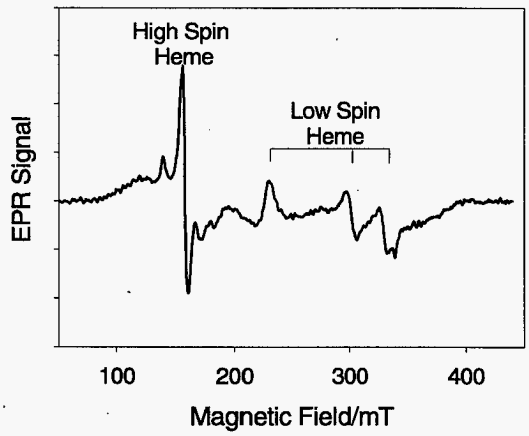

Figure 3. EPR Spectrum of the 37 kDa cytochrome with peaks from high-spin and low-spin hemes. Recorded at 8 K with 1.0 mW microwave power at 9.49 GHz with 100 kHz field modulation of 0.94 mT amplitude.

The presence of copper was confirmed by plasma emission (ICP) spectroscopy which found iron, zinc, and copper in a 3:1:1 molar ratio. This measurement, together with the

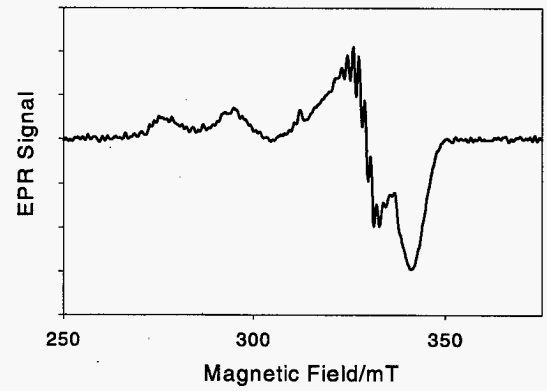

Figure 4. EPR spectrum of the 37 kDa cytochrome recorded at 77 K with the heme signals broadened beyond delectability. Recorded with 2.0 mW microwave power at 9.44 GHz with 100 kHz field modulation of 0.84 mT amplitude.

observation of both high- and low-spin heme, strongly suggests that the 37 kDa protein contains three hemes and two strong binding sites for divalent metal ions.

We expect the TIR to have a binding site for its metal ion substrate. In addition, metal reductase activity is inhibited by copper. Our working hypothesis is that the 37 kDa protein is the TIR and that it has a substrate binding site and an inhibitory copper binding site occupied during protein purification by zinc and copper impurities in the concentrated salt solutions used. Finally, we note that although the mobility of the protein on SDS-PAGE is that of a nonmembrane protein with a mass of 37 kDa, electrospray ionization mass spectrometry (ESI-MS) of the denatured protein reports a mass of 25078 +/- 4 Da, Figure 5.

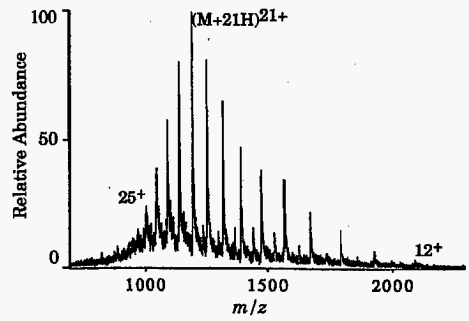

Figure 5. ESI-MS spectrum of the denatured 37 kDa cytochrome showing the multiple charged states.

Evaluation of Cellular Response to Insult

Charles G. Edmonds, Toyoko Tsukuda (Macromolecular Structure and Dynamics)
Margaret F. Romine (Earth Systems and Science)

Study Control Number: PN95033/1009

Project Description

The study of gene expression may be approached by the separation, isolation, and structural characterization of the relevant gene product(s). Derived amino acid sequence, even if only partial, allows the design of reverse translated nucleotide probes to identify, map, and isolate the corresponding gene. Alternatively, with the complete genome sequence, this task may be accomplished by searching the grand sequence database. Two-dimensional polyacrylamide gel electrophoresis (2D-PAGE) is among the most highly resolving methods in analytical biochemistry. It is well suited for the evaluation of new gene products and changes in abundance of virtually the complete array of proteins expressed (the proteome) in bacterial systems. We have developed and are refining a combined methodological approach for the "pico-scale" sample handling, chemical and/or enzymatic digestion, isolation, and concentration of such proteins. These methods will include matrix-assisted laser desorption ionization mass spectrometry and capillary zone electrophoresis and capillary isotachophoresis in dynamic combination with electrospray ionization mass spectrometry. This combination will add a new and sensitive axis of selectivity to the 2D-PAGE experiment which includes data on primary amino acid sequence and also the nature, the extent, and the residue location of post-translational modifications. Such developments will have wide applicability in the mass spectrometric extension of 2D-PAGE protein databases, correlation of cDNA sequences generated by the DOE Microbial Genome Project, the cataloging of functional relationships among sets of proteins, and the evaluation of co-regulation of gene expression in a variety of induced processes.

Technical Accomplishments

Our new mass spectrometric methods will permit the evaluation in 2D-PAGE analysis of the co-regulation of induced gene expression. This information will be invaluable in the studies of bacterial genes and gene products and in the highlighting of pathways which are induced by changes in environmental conditions and that are responsible for the metabolic transformation of environmental contaminants.

Aromatic hydrocarbons are common contaminants in groundwater nationwide. The Department of Energy supports investigations aimed at the use of the endogenous microorganism for in situ bioremediation of contaminated subsurface sediments and groundwater. Fredrickson and coworkers have isolated a subsurface bacterium *Sphingomonas* strain F199 from the sediments at 407 m below the soil surface. The subsurface bacterium *Sphingomonas* was shown to have the ability to use all xylene isomers, *p*-cresol, naphthalene, and toluene as a sole carbon and energy source.

We report the recognition of the proteins that are involved in the degradation of aromatic hydrocarbon in *Sphingomonas* F199. Two-dimensional gel electrophoresis provides an effective tool to identify the proteins that are induced, altered, or eliminated in response to environmental or genetic changes. The 2D-PAGE resolves the proteins on the basis of the polypeptide net charge in the first dimension and of the molecular sizes in the second dimension. The first dimension isofocusing gel (17 cm in length x 1.5 mm in diameter) consists of 3% polyacrylamide gel containing 9 M urea and ampholytes pH 310 (40%) and pH 4.56 (60%). After applying 900 voltage for 17 hours to the first dimension gel, the gel was laid on the second dimension 12% SDS polyacrylamide gel (19 x 21 cm) to separate the proteins according to their sizes. The resolved proteins in the gel were detected with the ammoniacal silver staining. With greater than 100 µg of the crude cell lysate, approximately 200 proteins between the molecular sizes for 80,000 to 17,000 daltons and the PI ranges of 4.5 to 6.3 were detected.

Various factors influence isofocusing of the proteins and the integrity of the first dimension gel. For example, isofocusing the F199 cell lysat resulted in breakage of the gel at the region where the pH is 7 to 8. However, electrofocusing the crude lysates form other species, or the strain of bacteria did not cause the gel breakage even when they were run under the same conditions. Varying the ratio and the type of ampholyte and the duration of electrophoresis minimized the breakage of the gels containing the F199 lysate. The gel breakage after isofocusing has often been documented—the explanations for the problems were not consistent. Since the first dimension gel is very thin (1 mm

in diameter) the salt concentration, nucleic acid contamination, and cell membrane components in lysate may attribute to the aberrant resolution of the proteins or/and the breakage of the gel. The component of the cell lysate varies from one strain of bacteria to the other. Therefore, the optimum condition for the isoelectrofocusing has been determined empirically for each species and strain of bacteria. The cell growing condition was established for each aromatic hydrocarbon source in the medium. For the *m*-xylene, its vapor was applied in the culture flask and the cell culture was incubated statically for 4 days at 30°C. For *p*-cresol, the cell were grown in 0.01% *p*-cresol which was added to the media every 24 hours for 4 days with aeration.

The induced proteins by *p*-cresol and *m*-xylene carbon source were identified by comparing to the control lactate carbon source. Using the 2-DE molecules standards, the size and the values of the electrofocusing points (PI) of the induced proteins were estimated (Table 1).

Publication

C.E. Edmonds. "Identification of the proteins involved in the degradation of *m*-xylene in a subsurface bacterium *Sphingomonas* F199." (in preparation).

Table 1. The estimated molecular weight (M.W.) and pI of proteins induced with m-Xylene and p-Cresol.

m-Xylene Induced Proteins				*p*-Cresol Induced Proteins	
Estimated		Estimated		Estimated	
M.W. (kd)	Predicted pI	M.W. (kd)	Predicted pI	M.W. (kd)	Predicted pI
53.2	5.1	40	4.85	55	5.6
52.6	5.2	39.3	5	49	5.8
52.4	5.3	37.2	5.05	43	5.6
51.0	5.7	36	5.85	37	5.8
51	5.7	36	5.8	33	5.8
50.8	5.85	35	5.05	31	5.8
50.8	5.8	35	4.95	29	6.4
50.4	5.6	35	4.85		
50.2	5.7	34	5.3		
46.7	4.55	31	5.5		
43.3	4.85	30.7	5.05		
43.2	5.25	29.2	4.6		
42.7	4.95	28	5.15		
40	4.95	27.2	5.2		

Mechanism of Biotransformation of Environmental Contaminants

Michael K. Bowman (Macromolecular Structure and Dynamics)

Study Control Number: PN96045/1112

Project Description

This project developed and applied macromolecular structural techniques, particularly Fourier transform electron paramagnetic resonance (EPR) spectrometry to study degradative enzymes and reactions at metal oxide surfaces. We developed methods to determine the conformation of substrates and the catalytically active site in order to understand the mechanism, the binding affinity, and the selectivity of these systems. We developed new spectroscopic methods such as HYSCORE for unoriented samples and three-dimensional HYSCORE-like experiments to obtain high-resolution spectroscopic data. These data, in the form of the spectroscopic coupling parameters, are related to structural and chemical properties of the active site or substrate using molecular modeling methods. The resulting molecular insights into structure and reactivity were applied, within the limited scope of this project, to purposefully alter the properties of an enzymatic or surface reaction.

Technical Accomplishments

This project has partially characterized the Rieske iron-sulfur center in 2,4,5-T monooxygenase, a multicomponent enzyme that helps degrade Agent Orange and other related persistent pesticides. This Rieske-type center shows differences in the HYSCORE spectra of the iron-sulfur center from the Rieske center in the prototypical eukaryotic, electron transport proteins. This is not surprising given the evolutionary distance between these proteins. However, it is more surprising that the spectra from this protein differs in some details from those recently published by the Cammack group on other oxygenases. The origin of these differences is not apparent, but may be related to changes in the structure or the environment of the iron-sulfur center that the protein uses to help tune the redox potential of the cluster. Since there is only a single x-ray crystal structure of a Rieske center, we turned to the plant-type two-iron, two-sulfur centers found in ferredoxins and many other proteins. There are a half dozen crystals structures for these, the best existing for the ferredoxin from *Spirulina platensis*, by all evidence nearly identical to the analogous protein from *Porphyria umbilicalis*.

A significant body of work exists that links, both theoretically and experimentally, the protein conformation around the iron sulfur center and the isotropic hyperfine couplings to the β-cysteine protons of the iron ligands. Because these structural details are quite difficult to obtain by diffraction or NMR methods and because the immediate conformation has been implicated as a determining factor in controlling the redox potentials, we have worked on developing methods to accurately and rapidly characterize this structure in unoriented protein samples.

We have developed a graphical spectral analysis method to determine the hyperfine couplings of weakly-coupled I=1/2 nuclei from HYSCORE spectra. We have applied this to the ferredoxin of *P. umbilicalis* and compared the protein conformation with the x-ray crystal structure (Figure 1).

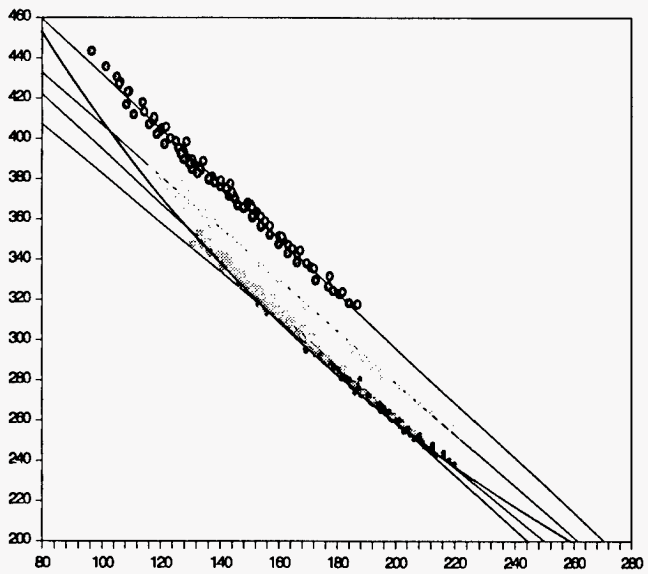

Figure 1. Peaks of non-exchangeable protons from the HYSCORE spectrum of a ferredoxin of *P. umbilicalis* in frozen solution. Four sets of points fall along the four straight lines indicated. The locations at which each line crosses the curve give the ENDOR frequencies of the principal directions of the hyperfine tensors. The coordinates are the squares of the frequencies in the HYSCORE spectrum and convert the curved arcs in the typical proton HYSCORE spectrum into the straight lines seen here.

Right around the iron-sulfur center, the HYSCORE-derived structure is in excellent agreement with the x-ray structure. These measurements have been extended to three-iron, four-sulfur centers in bacterial hydrogenases where there is a significant controversy over the role of those centers despite a good x-ray diffraction structure for the protein (Table 1).

Table 1. Iron-sulfur-carbon-proton dihedral angles for the β-cysteine protons in the ferredoxin of *P. umbilicalis* as determined here by HYSCORE and from two successive published refinements of the x-ray diffraction data.

		HYSCORE	X-Ray 4FXC	X-Ray 3FXC
Fe(II)	Cys-41	37	39	4
		157	159	124
	Cys-46	37	40	45
		157	160	165
Fe(III)	Cys-49	30	-3	-41
		150	117	79
	Cys-79	30	0	20
		150	120	140

The structure of a widely used active site probe was improved based on pulsed EPR data obtained in this project. The advanced HYSCORE spectroscopy measurements used here were able to distinguish the involvement of the amine nitrogen of histidine as a direct ligand of oxovanadium in complexes modeling active metal sites in xylose isomerase and other enzymes.

The relationship between the spectroscopic parameters that can be measured in pulsed EPR experiments and the structure of active sites in metalloproteins and oxide surfaces have been explored in an ongoing series of calculations. We have completed a study of the ligand conformation and isotropic hyperfine coupling for a series of model structures involving cysteine and Co(II) and are in the midst of a mixed-valent calculation for a two-iron, two-sulfur center. In addition, we have calculated results for an anthraquinone reporter molecule at surface sites of an aluminum oxide cluster. One such structure predicts couplings that match well with the experimental results obtained for anthraquinone at an active site on alumina. Completion of these calculations will allow us to assign specific structures to several of the species observed and to serve as a guide for extension to other metal oxide surfaces.

Publication

R.I. Samoilova, S.A. Dikanov, A.V. Fionov, A.M. Tyryshkin, E.V. Lunina, and M.K. Bowman. 1996. "Pulsed EPR Study of Orthophosphoric and Boric Acid Modified γ-Alumina." *J. Phys. Chem.* 100, 17621-17629.

Microbial Gene Expression and Genetic Engineering

Kwong-Kwok Wong, Jeffrey D. Saffer (Molecular Biosciences)

Study Control Number: PN95056/1032

Project Description

The objective of this research was to develop gene expression technology for the expression of diverse enzymes to support microbial biotechnology applications. In order to develop an expression technology, genetic elements or genes that are regulated by environmental signals have to be defined, and appropriate vectors have to be developed. In this study, we used a method developed in FY 1996 to clone and sequence RNA from the Columbia River sediment, for identification of genetic elements that are expressing in the natural environment.

Technical Accomplishments

Established Method to Amplify Partial cDNAs from Minute Amounts of RNA

By modifying the TRHA method, which was developed in FY 1996, we successfully amplified partial cDNA fragments from minute amounts of RNA isolated from 10 g of Columbia River sediment. The isolated RNA was analyzed (Figure 1, lane 1 to lane 3), and we were able to amplify enough cDNA with size ranges from 0.5 kb to 2 kb for visualization in the agarose gel (Figure 1, lane 4). We have cloned the TRHA-amplified cDNA products into the pCR-blunt cloning vector (Invitrogen). From the initial sequencing analysis of 12 clones, we were able to assign putative functions to five, including NADH dehydrogenase I, assimilatory sulfite reductase, surface glycoprotein, and two RNA virus proteins. The latter clones suggest that the gene expression profile is likely to include information about bacteriophage that contribute to the community structure such as potential for gene transfer. The partial cDNAs represent potential genetic elements for future development.

Demonstrated Plasmid Transfer Occurring Among Surface Bacteria

We have completely sequenced a 180 kb plasmid from a subsurface bacteria *Sphingomonas* F199. It was found that the plasmid carries a set of genes for conjugal transfer of this plasmid from one bacterium to another. To substantiate this hypothesis, we have cloned and sequenced several *Eco*RV fragments from another *Sphingomonas* strain B0695.

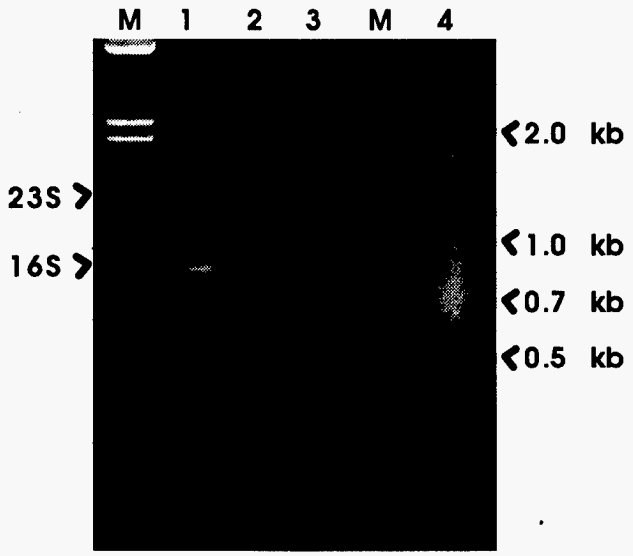

Figure 1. Agarose gel analysis of total RNA preparation from Columbia River sediment and TRHA product form total RNA. M, size markers; lane 1 to 3, RNA samples; lane 4, TRHA cDNA products from RNA. The locations of 23S rRNA and 16S rRNA molecules are indicated on the left. The sizes of the markers are indicated on the right.

The result indicated that strain B0695 carries the same plasmid with an identical sequence. Since strains F199 and B0695 were isolated from two different geological locations 25 miles apart, this suggests that one of the bacteria has been transferred from one site to another site and the plasmid pNL1 was transferred from one bacterium to another during this event. This property of the plasmid pNL1 further substantiates the notion that pNL1 will be a good candidate for use as a vector system for expressing genes usable for bioremediation in subsurface environment.

A Novel Partial Digestion for Analysis of Genetic Elements

To define the minimal genetic element required for gene expression, deletion mapping is usually used. Deletion mapping by conventional methods, however, is relatively tedious. We have developed a novel partial digestion method which will be useful for defining minimal genetic elements for gene expression as well as for sequencing analysis.

Publications and Presentations

K.K. Wong, L.M. Markillie, and J.D. Saffer. 1997. "A novel method for producing partial restriction digestion of DNA fragments by PCR with 5-methyl-dCTP." *Nucleic Acids Res.* 25:4169-4171.

K.K. Wong, L.C. Stillwell, S.J. Thurston, S.M. Varnum, E.C. Sisk, C. Dockery, and J.D. Saffer. 1996. "Complete DNA sequence of a 180 kb catabolic plasmid from a subsurface *Sphingomonas*." *Microbial & Comparative Genomics* 1:388, and Presented at Small Genomes: Sequencing, Functional Characterization and Comparative Genomics conference at Hilton Head, South Carolina, January 25-28, 1997.

Microbial Informatics

Margaret F. Romine (Environmental and Health Sciences)

Study Control Number: PN95057/1033

Project Description

The objective of this project was to provide bioinformatics support for the DNA sequence analysis of a 185 Kb plasmid extracted from *Sphingomonas aromaticivorans* strain F199. The scope of the work included both acquiring computer skills and tools to accomplish this project as well as assembly and annotation of the plasmid sequence.

Technical Accomplishments

DNA sequences generated from a catabolic plasmid, designated pNL1, have been assembled into a single contiguous fragment of 184,714 bp. This task was completed by assembling 2,693 templates using the Staden UNIX-based software package. We anticipate requiring less than 25 additional sequence files to complete the sequence of this plasmid on both DNA strands.

A preliminary annotation of the plasmid using blastn, blastx, and blastp was used to identify 110 genes within this sequence. A contiguous stretch of approximately 54,000 bp encodes open reading frames with extensive homology to genes known to be required for degradation of aromatic compounds such as naphthalene, biphenyl, *p*-cresol, and *m*-xylene. Discussions with Dr. Gerben Zylstra from Rutgers University revealed that sequences which his group generated from another bacterium, *Sphingomonas yanoikuyae* strain B1 are remarkably similar. Not only do the DNA sequences of the two bacteria possess more homology with each other than to sequences from other bacteria with similar genes, but the gene order of 35 genes is identical. The features that distinguish these regions are that

- F199 possesses an additional gene in this region for which no closely related genes involved in biodegradation of aromatics are known
- these 35 genes are flanked by insertion sequences in B1
- the F199 genes are plasmid-encoded while those in B1 are found on the chromosome.

Additional open reading frames likely to encode aromatic biodegradative genes are found in the adjacent 23,500 bp. Also found here are open reading frames with homology to genes associated with multidrug resistance efflux pumps and several genes whose function, if known, has no clear role in biodegradation of aromatic compounds. The presence of efflux gene homologues among biodegradative gene homologues suggests that a function of this pump may be to prevent toxic buildup of aromatic compounds within the cell. Although F199 is able to degrade a variety of aromatic compounds, it is sensitive to high levels of these materials in laboratory conditions. The presence of the pump suggests that F199 can be adapted to tolerate higher levels of aromatics by gradually increasing the concentration of aromatics to induce expression of the efflux pump. The association of an efflux pump with degradation of aromatics by *Sphingomonas* would be novel.

The remainder of the plasmid appears to encode genes involved in replication and conjugation (transfer of the plasmid to other bacteria). Only one long stretch of sequence (approximately 12,000 bp) with no known homology to genes deposited in public databases occurs here. It is possible that weak homologies to known genes will be found by using additional analytical software to survey this region. Additional interesting findings in this region include the presence of three transposase genes, two Group II introns, and a large open reading frame (4.3 kb) with significant homology to an insect gene that encodes a soluble mixed function monooxygenase responsible for detoxification of pyrrolizidine alkaloids.

Among the plasmid-encoded genes, there are several genes that can be grouped in the same gene family and therefore likely encode similar functions. Seven sets of genes encode large and small subunit dioxygenase components, which are responsible for recognition of the target aromatic substrate by the holoenzyme. Their gene products, when combined with ferredoxin and ferredoxin reductase, form an enzyme that is responsible for the first step in degradation of aromatic compounds such as *m*-xylene, toluene, naphthalene, and biphenyl. There appears to be only one gene, each, for the ferredoxin and ferredoxin reductase present on the plasmid. This finding suggests that this F199 may be able to combine any of the seven large and small dioxygenase subunits with the ferredoxin and ferredoxin reductase to create a different dioxygenase enzyme, each with unique affinities for different aromatic substrates. Other gene duplications include two *p*-cresol

monooxygenase flavoprotein subcomponents, two maturases (Group II introns), and two sets of the hydrolase, hydratase, and aldolase enzymes responsible for three of the enzymatic reactions that take place after meta cleavage of the catechol intermediate (lower pathway enzymes).

A comparison of the biodegradative genes found on pNL1 to pathways described for degradation of m-xylene and biphenyl reveals that only one enzyme, the toluate dioxygenase ferredoxin reductase subcomponent, is missing. Dr. Zylstra was also unable to find this gene in strain B1 and demonstrated that the ferredoxin and ferredoxin reductase genes could substitute for this subcomponent. The toluate dioxygenase ferredoxin reductase subcomponent possesses both the ferredoxin and ferredoxin reductase activities in a single protein molecule. Also missing is the cytochrome component of the *p*-cresol monooxygenase. Conjugative transfer of pNL1 into another *Sphingomonas* sp., which is unable to degrade aromatic compounds, enables the new host to grow on *p*-cresol. These findings suggest that all genes necessary for growth on p-cresol are plasmid-encoded and that no cytochrome subunit is needed for the monooxygenase activity.

The completion of the sequence of this plasmid is the first for a catabolic plasmid and the second for a megaplasmid.

Microbiosystems Development

Jeffrey D. Saffer, Kevin M. Groch (Molecular Biosciences)

Study Control Number: PN97071/1212

Project Description

The long-term objective of the project was to couple state-of-the-art microtechnology with molecular and cellular biology to produce biomedical systems including artificial organs and implantable therapeutic devices. The specific goals for this project were 1) identify functional criteria for specific operating devices and developing conceptual designs to serve as bases for focusing research and development efforts on critical feasibility issues, and 2) provide integration across the separate activities which would constitute the early efforts of the project.

Technical Accomplishments

Medical devices such as renal dialysis machines are and will continue to be essential for human health. Advances in molecular and cell biology, microtechnology and fabrication, and materials science suggest that the current armamentarium of medical devices available to the clinician represents only a fraction of the identifiable applications in the future. For example, advances in our understanding of liver cell biology suggest that an implantable device containing functioning liver tissue can be developed to replace the transplanted livers obtained from cadaveric donors. However, progress toward developing additional devices such as artificial livers has been hampered by a lack of scientific infrastructures that allow basic scientists in the medical, biological, and engineering disciplines to interact for integrating state-of-the-art knowledge in their respective fields. At its roots, this project was envisioned to address this void with an initial focus on defining a limited but specific series of potential devices for development.

Initial efforts included an analysis of the clinical need as well as the economics and feasibility of developing an implantable version of each of the five commonly transplanted organs (kidney, heart, lung, liver, and endocrine pancreas). Two major conclusions emerged from this analysis. First, successfully developing these organs would not only save lives and improve the quality of life for individuals suffering from the underlying diseases, but would have a profound impact on the U.S. economy. Of these organs, our analysis indicated that the greatest positive societal impact would come from a functioning artificial endocrine pancreas. Moreover, our analysis revealed that the technologies that would most likely be required for developing an artificial endocrine pancreas would also be directly applicable toward developing a broad spectrum of devices such as an artificial liver and indwelling bioreactors for housing genetically engineered cells producing biological products of therapeutic value.

The critical feasibility issues in developing a hybrid system capable of serving as an artificial endrocrine pancreas or indwelling bioreactor include 1) isolating viable cells from the host's immune systems, and 2) maximizing exchange between the cellular components of implantable devices and the systemic circulation. While substantial progress had already been made by others in developing methods to isolate implanted cells, we found that little progress has been made on the second issue. Given these conclusions and the state of the art, a technical analysis indicated that integrating micromechanical devices into solutions for addressing the exchange issue was premature and that biological solutions to the issue were more likely to succeed over the long run. Moreover, our analysis indicated an approach that integrated the appropriate combination of bioactive molecules known to induce the formation of vasculature such as vascular endothelial growth factor (VEGF) and biocompatible scaffolding to physically support the new tissue. A review of the open literature and communication with investigators active in the field indicated that this was a novel approach.

With these technical considerations in mind, a conceptual design for guiding the first research and development efforts was developed. The key question to be addressed is whether stimulating the ingrowth of new vasculature around immunoprivileged sites embedded within a porous, biocompatible scaffolding improves the function of grafted cells. Subsequent efforts would then be aimed at optimizing the subsystems as a prelude to preclinical testing as well as identifying novel scaffolding biomaterials which may provide superior performance.

Molecular and Functional Analyses for Evaluating Microbial Treatment Process Performance

Fred J. Brockman, Darrell P. Chandler (Biogeochemistry)

Study Control Number: PN97074/1215

Project Description

Microbial processes are widely used to destroy and detoxify organic and inorganic contaminants in groundwater pump-and-treat systems, petroleum refining, and other industrial wastewaters. However, these systems often experience process upsets and poor efficiency due to changes in the composition of the wastewater and/or changes in the functioning or population structure of the microbial community. Currently, only rudimentary efforts have been made to understand what is happening, at a microbial community structure level, during periods of poor system performance. Thus, engineers have a poor understanding of the specific microorganisms responsible for optimal system performance and how the treatment process could be enhanced. This project will develop and use a genosensor microarray to identify and characterize the types of micro-organisms in petroleum refinery wastewater during efficient and inefficient periods of operation. This information will provide an enabling technology for informed operational decisions, improved management of the treatment process, and minimization of the environmental impacts of wastewaters.

Technical Accomplishments

Substantial effort was made to assess the materials, architecture, and operating principles of genosensor microarrays being developed by various microelectronic companies engaged in biotechnology research and development. This activity was undertaken to take advantage of the extensive fabrication and biophysics expertise that exists in the private sector and that has been applied toward drug discovery and medical research diagnostics and mutation mapping. A range of technologies varying in the form of the sample DNA, method of labeling, array density, method of detection, and detection sensitivity exists. A company that possesses technology suitable for analysis of environmental samples and willing to co-develop wastewater microarrays was identified.

A companion LDRD project exists at Lawrence Berkeley National Laboratory (LBNL). In FY 1997 the LBNL project focused on gaining an understanding of the microbiological community of an Exxon activated sludge wastewater process (BIOX) using culturing methods and community level physiological profiling. LBNL found that knowledge of the dominant microorganisms present in the BIOX was not possible due to the inability to remove >0.1% of the biomass from the activated carbon.

In an effort to better understand the community and to determine what portions of the community the microarray should target most strongly, PNNL staff extracted DNA from a BIOX sample and the DNA was cloned. Randomly selected clones (244) were screened to (conservatively) identify different types, and one clone from each type was sequenced (ca. 650 bases). Each sequence was analyzed by computer against sequence databases to identify the most closely related sequences (i.e., BLAST analysis).
A BLAST score of >200, representing a sequence similarity of approximately >90%, was selected as the cutoff value for allowing genera-level phylogenetic and metabolic inferences. In contrast to most published studies on analysis of community 16S rDNA, a majority of the types in the BIOX sample (39/56 or 70%) were >90% similar to sequences in databases (Table 1). However, only two genera (*zospirillum Pseudomonas*) were identified in both the cultural approach (LBNL) and the direct extraction approach, highlighting the importance of analyzing communities directly and without culturing.

Among the 39 types with >90% similarity to database sequences, only one *Mycobacterium* represented a Gram-positive genera. This could have been due to poor lysis of the more recalcitrant Gram-positive bacteria. However, in several other environments we have obtained a large fraction of sequences corresponding to Gram-positive bacteria using the same protocols, so we conclude that few Gram-positive microorganisms exist in the BIOX sample. Among the 39 types, sequences corresponding to alpha, beta, gamma, and delta proteobacteria were, respectively, 41%, 26%, 18%, and 13%.

Only one type corresponded to an inferred genera (*Pelobacter/Geobacter*) that was strictly anaerobic; this genera performs sulfur and/or iron reduction. At least six of the inferred genera contained facultative anaerobes, four of which could denitrify. Other metabolic capabilities corresponding to the inferred genera included ammonia (*Nitrosomonas*), manganese (*Leptothrix*), and sulfur (*Thiobacillus*) oxidation.

Three types corresponded to uncultivated endosymbionts of marine benthic macroeukaryotes; these endosymbionts are known (based on the chemistry of the symbiosis) to perform sulfur oxidation. Although the similarity values are approximately 95%, these bacteria likely reflect non-marine microeukaryotic endosymbionts. A fourth type corresponded to a microeukaryote (ciliate) endosymbiont. These data have identified the portions of the microbial community that the microarray should target most strongly. In addition, sequences targeting microorganisms involved in undesirable foaming and floc bulking (usually *Nocardia* and other actinomycetes) will be placed on the microarray.

Table 1. Number of sequence types identified in the BIOX sample.

Category	Number of types[a]
>90% similarity	
Cultivated bacterium as closest match	36
Uncultivated bacterium as closest match	3
<90% similarity	
Cultivated bacterium as closest match	5
Uncultivated bacterium as closest match	12
No sequence[b]	10

(a) Types were based on restriction pattern. The exception was that sequence specified the type when different restriction patterns (on ca. 1365 bases) yielded the identical ca. 650 bases of sequence.
(b) Due to lack of homology between the internal sequencing primer and the clone, or due to two superimposed sequences.

Molecular Biology Infrastructure

Lisa C. Stillwell (Molecular Biosciences)

Study Control Number: PN96050/1117

Project Description

The principal objective of this project is to develop critical capabilities in molecular biology in a central facility to facilitate a wide range of molecular studies.

One area of interest is site-directed mutagenesis. This technique will be critical to new programs in structure-function analysis, where specific protein mutations will be required to test hypotheses about the functional contribution of key amino acids. This capability will contribute to research potential in several ongoing and planned research areas.

A second area requiring capability development is in gap closure in DNA sequencing projects. The Laboratory has previously developed approaches for doing medium-scale DNA sequencing. However, it has become apparent that for long DNA sequences, the final gap closure activities are requiring a much greater effort than the initial sequencing. Since many projects in several groups are planned that would require this capability, this project will refine existing methods and approaches for gap closure. This work will provide additional capability and speed to DNA sequencing projects and be widely applicable.

Technical Accomplishments

Protein Expression

Over the past year, this project has established capabilities for cloning, expression, and purification of proteins for structural biology studies. Much of this effort focused on XPA, a DNA damage recognition protein. In those efforts, approaches were refined for cloning genes into expression vectors by reverse transcription polymerase chain reaction (RT-PCR). In addition, various schemes for over-expression and purification were evaluated and modified to produce sufficient quantities for NMR analysis. These capabilities and those developed in protein site directed mutagenesis will enable future protein structure/function studies designed to understand the effects of single nucleotide polymorphisms in cell signaling proteins in disease susceptibility.

Bioremediation

The microbial genome research program at PNNL has focused on the subsurface *Sphingomonas* species F199, which has capability for aromatic hydrocarbon degradation. The majority of genes responsible for this activity were identified using genomic approaches and localized on a 180 kilobase pair megaplasmid. The complete DNA sequence of this megaplasmid has just been completed revealing important information regarding the organization and regulation of the degradative pathways encoded on the plasmid. Over the past year, the core facility developed polymerase chain reaction-based strategies for completing the sequence of pNL1 for which several gaps remained. Annotation and publication in a peer review journal are pending and a poster will be presented at the upcoming Microbial Genomes Conference hosted by The Institute for Genome Research.

Mutation Screening

The study of carcinogenesis, molecular genetics, molecular toxicology, and structural biology includes the study of DNA base changes in protein coding regions. These changes, or mutations, are often the underlying cause of a change in functionality of a protein which can contribute to uncontrolled cell division and tumor growth. How DNA base changes alter enzyme activity or efficiency is of interest to structural biologists as well since the structure and function of a protein is known to be integral to the DNA coding sequence. We have initiated efforts to develop procedures in the core facility for screening for mutations in polymerase chain reaction products without prior subcloning. These polymerase chain reaction products are often a mixture of wild type mixed with tumor, or mutated, sequences since it is difficult to completely separate tumor cells from the normal cell population. To circumvent this problem, an initial time-consuming step of subcloning each product into a sequencing vector is currently required. There is a danger of introduction and fixation of mutations in the subcloning process as well as potential for distorting the ratio of normal to mutant sequences. With the increased sensitivity of our sequencing system, however, we should be able to estimate the percentage of the polymerase chain reaction products

within the mixed population that have the wild type sequence and the percentage with the altered genotype.

While it is known that certain changes in DNA coding sequences can lead to a disease state such as cancer or sickle cell anemia, the effects of polymorphisms found in cellular proteins across populations are less understood. One hypothesis is that there are less obvious outcomes such as increased susceptibility to the harmful effects of chemicals we encounter in the environment. A future project is planned aimed at testing this theory by sequencing a number of cell signaling proteins from several strains of mice commonly used in molecular toxicology studies and known to have variations in susceptibility to liver cancer. The above capability of being able to detect a mixed population at each base will be instrumental in the success of this project. Once the system is optimized, we will be able to analyze four or five samples at time to screen for differences. Those sample mixes with a background level of alternate bases will be resequenced individually in order to identify polymorhisms from individual strains.

Novel Foreign Protein Production from Waste Starch

Jianwei Gao, Brian S. Hooker (Environmental and Health Sciences)

Study Control Number: PN97080/1223

Project Description

The objective of this project is to identify starch-degrading yeast strains, test starch use, and genetically engineer these strains to produce foreign protein from waste starch. The results obtained in this project provide information to evaluate biomass growth on starch material, genetic transformation, and the possibilities of foreign protein expression in starch-degrading yeast strains.

Technical Accomplishments

The agricultural and food industry disposes a significant amount of biomass byproducts during manufacturing processes. For example, a typical potato processing plant can produce as much as 340,000 pounds of biomass byproduct (wet potato waste) per day. Biomass byproducts are low-value and high volume products (much of it sold as livestock feed or even disposed as waste). Biomass byproducts are usually rich in starch, sugar, cellulose, and hemicellulose and therefore, are an inexpensive yet robust feedstock for biotechnological processes. As for potato waste, it is rich in starch and other nutritional factors, which can be directly used as a growth medium by bacteria and fungi. Through the use of molecular biology and advanced bioprocessing techniques, fungi (yeast or molds), which can be grown directly on starch substrate, may be modified for the production of novel foreign proteins.

Starch-degrading yeast strains can directly hydrolyze starch as their primary carbon source. Refined substrates such as glucose, galactose, and methanol are unnecessary. During FY 1997, starch-degrading yeast strains have been identified and obtained from American Type Culture Collection (ATCC) and researchers in universities. To characterize starch utilization of identified starch-degrading yeast strains, batch cultures of starch-degrading yeast were conducted in 250-mL flasks with 50-mL culture medium containing waste potato starch as the primary carbon source. Waste potato starch was obtained from a local potato processing plant.

In this project, two expression vector systems were evaluated to test genetic transformation and expression of foreign protein in starch-degrading yeast strains.

Phylogenetic Analysis of Anaerobic Dechlorinators

Margaret F. Romine, Darrell P. Chandler, Jim K. Fredrickson (Environmental Microbiology)

Study Control Number: PN96056/1123

Project Description

The focus of this work is to monitor the progress of enrichments for bacteria capable of deriving energy for anaerobic growth from perchloroethene (PCE). Only a few such bacteria have been found, and of these, only one is able to fully dechlorinate this compound. Isolation of functionally related bacteria is difficult because they often form symbiotic relationships with other bacteria or they compete for the same nutrients. By monitoring the types of bacteria that predominate during the course of enrichment, we hope to better understand the dynamics of the interactions between the PCE degraders and other community members.

Technical Accomplishments

An enrichment sample was obtained from Cornell University and analyzed for bacterial types. This enrichment was known to harbor a bacterium, designated *Dehalococcoides ethenogenes* strain 195, the only bacterial isolate known to date, which is able to completely dechlorinate PCE. Although this bacterium can be grown in pure culture, its growth requirements are quite complex and do not result in production of high biomass. Addition of sonicated cell pellets from the original enrichment greatly enhanced the amount of ethene produced from PCE, suggesting that other bacterial members provide growth requirements for strain 195.

16s rDNA was selectively amplified, by the polymerase chain reaction (PCR), from DNA extracted from this enrichment sample. The products were cloned into a plasmid and expressed in *Escherichia coli*. One hundred randomly selected clones were selected for restriction analysis to identify clones that differed from one another. Approximately 500 bp were sequenced from each of the 30 unique clones identified. Surprisingly, sequence analysis confirmed that there were only fifteen 16s rDNA types.

The restriction pattern between clones with similar sequences was very similar (some restriction fragments were identical in size while the remainder, when combined, could result in a similar sized fragment). The disparity between the number of unique clones identified by 16s rDNA fingerprinting versus sequencing may be accounted for by errors incorporated during PCR. Alternatively, unique fingerprints can represent different alleles of the 16s rDNA from the same bacterium. Many bacteria possess more than one copy of the 16s rRNA gene. Minor differences in their sequence are possible without affecting their function or the identification of the bacterium based on 16s rDNA sequencing. A final explanation is that the 16s rDNA PCR product was, in some cases, partially resistant to restriction digestion.

The 15 unique 16s rRNA sequences were compared to the Genbank database of DNA sequences to determine if similar sequences have been deposited by other researchers. The predominant clone type (31% of the total tested) was identical to the sequence of *D. ethenogenes*. There were three moderately predominant clone types (14, 12, and 11% of the total). One of these was closely related to *Desulfovibrio* sp., while the other two represent bacteria distantly related to any bacteria whose 16s rRNA sequence has been deposited in Genbank.

Our findings demonstrated that this method of community analysis can be used to identify predominant bacterial types in environmental samples. The initial identification of unique fingerprints should be very carefully evaluated to determine if any of the fingerprints differed only by a single restriction site. It would be worthwhile to determine the cause of the variations in fingerprints resulting from analysis of clones with similar sequences. If the disparity is due to purity of the DNA used in restriction analyses or to the use of small restriction fragments, the technique can be modified accordingly. An improvement in our ability to identify unique clones will reduce the number of clones that need to be sequenced for phylogenetic typing of the community.

Production of Foreign Protein Pharmaceuticals Using Transgenic Whole Plant and Cell Culture

Brian S. Hooker, Jianwei Gao, Ziyu Dai (Bioprocessing)

Study Control Number: PN96059/1126

Project Description

The objective of this project is to complete proof-of-concept tasks toward formulating commercially viable methods for production of functional foreign proteins using whole plants as well as plant cell suspensions transformed with appropriately constructed vector plasmids. The scope of this work focused on achieving stable expression of foreign proteins of interest in three product areas: pharmaceuticals, industrial enzymes, and phytoremediation. Proteins produced in *Nicotiana tabacum* (tobacco) whole plants and suspensions included human epidermal growth factor (hEGF), cellobiohydrolase (CBH1), and dinitrotoluene dioxygenase (DNTase).

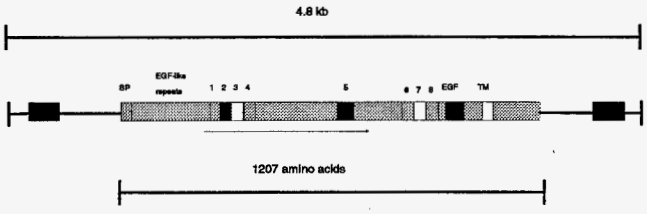

Figure 1. Structure of human kidney pre-pro-EGF (Bell et al. 1986).

Technical Accomplishments

Human Epidermal Growth Factor

Cloning efforts for hEGF were focused on obtaining an active portion of the larger pro-EGF protein for targeting of non-small cell lung cancer, with less rapid clearance properties than smaller, correctly processed hEGF. Correctly processed hEGF, at 53 amino acids, is cleared within minutes of introduction into the circulatory system, and therefore may not be used effectively for tumor targeting. The bacteriophage λEGF116 (ATCC No. 59956) containing the gene encoding the full length polypeptide of human kidney pre-pro-EGF was obtained from ATCC. Pro-EGF (Figure 1) is the 1207 amino acid precursor in which hEGF is flanked by polypeptide segments of 907 and 184 residues at its NH_2- and COOH-termini, respectively (Bell et al. 1986). The remainder of the 4.8 kb pre-pro-EGF gene encodes signal peptides at both the NH_2- and COOH- termini of pro-EGF. The polypeptide contains a transmembrane (TM) binding region that facilitates proper cleavage in the endoplasmic reticulum.

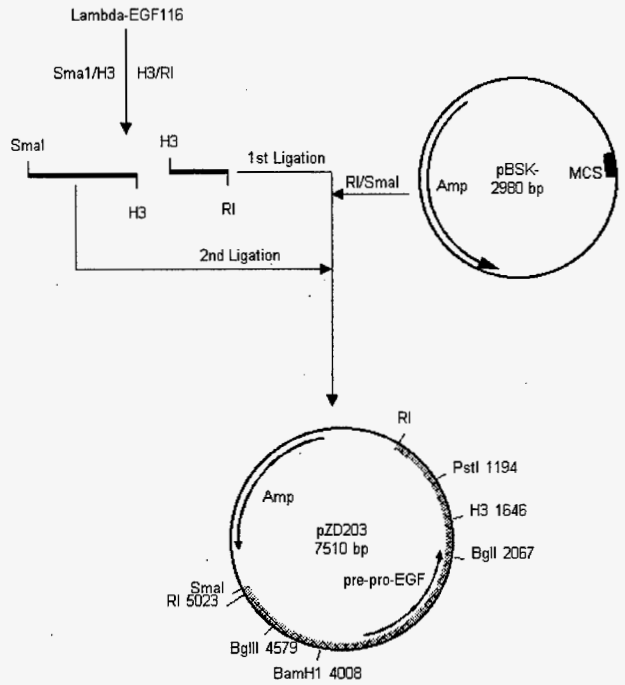

Figure 2. Insertion of human kidney pre-pro-EGF gene into pBluescript® to form pZD203. Amp: ampicillin resistance gene; MCS: multiple cloning site; SmaI, H3, RI, PstI, BglI, BamHI, BglII: specific restriction endonuclease cleavage sites; pBSK-: pBluescript.

The full length of cDNA was excised with Sma I, Hind III, and Eco RI restriction enzymes, as shown on Figure 2, producing two separate fragments. These were sequentially ligated into compatible Sma I and Eco RI sites in pBluescript- creating the 7.5 kb plasmid pZD203. After proper orientation was confirmed, pre-pro-EGF cDNA was further excised with Xba I and Cla I restriction enzymes and ligated into compatible sites located between the CaMV 35S promoter and T_7 transcription terminator of binary vector pGA643, forming the 16 kb plasmid pZD204 (Figure 3). The gene was introduced into tobacco whole plants (by leaf disks) and calli (by suspension culture) using an *Agrobacterium*-mediated system. Positive transformants were screened under kanamycin selection pressure and

preliminary ELISA results indicate the presence of hEGF in tobacco calli. Western blot analysis preliminarily indicate a protein size of 30 kD, as compared to correctly processed hEGF standard at 6 kD.

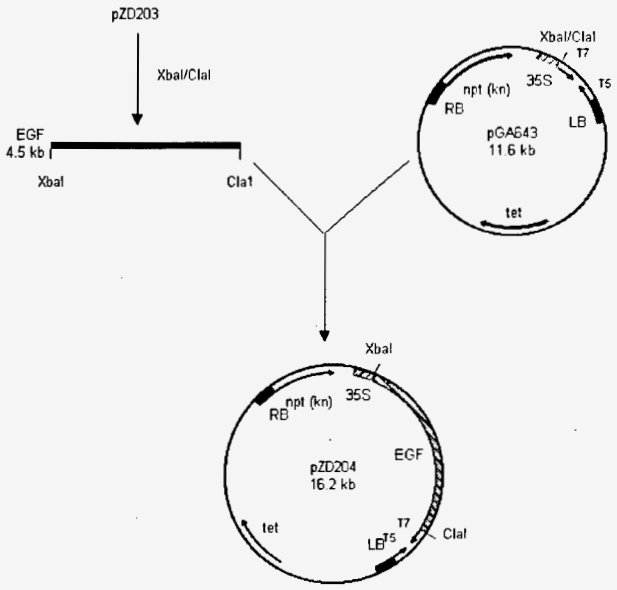

Figure 3. Insertion of human kidney pre-pro-EGF gene with proper ligation sites into the binary vector pGA643 to form pZD204. XbaI, ClaI: specific restriction endonuclease cleavage sites; 35S: CaMV 35S promoter; T7/T5: T7 transcription terminator; tet: tetracycline resistance gene; npt (kn): neomycin phosphotransferase gene (kanamycin resistance).

Cellobiohydrolase 1

CBH1, derived from *Trichoderma reesei* strain L27 (Shoemaker et al. 1983) catalyzes the exo-conversion of cellulose to cellobiose, the β(1-4) dimer of glucose. This enzyme is extremely important in the overall conversion of cellulose to ethanol-based fuels.

The plasmid pB210-5A containing the gene encoding the full sequence of CBH1 was obtained from Dr. Steve Thomas at National Renewable Energy Laboratory (NREL), Golden, Colorado. The full length of CBH1 cDNA (1.5 kb) was excised with Pst I/Xho I restriction enzymes and ligated into a compatible Hpa I site located between the CaMV 35S promoter and T_7 transcription terminator of the binary vector pGA643, forming the 13 kb plasmid pZD215. The orientation of the insertion was determined by restriction mapping. The gene was introduced into tobacco whole plants (by leaf disks) and calli (by suspension culture) using an *Agrobacterium*-mediated system. Transformants were screened under kanamycin selection pressure. Dot-blot immunoassay was used to confirm the presence of CBH1 in 184 of 202 separate transformants, representing three separate transformation events. CBH1 functional assays and Western blot analysis will be used to determine enzyme strength/concentration and protein size, respectively.

Dinitrotoluene Dioxygenase

The degradation of 2,4 dinitrotoluene (DNT) by *Pseudomonas* sp. strain DNT is initiated by dioxygenase attack to yield 4-methyl-5-nitrocatechol (MNC) and nitrate (Suen and Spain 1993). This degradative enzyme is important and may have some benefit in phytoremediation, since DNT is the major impurity resulting from the manufacture of 2,4,6 trinitrotoluene (TNT) (Spanggord et al. 1991).

The plasmid pJS33 containing the gene encoding the full sequence for DNTase was obtain from Dr. Jim Spain, Tyndall AFB, Florida. The full length of DNTase (3.22 kb) was excised with Bgl II/Nsi I restriction enzymes and ligated into compatible Pst I and BamH I sites in pBluescript - creating the 6.2 kb plasmid pZD209. After proper orientation was confirmed, the DNTase cDNA was further excised with Eco RV and Xba I restriction enzymes and ligated into compatible sites located between the CaMV 35S promoter and T_7 transcription terminator of binary vector pGA643, forming the 14.9 kb plasmid pZD213. The orientation of the insertion was determined by restriction mapping. The gene was introduced into tobacco whole plants (by leaf disks) and calli (by suspension culture) using an *Agrobacterium*-mediated system. Transformants were screened under kanamycin selection pressure. Additionally, functional assays will be used to determine the presence and strength of the DNTase in plant extracts.

References

G.I. Bell, N.M. Fong, M.M. Stempien, M.A. Wormsted, D. Caput, L. Ku, M.S. Urdea, L.B. Rall, and R. Sanchez-Pescador. 1986. *Nucleic Acids Res* 14:8427-8446.

R.J. Spanggord, J.C. Spain, S.F. Nishino, and K.E. Mortelmans. 1991. *Appl Environ Microb* 57:3200-3205.

W. Suen and J.C. Spain. 1993. *J Bacteriol* 175:1831-1837.

Presentations

Z. Dai, J. Gao, and B.S. Hooker. 1996. "Production and Characterization of Foreign Protein Pharmaceuticals in Transgenic Whole Plants and Cell Culture." Presented at the 1996 Annual Meeting of the American Institute of Chemical Engineers, Chicago, November.

Z. Dai, J. Gao, and B. S. Hooker. 1997. "Production and Characterization of Foreign Proteins in Transgenic Whole Plants and Cell Culture." Presented at the IBC Transgenic Therapeutics Conference, West Palm Beach, Florida, February.

B.S. Hooker, Z. Dai, and J. Gao. 1997. "Production of Cellulases in Transgenic Tobacco Whole Plants and Cell Culture." Presented at the 19th Symposium on Biotechnology of Fuels and Chemicals, Colorado Springs, Colorado, May.

Z. Dai, J. Gao, and B. S. Hooker. 1997. "Expression of Trichoderma reesei exocellobiohydrolase I in transgenic tobacco plants." Presented at the Quadrennial Joint Annual Meetings of The American Society of Plant Physiologists and Canadian Society of Plant Physiologists with the participation of the Japanese Society of Plant Physiologists and The Australian Society of Plant Physiologists, Inc, Vancouver, British Columbia, Canada, August.

Radium Complexation and Linkage to Monoclonal Antibodies for Cancer Therapy

Darrell R. Fisher (Radiochemical Processing Group)
Chien M. Wai (University of Idaho, Department of Chemistry)

Study Control Number: PN96062/1129

Project Description

The purpose of this project was to design and synthesize new macrocyclic ligands that complex radium (Ra^{2+}), that can be linked covalently to protein monoclonal antibodies, and that exhibit chemical stability in physiological media. The objective was to identify at least one preferred complexing agent that exhibited both high selectivity (preference for radium over all other competing metal cations), and high stability (binding strength with radium). The aim of this work was to find a complexing agent for the short-lived alpha emitter radium-223 ($T_{1/2}$ = 11.4 d), so that the complexed Ra-223 could be linked to a monoclonal antibody and constitute a new radiopharmaceutical for cell-directed radioimmunotherapy of cancer. Central to this effort was the goal of finding a chelate for radium that would remain stable in body fluids without exchanging radium for other metal cations (such as calcium, manganese, and zinc) present in relatively high concentrations.

The IIA element radium is highly electropositive and ionic in solution, and Ra^{2+} is therefore difficult to complex with chelating agents. It is also difficult to link the chelating agent to a protein molecule. This project involved three specific efforts: 1) molecular design of radium-complexing agents, 2) synthesis and testing of radium-complexing agents, and 3) linkage of the complexing radium-complexing agent to proteins. Animal testing of the radiolabeled immunoconjugate is a separate study under "Radium-223 Immunoconjugates for Cancer Therapy" (elsewhere in this report).

Technical Accomplishments

The coordination chemistry of Ra^{2+} is not well known. A computer model was developed to study the molecular dynamics of Ra^{2+} gas-phase ionic hydrates and of Ra^{2+} ion hydration in liquid water. Results of this work agreed well with predictions based on experimental values for IIA elements strontium (Sr^{2+}) and barium (Ba^{2+}). However, the computer model was not capable of testing Ra^{2+} interactions with more complicated types of macrocyclic compounds (such as calixarenes and calixarene-crown ethers) that have an optimal cavity size for the Ra^{2+} ion. Therefore, a number of different compounds (more than 30) were synthesized one by one and tested (by trial and error) as candidate radium chelates.

Previous studies showed that radium could be extracted from solvents with crown ether carboxylic acids (Beklemishev et al. 1995). Due to their translational flexibility, however, common crown ethers showed selectivity for Ra^{2+} over other metal ions but not high binding constants. Acyclic (open) crown derivatives were found to complex Ra^{2+} more tightly than closed crown ethers, but were not selective for Ra^{2+} over other alkaline earths (barium, calcium, and strontium).

The discovery (Gutsche 1989) of calixarenes (cyclic oligomers made up of phenolic units meta-linked by methylene bridges) provided another option for radium complexation. Recent reports suggested that calixarenes might undergo dimerization, forming a cage that could trap guest atoms or molecules. We found during chemistry experiments that commercially available calixarenes were not effective chelates for Ra^{2+}. We then reviewed published work by Bocchi et al. (1995) showing that calix[4]arene-crown-6 was selective for the cesium ion. We then synthesized calix[4]arene-crown-6, added two carboxylic acid groups, and found that this new ligand (Figure 1) showed both exceptionally high binding stability *and* selectivity for Ra^{2+} (Table 1).

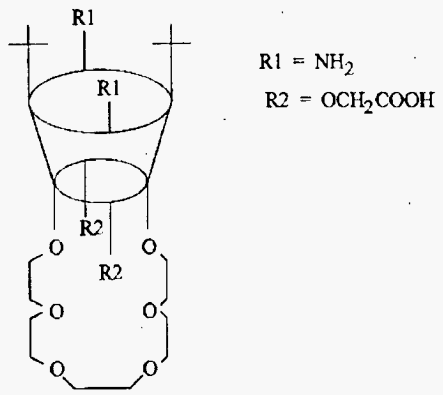

Figure 1. Schematic of a radium complexing agent: calix[4]arene-crown-6-dicarboxylic acid with amide linker positions and two *tert*-butyl stabilizers.

Table 1. Percent extraction of alkaline earth metal ions from water to $CHCl_3$ at pH 8.9 and at 25°C and distribution coefficient (D value).

	Extractability, percent (or D value)				
Ionophore	Mg(2+)	Ca(2+)	Sr(2+)	Ba(2+)	Ra(2+)
calix[4]crown(6)-DCA	0 (0)	15.6 (0.18)	73.5 (2.8)	98.7 (76)	100 (>100)
t-butyl(16)crown(5)-CBA	12.4	17.8	13.8	12.5	13.4
acyclic polyether-DCA	93.8	92.5	90.3	87	89

D value = concentration of metal complex versus uncomplexed metal

Table 1 shows the results of a two-phase solvent extraction experiment to compare the relative stabilities of Ra^{2+} with three different ligands: calix[r]arene-crown-6- dicarboxylic acid, *tert*-butyl-16-crown-5 carboxylic acid, and acyclic-polyether-dicarboxylic acid. The pH of the aqueous phase was adjusted with succinic acid-NH_4OH for pH = 4-6, Tris-HCl for pH = 7-9, and Tris-Me_4NaOH for pH >10. The distribution coefficient referred to in Table 1 is the concentration ratio of complexed metal to the uncomplexed metal.

Table 1 shows that the complexing agent calix[4]arene-crown-6-dicarboxylic acid exhibited selectivity for Ra^{2+} over other divalent alkaline earth metal cations (Mg^{2+}, Ca^{2+}, Sr^{2+}, and Ba^{2+}), greater binding strength compared to the second compound (*t*-butyl-16-crown-5-carboxylic acid), and greater selectivity for Ra^{2+} compared to the third compound (acyclic polyether dicarboxylic acid).

The preferred complexing agent (Figure 1) shows two *tert*-butyl groups and two amide (NH^2) groups on the aromatic ring of the calixarene. The amide groups serve as positions for linking the complexing agent to a monoclonal antibody using aminocaproic acid.

Initially, synthesis of complexing agents with one or two amides proved to be difficult. Ipso-nitration of the calixarene resulted in a mixture of one, two, three, or four amides, and concentrated nitric acid broke down the crown-6-ether. We then modified the procedure to nitrate the complexing agent under more mild conditions at lower reaction temperatures, and succeeded in obtaining the structure shown in Figure 1. Purification of the compound by HPLC may result in selective yield of the fraction with only a single amide group. This compound will be used for further antibody labeling studies.

References

M.K. Beklemishev, S. Elshani, and C.M. Wai. 1994. "Solvent Extraction of Radium with Crown Ether Carboxylic Acids." *Anal. Chem.* 66:3521-3524.

C. Bocchi, M. Careri, A. Casnati, and G. Mori. 1995. "Selectivity of Calix[4]arene-crown-6 for Cesium Ion in ISE: Effect of the Conformation." *Anal. Chem.* 67:4234-4238.

C.D. Gutsche. 1989. "Calixarenes." In *Monographs in Supramolecular Chemistry.* Ed. by Stoddart, J.F., Royal Society of Chemistry, London.

Publication

K. Miaskiewicz and M.A. Thompson. "Sr^{2+}, Ba^{2+}, $Ra^{2+}H_2O$ Interactions: Computer Simulations using a Polarizable Intermolecular Potential." *J. Phys. Chem.* (in press).

Sequencing and Functional Analysis of Thermus *Strain IRB-SA*

Margaret F. Romine, Jim K. Fredrickson, Yuri A. Gorby,
F. Blaine Metting (Earth Systems Science)

Study Control Number: PN97095/1236

Project Description

The focus of this work is to study the physiological and genetic basis for anaerobic respiratory pathways in *Thermus* strain IRB-SA. This bacterium was isolated from groundwater samples collected 3.2 km below the surface in a South African gold mine. Preliminary data on the physiology of this bacterium suggest that it is remarkably versatile in its anaerobic respiratory capability and thrives at elevated temperatures (60 to 70°C). The existence of this metabolism in a thermophilic bacterium is novel and suggests that this bacterium can be useful in the bioremediation of metals and radionuclides.

Technical Accomplishments

The 16s rDNA sequence of *Thermus* SA-01 (formerly IRB-SA) is greater than 98% identical to that of *Thermus* sp. strain NMX2, which was isolated by other investigators from a thermal spring in New Mexico. These investigators confirmed to us that strain NMX2 also appears to use iron as a terminal electron acceptor for anaerobic growth. *Thermus* NMX2 was obtained from these investigators and tested in parallel with *Thermus* SA-01 for iron-reducing capability. *Thermus aquaticus* (ATCC 25104) and *Thermus filiformis* (ATCC 43280) were also tested, but found to lack Fe(III) reducing capability. Strains SA-01 and NMX2 reduced Fe(III) in the form of amorphous Fe(III)-oxide and also Fe(III) complexed with citrate or nitrilotriacetic acid (NTA). Fe(III) is reduced to Fe(II); magnetite is not formed. Electron donors for growth coupled to Fe(III) reduction include lactate and acetate. These strains are able to mineralize nitrilotriacetic acid and appear to couple its oxidation to Fe(III) reduction. Lactate is oxidized to CO_2.

Neither of the Fe-reducing strains grew fermentatively, i.e., addition of an external electron acceptor was required for growth. *Thermus* SA-01 was also able to reduce Mn(IV), Co(III), and anthraquinone disulfonate (AQDS; a humic acid analog). Low concentrations of AQDS in the growth media improve the rate of iron reduction. Nitrate is reduced to nitrite. We have been unable to demonstrate reduction of elemental sulfur, sulfate, thiosulfate, or U(VI).

Thermus SA-01 grows in a temperature range of approximately 45 to 75°C and optimally at 65°C. Range of pH for growth and iron reduction is approximately 5 to 9 with an optimum of 6.5 to 7 (Figures 1, 2, and 3).

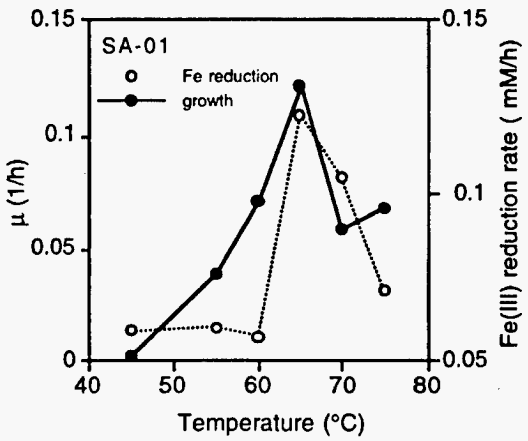

Figure 1. *Thermus* SA-01 (temperature).

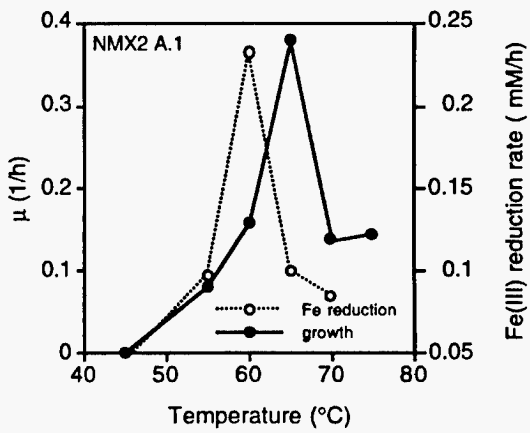

Figure 2. *Thermus* NMX2 (temperature).

Thermus sp. are most closely related phylogenetically to *Deinococcus* sp., which are best known for their remarkable radiation resistance. In collaboration with Dr. Michael Daly, we tested the effect of several doses

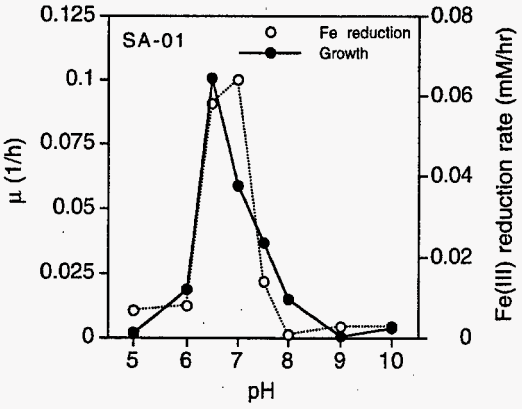

Figure 3. *Thermus* SA-01 (pH).

of ionizing radiation on survival of stationary cells. Bacterial survival was evident (visual growth in liquid culture) after exposure to 1000 and 2000 Gy, but not at doses of 3000 Gy or higher. *Escherichia coli* typically shows no survival at doses above 300 Gy, while *D. radiodurans* can survive 5000 Gy with no lethal effect. *Thermus* SA-01 is clearly not highly radiation resistant but is significantly more resistant than *E. coli*.

The ability of *D. radiodurans* to grow anaerobically was also tested. According to the literature, this bacterium is a strict anaerobe. We were, however, able to confirm that this bacterium is able to grow fermentatively on glucose in both rich and defined media. No growth was observed on nitrate. Analyses of the preliminary release of its genomic sequence suggest that several genes are present that could encode fermentative pathway enzymes. No extensive homology was found with other known genes that encode enzymes from other respiratory pathways (such as nitrate reductases, nitrite reductase, TMAO reductase, and DMSO reductase). Contrary to literature reports, these data suggest that *D. radiodurans* is able to grow anaerobically by fermentation.

The results of this work confirm that *Thermus* sp. SA-01 and NMX-2 are capable of anaerobically respiring on a variety of different compounds. These isolates are the first facultative anaerobic thermophilic Fe(III)-reducers to be identified. This work also is the first to demonstrate anaerobic growth in *Deinococcus* sp. These two species are phylogenetically related. As such, they make good partners for functional comparison, evolutionary studies, and gene exchange.

Use of Extremophillic Microorganisms for Use in Targeted Industrial Applications

Robert Romine (Environmental Technologies)

Study Control Number: PN97103/1244

Project Description

There are a growing number of research efforts for developing bioprocesses to compliment or provide alternate approaches to traditional process chemistry. There has been particular interest in bioprocesses using microorganisms because many thrive in extreme environments (i.e., high or low temperature or pH, high salinity or pressure) much like those required for bioprocessing. Extremophillic microorganisms are currently being screened for thermally stable enzymes such as xylanases and proteases for bioprocessing. Only a fraction of the potential capabilities of these microbes has been determined. The emphasis of past research has been on discovery and genetic characterization of the microorganism, while the determination of potential industrial uses has largely been overlooked.

Several microorganisms will have been identified in the screening process which warrant further investigation for developing a bench-scale (5 L to 10 L) bioprocess for desulfurizing crude oil and/or cleaning spent catalyst. Through the process of identification and screening of candidate microorganisms, we will have greatly expanded our capabilities to use extremophiles in developing novel bioprocesses.

Technical Accomplishments

Screening Experiments

The process that was originally targeted for this work was the desulfurization of crude oil. Shortly after the start of the fiscal year the targeted application was changed to the desulfurization of gasoline, based on discussions with DOE-HQ and petroleum industry contacts. Based on this change, thiophene was selected for use as a model compound for sulfur-containing species in gasoline.

Twelve purified microorganisms and one mixed culture were evaluated for their ability to degrade thiophene. Thiophene (50 ppm) was introduced into robust cultures in logarithmic growth phase. Degradation of thiophene was determined by HPLC measurements. Many of the microorganisms were unable to degrade thiophene and in some cases the presence of thiophene was lethal to the bacteria. Three organisms, *Rhodococcus rhodochrous*-IGTS8, *Sulfolobus acidocaldarius*, and *S. sulfataricus*, were selected for further evaluation based on the results of these initial screening experiments. These more detailed experiments included development a fine aerosol microencapsulation system.

Fine Aerosol Microencapsulation System

Overcoming problems associated with cell mortality in the presence of organics is a major issue with developing bioprocesses which must operate with a significant organic phase. Physically separating the bacteria from the organic phase (via the use of polymeric films and beads) has been successful in mediating mortality problems in similar applications. Development of a microencapsulation system was critical to protecting the bacteria from the thiophene organic phase. A bench-scale fine aerosol microencapsulation system was constructed that is capable of consistently producing microbeads in the 5μ -10μ particle size range. Bacteria were encapsulated in alginate, polyurethane, and polyacrylamide microbeads. Figure 1 is a photograph of the fine aerosol microencapsulation system.

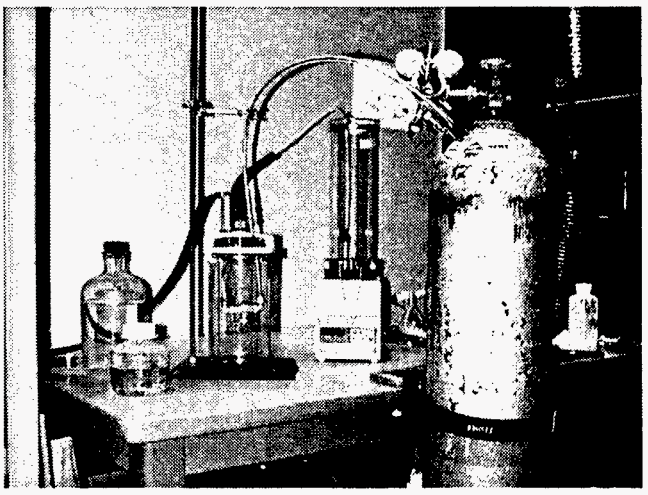

Figure 1. Fine aerosol microencapsulation system.

Encapsulation Experiments

R. rhodochrous, *S. acidocaldarius*, and *S. sulfataricus* were encapsulated in three different medium: alginate, polyurethane, and polyacrylamide. These encapsulated cells were exposed to 500 ppm thiophene (under the optimum

condition for the specific bacteria). The degradation of thiophene was again analyzed by HPLC. The results of these experiments can be found in Table 1.

It can be seen that the degradation of thiophene was significantly improved in the *R. rhodochrous* experiments, but was still lower than that of the free cell experiments with *S. acidocaldarius* and *S. sulfataricus*. Experimental results for the encapsulated strains of *Sulfolobus* were not improved. Alginate was a poor encapsulation medium for use with the acidophilic *Sulfolobus*. The alginate was severely destabilized by the elevated temperature (70°C) and low pH required (pH 2.5) to grow the *S. acidocaldarius* and *S. sulfataricus*. The poor results for the *Sulfolobus* strains encapsulated in polyurethane and polyacrylamide can be attributed to the pH sensitivity of the microorganisms. It is believed that the microenvironment within these polymer beads was not acidic enough and was not compatible with the biological requirements of these bacteria. New polymers which are more acidic in nature are being sought for future experimentation.

Construction and demonstration of the fine aerosol encapsulation system has expanded the bioprocessing/bioengineering capabilities of the Laboratory. This capability will be employed to address other research issues, such as biological treatment of low pH and high salt wastewater streams, low pH production of lactic acid and succinic acid from renewable resources.

Table 1. Degradation rates[a] of thiophene for encapsulated cells.

	Microorganism					
Bead Type	***R. Rhodochrous***		***S. Acidocaldarius***		***S. Sulfataricus***	
	FC[b]	ENC[c,d]	FC	ENC	FC	ENC
Alginate	0.32	2.8	6.9	2.1	5.8	1.9
Polyurethane		2.2		5.5		4.1
Polyacrylamide		2.6		0.9		0.5

(a) All rates expressed as milligrams of thiophene per 10^{10} cells per hour.
(b) Free cells.
(c) Encapsulated cells.
(d) 500 ppm thiophene vs. 50 ppm in FC experiments. 500 ppm thiophene ~100% lethal.

Chemical Instrumentation and Analysis

A Flow Injection/Electrochemical System for Detection of DNA Damage

Cindy J. Bruckner-Lea (Interfacial and Processing Science)

Study Control Number: PN96001/1068

Project Description

The goal of this project is to develop an automated in vitro microanalysis method for detection of DNA. Detectable changes in DNA structure can be used to screen for DNA damage due to chemical or radiation exposure. In addition, DNA detection is important for clinical applications (e.g., genetic screening, drug screening), and it can also be used to monitor bacterial DNA in water, soil, and air samples. Electrochemical detection of DNA is ideal for determining total DNA concentration in a sample, and electrochemical detection of DNA hybridization is also possible (Mikkelsen 1996). This project combines the sensitivity of electrochemical methods to changes in DNA structure with the small volume, precise control, and automation provided by flow injection analysis.

Electrochemical detection of unlabeled DNA is possible using two electrodes: mercury or carbon. From an electrochemical point of view, mercury is preferable since reduction of the bases guanine, cytosine, and adenine occurs at negative potentials that are only attainable using a mercury electrode. In addition, electrode fouling and contamination is not a problem because mercury is a renewable electrode that is freshly extruded for each measurement. During the first year of this project, we focused on using mercury electrodes for DNA detection. During the second year, we designed a flow system for automatically perfusing the electrode, and studied the alternating-current voltammetry of native and denatured DNA. The system proved to be useful for studying DNA electrochemistry, but is not suitable for instrument development since it is quite large and uses a few microliters of mercury per sample.

We are now evaluating two alternative renewable electrodes for DNA detection. Mayer and Ruzicka (1996) have shown that such a renewable electrode is feasible, and Wang et al. (1996) have shown that carbon electrodes may be used for electrochemical detection of DNA.

The flow injection system provides precise, automated control of the electrode renewal process as well as sample volumes and flow rates. In addition, renewable electrodes may be useful for other electrochemical detection systems where electrode fouling is a problem.

Technical Accomplishments

Mercury Sessile Drop Electrode

At the beginning of the project, Professor Emil Palecek from the Czech Republic, an expert in DNA electrochemistry, visited PNNL for 4 days. During this time, we discussed techniques for storing and handling DNA samples and conducted electrochemical impedance measurements using calf thymus DNA. In addition, a fluid delivery system was designed with the assistance of Professor J. Ruzicka from the University of Washington.

The DNA-modified electrode was electrochemically characterized by both manual operation and automated sample handling using the flow injection system. This work was conducted by Dr. F. Jelen (a visiting scientist from Professor Palecek's lab) and Dr. C. Bruckner-Lea. The parameters investigated were the effect of DNA concentration, the effect of DNA accumulation time, and the effect of electrode area (sessile drop size) on the electrochemical response. These experiments showed that less than 1 μg/mL of DNA can be detected, and that each measurement requires only a few minutes. The detection of DNA hybridization is the basis for identifying the genes of organisms ranging from humans to bacteria, and therefore has many potential applications. A paper describing the results of these experiments is currently in preparation.

Although mercury sessile drops are useful for studying DNA electrochemistry and our results indicate that it is possible to automate DNA detection using a mercury sessile drop electrode in conjunction with a flow injection system, the mercury sessile drop electrode is not suitable for instrument development since it requires careful handling and uses relatively large amounts (microliters) of mercury per sample. We conducted literature searches in these areas and began developing alternative approaches.

The principal investigator attended a "DNA Biochip Arrays" conference in February 1997, in San Diego, California, in order to become up to date on the development of DNA detection systems. No work was presented at this conference regarding renewable electrode systems, and the detection limits of many of the fluorescent labeling techniques were similar to electrochemical methods

(<μg/mL). This indicated that renewable electrodes should be investigated further for DNA detection, and we subsequently developed such an electrode.

References

S.R. Mikkelsen. 1996. *Electroanalysis*, 8(1), 15.

M. Mayer and J. Ruzicka. 1996. *Anal. Chem.* 68, 3808.

J. Wang, X. Cai, C. Jonsson, and M. Balakrishnan. 1996. *Electroanalysis*, 8(1), 20.

Publications and Presentations

C.J. Bruckner-Lea, F. Jelen, J. Janata. "A mercury sessile drop system for detection of DNA." (in preparation).

C.J. Bruckner-Lea. 1997. "Development of Flow Injection Systems for Biological Cells and Biomolecules." Invited seminar, Oregon Graduate Institute, March 14.

Aerosol Analysis by Laser Desorption in an Ion Trap Mass Spectrometer—Determination of Design Specifications for On-Line Instrumentation

Michael L. Alexander (Interfacial and Processing Science)
James Huckaby (Environmental Technology and Design)

Study Control Number: PN97010/1151

Project Description

The objective of this project was to build a prototype aerosol interface to take advantage of existing instrumentation and to demonstrate the feasibility of this concept for aerosol measurements. We proposed to add an aerosol interface to a new laser desorption ion trap mass spectrometer (LD-ITMS) currently under construction in the EMSL for the purpose of developing laser and ion trap-based on-line analysis methods. This unique device uses a proprietary PNNL ion trap design (patent applied for) and bipolar detection to simultaneously observe the mass spectrum of both positive and negative ions produced by laser desorption on a single shot basis. These characteristics of this device make it ideally suited to study the process of laser desorption of aerosols, to determine the physical and chemical characteristics of aerosols produced from various processes, and to provide the design parameters for portable aerosol analysis instruments. It can observe phenomena on a single particle basis or acquire average quantities. Although funding is in place for the construction of this instrumentation, no funding exists for its application to specific problems.

Technical Accomplishments

The results of this project are summarized below:

- particle interface was constructed and installed on ion trap mass spectrometer
- particle size measurement by laser light scattering was demonstrated from 0.5 to 2 microns
  - velocity measurement - aerodynamic sizing
  - light scattering cross-section
- mass spectra were taken for several particle sizes.

A schematic of the instrument is shown in Figure 1.

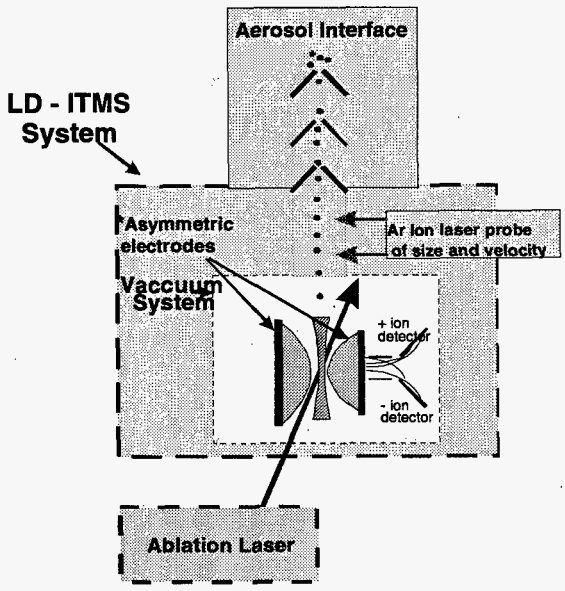

Figure 1. Aerosol interface on LD-ITMS. (The asymmetric electrode design is patented by PNNL.)

The interface was based on a design by Stoffels of PNNL. A programmatic program has been identified to demonstrate the aerosol interface as part of the iodine speciation program at PNNL. A U.S. patent was granted for the design of the asymmetric trap that is part of the LD-ITMS. The primary motivation for the asymmetric design is to allow the analysis of individual aerosol particles. The interface developed as part of this project is fundamental in applying this ion trap design.

Chemical Speciation of Radionuclides and Tritium in Nuclear Process Effluents

Bob W. Wright, Harry S. Miley (Radiological and Chemical Sciences)
John F. Wacker (Isotopic Separations and Analysis)

Study Control Number: PN97024/1165

Project Description

The objective of this project is to obtain preliminary information on the value of newly identified nuclear proliferation signatures. The overall results will be documented in a report that records the measured signatures, outlines the preliminary analytical procedures, and recommends developments for improved analytical capabilities. The information that will be gained in this work is needed as a basis for developing additional sample collection and analysis capabilities. These improved capabilities could possibly be used at other nuclear facilities to obtain further information.

Background

A document recently prepared by PNNL staff identifies several unique airborne radionuclide signatures of proliferation processes. Traditional signatures are compared to newly identified and more unique types of signatures. Unique signatures are identified for 1) nuclear fuel reprocessing (metal), 2) nuclear fuel reprocessing (oxide), 3) tritium production, 4) tritium recycling, 5) Hanford-type reactor operations, 6) light-water reactors, 7) heavy-water reactors, and 8) gas cooled reactors. The approximate emission rates, or relative amounts of the signature radionuclides (chemical species) are identified, as well as their potential utility in monitoring nuclear processes. The report also provides a basis for selecting the radionuclides and the chemical species which currently appear to provide the greatest sensitivity for detection of specific nuclear processes which may be indicative of nuclear proliferation. Many of these signatures must be investigated further to determine their precise ratio in effluents, the quantities which are released during various phases of plant operation, and variations in release rates from similar but separate operations. This document provides the justification for conducting the experimental work. At present, only limited information is available on the more unique signatures. The data that exists were developed many years ago during operation of the Hanford plants primarily for radiation exposure purposes. Other data from foreign operations that were published in the open literature also have been obtained and used as the basis for predicting probable signature compounds. Data obtained from experimental measurements made at the Hanford Site have collaborated the existence of specific new signature compounds. Analytical capabilities developed in this project are being used to characterize samples collected at the Savannah River 291-F reprocessing plant and from collection stations several kilometers remote from the plant.

Approach

Air samples from the Savannah River 291-F reprocessing plant ventilation stack and from the Williston Barricade have been collected. Savannah River personnel developed an isokinetic stack sampling system that was operated to collect specific samples for PNNL. This system has been approved to meet all of the Savannah River Site safety issues, and consequently provides certain limitations on what can be done. For instance, approvals do not presently exist to allow sampling directly from the dissolution or extraction off-gases. Sampling from the stack is also limited to certain volumetric flow rates to ensure that the flow dynamics are not upset. Two types of stack gas samples were collected; whole air samples in 500 mL evacuated steel canisters and various types of adsorption tube samples optimized to maximize collection efficiency for various species. Approximately 1 cubic meter air was sampled through each of the adsorbent tubes. Samples were collected during dissolution and extraction. Based on Savannah River sample processing schedules, it appears that various sampling opportunities will be available during 1998. Environmental air samples were also collected several kilometers downwind of the 291-F and H plants at the Williston Barricade. Two types of air samples were collected. Savannah River Site shipped the samples back to PNNL for analysis. Several types of analytical procedures were used. Iodine measurements will be made using established capabilities available at the laboratory. Specialty organic analyses were made using multi-dimensional gas chromatography/mass spectrometry. This technique continues to be developed to improve analytical capabilities.

Data from the various samples and analysis techniques will be compared and correlated to obtain a more definitive characterization of the signature compound spectrum. The early data already collected will allow sampling and analysis efforts to be further refined and optimized.

Ideally, development efforts for the specific signature compounds would have been completed prior to sample collection. However, the time-critical path required in this work demands that real sample collection and analysis be done concurrently with analysis methodology development.

Technical Accomplishments

During FY 1997 several significant activities were completed. They are as follows:

1. A follow-on document, PNNL-NSD-0597, was prepared that further assessed the known technical literature as it relates to the identification of various signature compounds and their significance in detecting proliferation processes. Predictions on the concentrations of various signature compounds were made based on straightforward assumptions to serve as guides in collecting samples. This document also provided potential directions for developing field detection capabilities.

2. Sampling hardware for collecting organics, iodine, and tritium species was assembled, tested, and sent to the Savannah River Site for their use to collect both field samples (remote location from the reprocessing plant at the Williston Barricade) and stack samples from the 291-F reprocessing plant. Sampling was based on collection of whole air samples and collection of specific species in custom adsorbent samplers.

3. Arrangements were made to have our samplers used during various relevant activities at the SRS canyon, e.g., decladding, dissolution, and solvent extraction of irradiated fuel elements. Four types of samples were collected at the stack and two types of samples at the Williston Barricade. The field samples were collected straightforwardly, but it took several months longer than we envisioned to successfully schedule collection of the stack samples. SRS had an ongoing stack sampling program that we were able to leverage to obtain our samples. Since our samplers were different, it took some effort to get them integrated into the existing system.

4. The collected samples were returned to PNNL for analysis.

5. Whole air samples were subjected to gamma ray spectroscopy and T0-14 organic analyses. The quantity of expected radionuclides found in the samples was less than expected based on first-order modeling predictions.

6. Significant effort was devoted to developing and refining on-line organic chemical analysis methods based on supercritical fluid extraction and tandem gas chromatography mass spectrometry to detect the ultralow levels of specific signature compounds. Selected field samples and stack samples were analyzed using the technique with a range of results obtained.

7. Traditional analysis methods for total iodine were applied to selected field samples with the results being consistent with our expectations.

Component Interface

Steve C. Goheen (Chemical Sciences)

Study Control Number: PN97025/1166

Project Description

This project is designed to develop a systematic approach to properly assemble components of a pathogen detector/analyzer. Examples of issues include the order of components, pathogen losses to the system, quality control, and sample preparation requirements.

Technical Progress

This project was initiated for the purpose of integrating the components of a pathogen detector from a chemical perspective. The main issue that was addressed was determining the order of the various components to identify and quantify pathogens. As efforts progressed, additional questions arose regarding quality control, standardization, solutions to be used, and the adequacy of the components to meet client needs. The components used to detect, identify, and measure pathogens included an optical technique, a mass spectrometric method, and potentially two DNA-enhancing methods, such as those that depend on the polymerase chain reaction (PCR). There were also some sampling methods under development, which would be used in the front end of the system.

The sampling technologies initially examined were for the gas phase. While the examined sampling methods initially were designed to convert aerosol to the liquid phase, this was not a requirement. The principal investigators were interviewed to determine their chemical requirements. Each detection/analytical component had some concept of how many cells or cell equivalents would be needed to perform a successful analysis. These are indicated in Table 1. These requirements were examined and the preliminary design was put before the principal investigators.

This project is also involved in developing standard criteria for the detection system. One criterion that needed to be resolved right away was a list of simulants that could be used to test each device. The simulant list was chosen to target suspected biological warfare categories of organisms/agents. The list of simulants is shown in Table 2.

Table 1. Component requirements for successful analyses.

Component	Input Buffer Requirements	Input Bacterial Requirements (number/volume)	Output/Comments
Sampling	TBD (airborne contaminants as well as buffer/solution used)	TBD from tests	Output targets to be determined by requirements of other components
Optical	TBD	TBD	Media probably needs to be transparent
Mass Spectrometry	TBD	100-1,000/μL	Some of the sample will be destroyed in analysis
PCR	0.1 mm Phosphate buffer, pH 8	>10,000 if background is minimal	Cells will be destroyed during processing

Table 2. Pathogen simulants.

Pathogen Class	Pathogen (e.g.)	Simulant	Other Names for Simulant
Gram negative bacteria	*Yersinia pestis*	*Erwinia herbicola*	*Pantoea agglomerans*
Gram positive bacteria	*Bacillus anthracis*	*B. subtilis* var. *niger*	*Bacillus subtilis*
virus	Yellow fever	MS-2 *E. coli* phage	
toxin	Botulinum	Bovine serum albumin	

Order of Detectors

In a pathogen detector system, the components should be assembled in the following order:

1. *Collector*

2. *Trigger Mechanism*—The trigger mechanism would identify whether an event had occurred or not. The trigger should be fast, and have few sample preparation requirements. Optical methods are good candidates for a trigger mechanism.

3. *Recognition*—The third component in a pathogen detector should be recognition. The mass spectrometry and polymerase chain reaction methods fall into this category.

The next step in this project dealt with quality control. How well do we need to know what we are measuring? The precision and accuracy of the analytical device needs to be defined before a device can be fully useful. Examples of variables that need to be defined for such a measurement device include the following:

1. Quantity of cells - What should our detection limit be? Under what background conditions?

2. Type of cells - How well do we need to know the cell type?

3. Viability of cells - Do they need to be viable? If so, what percentage of them?

4. Are the cells intact? How many of them are intact? How many need to be?

5. How accurately do we need to know the number of cells/volume?

To answer the above questions, some of the quality parameters were identified. Using these quality parameters and the initial selection and sequence of instruments, the ability of the proposed system to analyze airborne pathogens will be evaluated starting in FY 1998.

Development of a Field Portable Matrix-Assisted Laser Desorption/Ionization Mass Spectrometer for Pathogen Detection

Karen L. Wahl, Bruce D. Lerner, Joseph G. Birmingham, Charles J. Call
(Environment and Health Sciences, Environmental Technologies)

Study Control Number: PN97034/1175

Project Description

The objective of this project is to develop a mesoscale matrix-assisted laser desorption/ionization mass spectrometry (MALDI-MS) instrument that could be used in remote sites and integrated into the mesoscale aerosol sample collection and handling platform. The focus was to adapt this technique to the mesoscale by automating sample preparation and handling and reduce the physical size of the MALDI-MS instrumentation.

Technical Accomplishments

Commercially available MALDI time-of-flight mass spectrometry instrumentation is bench scale and portable for large vehicle deployment. However, for truly portable (hand-held) applications, a further reduction of size and weight of such instrumentation is required. In addition to size reduction, a simple on-line method for introducing samples into the mass spectrometer is needed. To make efficient use of resources, a literature and web-based search was performed to identify other efforts in miniaturizing MALDI mass spectrometry instrumentation and on-line sampling techniques for MALDI-MS. Several attempts at linking MALDI-MS to on-line separations and flow techniques have been attempted with limited success. The majority of MALDI-MS work is performed off-line where sample spots are prepared, dried, and then the sampling plate is inserted into the vacuum system of the mass spectrometer. Automated sample plate spotting has been developed; however, manual placement of the sample plate into the mass spectrometer interface region is still required. A tape-drive system would be ideal for continuous feeding of sample into the vacuum system, but engineering a robust system through the atmosphere/vacuum interface is not trivial.

Several processes of the MALDI technique could affect the integrity of the microbial cells and therefore play a role in which cellular components are sampled and detected by MALDI-MS. The cells were dried in the presence of a small organic matrix molecule, inserted into the vacuum system, and then sampled by a nitrogen laser beam. Efforts to sample the cells from the MALDI target surface after MALDI analysis for determination of cell membrane integrity were unsuccessful. Scanning electron microscopy was employed to provide insight into the plight of the cells during the laser desorption process. The majority of the cells appeared to be intact on the MALDI target surface before and after MALDI analysis. This suggests that cell lysis is not a facile process during MALDI sample preparation and analysis. While no direct cell damage resulting from the laser beam was visualized on the MALDI target surface, valuable information on ways to improve the sample preparation on the MALDI target for cell analysis was obtained. Efforts to reduce the number of cells applied to the target and improve the homogeneity are being implemented.

It was determined that efforts to miniaturize time-of-flight mass spectrometry and automate sample introduction were in progress at Johns Hopkins Applied Physics Laboratory (APL). A site visit provided an opportunity to initiate a collaboration. Collaboration between CoronaCat and Johns Hopkins was initiated for developing direct sampling methods into the mass spectrometer. PNNL researchers are consulting with the local small business to assist in developing the front-end sampling system compatible with MALDI analysis.

Once duplicate efforts were identified and a collaboration with the Johns Hopkins Applied Physics Laboratory initiated, efforts were redirected toward supplementing the analytical method development for MALDI analysis of microorganisms.

Development of High Performance Field-Portable Electrospray Ionization Fourier Transform Ion Cyclotron Resonance Mass Spectrometer

Richard D. Smith, Harold R. Udseth (Macromolecular Structure and Dynamics)

Study Control Number: PN97036/1177

Project Description

This project will develop a novel approach for decreasing the size of mass spectrometric instrumentation for the rapid detection and definitive identification of biological agents based upon concepts for field portable electrospray ionization (ESI) and ion trapping instrumentation. The method will use compact and ultra-sensitive multi-stage mass spectrometry and novel ion accumulation methods in a new manner that moves many lengthy laboratory sample manipulation steps (that require times on the order of hours) into the mass spectrometer where they can be conducted in an automated fashion on a time scale of seconds. The use of a novel ion accumulation device and high speed microvalve will greatly decrease the pumping requirements while a new method of activation and ion dissociation in the ESI interface will afford greater information from the mass spectra.

Technical Accomplishments

This project was initiated in the early summer of 1997, and thus limited progress was made in this fiscal year. The aim is to demonstrate convincingly proof of principle for concepts designed to enable the development of smaller, less massive and more sensitive instrumentation for biological warfare (BW) threat detection and/or identification. The technological focus of this project is the ESI-ion trap or FTICR technology that aims to provide sensitivity and the selectivity needed for the definite identification of distinctive polypeptides and proteins from the crude microorganism lysates that are provided by the rapid processing steps. Polypeptide biomarkers are selected due to their species-specific nature (as gene products, they reflect the sequence of DNA segments), and are selected for this purpose primarily on the basis of their size (smaller is better) and abundance. (The approach, however, can also target other classes of cellular constituents, such as fatty acids, and DNA after amplification by the polymerase chain reaction.) Thus, the approach is based upon the highly sensitive identification of these marker proteins, and thus poses extreme demands upon the analysis technology—a demand that is not currently met by any approach, even in the most sophisticated laboratory setting.

The approach depends on the capability of ion traps or FTICR to isolate trace-level species from highly complex mixtures containing both biological and other environmental components. The capability for identification is derived from the high selectivity afforded by the MS/MS capabilities that allow polypeptide identification.

The development and evaluation of a new approach to ESI-mass spectrometer interfacing to allow a small, compact and lightweight vacuum system to be utilized. There are two main elements to our approach: 1) inclusion of novel methods for improved ion focusing, trapping, and transmission from higher pressure regions; and 2) the use of methods to eliminate the gas introduction or transmission between differentially pumped regions, except during periods of ion introduction and transmission between these differentially pumped regions of the vacuum system. The significance of this approach is that it provides a decrease in the pumping speeds required by a factor of between 10 and 100, which is directly reflected by a reduction of the weight and size of the vacuum system. In our initial efforts a high speed micro-valve has been designed for the ESI interface of an ion trap mass spectrometer, and is currently under construction.

Flow Injection Analysis

Jay W. Grate (Interfacial and Processing Science)

Study Control Number: PN95034/1010

Project Description

Flow injection analysis constitutes a combination between wet analytical chemistry and instrumentation that automates analyses and processes in miniature form. Flow injection techniques are extremely flexible and analyses have been developed for a great variety of inorganic and organic chemicals on samples ranging from soils, wastewater, and industrial process streams. The purpose of this project was to enhance the flow injection analysis technique and conduct proof-of-principle experiments that will demonstrate the usefulness of these methods in addressing a variety of problems at Hanford and other DOE sites. Specific areas of interest include radiochemical analysis, soil and groundwater analysis, and process simulation.

Technical Accomplishments

Automation of radiochemical analysis was the focus of the work in FY 1996. We submitted a successful proposal entitled "Automation of Radiochemical Analysis by Flow Injection and Sequential Injection Methods" under the Wolf-Broido Initiative. Further radiochemical analysis research related to tank waste characterization problems was continued under this program and the LDRD project was shifted to other topics.

We demonstrated that sequential injection techniques could be used to automate the separation of isotopes for medical purposes.

The isolation of radioisotopes for medical use typically involves a mixture of a longer-lived parent isotope and shorter-lived daughter isotope in secular equilibrium. The purpose of the generator is to separate the daughter isotope from the parent and other radionuclide and stable interferences. If the daughter isotope has a short radioactive half-life, it needs to be separated from its parent at the user's facilities, as it cannot be produced and shipped. The medium containing the parent isotope is often referred to as the "cow." The cow is extremely valuable. One approach for medical isotope generation lies in storing the parent/daughter mixture in solution, and then using separation chemistry steps to isolate the daughter isotope from the parent. The parent (cow) is recovered and saved for additional use. An example of this approach is the Ac-225/Bi-213 separation method recently developed at PNNL. It would be highly advantageous to automate these types of separations.

Flow injection and sequential injection represent automated solution handling approaches that are highly suitable for this task. Under this project, we previously developed a rapid, automated, microanalytical procedure for the determination of Sr-90 in aged nuclear waste. It was based on a sequential injection system that rapidly separates Sr-90 from Y-90, Cs-137, and other radionuclides. The separation was achieved using a sorbent extraction minicolumn containing sorbent material that selectively binds strontium from nitric acid solutions. The separated Sr can be eluted with water. The eluted Sr-90 zone was mixed with a liquid scintillation cocktail and detected on-line with a flow-through liquid scintillation counter. The effectiveness of the new methodology for this load, wash, and elute separation was demonstrated in the analysis of tank waste samples. In addition, this instrumental approach is useful for studying new radiochemical separation methods.

In the medical isotope area, we set out to demonstrate applicability of the sequential injection methodology to the separation of Bi-213 from the Ac-225 parent. In a series of experiments in collaboration with Lane Bray, we demonstrated that the manual ion exchange generator procedure developed at PNNL can be efficiently automated. We demonstrated that the product isotope could be successfully separated from the parent in the automated format with excellent recovery efficiency. In addition, the cow was efficiently recovered for future "milking."

This work received ALARA recognition. This technology will not only save extremity and whole body dose taken by research staff at PNNL, but will also reduce dose to medical personnel administering the radioisotopes in hospitals when this technology is applied. The flow injection capability we developed has also now been applied to a number of bioanalytical applications.

In summary, flow injection and sequential injection have led to demonstrated applicability in a wide range of disciplines, including radiochemical separations and the automated analysis of nuclear waste, microanalytical determination of contaminants in soil and groundwater,

miniaturization of unit operations for nuclear waste separations for laboratory-scale research, development of generators for medical isotopes, and a variety of bioanalytical applications.

Presentations

J.W. Grate, O. Egorov, and J. Ruzicka. 1997. "Automation of Radiochemical Separations using Sorbent Extraction Techniques and Flow Injection Methodologies." Canadian Society for Chemistry 80th Conference and Exposition, Windsor, Canada, June 1-4.

J.W. Grate, O. Egorov, and J. Ruzicka. 1997. "Advancing FIA Applications in Radiochemistry: Rapid Automated Separation of Actinides by Flow Injection Analysis." Eighth International Conference on Flow Injection Analysis - ICFIA 97, Orlando, Florida, January 12-16.

O. Egorov and J.W. Grate. 1997. "Automation of Radiochemical Analysis by Flow Injection Techniques: Fast Actinides Separations by Flow Injection Analysis." 4th International Conference on Methods and Applications of Radioanalytical Chemistry, American Nuclear Society Topical Conference, Kailua-Kona, Hawaii, April 6-11.

O. Egorov, M. O'Hara, and J.W. Grate. 1997. "Flow Injection Based Radionuclide Analyzers: Automated Analysis of Sr-90 and Tc-99." 4th International Conference on Methods and Applications of Radioanalytical Chemistry, American Nuclear Society Topical Conference, Kailua-Kona, Hawaii, April 6-11.

Immunochromatographic Sorbents for the Selective Collection of Chemical and Biological Warfare Agents

Scott D. Harvey, Bob W. Wright (Radiological and Chemical Sciences)

Study Control Number: PN97052/1193

Project Description

A significant problem in the collection of environmental samples for analysis of biological and chemical warfare related chemicals is the nondiscriminate collection of numerous interfering compounds that occurs along with concentration of target analyte. One approach for isolating pure toxin from a preconcentrated environmental sample is to process the sample through a complex array of successive chromatographic separations. The approach presented here focuses on simplifying this analytical approach by implementing an initial selective preconcentration stage that will collect only the analyte of interest. We plan on exploiting the highly specific antigen/antibody interaction for this preconcentration stage by preparing custom immunochromatographic sorbents. The sorbents will be evaluated for their ability to quantitatively remove trace-level chemical warfare (CW) surrogates or biological warfare (BW) toxins from water samples. The target analytes will be eluted from the immunosorbent and analyzed by HPLC in an on-line configuration.

To produce a silica-based immunosorbent, a large quantity of purified IgG (approximately 100 mg/g sorbent) was required as a requisite to covalent bonding to the chromatographic support. Accordingly, the first goal of these studies was to develop improved methods for the semi-preparative isolation of antibodies from serum. Previously, we had used commercially available kits that used gravity-fed Protein A columns followed by gel-permeation chromatography to desalt the IgG fraction. Using these techniques, we purified antibodies to the mycotoxin zearalenone from rabbit serum; however, this approach was time-consuming and labor intensive. This LDRD describes an improved IgG isolation method. The second goal was to consolidate data created during previous zearalenone studies. Chromatograms from this study were transferred from strip chart tracings to electronic files to facilitate data use for publications and presentations.

Technical Accomplishments

A commercially available Protein A HPLC column (Shodex AFpak APA-894, 50 mm x 8 mm i.d.) was used for IgG purification. Various buffers and solvent combinations were explored using this column. A representative separation of serum on the Protein A column is shown in Figure 1. The arrow indicates when the step gradient to low pH buffer was initiated. Figure 1 illustrates approximately 1.33 mg of IgG eluting with a retention time of 19.63 minutes. The Protein A column was equilibrated for 20 minutes with the initial mobile phase before injection of the next sample. Alternative mobile phase systems, including a comparable phosphate buffer combination and a commercially available elution buffer system from Pierce (ImmunoPure®), did not yield acceptable chromatography for IgG.

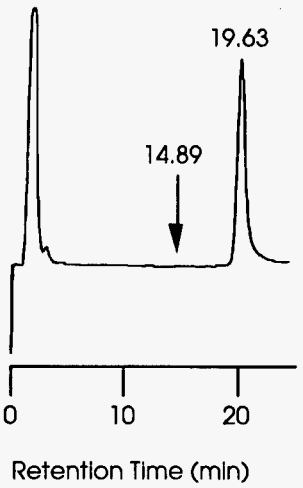

Figure 1. Representative chromatogram of semi-preparative IgG isolation from rabbit serum on a Protein A HPLC column. The arrow at 14.89 minutes indicates a step change to an acidic acetate mobile phase. IgG elutes with a retention of 19.63 minutes.

The Protein A-purified IgG fraction pool was neutralized to pH of 7.0 with a dilute sodium hydroxide solution. The solution was then processed through membrane filtration centrifuge tubes (Centriprep-30, 30 kDa cut-off, Millipore, Bedford, Massachusetts). During this step the antibody was desalted, the buffer exchanged to phosphate buffered saline (PBS), and the antibody concentrated. Future work could take advantage of a new membrane filtration advancement (i.e., Centricon Plus-20, 30 kDa cut-off, Millipore). Advantages include very low membrane binding, higher possible concentration factors, and faster sample processing. Larger versions of this membrane unit are capable of processing 80 mL of column eluate at a time.

Protein A column breakthrough studies were essential to ensure that IgG was not being discarded in the dead volume peak. These studies were performed by collecting the dead volume peak under actual semi-preparative chromatographic runs. This material was desalted (by dialysis) and concentrated (by lyophilization) before being reinjected on the Protein A column. The peak area for IgG was compared between the dead volume fraction and a similarly treated solvent blank (initial buffer that had been identically desalted and concentrated). This comparison indicated that breakthrough of IgG through the Protein A column during semi-preparative runs was less than 0.5%.

To further characterize the IgG and dead volume fractions, a specialized form of capillary electrophoresis (CE) was implemented. In this technique, proteins are first treated with sodium dodecyl sulfate (SDS). This surfactant denatures and binds to the hydrophobic portions of the protein in such way that a constant negative charge is imparted to the molecule per unit protein. Further, the SDS-induced charge overwhelms the native charge of the protein. The negatively charged proteins are then separated in an entangled polymer buffer. Under these conditions (designated CE-SDS), the sieving effect of the viscous hydrophilic buffer causes the larger proteins to migrate slower than smaller proteins. In fact, as observed in traditional SDS-polyacrylamide gel electrophoresis (SDS-PAGE), a linear log molecular weight versus migration time is observed. Initial experiments verified this linear relationship for CE-SDS with protein standards ranging from 14.4 to 200 kDa. The regression line equation derived from the linear plot allowed estimation of an unknown protein's molecular weight.

Analysis of the desalted and concentrated Protein A column dead volume fraction by CE-SDS indicated that serum albumin was the principal component. Although several very small peaks were also observed, IgG was not present, a result consistent with other breakthrough studies described above. The CE-SDS electropherogram of the IgG fraction was dominated by a broad peak having a molecular weight that corresponded to IgG. We hypothesize this peak was broad because antibodies were polyclonal and, therefore, contained structural heterogeneity. Surprisingly, there were other components present in the profile as well. It was noted that these additional minor components had molecular weights corresponding to the light and heavy chains that make up IgG. To test whether IgG was decomposing into its constituent polypeptide chains, all disulfide bonds were reduced by addition of 10 mM dithiothreitol. The electropherogram of the reduced IgG fraction verified that IgG had been quantitatively reduced to the light and heavy chains. Some of the fronting on the IgG peak could be due to combinations of partially reduced IgG that contain two heavy chains (110 kDa) and a heavy/heavy/light chain combination (132 kDa). The 77 kDa light and heavy chain combination (if present) would elute well before the IgG peak.

Immunosorbent was produced by covalently coupling IgG amino groups (*N*-terminal peptide and lysine amino groups) with an activated silica. This resulted in IgG being bound to the silica with a random orientation. Immunosorbents produced in this fashion have reasonable chromatographic properties, although two characteristics can be expected to limit performance. First, antibodies are bound in a region immediately adjacent to the solid silica phase. Diffusion in this interficial boundary layer is very sluggish and counter-productive to conducting efficient chromatography. Additionally, because IgG molecules are bound in a random fashion, many are unable to interact with analyte based on stearic considerations. We have proposed bonding strategies that address both shortcomings by incorporating a spacer molecule to distance IgG from the silica surface. This, combined with specific reaction chemistry that is designed to orient the antigen recognition sites toward solution, will result in a sorbent with a higher antigen capacity and more desirable chromatographic diffusion properties.

The example given below is taken from previous zearalenone studies. Once an immunosorbent has been prepared, a small precolumn containing this material is placed in-line with a reversed-phase chromatographic column. An HPLC trace enrichment valving configuration conveniently serves this purpose (Harvey and Clauss 1996). Figure 2 shows the analysis of 10.0 mL of 10-fold diluted urine that had been fortified with 5.0 ppb (ng/mL) zearalenone. The peak that elutes with a retention time of 9.27 minute is due to the mycotoxin zearalenone. Given the extreme complexity of the urine matrix, the background observed in this analysis is notably low. This example emphasizes the very high selectivity available through the immunochromatographic preconcentration approach.

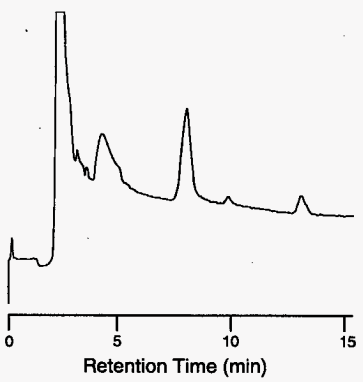

Figure 2. Immuno preconcentration followed by on-line reversed phase HPLC of 10.0 mL of 10-fold diluted urine that had been fortified with 5.0 ppb zearalenone. Zearalenone elutes with a retention time of 9.27 minutes.

Reference

S.D. Harvey and T.R.W. Clauss. 1996. "Rapid On-line Chromatographic HPLC Determination of Trace-level Munitions in Aqueous Samples." *J. Chromatogr. A*, 753:81-89.

Publication

S.D. Harvey, A.L. Tubaugh, and A. Krupsha. "Immunochromatographic trace enrichment with on-line HPLC analysis of the mycotoxin zearalenone." *J. Chromatogr. A* (in preparation).

Micromachined Aerosol Collection System for Pathogen Detection

Joseph G. Birmingham, Donald J. Hammerstrom, Charles J. Call, Jianwei Gao, Nancy B. Valentine, Brian S. Hooker (Process Technology)

Study Control Number: PN97072/1213

Project Description

A micromachined aerosol collection system for biological warfare agents will be designed, fabricated, and tested. This device can be coupled with a detection technology for use on the traditional battlefield and in counter-terrorism applications. The aerosol collection system we propose to build uses a combination of microelectromechanical and microfluidic technologies capable of trapping airborne viruses, bacteria, molds, and spores; and eliminating smoke, dust, and other large particulate interferences.

We will use advances in precision engineering techniques to develop a system with miniaturized components. The system will consist of micromachined electrostatic precipitation, microchanneled liquid collection. This flexible system can be assembled into smaller or larger architectures for a range of applications. It will overcome several limitations of the current biological detector system (BIDS): micromachined sheet substrate material choice is not limited; silicon, Teflon, plastics, ceramics and metals can be micromachined to be lightweight and compact; laminar flow in micromachined electrostatic precipitators reduces the destruction of biological samples by impaction and increases collection efficiency; the particle size range that can be effectively collected will be improved by an order of magnitude over current devices while power consumption is reduced; and compact micro-architecture reduces size and is ideal for mobile or battlefield applications.

Background

The experimental work performed in FY 1997 revealed that a 1000 liter per minute microelectrostatic precipitator (μESP) was able to collect polystyrene latex sphere aerosols at an efficiency of greater than 70% for several sizes. As a point of comparison, the state-of-the-art aerosol collectors are expected to be about 35% efficient.

The efficient collection of aerosols for subsequent analysis has become an important military objective after the Gulf War. One approach to the collection of aerosols is the electrical charging of the particulate followed by deposition in an electric field. This use of electrical forces to effect the efficient collection of aerosols of biological origin in micromachined devices is the focus of this project.

The prototype electrostatic precipitator was built at full scale for a flow rate of 1000 liters per minute of gas flow. Air flows were determined in a smaller diameter 2-inch section of tubing downstream of the evaporation section. The velocity head was measured with an inclined manometer.

The first-generation electrostatic precipitator did not have a fully integrated fluidic collection system due to excessive fabrication. Therefore, we used a batch collection process that deposited collected particles into a fluid at the end of a collection run. The collector plates were washed with water and then rinsed with tetrahydrofuran to remove all of the particles.

A Sequoia-Turner model 450 fluorometer was used to measure the fluorescence of our liquid samples. The instrument was used with the excitation and emission filters appropriate to the fluorescein dye which tagged the microspheres. For each sample, the measured fluorescence was scaled by the fluorescence from a standard solution of microspheres. Each standard contained a known number density N_{std} of microspheres, enabling the number density N_{sam} in the sample to be determined from:

N_{sam} = (fluorescence of sample/fluorescence of standard) N_{std}

The span setting of the instrument was adjusted such that N_{std} was constant over a series of measurements, thus compensating for instrument drift.

In general, each standard solution was prepared by diluting 0.01 mL of the standard 2.6 wt% solids solution (from Polysciences, Inc.) in 500 mL of deionized water. This concentration for the standards gave fluorescence emissions of the same order of magnitude as those from our influent and effluent samples. These solutions were transparent and were of sufficiently low concentration to yield emission intensities which were linear with concentration. Experimental samples which were not sufficiently transparent were diluted prior to measurement.

The overall design philosophy of the use of microfluidics, laminar flow, and massive parallel processing was

followed. This strategy has proved to be successful with other micromachined aerosol collectors. The power consumption of the μESP was found to be a fraction of a watt. It required about 14 watts to operate the air fan. This electric force is sufficient to remove the particulate to the collection electrode.

Technical Accomplishments

The efficient collection of aerosols using various sizes of polystyrene latex spheres has been demonstrated during FY 1997. The design was based on several considerations that differentiate the micromachined electrostatic precipitator (μESP) from conventional designs.

Some of these design anomalies will be modified for wind tunnel studies conducted with bacterial and viral simulants.

We did not include the charging section in the first series of tests because of the intrinsic negative charge of polystyrene latex spheres. Collection efficiency was determined by comparing the number of particles in the influent subsample air with the number in the effluent subsample air (i.e., after passing through the collector). We also measured the number of particles in the fluid collected from the plates. These amounts were roughly equivalent with the number of particles nebulized into the influent airstream, suggesting nearly 100% collection efficiency. These results are summarized in the following table:

Particle Size, μm	Avg. Collection Efficiency, %
0.485	84
0.752	72
0.930	77
0.973	90
1.871	71
5.47	48*

* Problems with the power supply during the test.

The efficiency of collection of polystyrene latex spheres by a μESP is shown in Figure 1. The two curves represent the predicted performance (top curve) using the Duetch-Anderson equation and the experimental results (bottom curve). The significance of the experimental results are that the current state-of-the-art aerosol capture devices have typically 35% collection efficiency whereas for almost every aerosol size the μESP collection efficiency was greater than 70%. The μESP performance as predicted from the Duetch-Anderson equation suggested that as the particulate size increased, the collection efficiency should increase commensurately. However, the experimental collection efficiency decline at the largest aerosol diameter was due to the loss of power during the experiment which allowed the polystyrene latex to pass through uncollected. Another explanation suggested by the data is that the mobility of larger aerosols may be reduced to the point that the collection efficiency is reduced. Whether the collection efficiency decline of larger aerosols is an experiment anomaly or reflects a reduced mobility condition will be determined in additional tests. In summation, the direct-current powered electrostatic precipitator has exceeded initial expectations for particulate collection.

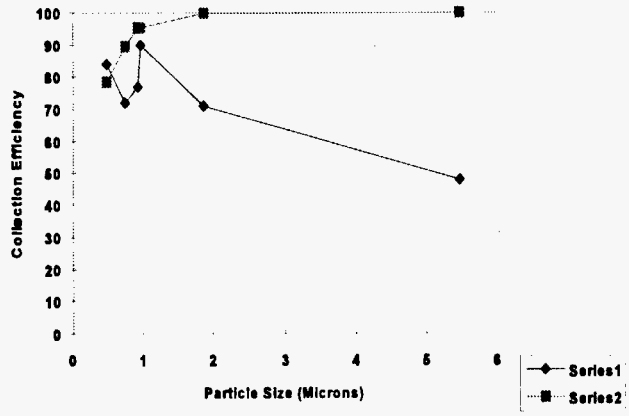

Figure 1. Microelectrostatic precipitator performance.

Multispectral Imaging for the Detection of Leaking Explosives from UXO

Khris B. Olsen, Edward C. Thornton, Christopher J. Thompson (Water and Land Resources)
Randy R. Kirkham (Hydrology)

Study Control Number: PN97078/1219

Project Description

This project evaluated the use of ultraviolet-visible-near infrared spectroscopy as a tool to identify explosives associated with explosive production and unexploded ordnance (UXO). Project activity focused on explosive detection in a soil matrix during dig-face activities.

Technical Accomplishments

A thorough literature search was conducted on optical methods associated with the detection of explosives. Results from the literature search suggest fluorescence techniques are not suitable for direct measurement of explosives in a soil matrix. Photon yields for explosives typically fall below 0.001 (1 photon emitted/1000 photons absorbed by molecules). This response factor is sufficiently low to prevent detection by fluorescence. Therefore, no further consideration was given to the use of fluorescence measurements during the course of this project.

The literature search suggested the ultraviolet-visible-near infrared portion of the light spectrum may provide reasonable sensitivity to detect explosives in soil matrix at or about 100 mg/kg. Based on this conclusion, ultraviolet-visible scans were conducted on liquid standards of TNT, RDX, and tetryl. The solution scans suggested the region of interest is between 200 to 350 nm for these three compounds (Figure 1). The feasibility of measuring explosives in sediments by ultraviolet reflectance was evaluated by examining spectra of silica and samples of silica that had been spiked with HMX, RDX, tetryl, and TNT (Figure 2). The spike concentrations were 4858 mg/kg HMX, 4230 mg/kg RDX, 4495 mg/kg tetryl, and 4322 mg/kg TNT. In general, the raw spectra are similar in shape, with a dip in the reflectance near 228 nm and gradually increasing reflectance values at longer wavelengths. The sample of unspiked silica was the most reflective, followed by the spikes of HMX, RDX, tetryl, and TNT. In order to convert the spectra into a form more useful for quantitation, each sample spectrum was divided by the SiO_2 spectrum, and the logarithm of the inverse of this ratio (i.e., log 1/R) was calculated. The results of this transformation are shown in Figure 3. The transformed

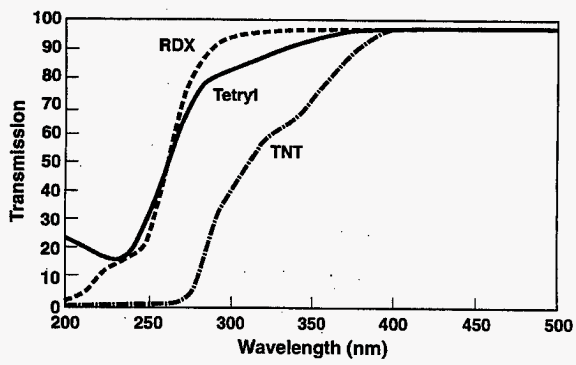

Figure 1. Transmission spectra of explosives.

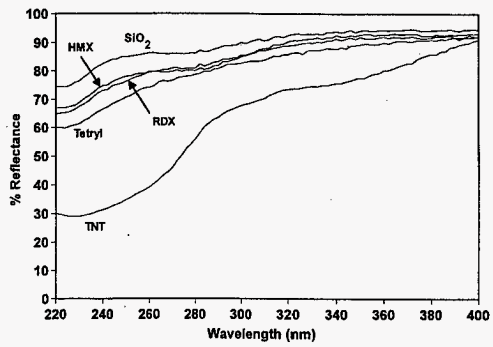

Figure 2. Raw UV-reflectance spectra of explosives in SiO_2.

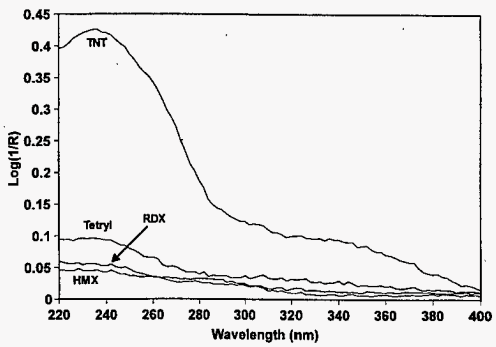

Figure 3. Transformed UV-reflectance spectra of explosives in SiO_2.

spectrum of the TNT sample shows an intense band centered at 240 nm. Much weaker bands in the same region are also apparent in the transformed spectra of the other spiked samples. This limited analysis shows that the spectral measurement appears to be much more sensitive to TNT than HMX, RDX, and tetryl. Consequently, a more detailed analysis of TNT in silica was performed. Figure 4 shows the log(1/R) spectra of six silica samples with TNT spikes ranging from 513 mg/kg to 5440 mg/kg. For quantitation purposes, the intensity of the bands should vary in a systematic fashion with concentration. While the three lowest concentration spectra appear to follow a linear trend, the relationship between intensity and concentration is not obvious for TNT concentrations greater than 2049 mg/kg. This is probably the result of a saturation effect that results from the strong absorbance of TNT and the influence of stray light. The detection limit for TNT in silica was estimated to be 110 mg/kg based on the intensity of the 513 mg/kg spectrum at 236 nm and an estimate of the noise in the baseline. A similar analysis was also conducted for the other explosives using the data in Figure 2. The detection limit estimates for tetryl, RDX, and HMX were 400 mg/kg (based on the intensity at 234 nm), 670 mg/kg (228 nm), and 940 mg/kg (228 nm), respectively. Since SiO_2 is a clean, highly reflective matrix, these values represent the "best-case" scenario for the measurement of explosives in sediments by ultraviolet reflectance spectroscopy.

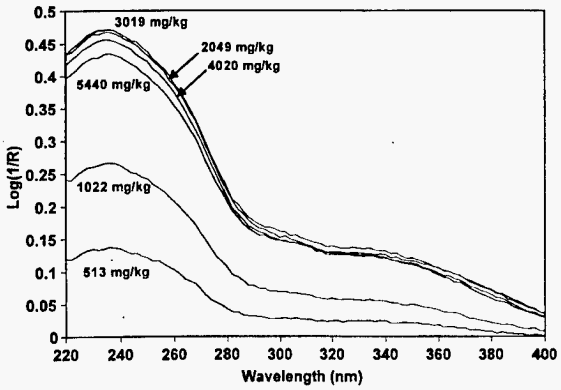

Figure 4. Transformed UV-reflectance spectra of TNT in SiO_2.

The effects of natural sediment matrices were evaluated by acquiring reflectance spectra of sand, clay, and silt samples (Figure 5). The sand, clay, and silt samples were collected from various locations around and on the Hanford Site. The sand fraction was collected from a road cut along the Columbia River in North Richland. The clay fraction was collected from a clastic dike adjacent to the Hanford highway. The silt fraction was collected from a burrow pit at the McGee Ranch near the Yakima Barricade. The samples were dried at room temperature over an extended period of time, spiked with the respective explosive,

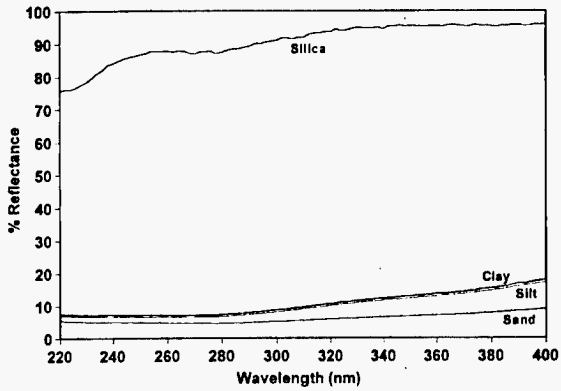

Figure 5. Raw UV-reflectance spectra of silica, sand, silt and clay.

homogenized, and packed into mounts. Representative spectra of these matrices are plotted in Figure 5 along with a raw spectrum of SiO_2. The graph shows that clay, silt, and sand are very highly absorbing matrices, compared to silica. In fact, the low reflectance values of these materials suggest that detection of explosives in clay, silt, or sand would be very difficult. This hypothesis was tested by spiking silt samples with 276, 633, and 1525 mg/kg of TNT. TNT was selected since it provided the best reflectance response on the silica matrix. Figure 6 shows the raw reflectance spectra of these samples and the average spectrum of three unspiked silt samples. The spectra of the three samples containing TNT are very similar to each other and have slightly higher percent reflectance values than the unspiked silt spectrum. Figure 7 shows the corresponding log(1/R) spectra for the TNT spikes. No obvious correlation exists between spectral intensity and concentration. Moreover, the spectra appear to be dominated by random noise. The detection limit for TNT in silt is therefore estimated at greater than 1525 mg/kg. Greater sensitivity might be achieved by using a brighter source of incident light, but the detection limit would never approach that observed for a silica

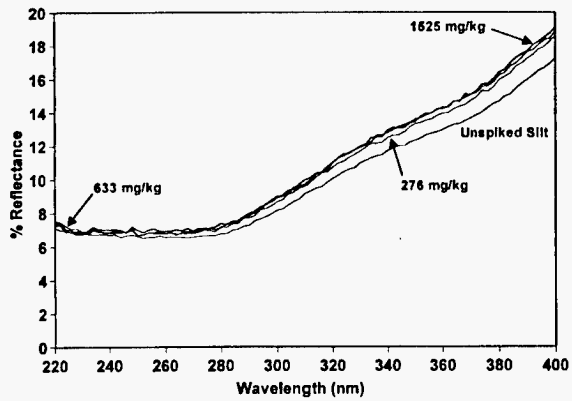

Figure 6. Raw UV-reflectance spectra of TNT in silt.

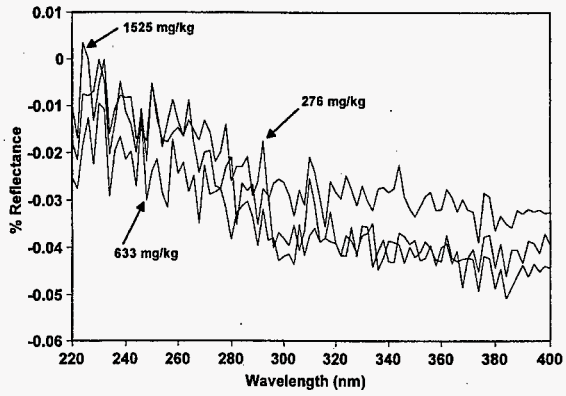

Figure 7. Transformed UV-reflectance spectra of TNT in silt.

matrix. These results, together with the less promising results obtained on tetryl, HMX, and RDX in silica, demonstrate that the detection of explosives in silt, sand, and clay by ultraviolet reflectance spectroscopy is not feasible at practical concentrations of explosives.

Near-infrared reflectance scans were also taken of the fine-grained silica sand standards (TNT, tetryl, HMX, and RDX) used for ultraviolet analysis. As before the concentrations of explosives were as high as 4858 mg/kg and the spectra were normalized by the log(1/R) transformation. In general, the spectra did not appear to contain any features that would be useful for the detection of explosives, although HMX and RDX may have weak absorbance bands at about 2300 nm. No further consideration was given to the use of the near-infrared spectral region for detection of explosives in sediments.

Conclusion

- Based on the results of an extensive literature search, the measurement of explosives by fluorescence was not conducted because of poor photon yields.
- Using ultraviolet reflectance and a silica-sand matrix, detection limits for TNT, tetryl, RDX, and HMX were determined to be 110 ppm, 400 ppm, 670 ppm, and 940 ppm, respectively.
- Ultraviolet-reflectance detection limits for explosives in natural sand, silt, and clays were determined to be greater than 1525 ppm.
- Laboratory testing of the near-infrared region of the light spectrum failed to identify any specific distinguishing bands associated with explosive compounds.

Acknowledgments

The assistance of Tim Stewart in acquiring the ultraviolet-visible-near infrared data for this study is gratefully acknowledged.

Rapid Detection of Bacterial Fingerprints by Matrix-Assisted Laser Desorption/Ionization Mass Spectrometry (MALDI-MS)

Karen L. Wahl, James A. Campbell, Mark T. Kingsley (Materials and Chemical Sciences)

Study Control Number: PN97089/1230

Project Description

The objective of this project was to develop a rapid screening tool for detection of microorganisms based on unique fingerprints produced by matrix-assisted laser desorption/ionization mass spectrometry (MALDI-MS). Unique ion fingerprints have been obtained from different microbial cells. However, a better understanding of the effects of experimental parameters, in addition to a fundamental understanding of the microbial origin of the fingerprint ions is needed.

Technical Accomplishments

Rapid detection and classification of microorganisms is important for public health, biotechnology, food processing, monitoring of biological warfare, and counterterrorism response. Most analytical methods developed for such detection required significant sample handling and preparation time, or exhibited indirect evidence of the presence of specific microorganisms. Recent advances in analytical instrumentation, such as MALDI-MS, have made it possible to rapidly and efficiently analyze biological components such as proteins, peptides, oligonucleotides, and phospholipids intact. MALDI-MS was chosen for detection of the microorganisms for this project due to its rapid analysis time (less than 5 minutes), minimal sample requirement (microliters), and for providing molecular weight information of biological components.

During FY 1996, preliminary MALDI-MS analysis directly from intact microbial cells was developed. Separation of whole bacterial cells from the soy broth growing media was required prior to mass spectral analysis using simple washing techniques. Distinct ions from 13 bacterial samples were obtained. A preliminary blind unknown test of sample preparation and MALDI analysis of the 13 samples was 50% successful in identifying the bacteria based on comparison with the known MALDI spectra. These results show the potential of this rapid analysis technique for screening for the presence of microorganisms such as bacteria.

In FY 1997, the effects of experimental variables, such as cell culture age and analytical matrix, on the bacterial fingerprints was investigated. The MALDI fingerprint spectra are reproducibly generated when the bacterial samples are in the same growth phase, and the matrix used for the MALDI analysis is the same. However, altering either culture age or matrix has a significant impact on the ions observed. For example, the Gram-negative bacterium *Shewanella alga* (BrY) has a very reproducible fingerprint of ions when 1) the bacterial sample is fresh, 2) the cells are in the log phase, and 3) when sinapinic acid is used as the MALDI matrix. When the cell sample has aged, so that the cells are in death phase, the MALDI-MS spectra differ from those obtained with fresh cultures. An example of changes in the MALDI-MS spectra based on cell culture age is shown in Figure 1. This may prove valuable if MALDI-MS can provide information on cell viability or growth state. Continuing work is in progress to assess this value.

A series of 13 *Bacillus* cultures was obtained from various sources. Analysis of these cultures by traditional DNA extraction, followed by polymerase chain reaction (PCR) gel electrophoresis, revealed that many were homologous (Table 1). The *Bacillus* strains that appear homologous based on PCR gel traces produce very similar MALDI mass spectra (Figure 2a,b). Bacteria that are found to be different by PCR gel also produce noticeably different MALDI mass spectra (Figure 2c). The MALDI-MS results and the PCR nucleic acid determinations are in agreement for comparative analyses of bacterial cultures.

Matrix-assisted laser desorption/ionization mass spectrometry is a powerful rapid screening tool for microorganism identification. Reproducible mass spectral fingerprints are obtained from intact microbial cells with minimal sample handling. Several experimental variables, such as microbial cell growth conditions and analytical matrix selection, affect the mass spectral fingerprints. However, the MALDI mass spectra are reproducible under identical parameters. Aged cells with consistent analytical conditions yield reproducible MALDI-MS fingerprints, but are different compared to viable cells. These variations may in fact provide valuable information to identify the origin and viability of the microbial sample. The MALDI-MS results and the PCR nucleic acid determinations are in agreement for comparative analyses of bacterial cultures.

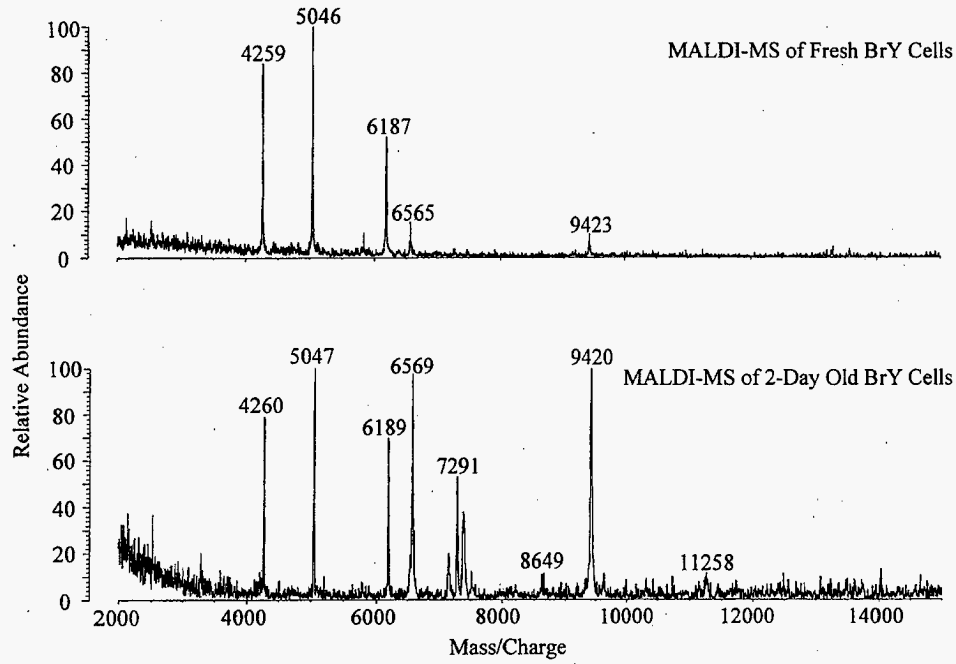

Figure 1. Culture age effect on MALDI mass spectra of gram-negative bacterium BrY.

Table 1. PCR fingerprinting of "BG" strains/repeat DNA primer sets.

Strains		Primer Sets		
		Rep (1)(a)	Eric(a)	Box(a
ATCC 9372	(*B. subtilis*)	1	A	a
ATCC 31028	(*B. subtilis*)	1	A	a
ATCC 51189	(*B. subtilis*)	1	A	a
ATCC 49822	(*B. subtilis*, formerly *B. globigii*)	1	A	a
ATCC 49760	(*B. subtilis*, formerly *B. globigii*)	1	A	a
DPG BG	(orange from simulant powder)	1	A	a
BMI BG	(purified from DPG)	1	A	a
ATCC 7972	(*B. subtilis*)	1*	A*	a*
ATCC 6455	(*B. atrophaeus*, formerly *B.s.*)	1*	A*	a*
ATCC 49337	(*B. atrophaeus*, formerly *B.s.* var *niger*)	1*	A*	a*
ATCC 4516	(*B. circulans*)	2	B	b
ATCC 6501	(*B. subtilis*)	3	C	c
ATCC 14580	(*B. licheniformis*)	4	D	d
ATCC 14579	(*B. cereus*)	5	E	e
ATCC 14577	(*B. sphaericus*)	6	F	f
•ENVI	(white culture)	7	G	g

1 Patterns with same number or letter are identical
* indicates similar but slightly different (additional bands, etc.)
• different from "BG" and controls
(a) amplification protocols essentially as Louws et al., 1994, *Appl. Environ. Microbiol.* 60, 2286.

ATTC - American Type Culture Collection
BMI - Battelle Memorial Institute
DPG - Dugway Proving Ground
ENVI - random environmental isolate

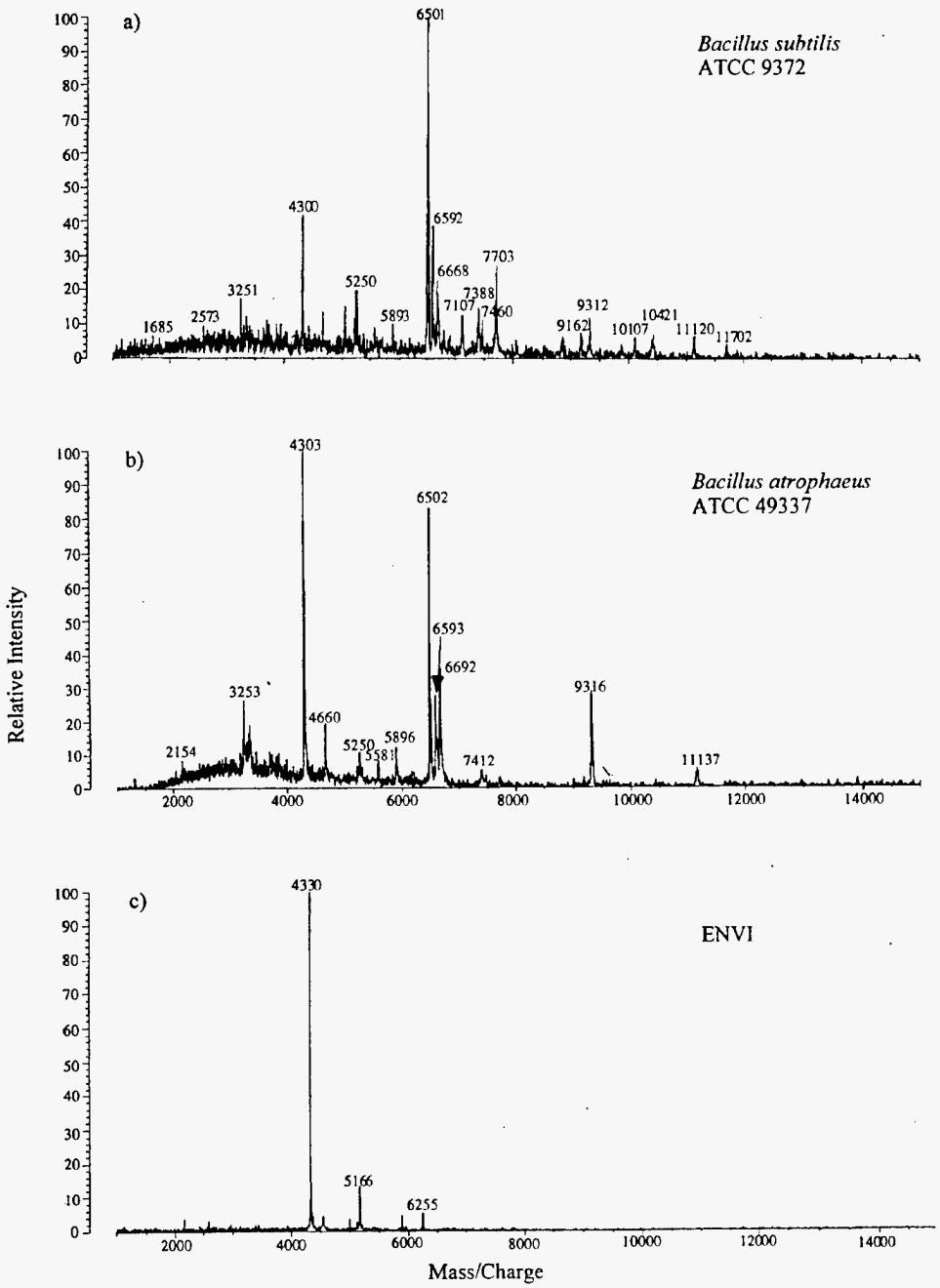

Figure 2. Comparison of two gram-positive *Bacillus* cells and one unknown isolate by MALDI-MS.

Publication and Presentation

K.L. Wahl, N.B. Valentine, S.L. Gantt, A Saenz, S.A. Clauss, and M.T. Kingsley. 1997. "Investigation of the MALDI-MS of Intact Microbial Cells and the Factors Affecting Them." *In Proceedings of the First Joint Services Biological Mass Spectrometry Workshop*, Baltimore, Maryland, July 28-30.

Versatile Synthesis Method for Sensing Materials

Jay W. Grate (Interfacial and Processing Science)

Study Control Number: PN97104/1245

Project Description

The objective of this research is to develop a versatile and generic approach to the synthesis of polymeric materials for chemical sensors and arrays. The approach and the resulting materials will be applicable to many different sensing platforms, including acoustic wave, fiber optic, planar optical waveguide, and field effect transistor sensors. The synthetic approach will be designed so that the following physical properties and capabilities are built into the materials: a) low glass-to-rubber transition temperature for rapid vapor diffusion and hence rapid sensor responses; b) tunable physical properties such as viscosity, refractive index, etc.; c) polymer end groups tailored for cross-linking to cure materials on sensor surfaces; d) incorporation of functional groups and binding sites to absorb the analytes of interest; and e) optional incorporation of molecularly dispersed groups to facilitate in signal transduction. Development of this capability will provide a significant advantage in developing chemical sensors and sensor arrays for particular client applications.

Technical Accomplishments

Just over a decade ago, the development of sensing materials for acoustic wave and other chemical sensors was an empirical approach based on testing candidate materials and seeing if they worked. The process was sometimes but often not informed by chemical intuition. Since that time, systematic studies by Grate, Abraham, and coworkers, using solvation parameters and linear solvation energy relationships, have established and quantified the interactions governing the sorption of organic vapors by sorbent polymers. With this understanding in hand, it should follow logically that sensing polymers can be rationally designed and synthesized at will. However, a number of practical considerations render this task more difficult than one might expect. Most synthetic approaches for polymer synthesis suffer from one or both of the following problems: 1) the polymer backbone and substituents lead to glassy or crystalline polymers leading to very slow vapor diffusion and hence slow sensor responses, and 2) the chemistries used to create covalent bonds create polar sites that may conflict with the desired selectivity of the material.

A useful sensor material must not only have the interactive properties of interest, it must also have other physical properties necessary for fabrication and reliable operation of a sensor device using a thin film of the material. For example, it must wet and adhere to the sensor surface. For optical applications, it may be necessary to tailor the refractive index. For acoustic wave applications, it may be necessary to be sure the material is not excessively lossy (thus, attenuating the acoustic waves) at the temperature and operating frequency of the device. Viscosity may need to be within a particular range for some applications, and in some cases it may be required that oily or gummy materials can be cross-linked to yield solid elastomers (on optical fibers, for example). In addition, it may also be necessary to adjust other properties for the transduction mechanism of the particular sensing platform. For example, optical sensors may require that absorbent or fluorescent sites be incorporated. Work function sensors require a suitable initial work function and electrical conductivity of the sensing materials.

Given the number of requirements placed on a sensing material when it is designed for a particular sensing platform and analytical application, it might appear that a new approach would be required for each case, and that some trial and error might be necessary to obtain all the desired properties. However, such an approach would be inefficient. It would be advantageous if a versatile and generic approach could be developed to deliberately synthesize materials to obtain the full range of required properties in a predictable way, and be able to apply this approach to multiple sensing platforms.

We are developing a versatile synthetic approach that will enable the existing rational understanding of vapor/polymer interactions to be extended to the rational design and synthesis of sensing materials. In addition, by careful attention to polymer physical properties, material cross-linking, and interfacial issues, we will greatly improve the reliability of chemical sensor devices employing sorbent thin films.

This approach is being used to help prepare a set of sorbent materials covering all the solubility properties that one would wish to put in a sensor array for organic vapors, and to prepare these polymers in formulations that can be cross-linked in thin films. The properties to be covered include a non-polar polymer, a polarizable polymer, a dipolar polymer, a dipolar basic polymer, a basic polymer, and a hydrogen-bond acidic polymer. Thus far we have found or

synthesized materials that cover four of these categories, and we have strategies in place for the remaining two.

A critical issue in the development and deployment of polymer-coated sensors is the reproduciblity and reliability of such sensors. This is critically dependent on the behavior of the polymer as a thin film. We have observed that the overall performance is dependent on factors such as film morphology, the surface to which the film is applied, and the ambient humidity. We are performing experiments to determine which of these factors are most important under what conditions, and whether or not cross-linking is necessary or beneficial. With discontinuous films, cross-linking alone is not sufficient to prevent performance problems with some polymers. On the other hand, one of our newly synthesized materials is well behaved regardless of the film morphology or humidity, even without cross-linking.

Presentations

J.W. Grate and S.N. Kaganove. 1997. "Hybrid Organic-Inorganic Copolymer Films with Strong Hydrogen Bond Acidic Properties for Vapor Sensing." 213th National Meeting of the American Chemical Society, San Francisco, California, April 13-18, and Canadian Society for Chemistry 80th Conference and Exposition, invited talk, Windsor, Canada, June 1-4.

Computer and Information Science

A Metadata-Based Approach for Retrieval of Heterogeneous Data

Daniel R. Adams, James C. Brown,
David M. Hansen, Mark A. Whiting (Information Sciences)

Study Control Number: PN97001/1142

Project Description

The purpose of this project is to explore and develop new techniques for locating and retrieving heterogeneous, multimedia data sources using search and visualization techniques that exploit both the content of data sources as well as the context in which those sources exist. We must move beyond the simple text indexes used with World Wide Web search engines to richer and more adaptable forms of metadata (i.e., information that describes the actual data sources) in order to deal with the wealth of data and data types available today. The research focuses on developing a malleable and extensible metadata structure that can describe the contents of heterogeneous data types (text, audio, video, imagery, etc.), as well as describe the relationships between various data sources. From this base we will move forward to develop advanced search capabilities, visual exploitation tools, and new approaches for extracting and exploiting metadata.

Technical Accomplishments

As the amount and variety of data available increases, new techniques for locating data sources that are relevant to a given problem are needed. At present, most techniques for locating electronic information rely on textual descriptions of data sources and Boolean searches of word indexes to locate relevant information. (There is a growing body of work on performing image queries, but these efforts rely on textual descriptions of images or they use feature/attribute extraction and recognition algorithms that are not readily combined with other data types.) These approaches are not cognizant of, and cannot exploit, contextual clues in locating relevant information. A significant amount of information relevant to locating data that is germane to a given problem is actually found in the correlations and relationships between data sources. One perspective on the Galaxies, SPIRE™, and ThemeScapes™ approaches to data visualization is that these are techniques for finding, visualizing, and exploiting the relationships and correlations between textual documents. This research attempts to broaden the types of relationships that can be modeled, extend these relationships to multimedia data, and explore how the content and context metadata can be effectively exploited.

The metadata construct for individual data sources is relatively straightforward and quite general. We capture the information needed to retrieve an object (including location, ownership, access limitations, etc.), keyword=value pairs that describe the data objects, and links which document and describe relationships between data objects. Furthermore, we determined that any implementation of a metadata repository for information extraction must be dynamic. That is, it must be possible to add metadata and relationships over time, and systems must be able to easily accommodate the addition of items and forms of metadata that were not anticipated at the time the system was designed.

Although we evaluated several products, we chose to implement the metadata repository using the Gemstone Object Oriented Data Base Management System because it is highly extensible, can adapt to new and changing metadata components at run time, and can be used to model both static and active relationships. To demonstrate the basic concepts of the research platform and to validate our design, we prototyped a system (Figure 1) that

- drills down through a Windows file system
- identifies files from which text can be extracted (e.g., word processing files, spreadsheets, presentations, Postscript, etc.)
- extracts the text and any keyword=value pairs that can be identified (e.g., components of the "Properties" sheet in Microsoft Office products)
- summarizes any text extracted from files
- populates the Metadata Repository with the keyword=value pairs, text summaries, and location and retrieval information
- builds a searchable index of the text
- provides tools to subsequently locate and examine data based on queries of the text and keywords.

This project will provide the foundation for research proposed in FY 1998. This research proposes to expand into working with audio data, discovering and establishing connections and relationships between data source through the use of information models impressed onto a data space, and developing new approaches to visualize the web of data and information represented within the metadata repository.

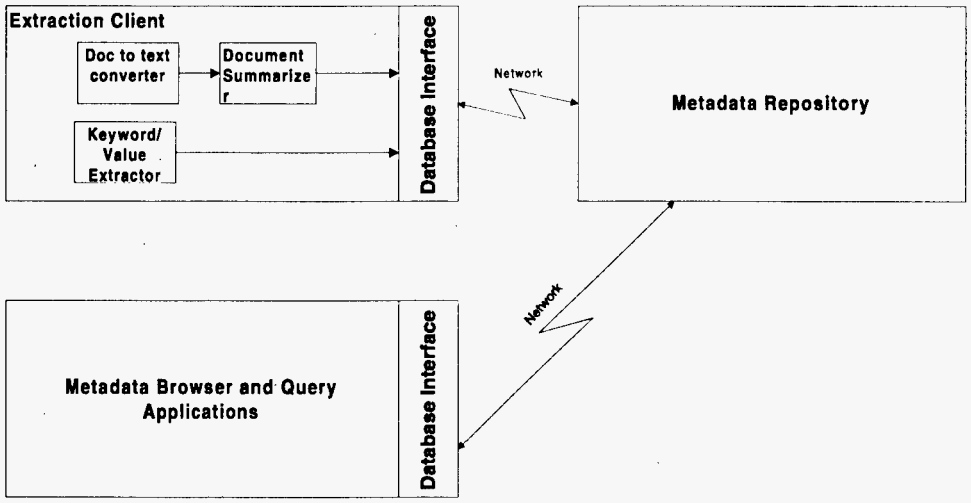

Figure 1. System prototype.

Applied Intelligence Systems

Tamara S. Stewart (Information Sciences)

Study Control Number: PN97013/1154

Project Description

Information tools of the future will provide services to the full spectrum of information manipulation tasks of customers. This includes software/hardware components for cognitive processing, providing opportunities to better extract meaning from information in a context, and fit into architectures that conform to "good design practices" for a specific application. This project's objectives were to make initial inroads to 1) identify cognitive processing approaches that could assist in information manipulation tasks, 2) identify which cognitive processing approaches were appropriate for current information technology projects, and 3) identify a methodology to determine task-appropriate information theories/structures/logics for use in system design.

Technical Accomplishments

There are underlying theoretical principles which support or give meaning to our work, any of our work, and we as human analysts draw conclusions and implications and take action based on the meanings derived from those principles applied to specific situations.

In the information technology arena, theoretical principles have dictated the bounds of computability, the nature of information, and the design of systems to manipulate that information. When we modify those principles or the environmental situation they operate within, we should expect the entire system to react. The valid range of problems and applicable analysis methods for them will change, a shift in the types of conclusions which may be drawn will occur, and implications and subsequent user actions will be altered.

For information technology, a recent paradigm shift has been data visualization. The explosion of information available has not only "pushed" the need for new ways of viewing and reviewing data, but "pulled" a reassessment of the nature of information in order to focus automation tools on issues critical to relieving the overburdened analyst.

At today's stage of information system development, researchers are still identifying information components, their appropriate representations, boundaries for reasonable application of new display technologies, and information systems to assist in manipulating new forms of information. However, it is clear that to design a system that assists in revealing an information set's meaning and relevance in a context or the variable situations that a context occupies in time, the information modeled will have to contain conceptual components.

There is a strong relationship between information, knowledge structures, and their representations on one hand; and design, architecture methods, and algorithms. How we design or how we think in structured ways is influenced by how we define information and knowledge and how we hold that knowledge for processing. If we can understand how design takes place at a cognitive level, then we may identify principles that are closely related to thought processes and assist in designing information manipulation tools that assist analysts in their tasks.

Modeling conceptual information will extend current information technology capabilities, integrate organizational science and human factors research more closely using new information technologies, and lead to significant applications using conceptual and cognitive structures as the principal basis for each application.

This project initially focused on the underlying structure and theoretical relationships describing data, information, knowledge, and system design. This inquiry led to an understanding of the importance of conceptual structures and context/situation.

Conceptual structures research and tools exist in both academic and commercial settings. Only very recently have commercial tools been released that provide conceptual representations. They are still immature in their feature sets, but indicate support and a wide potential of applications for the technology.

Publication

T.S. Stewart and D. Kashporenko. "Conceptual Structures." Pacific Northwest National Laboratory, Richland, Washington. (in preparation)

Applied Mathematics and Computer Science

George I. Fann, Joel M.J. Malard (Theory, Modeling and Simulation)

Study Control Number: PN97014/1155

Project Description

Four decades of production, testing, and operations at the U.S. Department of Energy facilities across the nation have resulted in the interim storage of millions of gallons of highly radioactive mixed wastes in hundreds of underground tanks, extensive contamination of the soil and groundwater at thousands of sites, and hundreds of facilities that must be decontaminated and decommissioned. One method of developing and evaluating remediation strategies is to apply computer simulations. It has long been recognized that modeling of the transport, fate, and processing of contaminants is a computational challenge of the first magnitude, a "Grand Challenge," because of the complexity, variation in temporal and spatial scales, requirements for accuracy, and urgency of the problems at hand due to safety and risk considerations.

In order to best utilize current and future computational resources, simulation software will need to take advantage of clustered shared memory computers. Our work develops the computer science and computational mathematics capabilities that are required for the fast, accurate, and scalable subsurface modeling needed for environmental remediation and restoration efforts using massively parallel computers. During 1997, we developed a library of iterative linear equation solvers with preconditioners that is suitable for groundwater simulations with wells. In addition, we assisted the groundwater modelers with interfacing their simulation codes with post-processing and parallel visualization of their results.

The iterative solution methods are scalable and portable to MPPs and clusters of SMPs using the UNIX operating system with MPI for communication.

Technical Accomplishments

The discretization of partial differential equations occurring in groundwater modeling, e.g., the reservoir equations, leads to systems of linear equations whose coefficient matrices are large and sparse. For example, a three-dimensional simulation of an aquifer discretized as a 100 x 100 x 100 grid yields a linear system of a million equations. The efficient and accurate solution of such large systems is essential to further our understanding and the predictability of subsurface flows and reactive transport of chemical species. The linear system is typically ill-conditioned and block banded in structure. Ill-conditioning is characterized by real and small eigenvalues whose norm is near the numerical machine precision. Banded direct solvers are typically used on serial computers and in optimized codes. However, they do not scale well to parallel computers when using a relatively small number of grid points. Iterative methods such as SOR and SLOR are applicable; however, their rate of convergence is slow because of the small eigenvalues. Complex eigenvalues render the use of traditional non-symmetric iterative solvers such as SSOR or BiCG prohibitive. Newer techniques such as Generalized Minimal Residual (GMRES) (Saad and Schultz 1986), Quasi-Minimal Residual (QMR) (Freud and Nachtigal 1991), Biconjugate Conjugate Gradient Stabilized (BICGStab(L)) (Sleijpen and Fokkema 1993), and BiConjugate Gradient (BiCG) exhibit better numerical robustness and scalability than previous methods and can handle the presence of complex eigenvalues.

We have implemented GMRES, QMR, BiCGStab(L), and BiCG. The QMR, BiCG, and BiCGStab(L) have been incorporated with preconditioners into the PNNL groundwater code STOMP. The performance of the QMR was excellent when the error tolerance requirement was greater than 10^{-7}; however, it was disappointing when tolerance of less than 10^{-13}, needed for groundwater simulation, was required. The performance and convergence of BiCGStab(L) was better than QMR in this tight tolerance regime. We investigated the performance of BiCGStab(L) as a function of L, the number of Lanczo search directions, and as a function of data distribution on the Silicon Graphics PowerChallenge computer.

The structure of linear systems arising in groundwater modeling and reactive transport has a strong impact on the scalability of iterative solvers. The matrices underlying these systems are typically block-banded and the size of the block is closely tied to the number of coupled equations in the original system of the differential equations. In the type of applications that are relevant for this part of the effort, the bands are typical, about 7, and the blocks are small, no more than 10. In effect, there is little arithmetic involved to amortize synchronization costs on SMPs or communication latency across processors on MPPs.

Within this project, we have developed distributed data structures for storing block-banded matrices that are compatible with groundwater application software and yet

allow for scalable implementations of the sparse matrix-vector multiplication kernels that are commonly found in sparse iterative solvers. Moreover, our codes were written to take full advantage of the three-dimensional nature of physical problems. For example, the number of processors effectively used by our implementations of matrix-vector multiplication for three-dimensional problems scales proportional to $p^{2/3}$ where p is the number of nodes compared to $p^{1/2}$ scaling for three-dimensional problems. We also take advantage of the matrix structure so that only nearest neighbor communications are needed in several of the mathematical kernels, e.g., matrix-vector multiply, Schur Complement.

Using these data structures, we have implemented solvers for banded and block-banded linear systems arising in groundwater simulation. Our solvers library contains QMR, BiCGStab(L), CGS, and BiCG with application interfaces for FORTRAN 90 and FORTRAN 77. For our implementation of BiCGStab(L), we obtained a novel implementation of QR factorization that combines the numerical accuracy achievable via modified Gram-Schmidt and the scalability of solving the normal equations. The groundwater simulation component of the STOMP code has already achieved a speed-up of more than 6 using our serial implementation of BiCGStab(L) on a single processor. (See Figure 1.)

We have continued interactions with the compiler tool component of the initiative to ensure that the FORTRAN Pre-Processor (FPP) tool being developed by Matt Rosing for the subsurface reactive transport project can take full advantage of the parallelism available in our iterative solvers.

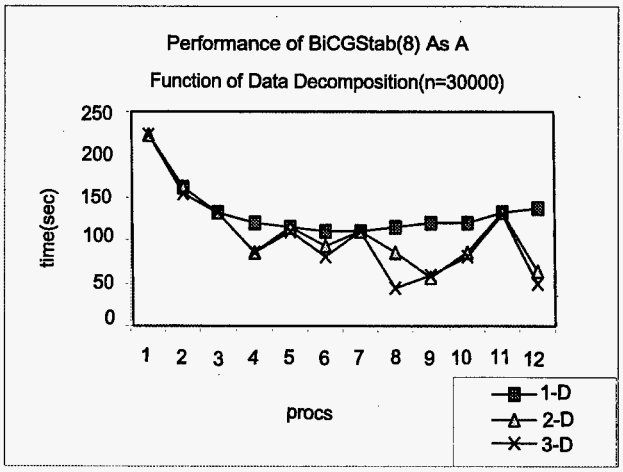

Figure 1. Parallel performance and scalability of the iterative solver BiCGStab(L) as a function of L and as a function of the dimension of the data decomposition.

References

R.W. Freud and N.M. Nachtigal. 1991. "QMR: a quasi-minimal residual method for non-Hermitian linear systems." *Numer. Math.*, 60:315-339.

Y. Saad and M.H. Schultz. 1986. SIAM *J. Sci.Stat.Comp.* 7:856.

G.L.G. Sleijpen and D.R. Fokkema. 1993. *BiCGSTAB(L) For Linear Equations Involving Unsymmetric Matrices With Complex Spectrum.* ETNA, Kent State University, pp. 11-32.

Automated Document and Text Processing

Grant C. Nakamura (Information Technologies/Sciences)

Study Control Number: PN95007/983

Project Description

There exists innumerable collections of text documents that require content exploration and analysis in order to be used effectively. Due to the amount of text involved, it is usually impractical to manually explore and analyze such a collection. Automated approaches show promise, but must be developed further with respect to accuracy, efficiency, and interpretability. The goal of this project was to develop and test new automated text analysis approaches, measures, and algorithms.

In previous years, this project formulated a text analysis approach and developed that approach into the SID (System for Information Discovery) text analysis software. In FY 1997, the project primarily explored possible alternatives to the SID methods, ways to tailor SID algorithms to focus analysis on specific areas of interest, and ways of using the SID algorithms to incrementally process text.

Technical Accomplishments

The project's FY 1997 research was spread over five areas:

- Incremental processing methods
- Alternative text analysis
- Multiple vector representation
- Predefined information
- Loose integration with the Metadata Repository.

Incremental Processing Methods

SID processing creates a context vector model for a set of documents. SID identifies key terms from the set, and relationships between those terms, to generate the model. Because SID processing uses terms from the entire set, the technique requires that all documents be processed within one SID run.

Sometimes it may be desirable to process a set of documents in piece-wise fashion rather than all at once. One motivation for piece-wise processing is to reduce the time that the user must wait before beginning to interact with a large data set. Another motivation is that some data sets, by their nature, grow incrementally. The project created variants of SID algorithms that could perform partial reprocessing, yielding approximately the same vectors that would have been produced by full reprocessing.

We conceived two approaches for the reduction of time to first interaction, one involving piece-wise processing of each document in the data set, the second involving processing of full documents chosen at random from the data set. The theory was that the user could begin to interact with an approximate representation of the data set while SID continued to process subsequent increments in the background. When background processing was completed, the results would have converged to those of a single, one-step SID run. The basic technique we tried was to monitor word usage, and limit reprocessing to words with significantly changed usage, as measured by heuristics. Initial testing in late FY 1996 and early FY 1997 suggested that the technique produced acceptable context vectors, but it was uncertain whether the time saved was substantial enough to warrant avoiding full reprocessing. This uncertainty was due to having an insufficiently large test set, and not having a fully optimized version of SID.

In FY 1997, we sought to remove both areas of uncertainty. We acquired a substantially larger test data set. More importantly, we profiled and optimized the existing SID algorithms. We modified many of SID's I/O-intensive operations, relying more heavily on the use of in-memory operations, and increasing virtual memory usage to accommodate the large amounts of information. In doing so, we took advantage of empirical data gathered during the preceding year about system run-time requirements. We made optimizing assumptions based on these observations, allowing further improvements in the algorithms. As a result of these efforts, SID processing is now approximately an order of magnitude faster than before.

Once this optimization process was completed, it became clear that our intended approach to incremental processing would not sufficiently reduce the time to first interaction; full reprocessing would be a better option. Our plan was to use a B-tree data structure to manage the increasing vocabulary associated with incremental processing, but this proved to be too inefficient. The major problem was that the preparation time for each incremental pass through the set of documents can be greater than the time saved by processing a smaller amount of text. Reducing the size of the text increment processed each pass made each pass

complete sooner, but required more passes to converge to useful results. Therefore, we abandoned the notion that incremental processing could be useful in reducing the time to first-user interaction.

The second motivation, processing incrementally growing data sets, remains a strong one. During the last half of FY 1997, we began to investigate ways to reengineer SID such that documents could be added to the data set and the context vectors recomputed by reusing and expanding, rather than completely recalculating, many of SID's intermediate bookkeeping tables.

Alternative Text Analysis

In FY 1996, this project began to investigate alternatives to the current SID methodology. In FY 1997, this task sought to continue that investigation. The project explored the modification of SID algorithms and alternative vector generation algorithms. To better understand the results, we also added new evaluation techniques to our testing.

This latter item is related to an important observation of our research, the difficulty of comparison of results. In evaluating alternatives to the existing methodology, it is necessary to compare results from the two methods for the same data sets. Our current comparison techniques rely heavily on subjective judgments, such as comparing similar visualizations produced using different vector generation techniques. Objective measures would seem to be preferable, but in our view, effective methods for objectively measuring subtle differences between approaches do not yet exist. Precision and recall measures, the de facto standard of the information retrieval community, cannot effectively differentiate between small differences in performance.

Because of our lack of confidence in precision and recall, we naively set out to create objective measures for model accuracy, but soon found this to be an extremely difficult problem that could not and should not be addressed in the scope of this project. Therefore, until better objective measures are established, many of our research results are necessarily based on subjective comparisons.

During FY 1997, the project investigated several alternative association measures for use in SID. These measures are used to calculate strength of relationship between important words identified by the SID algorithms. Several modifications studied are apparently viable alternatives to the current measure and need to be studied further once more objective evaluation techniques are developed.

Once SID was optimized, larger test sets could be processed, giving an indication of performance over a larger sample of corpus sizes. Unfortunately, our visualization techniques were too computationally intensive to use if there were more than about 3000 documents. We developed software to support the well-known k-means clustering technique and have successfully visualized larger data sets with it.

The project continued development and validation of an iterative vector generation method. This approach iterates simultaneously on both word and document context vectors. As an approximation, one can treat documents as being defined by the words they contain, and words as being defined by the documents that contain them. Using this approximation leads to a symmetrical relationship between words and documents that can be expressed as a large linear system of equations. Approximate iterative solutions of this system are then used as the basis for both word and document vectors.

Based on visualization of topical relationships, this method appears to be more effective than the current SID method at modeling those relationships. However, there is a stability issue with the linear system. Iteration can proceed too far, causing simpler relationships to be reinforced at the expense of losing more complex relationships.

The project developed software implementing an n-gram vector generation method. The method uses contiguous and overlapping blocks of n characters and uses the frequencies of blocks within a document to form a context vector. Initial results clustering tri-gram results show noticeable differences from clustering of the same data with SID. Additional investigation of this method is needed. One particularly promising aspect of the technique is that it can be used to generate a vector for a document based solely on the contents of that document, making the method a potentially good choice for incremental processing applications.

In order to gain further insight into the effectiveness of alternative methods, the project developed several new or modified techniques for transforming the n-dimensional vector model to a visualizable form. The project also developed an objective measure for assessing the amount of error introduced by these and other methods of transforming from n-space to 2-space.

Multiple Component Vectors

The project conducted preliminary work in splitting SID-generated context vectors into multiple components. The idea was that some documents cover a broad range of topics, and might better be represented by multiple vectors. We had hypothesized that separation of SID vectors into primary components might be sufficient to create such a multiple vector representation. We developed software to test this hypothesis.

Topic and document vectors are assumed to have already been generated by the SID text engine. Topic vectors are then projected using a PCA algorithm. Each document is initially positioned at the same two-dimensional

coordinates as its most significant topic. The position is then adjusted for each other topic in order of significance. If a move would exceed a preset tolerance, another position is introduced instead, with each position representing different components of the original document vector. In this way, a document can appear in more than one place if it contains diverse topics.

We ultimately concluded that SID vectors are not sufficiently discriminated to support division into parts. If SID is to be used for this purpose, a different approach will be needed, perhaps one based on first automatically identifying different thematic sections of documents, then applying SID techniques to the sections.

Predefined Information

The project developed techniques for using predefined information to influence the SID text analysis. For any given domain area, certain words and relationships between words will be known beforehand to be significant. By developing the capability to predefine some of this information for SID, we hoped to both simplify computation and improve accuracy of analysis. We developed proof-of-concept software for predefined topics, predefined vocabulary, and a predefined association matrix.

Normally, SID processing estimates the importance of terms, and uses only the most important terms for the purpose of generating context vectors for documents. The idea behind predefined topics is to be able to specify the "topicality level" for some or all terms, in order to significantly influence the focus of a SID analysis. Our software uses a file of term "pre-definitions" where listed terms are followed by any or all of the three possible topicality levels.

Another area for pre-definition is to allow the user to specify the entire vocabulary, and let SID perform the rest of its processing based on that vocabulary. Tests have been done by running SID with a predefined vocabulary, then running SID normally, and comparing SPIRE visualizations of the results. As expected, the visualizations are different, and terms in the original vocabulary do not show up if they were not included in the predefined vocabulary.

The final predefined item that has been implemented is a predefined association matrix. If a predefined matrix is supplied to SID, then SID computes context vectors based on it, instead of a SID-computed matrix. As with predefined vocabularies, merging a predefined matrix with a SID-computed matrix is left as a future research area.

Feature Extraction and Signature Tracking (FEAST)

Brent M. Pulsipher, Don S. Daly (Engineering and Analytic Sciences)

Study Control Number: PN97045/1186

Project Description

The development and deployment of high-speed, high-dimensional data generators, such as multivariate sensors and sensor arrays, are accelerating. The ability to collect and store the ever larger, more complex datasets and data streams is keeping pace. However, the ability to identify, extract and track key features in these datasets and data streams lags further and further behind. The data generating, collecting, and storing components are now far more sophisticated than the analysis component; the advanced capabilities of the former are not exploited due to the simplicity of the latter. The Feature Extraction and Signature Tracking (FEAST) project was posed to bridge this sophistication gap by developing a system keyed to the efficient and comprehensive analysis of multivariate spatio-temporal datasets and data streams.

The long-term goal of this effort is to improve significantly the development of defensible, costeffective, comprehensive solutions to stochastic feature extraction and signature tracking (FEAST) problems. The long-term objective of this project is to develop an analysis system keyed the efficient and comprehensive analysis of complex multivariate spatio-temporal data problems. The FEAST system would provide a flexible, supportive environment featuring interconnected custom and commercial multivariate analysis and visualization tools for feature extraction and signature tracking. This year's efforts were focused on three objectives (which were achieved): defining the FEAST paradigm (the foundation of a successful FEAST system) bringing that paradigm to life in a prototype FEAST system, and refining the FEAST roadmap leading from paradigm to functioning system.

Technical Accomplishments

During 1997, we defined a FEAST paradigm describing an analysis system to identify and extract features from, and to track signatures embedded in, large-volume, high-dimensional, spatiotemporal datasets and data streams. We embodied this paradigm in a fast FEAST prototype.

Four elements capture the essence of the FEAST paradigm:

1. a collaborative analysis environment featuring a flexible, supportive technical study manager
2. the integration of multivariate data conversion, analysis, and visualization tools
3. custom tools to fill critical conversion, analysis, and visualization niches left uncovered by the available commercial tools
4. analysis support provided by an "expert's assistant."

Under our paradigm, the FEAST analysis environment incorporates a technical study manager that

- assists in directory, file, and content management
- provides defensibility/traceability through cross-referencing, hyperlinking, journaling, and revision control
- facilitates "collaboratory" communications: study participants can access some or all on-line study materials at their leisure since an ongoing study is an evolving web document
- streamlines the production of analysis algorithms, journal articles, protocols, technical reports, and presentations
- eases study archival, retrieval, and review
- acts as an intermediary for diverse collections of commercial and custom data conversion, analysis, and visualization tools
- adapts to the analyst's style; does not coerce the analyst to adopt a new style.

The FEAST study manager may be realized in a web-based setting using a web-browser; web-based programming languages such as HTML, Java, and CGI; and systems-level programming languages such as Pearl.

A multitude of commercial multivariate software is available. Two significant shortcomings are common to these codes: they are not comprehensive, and they are not integrated with their competitor's products. The first can be cured by identifying the holes and then developing niche analysis codes; the second can be cured by providing product-to-product data conversion software, and by

smoothing inter-product usage via a high-level intermediary, ala the study manager.

Identifying and then tailoring sophisticated analyses and algorithms to complex datasets and data streams can be aided greatly by an expert's assistant. An expert's assistant is closely related to an expert system. The key difference is that an expert's assistant never takes over the analysis; it only assists. The human analyst retains complete control over the analysis. The simplest form of an expert's assistant provides reference materials. A more advanced expert's assistant provides on-line help. The most advanced expert's assistant actively suggests alternatives to the analyst and provides draft code segments. FEAST knowledge is embedded in our studies. Eventually, it will fall upon the expert's assistant to help us extract that knowledge from our studies.

The FEAST System Prototype

The FEAST system prototype is a partial realization of the FEAST paradigm. Though not a fully functioning FEAST system, the prototype does illustrate almost all aspects of the FEAST paradigm.

In the prototype, the technical substance of a study (i.e., text commentary, data, graphs, and tables, analysis journals and logs, and source code segments) is managed within a dynamic document-like "Abstract to Conclusions/ Recommendations" framework. The materials are thoroughly cross-referenced using hyperlinks; e.g., text commentary to graphs to source code segments. The study manager, through a web-based interface, provides the analyst free-wheeling access to generate, update, or remove study materials through editing, analysis, and visualization software chosen by the analyst.

In the FEAST system, a technical study is purposefully immersed in a web-based world. Hence, it is straightforward to navigate among study materials. Dynamic technical communications among study participants are easy to carry out. A technical study in a web-based format is easy to archive, retrieve, and review. To aid a new study, it is easy to search a collection of FEAST studies for relevant materials, and in particular, relevant methodologies.

Heterogeneous Information Systems Linkages

James C. Brown, Mark A. Whiting (Information Technologies)

Study Control Number: PN95038/1014

Project Description

Development for this final year of this project consisted of efforts toward completing implementation and integration of the independent metadata search, analysis, retrieval, and maintenance processes of the metadata repository. Several processes and software agents had been designed and partially developed for handling the metadata related to heterogeneous information sources. The tasks for FY 1997 were targeted at completing a representative set of the agent process to prove viability and to integrate the metadata repository and associated processes with other research efforts. To accomplish this, we set up the following five tasks to be completed.

- Metadata Repository Agent Processes - Design and implement agent processes for identifying and managing physical and semantic linkages.
- Agent Processes for Metadata Mining and Maintenance - Implement agent processes to perform user-directed mining of information sources for data of interest.
- Enhanced Iterative Query Tool - Construct a query mechanism to enable expansion /generalization of queries.
- Baseline Testing - Evaluate effectiveness of iterative query mechanism against known data sets.
- Integration - Integrate ITI Tasks 1 and 2 for evaluation on at least two demonstration problems.

Technical Accomplishments

Physical and Semantic Linkages

Implementation and integration of physical and semantic linkages was accomplished by extending the object model for metadata. The metadata model was extended to allow for the entry of attribute/value pairs where the attribute represented the type of linkage between the objects (either physical or semantic) and the value was the keyword or property that forced the linkage.

Agent processes were developed to automatically identify and populate these linkages into the metadata repository for use later in the query and retrieval stages of information collection and analysis.

Metadata Mining Process

A process was developed for mining and maintaining metadata from multiple information source types. We split the process into two parts, one to collect physical metadata and one to collect semantic (content based) metadata. For physical metadata, we put in place mechanisms to collect information on the characteristics of the information object such as size, source, format, IP address, object type (image, document, video, etc.), database, and table for relational information. This information was instantiated in the metadata repository attached to the information object. This information is then made available for searching for information objects applicable to the users' interests. This proved to be highly effective. Potentially, this could be extended to do more advanced metadata generation. For instance, we could pull the IP address apart and access other systems that could tell us what country the address is assigned to. This would enable you to make a query against the metadata repository by asking for all messages from a specific country in the world.

The semantic metadata is based on the textual content contained in the title, description, and/or body of the information object. For this effort, we concatenated the title (for non-database objects) and the first 2000 bytes of content. While this did not give us a completely representative sampling of the overall content, it did give us enough variability to test the viability of searching, analyzing, and visualizing metadata as a means of rapidly scanning information.

The results we received were mixed. On one hand, we were able to collect, manage, and query on the metadata. This gave us the ability to quickly scan through information objects without the need to read the entire object first.

On the other hand, though, our results indicate the need to have a text summarization capability to more effectively produce a true summary of large textual information objects rather than simply capturing the first x-number of bytes. This was especially noticeable when dealing with web-based information objects. There was not enough variability in the captured semantic metadata to provide a sufficient analysis. The results from using database records

was more satisfactory since the records were normally captured in whole since their total field length was normally less than 2000 bytes.

Iterative Query Processing

To develop a paradigm for iterative processing and refining of an information query, we first looked at the processes one uses to manually search for information on the Internet and from structured databases. This led to the identification of several principal characteristics of query refinement; regardless of whether the purpose of the refinement was for expansion or reduction in the query results.

The primary steps we identified included

- Select an information source type to query, such as web pages, news groups, relational database.
- In the case of a relational database, the user typically must select a beginning database table.
- Select one or more key words to return an initial set of results.
- Based on a manual review of the results, make possible modifications to the sources being searched.
- Modify the search terms used by selecting one or more to either add to or restrict from the result set.

These basic steps were consistent during searches for various types of information. Through the use of the metadata repository, we extend the search capability by enabling a user to select specific domains, IP address ranges, etc., to further modify the query parameters. This was possible by allowing the user to specify search criteria on the metadata as well as the content of the data objects. We also enable users to search across all the tables in a relational database at one time. This enables the user to make broader searches across large data sets. This can be done without the need for prior knowledge of the physical designs of structured data systems.

Another method of extending the query modification capabilities that we investigated was through the use of visualization tools. To do this, we made an initial, broad search for information, imported the metadata into the metadata repository, and then exported the metadata set in a format that could be imported into both the SPIRE and Starlight visualization tools.

Query Effectiveness

The fourth task was to evaluate the effectiveness of the query and retrieval mechanisms to return appropriate information.

To accomplish this, we needed to have 1) a known information set to be used as a baseline, and 2) the query paradigms developed under this effort. Together, these were to be measured against known and confirmed results. We were not able to complete this task.

Integration

The last task planned for this effort involved the integration of the two tasks: heterogeneous information access and document understanding. The purpose was to show the overall complimentary nature of the two efforts. It was our intention to demonstrate this integration, even if it was only a loose integration. It was this loose integration that was accomplished.

There were three primary sub-tasks involved in doing this:

- The query refinement process needed be connected to the document understanding algorithms. To do this, we manipulated the structure and information of the metadata repository content to enable it to be fed into both SPIRE and Starlight.
- The output from the document understanding task needed to be fed back into the metadata repository to supply another form of linkage among information objects. This element was not completed. Because the context vector created by SPIRE was specific to the set of data processed, we decided that it would not be helpful to store that "corpus specific" vector in the metadata repository since it is non-corpus specific.
- Investigate finding a common platform for the metadata repository and the visualization tools. The investigation resulted in a determination that it was more appropriate to host each tool on the platform best suited for that functionality. The loose connection accomplished via network connections was adequate for this effort.

Private Information Spaces

During the work performed (as described above), a concept that became obviously necessary was that of private information spaces. We extended the metadata repository to include the ability for the user to create and manage information spaces where they could maintain pointers back into the metadata repository for subject- or domain-specific information. This feature of the metadata repository enabled us to create, add to, delete from, and combine sub-sets of information for further export to other analysis tools.

To evaluate the capabilities implemented under this effort, we tested these capabilities through the end-to-end process of information analysis. The case established involved

1) collecting information from the open Internet and structured databases, 2) sub-setting that information using the tools of the metadata repository, 3) exporting a sub-set of metadata to visual analysis tools, 4) refining the information set using the metadata repository tools, and 5) re-visualizing the information for final analysis.

Through the visualization of the metadata, it was possible to rapidly categorize and create clusters from the information without the need for the user to review or read all entries. This capability impacted step 4 in the process above. In one of our test cases, in the visual representation of the metadata, we found one cluster that was significantly different from the majority of the objects. This cluster contained 64 objects (out of a total of 3500+) that contained no actual data even though the original search mechanism included them based on the content of the "title" of the object.

Using the capabilities of the visualization tool, we identified that each of these objects contained the phrase "NOT FOUND" as the actual content. These were clearly brought back by the search engine based on the titles only.

Once this phrase was identified, we went through the following process:

1. returned to the metadata repository
2. queried the private information space to identify the records containing the phrase "NOT FOUND"
3. removed them from the private information space
4. exported the new metadata space
5. re-visualized the metadata.

The elapsed time from when we initially recognized the cluster (that skewed the visualization) to the time we re-visualized the reduced metadata set was less than 2 minutes. To accomplish this through a totally manual process would have taken tens of minutes for a person to review the content of all the metadata objects to locate the offending entries. The ability to manage visualization metadata prior to visualization of the entire content of an information collection greatly reduced the processing time required to get a basic understanding of the total information set. The use of private information spaces, which act like a scratch pad for rapidly manipulating a set of information, added the information set generation capability that is too often missing in information analysis processes.

Application and Presentation of the Technology

The metadata repository architecture and interface were used as the basis for locating and retrieving information for the United States Air Force Modular Aircraft Support System Information server at Wright-Patterson Air Force Base. They have called their resulting system "Info Server."

Presentation

The test case described above was presented and demonstrated to a wide audience of intelligence community representatives at the Advanced Information Processing and Analysis (AIPA97) Symposium in March 1997.

Individual Document Analysis and Comparison

Elizabeth G. Hetzler, Vernon L. Crow, Shelly Harris,
Don Jones, Nancy Miller, Grant Nakamura (Information Sciences)

Study Control Number: PN97054/1195

Project Description

This project will explore textual information. A visual representation of a document could show document attributes, length, distribution of themes within the text, and relevance to a particular user context (such as search history). User could visually compare several documents simultaneously, quickly get a more in-depth understanding of their contents, and then narrow in on what to actually read.

This project will develop the ideas for document overview and comparison to the point where a proof of concept can be demonstrated to potential clients. This will include initial research into visualization and analysis options, selection of promising approach(es), and experiments to show viability of the approach. What we will discover is how well various approaches actually work n conveying useful information. If we are successful in demonstrating a method that allows users to better understand and compare individual documents, the impact will be significant.

Technical Accomplishments

The investigation focused on three main approaches:

1. The thematic content of documents can be represented in detail by subdividing a single document into a collection of pieces and constructing a Themescape showing the variety of detailed topics addressed by the document.

2. The content of the document can be represented as a curve showing the strength of thematic topics, allowing the user to display multiple document curves for comparison.

3. Document attribute information can be represented by showing documents as rich graphic elements.

Each approach will be discussed in turn, including details of the method, results achieved, and knowledge learned.

Single Document Themescape

In this approach, a document is first divided into subpieces to form a pseudo-corpus. This pseudo-corpus can then be visualized either as a standalone corpus or in the context of the original. Both methods were investigated. Figure 1 illustrates the results.

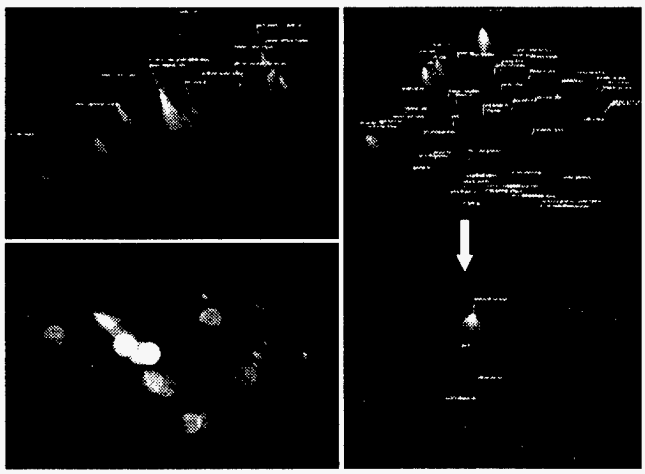

Figure 1. Single document Themescapes: upper left - document split into pseudo-corpus; lower left - circular "clouds" over document Themescape show prevalence and strength of descriptive theme; right-transition from full Themescape to encapsulated pieces.

For subdividing the documents, we used a method developed in a previous project, enhancing the implementation and tailoring its use. As expected, we found that the subpieces could be analyzed and visualized using the current SPIRE™ system, although we found that optimal parameter settings for this analysis were different from normal defaults.

Working with the visualizations, a key discovery became clear. Our current text analysis methods focus on finding themes that distinguish document subsets within the corpus. When visualizing an individual document, it is equally important to identify and visualize the themes that describe the document as a whole. By experimenting with parameter inputs, we were able to use the SPIRE analysis engine to generate a first pass at such descriptive terms, which we used to investigate visualization methods. The most promising of these builds on the Themescape metaphor by portraying a layer of translucent clouds representing the distribution of one or more prevalent themes.

As an alternate approach, we investigated analyzing document subpieces in the context of the larger document collection. The resulting visualization shows how the various sub-themes within the document relate to the rest of the collection; it can also reveal the thematic cohesiveness of the document. A particularly effective method for demonstrating this visualization was developed using a morph technique to show the correspondence between the collection and the document subpieces.

Theme Curve Visualization

A frequent question that arises with current visualization systems based on clustering, is "why are these documents together?" or alternatively, "why are these documents not together?" The theme curve visualization addresses this question by allowing the user to examine the relative theme strengths of a small group of selected documents. The presentation method is designed to focus on those themes that most strongly characterize the documents, to help the user determine which themes will cause the documents to cluster together or which theme differences will cause them not to cluster together.

A functional prototype was developed and proved quite effective; the visualization clearly distinguishes documents that have close relations across various themes from ones that do not (see Figure 2). A user can view the topics in a selected group of documents, determine which of the documents contain the topic words themselves, and even determine which other topics and themes are related to a selected topic. It helps users to better understand the nature of the relationships identified and the nature of the themes in the document corpus.

Representing Multiple Document Attributes

Displaying multiple document attributes can provide useful information to a user, both in selecting specific documents for closer examination and/or in understanding the document collection itself. This part of the project investigated using "glyphs" or graphic elements to convey useful document attributes. Examples of potential attribute mappings include:

- document length - glyph size
- document source - glyph color
- document age - glyph brightness.

Ideally, the level of complexity of the document glyph would vary with zoom scale. Like gradually adjusting the view through a lens, the representation can expand from several single document points, to simple glyphs providing a general group sense of few attributes, to more complex glyphs showing detailed document attribute information, to expanded glyphs portraying attributes of narrative segments of the document.

We selected a simple base glyph and experimented with various assignments for document attributes and methods for interacting with the graphic elements (see Figure 3). An interactive mock-up was created to demonstrate a number of options. For example, eight "petals" of a single document glyph can show the relative strengths of eight themes in the document with varying brightness. Additional attributes can be represented by the color and size of glyph elements and by refining or adding additional

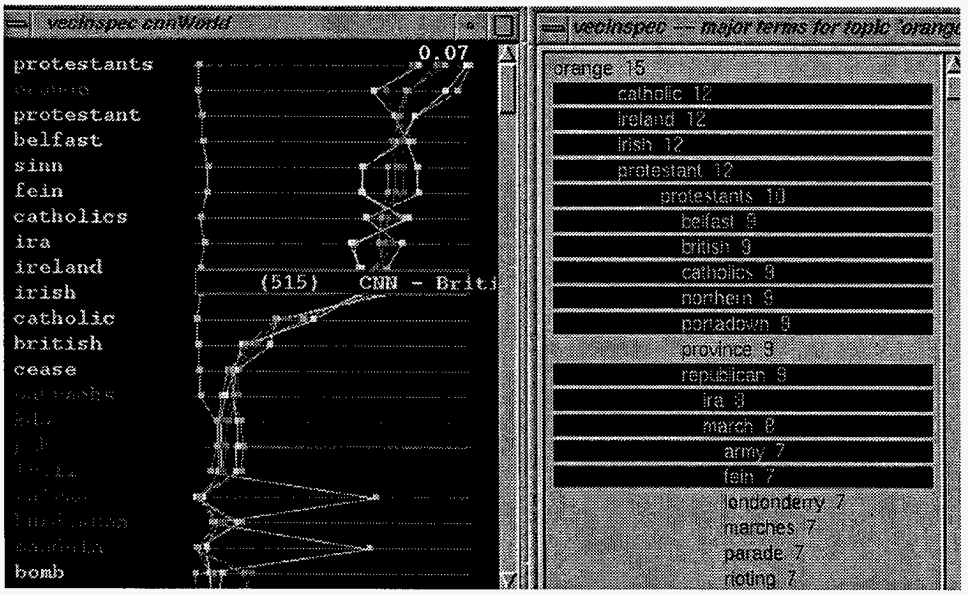

Figure 2. Theme curves (left) show thematic differences between group of related documents and single document from another cluster; right side window shows major terms related to the topic "orange" in this collection.

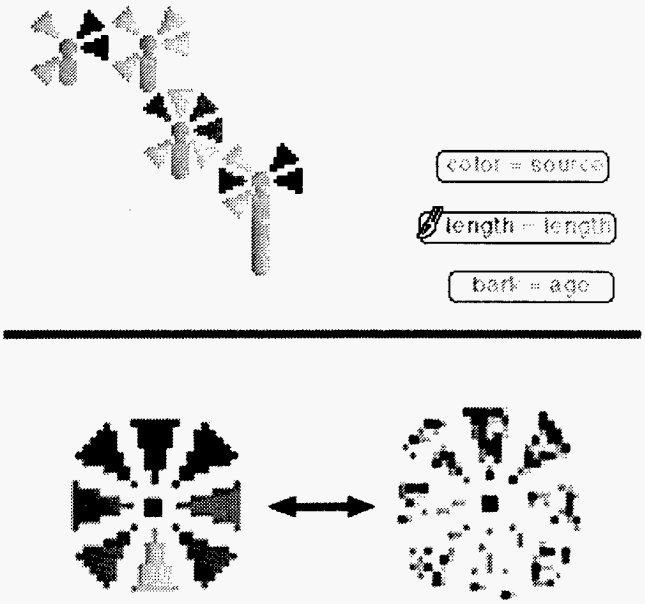

Figure 3. Glyphs: top - document attribute glyphs; bottom - strength of eight themes shown both averaged over whole document (darkness of the petal indicates strength of that theme) and within each document subpiece.

elements to the glyph. At a more detailed level, each theme petal can be separated into sequential segments, with each segment showing the relative strength of the theme in the corresponding document segment. Interaction methods incorporated in the demonstration include the ability to turn on or off various graphic elements and the ability to "paint" graphic elements on selected document glyphs.

This approach has the potential to add significant value to our visualizations. To refine the selection of graphic elements and user interactions, a functional prototype should be developed to allow users to experiment with the various options applied to multiple document groups.

Summary

The project focus was to explore and identify new capabilities which are lacking in our current text visualization methods. Three approaches were identified and investigated: Single Document Themescapes, Theme Curve Visualization, and Representing Multiple Document Attributes. These investigations added to our base understanding of text visualization, produced a functional prototype, and several interactive demonstrations, all of which have been and will continue to be demonstrated to current and potential clients.

Internet Platform Technology

Larry E. Skelly (Information Sciences)

Study Control Number: PN97061/1202

Project Description

The purpose of this LDRD investment is to build a useful, working decision support tool incorporating the best of our thinking surrounding human interaction (knowledge sharing) in an Internet-centric environment to bring widely disparate points of view into a common, interactive, integrated decision process. The process deals with asset analysis, resource allocation, and decision consequence evaluation to first determine the optimal investment path, then measure accomplishment of investment goals after managers make investment decisions.

The objective of this project is to produce an integrated decision support system composed of a "toolkit" which enables strategic and tactical level decision makers, with their respective staffs, to interact in a virtual decision work space to define the optimal investment portfolio for the organization. The decision support system will support predictive analysis based on existing data ("past"), modeling to examine possible scenarios ("future"), and consequence analysis to evaluate possible outcomes ("what if"). The system also will provide a feedback mechanism to compare actual results with predicted results after an investment decision has been made ("what we thought would happen" with "what really happened") to support post-decision course corrections.

Background

DOE lacks a formal research and development portfolio management process that examines the totality of DOE investments from a corporate-level ROI payoff perspective (the corporate "stockholders" are the U.S. taxpayers). Low payoff programs (low "ROI") continue to compete with higher payoff programs for scarce DOE resources. This occurs in some cases because DOE senior managers are not aware of the relative comparative merits of the competing programs. Judgments are made on a case-by-case basis rather than a portfolio basis. It also occurs in some cases where political rather than fiscal or public benefit factors determine program continuation.

For the last few years PNNL has assisted the DOE Assistant Secretary for EE/RE, Office of Planning and Analysis, in examining the EE/RE research and development portfolio. David Eike, BWO, developed a stand-alone, Windows™ based portfolio analysis tool to aid EE/RE in its annual research and development budget planning process. This tool has proven very useful in portfolio analysis from a budget development perspective but has played only a minor role in actual management of the portfolio. Expanding the tool to a network-wide environment and broadening its use to other research and development management offices in DOE could significantly enhance the Secretary's ability to evaluate the effectiveness of all DOE research and development investments. Such an analysis could prove extremely valuable in advocating DOE requirements in Congress.

Since 1993, PNNL has worked on developing an integrated, multi-user distributed data decision support system containing predictive models, geographical and relational databases, and planning/response tools for the U.S. Army's Chemical Stockpile Emergency Preparedness Program. The system supports planning, daily operations, response, and training of civilian and federal emergency management decision makers to enable them to employ their scarce resources (portfolio) in the most effective manner to protect lives and property (ROI). The system, called FEMIS (Federal Emergency Management Information System), consists of a suite of commercial off-the-shelf (COTS) products, government models, and communications applications working together under a PNNL-developed user interface. Our experience in integrating stand-alone COTS products, the disparate informational requirements of multiple agencies, and a variety of communications protocols under a common user interface to produce a multi-agency decision support system is highly applicable to building a portfolio analysis system. At its core, managing a portfolio involves allocation of resources to achieve a desired goal and then measuring the results of the resource allocation decisions to determine if the goals will indeed be met or exceeded.

Technical Accomplishments

The original 4-year development plan was built around 3 years of LDRD support, based on rapid prototype approach to develop working, useful modules, which then could be implemented with users to gain feedback and new ideas. The modules were to be integrated into the larger system as they were produced. Maximum use of COTS products was planned to avoid "reinventing the wheel" and to reduce development costs.

1. The project team developed prototype modules in the following areas.

- First generation Web-based "bubble viewer"
  - limited number of parameters
  - four-dimensional display (x,y,z, and color)
  - zoom/pan
  - connectivity with standard databases

- Data design
  - definition of relationships between significant elements
  - access control and roles definitions
  - interface (data input/view)
  - relationship map between different data elements, establishment of hierarchy of data.

- Asynchronous communication between participants
  - discussion areas
  - feedback loops
  - voting:
    simple majority
    weighted scoring

- Synchronous communication
  - teleconferencing (testing)
  - chat (several COTS products tested)
  - viewboard: a method of viewing/sharing public and private views of scenario alternatives

- Alternatives analysis
  - definition of scenarios and how they interact with decision process
  - influence of outside factors

- Feedback
  - performance results

2. Process Map. The team developed a map of the investment decision-making process within DOE after conducting interviews with selected senior policymakers.

With the revision in funding in FY 1998, the emphasis of the project is to produce a working version that can demonstrate the utility of an interactive, group-based decision analysis tool for an organization. The experience of the first year's effort demonstrated that using COTS tools whenever possible significantly reduces costs, but increases the potential for integration bottlenecks. The real-time aspect of the interaction modules did not yield as significant a value to the process as originally anticipated.

In FY 1998, we will deliver a web-based tool using commercial groupware products with a customized front-end for data analysis and group decision collection/ interaction. The emphasis will shift from a real-time tool to an iterative, contribute-when-you-can model that allows participants to contribute to the decision process whenever and wherever they are.

On-Line Collaborative Instruments

John M. Price (Computing and Information Sciences)

Study Control Number: PN96055/1122

Project Description

The focus of this work is to build a set of working prototypes for the next generation of PNNL's collaborative research instruments. To do this, we are constructing a group of on-line, network-based applications to support data sharing, remote instrument control/monitoring, and scientific data management across the Internet. This work exploits many of the new technologies that will be central to effective collaborative experimental research in the future and is helping us build capabilities to compete aggressively for new projects. In FY 1996 and FY 1997, we greatly extended the capabilities of a new EMSL radio frequency (RF) ion trapping experimental apparatus, making significant progress toward the goal of providing full, network access to the instrument, the data, and the researchers involved in the experiment. From this work, a highly visible system has been developed for use by EMSL scientists and their collaborators that demonstrates our unique capabilities in a new and growing area. In addition, the project has had successful "spin-offs" in several areas, including instrumentation development and science education.

Overview

Communication and data management software exploiting the Internet have made long-distance collaborative research projects easier and more productive. These technologies are in the process of revolutionizing scientific research across a wide range of fields and "scales" of experiment, from large to small. In response to these new developments, DOE-ER has recently begun to emphasize the importance of putting its "Facilities On-line" as a way to help stimulate better collaborative science and make the most effective use of unique DOE resources. Several new research programs have been implemented under this framework. (One example is the DOE 2000 initiative launched last year in Washington, D.C.) The *On-line Collaborative Research Instruments (EMSL On-line)* project was funded under LDRD to build capabilities to help us to compete effectively for programmatic funding in this area.

The objective of this work is to greatly extend the functionality of the instrumentation and software used in a pilot group of representative EMSL experiments and build capabilities we can use on future projects. The vision is to provide full "on-line" connectivity to these instruments and give researchers increased access to their data, instrument resources, and collaborators. Under this proposal, a radio frequency ion trapping experiment is being used as the first technology test bed and its capabilities are being extended in the following ways:

1. Existing instrument control, data acquisition, and analysis software are being modified and enhanced to provide wide-area-network (WAN) based monitoring and control of the instrument.

2. Data and meta-data about the experiments will be automatically saved to a network database system in a way that is fully integrated with the instrument control software.

3. Internet groupware and communication tools are being developed and integrated with the instrument software to give remote collaborators better access to their coworkers.

Technical Accomplishments

Since work started in January 1997, a virtual research facility has been created. As described below, the EMSL NMR spectrometers were made available across the Internet, collaborative software was deployed, new means of sharing and visualizing NMR data were created, and an NMR collaboration linking researchers at LBNL and PNNL was set up, the researchers trained to work using collaborative tools, and experiments begun. The researchers are continuing their experiments in FY 1998 and are continuing to use collaborative tools to communicate and to remotely run experiments on EMSL NMR spectrometers.

Work built on the work of the previous year, extending the capabilities of both the instrument and the suite of software supporting network use of the device. Several new applications were developed to support "real-time" interactions between researchers at the laboratory with outside collaborators. A Java client was developed to permit cross-platform use of the instrument from any computer connected to the Internet through a web browser. Experiments were performed to characterize the performance of a novel operating mode for the ion trap.

The work in FY 1997 can be broken down into three main areas: instrument development tasks, software development tasks, and applications of the technology.

Instrument Development Tasks

The radio frequency ion trap test bed was made operational in FY 1996. Since then, the instrument has been disassembled, moved to the new EMSL facility, reassembled, and tested. In FY 1997, the instrument control and monitoring functions were augmented, new electrode designs were tested, and work has been done to move the system from a prototype toward a more robust "production" system for performing routine analyses remotely.

Currently, computer control over a range of parameters is possible including: instrument timing, radio frequency trapping levels, mass ranges, and data collection modes. A computer-controlled sample handling system was also constructed in FY 1996-1997. This system includes a gas mixing manifold with pressure monitoring sensors, solenoid valves, mass flow controllers, and a solid sample laser ablation source making use of a pulsed Nd-YAG laser. In FY 1997 this system was interfaced to the laboratory computer.

During the interfacing task in FY 1996, new operating modes for the radio frequency ion trap were developed. In FY 1997, detailed studies were made of the method to evaluate its applicability to portable mass spectrometric applications. Results from these studies were presented at international conferences and a publication on the method has been prepared for the *Journal of the American Society of Mass Spectrometry*.

It should be noted that this part of the work was a synergistic outcome of the interfacing task. With so many of the instrument's parameters under computer control, it was easy to experiment with novel experimental conditions. This led to the observation that certain methods traditionally used for ion excitation or isolation could be used to obtain mass spectra as well. Our unique setup permitted us to perform these measurements at scan rates much higher than had been used previously. The method shows promise for portable applications as it relies on significantly lower radio frequency voltages than are traditionally used in ion trap mass spectrometry, reducing the needed size of the radio frequency power supplies considerably.

Software Development Tasks

In FY 1996 we developed a flexible software architecture for supporting distributed instrument control, monitoring, and remote data acquisition. A client-server model was used, allowing for a single client to connect up to one or more data acquisition servers to acquire data and set/read instrument parameters from each. A Windows95 client application was developed that could connect to a server running on the ion trap laboratory computer from anywhere across the Internet, request changes to the instrument parameters, acquire data, and display the information in nearly real time. The server was built to evaluate these requests and execute them if they fall within predefined parameters and put the machine into a safe "idle" state if network communications are lost unexpectedly.

In FY 1997, we extended the capabilities of the server to allow for more control and monitoring functions and explored the possibility of including new advanced network security features into the application. CORBA, (Common Object Request Broker Architecture) was evaluated in FY 1997, and some small test applications are being written under this secure framework to see how easy it might be to use this as the underlying architecture.

The client was also extended and a Java programming language version was written to supplement the earlier Windows95 client. Java has the advantage of being an inherently cross-platform language and a data acquisition client written in that language allows for a wider range of users; e.g., scientists using UNIX and Macintosh computer systems as well as Windows95 and WindowsNT. Work for FY 1998 will be in improving this client and adding joint analysis capability and database access through the client interface.

Network aware programs were also developed in Java for communicating with laboratory instruments. Devon St. Pierre, developed an architecture for communicating with GPIB (General Purpose Interface Bus) devices across the network and Ken Swanson implemented a server side GPIB interface. In FY 1998 a Java-based remote instrument server architecture will be developed using this work.

In FY 1996 we developed a data model for the object oriented database system to use to store and classify the instrument data and meta-data. This model is generic enough to cover a range of experiment types and can be extended (by virtue of the object oriented nature of the system) to cover new cases as they arise. In FY 1997 we began setting up the database to house the information coming off of the instrument and replace the file-based archive system we have implemented so far. This work will include building a database "loader" process to communicate with the client applications, a browser application (possibly written in Java) to allow users to search the database.

Several "real-time" tools were developed this year as well. An OLE-based tool for synchronizing web browsers with an interactive pointer was developed and used in a series of presentations given between PNNL and Heritage College's department of chemistry. (See below.) A multipoint audio

conferencing tool and a stand-alone camera pan-tilt system that remote users can manipulate in a videoconference were also added to the suite.

Applications of the Technology

In FY 1997 the EMSL On-line (EOL) system has seen applications in experimental research in mass spectrometry, education, and spin-offs of the architecture for other instruments at the laboratory.

Using the new frequency sweep method, the on-line instrument has been used to study the application of metal ions as selective chemical ionization reagents and to study the kinetics of dehalogenation reactions. These data will be part of a paper that will be submitted in the next year.

Collaborating with Professor Hossein Divanfard, Dr. Jeffrey Mack has used the EOL software to deliver remote lectures on mass spectrometry to chemistry classes at Heritage College (Toppenish, Washington). As part of this short course in mass spectrometry, he has provided access to the instrument so that students may operate it from the college.

Finally, the software architecture used on the project has been applied in two EMSL projects undertaken by the Instrument Development Laboratory (IDL). In the first, the server program was modified to provide an interface to a motion control system that was part of a femtosecond pulsed laser system in the laboratory of John Daschbach. In this case, the server provided access to the laser and the PC-based motion control hardware to a client program running on a UNIX computer. The client program was written by Daschbach and this architecture allowed him to take advantage of both the speed of the UNIX workstation for display and analysis and the motion control hardware made specifically for PCS from the same program.

Similar tools are being used on a program for Bruce Kay that controls a pair of high voltage power supplies used on an ion beam line. These devices provide computer controllable outputs to ~50 independent direct-current voltages from -6KV to +6KV. The power supplies are controlled by onboard computers with their own Internet protocol addresses and the control software written by the IDL that communicates with them is based on a similar architecture to the EOL client.

Publications and Presentations

J.M. Price, J.A. Mack, and M.V. Gorshkov. 1997. "Laser Desorption Ion Trap Mass Spectrometry With Frequency Sweep Detection." *In proceedings of the 45th ASMS Conference on Mass Spectrometry and Allied Topics.* Palm Springs, California, June 1-5.

D. St. Pierre. 1997. "Web Interface for Remote Control of Scientific Instruments." Class Project in Support of Masters Degree. Computer Science 155, Washington State University. (http://www.tricity.wsu.edu/~dstpierr/cs555proj.html)

J.A. Mack, M.V. Gorshkov, and J.M. Price. 1997. "Frequency Sweep Quadrupole Ion Trap Mass Spectrometry." 9th Sanibel Conference on Mass Spectrometry, Sanibel, Florida, January 25-28.

PNNL-LBNL Virtual Research Facility

James D. Myers, Raymond A. Bair (Computing and Information Sciences)
Paul D. Ellis (Macromolecular Structure Dynamics)

Study Control Number: PN97085/1226

Project Description

Discussions between PNNL and Lawrence Berkeley National Laboratory (LBNL) have identified a range of significant collaboration opportunities with compatible research program objectives and complementary research facilities and expertise. This project exploited advances in electronic communication and computational technologies that will enable scientists to work more closely together. It was coordinated with a complementary LDRD project at LBNL entitled, "Enhanced Scientific Collaboration Through Computer-Based Communication: The LBNL-PNNL Joint Collaboratory."

This project created a virtual research facility (with instruments, data, software, and expertise distributed among the sites) by providing Internet support for in-depth, interlab research in nuclear magnetic resonance spectroscopy and x-ray crystallography. Several ongoing and new collaborations between NMR scientists at PNNL and synthetic chemists at LBNL were focal points of the system. Our pilot project coupled PNNL's developing Collaboratory software (including the TeleViewer shared computer display, the World Wide Web (WWW) based electronic notebook, and LBNL's MBONE videoconferencing tools), with specific software built upon this infrastructure to allow an interlaboratory group of researchers to monitor NMR and crystallography experiments; "access data"; analyze and visualize results; discuss findings; and prepare proposals, presentations, and papers, all via the Internet and WWW. In FY 1997, PNNL led the effort to develop remote NMR capabilities. In FY 1998, LBNL will lead the effort to provide similar capabilities for crystallography experiments with the Advanced Light Source. The chemical characterization undertaken in this project requires information from complementary experiments done using these two techniques, and therefore relies on the combined capabilities and expertise to be made available in this virtual research facility.

Overview

Using LBNL videoconferencing, the EMSL TeleViewer shared computer display, World Wide Web (WWW) based electronic notebook, and software for secure remote access to the EMSL NMR spectrometers, Dr. Kelly Keating (PNNL) and Dr. Jeff Pelton (LBNL) conducted a series of experiments on a heat shock factor (HSF) protein. The HSF protein was prepared at LBNL and shipped to PNNL for analysis to take advantage of the enhanced resolution available on the EMSL 750 MHz spectrometer. Researchers have been experimenting with the electronic notebook and other tools for several months and started acquiring HSF data under remote control in September. They have desktop videoconference capabilities, can store and view three-dimensional protein structures through the electronic notebook, and collaborate directly on data acquisition and analysis tasks, viewing each other's computer screen in real time.

One major objective of this project was to enable inter-lab chemistry research between PNNL and LBNL (and other locations) through the use of recently developed collaboration tools. Despite the reduced scope, this has been achieved. A second major objective was to demonstrate how the core collaboration technologies that have been developed at PNNL and LBNL can be extended to DOE and other clients with project-specific additions to create virtual research facilities for distributed research teams. Many of the activities related to this objective that would have provided for automation of many data transfer, translation, and visualization steps; simplified and sped remote data access; and guaranteed Internet bandwidth during data acquisition were removed from the project. Nevertheless, the integration of secure instrument access with conferencing and application sharing tools, and the support for viewing three-dimensional protein structures that was integrated into the notebook, do provide some demonstration of the additional work needed to bring project-specific scientific resources into a collaborative environment, and the benefits this work provides to the distributed team.

Technical Accomplishments

In FY 1997, a virtual research facility was created. The EMSL NMR spectrometers were made available across the Internet, collaborative software was deployed, new means of sharing and visualizing NMR data were created, and an NMR collaboration linking researchers at LBNL and PNNL was set up, the researchers trained to work using collaborative tools, and experiments begun. The researchers are continuing their experiments in FY 1998,

and are continuing to use collaborative tools to communicate and to remotely run experiments on EMSL NMR spectrometers.

Tasks on this project were divided into five areas:

1. Research Scientist and Evaluation

- Dr. Kelly Keating, an NMR researcher tasked to work with Jeff Pelton at LBNL performed NMR experiments collaboratively. Dr. Keating helped to develop requirements and validate approaches, testing and improving software, and discovering new ways of doing research using the collaborative tools. She is now successfully using collaborative tools to perform experiments with Jeff Pelton.

- *Organizational/Sociological/HCI Analysis.* The interactions of the NMR researchers, and their interactions with the tools, have been monitored and analyzed to provide feedback to the development team. This information has contributed to the redesign of our notebook interface, identification of protein viewers for the notebook, etc.

2. Remote Data Acquisition, Monitoring, and Control of the NMR Spectrometers at PNNL

- *Secure Remote Access.* Work was completed to integrate the "secure shell (ssh)" application with the EMSL's distributed computing environment (DCE) security infrastructure (in collaboration with Tom Harper of the Computing and Network Services group). This allows secure remote login to the NMR spectrometer console and encrypted transmission of the console display back to the remote user.

- *Secure Collaborative Access.* Providing a secure shared view of the console to multiple sites to allow consultation and training was demonstrated by integrating "ssh" with the EMSL TeleViewer.

3. Remote Laboratory Notebook with Custom NMR Data Viewers

- *Identification of Data Types.* Work was completed to document all data/metadata generated during an NMR experiment that would be useful to share with colleagues, to identify the format of this information, and to prioritize integration of these data types with the notebook software.

- *Integration of Three-Dimensional Protein Structures in Brookhaven Protein Data Bank Format.* Top priority was given to developing the capability to view three-dimensional molecular structures within the notebook. Two iterations of this work were completed during the year. The first provided a simple, rotatable view of the protein. The second, integrating the publicly available WebMol viewer, provides multiple types of color, depth cued views, and allows simple querying of inter-atomic distances and angles.

4. Real-Time Videoconferencing and Shared Work Environment.

- *Hardware Deployment.* A desktop workstation with camera, graphics tablet, was acquired for Dr. Keating. LBNL provided a workstation to Jeff Pelton (the LBNL NMR researcher).

- *Software Deployment.* Deployment and support of tools (including user training) at PNNL and LBNL. This work included deploying EMSL's integrated collaboration environment with videoconferencing, TeleViewer application sharing software, chat, etc., the electronic notebook client, and security software, as well as installing a password-protected "NMR" notebook server at PNNL for project use. Training was provided via phone and the Internet, as well as during visits to LBNL.

Publications and Presentations

A. Schur, K.A. Keating, D.A. Payne, T. Valdez, K. Yates, J.D. Myers. "The Impact of Collaborative Tools on Experiment Oriented Scientific Research." ACM Interactions, special topic issue on Collaboratories (submitted).

This project has been a part of over 50 demonstrations to visitors to PNNL, including staff from industry, academia, the national lab system, the U.S. Army, and the program offices of DOE and other government agencies.

February 12-18, 1997, AAAS AMSIE '97, Seattle, Washington.

June 12, 1997, 1997 International Technology Summit: Science Based Companies for the 21st Century: The Convergence of Information Technology and Biotechnology, Seattle, Washington.

July 24, 1997, "Scientific Collaboratories: Remote Research and Education Via the Internet," AWU Distinguished Lecture, multiple invited presentations to AWU schools, spring and fall 1997, presentation to the Collaborative Electronic Notebook Systems Association (CENSA), Chicago, Illinois.

August 28, 1997, Secretary of Energy Federico Peña, PNNL, Richland, Washington.

October 16-18, 1997, EMSL Symposium and Open House, PNNL, Richland, Washington.

November 15-20, 1997, Supercomputing '97, San Jose, California.

Design and Manufacturing Engineering

A Multicontinuum Approach to Composite Material Characterization and Predictive Analysis for Composite Structures

Mark R. Garnich (Engineering and Analytic Sciences)

Study Control Number: PN97002/1143

Project Description

The primary objective of this project was to establish and demonstrate the analysis tools that will form the core of a multicontinuum analysis capability for structural composites at PNNL. This new approach was based on multiple continuum fields (multicontinuum). The ability to design complex composite structures and accurately predict their performance and reliability does not exist. This project helped to address these issues. Inherent to the approach was the analytical prediction of composite material properties using micromechanics. Such analyses reduced the need for costly experiments (empiricism) and institutionalized a valuable capability through the development of a library of micromechanics models.

Technical Accomplishments

Efforts in FY 1997 focused on implementing multi-continuum analysis capabilities for linear thermal-elastic composites in a commercial finite element code and beginning implementation of capabilities for linear viscoelastic composites. The MARC general purpose finite element code was identified as the best candidate for multicontinuum application. This choice was based on experience with and existence of the code on PNNL engineering workstations (ongoing lease), and the fact that the MARC code permits interfacing with the internal numerical solution process through a system of FORTRAN user subroutines. Also, the graphical pre- and post-processor (MENTAT) permits the storage of additional solution variables so that multicontinuum variables are accessed and manipulated in the same manner as conventional structural solution results. The linear thermal-elastic multicontinuum equations were successfully implemented and an example structural analysis was performed and verified by comparison with previous results published in the dissertation of Dr. Mark Garnich.

Preliminary to implementing viscoelastic capabilities, a previously developed finite element micromechanics model was resurrected to generate the necessary material data for multicontinuum application and demonstration using a representative viscoelastic composite material. Previous data had been in the form of creep compliances, however, the MARC code requires the equivalent set of relaxation moduli. Also, a deficiency in the MARC code was identified that will result in additional work to accommodate the more general viscoelastic constitutive law required by the multicontinuum formulation. A strategy for implementing the viscoelastic equations was developed but significant progress on the required user subroutines was not achieved.

BW System Integration: Mesofluidics Motherboard

Charles J. Call, Joseph G. Birmingham (Process Technology)

Study Control Number: PN97021/1162

Project Description

Dramatic gains in detector system performance can be expected through the seamless integration of miniature and microfluidics sample handling components with microscale chemical and biosensors through a novel motherboard technology: the Mesofluidics System Integration Motherboard. This project developed and demonstrated this motherboard technology, including the unique microfabrication technology required. It should find application for hand-held or field-portable systems for the detection and identification of hazardous chemical and biological organisms. The purpose of this technology is to facilitate the tight integration of a number of electronic, fluid handling, and sensor components of these systems.

Technical Accomplishments

Current detector systems for biological materials are large (not portable by an individual) and have slow response times (approximately 15 minutes for air sample collection to data output). They require highly specialized personnel to operate the equipment. Sensor technology is rapidly advancing, but the balance of the system has not evolved significantly. The mesofluidics system integration motherboard for agent and hazardous materials detection and identification will have the following features:

1. Creates a new motherboard technology for mixed microelectronics and microfluidics systems. The mesoscale platform is tightly integrated and solid-state (e.g., all liquid flows are in microchannels) eliminating the need for tubing for fluid distribution and connectivity.

2. System optimized by incorporation of best and smallest available technology for each sub-system function.

3. Accepts third-party components and sensors through definition of standards for power, form, and function, thereby anticipating the need to integrate emerging and not-yet-conceived technology.

4. Allows field upgrades and repairs of hardware and software by incorporating the "plug and play" concepts now standard.

5. Mass-producible via micromanufacturing, allowing low initial cost per system.

The need for an effective aerosol collection system for biological material detectors addresses a vital national concern to protect against biological warfare agents in battlefield and other military and civil defense applications, such as airborne pathogenic agents released by terrorist groups; and infectious organisms contaminating air in hospitals, research laboratories, public buildings, and confined spaces, such as subway systems.

The following accomplishments have been achieved to date:

1. An initial demonstration of seals produced with PDMS (polydimethylsiloxone) polymer using a lithographic technique was performed.

2. An initial demonstration of laminate seal fabrication using a laser micromachining tool was completed.

3. Several generations of microfabricated capillary electrophoresis units have been fabricated. Electro-osmotic pumping has been demonstrated. A second-generation unit is currently being tested for the separation of DNA.

4. A prototype of a complete motherboard was fabricated. Several technical challenges were addressed, including

   - development of a custom in-house circuit to drive the micropumps
   - attempt to seal laminates over a 16 sq. in. area
   - integration of microfluidics and microelectronics
   - embedding of micropumps/valves in a motherboard.

Freeform Fabrication of Structural Metal Components

Suresh Baskaran, Gary Maupin, Gordon L. Graff (Environmental and Health Sciences)

Study Control Number: PN97046/1187

Project Description

Solid freeform fabrication is the machine capability to convert "virtual objects," such as in a CAD file, to solid objects without part-specific tooling. In solid freeform fabrication, a CAD model is electronically sectioned into layers, and the data transmitted to a solid freeform fabrication machine which then builds the component using a sequential, layered, or lithographic approach. Solid freeform fabrication technology is currently used for rapid prototyping for short-run production, for mold/die making, and has the potential to significantly impact manufacturing.

Solid freeform fabrication methods using polymeric build materials have attained sufficient technological maturity. The critical technological need now is direct fabrication of functional (structural) ceramic or metal components and tooling. In FY 1995, PNNL began research on the use of chemical drop-gelation on slurry layers to fabricate ceramic components without molds or dies. In this fabrication approach, ceramic powder slurries containing poly-saccharide alginate binders are applied as thin layers on a build table. Selected areas of a slurry layer are gelled by impact of droplets of a salt solution. Samples are fabricated by repeatedly applying and gelling layers of the slurry. The gelled part is finally removed from the slurry, washed to remove impurity ions, dried, and sintered. High density engineering components in alumina have been demonstrated with this process.

For metals, the current methods of freeform fabrication use coarse powder, molten droplets, or cut-metal sheets as the build materials. The key requirements in fabricated parts are dimensional accuracy, surface finish, cost, and functional properties. In this project, PNNL's layered slurry gelation approach was investigated for fabrication of metal components from metal powder slurries.

Technical Accomplishments

Initial experiments focused on developing iron powder slurries containing alginates, that could be dispensed and leveled to form thin layers on a build table. The smallest ($\approx$1 to 6 μm size) commercially available spherical iron powder was used in this study. A semi-automated machine was assembled at PNNL and used for these layered fabrication experiments.

The gelling agent was dispensed from a commercial HP Deskjet 600C printer mounted on a gantry positioned over the build chamber in this machine. After gelation, the build table was lowered, additional slurry added, and another layer leveled with the doctor blade. Machine parameters including print pattern, layer thickness, and gelling agent concentration was optimized for the metal slurry experiments. Gelled rectangular bars were fabricated by layered gelation. Samples were dried slowly (over 2 days) to prevent warping or cracking during drying.

Iron bar samples fabricated by layered gelation were sintered in H_2 at 1300°C for 1 hour. SEM micrographs show fracture surfaces of unfired and fired bar samples. The green microstructure showing the highly spherical carbonyl-derived powders was uniform over the thickness of the sample, with no evidence of impurities, interlayer porosity, or segregation of particles in the slurry during fabrication. The fired density was 6.98 g/cc (bulk density), with 5% open porosity. These initial results compare well with the reported sintered density of injection molded samples prepared from similar powders, which are in the range 7.04 to 7.70 g/cc.

Simple rectangular bars of high quality were fabricated, with the wet strength and edge definition being comparable to the alumina body, but more complex gear wheels either contained cracks or were characterized by rounded edges. Since the iron powders are larger and heavier compared to most oxide ceramic powders, the rheological behavior of the slurry caused difficulties in removing gelled gear wheels from the unreacted metal slurries and retaining sharp features consistently. The impurities in gelled iron bodies also could not be washed extensively due to oxidation of iron. This study demonstrates that iron components can be fabricated by a layered slurry gelation approach, but future work should concentrate on more oxidation-resistant (e.g., stainless steel) metal powders.

Power Line Robot Conceptual Design

Bernie F. Saffell (Engineering and Analytic Sciences)

Study Control Number: PN97087/1228

Project Description

The objectives of the project are to develop a feasible, conceptual design for an untethered power line robot that can serve as a platform for live-line inspection, mapping, and maintenance. This will be accomplished through two tasks:

1. Power Line Mobile Robot. A conceptual design for an untethered power line robot was developed for inspection of power transmission lines. The robot reduces operation and maintenance costs by providing a low-cost method for completely inspecting transmission lines between substations. The robot clamps onto the transmission line and navigates various obstacles. Transmission lines will be inspected with infrared and visible light video cameras.

2. QuickTime VR Cyberhiking. QuickTime VR cyberhiking will provide additional 360-degree video nodes used for navigation, determining a clear right-of-way, and detailed information at user-defined segments of the power line. The robot is powered directly by the transmission line and communicates with maintenance personnel via radio frequency transmissions.

Background

Power system operation and maintenance represents a significant component of the total cost of the electric delivery system. This cost in a regulated environment was simply passed on to the customer with little incentive to develop and deploy innovative concepts for improving the cost effectiveness of the operation and maintenance process. Operation and maintenance costs in a deregulated environment are emerging as a significant competitive element in the energy delivery industry and as such are receiving increasing attention. Utilities are cutting costs in this area by reducing operation and maintenance activity. While utility costs and profitability are clearly not within the DOE mission, the reliability and dependability of the country's energy delivery infrastructure represents a clear mission element. Evidence is DOE's current intense examination in response to a White House request of the energy infrastructure vulnerability.

This industrial segment, today and for the foreseeable future, represents a significant opportunity for the innovative application of technology as a means of ensuring the dependability and reliability of the energy delivery infrastructure.

Application of robots for the purpose of power line inspection and maintenance has only recently been aggressively pursued with the focus being on tele-operated systems which enable work to be performed on live lines by a maintenance person. Power line inspection and maintenance focused on connectors and insulators represents a clear and impactful need that could be met by a small robotics vehicle. Alaska's Railway Utility Group is very interested in a robotics device for keeping power lines clear of snow and ice. Desirable features of such a power line robot include autonomous operation, a geographical positioning system, the ability to inspect and clean connectors and insulators, and the ability to traverse power line towers. To our knowledge, concepts have focused on tethered vehicles with only one autonomous concept supported by the Tennessee Valley Authority currently being pursued.

Technical Accomplishments

The following accomplishments were achieved in FY 1997:

- *Conceptual Design of the Transmission Power Line Robot.* PNNL researchers have developed a conceptual design for an innovative, untethered, transmission power line robot. The robot has the capability to autonomously traverse miles of transmission power lines and negotiate the associated in-line obstacles. Inspection information gathered by the robot will reduce the operation and maintenance costs associated with the transmission power lines while increasing the reliability and dependability of the country's energy delivery infrastructure. The conceptual design is of sufficient detail to develop a prototype.

- *QuickTime VR Cyberhiking.* A mobile-based QuickTime VR capable image capture and process system has been assembled to demonstrate the cost-effectiveness of gathering images from a wirelessly tethered camera system and on-site node processing label where each panoramic node is converted immediately and placed into the final virtual tour in real time.

Ecological Science

Ecological Modeling of Regional Responses to Global Change

Edward J. Rykiel Jr. (Environmental Technologies)

Study Control Number: PN95209/1005

Project Description

Humans are changing the chemical composition of the atmosphere, the land cover of the continents, and the biological composition of the ecosphere without understanding the consequences of these changes. The major task of global change research is to provide a level of scientific knowledge that enables us to understand how human activities affect the ecological mechanisms that support sustainability. The goals of this project are 1) to explore new theoretical approaches to global change problems, 2) to develop an integrated framework for simulating regional ecological responses to climate change, and 3) to provide scientific support to the policy community concerning global change issues by developing a strong knowledge of the interaction between earth and life sciences. The FY 1997 goal was to estimate the net primary productivity (total carbon fixed by plants annually) of the Pacific Northwest region (Washington, Oregon, Idaho). Funding for this project will extend PNNL's ecological modeling capability through the development of state-of-the-art ecosystem models.

Technical Accomplishments

Work in FY 1997 focused on developing a modeling strategy for estimating the total annual net primary productivity (NPP) of the Pacific Northwest region (PNW) defined as Washington, Oregon, and Idaho. Net primary productivity is a fundamental ecological quantity because it is the energy base for ecosystem processes. Changes in NPP that may result from land use and climate change are therefore of considerable socioeconomic and ecological interest. Estimates of NPP for the PNW region were developed in three ways: 1) down-scaling simulations using the CASA global vegetation model (Potter et al. 1993); 2) summarizing NPP values from the Vemap project (Vemap 1995); and 3) generating a biogeographic estimate based on literature values for NPP obtained by field sampling. We compared the results to assess whether available data is sufficient to choose a best estimate from these alternatives.

CASA

We used the CASA NPP model (Potter et al. 1993), which is a global vegetation model designed for a 1° x 1° spatial scale, to run simulations for the PNW. We ran simulations at spatial scales of 1° x 1°, and then downscaled the model to 0.5° x 0.5°, and 0.1° x 0.1° (about 120 km^2) to determine the effect of increasing the resolution of climatic data. One set of simulations used the original 1° x 1° climate data for temperature, precipitation, and solar radiation. As expected, merely increasing the spatial resolution did not change the total regional NPP. For the next set of simulations, we generated temperature and precipitation data sets for the PNW at all three spatial scales using data from weather stations in the region. The problem of mapping the scattered meteorological observations in the region to produce values on regular uniform grids for ecosystem modeling has presented meteorologists with a significant challenge because topography and vegetation are prominent features in this region. We applied the Multi-Quadric Interpolation Method (MQIM) to map the scattered meteorological observations in the PNW region. Simulated NPP increased with better spatial resolution of climate. For the last set of CASA simulations, we used our weather data and Vemap 0.5° x 0.5° solar-radiation data. The effect of better spatial resolution is to increase the simulated NPP by 13% (Table 1). In all these simulations, the land cover types were as described in the original CASA model for the PNW region. Thus, we have not yet tested the effect of improving the spatial definition of the land cover. However, since the 1° x 1° scale masks substantial differences in PNW vegetation, we suspect that simulated NPP would again differ as spatial resolution improves.

Vemap

The Vemap project combines three biogeochemical models (Biome BGC, Century, TEM) with three global vegetation models (MAPPS, DOLY, Biome) to simulate NPP for the conterminus United States. These data have a spatial scale of 0.5° x 0.5°. We assembled the nine data sets of NPP values for the PNW, but report only the range of values here (Table 2).

Table 1. Effect of spatial down-scaling of temperature and recipitation on CASA model NPP estimates (Tg C) for the Paccific Northwest (WA, OR, ID).

1° x 1°	190
0.5° x 0.5°	207
0.1° x 0.1°	214

Table 2. Comparison of estimates of total amount net primary productivity of the Pacific Northwest Region under current climatic conditions in Tg C.

Biogeographic	CASA Model	Vemap Models
229	190 - 214	183 - 315

Biogeographic Estimation of NPP

We used a map of the potential natural vegetation of the PNW to obtain areas for general vegetation types, and then modified these areas based on more specific information. The major land cover types included: forest (11 types), woodland (1 type), shrubland (2 types), grassland (2 types), forest/shrub/grass complex (2 types), cropland (6 types), farmland (3 types), and developed land (including metropolitan vegetation). Aquatic ecosystems were not included, which is typical for global and regional NPP models. Cropland area was subtracted from shrubland, grassland, and complex types. Most of the agricultural data we used were for 1992. Once we assigned an area to the vegetation types, we multiplied the area by the NPP value that we developed from the ecological literature to generate an estimate of total regional NPP under the ambient climate (Table 2).

Comparisons

Before evaluating the estimates from the three approaches, some limitations include the following. The biogeographic estimates are generally based on investigations at small spatial scales, below-ground carbon is often not measured directly, plant community types are sometimes transitional and do not correspond to those used by global modelers, and more data are available for vegetation types that contain economically important plants such as merchantable tree species. The global and regional vegetation models have relatively few vegetation types. CASA uses 12 types, which have not been refined for the PNW, and do not include regional topographic effects. The data in Table 2 indicate that there is considerable overlap among all the estimates of total regional NPP. Thus, with the data currently available, it is not possible to determine which model is best. The biogeographic estimate suggests that some of the models underestimate NPP by masking heterogeneity in the vegetation and the environment that exists below the spatial scale of the models. To reduce the uncertainty of regional estimates below a factor of two, more detailed vegetation models are likely to be needed. Estimates of annual global terrestrial NPP are in the range of 48 to 62 Pg C. PNW NPP of 229 Tg C is 0.229 Pg, which is 0.4 to 0.5% of the global amount. The land area of the PNW is 0.42% of the global land area. The high productivity areas of the PNW are balanced by low productivity arid and semi-arid areas with the result that the regional contribution to global NPP is consistent with its land area on a percentage basis. This regional response to global climate change may, therefore, be of greater significance than is indicated by its relative size.

References

C.S. Potter, J.T. Randerson, C.B. Field, P.A. Matson, P.M. Vitousek, H.A. Mooney, and S.A. Klooster. 1993. "Terrestrial ecosystem production: A process model based on global satellite and surface data." *Global Biogeochemical Cycles* 7(4): 811-841.

"Vegetation/Ecosystem Modeling and Analysis Project (VEMAP): Comparing biogeography and biogeochemistry models in a continental-scale study of terrestrial ecosystem responses to climate change and CO2 doubling." 1995. *Global Biogeochemical Cycles* 9(4): 407-437.

Publications and Presentations

E.J. Rykiel, Jr., R.N. Kickert, and W.H. Reid. "Net primary productivity in the Pacific Northwest Region." (in preparation).

X. Bian, L.R. Leung, and E.J. Rykiel. 1997. "Application of multi-quadric interpolation method to meteorological mapping in the Pacific Northwest Region. The 1997 International Conference on Computational Physics, August 25-28, Santa Cruz, California (paper in preparation).

Integration of Acoustic Doppler Current Profiler Subsurface Sensing and Global Positioning Systems Technology

Ted M. Poston, David R. Geist, Andrew T. Cooper (Environmental Technologies)

Study Control Number: PN97057/1198

Project Description

The objective of this research was to measure groundwater upwelling (i.e., contaminant infiltration) into a large fast-flowing river with a cobble bed. Electrical conductivity was measured as a surrogate indicator of contaminants because contaminants are carried primarily via groundwater. Groundwater at Hanford contains comparatively high concentrations of dissolved minerals and typically has conductivity readings greater than the Columbia River. Other available probes are designed for mud-bottom rivers and are prone to seepage of river water around the electrodes due to the uneven cobble bottom of the Columbia River. A system was developed that incorporated a global positioning system with a pair of temperature-conductivity probes to measure, in real time, the differential conductivity at the sediment water interface and in river water approximately 6 cm above the surface.

This system minimizes surface water contact with the conductivity bridge electrodes and provides for a reference measurement against river background in real time. Laboratory testing of a prototype model indicated a sensitivity of about 5 microsiemens per centimeter (µS/cm). A second model was constructed of heavier materials and equipped with an underwater camera for field testing.

Technical Accomplishments

A prototype probe was developed and tested in a recirculating tank containing a cobble bed. A magnesium chloride solution was injected into the cobble substrate to simulate groundwater upwelling in a controlled setting. Nineteen trials were performed with flows of 1, 2, or 3 ft/s. These laboratory trials indicated that the prototype design was functional at flows as high as 3 ft/s. Additionally, the ability to measure upwelling relative to background river water indicated a minimum sensitivity of about 4 to 5 µS/cm.

Field testing confirmed that the system could locate and measure underwater seepage, and based on trials at known seeps, could detect differences as low as 4 to 5 microsiemens. Additional modifications to the sediment-sensing probe facilitated its use in silt-mud bottoms in river sloughs. Maps were created and data logged by time to monitor areas of upwelling in areas of the Columbia River that support salmon spawning. The system was envisioned to be coupled with an acoustic Doppler current profiler, however, the initial trials performed during the study used a portable electromagnetic flow sensor. This was ineffective due to electrical interference from the boat motor.

Field testing was performed twice at White Bluffs Slough, twice at 100-H area, and at the old Hanford Townsite, Wooded Island, and the 300 Area. Groundwater upwelling was detected at the White Bluffs Slough, 100-H area, Wooded Island, and the 300 Area. Because of stagnation and closed circulation, the conductivity of White Bluffs slough was elevated above river background and the prevalence of upwelling was significant. Figure 1 shows the results of a transect within White Bluffs slough. Two passes over the same area are shown. The initial detection occurred at about 9:51:50 where the bottom probe detected a conductivity difference of about 80 µS/cm. The boat returned to this area and passed over the edge of the upwelling where the difference was about 40 µS/cm. At 100-H, there is a known seep that was detected at about 4 to 5 µS/cm above river background. This represents the lower limit of sensitivity of the probe based on laboratory studies with the first prototype.

Presentations

R. Sternbeerg, T.M. Poston, A.T. Cooper, and D.R. Geist. 1997. A Bottom Contacting Sediment Probe for Detecting Ground-water Upwelling in a Large Cobble-bed River. Student Poster Presentation, Presented at Sixth Annual Meeting of the Pacific Northwest Chapter, Society of Environmental Contamination and Toxicology, Richland, Washington, May 8-10.

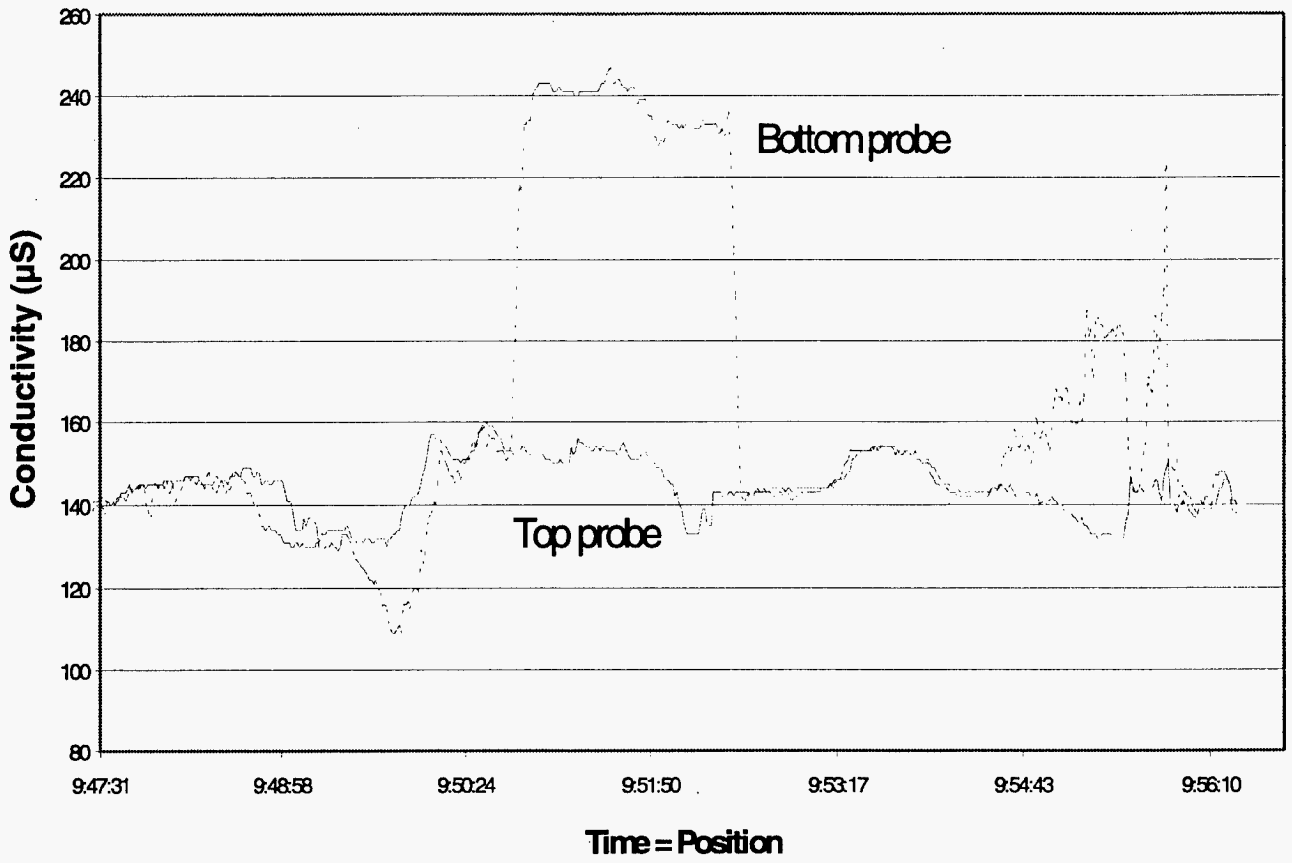

Figure 1. Conductivity measurements taken at White Bluffs Slough on 9/15/97.

Integration of Unmanaged Ecosystems into the Global Change Assessment Model

R. César Izaurralde, Norman J. Rosenberg (Global Change)

Study Control Number: PN97059/1200

Project Description

The objective of this project is to model the response of unmanaged ecosystems to climatic change within PNNL's Global Change Assessment Model (GCAM). GCAM consists of four interacting modules that compute

1. how economic activity influences greenhouse gas emissions
2. how these emissions lead to changes in atmospheric composition and alter global mean temperature
3. how changes in global mean temperature affect the geographic distribution of climate change predicted by several general circulation models
4. how altered climates affect agricultural productivity, water resources, and unmanaged ecosystems.

Adding the capability to model unmanaged ecosystems to GCAM is an essential step toward answering questions regarding vegetation dynamics, carbon balance, and biodiversity in response to climate change.

Technical Accomplishments

Work on this project began in August 1997. We have initiated the evaluation of BIOME3, a biophysical and biogeochemical model by Haxeltine and Prentice that simulates large-scale vegetation patterns. Photosynthesis in BIOME3 is a function of environmental and leaf parameters. The maximum rate of photosynthesis achievable under light-saturated conditions is regulated by the catalytic capacity of the Rubisco (ribulose biphosphate carboxylase oxygenase) enzyme and leaf N content.

BIOME3 uses a minimal set of five woody and two grass plant types for large-scale (global) modeling. Variables calculated include leaf area index and net primary productivity. Semiempirical rules capture the opposing effect of succession driven by light competition and natural disturbance by fire. Dominant plant types arise from highest net primary productivity values. Environmental factors (e.g., CO_2) influence photosynthesis, stomatal conductance, and leaf area.

Test runs have been conducted in our laboratory on a UNIX workstation. Model initialization included data on latitude, CO_2 concentration, monthly climatic values (temperature, precipitation, and sunshine hours), and soil texture on a 0.5° grid. The model predicts global natural vegetation patterns (Figure 1) by using a rule-based algorithm to determine plant functional type and by determining the leaf area index that maximizes net primary productivity (Figure 2). In its current form, BIOME3 simulates vegetation patterns at steady state; i.e., it does not predict the time course of vegetational composition and structural adaptation to change.

In FY 1998, we will compare model outputs of functional plant types, net primary productivity, and leaf area index for the conterminous U.S. against measured or remotely sensed data. We will simulate changes in net primary productivity and ecosystem distribution in the conterminous U.S. in response to a matrix of climate change, time periods (represented by increasing global mean temperatures), and atmospheric CO_2 concentrations (3 GCMs x 3 periods x 3 CO_2 concentrations = 27 scenarios). Impacts on total land area in each major ecosystem and on biomass (carbon sequestration) will be computed for each scenario. These results will be coupled with results of crop yield simulations under the same climatic change scenarios to determine, with the aide of the GCAM economics module, where and by how much land use will change in response to the climatic change scenarios.

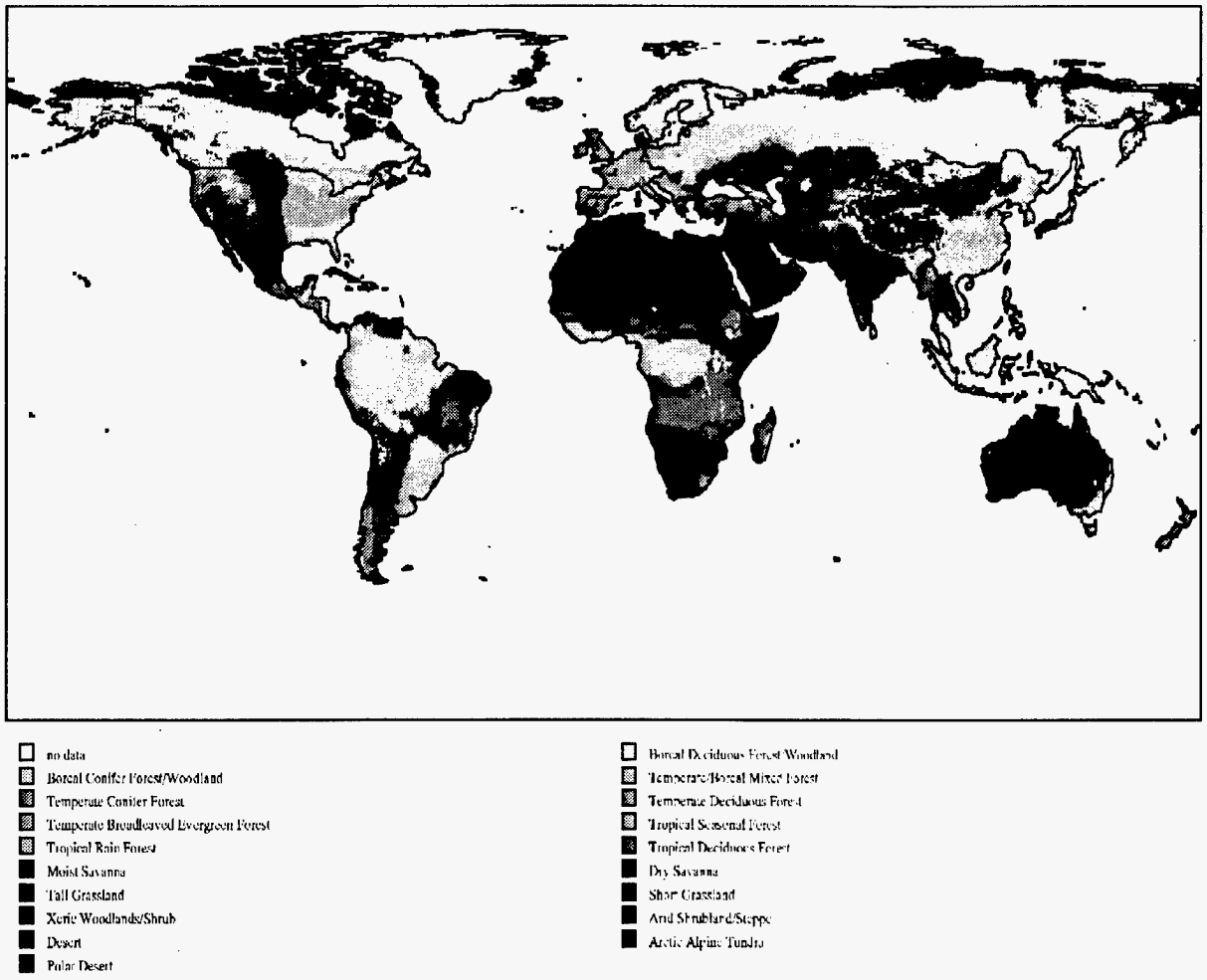

Figure 1. Predicted global vegetation patterns using the BIOME3 model.

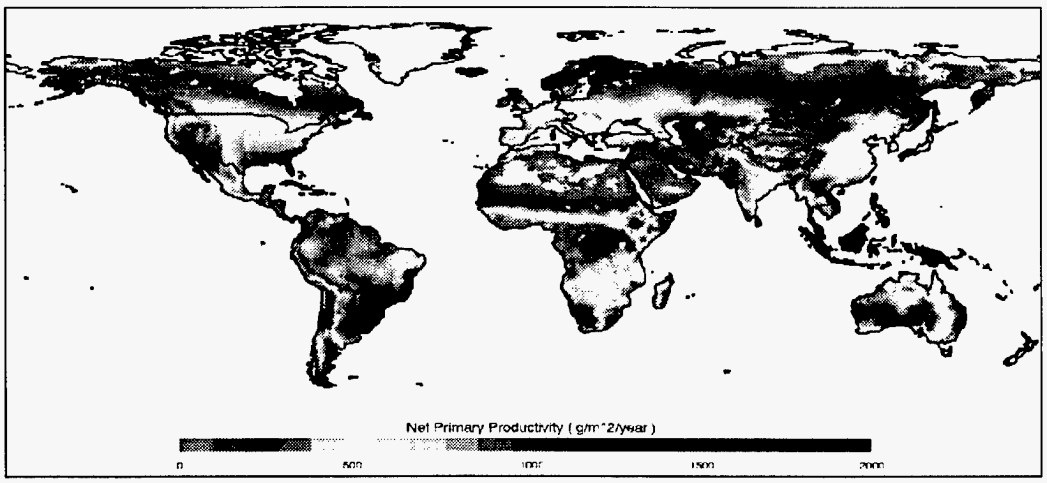

Figure 2. Predicted global net primary productivity (g m-2 yr-1) using the BIOME3 model.

Electronics and Sensors

Automated Electrooptical Identification of Pathogenic Microorganisms

Charles R. Batishko (Sensors and Measurements Systems)
David A. Nelson (Materials and Chemical Sciences)

Study Control Number: PN97015/1156

Project Description

The objective of the research is to define the limitations of the application of optical pattern recognition technology, and to apply that technology to the identification of microorganisms within those limitations. It is of particular importance to identify and apply algorithms reported in the literature which would provide the most robust identification in the presence of subject rotation and scaling variations and in the presence of significant clutter.

Technical Accomplishments

This project was divided into several tasks: the optical correlator, sample images (microorganism database development and image acquisition), and correlation filter development.

Optical Correlator

When initiated, the project intended to take advantage of the anticipated commercial availability of a personal computer expansion board-based optical correlator. When the vendor failed to bring the device to market, other options were explored including other correlators and use of a wedge-ring detector for reading spatial Fourier transforms. In the meantime, digital simulations were performed to begin to define the issues which would be presented in algorithm design. Eventually a correlator was procured from Boulder Nonlinear Systems of Boulder, Colorado. The correlator was a 256 x 256 pixel binary SLM device. While adequate for initial demonstration and testing, this system will likely require an upgrade to a 256 x 256 or 512 x 512 pixel gray scale SLM in the second year. Unfortunately, the correlator was delivered too late in the fiscal year for anything other than acceptance testing.

Correlation Filter Development

The optical image processing literature was reviewed with particular attention to the state of optical correlation filter algorithms. NASA-developed software was acquired in preparation for filter algorithm development once the correlator was delivered. There was a significant learning curve as existing expertise was too superficial to support filter algorithm development.

Sample Images

For preliminary testing, an extensive number of images were acquired from the Internet and photographs. These were predominantly microorganisms currently on the Australian List (potential BW-agents). It quickly became obvious that, at least until concept feasibility is demonstrated, image acquisition would be limited to optical microscopy. This meant generally limiting the sample microorganisms to those in the range of bacteria (>0.5 micrometers). While most virus and rickettsia will be unobservable, most of the readily cultured and weaponizable microorganisms are bacteria (e.g., *Bacillus anthracis, Yersinia pestis,* and Vibrio cholerae). During the first year, a number of surrogates for *B. anthracis* and *Y. pestis* have been examined. These are listed in Table 1. Images were acquired with a Nikon microscope, 100X oil immersion objective and 10X secondary magnification resulting in a net magnification of 1000X.

This investigation indicated that the rod-shaped Bacillus can be observed as such, but further magnification/ resolution may be necessary for identification of the oval-shaped *Erwinia herbicola*, the surrogate for *Y. Pestis*. Differentiation of cocci (sphere-shaped) microorganisms may be problematic. Rod-shaped organisms include *Bacillus*, *Clostridium*, *Legionella*, and *Pseudomonas*; all of which are pathogenic to man. Gram stained smears, using buccal (cheek/gum) swabs, were examined in an attempt to obtain spirochete signatures. However, only *Bacillus spp.* were observed.

At the end of the year, the focus was to develop a set of test images which would include multiple reference images of microorganisms of a single class—at least one class each representing microorganisms geometrically similar to a preselected test microorganism.

Table 1. Microorganisms grown as surrogates for BW-agents.

Microorganisms	Medium	Morphology
Bacillus thuringiensis	Nutrient agar	Spore forming rods
Bacillus aetrophaeus	Nutrient agar	Rods
Shewanella alga (BrY)	Tryptic soy broth (TSB)	Rods to longish rods
Pseudomonas cepacia (3N3A)	TSB 3 g/L	Short rods
Thermus sp.	Minimal iron-NTA medium	Short to very long polymorphic rods
Escherichia coli	Nutrient agar/nutrient broth	Rods
Erwinia herbicola	LB agar	Short rods (may have heavy capsule formation)
Deinococcus radiodurans	TYG broth*	Large diplococci

* TYG broth= 0.5% tryptone, 0.3% yeast extract, 0.1% glucose

Collaboration for FY 1998 was established with Dr. Guy Cook of the Montana State University Biofilm Center. The Center should be able to provide photos and samples necessary for the optical collator.

Enhanced RF Tags

**Ronald W. Gilbert, Kerry D. Steele, Brenda G. Gray,
Tom R. Heimbigner (Engineering and Analytic Sciences)**

Study Control Number: PN97041/1182

Project Description

Development of advanced/enhanced RF (radio frequency) tags would open a multitude of applications for which there are no competing technologies. A radio frequency tag is a passive (no battery), miniature device that when interrogated by an external radio-frequency source, returns a unique identification code. This tag has been used primarily in limited industrial applications for inventory control and object tracking.

The present commercial tags, of which there is only a handful of manufacturers, have several limitations preventing their exploitation. The enhanced radio frequency tag development idea would expand the capability of the radio frequency tag by adding key features and refinements.

Previous research conducted on radio frequency tags will be evaluated as a starting point for understanding the use of existing radio frequency tags. From this research, we will define the next steps for expanding the capability of radio frequency tags by adding key features and refinements. Last, we will fabricate radio frequency tags for demonstration purposes. The outcome of this project will be an assortment of tags—each with specific features. Follow-on programmatic funding will be obtained to further refine the tags for specific needs.

Technical Accomplishments

Two unique paths were followed to yield designs which met two requirements. Each path was aimed at showing design validation by building a working prototype. The prototypes were successfully demonstrated in the laboratory and will serve as candidates for future research and development.

The task to allow multiple tags to be quickly interrogated involved expanding the number of digital bits in the identification code plus frequency hopping the tags retransmission frequency (narrow bands). The existing concept for reading tags uses a serial concept meaning only one tag, the strongest tag, is read in the radio frequency field. The enhanced concept involves tags with inherent properties of both an identification code and a selective retransmit frequency.

The read/write effort involved enhancing the existing technology to provide additional circuitry to acquire both the incoming data stream and to store it into nonvolatile memory. Since the tags are passive (no battery), enhancements were also added to acquire the additional power (from the radio frequency incoming stream) to accommodate the new write feature. This design impacted tag/reader antenna design and reader transmission features.

Presentation

An internal demonstration/presentation of "multiple tags in an RF field" and "read/write backscatter tags" was held for an internal PNNL review committee on October 3, 1997.

Fiber Optic Sensor Platform[(a)]

Norman C. Anheier (Sensors and Measurement Systems)

Study Control Number: PN95051/1027

Project Description

Conventional iron core current transformers (CTs) and capacitive potential transformers (CPTs) are used to measure current and voltage on power lines. The costs associated with electrical isolation and shielding materials (porcelain) used on CTs and CPTs are high. CTs and CPTs also are costly from the standpoint of installation because they are very large and heavy. In addition, these current and voltage transformers suffer from nonlinearity and saturation. CTs also have been noted to explode due to the buildup of hot gases when the pressure relief valve fails.

The objective of this project was to develop an optically powered smart sensor platform capable of accepting analog current or voltage values from power line sensors and then transmitting those values, via a low-power optical data link, to a ground-based data acquisition system. The measurement of power line parameters, such as current and voltage, requires great care to achieve electro-magnetic interference (EMI) immunity and flashover protection. An optical interconnect provides the ideal EMI immunity, ground potential rise isolation, and electrical isolation during power line monitoring. Such an interconnect can be easily interfaced between existing sensors and ground-based data acquisition systems.

Technical Accomplishments

In FY 1996, PNNL staff collaborated with Bonneville Power Administration to understand electric power utility needs for power metering, fault, and protection applications. A commercial fiber-optic-based current sensor was field tested for 4 weeks at BPA's Slat substation in Arlington, Oregon. This field test allowed PNNL staff to observe actual substation monitoring conditions and constraints. Lessons learned from the field test were useful in defining the next generation optically powered smart sensor platform.

In FY 1997, technical efforts were directed at designing a 16-bit resolution smart sensor platform useful for power utility and other applications (Figure 1). The PNNL developed sensor board is optically linked to a ground-based controller using two fiber optic channels. The first channel is used to optically power the sensor board. The second channel is used for a fiber optic data link.

Key features developed in this system include a 16-bit analog-to-digital converter (ADC), a high-speed, high power laser diode driver, and a robust fiber optic data link. The ADC incorporates sigma-delta modulation to obtain the required signal fidelity and resolution needed for power metering. In addition, the data acquisition is capable of acquiring analog current values at 12.5 thousand samples per second. Sampling at this rate permits a unique look at actual power line fault events.

A 1-watt diode laser driver, capable of modulation up to 4 MHz, was designed and built. The driver controls the diode laser used to optically power the remote sensor board and to supply the ADC clock using the 4 MHz modulation.

The fiber optic communication link was designed based on a biphase mark-encoding scheme. This link has a bit rate exceeding 10 Mbit digital, that easily handles the required 16-bit analog bandwidth of 12.5 kHz (208th harmonic of 60 Hz). The fiber link also supports a closed-loop fiber safety monitor. This monitor verifies the integrity of the optical power fiber link. If the link is broken or otherwise disconnected from the laser diode, the safety monitor powers down the diode laser to prevent possible eye damage.

(a) Project was formerly entitled, "Low Cost Sensing Technology for Operations and Maintenance Applications."

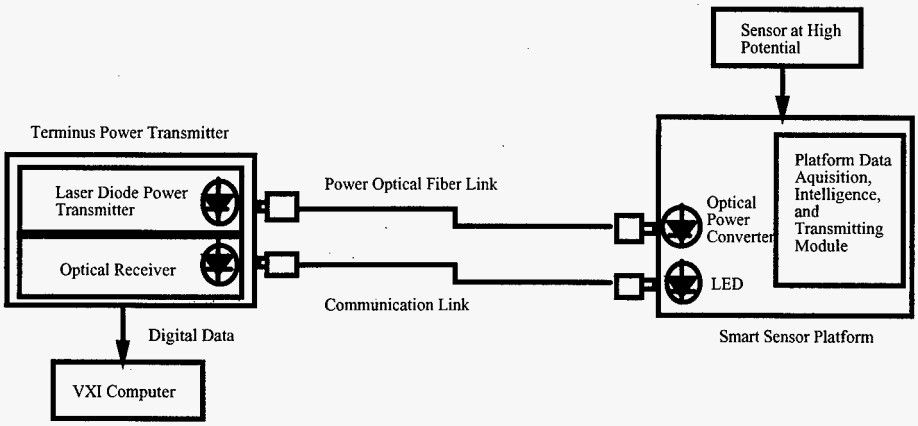

Figure 1. Optically powered smart sensor platform.

Gas Composition Instrument[(a)]

Chester L. Shepard (Engineering and Analytic Sciences)

Study Control Number: PN95051/1027

Project Description

In this project we built and demonstrated a prototype laboratory instrument for the measurement of the composition of gaseous mixtures. The instrument uses special membranes as the front end to typical laboratory instruments, such as mass spectrometers and optical spectrometers. The advantage of the membranes is that enhancement of instrument performance is accomplished with greater simplicity and much lower cost than present instruments provide. The concept takes advantage of the time dependence of signals collected by the mass spectrometer, which is related to the properties of the membrane through which the gas sample diffuses. For instance, it may be possible to replace the entire GC part of a GC/MS with a membrane system and accomplish similar detection capabilities. A prototype was built, and in FY 1997, we tested the instrument with several different kinds of membranes.

Technical Accomplishments

Success on this project required the availability of an ion trap mass spectrometer with which to perform experiments. A new ion trap mass spectrometer became available during the year and we planned to use this for our studies. However, the instrument did not function properly and no useful data were obtained with it, in spite of repeated attempts. A suitable replacement mass spectrometer was not identified during the year.

We attempted to obtain data using another mass spectrometer designed for use at atmospheric pressures. This instrument was intended for use in direct sampling of air. It relied on the breakdown of air in an intense electric field at the inlet of the mass spectrometer to create the charged particles needed for creation of ions which could then be analyzed with the mass spectrometer. This instrument did not have sufficient stability to allow time-resolved measurements needed for testing the measurement concept. In addition, it could not be operated at low gas pressures or with more appropriate carrier gases such as argon. The data obtained in these tests were sufficient to show that it did not appear likely that even a suitable mass spectrometer would show the results which we desired, at least for a natural gas sample. Natural gas is composed of molecules which contain only carbon and hydrogen atoms, and they differ from each other only in the numbers of these elements. All of these molecules are easily ionized in a mass spectrometer with the resultant creation of a host of molecular fragments. The problem is that many of these fragments are similar regardless of the parent molecule from which they came. As a result, a prominent peak in a mass spectrum can contain contributions from as many as seven or eight of the constituents which make up natural gas. This is particularly true at low mass numbers corresponding to methane or ethane or propane. It would be extremely difficult to arrive at a constituent analysis of natural gas using this method, which was our goal.

A more suitable instrument for measurement of natural gas composition might be a Fourier transform infrared (FTIR) spectrometer. This instrument is useful for analysis of molecules which have an infrared spectrum, such as most of the components of natural gas. Some components, such as carbon dioxide or nitrogen cannot be analyzed with FTIR spectrometers. However it may be possible to obtain the relative concentrations of the hydrocarbons present in a sample. The membrane system that we have developed can be useful in conjunction with several analytical instruments. In all cases it provides another dimension in capability, namely time resolved measurements which can be used to quantify gas composition. We used the membrane system in conjunction with a gas cell used with FTIR measurements. The cell, a glass unit about 20 cm long and 3 cm in diameter, was filled with natural gas to a low pressure of about 10 mm Hg and this mixture diffused out of the cell through the membrane and to a vacuum pump. FTIR measurements were performed while the cell went from its original pressure down to vacuum. While the FTIR data looked reasonable, the results obtained were not consistent with our understanding of the experiment. For instance, we fully expect that the ratio of the amount of methane in the sample to the amount of ethane should decrease in time, since the methane is lighter and should

(a) Project was entitled "Low Cost Sensing Technology for Operations and Maintenance Applications," in FY 1995.

escape the volume through the membrane at a faster rate than ethane. We observed that the ratio of methane to ethane actually increased over the several hours of the experiment, implying that ethane leaves the volume at a faster rate than methane. This simply cannot be the case. Even though, efforts to understand what went wrong with the experiment are still being carried forward. This project is now complete and no funds have been requested for carrying on the work. It does not appear that the method of determining gas composition using the concept described here is suitable for use with natural gas or with very complex gases having a multitude of components.

Genetically Engineered Sensors

Peter C. Rieke (Materials and Chemical Sciences)
Fred J. Brockman (Molecular Biology)
Cynthia J. Bruckner-Lee (Materials Interfaces and Process)

Study Control Number: PN96028/1095

Project Description

The objective of this project was to develop a general bioengineering strategy for the use of cellular organisms as sensors and to demonstrate the feasibility of the necessary steps required to achieve complete engineering for detection of a specific analyte. We planned to use this biochemistry to prepare sensors using either the live organisms or, if possible, selected portions of the protein synthetic scheme associated with response to the toxin. These genetically engineered sensors should have considerable application to problems encountered on the Hanford Site. Candidate organisms might even be selected from bioremediation studies currently ongoing in the area. Organisms have remarkable selectivity and sensitivity to environmental stimuli including chemical toxins. High sensitivity and high selectivity are highly desirable in sensors used in complex analyte matrices such as those found at the Hanford Site.

Technical Accomplishments

During FY 1997, our objective was to develop an analytical scheme for monitoring the luminescent response of organisms to the presence of desired analytes. The Pseudomonas fluorescens 5RL bacteria that degrades salicylate was used for this purpose. The primary difficulty is design of a microflow system that allows manipulation of small aliquots of bacteria as well as the necessary reagents for inducing luminescence and maintaining viability of the cells.

Three approaches were used to develop flow systems for the analysis of bacterial cell luminescence: a batch fluid cell, a flow-through cell, and a jet-ring cell. The jet-ring cell proved the most versatile and repeatable and was used for further studies with the specific objective of determining the sensitivity and dynamic range of the technique. Early efforts focused on glass beads derivatized with trifluoro acetic acid terminated silanes. While these worked, the hydrophobicity caused clumping of the beads and irreproducible pumping characteristics. Different quantities of glass beads were trapped in the jet-ring cell each time. Considerable effort was focused on different cell to bead attachment schemes to overcome this problem. Further, this effort improved flow characteristics of the cell and improved the viability, distribution, and quantity of cells on the bead surface. The reproducibility of measurements was substantially improved by these techniques.

The nature of the cell growth curve and growth conditions and the influence on chemiluminescent response was investigated. For this investigation a bioreactor was set up for the 5RL bacteria. It was found that cells in the early stages of growth were more responsive than those in the latter stages of growth. We surmised that this was due to the relative nutrient needs of the cells. Young cells undergoing more rapid division will seek alternative nutrient sources to maintain viability. Older cells will be more selective in their metabolic behavior and will pass over salicylate in favor of more conventional food sources.

The secondary nature of the salicylate metabolic pathway also slowed the chemiluminescent response of the cells. The cells were maintained in a certain growth stage in the reactor with a standard nutrient media that did not contain salicylate. Upon introduction to the flow cell and attachment to beads, the nutrient media was removed from the cells and upon introduction of the salicylate the cells were forced to modify their metabolic pathways to use the salicylate. We found that maximum response of the cells occurred 3 hours after exposure to salicylate. Plug exposure and continuous exposure resulted in varied magnitude of signal but did not significantly influence the response time. Apparently it takes some considerable time to turn on the salicylate pathways.

Publications and Presentations

C.J. Bruckner-Lea, F.J. Brockman, D.P. Chandler, F.S. Lai, C.R. Martin, N.B. Valentine, and P.C. Rieke. "Development of a Flow Injection System for Monitoring Luminescent Bacterial Cells." (in preparation).

This work was presented at the Eighth International Conference on Flow Injection Analysis (ICFIA 97), Orlando, Florida, January 12-16.

Imaging the Neurological Mental Processing of the Human Brain

David M. Sheen, H. Dale Collins (Engineering and Analytic Sciences)

Study Control Number: PN96033/1100

Project Description

The major objective of this project was to conduct basic imaging research of the EEG signals generated in the cortex of the human brain. This project includes collaborations with two or more major medical institutions in the United States. Their medical expertise, coupled with PNNL's holographic imaging technology, should provide the best possible combination to ensure success in this area. Successful results from imaging the functional cortex EEG signals should lead to many potential applications within the medical community.

Introduction

We have proposed a new medical science program, "electroholoencephlography" (EHEC) that will merge the results of both positron emission tomography (PET) and computerized electroencephalographic tomography (CET) that is, image the electroencephalographic signals (EEG) emitted from the brain and display, in real time the thinking processes in the cortex as demonstrated in non-real time with PET. PET requires the use of radioactive oxygen which, injected into the blood stream, is transported to the brain. This diffusion process may not be a true indicator of the electrical activity (thinking processes) of the brain and, in addition to being relatively slow, the brain's activities can never be displayed in real time using this process. Real-time imaging of the brain's electrical activities in the cortex is of major significance to researchers in the field. If made available, this technology would allow them to see, in real time, how the different areas of the cortex light up in response to the functional processes of the human brain (Figure 1).

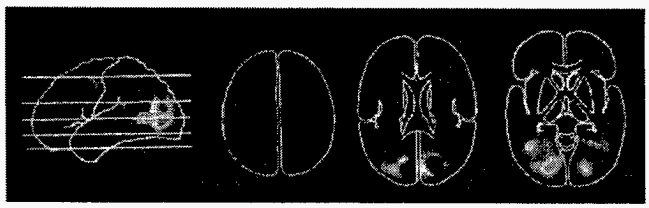

Figure 1. PET scan images of the neurological processes.

Using a near-field phase multiplication holographic technique, this new EHEC imaging concept shows excellent potential for imaging electrical signals generated in the brain's cortex as a result of functional processes like thinking in real time (Figure 2). Figure 2 is the first holographic image of nerve activity in the human cortex. The white dot is the image of evoked potential (electrically stimulated right index finger) in the motor sensory region of the cortex. The magnetic resonance image is used to locate cortex function regions in the brain.

● **Motor System Region of the Brain**

Figure 2. Holographic EEG images of the neurological processes.

This noninvasive technique uses existing EEG signals from an array of electrodes that are attached to the skull. The signals are then processed as images in the computer. The images, which are generated in real time dynamically display the brain's cortex where the functionally derived signals originate. The static EHEC images appear to compare with the PET images in this first image.

Technical Accomplishments

Brain Images of EEG Evoked Potential Scalp Data (Electrically Stimulated Right Index Finger)

EEG-evoked potential two-dimensional array data were acquired from Dr. Jeff Eriksen (Good Samaritan Hospital). The 80 sample point data were sampled every 1 cm and the aperture centered at the Cz point on the scalp. There are 8 rows of 10 data points spaced 1 cm apart. The time series EEG data revealed a low frequency single sine wave cycle (noisy) at approximately 60 ms from the initiation of the shock stimulation of the

right index finger. Fourier transform of the signal revealed the time frequency bandwidth to be very low (less than 30 Hz) as expected.

An 8 Hz hologram was extracted from the two-dimensional array of data and then phase multiplied by 3 (Figure 3a) and then reconstructed into an image as shown in Figure 3b. The bright point image in the left side of the brain shows where maximum nerve activity is taking place with respect to the overall low-level activity. The low-level activity appears as a grid resembling diamond shaped areas over the cortex. The depth of the nerve activity is approximately 1.5 cm to 2 cm below the scalp surface.

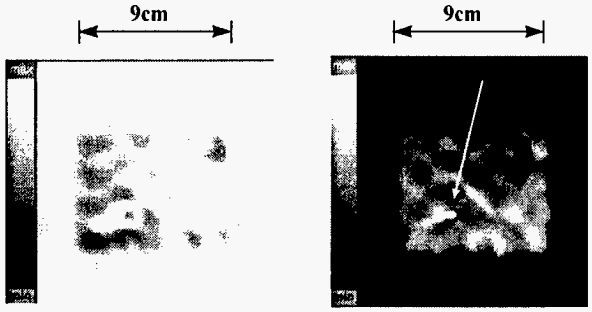

Figure 3. Hologram and image of EEG somatosensory evoked potentials.

The assumed average phase velocity in the scalp media (between the cortex and scalp) is approximately 30 cm/s. This range of values fits the data and produces the optimum image of the somatic sensory evoked potentials. The assumption is that the excessively high attenuation in the various layers between the cortex and scalp results in this low phase velocity. The velocity was also computed using the EEG time signal (after subtraction of the cortex propagation time ~9 ms) of the signal from the finger tothe cortex). The average velocity from the surface of the cortex to the scalp was computed to be approximately 30 cm/s using a distance of 1.5 cm and a propagation time of 51 ms.

Figure 4 is the image imposed on the magnetic resonance images and the scalp surface along with some of the data point positions. The dark dot is the motor region where the nerve activity is generated for electrical stimulation of the right index finger. The white dot (image) is very close to the correct position. The data (grid) are numbered starting from left to right 1, 2, 3 to 80 in 8 rows. The aperture was centered on the Cz point on the scalp and sampling density ~1 cm.

Comparison of Brain Images of EEG Evoked Potential Scalp Data (Electrically Stimulated Right Index Finger) and Computer Model Images

Figure 5 compares the computer model and actual EEG image data for the somatic sensory two-dimensional array data. The computer modeled and actual EEG holograms and images are amazingly similar and support the theory in that we are able to essentially reproduce the results with the model.

Conclusions

The initial imaging results with high-density array EEG somatic sensory data are very encouraging and support the proposed theory. Hopefully this work will motivate others to pursue high-density sampling EEG imaging experiments. More research is required to verify the above results and raise the level of effort in this area. We believe this is only the beginning in this very exciting field with infinite possibilities left to the non-timid.

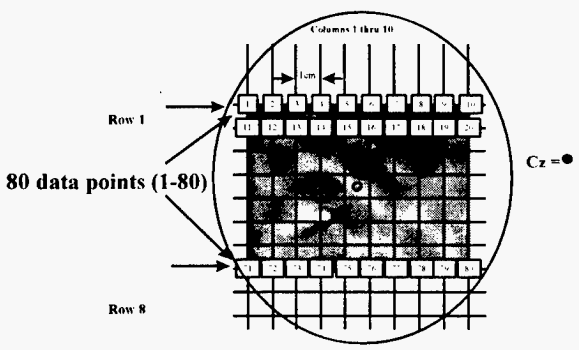

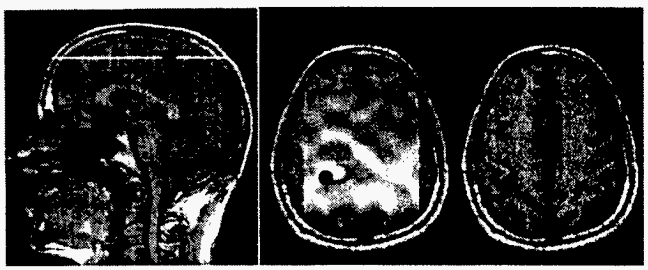

● Motor System Region of the Brain

Figure 4. Image imposed on the magnetic resonance images and the scalp surface along with some of the data point positions.

Computer Model Data

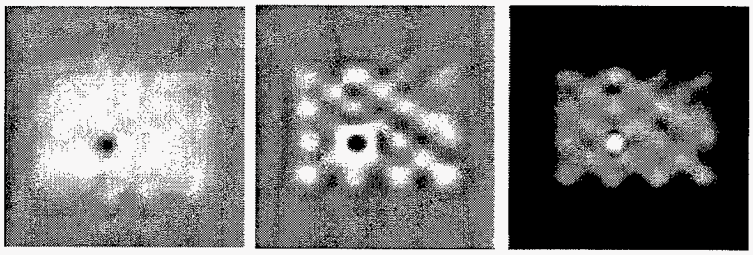

Hologram 3X Hologram Image

EEG Scalp Image

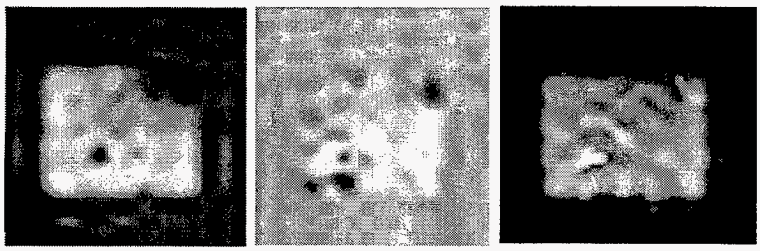

Hologram 3X Hologram Image

Figure 5. Computer model and actual EEG image data.

Investigation of OSL Materials for IR/UV IFF Tags

Steven D. Miller (Environmental Technology Division), Chuck Batishko (Energy Division)

Study Control Number: PN97062/1203

Project Description

The focus of this LDRD project is the application of optically stimulated luminescence (OSL) for the purpose of marking and tracking. Identification-friend-or-foe (IFF) is also included in potential applications. The application of infrared OSL phosphors and the development of ultraviolet-emitting phosphors are the technical activities. Production of useful quantities and the development of polymer composites were deliverables. The generation of ultraviolet OSL phosphors was also successful and will be optimized next fiscal year.

Technical Accomplishments

Production of infrared active OSL materials is accomplished through the application of mechanical stress to crystalline solids. The action of mechanical stress produces profound changes in the crystal lattice that acts as electron traps. The action of ionizing radiation on the pressed crystals produces free electrons that become trapped in the pressure-induced defects. These trapped electrons, when illuminated with the proper wavelengths, absorb the light and "shift" the light to a longer wavelength.

Small quantities of infrared-active phosphors have been made using a small mechanical press contained within the principal investigator's laboratory. One of the important outcomes this year was to identify a large-scale mechanical press that would enable large quantities of pressed crystals to be produced conveniently. A large mechanical press was located in the 300 Area of Hanford and permission to use the equipment was obtained. When a metal dye was fabricated to press the powder to the necessary pressures, it was quickly determined that the necessary pressure exceeded the mechanical strength of the metal dye parts. We spent a great deal of effort on this issue before we obtained a heat-treated metal dye that could withstand the necessary pressures. A large quantity of phosphor was made and processed for later use.

Some of the phosphor material was made into polymer "swatches" for future testing. Besides the fabrication of fairly opaque polymer "swatches," some phosphor was loaded into polymers that were index-of-refraction matched. These polymer samples produced nearly optically transparent layers since the phosphor grains "disappear" when the polymer/phosphor composite becomes a good refractive index match. This will be important to such applications as a clear wax marker or other covert applications. The invisibility of the phosphor/polymer composite enables the application of invisible codes to the object being marked. For example, an object could be marked with a serial number that would be invisible to the naked eye but that is machine-readable. It may be possible to read the serial number even at high speed using an intense laser pulse or flashlamp.

The U.S. military is conducting some development toward special goggles that permit ultraviolet vision. For this reason, PNNL has been investigating phosphor materials that emit ultraviolet light. Metal doped alkali-halides have been demonstrated to emit ultraviolet light when irradiated, followed by illumination with visible light. The emission spectrum of one phosphor is centered near 250 nm. The current ultraviolet emitting materials have demonstrated instability with time indicating the electron trapping levels are fairly shallow. Further development of this promising system will be completed next fiscal year in order to improve the stability characteristics of the ultraviolet emitting materials.

The objective of the range analysis task is to upgrade a previously written white paper covering an analysis of the potential detection range of an OSL tag using current or near future laser designator and detection hardware. To keep the former analysis unclassified, only ratios of transmitted excitation laser energy and detection sensitivity were used, and lacking hard data on OSL fluorescence efficiency, approximations were used. Nevertheless, the results suggested that 3 km range was potentially feasible. In this task, actual radiometric measurements of fluorescence efficiency will be used, and actual radiometric performance of tactical designator/ detector systems will be used.

A classified literature search was initiated to find a source for radiometric specifications for current or near future military systems. At this time, this preliminary search has not identified any readily accessible, sufficient data. A more extensive search will be conducted. Radiometric

measurements were attempted using an existing radiometer, but the levels measured were near the sensitivity limit of the instrument. A new InGaAs-based radiometer with several orders of magnitude greater sensitivity in the 0.8 to 1.6 micrometer wavelength of interest range was ordered and received in mid-September and is currently being readied for measurements.

Low Cost Demodulator - Novel Fiber Grating Sensor

Norman C. Anheier, Richard A. Craig (Engineering and Analytic Sciences)
Mary Bliss (Radiation Instrumentation and Application)

Study Control Number: PN97066/1207

Project Description

The introduction of fiber-optic sensor technology has revolutionized many industries. The Bragg fiber-grating sensor is one of the most current and promising fiber-optic sensor development areas. Fiber-grating sensors are intrinsic sensors that can be distributed within a single optical fiber. Fiber gratings have applications in communications, sensing, and signal processing. As a sensor, fiber gratings respond principally to temperature and strain. They can be used as a generic transducer to measure many different physical parameters indirectly through a strain measurement. Fiber-grating sensors have been installed in many civil structures, such as bridges and dams to measure the integrity of the structures.

Technical Accomplishments

The fiber grating was strained using an aluminum cantilever beam (Figure 1). The cantilever beam was convenient for the application of low levels of static and dynamic strain. A direct measure of the surface strain was made with a resistance strain gauge epoxied near the fiber-grating sensor. A micrometer allowed fine control of the vertical deflection.

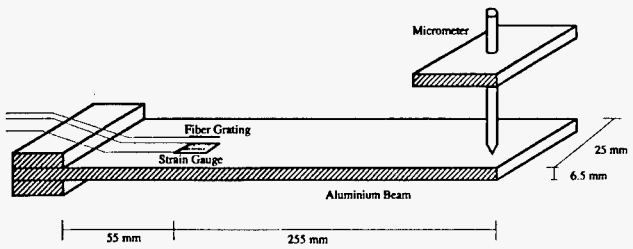

Figure 1. Aluminum cantilever beam.

Wavelength tunable light from a temperature-cooled diode laser was used to interrogate the Bragg fiber grating (Figure 2). Lens L1 collimated the diode laser light, and an optical isolator, I1, prevented retroreflected light from re-entering the diode laser. Lens L2 focused the diode laser light into a single mode branch coupler, BC1. The grating fiber pigtail was fusion-spliced to the branch coupler. Light in resonance with the Bragg grating period was highly reflected back into the branch coupler and then onto the demodulator experiment.

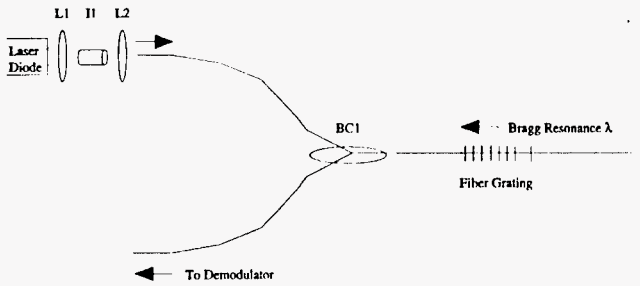

Figure 2. Fiber-grating wavelength source.

A variation of a Lloyd's mirror interferometer was assembled and tested in the lab (Figure 3). Light that is reflected by the Bragg grating is launched into the demodulator using the single mode optical fiber pigtail. Monochromatic light exiting the single mode fiber can reach the photodiode array (PDA) detector by either of two paths: direct or via reflection from the mirror. The difference in path lengths between the two paths (plus the phase shift induced by the reflection on the mirror surface) induces a phase shift between the two wave fronts. These two signals combine constructively or destructively to form an interference pattern on the PDA detector. The reflected ray appears to be coming from an "image" fiber a distance *d* below the plane of the mirror. The fringe pattern detected by the PDA detector is acquired by a computer and analyzed using LabView software. Digital filtering and a power spectrum is computed to determine the spatial frequency of the fringe pattern.

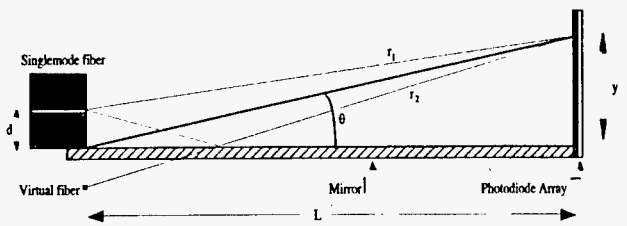

Figure 3. Novel fiber-grating sensor demodulator.

The resultant irradiance at the photodiode array is given by:

$$I = 4I_0 \cos^2(yd\pi/L\lambda)$$

The period of the fringe spacing is given by:

$$\Delta = L\lambda/2d$$

A typical interferogram is shown in Figure 4 (the pinhole separation is 2d). By performing a power spectrum on this data set, the spatial frequency and its corresponding strain on the fiber-grating sensor can be ascertained.

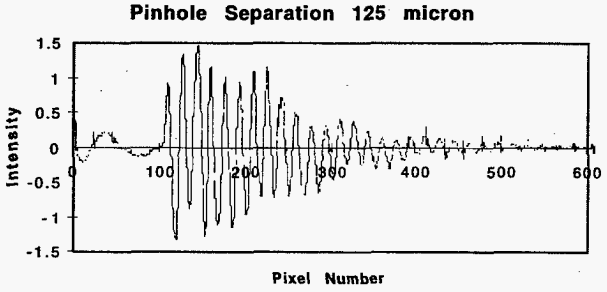

Figure 4. A demodulator interferogram.

Conclusion

With a handful of components that would cost less than $200 to manufacture,[(a)] we have been able to acquire interferograms from the Bragg grating strain sensor. A literature survey of similar technology was performed. The literature survey showed that no equivalent technology exists. While there was not enough time to experimentally determine the full resolution of this instrument, the data sets did show that the demodulator has merit. Finally, for a future study, we have identified several techniques to improve the demodulator analysis software, such as summing the interferograms, curve-fitting the data, and factoring in the phase information.

(a) The demodulator was assembled with low-cost components consisting of a single mode fiber-optic branch coupler, front surface mirror, a PDA detector, single channel digitizer, desktop computer, and some rudimentary software. The demodulator itself could cost less than $200 to manufacture.

Low Cost Endoscope for Viewing Inaccessible Areas

Jeffrey W. Griffin (Sensors and Measurement Systems)

Study Control Number: PN97067/1208

Project Description

The objective of this project was to design and demonstrate a new concept in fiber optic endoscopes. Unlike conventional fiber optic endoscopes based on a coherent array of optical fibers, the new concept employs a fiber optic ribbon consisting of individual optical fibers laid side-by-side.

Technical Accomplishments

During FY 1997, efforts focused on developing a method to fabricate the required fiber optic ribbon. These ribbons were formed using small-diameter plastic optical fibers obtained from two commercial vendors. The fibers purchased from General Fiber Optics had a numerical aperture of 0.58 and an outer diameter of 125 microns. Fibers procured from Moritex had an outer diameter of 250 microns. Ribbons were fabricated by winding multiple turns of fiber onto a 12-inch-diameter aluminum mandrel. This mandrel was mounted on a machine lathe and rotated at low speed to achieve accurate placement of the fibers side-by-side with no overlap or gaps. When the desired ribbon width was attained (typically ½ inch to ¾ inch), the winding process was terminated and a short section of the ribbon (1 to 2 inches) was glued in-place using an ultraviolet-curing optical adhesive. To remove the ribbon from the mandrel the ribbon was sliced crosswise through the glued portion. The ribbon could then be removed and the ends polished to obtain good optical transmission through the ribbon length (approximately 3 feet).

Implementation of the ribbon fiber endoscope concept requires that the two ends of the ribbon be fluttered in synchronization. Our initial attempt to achieve this involved cementing piezoelectric actuators to the two ribbon ends. These actuators, obtained from Amp Inc. are plastic bimorphs fabricated from PVDF. It was found, however, that these actuators did not provide adequate displacement to achieve the desired high-amplitude flutter of the fiber ribbon ends. Our second (and more successful) attempt at fabricating ribbon drivers involved fastening the ends of the ribbon to the cones of two audio speakers driven in synchronization. Using this method of synchronized ribbon displacement we were able to convey the image of a USAF test target from one end of the ribbon to the other.

Conclusions

In FY 1997 we were able to successfully demonstrate the concept for a low-cost endoscope based on a coherent fiber optic ribbon. Further refinements of the concept and a determination of the ultimate limits of attainable image quality will require contract funding.

Portable Ultrasensitive Biological Sensor

Brion J. Burghard, Chester L. Shepard (Engineering and Analytic Sciences)
Manish Shah (Materials and Chemical Sciences)

Study Control Number: PN96057/1124

Project Description

The objective of this project was to develop low cost, quantitative sensors capable of detecting the presence of specific chemical and biological materials at low (part per billion to part per trillion) concentration levels. Antibody/antigen enabled agglutination of molecules is one of the newest approaches in the detection of biomolecules. Recently, rapid (2 to 10 minute) whole blood test assays based on red blood cell agglutination (or agglutination inhibition) have been developed for a variety of pathogens and disease indicators (endotoxins, HIV-1 and HIV-2 antibodies, hepatitis B virus, and the fibrin component D-dimer). Similar agglutination tests have been demonstrated that use latex beads coated with the target analyte (in place of the red blood cells). Rapid diagnostic tests using latex bead agglutination have also been developed for meningococcal meningitis, H. influenza, pneumococcal bacteremia, and others. The results of these assays indicate the presence or absence of the targeted pathogen but do not provide concentration levels. We have been working toward developing a method to automatically and quantitatively measure the agglutination rate. We believe this could lead to low cost, quantitative sensors for a large number of specific pathogens and disease indicators.

Technical Accomplishments

Most agglutination assay kits include a fluid containing a colloidal suspension of latex beads. These beads are coated with a specific antigen for the detection of a corresponding specific antibody. The kit is used by depositing a sample under test into a sample of the kit solution containing the beads. The mixture is then gently rocked and swirled by hand. If the beads agglutinate after several minutes, then the specific antibody is present in the sample. The test is simply a yes/no test rather than quantitative (how much antibody was present in the sample). The agglutination is observed visually. The main thrust of our efforts has been to make this test quantitative, simple, and automatic.

We built a testing device which allows a measurement of light transmission through the mixture of beads and sample and also provides for mixing of the sample.

A schematic drawing of the apparatus is shown in Figure 1. Light from an incandescent source was first filtered to produce light in the blue region of the visible spectrum and then transmitted through a pinhole, collected by a lens, passed through the sample, and finally focused onto another pinhole covering a silicon light detector. The final pinhole discriminates against scattered light and, to a large extent, allows only light directly transmitted through the sample to arrive at the detector for recording.

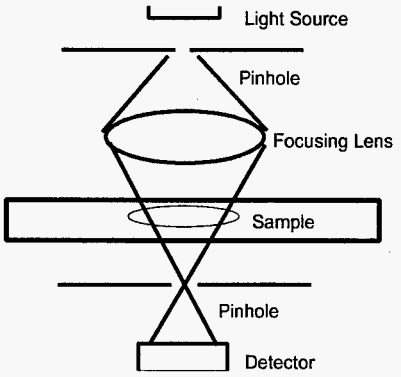

Figure 1. Experimental setup.

Dr. Nathan Smith helped us in the performance of this work. He provided a solution containing latex beads and another solution containing the corresponding antibodies. The beads were about 1 micron in diameter.

The experimental procedure was to deposit a small sample of the bead solution into the sample holder and then add and mix the antibody solution with the beads. The sample was then placed inside our measurement system and the light transmission was measured as a function of time while the mixture was continually agitated within the sample holder. The amount of antibody solution added to the beads was carefully measured and the same amount was used for each test. The concentration of antibodies was varied by diluting the antibody mixture with a saline solution.

In order to obtain a quantitative test, some ideas concerning the agglutination of the beads needed to be formulated. We have developed a first order theory describing bead agglutination and we have related this

to our measurement parameter, which in this case, is the amount of light directly transmitted through the bead mixture. The scattering of light by spherical particles is described by the theory of Mie scattering which is a complete and exact theory based on Maxwell's electromagnetic equations. In its most general form, the theory is quite complicated. For opaque spherical particles of a diameter greater than several times the wavelength of irradiating light, each particle removes light from the beam with an effective diameter of about twice its true diameter. Half of the light is simply blocked or reflected while a similar amount is lost due to diffraction as light passes by the particle. We will make the simplifying assumption that the amount of light occluded from the irradiating light beam by a particle is proportional to the particle size. Over the range of particle sizes appropriate for the experiments described later, this assumption is probably not exactly correct, but it should be fairly accurate. A more complete theory can be formulated which properly accounts for particle size. In our case the individual particles are of about 1 micron diameter while the light wavelength is about 0.5 micron. As agglutination proceeds the average particle size increases and so the condition that particle size must be several times the light wavelength is met.

Consider a suspension of particles of fixed number N which are undergoing agglutination. As agglutination proceeds the size of the particles increases while the total number of particles decreases. The amount of light lost due to scattering depends upon the total number of scatterers and, as described above, their size. The number density of particles will fall faster than the particle size increases, assuming that the particles pack spherically. As a result, light transmission increases as agglutination proceeds. The expression relating light transmission to particle diameter is

$$I = I_0 \exp\left(-\frac{A}{D}\right) \tag{1}$$

where I_0 is the incident light intensity, I is the intensity after passage through the particles, D is the average particle diameter, and A is a constant which depends upon geometry and the initial number density of the beads.

Consider the mechanism for agglutination as it applies to this case. The beads are completely coated with antibodies and the beads are much larger than the antigens. Antigens that collide with a bead are immediately attached to it. When we mix the antigen-containing solution with the beads, the first consequence is that all of the antigens get distributed among the beads. The number of antigens on each bead probably follows a Poisson distribution, but we will for simplicity assume each bead obtains a number of antigens equal to the expected average given by

$$a = \frac{M}{N} \tag{2}$$

where M is the total number of antigens within the test solution and N is the number of beads to which the test solution is added and mixed.

Mixing causes the beads to collide with each other. The probability that two beads will stick together after collision depends on the number a. In order to stick, an antigen on one bead has to be in proximity to the surface of the other bead. If the beads collide in a region where both beads are devoid of attached antigens, they will not stick. Assume that mixing occurs in a uniform manner and that all beads are in motion at about the same velocity. If a is low, we require, on average, more collisions (and therefore more time) in order for two beads to stick. In any case it is also clear that the agglutination rate must depend linearly on the collision rate. The agglutination rate is then given by

$$\eta = const \cdot a \cdot R \tag{3}$$

where η is the agglutination rate and R is the collision rate. The collision rate is a function of the number density of beads, the cross-sectional area of the beads, and the velocity of the beads, and the relation is

$$R = n\sigma v \tag{4}$$

where σ is the bead cross-sectional area, n is the number density of beads, and v is the average bead velocity.

Several effects occur with the onset of agglutination. First, the number density of the beads decreases since there are fewer total particles when individual particles start sticking. The particle cross-sectional area increases since the size of several particles stuck together is greater than the original particle size. The total mass of particles is constant, however. Therefore,

$$n \cdot V = const \tag{5}$$

where V is the average particle volume. The particle volume is proportional to the cube of the particle diameter, D, and the cross section is proportional to D^2 so we have

$$n \cdot \sigma \cdot D = const \tag{6}$$

Then from the expression for the collision rate we obtain

$$R = const \cdot v / D \tag{7}$$

and conclude that the collision rate will decrease as agglutination proceeds. We need an expression relating the agglutination rate with time. The relative change in particle size will be proportional to the agglutination rate, so

$$\frac{1}{D}\frac{dD}{dt} = const \cdot \eta = const \cdot a \cdot R \qquad (8)$$

Since $R \propto 1/D$ we find

$$D = D_0 + const \cdot a \cdot \nu \cdot t \qquad (9)$$

where D_0 is the initial bead size. The particle size will grow linearly in time. Also,

$$\eta = \eta_0 \left(\frac{1}{1 + const \cdot t}\right) \qquad (10)$$

where η_0 is the initial agglutination rate. Hence the agglutination rate decreases with time. We can solve for the measured unscattered light intensity as a function of time and we obtain, finally,

$$I = I_0 \exp\left(\frac{-C_1}{D_0}\left[\frac{1}{1 + C_2 \cdot a \cdot t}\right]\right) \qquad (11)$$

where C_1 and C_2 are constants. In the material provided by Dr. Smith we do not know the original particle concentration or the antigen concentration in the test solution. Therefore, we cannot directly test the theory without admitting some (two) unknown constants. However, the functional form of the theory can certainly be tested experimentally. We have performed one test of the theory. In this experiment the bead suspension by itself was placed in the light beam and the light transmission was measured for 8 minutes at 1-minute intervals. Immediately after the eighth minute, a dilute antigen solution was added to the beads and light transmission was measured over the next 5 minutes. The data are shown in Figure 2. The constant signal up to 8 minutes shows that no agglutination is occurring. After 8 minutes, the transmission starts to increase. In this experiment the initial intensity I_0 is not measured, but rather the intensity after passage first through the bead solution without antigen and then through the mixture with antigen present.

For these experimental conditions the expected light transmission is obtained by following the same reasoning as outlined above and is given by

$$\frac{I(t)}{I_\gamma} = \exp\left(-A\left[\frac{1}{1 + b \cdot t} - 1\right]\right) \qquad (12)$$

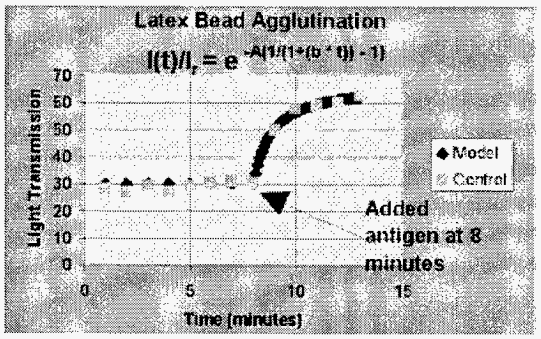

Figure 2. Light transmission data.

where I_r is the initial transmitted intensity and A and b are undetermined constants and t is measured starting from 8 minutes. The data show that for suitable choice of A and b the model fits the data very well. The constant b is proportional to the concentration of antigens in the test solution and in practice, determination of this constant would provide a quantitative measure of the amount of antigens present in a test sample.

Unfortunately, no other experiments were conducted to further test the hypothesis. Later attempts were not successful due presumably to aging of the samples. They did not behave in a reliable manner. For instance, later it was not possible to obtain the relatively constant background signal when only the bead solution was present in the light beam, which suggests that agglutination was occurring even without the presence of an antigen. Attempts to obtain additional samples from Dr. Smith were not successful. It is imperative that this problem be revisited and verification of the theory be accomplished before proceeding with the further development of this measurement concept. While the data are supportive of our simple model, there simply is not enough data at present to warrant a high level of confidence. If the model can be verified, then we indeed have a very useful method for measurement of pathogen concentration in fluid samples which can be automated and incorporated into a field instrument. Significant work would remain to reach this goal. However, other members of the Pathogen Detection team at PNNL are already doing some of the necessary steps in sample handling and preparation and this work would be very helpful in forwarding the concept.

Position Sensing for Hand-Held Wand

James M. Prince (Engineering and Analytic Sciences)

Study Control Number: PN97086/1227

Project Description

The objective of this project was to develop and check out an electronic technique based on recently released monolithic single chip accelerometers that we felt were accurate enough to provide adequate position sensing for holographic imaging. The challenge was to generate accurate information on the position of a hand-held device with gravitational effects (noise) removed. In typical hand scanning motions, the acceleration is less than 1 g. Therefore, we had a signal-to-noise ratio of less than 1:1.

Electronic circuitry was to be developed to support two or three accelerometers attached to a hand-held wand. The accelerometer data would be processed in such a way as to provide accurate data on the position of the wand. The performance would be evaluated by hand-scanning the wand above a grid to provide the positional reference.

This project ended early due to programmatic funding from the Air Force.

Technical Accomplishments

A mathematical model was developed using Mathematica to simulate and evaluate various acceleration-to-velocity signal processing algorithms. The velocity was to be converted to sample-points per unit length in electronics using a voltage-to-frequency converter. This could provide the evenly spaced samples of a hand-held wand's linear array for holographic processing.

We determined that there was no practical solution for obtaining wand velocity using a single tri-axial set of accelerometers, i.e., three equations and five unknowns.

At the point where we concluded this project, a design incorporating a second set of accelerometers was being analyzed. The second set was positioned such that it would sense wand tilt but no lateral acceleration. This configuration would eliminate two of the unknowns allowing the scan acceleration component to be calculated with minimal gravitational effects.

Special electronic integrators were designed to eliminate long-term direct-current offset drifting, while providing accurate conversion from acceleration to velocity.

The project ended before any signal processing algorithms could be verified using hardware.

Sensors and Controls for Advanced Manufacturing

John S. Hartman, Peter A. Eschbach (Sensors and Measurement Systems)

Study Control Number: PN97093/1234

Project Description

This project developed sensing capabilities for shaping, cutting, and boring processes (e.g., monitoring tool wear, developing feedback for adaptive control systems, and providing feedback to enhance the performance of cutting, shaping, and boring operations).

Technical Accomplishments

Three tasks were undertaken in FY 1997:

- literature search on commercially available machine tool monitors
- development and subsequent demonstration of a prototype temperature sensor
- design of an optical system to characterize periodic shear bands in chips.

Literature Search

A literature search revealed that machine tool monitors are commercially available. We searched all of the trade journals and found several tool monitoring systems (manufactured by Montronix, Sandvig, and Aspec). The Montronix system was the most readily adaptable. This system used load cells for force measurements and also monitored power consumption and acoustic emission as part of the diagnostics package. Measurement of temperature at the tool-part interface was not included in any of the commercial systems.

Prototype Temperature Sensor

A prototype temperature sensor was developed and demonstrated. The temperature sensing probe was made using a brass brush as a contact to the drill bit while a brass screw mounted into a Plexiglas base was in contact with the machined part. Temperatures of 150°C were measured by hooking the two contacts to the input of an electrometer. The voltage measured was on the order of 1 millivolt and was due to the Seeback effect between the dissimilar metals (the high carbon steel drill bit and the aluminum part being machined). The sensing method worked well in static tests (where the junction was heated with a heat gun. However, the signal voltage was overwhelmed by induced noise when the drill press was in actual operation. Future efforts will be directed at overcoming this problem.

Optical System Development

Very late in the year, we learned that the basic understanding of high speed machining could be greatly advanced if the metal chips resulting from this process could be characterized as they were being produced. If such a measurement could be made then, process advances could be made by utilizing the data in modeling and simulation. A very high speed optical system would be necessary in order to characterize the chips.

The chips crinkle just prior to being removed from the work piece and an optical measurement of the spatial frequency of the undulations present in the chips would provide the necessary information. An optical system to characterize the periodic shear bands in chips spalled from the machining process was designed. This system looks for periodic structures with the aid of Fourier optics. Periodic structures will appear in the Fourier transformed image of the machined part. The fiscal year terminated before the designed system could be completed. Initial work has shown flaws in the original concept and further efforts will be aimed at improving the concept.

Ultrasound Vector Velocity

Charles R. Batishko, Byron B. Brenden (Sensors and Measurement Systems)

Study Control Number: PN96071/1138

Project Description

The feasibility of visualizing blood flow for medical diagnostics using the PNNL Real-time Ultrasonic Imaging System (RTUIS) was investigated. Ultrasonic waves passing through a moving medium (blood) experience a shift in frequency when they are scattered by moving particles (corpuscles). In RTUIS, this shift in frequency produces a speckle field which is modulated at the shift frequency rate. In the simplest case, the speckle pattern becomes a pattern of light and dark bars moving at a rate linearly proportional to the frequency shift. These changes in the speckle pattern occur only in the region of the image where moving scattering centers interact with the ultrasound waves. A successful implementation of these principles could render blood flow visible in the ultrasonic imaging system. The objective of this project was to investigate, and if possible, demonstrate feasibility of the concept of adapting RTUIS technology to the visualization and measurement of blood flow.

Technical Accomplishments

A relatively straightforward approach to demonstrating the feasibility of visualizing blood flow using RTUIS was first attempted. Water, loaded with up to 21% volume fraction of 14 μm diameter particles (acrylic spheres), was pumped through a flow cell at rates of 5 to 50 mL/s. No speckle field changes corresponding to flow were observed. In retrospect, we conclude that changes, if any, would have been too rapid to be visually observed using the current RTUIS hardware.

To reduce the complexity of the experiment, the flow cell was replaced by a transducer which could be shifted in frequency to simulate frequency shifted waves scattered from a moving particle. Frequency shifts in the range from 0 to 15 kHz corresponding to a particle velocity of up to 200 cm/s produced the expected change in the speckle pattern. Blood velocities less than 200 cm/s should thus be detectable, with measurement of very low velocities feasible. This finding is favorable to the use of RTUIS because, in most instances, the main component of blood flow velocity would be perpendicular to the direction of propagation of ultrasound (the line-of-sight) with only a small parallel component to which RTUIS would be sensitive.

Spatial filters were constructed and installed on both the optical and acoustical sides of RTUIS's imaging detector. Those on the optical side enhanced both the image brightness and the contrast in the speckle pattern. Those on the acoustical side were designed to eliminate the main ultrasonic beam and transmit only scattered ultrasonic energy. The ultrasonic spatial filters did not produce any useful results other than to make us aware that forward scattering angles are small (i.e., the forward scatter energy propagates very close to the direction of the unscattered energy resulting in lowered fringe contrast due to the stronger unscattered component).

The apparatus was constructed to measure the angular scattering distribution of ultrasonic energy relative to the flow direction of a moving stream of water carrying a mixture of acrylic spheres ranging in size up to 43 μm in diameter. Experiments confirmed that forward scattering angles are small. Our conclusion, based upon these findings, is that noninvasive detection of blood flow and the measurement of blood flow velocities using a RTUIS-type device appears to be feasible, although this has not been fully proven.

Factors supporting this conclusion include

- RTUIS images by transmission of ultrasound, therefore the predominant forward scattering is a good match for the instrument.
- Shifts in the speckle pattern imaged by RTUIS have been observed verifying the underlying assumption.
- RTUIS is capable of measuring the very small shifts in frequency predicted for the practical application, due to the small component of velocity nominally parallel to the axis of the ultrasound beam.

It appears that the requirements for further progress in detecting blood flow using RTUIS include development of a means for electronic detection of the frequency shift signal, and demonstration of detection using a flow loop of suspended particles in water.

Factors which will make practical application difficult include

- the open channel of the blood vessel (the lumen) of most blood vessels is too small to be resolved in the image. Nevertheless, frequency shifts may be detectable.

- the concentration of scattering centers (corpuscles) contributing to the frequency shift will be small resulting in very scattered (low frequency shifted) energy relative to unscattered energy. This results in a low fringe contrast, and subsequently a low S/N.

References

P.A.J. Bascom and R.S.C. Cobbold. 1995. "On a Fractal Packing Approach for Understanding Ultrasonic Backscattering from Blood." *Journal of the Acoustic Society of America*, vol. 98, no. 6.

B.B. Brenden. 1994. "Ultrasonic Holography Using a Liquid Surface Sensor." *International Advances in Nondestructive Testing*, vol 17, ed. by Warren J. McGonnagle, Gordon and Breach Science Publishers, Langhorne, Pennsylvania, pp. 31 - 62.

Experimental Toxicology

Determination of Estrogenic Effects of Environmental Contaminants

Ann S. Drum (Marine Sciences Laboratory)

Study Control Number: PN97029/1170

Project Description

The objective of this project is to develop a model using male rainbow trout to screen for endocrine-disruptors in the environment. Controlled laboratory experiments were used to establish a dose-response relationship based on the internal dose of a synthetic estrogen and the induction of a biomarker (vitellogenin) in the blood of rainbow trout. This pharmacokinetic - pharmacodynamic model describes the changing plasma levels of an environmental estrogen and the appearance and decline of vitellogenin. These parameters can be measured for various xenobiotics and compared to estimates for estrogen. Also, the model can be used to simulate vitellogenin levels in wild fish populations potentially exposed to environmental estrogens. These studies will provide support for the use of fish to screen for potential health effects of endocrine-disrupting compounds in the environment for both human and environmental risk characterization and will have wide application in environmental monitoring programs.

Technical Accomplishments

A number of in vivo and in vitro bioassays have been developed to assess the estrogen-like activity of xenobiotics in animals. A commonly used endpoint with in vivo studies is the induction of the female egg protein vitellogenin (Vg) in male fish. The presence of vitellogenin in the plasma is especially significant in male fish, which only produce this protein if exposed to estrogen or estrogenic compounds. Typically, these studies administer the xenoestrogen via water exposure or intraperitoneal injection and sacrifice fish at one or at most a few time points to monitor plasma levels of vitellogenin. However, induction of vitellogenin is a dynamic process, and the lack of detailed knowledge regarding induction and elimination rates of vitellogenin in fish can make it difficult to assess the degree of induction following exposure to a xenobiotic.

This study combined pharmacokinetic approaches to estimating target organ concentrations of a xenobiotic with simultaneous measurement of the vitellogenin plasma-time profile for individual fish. Internal dose is based on the plasma concentrations of tested chemicals using trout fitted with intravenous cannulas (Figure 1). This experimental design allows for serial removal of blood and calculation of the plasma area under the curve. This will permit interspecies comparisons of sensitivity to environmental estrogens based on internal dose and allow for a more valid estimation of risk to humans to be calculated.

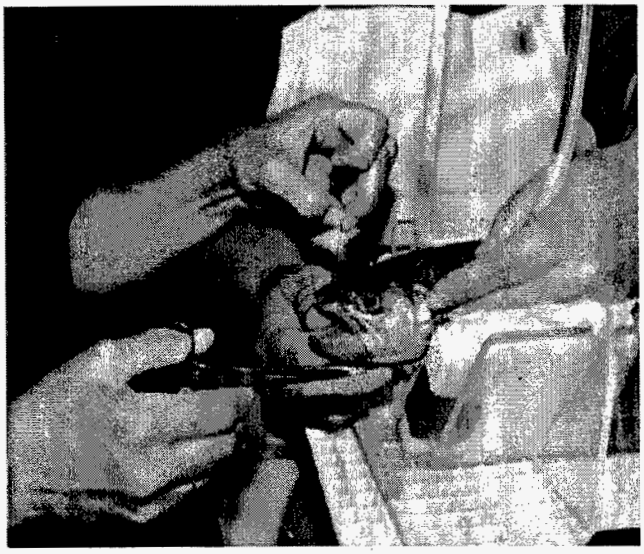

Figure 1. Fitting a male rainbow trout with an intravenous cannula while the fish is under a general anesthesia.

A range of doses of a potent synthetic human estrogenic compound—ethynlestradiol—was administered, and blood samples were collected via cannula (intravenous system) from individual fish over time. In this study, we administered ethynlestradiol (0.1, 1.0, and 10.0 mg/kg) to male rainbow trout via a dorsal aortic cannula, which allowed repetitive blood sampling from individual fish for up to 48 days after injection. The biomarker, rainbow trout vitellogenin was purified, and antibodies were

produced for use in an enzyme-linked immunosorbant assay. The pattern of induction of vitellogenin in plasma was similar for all doses of ethynlestradiol, which increased sharply after 24 hours and reached maximum levels by days 8 to 12 (Cmax = 12; 25 and 42 mg/mL Vg). The levels then rapidly returned to near basal levels by days 16 to 24 (Figure 2).

In addition to the synthetic estrogen, rainbow trout were exposed to DDT, an environmentally persistent pesticide that is known to disrupt the reproductive systems of a wide range of organisms.

Semipermeable membrane devices (SPMDs) consist of polyethylene sheets and have been shown to concentrate organic compounds in water. For this study, SPMDs were deployed for 2 weeks in the effluent stream of a Puget Sound municipality wastewater treatment plant. Plasma vitellogenin was not induced in male rainbow trout administered concentrated extracts from the SPMDs.

These studies will provide support for the use of fish to screen for potential health effects of endocrine-disrupting compounds in the environment for both human and environmental risk characterization and will have wide application in environmental monitoring programs.

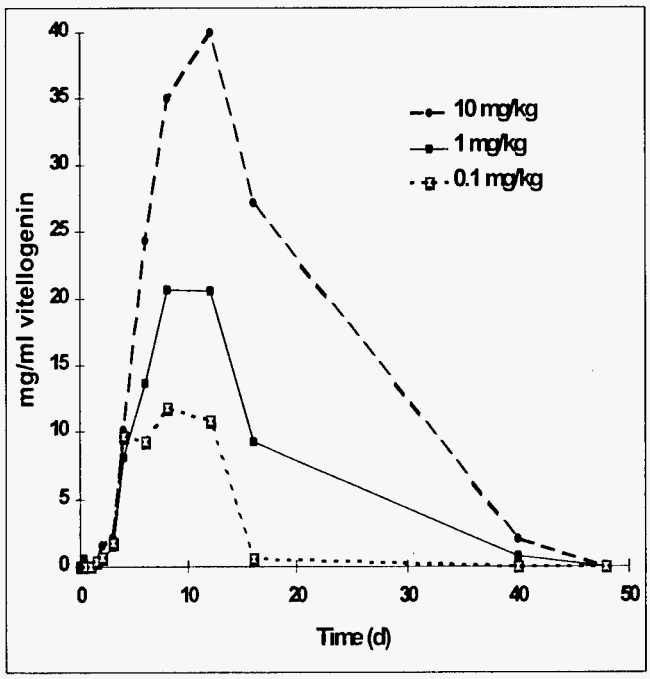

Figure 2. Plasma levels of vitellogenin in male rainbow trout administered ethynlestradiol (0.1, 1.0, and 10 mg/kg) via a dorsal aortic cannula.

Health Protection and Dosimetry

Detection of the Helicobacter Pylori *Infection Using Infrared Laser Breath Analysis*

James J. Toth (Systems Analysis)
Steven W. Sharpe (Chemical Structure and Dynamics)
Karla D. Thrall (Environmental and Health Sciences)

Study Control Number: PN95022/998

Project Description

The objective of this project was to identify disease-specific biomarkers in expired breath through the use of highly sensitive infrared laser detection. Breath analysis is an advancing technique that can help the physician diagnose disease in its earliest and most treatable stages. Spectroscopic interrogation of biomarkers in the breath using near-infrared lasers provides new measurement capability for simple, noninvasive testing. In this project, near-infrared lasers were used for the identification and speciation of breath ammonia.

Analysis of exhaled breath for the presence of chemical species indicative of specific diseases or as a means of following metabolic processes can be accomplished in several ways, including 1) measuring absolute concentrations of chemical species, 2) measuring altered ratios, or 3) measuring species after the administration of specific metabolites. In the third approach, the species should ideally contain a nonradioactive biomarker with a small natural abundance such as the isotope ^{15}N. A case in point is the measurement of exhaled ammonia, NH_3, for the diagnosis of *Helicobacter Pylori* infection.

The *H. Pylori* infection has been shown to be the major cause of duodenal ulcers and is implicated in gastric ulcers and in gastric cancer. In general, *H. Pylori* affects about 20% of persons below the age of 40, and 50% of those above the age of 60. Low socioeconomic status predicts the *H. Pylori* infection.

Since the *H. Pylori* bacterium is known to break urea down into CO_2 and NH_3, a large change in the ratio of $^{15}NH_3$ to $^{14}NH_3$ post-dosing is indicative of the presence of the *H. Pylori* infection. The ammonia biomarker may potentially be used to identify other disease states, such as the increased metabolism of certain amino acids, and perhaps as an indicator for physical or chemical trauma.

Technical Accomplishments

During FY 1997, a real-time bench-top apparatus for near-infrared breath analysis was developed, and most of the preliminary issues concerning laser-based breath analysis for ammonia in humans were addressed. Protocols for human subject testing were prepared, reviewed, and approved by PNNL's Human Subjects Review Committee. The effects of fasting on breath-ammonia were determined. Administration of standard meals prior to testing were found to reduce breath-ammonia measurement levels. Therefore, all breath tests were conducted on fasted human subjects.

The methodology developed for human breath sampling and measurement permitted the ability to measure breath-ammonia as it is exhaled. Approximately 20 human subjects were fed non-isotopically enhanced urea (300 mg urea in 200 mL of water) and their breath ammonia levels monitored over a 20-minute period. Unfortunately, we were unable to clearly define the discriminating feature of ammonia exhalation for *H. Pylori* positive subjects because of the large natural abundance of ammonia in human breath, the wide variation of ammonia exhalation patterns in human subjects, and the effect of body weight upon ammonia exhalation patterns. Thus, collecting clean biokinetic exhalation data may necessitate the administration of urea tagged with a nonradioactive biomarker such as ^{15}N, to discriminate ammonia exhaled from the hydrolysis of urea as a result of the presence of *H. Pylori*.

A typical exhalation pattern of ammonia before and after ingesting urea is shown on Figure 1. Further development of the detection of *H. pylori* infection using the near-infrared laser-based breath analysis is dependent upon the measure of exhaled ammonia tagged with nitrogen ^{15}N following administration of tagged urea.

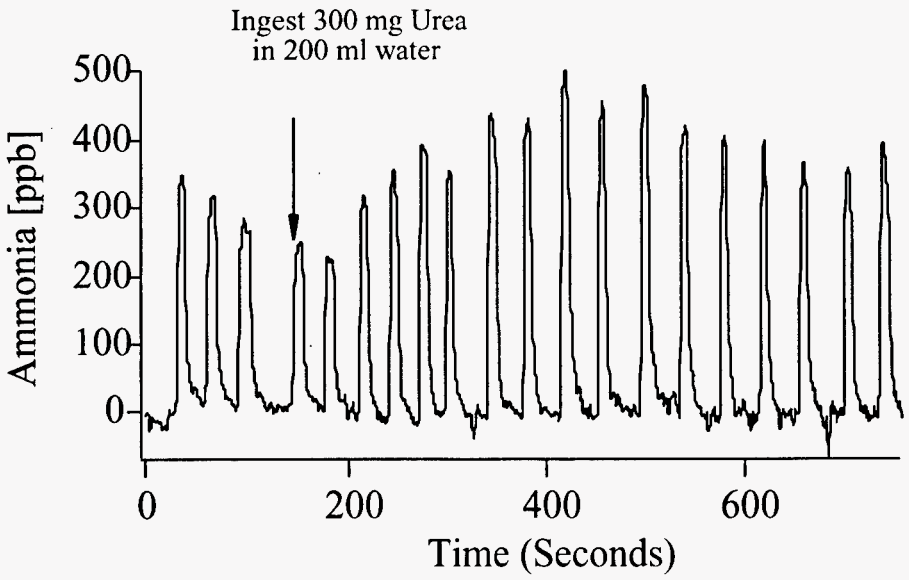

Figure 1. Test data from *H. Pylori* negative patient. Each feature or "blip" corresponds to an individual exhalation into the instrument. Note the apparent decrease followed by increase of ammonia after ingesting sample.

Development of PBPK Modeling for Mixed Waste Applications

Karla D. Thrall, Richard A. Corley, Charles Timchalk, Richard Traub (Environmental and Health Sciences)

Study Control Number: PN97037/1178

Project Description

Physiologically based pharmacokinetic (PBPK) models continue to increase in popularity in the field of chemical toxicology. This is attributed, in part, to demonstrated success in using scientifically validated PBPK models to replace conservative default assumptions in regulatory risk assessments, and in setting threshold limit values for ACGIH (American Conference of Governmental Industrial Hygienists), and reference doses and reference concentrations for the Environmental Protection Agency.

Background

An ongoing challenge to the cleanup efforts at DOE sites has been the potential for exposures to mixed radionuclide and chemical wastes. The objective of this project was to begin to address the health issues associated with exposures to complex mixtures by initiating a collaborative effort between investigators conducting PBPK modeling of chemicals and investigators conducting anatomical modeling of energy deposition from radionuclides. The ultimate goal is to develop models that accurately predict the target tissue dosimetry and potential for interactions between chemicals and radionuclides in humans exposed to mixed waste.

A PBPK model is used to simulate the absorption, distribution, metabolism, and elimination of a compound (and its metabolites, if applicable) in the body. The models have a biological basis which incorporates important organs and tissues, and links them by arterial and venous blood flows. Chemical-specific information, such as absorption rates, tissue to blood partition coefficients, metabolism, and elimination rates are incorporated into the physiological models to describe chemical disposition dynamics in any species under a variety of exposure conditions.

Radionuclide modeling has developed using biokinetic models to describe the deposition of energy (e.g., α, β, or γ) from radionuclides based on the anatomical location of the nuclide, decay rates, and elemental composition of the tissues. Absorption, distribution, and elimination of the radionuclide is generally modeled as a first-order process between compartments.

Each modeling approach offers unique advantages that can significantly improve mixed chemical and radionuclide modeling if properly integrated.

Technical Accomplishments

A significant challenge in the integration of the two modeling disciplines was to develop a common understanding of the language, model structures, and software. The most widely used software product in PBPK modeling is SimuSolv (The Dow Chemical Co.). This multifunctional package is designed to allow for simulation of behavior of a system (physical or biological), optimization of performance, and estimation of best values for model parameters. This software was selected for integration of PBPK modeling with radionuclide biokinetic modeling because of the simple interface between the user and the Fortran subroutines.

A simple one-compartment saturable elimination model was developed to compare the physiological model to the biokinetic model where material is transferred by empirical zero- or first-order rates. Additional physiological reality was added to the one-compartment model to develop an isolated perfused liver model with a known volume, blood flow rate, and metabolic capacity. In this model, the concepts of blood flow limitations versus metabolism limitations on the elimination of the compound were compared.

A complete PBPK model containing all relevant tissue groups was developed for the test chemical—methylene chloride. This model was used to demonstrate the experimental basis behind the estimation of the critical chemical-specific parameters used in the PBPK model: tissue to blood and blood to air partition coefficients and rate constants for the two competing metabolic pathways for methylene chloride. Using this model, route-to-route extrapolations of administration (oral, inhalation, intravenous injection, etc.), high to low dose extrapolations, and the impact of dose-rate on simulated internal doses of toxic metabolites at target tissues were compared across species.

This process of building a PBPK model was compared with the process of building a biokinetic model for a

radionuclide to develop a common understanding of terminology and modeling philosophy. An outcome of this project will be a collaborative proposal directed at DOE for development of a biologically based model for a combined exposure to a chemical and a radionuclide. Such a model can form the basis for sound, biologically based assessments of potential human health risks to mixed wastes, and thus enhance DOE's cleanup efforts.

Development of Specific Absorption Rate (SAR) Measurement

Matthew H. Smith (Environmental Technologies)

Study Control Number: PN97038/1179

Project Description

The objective of this project is to develop the capability to measure specific absorption rate (SAR) for electromagnetic radiation. This type of radiation is emitted by products such as cellular telephones.

In recent years, there has been increased attention paid to the safety of devices that emit radio frequency (RF) and microwave (MW) radiation. The most common device to receive scrutiny is the hand-held cellular phone. In response to public concerns regarding RF/MW safety and directives given in the Telecommunications Act of 1996, the Federal Communications Commission (FCC) has developed rules on the subject of RF/MW safety for emitters that require a FCC license.

A component of these rules calls for the evaluation of SAR for RF/MW devices designed to be held within 20 cm of the human body. Accurate measurement of SAR requires small electric field probes and realistic human phantom models.

Technical Accomplishments

During FY 1997 progress was made in the areas of electric field probe procurement and the development of a standard human model for SAR measurements.

A miniature broadband electric field probe was procured from Loral Microwave-Narda. This probe works with existing equipment at PNNL and allows the evaluation of electric fields in the frequency range 400 MHz to 26 GHz. Initial tests of the probe showed that emissions from current generation cellular phones in the 825 MHz to 890 MHz frequency range could be measured. Electric field strength values at 1 m from phone were typically <3 V/m. The broadband nature of the probe will also allow measurements to be made on "next generation" PCS phones that operate in the 1800 to 2200 MHz range.

Development of an appropriate human phantom model was enhanced by PNNL's participation on IEEE Standards Coordinating Committee (SCC) 34. This standards body is currently working on recommendations for performing SAR measurements. Their work is continuing at a rapid pace due to the impending FCC rules and requirements. Prior to the work by this committee, no standard method for SAR measurement was defined. PNNL's participation on this committee gives us a "ground floor" entry into SAR measurement work.

By year end, SCC 34 had issued a draft of their recommendations for a human phantom. Once these are finalized, PNNL will proceed on the construction of a phantom for our SAR measurement system.

Performance Testing of Non-Radiological Instrumentation

Judson L. Kenoyer (Environmental Technologies)

Study Control Number: PN97083/1224

Project Description

The objective of this project was to initiate the development of performance testing capabilities for non-radioactive gas and aerosol monitoring and sampling instrumentation. Several pieces of equipment were moved to the 318 Building from LSL-II and transferred from the Toxicology Department. This equipment included aerosol monitoring instruments and exposure equipment. Efforts performed included setting up the exposure equipment and making it operational and establishing the capability to use the aerosol monitoring instrumentation. The majority of the effort was focused on the development of specific performance testing criteria, establishing a relationship with NIOSH instrument performance testing personnel and selected instrument vendors, and conducting research to determine the optimum testing parameters. Initial testing of gas and aerosol instruments using the exposure system was planned.

Technical Accomplishments

For several years, the Health Protection Department has had the equipment and expertise to perform performance testing of radiation detection monitoring instrumentation. Several pieces of equipment were purchased with DOE funds in the 1980s to test instruments and evaluate draft ANSI standards in the N42.17 series. This equipment includes two environmental chambers, a vibration table, a shock testing system, radio frequency, microwave, and magnetic field exposure systems, electronic testing equipment, and an ambient pressure chamber.

Essentially all of the tests described in the ANSI standards for radiological instruments can be performed by personnel in the Environmental Technology Division with this equipment. There are some tests related to the testing of continuous air monitors (CAMs) that cannot currently be performed; the aerosol generation and monitoring equipment needed for the testing was not routinely available for use and a previously used exposure system is no longer available. With the transfer of the Toxicology personnel to BCO, some of the needed equipment became available for use in DOE projects. The equipment can be used to complete most of the capabilities needed to evaluate instruments against all of the testing criteria in the N42.17 standards and also begin to establish the capabilities for testing non-radiological instrumentation such as gas and aerosol monitors.

The exposure and aerosol monitoring equipment moved to the 318 Building had been used by personnel who are now working for BCO; they were able to assist in the establishment of the exposure system as operational.

During the past year, we have been able to obtain the exposure chamber and many pieces of aerosol monitoring equipment. The chamber is usable at restricted levels until the exhaust is connected into the facility exhaust system.

The involvement of PNNL staff on the AIHA Aerosol Technology Committee and the ACGIH Air Sampling Instruments Committee and the initial efforts to establish an in-lab performance testing capability have all had a positive influence on the interest of others to either be collaborators in the effort or to be potential clients of the services developed. A collaborative relationship has been initiated with NIOSH that will benefit both parties in the instrument performance-testing arena. Multiple instrument vendors have also expressed an interest in the possible use of the service once it has been established and have also offered to be part of the performance criteria development process.

The following were results from this year's efforts:

- Exposure and aerosol monitoring equipment was moved to the 318 Building in several phases. The exposure chamber has been set up in Room 122 and is operational at a restricted level; only non-toxic aerosols and gases can be used at this time. Toxicology personnel needed some of the aerosol equipment in on-going work until new equipment was purchased; all but two pieces of equipment have been delivered.

- The exposure chamber was made operational. This included manufacture of some hardware and interfaces and the loan of an air moving system from Toxicology. The operation of the system is being expanded. An effort within the facility to change to recirculating

ventilation within the building is affecting where the exhaust will be connected within the system; however, this will reduce the cost of the process of hooking up the exhaust.

- Development of standard operating procedures for the exposure system and the aerosol monitoring equipment is currently being performed (as needed).

- Discussions with NIOSH personnel have created a collaborative relationship where we will be able to develop performance-testing criteria together.

- Discussions with selected vendors have established collaborative relationships for the development of instrument performance-testing standards.

- Specific instrument performance-testing criteria have been developed and proposed testing procedures have been drafted and are ready for testing for the evaluation of instrument stability, accuracy, precision, temperature, and humidity. Other criteria being developed include ones for alarm setpoint, vibration, shock, and radio frequency, microwave, and magnetic field interferences.

- Discussions with other performance-testing researchers and decisions made based on past experience have resulted in the establishment of proposed optimal operating parameters.

- An initial plan has been made for a collaborative effort with NIOSH for the testing of NO_2 monitoring instrumentation.

Radium-223 Immunoconjugates for Cancer Therapy

Darrell R. Fisher (Radiochemical Processing)
D. Scott Wilbur (University of Washington, Department of Radiation Oncology)
William McBride (University of California at Los Angeles, Department of Radiation Oncology)

Study Control Number: PN96063/1130

Project Description

The purpose of this project is to prepare and test a radium-223-labeled immunoconjugate for therapy of cancer. An immunoconjugate is a protein antibody labeled with a radionuclide or other toxin. The protein recognizes a specific binding site on a cancer cell and directs the radionuclide to that cell. Radium-223 (half-life = 11.4 days) is a promising candidate for therapy of cancer because it emits four highly effective alpha particles and two beta particles in its rapid decay to stable lead-207. Radium-223 can be produced more readily and abundantly than other alpha emitters considered for radioimmunotherapy of cancer. It also emits gamma rays that are convenient for imaging and dosimetry.

The preparation and testing of a Ra-223 immunoconjugate involves several steps: 1) preparing a chemical cage for Ra-223, 2) functionalizing the cage with a linker position, 3) linking the cage to antibody, 4) testing the antibody-cage structure for chemical stability in serum, 5) evaluating whether the antibody retains immunoreactivity when it is linked to the Ra-223 cage, 6) studying the biodistribution of the labeled immunoconjugate in normal mice, and 7) studying the anti-tumor efficacy of the Ra-223-labeled immunoconjugate in tumor-bearing mice. This work is a follow-on effort to a separate project, "Radium Complexation and Linkage to Monoclonal Antibodies for Cancer Therapy" (elsewhere in this report). The purpose of that project was to develop a suitable cage structure for Ra-223.

Background

Radium is a highly electropositive element that is not easily chelated or linked to a protein antibody. The successful labeling of antibody with Ra-223 requires chemical bonds with sufficient thermodynamic and kinetic stability to remain intact in body fluids. Therefore, much of the early work on this project involved an effort to match the chemistry of the cage structure with the chemistry needed to attach the cage to the antibody.

Technical Accomplishments

A source of Ra-223 was prepared from purified actinium-227. Radium-223 was radiochemically separated and purified. Separate experiments were conducted to evaluate Ra-223 as a suitable radionuclide for applications in radioimmunotherapy. The short physical half-life of Ra-223 requires a separate extraction from Ac-227 for each experiment. Long-lived Ra-226 (1600 years) was used to test radium complexation.

A calix[4]arene-crown-6-dicarboxylic acid was discovered in FY 1997 to complex Ra-223 with high stability and selectivity over other competing metal and alkaline earth cations (see "Radium Complexation and Linkage to Monoclonal Antibodies for Cancer Therapy"). This cage has an optimum cavity size and oxygen electron sharing (covalent-coordination bonding) for high selectivity and stability.

The Ra-223 cage must be bifunctional, that is, it must hold Ra-223 at one end, and also bond covalently to the constant region of the antibody on the other end. Therefore, it was necessary to add a reactive group to the cage for linking to the antibody. The reactive may be an amide (NH_2) or carboxylate (COOH). However, it was not possible to link the cage to the antibody using carboxylate because both carboxylates at the bottom of the cage contributed to radium complexation. We tried to add an amide group at the top of the cage in place of one of the stabilizing *tert*-butyl groups. That synthesis proved to be more difficult than expected and produced a mixture of compounds containing one to four amides and a low yield of the monoanilino derivative.

Steps were then designed to resynthesize the radium cage using an anhydride calixarene as starting material. When available, the anhydride derivative of the radium cage will be reacted with mono-tBoc-protected diamine. The carboxylates at the bottom of the cage will be protected as esters. The cage will be hydrolyzed with base (leaving the tBoc intact). The tBoc will then be cleaved with trifluoroacetyl tetrafluorophenol (TFA) to make the

maleimide from the free amine. The linker will then react with the ϵ-amino group of lysine on the antibody at pH = 8.5 or through reduced disulfides (thiol conjugation) at pH = 6.5. This effort should result in an antibody-linker-cage structure, which can then be reacted with Ra-223 (chloride) to form the complete immunoconjugate. The Ra-223 immunoconjugate will then be evaluated as a potential therapeutic agent.

Plans for FY 1998 involve completing synthesis of a radium cage with amide linker group, testing the stability of the linker between the cage and the antibody, and testing the affinity and avidity of the antibody in vitro using the MCA-K cell line. Biodistribution studies will be made using normal and immunodeficient SCID mice, and the stability of the Ra-223 labeling will be determined. Of particular interest will be the comparative biodistribution of complexed Ra-223 and uncomplexed Pb-211 daughter in normal organs, tissues, and tumor implants. The tissues samples will be analyzed at PNNL by gamma spectroscopy. Tumor response studies will be conducted in collaboration with Professor Bill McBride at UCLA using an anti-CD44 human anti-breast carcinoma antibody and a transplantable human breast carcinoma (MCA-K) xenograft in SCID mice.

Other

During the search for a suitable ligand for Ra-223, two calix[4]arene derivatives were tested for their ability to chelate actinium-225. Actinium-225 is a 10-day alpha emitter (Geerlings et al. 1993) with radiological emissions similar to Ra-223 (four alpha and two beta particles). We found that 5,11,17,23-tetra-*t*-butyl-25,26,27,28-tetrakis(carboxymethoxy)calix[4]arene (Figure 1) and 5,11,17,23-hexa-*t*-butyl-37,38,39,40,41,42-hexakis (carboxymethoxy)calix[6]arene exhibited high selectivity for Ac-225 over alkaline, aline earth, and zinc metal ions under neutral and weak acidic conditions.

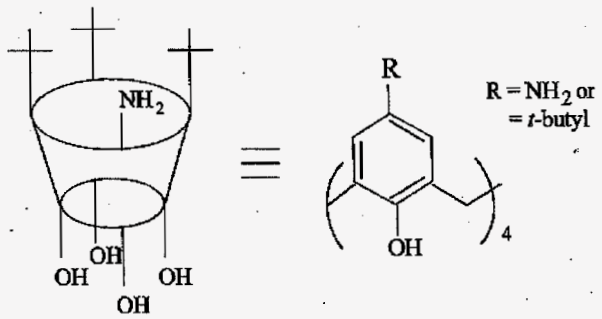

Figure 1. Structure of a tetrakis(carboxymethoxy)-calix[4]arene bifunctional ligand for actinium-225.

It was not possible to determine stability constants of the Ac-225 complexes using common spectroscopic or potentiometric titration methods because of the short physical half-life of Ac-225. However, relative stability constants were determined using a competition extraction method with ethylenediaminetetraacetic acid. This work showed the extraction constants of Ac-225 with either calixarene derivative to be on the order of 10^{12}. The discovery of a new complexing agent for Ac-225 provides future opportunities to develop and test an Ac-225 immunoconjugate in parallel with work on Ra-223 immunoconjugates.

Reference

M.W.Geerlings, F.M. Kaspersen, C. Apostolidis, and R. Van der Hout. 1993. "The Feasibility of ^{225}Ac as a Source of α-particles in Radioimmunotherapy." *Nucl. Med. Commun.* 14:121-125.

Publications

X Chen, M. Ji, D.R. Fisher, and C.M. Wai. "Carboxylate-Derived Calixarenes with High Selectivity for Actinium-225." *J. Chem. Soc., Chem. Commun.* (submitted).

D.R. Fisher and G. Sgouros. 1997. "Dosimetry of Ra-223 and Progeny." *Proc. 6th International Radiopharmaceutical Dosimetry Symposium*, Oak Ridge Associated Universities, Oak Ridge, Tennessee.

Hydrologic and Geologic Sciences

Determining Reactive-Well Design Parameters

Tyler J. Gilmore, Daniel I. Kaplan (Applied Geology and Geochemistry)
Mart Oostrom (Hydrology)

Study Control Number: PN97030/1171

Project Description

The reactive well technology is a new groundwater remediation method that modifies the typical groundwater well construction by replacing the filter pack sands with absorbents, bioamendments, oxidants, or reductants to form a selective reactive barrier around the well that detoxifies or stabilizes targeted contaminants. The filter pack reactant studied under this project was zero-valent iron (Fe^0).

Background

A filter pack in a well is a material, typically made of sand, that is placed between the well casing and the formation. The filter pack is designed to separate the formation material from the well screen and increase the effective hydraulic diameter of the well. The filter pack sand is replaced with, or impregnated with, absorbents, bioamendments, oxidants, or reductants to form a selective reactive barrier that would detoxify or stabilize targeted contaminants while permitting non-targeted groundwater constituents to pass through the filter pack freely. At least two configurations have been considered. The first configuration uses a re-circulating well, and the second uses a drain-field for reinjecting the treated water.

In an example application, the filter pack sand could be mixed with zero-valent iron metal. A groundwater pump would draw water into the well through the filter pack where the iron would reduce contaminants such as chlorinated solvents and some metals including chromium and uranium. The reduction detoxifies (e.g., TCE Cl^- + ethane) or stabilizes the contaminants (e.g., Cr^{6+} CR^{3+}) in place. The clean water drawn into the well could then be reinjected into a second zone within the well or injected into a drain field near the surface. The filter pack could also be modified with oxidants and/or absorbents to treat a wide range of contaminants.

This method greatly improves upon pump-and-treat approaches in that it treats the groundwater in the subsurface. There is no aboveground treatment or disposal required. Also, the re-circulating water "sweeps" through lower permeability zones that may not otherwise be influenced by typical pumping wells, decreasing the time required for remediation.

The well construction does not require specialized components or drilling methods. The primary difference from standard well construction is that the filter pack will include chemically reactive materials that will treat contaminated groundwater that flows through it.

Technical Accomplishments

This project provided the proof-of-principle testing in the laboratory by determining the required residence times of several common contaminants (Cr, TCE, TCA, and DCA) in a reactive filter pack composed of zero-valent iron (Fe^0) and sand. The reaction rates were found to vary based on the available iron surface area and water type. The reaction kinetics, determined from the laboratory-scale experiments were input into a multiphase flow and transport simulator (STOMP) to predict the effectiveness of the system in the field. These numerical investigations provided information required for designing these systems and will assist in identifying the environmental limits for which this technology is appropriate.

Publication

A technical white paper was prepared summarizing our laboratory and computer simulation results and provided to the Naval Research Center and the Naval Facilities Engineering Service Center.

Immobilizing DNAPL's Using Clathrate Hydrates

Daniel I. Kaplan (Applied Geology and Geochemistry)
Jagannadha R. Bontha (Chemical and Slurry Processing)

Study Control Number: PN97051/1192

Project Description

The use of the phenomena of clathrate hydrate formation by carbon tetrachloride (CCl_4), 1,1-DCE, TCE, and PCE in the presence of a help gas to stabilize the clathrate hydrate structure was examined with the objective of developing either an in situ or ex situ process for immobilizing or remediating DNAPL contaminated groundwater. Clathrate hydrates are ice-like structures that form under unique chemical, temperature, and pressure conditions. They differ significantly from ice in regard to their physical properties because they have a cage structure, as oppose to a sheet structure like common ice (ice Ih) (Figure 1). One important difference between common ice and clathrates is that the latter solid phase can exist at temperatures as high as 62°C (McMullan and Jeffrey 1959). Clathrate hydrates have been the subject of extensive research because enormous natural gas reserves exist within them (more fossil fuel exists as clathrate hydrates than as oil or coal [Sloan 1989]). The first objective of this study was to evaluate whether PCE, TCE, DCE, and CCl_4 could be included within clathrate hydrate structures through the use of help gases. Help gases lower the pressure and raise the temperature requirements for clathrate formation, thereby permitting their formation under conditions commonly found in the natural environment. The second objective was to evaluate the effect of two different help gases. The third objective was to evaluate the ability of clathrate hydrates to immobilize DNAPLs as dissolved species and as a separate phase.

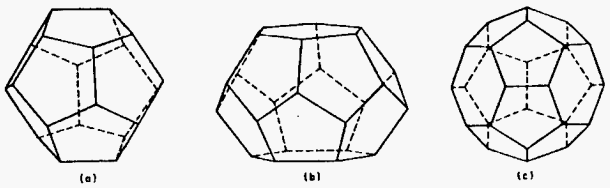

Figure 1. Three clathrate hydrate structures that can hold single DNAPL or gas molecules: (a) pentagonal dodecahedron, (b) tetrakaidecahedron, (c) hexakaidecahedron.

Technical Accomplishments

Clathrate hydrate dissociation temperatures (also referred to as hydrate melting point) for 1,1-DCE, CCl_4, PCE, and TCE with H_2S and xenon as help gases were determined at 1 atm (Figure 2). The melting point data for all the DNAPLs studied, except for 1,1-DCE, are close to or greater than 15°C. These results suggests that for groundwater contamination by CCl_4, TCE, and PCE, in situ immobilization of these DNAPLs may be accomplished by bubbling these gases into the plume, provided that the temperature of the groundwater is less than their melting point. Importantly, this process is not limited to the use of xenon, an expensive gas, or H_2S, a toxic gas. Based on thermodynamic consideration, it is quite likely that less expensive or less toxic gases such as CO_2 or mixtures of gases with CO_2 may also be used for this purpose.

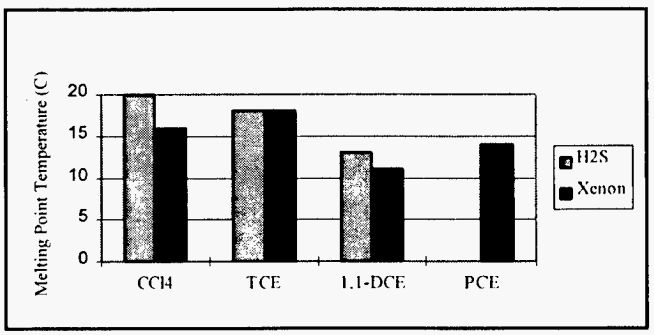

Figure 2. Melting point of various DNAPLs using hydrogen sulfide and xenon as help gases.

About 18% and 43% of the hydrate phase was determined to be composed of 1,1-DCE and CCl_4. These results have relevance to ex situ separation options (the DNAPL clathrates could be separated by filtration), as they provide an enrichment factors of 200 and 500 from an aqueous solution saturated with 1,1-DCE (saturation concentration in water at 25°C = 200 ppm) or CCl_4

(saturation concentration in water at 25°C = 800 ppm), respectively. Also, unlike conventional ex situ processes which are dependent on the separation medium (e.g., activated carbon absorption on membrane separation), the clathrate process involves just a simple solid-liquid separation step.

The ability of clathrates to incorporated dissolved CCl_4 (note: the CCl_4 is dissolved, not as a separate liquid phase) into their structures was determined at two CCl_4 concentrations. At 200 ppm CCl_4 in water, almost 92% of the CCl_4 was transferred to the hydrate phase. At 50 ppm CCl_4 in water, the separation factor was slightly lower (72%). It is likely that a much higher separation factors could have been achieved, had additional time been devoted to solid-liquid separation techniques. In conclusion, based on the melting point information and the long term stability tests, it appears that CCl_4, TCE, and PCE can be immobilized as stable clathrate hydrates in many groundwater plumes provided groundwater temperatures <13°C for PCE contamination and <15°C for both CCl_4 and TCE contamination. Through the use of other help gases, it is anticipated that the melting points of these DNAPL clathrate hydrates could be further increased, thereby increasing the range of temperatures that this immobilization technique can be employed.

References

R. McMullan and G.A. Jeffrey. 1959. *Journal of Chemical Physics.* 31:1231-1234.

E.D. Sloan. 1989. *Clathrate Hydrates of Natural Gases.* Mercel Dekker, Inc., New York.

Publication

J.R. Bontha and D.I. Kaplan. "Formation of DNAPL Clathrate Hydrates: Application for in situ Stabilization of Contaminated Groundwater." *Environ. Sci. Technol.* (in review).

In Situ Redox Manipulation Permeable Barrier Research

Mark D. Williams, Kirk J. Cantrell (Environmental Technologies)

Study Control Number: PN97053/1194

Project Description

A successful proof-of-principle in situ redox manipulation (ISRM) field experiment was conducted at the 100-H Area of the Hanford Site for determining the feasibility of altering the redox potential of an aquifer using a chemical reagent (sodium dithionite with a potassium carbonate/bicarbonate pH buffer). This technology is being developed to alter the redox potential of an aquifer in order to treat specific redox-sensitive contaminants in the groundwater (e.g., chromate, halogenated-hydrocarbon compounds). The goal of the first task is to develop a more efficient design for emplacement of a reduced zone in an aquifer to treat large contaminant plumes. The goal of the second task is to complete bench-scale experiments of the injection of Fe colloids in order to design a field experiment as another approach for creating a reduced zone in an aquifer.

Technical Accomplishments

LDRD research in FY 1997 for the first goal of this project involved with dithionite-treated sediment focused on the development of design tools to provide for the capabilities and confidence in the numerical modeling of the ISRM emplacement process. These studies included laboratory experiments, new capabilities in numerical modeling, and modeling of the 100-H Area field experiment as a means of validation for the methodology. Two features (a well function and first-order chemical reactions) were added to the STOMP (Subsurface Transport Over Multiple Phases) code.

An automated experimental system was designed and developed for measuring the reductive capacity and reaction rates of dithionite-reduced sediment using samples collected from both the Hanford 100-H Area and 100-D Area. This system features automated calibrations in order to determine probe drift over the multi-day experimental runs. Reactive transport parameters were determined by modeling/fitting of these column experiments. These parameters will then be used in the larger-scale reactive transport models of the field site. Differences were found in the formulation of the reaction kinetics to fit these column data from the earlier bench-scale experiments. Additional batch experiments are planned to investigate and resolve these differences obtained from the various scales of experiments.

TCE degradation experiments were also conducted using sediment reduced by dithionite which showed promising results. A 1-meter long column was constructed for these tests with a residence time of 1 week. The results showed that approximately 99% of the TCE was degraded ($\sim$1 day half-life) in the column effluent with the main degradation product of acetylene. The sediment treated about 30 pore volumes of groundwater with influent concentrations $\sim$1 ppm dissolved TCE. These results helped to support efforts for the application of the ISRM at sites with aquifers contaminated with dissolved TCE.

Proposed continuing research is the application of these tools in the testing and design of more efficient emplacement approaches for in situ redox manipulation in the treatment of large groundwater contaminant plumes. The goal of these refinements would be to decrease emplacement costs associated with well installation and reagents and to minimize wastewater and residual chemicals in the aquifer. The current design involves a single injection/withdrawal well where reaction rates and the geometry limit the radius of influence to about 10 m radially from each injection well. Long linear barriers are created by overlapping these 10 m radial cylindrical reduced zones. Alternative approaches to be tested using reactive-transport modeling include the use of horizontal wells or simultaneous operation of multiple injection and pumping wells to increase inter-well travel times. Accomplishments for the second part of this research project involving Fe colloids are discussed below. Fe shows great promise as an in situ reactive barrier material because of its applicability to a broad range of contaminants, rapid reaction kinetics, and the low cost and wide availability of the material. Several in situ reactive barriers composed of Fe have been constructed to date using trench-and-fill techniques, i.e., digging a trench in the flow path of a contaminant plume and backfilling the trench with reactant material or auger techniques. Although the trench-and-fill approach is effective, it is limited to sites where the aquifer material is porous, as opposed to fractured, depths that are shallower than about 20 m, and aquifers which are relatively thin (because excavations must be dewatered during construction).

Because of these factors and the fact that trench construction tends to be the single greatest expense for this remediation technique, innovative methods for installation of reactive barriers in the subsurface are needed. Our previous work has demonstrated the viability of an innovative approach for emplacement of an in situ treatment zone by the injection of a suspension of colloidal size (1 to 3 micron diameter) Fe particles into the subsurface. As the suspension of particles moves through the aquifer material, the particles are filtered out on the surfaces of the aquifer matrix.

During FY 1996, LDRD funds were used to develop the use of shear thinning or pseudoplastic viscosity amendments for improving the emplacement of the colloidal Fe suspensions in porous media. In contrast to a Newtonian fluid, whose viscosity is by definition independent of shear rate, certain non-Newtonian fluids are shear thinning, a phenomena in which the viscosity of the fluid decreases with increasing shear rate. Aqueous solutions of three polymers at different concentrations were investigated in this study: a synthetic high molecular weight polymer (partially hydrolyzed polyacrylamide, PA), a biopolymer (gum xanthan, GX), and a cellulose type polymer (carboxymethyl cellulose, CMC). The results of this work indicate that the use of shear-thinning fluids greatly improves the emplacement profile of suspensions of micron size Fe particles in porous media relative to suspensions without shear-thinning fluids. Use of these fluids will also permit the use of much lower flow rates than would be possible without them. Lower injection rates are desirable because it will decrease the number of injection wells required to emplace the barrier, thereby decreasing the installation cost of the barrier. This will greatly increase the range of subsurface environments that this emplacement technology can be used. The results of this work also indicate that additional data collected from column experiments at various suspension concentrations would allow the development of a simple empirical model for predicting the emplacement of the Fe colloids as a function of suspension flow rate, concentration, and total throughput.

Additional work conducted with porous media composed of quartz sand indicated that the technique would be applicable for pore velocities of between 0.010 cm/s and 0.154 cm/s. It was also demonstrated that the technique could be used for media with hydraulic conductivities between 1.0 x 10 m/s and 3.0 x 10.

During this work, a method was developed to measure the concentration of Fe in natural materials which contain Fe (as oxides and within basalt). As a result of this development, further work was modified such that it would be conducted with natural Hanford sediment instead of quartz sand.

Problems arose with the first column experiment conducted with the natural material. It was observed that a very high backpressure developed within the column during the injection of the Fe colloid suspension. This behavior was not observed with the quartz sand. A wide variety of experiments were conducted to determine the cause of this problem and if the problem could be circumvented. The results of these experiments indicated that it was not the Fe colloids that were clogging up the porous media and causing a high back pressure, but that the viscosity enhancers were adsorbing to the porous media and causing the columns to become clogged. The experiments were repeated with each viscosity enhanced previously used and a few that were not previously used. Attempts were also made to alleviate the problem by pretreating the columns with deionized water, a solution of 0.01 M CaCl, and the viscosity enhancers without the Fe colloids. Nothing that was done was able to prevent the viscosity enhancers from clogging up the column. As a result further work was discontinued until a more fundamental understanding of the interactions between the viscosity enhancers and natural media can be gained. With this knowledge it may be possible to determine the characteristics required for a viscosity enhancer that would not result in the clogging of the pores of natural media.

Publications and Presentations

K.J. Cantrell and D.I. Kaplan. 1997. "Injection of Colloidal Fe Particles in Sand Columns with Shearthining Fluids." *J. Environ. Eng.* 123:786-791.

K.J. Cantrell and D.I. Kaplan. 1997. *Injection of Colloidal Size Particles of Fe in Porous Media with Shearthinning Fluids as a Method to Emplace a Permeable Reactive Zone*. 1997 International Containment Technology Conference and Exhibition, St. Petersburg, Florida, February 9-12.

C.L. Wilson, M.D. Williams, J.E. Szecsody, and C.R. Cole. 1997. *Determination of Reaction Rates for the Reduction of Fe(III) to Fe(II) by Dithionite and Subsequent Oxidation of Fe(II) to Fe(III) by Dissolved Oxygen from Column Experiments*. Annual Meeting of the Geological Society of America, Salt Lake City, Utah, October 20-23.

Microbiologic Controls on Contaminant Behavior

Raymond E. Wildung (Environmental Science Research Center)

Study Control Number: PN95058/1034

Project Description

The primary objective of this investigation was to establish PNNL capability in organic geochemistry and in microbial physiology and biochemistry through joint appointments at Washington State University (in Pullman and at the Branch campus) that provided the advanced, long-term resources needed to link molecular-scale investigations in chemistry and microbiology to the solution of problems in environmental restoration.

Technical Accomplishments

Rapidly developing capabilities in molecular sciences at PNNL's Environmental and Molecular Sciences Laboratory (EMSL) must be linked to resolution of problems being faced by DOE in environmental restoration and waste treatment. Critical environmental issues addressed in this project included microbial biodegradation of contaminants and contaminant interactions at mineral-solution interfaces. In conjunction with hydrologic transport, these phenomena govern contaminant mobility in the subsurface and form the basis for development of new remediation concepts.

To address these issues, two new WSU positions were established, which in conjunction with developing capabilities at PNNL, will serve as a basis for proposed new research to define contaminant behavior and develop remediation concepts based on an integrated understanding of biological and chemical phenomena.

Microbial Physiology and Biochemistry

The position in microbiology is continuing to play an essential role in linking advanced capability in structural biology being developed in the EMSL with new capability in microbial physiology and biochemistry developed at WSU to bring new understanding to processes involved in degradation of organic contaminants in soils and groundwaters. In order to understand the reaction mechanisms and to improve the activities of a reductive dehalogenase, tetrachloro-*p*-hydroquinone (TeCH-RD) important in degradation of contaminants, a collaboration with EMSL was established to determine the three-dimensional structure and reaction mechanisms of the enzyme by NMR. Since TeCH-RD is a relatively large (20 kDa) protein, determining its structure requires NMR capabilities on the cutting edge of science, such as the 750 MHz NMR at PNNL. The protein has been over expressed and produced in sufficient quantities for NMR analysis. Significant progress has been made in stabilizing the protein, maintaining a monomer status, labeling it with N^{15}, and analyzing labeled and unlabeled products by two-dimensional NMR. Progress in determining the structure of the enzyme is described in another project by M.A. Kennedy, principal investigator.

Focus also has been on the molecular biology of nitrilotriacetate (NTA) degradation by Chelatobacter strain ATCC 29600. Nitrilotriacetate is a chelating agent, and its degradation is thought to decrease the mobility of heavy metals and radionuclides in the environment. An NTA monooxygenase (NTA-Mo) has been purified that catalyzes the oxidation of nitrilotriacetate to iminodiacetate and glyoxylate and its N-terminal amino acid sequence determined. The gene responsible for expression of this enzyme was cloned using an oligonucleotide probe developed on this project in collaboration with Dr. M. Kahn (Washington State University). The genes have been sequenced and a DOE project to apply this knowledge to mitigation of complexed radionuclide/metal was initiated under the DOE Natural and Accelerated Bioremediation Research (NABIR) Program in FY 1998.

The biochemistry of 2,4,5-trichlorophenoxyacetate (2,4,5-T) degradation by *Pseudomonas cepacia* AC1100 also has been under study. The compound 2,4,5-T is a chlorinated aromatic herbicide. In cooperation with Dr. A.M. Chakrabarty (University of Illinois) and Dr. R.L. Crawford (University of Idaho), this study focuses on understanding its biodegradation pathway and has provided much needed information on dehalogenation mechanisms. Three enzymes involved in the 2,4,5-T degradation pathway have now been purified and characterized.

The biochemistry of 3-chlorobenzoate degradation by *Desulfomonile tiedjei* is another exciting avenue of research instituted on this project. Reductive dehalogenation is the only known mechanism for remediation of many chlorinated compounds and this

research is challenging because *D. tiedjei* grows very slowly and requires strictly anaerobe conditions. In addition, the enzyme is a membrane protein. However, this research, in collaboration with Dr. W.W. Mohn (University of British Columbia), has successfully purified and characterized the enzyme, and has placed the WSU-PNNL team in the leading position to understand the reductive dehalogenation by anaerobic microorganisms. Research is continuing on cloning the corresponding genes.

Another continuing research effort is to define the biochemistry of ethylenediaminetetraacetic acid (EDTA) degradation by a newly isolated bacterium. EDTA is known to be responsible for mobilization of radionuclides in subsurface systems beneath DOE waste sites and to complicate separation of radionuclides in tank wastes. This research in collaboration with H. Bolton and J. Campbell at PNNL led to the first purification and characterization of an EDTA degrading enzyme. The purification of the monooxygenase is under way. Understanding the degradation of this chelate will provide the basis for technology to markedly reduce the likelihood of radionuclide mobility in the environment and during waste processing.

Two other efforts have been directly involved in bringing EMSL capabilities to bear on problems in microbial biotechnology. The first involves purification of a flavin-containing dehalogenase to examine the reaction at a single molecule level. A single protein image using a unique far-field microscope in the EMSL has been obtained in collaboration with S. Xie (principal investigator, related project). In an unprecedented observation, enzymatic turnover was observed at the single molecule level. These initial results led to a new project under the DOE NABIR Program. A second EMSL collaboration with M. Bowman (principal investigator, related project) involved purification of an iron-sulfur protein responsible for dehalogenation and subsequent analysis of the iron center by EPR.

Organic Geochemistry

These investigations focused on understanding the interactions between biodegradation processes as described above and physical and chemical partitioning phenomena in subsurface solute transport processes at multiple scales. Focus was on quantitative approaches for describing the kinetics of these reactions.

Research has been directed toward two thrust areas: degradation of refractory aromatic compounds and estimation of the impact of contaminant sorption on degradation. Biodegradation of naphthalene in multiphase systems containing nonaqueous phase liquids (NAPLs) indicated that relative to aqueous systems, conversion of naphthalene to CO_2 increased in the presence of decane, dodecane, and hexadecane. Biodegradation was apparent, but decreased in the presence of octane, and was negligible in the presence of hexane. Thus biodegradation was sustained in systems where log Kow of the NAPL was >5 and inhibited when log Kow of the NAPL was <4.

Research is continuing to elucidate the mechanisms controlling biodegradation in systems with residual NAPLs that are nontoxic to the bacteria, including the biodegradation of recalcitrant, 4-ring, polycyclic aromatic hydrocarbons. Five pure bacterial cultures that were able to use pyrene as a sole source of carbon and energy were isolated from contaminated soils. The organisms were classified by 16s rRNA analysis as *Pseudomonas* and *Arthrobacter* (genus level). This result is important for placing the organisms in an evolutionary framework and establishing the diversity of pyrene-degrading organisms. This was the first discovery of a gram-negative bacteria with the ability to degrade pyrene. Related research that addresses contaminant partitioning, mass transfer, and bacterial attachment at the NAPL-water interface will continue to explore the mechanisms governing biodegradation in systems that contain residual NAPLs.

A second research thrust, now complete, addressed the bioavailability of organic substrates in soil and groundwater systems. This research was directed toward developing simple methods for independently approximating biodegradation kinetics due to sorption of the contaminant on mineral surfaces in soil-water systems where availability of the substrate is decreased. An approach to accomplish this combined measured sorption parameters with the biodegradation rate constant that was determined in aqueous solution. This investigation indicated that the distribution of natural organic matter (NOM) between the solid and liquid phase significantly impacted both sorption and degradation processes in soils with natural organic matter $>5\%$. The natural organic matter accelerated other contaminant transport and the growth of the microbial population; increased microbial growth resulted in increased biodegradation. Biodegradation rates in soil-water systems were typically slower than the rates measured in aqueous suspension. An approach for predicting a decrease in the biodegradation rate was developed and evaluated for four soils. The approach worked well with the exception of a high organic matter soil where degradation was faster than predicted and explained by natural organic carbon in the system. The results have important implications for understanding bioremediation, reconciling observed differences between soil incubation and liquid culture rates, and predicting biodegradation rates in subsurface systems. For example, the approach can be used where cultured organisms will be inoculated into the subsurface. Research proposals are in preparation to further explore

the impact of natural organic matter on contaminant transport, information essential for understanding biogeochemical interactions that impact contaminant transport and persistence.

Publications

A. Chlopecka, A.P. Gamerdinger, R.K. Kolka, D.C. Adriano, and D.I. Kaplan. 1997. "Source and Practices Contributing to Soil Contamination." In: *Bioremediation of Contaminated Soils,* Soil Science Society of America (in press).

A.P. Gamerdinger, R.S. Achin, and R.W. Traxler. 1997. "Approximating the Impact of Sorption on Biodegradation Kinetics in Soil-water Systems." *Soil Sci. Soc. Amer. J.* 61:1618-1626.

A.P. Gamerdinger, R.S. Achin, and R.W. Traxler. 1997. "Impact of Sorption on the Kinetics of Naphthalene Biodegradation in Soil." *Soil Sci. Soc. Amer. J.* (in revision).

J.-Y Lee and L. Xun. "A Novel Biological Process for the Production of L-DOPA from L-tyrosine by p-hydroxyphenylacetate Hydroxylase." *Biotechn. Lett.* (submitted).

J.-Y Lee and L. Xun. 1997. "Purification and Characterization of 2,6-dichlorohydroquinone Chlorohydrolase from *Flavobacterium* sp. ATCC 39723." *J. Bacteriol.* 179:1521-1524.

J.W. Payne, H. Bolton, Jr., J.A. Campbell, and L. Xun. "Purification and Characterization of EDTA Monooxygenase from the EDTA-degrading Bacterium BNC1." *J. Bacteriol.* (submitted).

Y. Xu, M.W. Mortimer, T.S. Fisher, M.L. Kahn, F.J. Brockman, and L. Xun. 1997. "Cloning, Sequencing and Analysis of a Gene Cluster from *Chelatobacter heintzii* ATCC 29600 Encoding Nitrilotriacetate Monooxygenase and NADH:flavin Mononucleotide Oxidoreductase." *J. Bacteriol.* 179:1112-1116.

L. Xun "Purification and Characterization of Chlorophenol 4-monooxygenase from *Pseudomonas cepacia* AC1100." *J. Bacteriol.* (submitted).

Speciation of Uranyl Aqueous and Surface Complexes by Cryogenic Spectroscopic Methods

Donald M. Friedrich (Environmental Dynamics and Simulation)

Study Control Number: PN96067/1134

Project Description

The objective of this project is to develop cryogenic techniques for improving the resolution of optical spectra of actinide complexes in aqueous and mineral suspension phases. Improved spectroscopic resolution will provide greater detail in the speciation of the actinide complexes both in solution and at aqueous/mineral interfaces. The results obtained for aqueous speciation will serve as the baseline for the interpretation of surface speciation and help us understand the interrelationship between solution and surface species as well.

The goal of this project is to 1) determine speciation of uranyl complexes in aqueous-phase and on aqueous/clay interfaces and 2) elucidate structural detail about the complexes and their binding sites. In support of these goals, research will be focused toward the near-term objectives to 1) produce hyperquenched cryogenic films of uranyl complexes in aqueous solution and clay suspensions; 2) measure excitation and fluorescence spectra at high resolution by laser excitation methods, including laser-induced fluorescence line-narrowing and hole-burning spectroscopy; and 3) analyze the vibronic structure of the spectra in terms of structures determined for model uranyl complex systems (e.g., uranyl on alumina, silica). This research draws upon knowledge, technology, and instrumentation recently developed in the EMSL (amorphous water ice films, electrospray technique, and laser induced sorbate fluorescence) in order to exploit the well-known effect of cryogenic line-narrowing spectroscopy for the purpose of obtaining improved resolution of sorbate structural data. This is a new technical approach to the problem of surface complex speciation.

Technical Accomplishments

Aerosol Hyperquenching Vacuum Cryostat

The following modifications were made to the apparatus.

- The original turbo pumping system was replaced with a higher pumping-speed system capable of operating at higher inlet pressure during deposition.
- A differentially pumped chamber was added between the atmospheric pressure aerosol generation chamber and the vacuum cryostat.
- Conical skimmers were added to the inlet and outlet ports of the differentially pumped chamber.
- A fast electropneumatic gate valve was mounted at the outlet of the differentially pumped chamber to permit pulsed deposition of aerosols. Pulsed deposition will enable operation of the vacuum cryostat at a lower average pressure than possible with simple steady-state deposition.

High Resolution CW Dye-Laser Configured for Blue (460-500 nm) Excitation

Laser-induced fluorescence line-narrowing requires the use of a narrow line-width dye laser that can be tuned to vibronic bands near or at the electronic origin of the absorption band of the fluorescing electronic state. For excitation of uranyl cations, this requires a tunable laser in the 460 to 500 nm region. Our existing narrow line-width dye laser (an older model Coherent 899-29) was previously configured for longer wavelengths and had not been operated in the blue. In FY 1996 the dye-laser was fitted with optics for operation in this spectral region. Further testing in FY 1997 revealed the need for additional vendor servicing of this laser and training of PNNL staff on the alignment and short wavelength operation of the laser.

The vendor was contracted for a site visit in FY 1997 to bring the laser up to specifications and to train a PNNL laser scientist (Alan Joly) in short wavelength operations and techniques. An additional brief site visit is planned for early FY 1998 to bring the electromechanical wavelength scanning mechanism up to specifications.

Chemical Process Permit

Aqueous uranyl samples are less than 8.4 pCi/g total activity of depleted uranium and its progeny. The previous chemical process permit for handling the dilute uranyl samples was deemed invalid for EMSL, and another round of permitting was called for. This process is ongoing.

Nonradiological Model

The simple polynuclear aromatic hydrocarbon tetracene (2,3-benzanthracene) has been identified as a spectroscopic surrogate for the laser-induced fluorescence line-narrowing measurements proposed for uranyl. The fluorescence spectrum of tetracene lies in the same wavelength region (480 to 580 nm) as uranyl and also possesses a simple four-line vibronic structure. Site narrowed spectroscopy of tetracene is known in cryogenic polycrystalline solvents, which to the best of our knowledge, have not included aqueous media. The low solubility of tetracene in water (10^{-3} mg/L) sets its absorption coefficient (product of extinction coefficient and concentration) at approximately 4×10^{5} cm^{-1}—an excellent model for visible excitation of the proposed uranyl solutions (approximately 10^{4} cm^{-1}). We anticipate that the majority of preliminary work involving optimizing the experimental conditions for deposition, laser excitation, and spectroscopic measurement will be performed with the tetracene surrogate, which is not subject to unusual permitting or handling. The cryogenic aqueous tetracene spectra will be of environmental relevance in the field of PAH/water contamination, as well as in the area of fundamental understanding of solvent/solute interactions of large PAH compounds in water. The tetracene model will enable us to proceed immediately in developing the experimental methods, in anticipation of eventual permitting of uranyl use in EMSL.

Stochastic Methods for Bioremediation and Geochemical Modeling

Brian D. Wood, Ellyn M. Murphy, Tim R. Ginn (Interfacial Geochemistry)
Carver S. Simmons (Hydrology)

Study Control Number: PN97099/1240

Project Description

The objective of this project was to develop a statistically based (also known as a "stochastic") approach for subsurface solute transport where biologically mediated reactions may be involved. The descriptions of these processes are often complicated by the fact that they occur under transient flow conditions. Conventional stochastic approaches generally fail for transient flow conditions, and thus there have been few attempts to develop statistically based approaches. Through this research, we have developed a stochastic approach that is applicable to reactive transport under transient flow fields. This new approach has immediate applications to nonlinear reactions which are important in bioremediation processes. To accomplish this task, we applied unique mathematical tools borrowed from the fields of quantum electrodynamics and turbulent diffusion theory.

Technical Accomplishments

The prediction of transport and reactions of solutes in subsurface environments is a difficult problem because of uncertainty in the parameters involved. The variation in these parameters has been clearly indicated in field observations; for example, it is well known that field measurements of hydraulic conductivity show substantial spatial variation at multiple scales. Therefore, statistical information is used to characterize the distribution of relevant parameters. Stochastic models often provide the only feasible approach for describing transport and reactions in such environments.

Although there has been tremendous progress in the applications of stochastic theory to the problems of subsurface hydrology, the problems of reactive transport and transport under unsteady flow field conditions have only begun to be studied, even though these are the conditions that may prevail for many environmental remediation efforts.

Conventional approaches in subsurface hydrology generally describe transport from either the Eulerian (fixed frame of reference) or the Lagrangian (frame of reference that moves with the flow field) perspectives. We have developed a mixed Eulerian-Lagrangian method for describing the ensemble-average behavior of subsurface solutes. This has been accomplished by the use of particular operators that act to "translate" along the trajectories (i.e., the paths that particles released into the flow field would follow). These operators allow the equations that describe the reactive transport to be written from a Eulerian perspective. Additionally, under transient flows these translation operators do not in general commute with one another; that is, the order that the translation operators are applied is important. To handle this difficulty, we have relied on a technology that was developed for the theory of quantum electrodynamics known as the operational calculus of time-ordered exponentials.

One difficulty with conventional Eulerian approaches for developing the ensemble-averaged equations for transport is the so-called "closure problem." This arises because in conventional perturbation expansions, terms that are expressed as products of the perturbations arise. This leads to an infinite hierarchy of equations that must be solved ("closed") to obtain the final ensemble-averaged transport equation. We have adopted a renormalized cumulant expansion rather than a regular perturbation expansion. The resulting ensemble-average equations are closed by truncating this expansion. One advantage that this has over conventional techniques is that the conditions for which this truncation are appropriate can be precisely expressed in terms of a restriction. This restriction gives, in terms of dimensionless quantities, the conditions under which the truncation is valid. Under the conditions of such a restriction (which is known in the physics literature as a Kubo number restriction), a second-order accurate equation describing the reactive transport can be developed. For the case of linear, first-order reaction kinetics, the resulting ensemble-averaged equation can be

expressed in a form that resembles the conventional advection-dispersion-reaction equation (Figure 1).

$$\frac{\partial\langle c(\mathbf{x},t)\rangle}{\partial t} = \mathbf{D}^*(\mathbf{x},t):\nabla\nabla\langle c(\mathbf{x},t)\rangle - \mathbf{v}^*(\mathbf{x},t)\cdot\nabla\langle c(\mathbf{x},t)\rangle - \mu^*(\mathbf{x},t)\langle c(\mathbf{x},t)\rangle$$

Figure 1. The second-order-accurate transport equation developed by a renormalized cumulant expansion for a (first-order kinetic) reactive solute. The effective parameters (denoted by asterisks) are defined in terms of time integrals of Lagrangian covariance functions.

The ensemble-averaged transport equation contains effective parameters that are indicated by an asterisk in Figure 1. These effective parameters are nonlocal in time and space and time; in other words, they are defined by integrals of covariance functions along trajectories. The resulting transport equation is, however, local in the ensemble-average concentration. Some theories of stochastic subsurface transport result in equations that are nonlocal in the concentration, and are therefore very difficult to apply. The local form of the equations developed in this research, then, are an advantage when it comes to experimental and field applications.

The renormalized cumulant expansion method has some unique advantages for describing reactive transport in the subsurface. It has been successfully applied to develop the ensemble-averaged (upscaled) equation for reactive transport at the field scale, and has immediate applications for multicomponent reactive transport with nonlinear reactions. The theory is developed to a state that it is presently ready to be tested by applications to field data for reactive subsurface transport.

Publications

B.D. Wood and M.L. Kavvas. "Ensemble-averaged Equations for Reactive Transport Under Unsteady Flow Conditions." *Water Resources Research* (submitted).

B.D. Wood, T.R. Ginn, and M.L. Kavvas. "A Connection Between Stochastic-Convective and Cumulant Expansion Methods." *Advances in Water Resources* (in preparation).

Subsurface Reactive Transport

Steven B. Yabusaki (Hydrology)

Study Control Number: PN97100/1241

Project Description

This project will provide an efficient and flexible framework for performing fully-coupled, high-resolution, three-dimensional, nonisothermal, multiphase, multicomponent, high-ionic strength, reactive transport simulations. These simulations are necessary for fundamental advancements in the understanding of contaminant behavior in the subsurface and in the assessment of remediation strategies. Critical issues that will benefit from this level of analysis include: contaminant migration beneath the Hanford SX Tank Farm, low-level and high-level radioactive waste management design, natural attenuation efficacy, in situ treatment design and operation, and optimization of integrated remedial activities. In recognition of the importance and difficulty of modeling the subsurface, the Department of Energy has classified this analysis of multiple biological and chemical components reacting in complex subsurface environments as a scientific and computational "Grand Challenge." The approach is to build on PNNL strengths in subsurface simulation (multiphase fluid flow and reactive transport) and high performance computing (EMSL computational chemistry experience) to provide advanced applications software for these grand challenge problems, and to develop software tools and procedures that will be deployed on PNNL's massively parallel computer systems.

Technical Accomplishments

An interdisciplinary team of subsurface scientist/ engineers, applied mathematicians, and computational scientists is working on the parallel multiple-phase subsurface flow and reactive transport simulator. Over 35,000 lines of new source code were generated by the team. The high productivity of the code development is due, in large part, to the use of a parallel Fortran preprocessor (PFP) that was developed by one of the team members. The PFP allows the physics in the model to be programmed at a very high level without explicitly considering the low-level details of parallel processing (e.g., data distribution over processors, message passing, synchronization, parallel I/O). This approach preserves the software investment because the Fortran-90 coded algorithms are reusable. Furthermore, preliminary testing of the reactive transport module indicates that the PFP delivers extremely good performance and scaling on the newest configuration of NWMPP1, the EMSL massively parallel computer (Figure 1). It should be mentioned that the PFP generates portable Fortran code that runs on our SGI workstations, as well as the 512 processor IBM SP (NWMPP1) without modification of the high-level algorithms.

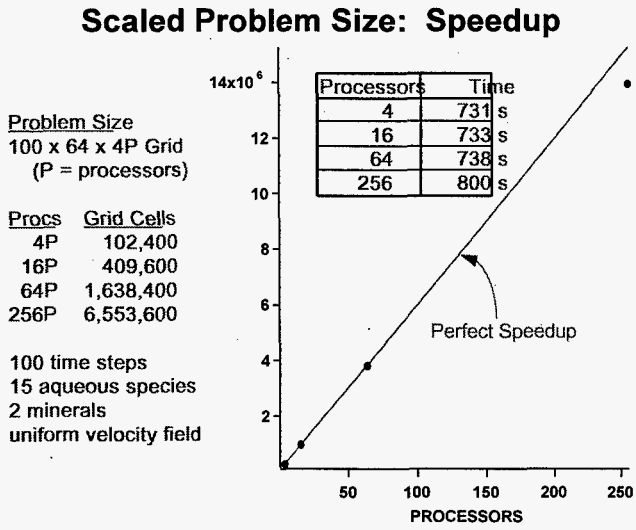

Figure 1. Scaling of processor performance for parallel reactive transport simulation.

We have written and performed verification simulations on three operational modes of the multiphase fluid flow module, giving it capabilities for solving hydrologic systems characterized as aqueous with a passive gas phase, aqueous-gas, and aqueous-gas with kinetic air dissolution. The use of distinct air quantities allows for kinetic dissolution (interphase mass transfer) of the air, a feature that will be required to accurately model the redox barrier technology on the Hanford Site.

The linear equation systems that result from numerical discretization and linearization of the governing partial differential equations that describe multiple-phase subsurface flow and transport generally are poorly conditioned. Iterative solution techniques frequently fail for these types of problems that can contain several numerically stiff zones within a single computational

domain. Parallel algorithms for the solution of these systems are being developed by Dr. Joel Malard. Dr. Malard designed and coded parallel Fortran 90 versions of the quasi-minimal residual (QMR), conjugate gradient squared, and bi-conjugate gradient stabilized (Bi-CGStab) non-symmetric iterative linear equation solvers, which have been incorporated into the water operational mode of the multiphase fluid module. A significant effort has been made to accelerate convergence by testing various starting vectors and making use of eigenvalue estimates from the Lanczos process. Performance improvements to the iterative solvers have been demonstrated by implementing improved matrix-vector multiplication schemes, by replacing "c-shift" structures with "for-all" structures, and by incorporating data information for cache, stride, and hops.

The chemical equilibrium model GMIN has successfully been linked with our transport module so that robust speciation calculations are now possible even with complex nonideal chemistry. We are evaluating the CPU requirements and the convergence success/failure rate for GMIN against other generic minimization algorithms so that guidelines can be established on when to opt for these solvers. A number of DAE solvers, including DASSL, RADAU5, LSODI, and LIMEX, have been evaluated for computational accuracy and speed on the mixed equilibrium/kinetic reaction module. We are currently addressing several issues regarding the numerical solution of initial-value DAE systems with these solvers.

A new "split-kinetics" approach for coupling reactions and transport has been developed. Initial tests on the transport of a radionuclide in a one dimensional column with a Langmuir isotherm showed that the approach is an order of magnitude faster than conventional techniques for solving this problem, while yielding a near-analytic solution. Multidimensional test problems with more complex reaction mechanisms remain to be tested. Additional analysis of the numerical schemes and their implementation is currently under way for nonlinear hyperbolic systems in multiple dimensions. A series of analytic solutions have been developed for the initial-boundary value advection-reaction problems in two dimensions with nonuniform flow patterns and nonlinear reactions. These analytic solutions will be used in testing the accuracy of new schemes and in code verification. We expect these problems and their analytic solutions to be adapted as tools for code verification by the transport modeling community.

In the course of model development and testing, several applications have been performed: chemistry - uranium redox, lead dissolution, and migration; reactive transport - organic carbon degradation and redox (15 species, 2 minerals, 4,194,304 grid cells); unsaturated reactive transport - injectable chemical treatment zones - redox manipulation at the 100-D Area. A visualization software package, pV3, designed for use with simulations on multiprocessor platforms, was successfully installed and tested on NWMPP1 and a 4-processor SGI workstation. pV3 permits real-time visualization and steering of complex, highly resolved three-dimensional simulations.

Publications and Presentations

S.B. Yabusaki, C.I. Steefel, and B.D. Wood. 1997. "Multidimensional, Multispecies Reactive Transport in Nonuniform Velocity Fields: Code Verification using an Advective Reactive Streamtube Approach." *Journal of Contaminant Hydrology* (accepted).

A. Chilakapati, T.R. Ginn, and J.A. Szecsody. 1997. "Complex Reaction Networks: Solvability." *Water Resources Research* (in review).

S.B. Yabusaki. 1996. "Subsurface Contaminant Transport Modeling." SuperComputing '96, Pittsburgh, Pennsylvania, November.

S.B. Yabusaki. 1996. "Subsurface Science and Engineering: High Performance Computing at PNNL." Advanced Simulation of Contaminants in the Subsurface, Research Triangle Park, North Carolina, December.

S.B. Yabusaki and J.A. Szecsody. 1997. "Subsurface Reactive Transport." AAAS Annual Meeting, Seattle, Washington, February.

S.B. Yabusaki. 1997. "(Molecular to) Pore to Continuum." Workshop on Pore to Continuum Scaling, Los Alamos, New Mexico, April.

S.B. Yabusaki, M.D. White, and A. Chilakapati. 1997. "Reactive Transport Science: Mechanistic Process Modeling and Engineering Analysis." SIAM Geosciences, Albuquerque, New Mexico, June.

S.B. Yabusaki 1997. Subsurface Contamination Interest Area Co-Chair for DOE MODSIM Workshop, Albuquerque, New Mexico, September.

Marine Sciences

An Integrated Capability for Remote Sensing of Bottom Conditions in Near Shore Coastal Systems

Ronald M. Thom, Paul J. Farley (Marine Sciences Laboratory)
Gregg M. Petrie (Remote Sensing)

Study Control Number: PN97011/1152

Project Description

The objective of this project was to develop the capability to conduct rapid, integrated, high resolution mapping of submerged coastal bottom conditions. The scope of the project consisted of testing and development of the system in local areas representative of coastal conditions in the Pacific Northwest that integrates remote sensed images. This technology is needed for very rapid mapping of coastal conditions, that can be applied to a number of different research questions including predicting the effects of changes in weather and sea conditions on bottom topography and habitats.

Technical Accomplishments

Field data collection was largely successful, and produced very high quality images of submersed vegetation and substrata at the sites. We were able to acquire data from four areas including: 1) South side of Travis Spit, 2) Washington Harbor Road, 3) Northwest Protection Island, and 4) between Travis Spit and Diamond Point. Although all areas provided good data, the best information was acquired from areas 2 and 3. We found that the tide was too low during the surveys to acquire broad coverage of eelgrass and other habitats at site 1. The following data were converted to files compatible with ArcInfo software.

- Sensor type and identification/serial number (if applicable) - EGG 260 towfish and transceiver side scan sonar; Interspace Technologies 480 series narrow beam precision depth recorder.

- Sensor technical specifications - Side scan used 100 KHz set at high gain. Bathymetry done at 100 KHz, narrow beam, with high gain fathometer.

- Sensor parameter settings, including calibration, filters used, gain settings, or other applicable sensor variables - Gain set, site variable, in mid gain range. Secondary image enhancement and threshold, site specific via ISIS image processing system.

- Significant problems encountered - Sidescan sonar survey of Travis Spit area was conducted during low tide (due to time constraints). Grazing angle of sonar too great to obtain wide coverage of bottom types. In addition, water contained unusually high densities of red tide plankton which interfered somewhat with the image.

We successfully pulled these files into MapInfo and other software packages.

Data Collection and Processing

Acquisition of fine scale bathymetry and side scan sonar data involved time in the water and data processing time. Time was also required to obtain the needed equipment, prepare for the cruise, and demobilization. The field work at the four sites was conducted over 3 days. Once in the water, we found that we could set the boat up and do both the bathymetry and side scan sonar acquisition in approximately 3 hours for a site that was approximately 50 ha. Travel times to the sites were less than 1 hour. Longer travel times between sites would add to the time required to complete the sites. Processing bathymetry data required approximately 1 hour for a site approximately 50 ha. Processing the side scan and bathymetry data to a point where the data were mosaiced by the ISIS system and were transferred to files on a map analysis program required about 8 hours for a 50 ha site. Post-processing of the image to delineate substrata, vegetated habitat types, and other major features, and to calculate the areas occupied by the major features required approximately 1 hour for a 50 ha site. Time to accomplish this latter task will likely vary with the complexity in cover types at a site. Plots of maps of the images from the side scan system required minimal time. Our best estimate is that, once set up on site, the system could acquire bathymetry and side scan data over a contiguous area approximately 500 ha in size in 1 day (i.e., 10 hours). For example, habitats within a 150 m-wide swath along an approximately 34 km stretch of coastline could be surveyed in 10 hours. This assumes a 2 knot travel speed and relatively calm weather. The data acquired from this area could be delineated into major habitat and bottom types in 1.5 days.

System Performance

A. Bathymetry - ±10 cm

B. Substrata - can readily distinguish between consolidated and unconsolidated substrata

- mud - distinguishable
- sand - distinguishable
- mixed fine - distinguishable
- gravel - distinguishable as mixed coarse
- cobble - distinguishable as mixed coarse
- mixed coarse - distinguishable as mixed coarse
- boulders - distinguishable
- bedrock - distinguishable
- artificial - distinguishable
- organic - somewhat distinguishable
- hardpan - distinguishable

C. Vegetation - can readily distinguish between vegetated (greater than 25% cover) and unvegetated areas

- kelp - distinguishable
- eelgrass - distinguishable
- other algae - distinguishable
- unvegetated - distinguishable
- brown algae - distinguishable as other algae

D. Minimum mapping units - less than 1.0 m^2

E. Positional Accuracy - sub 1.0 m^2

F. Amount of subtidal area covered per time period - potentially can cover 500 ha in 8 hours

G. Ability to distinguish habitat types and accuracy assessments - estimated approximate accuracy using classification levels as shown above within at least 10% of actual habitats. This estimate is based on visual observation made from the boat during the time of the surveys.

H. Positional accuracy of data and ability to mosaic data into complete area coverage - data as accurate as navigation as long as the towed fish is fixed in place. If towed away from the vessel and not fixed, correction must be made for the position of the fish. In shallow systems as were surveyed during the present study, positional accuracy was essentially the same as for navigation. Mosaic of data highly automated and easily accomplished.

I. Ability to work in a variety of habitat types - the system can produce accurate maps from intertidal to deep subtidal depths.

Publications and Presentations

R.M. Thom, P. Farley, A. Borde, L. Antrim, and G. Petric. "An integrated method for mapping seagrass systems using side scan sonar." (in preparation).

R.M. Thom. 1997. U.S. Environmental Protection Agency, Marine Environmental Research Laboratory, Newport , Oregon, August.

R.M. Thom. 1997. Washington State Department of Natural Resources. September.

R.M. Thom. 1997. Seattle District U.S. Army Corps of Engineers. October.

Materials Science and Engineering

A Smart Molecular Membrane System for Wastewater Treatment and Recycle

Xiangdong Feng, Lonnie M. Peurrung, Liang Liang (Process Technology)

Study Control Number: PN97005/1146

Project Description

Water purification and recycle at high efficiency and low cost could be one of the most important research and development areas in the next century. This project performs a proof-of-principle demonstration of an advanced membrane for wastewater treatment and recycle. The proposed membrane is based on a smart polymer system that changes when the membrane is subjected to a temperature change. Work in FY 1997 identified and synthesized such polymers. This polymer has been shown to reversely adsorb water from wastewater at over 20 times of its dry weight and discharge molecular pure water at a temperature change of only about 10 degrees around room temperature. This offers an excellent opportunity to produce ultrapure water at extremely low cost.

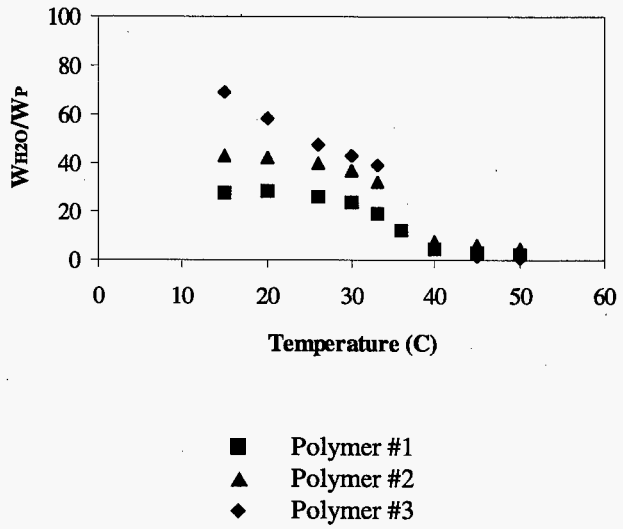

Figure 1. Water absorption capacity as a function of temperature.

Technical Accomplishments

In the present study, we have synthesized a membrane that exhibits the significant characteristics to switch on and off in response to the external temperature stimuli. Figure 1 illustrates the temperature-dependent swelling of the membrane in water. The membrane was completely swelled with water which discharges most of the water at temperatures below 40°C. The amount of water uptake is a function of polymer composition and temperature.

Figure 2 indicates the kinetics of water releasing (i.e., water releasing is faster at higher temperature). Substantial amounts of water can be released within a few minutes. The best economics may be derived from incomplete water delivery; however, this needs more investigation.

Further investigations and evaluations of the relationship between polymer composition and the amount of released water will be carried out by separating electrolytes from water.

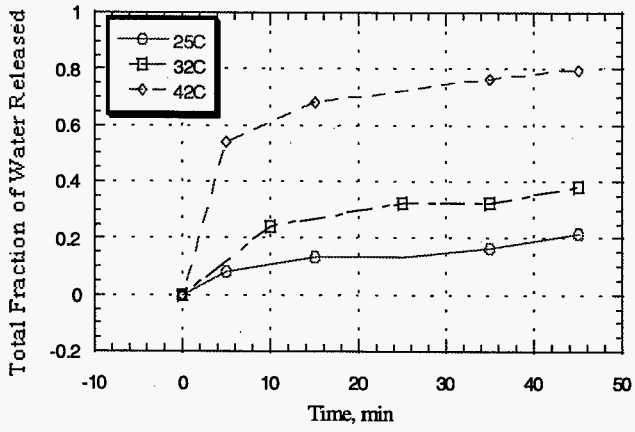

Figure 2. Water release versus time.

Conventional water treatment and recycle techniques such as distillation, crystallization, and solvent extraction have been supplemented by membrane separation processes, which appear to be more efficient and more economical than conventional separation technologies. Membranes are typically classified as being either size-exclusion membranes, molecular-sieve membranes, surface-diffusion membranes, or solution-diffusion membranes. The smart molecular membranes present do not rely on pore structure for filtration and are impermeable to ions, molecules, or any matter other than water molecules. Water transport in the membrane is achieved by changing the smart polymer's molecular configuration. The comparison of energy

consumption, product-water quality, and practical water recovery among different ways to purify water is listed in Table 1. It can be seen that the energy consumption in smart molecular membranes is much lower than conventional separation methods and almost the same as that in the reverse osmosis process which is the best method to purify water on a larger scale.

Table 1. Energy consumption, product-water quality, and practical water recovery by different technical methods. (Feed: 1 wt. % in water)

Method to Purify Water	Energy Consumed (kWh/1000 gal water)	Price (1000 gal water ($))	Product-Water Quality (ppm)	Recovery (%)
Flash distillation	140	6.02	5	25
Vapor compression distillation	90	3.87	5	57
Electrodialysis	40	1.72	500	33
Reverse osmosis	20	0.86	150	50
Smart molecular membrane	27	1.16	N/A	N/A

Advanced Multilayer Panels for Construction Applications

Kevin L. Simmons (Environment and Health Sciences), Mark R. Garnich (Energy)
Mark T. Smith (Environmental Technologies)

Study Control Number: PN97008/1149

Project Description

Multilayer polymer and polymer/metal panels that incorporate required structural performance and integrate mechanical and electrical functions are an emerging research priority within the buildings construction industry. The objective of this project was to develop fundamental materials joining and forming techniques for multilayer polymer-based construction panels. This requires a multidisciplinary approach that includes material testing, development of selective joining methods for polymer sheet, the application of structural design, energy efficiency measurement capabilities, and the sub-scale demonstration of the multilayer panel forming technology.

The technical approach used to develop multilayer polymer panel forming was based on the forming of sub-scale panels that demonstrate fundamental material, joining, and design requirements. The development of reactive phase joining for the bonding of multiple polymer sheets utilized research conducted at PNNL in displacement reactions for metals and ceramics.

Technical Accomplishments

During FY 1997, the first phase of the project was to focus on selecting materials and joining methods for the multilayer process. Five sheet materials were selected based on forming characteristics, as well as suitability for interior housing application. Sheet compounds having low-cost, fire retardant fill materials and fiber reinforced polymer sheet were also included in the evaluation, but the addition of other variables to the joining process led to these compounds being left out at this time. Standard forming tests were tried on each selected sheet material to generate temperature, flow stress, strain, and strain rate relations used in the forming process development effort. This effort is incomplete and needs to be continued to fill in our test matrix. Dynamic mechanical analysis was performed on the selected materials for determining the change in viscous properties of the material during heating.

Joining and Multilayer Forming Technology

Joining methods that have been evaluated include ultrasonic welding, heat (fusion), and plasma treated surfaces. Bonded tensile test specimens were used to evaluate joint strength and determine optimum conditions for forming. The results of the ultrasonically welded lap shear test specimens showed room temperature results of ABS to be very strong. Additional testing of lap shear specimens at elevated temperatures needs to be conducted on all materials.

The focus of the second phase of the multilayer-forming project was to develop and demonstrate joining and pressure forming techniques for simple 2- and 3-sheet polymer structures. An understanding of data generated from the phase 1 specimen tests was used to develop temperature programs for the forming of the multilayer panels. With the recommended material selected and welded together, a multilayer panel of 10-inch by 10-inch sub-scale panel was formed (Figure 1). This panel size was the basis for testing our multilayer panel designs and developing our forming process, which focused on demonstrating structural performance in combination with inner panel functions. An important aspect of panel design is the joining of multiple panels, and concepts for low thermal loss edge joints have yet to be developed as part of the analysis effort.

Presentation

G.J. Exarhos. 1997. "Synthesis and Processing of Advanced Materials." Polymer Workshop for DOE Center for Excellence, Task Center, Microstructural Engineering with Polymers. Alta, Utah, August 18-19.

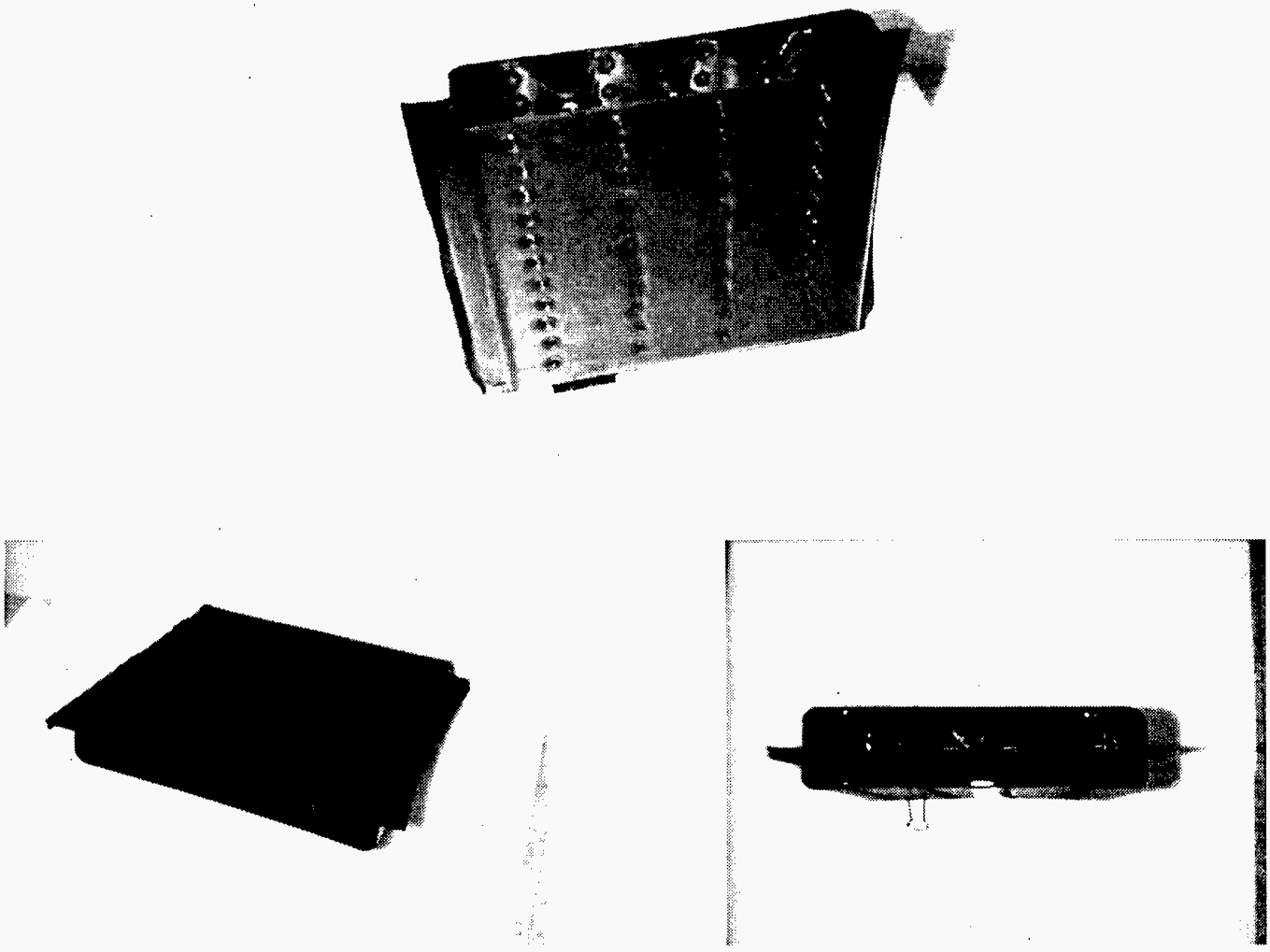

Figure 1. Constructed prototype panel.

Antimicrobial Coatings

Glen E. Fryxell, Manish M. Shah (Materials and Chemical Sciences)

Study Control Number: PN97012/1153

Project Description

The objective of this project is to install a surface active coating that is terminated with a biologically active antimicrobial peptide. We intend to demonstrate that 1) surface coatings can be installed on various catheter materials, 2) antimicrobials can be attached to the coated catheter, and 3) the coated catheter will inhibit microbial attachment and/or growth.

Background

Urinary tract infection is a serious concern in catheter use. The goal of this research is to impart antimicrobial activity to a catheter surface. Preliminary results suggest that coatings used to date inhibit the attachment of organisms, but does not inhibit their growth. Further refinement of these concepts is under way.

Technical Accomplishments

The need for antimicrobial materials is well-recognized in medical and food industries. Despite manufacturing advances, infection continues to be a frequent and serious issue. There is a fear of development of antimicrobial resistance strains. There are limited numbers of anti-microbial chemicals that can be used to develop the next generation of antimicrobial materials. Current techniques of evaluating performance of antimicrobial materials are not adequate for real-world situations for long-term use of antimicrobial materials. At PNNL, we are pursuing the development of antimicrobial materials that can be seen as environmentally safe, that do not prompt creation of antimicrobial resistance strains, and have a smart system approach. In addition to being antimicrobial, smart systems will involve sending a signal to doctors to inform them that there is an invasion of microorganisms on the surface. Results to date suggest that selected materials can completely inhibit the attachment of microorganisms even after 2 months of incubation. By far, one of the most pervasive complications associated with catheter use is infection. Half of the catheters that are left in place for more than 2.5 days undergo the formation of biofilms. Successful mitigation strategies include soaking the catheters in surfactant solutions or antibiotic solutions. However, soaking provides only short-term benefits. We propose to improve upon existing approaches significantly by coating the catheter surface with anti-microbial coatings, thereby establishing antimicrobial activity for prolonged durations.

Peptides with antimicrobial properties are found widely in nature. They exist in various taxonomic species, including plants, insects, amphibians, and mammals. Antimicrobial peptides are low molecular weight molecules characterized by highly compact structures. They show significant diversity, but in general, they are membrane active amphipathic molecules with a net positive charge. Many antimicrobial peptides contain unusual amino acid residues which contribute to their properties and functions. The hydrophilic portion of their molecules renders them water soluble, while the lipophilic portion is required for the penetration of microorganism membranes. The primarily observed mechanism of action is pore formation in the cytoplasmic membrane of the microorganism, and the disabling of its energy generating system. These peptides inhibit microbial growth effectively because they are able to invade microbial cells easily and rapidly. Bacteria are the primary target of all antimicrobial peptides. Although these peptides exhibit potent antimicrobial activity, they have very little effect on eukaryotes.

Since we have already developed methods to install monolayers on a wide variety of surfaces (metals, ceramics, polymers, etc.), future work should be directed toward imparting similar antimicrobial activity to a number of other important classes of biomaterials.

Accomplishments to date include an established procedure for coatings consisting of different types of biomolecules, and a procedure to test the antimicrobial performance of the coating material, using scanning electron microscopy (SEM). We incubated the coated surface for six weeks in a microbial solution and then analyzed the TPU surface by SEM. The SEM data suggests that the coating inhibited the attachment of microorganisms. However, we also found that an attached coating of antibiotic alone did not inhibit the growth of microorganisms.

It is possible that the organisms we worked with had developed resistance to the antibiotic. We are currently evaluating the effectiveness of the antibiotic in solution. It is also likely that the antibiotic had lost its ability to penetrate the microorganism membranes. We believe that

such problems are real and will be faced with any antimicrobial material.

The U.S. FDA has given approval of antimicrobial catheters and toys. Antimicrobial materials can replace several items currently used in public places, hospitals, and households with the advent of a new generation of antimicrobial materials. Catheters with chlorohexidine and silver compounds reduce infections. However, they have limited lifetime and efficacy when evaluated during clinical trials.

The future needs are in having smart antimicrobial materials with the ability to maintain antimicrobial activity for long times and to prevent the buildup of antibiotic resistance strains. There is also a need for antimicrobial resins, biosorbable antimicrobial implants, and surgical instruments. There is a need for environmentally safe and biocompatible antimicrobials. Our research will lead to the development of technology to impart antimicrobial activity.

Publications and Presentations

M.M. Shah and G.E. Fryxell. "On the antimicrobial performance of silica chips and TPU with covalently attached vancomycine and heparine." *Antimicrobial Agents and Chemotherapy* (to be submitted).

M.M. Shah and G.E. Fryxell. 1997. "Issues and Challenges in Development of Next Generation of Antimicrobial Materials." Presented at the American Society for Biomaterials, Annual National Meeting, San Diego, California, April 22-26.

Biocatalyst for Remediation

Manish M. Shah, James A. Campbell (Environmental and Health Sciences)

Study Control Number: PN97017/1158

Project Description

We are reporting an environmentally benign process for treatment of explosives. We find that explosives can be treated by naturally occurring enzymes. In addition to explosives, they can transform other nitroaromatics. We used nitrobenzene and TNT as model molecules to study. Nitrobenzene was reduced in a solution. The product of nitrobenzene was identified as phenylhydroxylamine (PHA) on 1:1 basis. In the case of TNT, we find that 4-hydroxylamine derivative of TNT was accumulated. We expect that this intermediate can be pursued for industrial applications for disposal of TNT stockpiles.

Background

Nitroaromatics and nitroheterocyclic chemicals are used by the pharmaceutical, dye, plastic, agrochemical, and defense industries. Nitrobenzene plays a major role as a solvent and in production of a variety of intermediates (Kirk-Othmer 1978). Naturally occurring redox enzymes such as dehydrogenases, reductases, and oxidases are known to react with a number of nitroaromatic and nitroheterocyclic chemicals (Orna and Mason 1989; Anzlezark 1992; Angermaier and Simon 1989; Middlebrook et al. 1993; Shah and Spain 1996). These enzymes are ubiquitous and can be obtained from plants, microorganisms, and animals. There is current interest in use of plants- and microorganism-based processes to remediate soil and sediments that are contaminated with nitroaromatic chemicals. It is important to understand the metabolism of nitroaromatic chemicals by redox enzymes. Interestingly, nitroaromatic or heterocyclic chemicals are not true substrates of these nitro reductase enzymes. As a result, substrate affinity of enzyme, the rate of reaction, and products of nitroaromatic transformation may vary with substrate and reaction conditions. In general, the mechanism of reduction of nitroaromatic chemicals by the nitro reductase enzymes could be either one or two electron based (Mason 1979; Bryant and McElroy 1992). Enzymes that catalyze one electron based reduction are generally oxygen sensitive. In the presence of oxygen, the oxygen sensitive nitroreductase enzymes reduce molecular oxygen to superoxide anion radical using nitroaromatic chemical as an electron mediator.

Although there are several reports describing the reactions between the "apparent" nitro reductase enzymes and nitroaromatic or nitroheterocyclic chemicals, there is very little or no knowledge on the reactions of these apparent nitro reductase enzymes with nitrobenzene. In the current communication, we are reporting the reduction of nitrobenzene to phenylhydroxylamine (PHA).

Technical Accomplishments

Figures 1A and B compare chromatograms of PHA standard and the reaction sample after the enzyme treatment. Figure 1A represents chromatogram of PHA. The retention time of PHA was about 3.7 minutes. The retention time and spectra of synthesized PHA standard matched exactly with the metabolite of nitrobenzene, formed after the enzyme treatment. Figure 1C shows the matching of the ultraviolet visible spectrum of the metabolite of nitrobenzene and PHA standard. Hence, the metabolite of nitrobenzene was identified as PHA. The metabolite was not detected in the absence of nitrobenzene. The metabolite was not observed under aerobic conditions. The kinetics and stoichiometry of nitrobenzene transformation is shown in Figure 2. About one mole of PHA is formed for every mole of nitrobenzene.

Our results demonstrate the transformation of nitrobenzene to PHA. Ferrodoxin NADP oxidoreductase (FNR) has been shown before to generate nitroanion radicals of nitrofurazone, nitrofurantoin, p-nitrobenzoate, and metronidazole (Orna and Mason 1989). Based on the results, they suggested that the rate determining step in the reduction of nitro chemicals by flavoenzymes is the initial single electron transfer step. The reduction of tetryl by the FNR leads to the elimination of nitramine nitro group of tetryl (Shah and Spain 1996) while the reduction of nitrobenzene leads to the formation of hydroxylamine. Future study is necessary to understand if under any condition, nitro group can be eliminated from nitroaromatic chemicals. Similar reactions were observed with TNT. It was possible to harvest the intermediate of TNT. In the case of TNT, we find that 4-hydroxylamine derivative of TNT was accumulated. A mass spectrum of 4-hydroxyaminedinitrotoluene is shown in Figure 3. The mass spectrum of the metabolite is shown in Figure 4. The metabolite was obtained from labeled-TNT (^{13}C and ^{15}N labeled). The resulting fragment ions differ by 10 amu from the standard, due to the labeling of the starting material. If the intermediate was not harvested, the reaction led to several reduced metabolites and they were not identified.

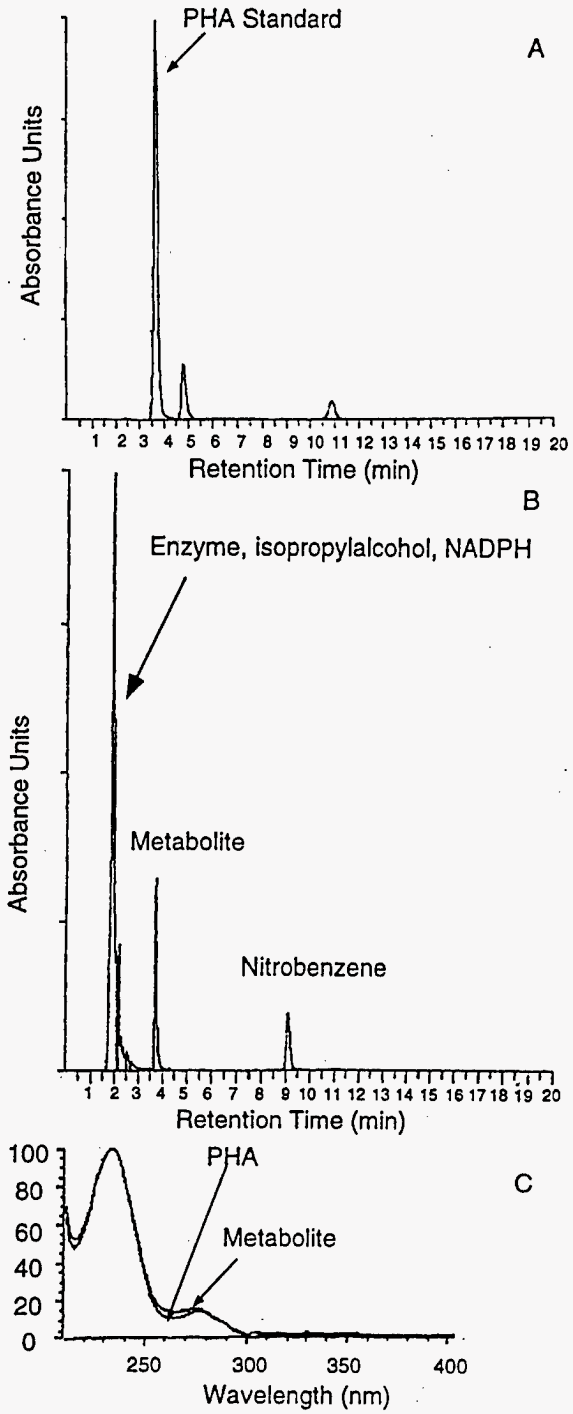

Figure 1. Comparison of HPLC retention times an authentic PHA standard (A) and the nitrobenzene metabolite (B) formed after enzymatic treatment and their UV-VIS spectra (C).

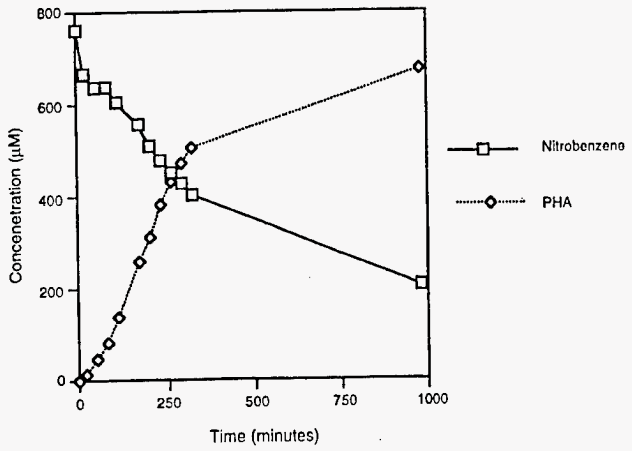

Figure 2. Kinetics and stoichiometry of nitrobenzene transformation. Reaction conditions are the same as that reported in Figure 1.

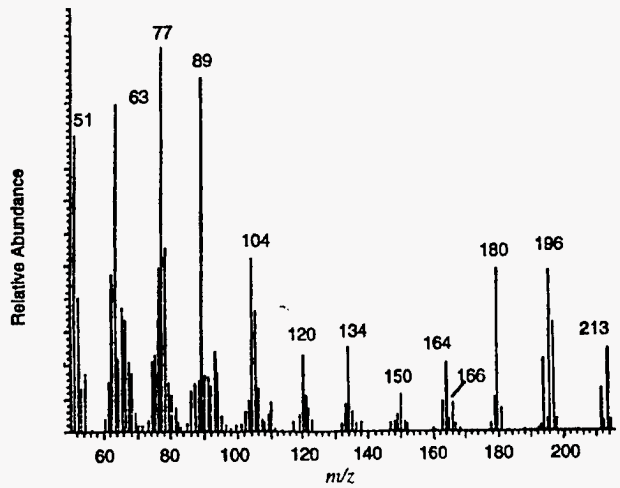

Figure 3. Mass spectrum of 4-hydroxyaminodinitrotoluene.

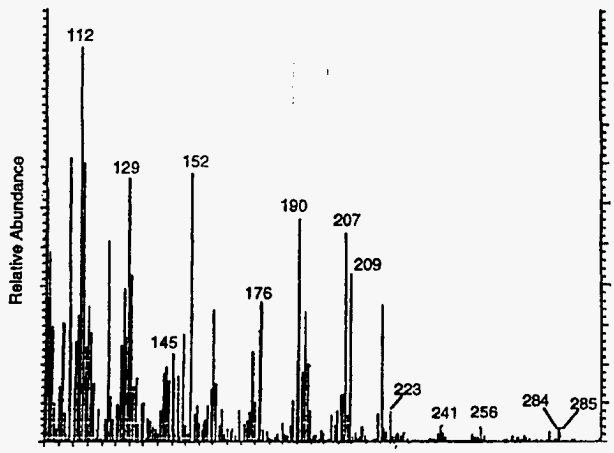

Figure 4. Mass spectrum of the TNT metabolite formed after enzyme reaction.

Acknowledgments

The authors would like to extend their thanks to Georgia Ruebsmen for artwork. Technical assistance provided by Scott Clauss and Gary Mong is gratefully acknowledged.

References

L. Angermaier and H. Simon. 1983. *Hoppe-Sp,Z. Physiol.Chem.* 364, 961-975.

Anlezark et al. 1992. *Biochem. Pharmacol.* 44, 2289-2295.

C. Bryant and W.D. McElroy. 1992. in *Chemistry and Biochemistry of Flavoenzymes*, Boca Raton, CRC Press, vol II, chapter 9, 291-304.

Kirk-Othmer. 1978. *Encycl. of Chem. Technol.*, 3rd ed., John Wiley & Sons, New York.

R.P. Mason. 1979. *Reviews in Biochemical Toxicology*, Elsevier North Holland, Inc., Vol. I, 151-201.

T.J. Middlebrook, S.E. Behnken, and W.R. Mitchell. 1993. *Haz. Wastes and Haz. Mater.*, 10, 347-355.

M.V. Orna and R.P. Mason. 1989. *J. Biol. Chem.*, 21, 12379-12384.

M.V. Orna and R.P. Mason. 1989. *J. Biol. Chem.* 21, 12379-12389.

M.M. Shah and J.C. Spain. 1996. "Reduction of the explosive tetryl by ferredoxin NADP oxidoreductase from spinach." *Biochem. Biophys. Res. Commun.*, 220, 563-568.

C. Sommerville, S.F. Nishino, and J.C. Spain. 1995. *J. Bacteriol.*, 177, 3837-3842.

A.I. Vogel. 1977. *A Text Book of Practical Organic Chemistry*, Third Edition, Longman Group Ltd, London, 628-630.

Publications and Presentations

M.M. Shah and J.A. Campbell. 1997. "Transformation of nitrobenzene by ferredoxin NADP oxidoreductase from spinach leaves." *Biochem. Biophys. Commun.*, 241, 794-796.

M.M. Shah and J.A. Campbell. 1997. Identification of Enzymatic Transformation Products of TNT Using Particle Beam LC/MS. ASMS Conference, Palm Springs, California, June 1-5.

Biological Interactions/Materials Biocompatibility

Barbara J. Tarasevich, Steven C. Goheen, Karen L. Wahl (Chemical Sciences)
D. L. Allara (Portland State University), B. Ratner (University of Washington)

Study Control Number: PN97019/1160

Project Description

Our objectives are to develop a fundamental understanding of how interfaces control biological responses. We wish to understand how interfacial properties affect protein adsorption and conformation and how protein adsorption, in turn, controls cell adhesion and growth. Biological interactions onto interfaces are of great importance to medical technologies such as artificial and resorbable implants, cell/tissue scaffolds, and invasive probes. The success of a biomaterial depends largely on how well its surface promotes or discourages specific protein and cellular responses. For example, the use of small bore vascular implants during heart surgery has been limited due to thrombotic occlusion at the surface. The role of surfaces in controlling this biological response, however, is not well understood. It is believed that protein adsorption initially occurs and then mediates interactions with cells via adhesion receptors. We have done studies of serum protein adsorption and endothelial cell growth onto model self-assembling monolayer surfaces and have developed a novel flow-through system to examine protein adsorption and binding onto chromatographic supports. These studies provide valuable insight on how to design new materials and surfaces to tailor biological responses.

Technical Accomplishments

Two approaches were used to examine protein adsorption and cell growth onto tailored surfaces:

1. Endothelial cell growth and serum protein adsorption and elution onto model self-assembling monolayers (SAMs) containing various functional groups was studied.

2. An in situ flow-through technique was developed to examine protein adsorption and retention onto chromatographic supports.

Endothelial cell growth was examined because endothelial cells are naturally antithrombogenic and their adhesion and growth onto vascular implants promotes biocompatibility. Also, their growth and proliferation are anchorage dependent, but there is confusion in the literature as to how surfaces affect cell anchorage and growth. Bovine aortic endothelial cells (BAEC) in 10% bovine serum were seeded onto SAM surfaces containing -CH_3, CO_2CH_3, and OH functional groups. Figure 1 shows images of cell growth patterns for cells cultured onto -CH_3, CO_2CH_3, OH, and CH_3 terminated SAMs. The hydroxyl surface, upper left, exhibited the fewest total number of cells. Cells on this surface primarily appeared rounded and were sparsely spread over the monolayer surface. The methyl ester surface exhibited an increased number of cells, cell spreading was observed in some of the cells. On the methyl monolayer, a higher cell density was observed relative to the OH and methyl ester SAMs. A significant increase in cell number was observed on the carboxyl surface, lower right. Cell spreading was evident in a majority of the cells observed on this surface. A nearly confluent monolayer was achieved after 5 days of culture on the COOH surface.

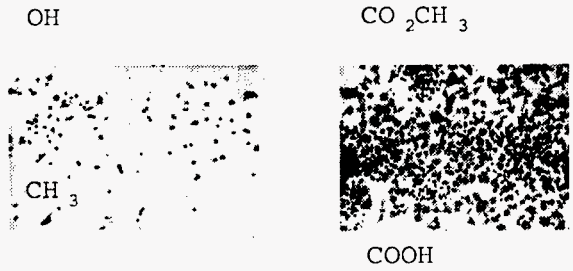

Figure 1. Endothelial cell growth onto functionalized SAMs.

Results indicate distinct differences in cell growth in response to the various functional groups present on the homogeneous SAM surfaces. The COOH functionality resulted in maximum cell growth promotion while the OH and CO_2CH_3 functionalities demonstrated poor cell growth characteristics. This work is interesting because two hydrophillic surfaces were examined (COOH, OH) and resulted in drastically different cell growth results. This is in contrast to previous studies which have suggested hydrophillic surfaces or oxygen-containing surfaces promote cell growth.

Since an adsorbed protein layer mediates interactions of cells with the surface, the adsorption of fibronectin and albumin were studied from serum solution by radiolabeling and gamma counting. Fibronectin (Fn) is a cell adhesion protein and albumin (Alb) is the most common serum protein. Slight differences in the amount of albumin adsorbed are observed in response to the presence of the

different surface functionalities. While albumin is considered a nonadhesive or blocking protein, the ability of a substrate to support cell growth does not appear to be negatively affected by the adsorption of albumin as evidenced by the superior cell growth observed on the COOH SAM which demonstrated the highest level of albumin adsorption. Fibronectin adsorption ranged from 0.8 ng/cm^2 on the OH surfaces to 2.54 ng/cm^2 on the COOH surface, a difference which is statistically significant. Fibronectin adsorption was significantly higher on the cell growth promoting surface, COOH, compared to the other surfaces. This indicates that higher serum fibronectin adsorption levels contribute to enhanced cell attachment and spreading. Fibronectin is known to promote cell adhesion and growth by interactions of RGD sequences with integrin receptor sites on the cell membrane. In addition, cells start to produce their own fibronectin which may then have higher affinity with the COOH SAM, resulting in further cell growth enhancement.

Further studies were done to understand protein adsorption and retention onto surfaces using a flow-through system. The adsorption properties of three representative plasma proteins, albumin, fibrinogen, and immunoglobulin G, were examined on hydrophilic surfaces containing either quaternary amine or sulfopropyl functional groups. The adsorption properties were studied at near-physiological conditions (37°C, pH 7.4) using a continuous flow rate of 1.0 mL/min in a 7.8 mm inner diameter flow chamber. The results from this study suggest a new way to study protein-surface interactions. The data obtained from this study may help us understand the chemistry and dynamics of protein adsorption. Results are discussed in relation to biocompatibility.

Calibration curves generated from the adsorption-testing device were used to determine the amount of protein recovered after it interacted with the cationic and anionic surfaces. We allowed each protein to rest on the hydrophilic surfaces for various periods of time and measured protein recoveries. The desorption of the proteins was attempted using a much higher salt content in the eluent than the protein would normally require for desorption (as determined from the adsorption index). On both the quaternary amine and the sulfopropyl surfaces (cationic and anionic, respectively), the amount of protein recovered dramatically decreased with increasing residence time on the surface. Put another way, the irreversible binding of all three proteins was time-dependent. The longer each protein was allowed to reside on the surface, the less would desorb. This is clearly a different mechanism that dictates the binding of those stagnant proteins as opposed to the dynamic (flowing) case. A reasonable explanation is that these proteins unfold on the surface in a time-dependent manner.

Our work involving tailored self-assembled surfaces and new methods to examine protein adsorption has elucidated aspects of the role of surfaces in controlling endothelial cell growth and protein adsorption and unfolding. These studies have already provided guidance on how to design surfaces and materials to control biological responses. Further work will examine cell growth onto more complex, mixed functionality surfaces as well as protein adsorption and time-dependent conformational changes.

Publications and Presentations

C.D. Tidwell, S.I. Ertel, B.D. Ratner, B.J. Tarasevich, S. Atre, and D.L. Allara. 1997. "Endothelial Cell Growth and Protein Adsorption onto Terminally Functionalized, Self-Assembled Monolayers of Alkanethiolates on Gold." *Langmuir* 13(13), 3404.

S.C Goheen and J.L Hilsenbeck. "Adsorption of Plasma Proteins on Polar Surfaces." *J. Colloid Interf. Sci.* (in preparation).

S.C. Goheen and J.L. Hilsenbeck. "Studies on the Separation of Plasma Proteins by HPIEC." *J. Chromatogr.* (in preparation).

C.D. Tidwell, A.M. Belu, B.D. Ratner, B.J. Tarasevich, S. Atre, and D.L. Allara. 1997. "Endothelial Cell Growth on Binary Composition Self-Assembled Monolayers: Effect of Surface Chemistry and the Adsorbed Protein Layer." Society for Biomaterials Annual Meeting, New Orleans, Louisiana, April 30 - May 4.

S.C. Goheen and J.L. Hilsenbeck. 1997. "The Adsorption of Plasma Proteins on Polar Surfaces." Presented at the Surfaces in Biomaterials '97 Conference, Minneapolis, Minnesota, September 3-6.

Development of Improved Oxygen Electrolyzer Membranes

Timothy R. Armstrong, Jeffry W. Stevenson, Suresh Baskaran (Materials and Chemical Sciences)

Study Control Number: PN96015/1082

Project Description

This project will develop and investigate new solid electrolyte materials for use as oxygen separation membranes in oxygen generators. The development of these new materials will allow the operation temperature of current electrolyzers to be decreased to approximately 600°C to 700°C from the current operating temperature of 1000°C. In addition, the development of these materials will improve electrolyzer efficiency, allow for miniaturization of the electrolyzer, and allow a faster initial start-up of the electrolyzer. The materials and components to be developed will be used in the manufacture of small-scale oxygen electrolyzers used to produce oxygen for the medical industry.

Technical Accomplishments

The objectives during FY 1997 were to determine: 1) the mechanical properties of lanthanum gallate and 2) the effect of A-site cation deficiency on the properties of lanthanum gallate. $La_{1-x}Sr_xGa_{1-y}Mg_yO_{3-\delta}$ compositions are designated by the abbreviation LSGM.

A-Site Nonstoichiometry

The selection of rich combustion conditions was based on a previous study on the synthesis of doped lanthanum gallate (Stevenson et al. 1997). While the as-synthesized powders contained substantial quantities of non-perovskite phases, the fraction of pervoskite present increased with increasing temperature. LSGM Composition 1 was a single-phase perovskite when sintered at 1400°C or higher; LSGM Composition 2 was single phase above 1500°C.

All of the compositions were readily sinterable to high densities at temperatures in the 1400 to 1500°C range. The decrease in sintered density observed at the highest sintering temperature may be attributable to the volatilization of gaseous Ga_2O and O_2 from the perovskite material:

$$2\,Ga_{Ga}^{x} + 3\,O_{O}^{x} \quad Ga_2O + O_2 + 2\,V_{Ga} + 3\,V_{O}^{\bullet\bullet}$$

The above reaction (Kroger-Vink notation) causes a net loss of specimen mass and possibly an increase in specimen volume due to bloating; the volatilization of Ga_2O from LSGM at high temperatures was verified in this study by mass spectroscopy.

Linear thermal expansion coefficients for LSGM Composition 1 and LSGM Composition 2 were measured on sintered specimens over the temperature range 20 to 1200°C. These values are somewhat higher than that of YSZ (approximately 10.4 x 10-6°C-1).

Mechanical Properties

Four-point bend strengths were measured as a function of temperature on machined bar samples for stoichiometric LSGM Composition 1. The measured strength at room temperature was ≈ 150 ± 25 MPa, which is comparable to the strength of alkaline earth-doped lanthanum chromites, and somewhat lower than the strength of cubic yttria-stabilized zirconia (≈ 250 MPa). The high temperature strengths at 600°C to 1000°C was ≈ 100 ± 10 MPa (Figure 1). SEM inspection of surfaces fractured at various temperatures showed that fracture was predominantly transgranular, with lower strengths corresponding to larger flaws.

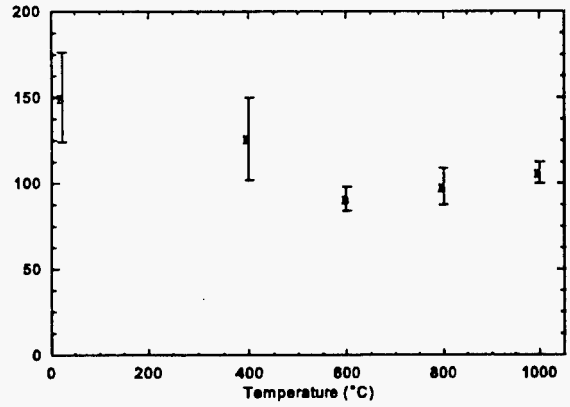

Figure 1. Flexural strength of LSGM as a function of temperature.

Fracture toughness as a function of temperature was estimated using single-edge notched beam specimens. Toughness measured by this technique was essentially invariant at 2.0 to 2.4 MPa$\sqrt{m}$ at room temperature decreasing to ≈ 1.0 MPa$\sqrt{m}$ at 1000°C, for stoichiometric LSGM Composition 1. The fracture toughness and

hardness was also estimated using the vickers indentation method. The fracture toughness obtained by this method is typically less than other macroscopic techniques such as the notched beam method, but is useful for comparison between various compositions. The literature values for indentation toughness and hardness of single crystal lanthanum gallate ($LaGaO_3$) are 0.7 MPa$\sqrt{m}$ and 9.4 GPA, respectively. The indentation toughness of polycrystalline LSGM compositions was in the range 0.9 to 1.1 MPa$\sqrt{m}$, while the hardness was 7.0 to 8.2 Gpa. The toughness is significantly lower than polycrystalline cubic-zirconia (KIc of 2 to 3 MPa$\sqrt{m}$). The lower hardness of polycrystalline LSGMs compared to the single crystal is indicative of the decreased resistance to penetration with a polycrystalline assemblage.

The fracture toughness of LSGM Compositon 1 was measured at room temperature and 1000°C using a single-edge notch beam. At both temperatures, the fracture toughness was 2.35 MPa$\sqrt{m}$, indicating that there is apparently no decrease in fracture toughness of this material with increasing temperature.

Publications

T.R. Armstrong, J.W. Stevenson, and L.R. Pederson. "Effect of A-Site Cation Nonstoichiometry on the Properties of Lanthanum Gallate." *Solid State Ionics* (submitted).

J.W. Stevenson, T.R. Armstrong, L.R. Pederson, and W.J. Weber. 1997. "Processing and Electrical Properties of Alkaline Earth-Doped Lanthanum Gallate." *J. Electrochem. Soc.*, 144, 3613-3620.

Dissolvable Stents

William D. Samuels (Materials Sciences)

Study Control Number: PN96018/1085

Project Description

There is a need for stents for the reconnection of veins and arteries. The optimum material would promote the natural healing process for the reconnected veins or arteries, prevent infection or thrombosis at the site, and dissolve into benign compounds. The unique attributes would provide a platform for the incorporation of antibiotics (penicillin-N), anticoagulants (4-hydroxycoumarin), a mixture of ethoxyated amino acids, and a trace (<0.1%) amount of a cross-linking agent for internal strength.

The ability to control both the chemical and physical properties of the polymeric materials to fit the requirements is a unique property of polyphosphazenes. Open literature work has indicated that the amino acid polyphosphazenes will hydrolyze into nonharmful compounds in 400 to 500 hours. The preparation of the proof-of-concept polymer will be an application of previous research.

Technical Accomplishments

In FY 1997, the synthesis of polyphosphazenes contained a number of different amino acid and phenols. The yields were consistent for similar synthesis reported in the literature. The use of a replacement for the base or amine hydrogenchloride scavenger was initiated with positive results. The complete replacement of P-Cl bonds was accomplished faster and to a higher degree than under standard conditions. Phenolic substitutions are known to be difficult requiring either high pressure or long reaction times at reflux. The use of some replacement materials improved yields, while low yields of polymer were found under other conditions.

Discussions with NuFlo Corporation, Seattle, Washington, suggested that the stents need to be stiffer than the initial formulation. Consequently, several side groups were investigated that would provide for a less pliant polymer. Incorporation of these side groups led to reaction yields that were acceptable.

Gas Selective Thin Film Barrier Materials

Peter M. Martin, Dean W. Matson (Material and Chemical Sciences)

Study Control Number: PN96027/1094

Project Description

This project focused on the development of sputtered thin, hydrogen permeable membranes on porous ceramic supports. Support geometries included both ceramic disks, to be used for testing at Washington State University, and ceramic tubes, for use in membrane reactors at PNNL. A primary effort was made in the development of an intermediate smoothing layer between the ceramic support and the sputtered coating. The purpose of this layer was to improve the characteristics of the coating as a gas barrier, yet still allow permeation of hydrogen. A secondary focus of the project was to adapt a cylindrical triode sputtering apparatus with RF capability for use in coating porous ceramic tubes with a Pd-Ag alloy for evaluation as permselective membranes at PNNL. Use of a cylindrical geometry for this application would allow improved materials efficiency and high rate sputtering possible with the triode system should allow for improved microstructural coating characteristics in this application.

Technical Accomplishments

Pd-25% Ag alloy coatings were sputtered onto porous alpha-alumina 1 inch disks provided by Washington State University. All of the disks were polished to 600 grit to remove gross surface irregularities and dried under vacuum. Some of the disks were coated "as polished." Others were surface modified. The boehmite-coated disks were subsequently heated to convert the boehmite into the gamma alumina phase. Some of the coated disks were then repolished back to the original alpha alumina surface prior to sputter coating. The Pd-Ag alloy was deposited onto all of the disks to a thickness approaching 5 microns using a 2 inch magnetron sputtering cathode. Coated samples were returned to Washington State University for gas selectivity analysis.

Preliminary results from Washington State University indicate that samples having the Pd-Ag barrier coating without the intermediate gamma alumina smoothing layer exhibit poor gas selectivity. Specifically, they are highly permeable to both hydrogen and nitrogen. Optical and SEM analysis of cross sectioned coatings on samples without the smoothing layer confirm that the coatings have a large number of defect structures producing a high coating porosity. At least some of the samples produced with the intermediate gamma alumina layer exhibit a high selectivity of hydrogen over nitrogen, at ratios of up to 56:1, suggesting a low degree of porosity in the barrier coating. Cross section analysis of the coatings with the intermediate layer confirm this interpretation. Gas selectivity evaluation of the coated disks is ongoing.

A secondary effort under this project was to adapt a triode sputtering system to allow sputter coating of porous ceramic tubes to be evaluated in gas membrane reactors. A system was modified to accommodate a cylindrical sputtering geometry with the tube to be coated running up the axis of the cylinder. The apparatus was further equipped with RF biasing capability to allow ion cleaning of the tube and bias sputtering during the deposit. This modification was completed and successfully tested using a dummy metal target. A Pd-Ag alloy target was received after completion of the project and no coated samples were produced for evaluation using this apparatus. However, the capability has been assembled and demonstrated for future projects.

High Functionality Surfaces and Structures in Microchannels

Xiangdong Feng, Timothy L. Hubler (Environmental Technologies)
Jun Liu, Donald Baer, Yong Liang, Liang Liang,
Glen E. Fryxell (Envioronmental and Health Sciences)

Study Control Number: PN97048/1189

Project Description

This project focus and overall goal is to develop scientific knowledge that will aid in the development and advancement of miniature chemical and energy devices. Specific objectives aimed at providing this scientific knowledge include 1) investigating methods for reducing the effect of fouling in microchannels, 2) developing a novel smart microsystem concept based on the integration of smart molecules and microsystems, and 3) investigating our ability to create nanoscale functional structures with possible applications as elements in microsystems. The project consists of the following two tasks.

Molecular and Polymeric Surfaces for Controlling Surface Hydrophobicity and Energy. Microchannel properties such as surface energy, surface hydrophobicity, surface charge, and charge density are critical to the functionality and efficiency of these microsystems and can be controlled through molecular and polymeric surface coatings. Microchannels are susceptible to fouling, which is closely related to these surface properties. Antifouling surfaces in microchannels are being used as a model for surface functionality modification and are being developed by rational design, modification, and testing controlled surfaces and interfaces. Desired surface coatings are being constructed using molecular self-assembly, biomimetic coating, and other innovative methods. The surface properties can be fine-tuned to reduce and eliminate fouling in microchannels.

Forced convection in a microseparator can greatly increase its separation efficiency and is being achieved using smart molecular surfaces without mechanical intervention. A model system to mimic this process is being designed. This involves a capillary tube immersed in two immiscible solvents (e.g., an aqueous solvent on top of a heavier organic solvent). The goal is to move the liquid surface in the capillary tube up and down across the interface of the two solvents without mechanical intervention. This is being achieved by first coating the interior of the tube with electroactive functional molecules. Without an electrical field, the coating in the capillary tube is hydrophilic and the meniscus is at the bottom of the capillary tube, while the meniscus level is expected to move to the top of the capillary tube when the coating becomes hydrophobic under an electrical field. This process can be regulated with an electrical field (or thermal field).

Creation of Functional Nanostructures. Metal/oxide systems are of great importance in heterogeneous catalysis and chemical sensors due to their high activity and specificity for molecules to be converted or monitored. A key issue in adapting these metal/oxide systems to microsystems is the control and miniaturization of the metal clusters on oxide surfaces.

Technical Accomplishments

Molecular and Polymeric Multiple-Function Surfaces in Microchannels

In 1997, three types of smart polymeric surfaces were explored: 1) thermoactive poly (N-Isopropylacrylamide), 2) electroactive polyacrylic acid-polyacrylamide, and 3) pH active polyacrylic acid-polyvinyl alcohol. The thermoactive surface was studied in detail.

Silicone wafers and glass pieces were employed as substrates for the smart surfaces. The substrate surface was first coated. The thickness of coated surface was measured by ellipsometry. A polymer layer was then formed that was bound to the surface of a silicone wafer and glass pieces. Figure 1 shows that the cross-linked material exhibits significant capacity for water (up to 70 g of water per gram of the polymer) when it is hydrophilic at room temperature and discards essentially all the water when temperature is increased to 40°C. The capacity of water absorption by the polymer can be controlled.

Temperature-dependence of the surface hydrophobicity was investigated by dynamic contact angle at the temperature ranging from 15°C to 50°C as shown in Figure 2. The surface is essentially hydrophilic at 30°C and becomes almost totally hydrophobic at 40°C. This behavior is illustrated in Figure 3.

This dramatic hydrophobicity change over a narrow temperature change represents a great achievement of this project this year, which will provide the foundation for the model systems to be demonstrated in the coming years, and it may lead to some breakthrough applications in many fields.

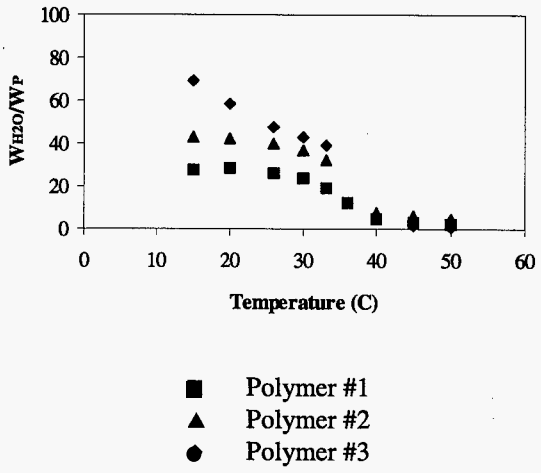

Figure 1. Water absorption capacity as a function of temperature.

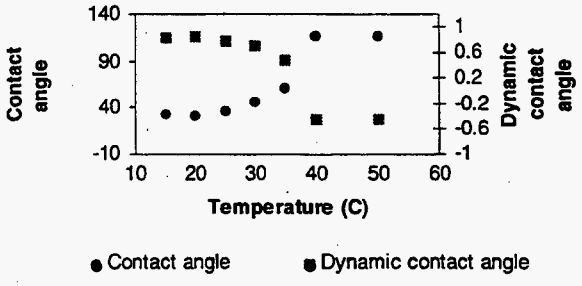

Figure 2. Temperature dependence for dynamic contact angle changes on a grafted surface.

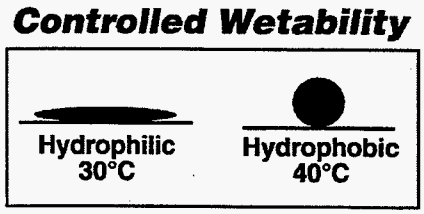

Figure 3. Surface hydrophobicity change versus temperature.

Creation of Functional Nanostructures

Our research focus was mainly on a simple catalyst system: Pt on carbon surface. Carbon (graphite) was selected not only because it is a common material widely used to support the catalysts, but also because of its flatness so that nano-scale features can be identified on the surface. We used STM to create nano-scale Pt clusters on carbon surface. By positioning the STM tip on the surface, an array of Pt clusters were fabricated. Figure 4 is a STM image showing an array of clusters deposited on the carbon surface. Before the Pt deposition, the carbon surface had been atomically flat with only a few atomic steps on the surface. After the Pt deposition, an array of clusters formed on the carbon surface, as shown in Figure 4. The height of those clusters is approximately 6 nm with a width of approximately 40 nm. The original atomic steps are still recognizable after the Pt deposition. In order to confirm that the clusters are Pt, we performed a high resolution scanning Auger microscopy measurements on the carbon surface. The results are shown in Figure 5. Before the Pt deposition, the surface was clean except for a small amount of oxygen due most likely to the adsorption of H_2O on the carbon surface. No Pt was found from the Auger measurements before the Pt deposition. After the Pt deposition, however, Auger spectrum taken in the region where Pt was deposited shows a noticeable amount of Pt on the surface, as illustrated in Figure 5. This suggests that the deposited clusters are indeed Pt transferred from the STM tip.

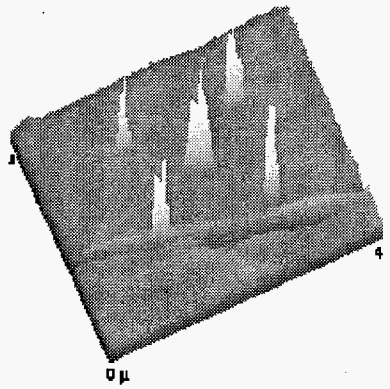

Figure 4. ASTM image showing an array of Pt clusters deposited on carbon surface.

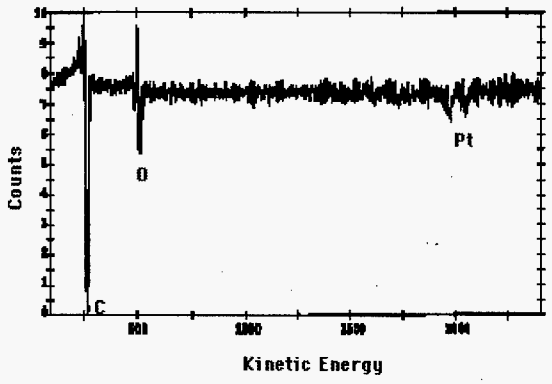

Figure 5. An Auger spectrum showing Pt on carbon surface.

Publication

X. Feng, G.E. Fryxell, L.-Q. Wang, A.Y. Kim, J. Liu, and K.M. Kemner. 1997. "Functionalized Monolayers on Ordered Mesoporous Supports." *Science* 276, 923.

High Precision Rapid Prototyping

Peter M. Martin, Dean W. Matson, William D. Bennett (Materials and Chemical Sciences)

Study Control Number: PN97049/1190

Project Description

This project aims to develop low-cost manufacturing, high precision microfabrication, rapid prototyping processes, and miniaturization of energy and chemical systems. A PNNL laser micromachining system can be used to fabricate features as small as 1 μm in plastics, semiconductors, metals, and insulators. This system will initially be used to fabricate micromolds in plastics for formation of microscale components by electroplating of metals. Component designs to be fabricated include micronozzles, very high aspect ratio microchannel heat exchangers, micromembranes for low-cost solvent extraction, spiral channels for liquid metal actuators, micropump diaphragms, microoptical components, and microjets.

This project will also develop advanced, mass-producible, microfabrication methods. FY 1997 activities focused on developing processes for laminated microchannels. The components developed include those with less strict dimensional constraints (low precision) and with medium precision. Low precision components include microchannel heat exchangers and microchannel devices fabricated by lamination. These processes will give PNNL a broad and unique technology in microfabrication not presently pursued by others. Using the lamination process, channels with high aspect ratios can be achieved with a variety of materials. Lamination techniques will be developed for metals using microcomponents developed at PNNL.

Technical Accomplishments

During FY 1997 the development of laser micromachining capabilities at PNNL was initiated. The Potomac model LMT-4000 excimer laser micromachining workstation that had been previously procured under non-LDRD funding was installed and staff became proficient with the CAD/CAM software and laser machining capabilities and limitations. The workstation was modified with a class I enclosure around the machining stages, machining software was upgraded to allow enhanced machining capabilities, and a z-stage was added to the system to improve focusing and machining depth control. A 351 nm XeF excimer laser was also procured to supplement the machining capabilities of the 248 nm KrF laser supplied with the laser workstation, and to provide capability for future microfabrication efforts using laser photopolymerization processes.

Laser machining capabilities and limitations were evaluated in a range of different substrate materials and a number of test/evaluation parts were fabricated. This piece of equipment has become one of the most valuable and widely used microfabrication capabilities thus far developed at PNNL. Among the designs investigated were microchannel arrays suitable for heat exchanger and chemical processing applications, microchannels arrays for fluid flow applications, hole arrays for use in flow control or chemical separations technologies, and gaskets for microscale fluid processing devices. Representative examples of laser micromachined products are shown in Figure 1. Channels and holes as small as 5 μm diameter were demonstrated. This equipment has also been used to fabricate microscale components for PNNL's Airborne Pathogen Initiative.

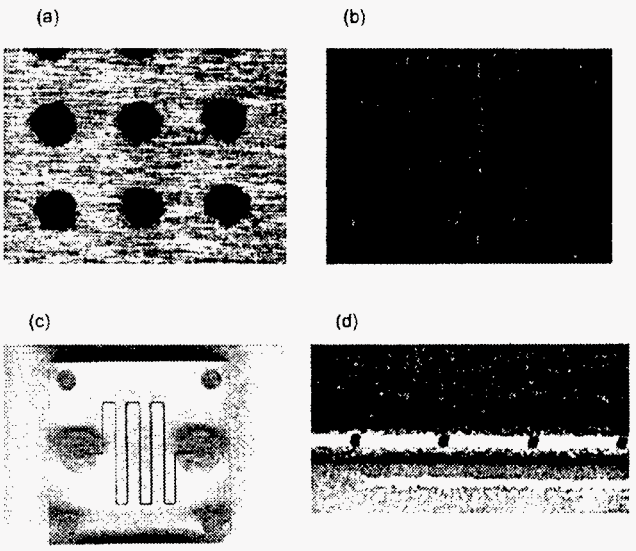

Figure 1. Examples of laser micromachined components. a) Hole array in 25 μm thick brass foil (hole diameter ~200 μm). b) Porous membrane produced by laser drilling in 50 μm thick polimide sheet. c) Channel (100 μm wide x 60 μm deep) with headers in 1.5 cm x 1.5 cm polycarbonate chip. d) Series of 50 μm diameter holes machined at an interval of 1.0 mm in a length of 0.020 inch diameter stainless steel hypodermic tubing.

An electrochemical deposition station was procured and installed for use in fabricating metal molds from micromachined designs to facilitate low cost, mass produced microcomponents, and to directly fabricate microscale heat exchangers and flow components. This equipment has the capability to build up metallic (e.g., Ni) structures in laser micromachined templates produced in polymers. After metallic electrodeposition the polymer can be removed either chemically or by plasma etching to leave the metallic mold. Figure 2 shows an example of a microchannel template produced in a 250 μm thick polyvinyl chloride plate attached to a copper backing piece and the nickel mold produced by depositing Ni in the template. The electroplated channels were about 75 μm wide and 375 μm deep, with an aspect ratio of 4:1. We expect to be able to fabricate structures with 10:1 aspect ratios in FY 1998.

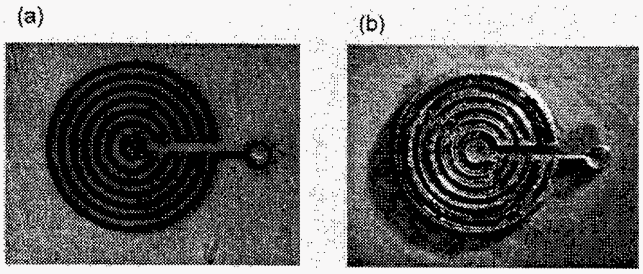

Figure 2. Microchannel template laser machined in polyvinyl chloride (a) and metal micromold (b) produced by electrodepositing nickel into the template. The polymer template was removed after the metal deposit using a chemical solvent.

Development of lamination processes for the fabrication of unique and/or low cost microchannel devices was pursued as a part of this project. We had previously submitted an invention disclosure covering production of solid structures containing microchannel arrays with very large aspect ratios. During the period of this project we submitted an additional invention disclosure expanding on the idea and covering additional configurations. This technology offers the potential to produce complex microscale components that cannot be formed by any other method. As an example, flow components containing microchannels having aspect ratios of greater than 100 are easily produced by this process. During the period covered by this project we were able to demonstrate the production of both stainless steel and aluminum components using this process. A stainless steel microchannel component is shown in Figure 3. An electrochemical machining station has been procured and set up to allow low cost fabrication of the shim layers to be used in such devices.

Among the additional capabilities developed at PNNL under this project is a video microscope/image capture

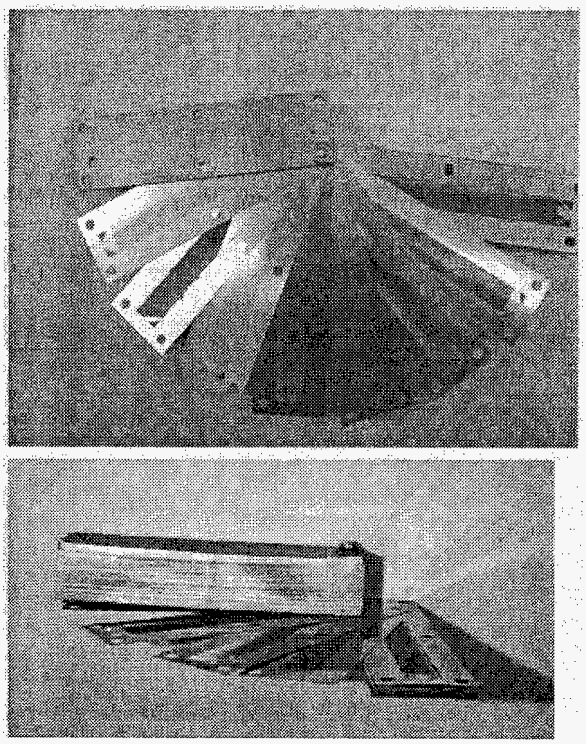

Figure 3. A solid stainless steel microchannel device produced using the lamination and diffusion bonding process. Additional nonbonded shims are shown to illustrate the form of the original layers prior to diffusion bonding.

station that allows detailed inspection, manipulation, and photography of microfabricated components. Using existing microscopes, magnifications of up to 180x can be obtained, and full zoom and/or macro capabilities exist.

Publications and Presentations

P.M. Martin, W.D. Bennett, D.J. Hammerstrom, J.W. Johnston, and D.W. Matson. 1997. "Laser Micromachined and Laminated Microchannel Components for Chemical Sensors and Heat Transfer Applications." In *Micromachined Devices and Components III, SPIE Conference Proceedings* Volume 3224, pp. 258-265, and presented at SPIE Conference on Micromachining and Microfabrication, Austin, Texas, September 29-30.

D.W. Matson, P.M. Martin, W.D. Bennett, D.C. Stewart, and J.W. Johnston. 1997. "Laser Micromachined Microchannel Solvent Separator." In *Micromachining and Microfabrication Process Technology III, SPIE Conference Proceedings* Volume 3223, pp. 253-259, and presented at SPIE conference on Micromachining and Microfabrication, Austin, Texas, September 29-30.

Interfacial Interactions of Biomolecules

Barbara J. Tarasevich, Allison A. Campbell (Materials Sciences)

Study Control Number: PN97060/1201

Project Description

Our objectives include developing a fundamental understanding of how interfaces control the adsorption of macromolecules. The interactions of macromolecules with surfaces are critical to many different industrial processes including biomaterials, enzyme synthesis, and the use of materials exposed to water/marine environments. Adsorption of an initial protein layer leads to a sequence of events such as microbial and cellular adhesion that can lead to material failure. Uncontrolled macromolecule adsorption or fouling often leads to corrosion or biological responses that result in implant failure. For example, the use of small bore vascular implants during heart surgery has been limited due to thrombotic occlusion (blood clotting) at the surface. The role of surfaces in controlling this response is not well understood, largely because the surfaces used have been complex and not well characterized. In addition, there are not very many well-developed experimental techniques to examine protein adsorption and conformation in situ.

We have developed self-assembling monolayers containing controlled surface site functionality as model systems to study protein adsorption. We also have developed the quartz crystal microbalance as an in situ real-time technique to examine protein adsorption kinetics. These studies have provided valuable insight on the nature of protein-surface interactions and conformational changes and have suggested ways to design surfaces to inhibit protein adsorption and fouling.

Technical Accomplishments

Self-assembling monolayers (SAMs) were developed. These molecules spontaneously adsorb from solution or vacuum and assemble by interchain van der Waals forces to form ordered arrays. SAMs make ideal model surface systems because site functionality, structure, and density can be systematically varied and controlled. The groups selected for the experiments were chosen in order to examine a hydrophobic, charged hydrophillic, and uncharged hydrophillic surface and were characterized by single wavelength ellipsometry, contact angle wetting, and external reflectance infrared spectroscopy (ER-FTIR).

A quartz crystal microbalance (QCM) apparatus was constructed that consists of gold electrodes vacuum deposited onto AT-cut quartz crystals attached to an oscillator probe via contact pins, a frequency counter, and a C program which collects the frequency data and displays it on screen. The QCM operates by application of a radio frequency to electrodes attached to an AT-cut quartz crystal which causes formation of an acoustic wave due to the converse piezoelectric effect. The oscillator circuit tracks the resonant frequency which corresponds to the formation of standing acoustic waves in the thickness shear vibrational mode. The addition of a rigid layer to the quartz surface increases the shear wave wavelength which reduces the resonance frequency. The Sauerbrey equation describes a linear relationship between mass and frequency change. Since very small changes in frequency can be detected, very small changes in mass can be determined on the order of 1 to 3 nanograms/cm^2.

A Plexiglas flow-through cell was constructed that could screw into the oscillator probe and allow flow of buffer and protein solution at rates of 1 to 500 μL/sec using a stepper motor controlled syringe pump. The flow cell volume was 0.1 mLs. SAMs were adsorbed onto the gold electrodes attached to the quartz crystals and the adsorption of albumin and fibrinogen was examined in pH 7.4, 25°C phosphate buffer solution. Albumin is the most common protein found in blood serum and fibrinogen is an adhesion protein associated with the attachment of platelets. Adsorption of fibrinogen is believed to start platelet adhesion and initiation of the platelet adhesion or thrombosis cascade. Figure 1a shows frequency changes associated with the introduction of protein solution into the flow cell at 5 μL/sec onto COOH SAMs after the frequency readings stabilized in buffer solution. The figure shows a decrease in frequency associated with protein adsorption. There is a slight increase in frequency after the protein solution is then flushed out with buffer. This most likely occurs because the solution viscosity affects the frequency reading and protein solution has a higher viscosity than the buffer solution. A kinetic plot of amount adsorbed versus time is shown in Figure 1b as determined by use of the Sauerbrey equation. This data shows two regions to protein adsorption, an initial region of high adsorption rate and a second region of much lower adsorption rate. The initial region occurs over time periods of 3 to 5 minutes and is

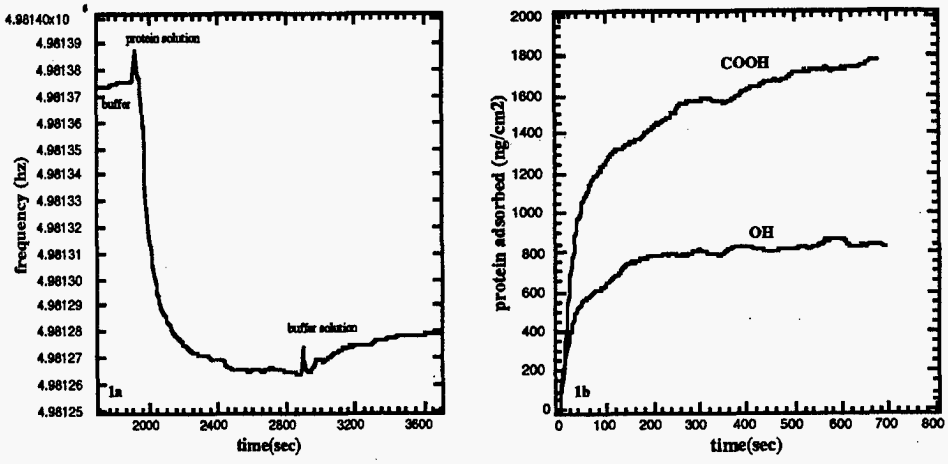

Figure 1a). Frequency changes associated with protein adsorption
1b). Adsorption kinetics on two different surfaces.

most likely associated with diffusion-limited adsorption of protein. In other words, the rate of adsorption is limited by diffusion to the surface. The second region represents surface-limited adsorption near the saturation plateau. This region occurs over longer time periods and represents adsorption that is limited by the magnitude of interaction with surface sites.

Examination of changes in frequency indicated that there were differences in protein adsorption depending on the protein used. In general, much more fibrinogen adsorbed than albumin. This may be expected because fibrinogen is larger (340K daltons) and has various charged and hydrophobic domains. Protein adsorption also depended on the surface site used and varied for fibrinogen as CH_3 (553 ng/cm^2) ≥COOH (476 ng/cm^2) >>>OH (60 ng/cm^2). These results are very interesting because they shed some light on the nature of interactions involved in protein adsorption and one surface, OH, resulted in very little protein adsorption. The large amount of protein adsorbed onto CH_3 indicates that hydrophobic interactions between nonpolar protein domains and nonpolar CH_3 surfaces are dominant here. Hydrophobic interactions are entropy-driven and result from interactions between nonpolar domains and surfaces which occur in order to reduce the amount of structured water surrounding nonpolar surfaces. The large amount of protein adsorbed onto COOH sites is in contrast to trends in the literature that show more protein adsorption onto hydrophobic surfaces. This suggests electrostatic interactions between charged amine residues and negative COO- sites. This suggests that different domains are involved in interactions with this surface than with the hydrophobic CH_3 surface. The small amounts of fibrinogen adsorption that occurred onto the OH surface (4Å) indicates that this surface may be of interest for applications involving inhibition and prevention of biofouling. Reduced adsorption may occur because of a lack of possible hydrophobic and electrostatic interactions. In addition, it is likely that a structured water layer is formed onto the OH surface which may create repulsive forces.

There was a difference in the mass changes obtained using the QCM (in situ) compared to those obtained using ellipsometry (ex situ). Mass changes were much larger for the QCM. This probably occurs because the QCM mass includes protein, as well as water due to hydration. It is not clear whether hydration results in a viscous or rigid component to the frequency change but this can be discerned from vector impedance analysis. Interestingly, the mass differences depended on the surface and were largest for the OH surface. This may occur due to protein unfolding which exposes hydrophillic domains to the surface and traps water there. Since there is very little known about which domains adsorb to surfaces, the QCM may be useful in elucidating these effects.

Our work involving self-assembled surfaces and new in situ methods to examine protein adsorption has elucidated aspects of the role of surfaces in controlling protein adsorption and unfolding. These studies have already provided guidance on how to design surfaces to reduce protein adsorption. Further work will examine protein adsorption onto more complex, mixed functionality surfaces and the use of other techniques to obtain molecular level information on protein binding.

Publication

B.J. Tarasevich and B. Jones. "Protein adsorption onto self-assembling monolayers using the quartz crystal microbalance." *Langmuir* (in preparation).

Light Emitting Polymers

John D. Affinito (Materials Sciences)

Study Control Number: PN97065/1206

Project Description

It was proposed to adapt PNNL's polymer multi-layer (PML) and liquid multi-layer (LML) vacuum deposition technologies to deposit light emitting polymer (LEP) materials in order to develop a low-cost, pollution-free, manufacturing process for fabrication of low voltage, wide area lighting and display panels. Such a process would revolutionize both the lighting and the flat panel display industries. We expected to demonstrate a single pass vacuum process for fabrication of wide area, flexible lighting panels that will make obsolete current methods that fabricate small, rigid panels in discrete multistep, air-vacuum-air processes. Further, as the current industry methods for depositing LEP materials rely on organic-solvent-based spin coating processes, substitution of solventless PML/LML methods will eliminate the main waste stream associated with the current industry approach to LEP devices. As well, spin coating is inherently a small-area, discrete-part fabrication method while PML/LML are inherently large area. It is further expected that with such low-cost, low-voltage, large-area, pollution-free, and high-efficiently lighting panels available, the adoption of this technology by the construction, transportation, military-aerospace, and electronics industries will be both rapid and wide spread.

Background

General Introduction to Light Emitting Polymers (LEPs)

Light emitting diodes (LEDs) based on organic materials (or LEP diodes) have attracted attention in the past few years because of their potential applicability to display technology. LEP technology could prove very attractive for low voltage, wide area lighting applications if a low cost fabrication process becomes available. Much of the cost of fabrication currently revolves around the multistep process that requires both vacuum deposition and atmospheric spin coating deposition.

In general, LEP displays are derived from sandwiching a thin film of semiconducting and light emitting polymer between a hole injecting (high work function) electrode and an electron injecting (low work function) electrode. In order to get the light out of such an electroluminescent device, one of the electrodes should be transparent.

As such, the hole injecting material used in polymer LEDs has almost exclusively been indium tin oxide (ITO) because of its transparency, high work function, and reasonably high conductivity. The electron injecting material is usually composed of a sputtered, or evaporated, metal layer. For a display device, the electrodes need to be patterned in orthogonal rows and columns and light is then emitted from the area of intersection of these lines upon applying an external potential (Gustafsson et al. 1993; Burroughes et al. 1990). For lighting applications, a simple, interdigitated sandwich structure is sufficient. Figure 1 displays a side view of the configuration of such an electroluminescent lighting device. One should note that, if the electroluminescent layer in Figure 1 is active LEP material dispersed in an polymer electrolyte matrix, the device is bi-polar and the work function of the electrodes does not matter. Such devices are called light emitting electrochemical cells (LECs).

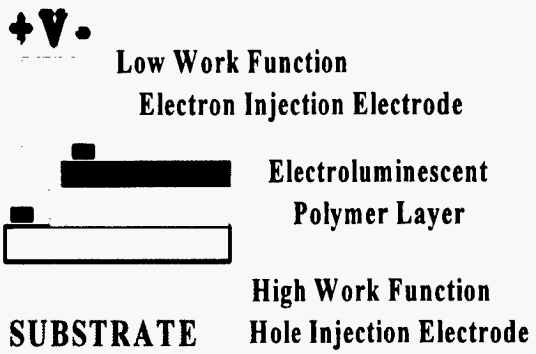

Figure 1. Schematic sketch of the Schottky type electroluminescence device.

When compared to conventional inorganic counterparts, such as liquid crystal displays (LCDs), there are several potential advantages for the use of LEPs. In contrast to LCDs or plasma displays, LEP devices can be fabricated on one sheet of glass or plastic, thus simplifying the manufacturing process and reducing the production cost. LEP devices are not limited to flat glass sandwiches which makes them more versatile than the conventional display technologies. Moreover, LEPs may be used for low-voltage lighting while LCDs are too expensive to be used

for lighting, and plasma displays are inherently high voltage and inefficient.

Polymers Used for Light Emitting Polymers

Until now three different processes have been explored for the fabrication of light emitting polymer devices:

1. A variety of organic, low molecular weight materials has been used for LEP fabrication. Discrete conjugated emitter center molecules are attached to the backbone of a non-conjugated polymer (Aguiar et al. 1995; Aguiar et al. 1996; Kido et al. 1993). These polymers are then put into solution and spin coated on glass or polymeric substrates that already have a transparent conducting coating, usually ITO or PolyANIline (PANI). The polymer film is then coated with a carrier transport layer, usually consisting of another highly conjugated organic material. After the transport layer, the low work function electrode (usually calcium) is deposited by evaporation. Three disadvantages to this approach are the crystallization of the organic layer that can occur, compromising interfacial contacts, the relatively high voltages required to inject charge carriers, and the instability of calcium (Tang and Vanslyke 1989).

2. Intrinsically emitting, conjugated polymers such as poly(p phenylenevinylene) (Kido et al. 1992) and poly(3 alkylthiophene)s (*Polymer Handbook 3rd edn* 1989) have been widely used as the emitting layers in LEDs because their p-electrons can be easily removed or injected forming ion radicals without affecting the s-bonds responsible for the integrity of the polymer. The most important drawback of these polymers is their insolubility in common solvents, making them difficult to process by well-established techniques such as spin casting or dip coating.

3. The molecular dispersion of charge transporting molecules in either inert inactive polymeric binders (for LEPs) or polymer electrolyte binders (for LECs) - also called molecularly doped polymers (MDPs). A good example of an MDP is the dispersion of the triphenyl diamine derivative N,N' diphenyl N,N' bis(3 methylphenyl) 1,' biphenyl 4,4' diamine (or TPD), which is a hole transporting emitting molecule, in poly (methylmethacrylate) (PMMA) at between 0.3 to 0.8 weight fraction (Kido et al. 1992). TPD is ideally suited because it has a high hole drift mobility of 10^3 cm^2/V s, while PMMA is optically and electronically inert and has good film forming properties with a high glass transition temperature of 105°C (*Polymer Handbook 3rd edn* 1989). Typically, a dichloromethane solution of the appropriate amount of PMMA is dip coated onto an ITO or PANI covered glass substrate. Then an electron transporting emitting layer composed of something like tris (8 quinolinolato) aluminum(III) (Alq) is vacuum deposited onto the polymer layer followed by a vacuum deposited metal electrode, usually a magnesium-silver alloy. Molecular structures for TPD and Alq are shown in Figure 2.

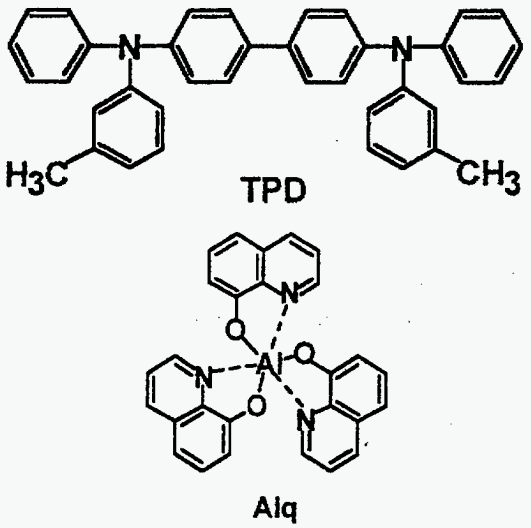

Figure 2. Molecular structure of TPD above and Alq below.

Advantages of this approach are that MDPs are much more versatile materials than the intrinsically conductive polymers, and their mechanical properties can be chosen by selecting the proper host polymer binder. Thus, they are more stable than the conjugated emitters attached to a polymer backbone. Another advantage is that, by using multiple emitter layers, broader band emission—approaching white light—can be attained.

Application of the PML Web Coater to the Production of Large Area Displays Based on LEPs

As mentioned before, one of the big advantages of LEPs over inorganic display devices is the potential to fabricate large area devices. PNNL has developed a vacuum web coater, and two unique processes, specifically for the high speed, low cost production of ultraviolet and electron beam curable polymeric films. Typically this sort of polymer process is carried out under atmospheric conditions. The unique vacuum deposition process has been developed at PNNL for a variety of applications that combine the polymeric layers with conventional vacuum deposited layers in an integrated manufacturing process. This integration reduces handling of the substrate between deposition of the individual layers which improves interlayer adhesion, gives better electrical contact, reduces contamination, and reduces fabrication costs as well. The coater, in its current configuration, is shown in Figure 3. The two unique PNNL processes for vacuum deposition of polymer films are called the PML (for Polymer Multi-Layer) and LML (for Liquid Multi-Layer) processes. A brief description of the PML process follows.

LAYOUT OF THE PML WEB COATER

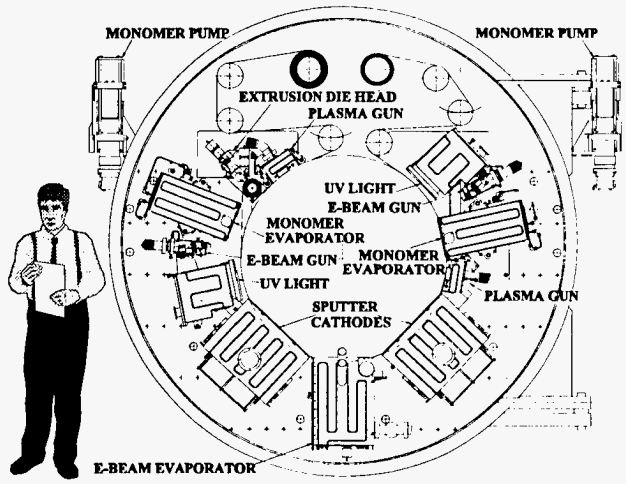

Figure 3. Schematic of PNNL's vacuum web coater that integrates PML flash evaporated polymer layers and LML extruded polymer layers with conventional vacuum deposited layers.

The PML process involves the flash evaporation, condensation, and subsequent polymerization of a monomer fluid. The technique used to evaporate the monomer is really quite simple. Monomer fluid is first degassed (stirred while the vapor is pumped away) to a suitable base pressure toprevent violent expansion when it is introduced to the vacuum environment. The degassed monomer is then sprayed into a very hot tube that has a very hot, pressure baffling, expansion nozzle on one end. By very hot, it is meant that the tube is hot enough to instantly vaporize the monomer spray, yet not hot enough to crack and/or polymerize the monomer on contact. Under these conditions the monomer evaporates as quickly as it is introduced into the tube and does not form a pool of liquid in the tube. The baffles in the tube/nozzle system serve to build the pressure (of the molecular gas of monomer molecules) in the nozzle expansion chamber. Building the pressure serves to make the molecular gas stream exiting the slit in the nozzle more uniform across the length of the nozzle slit. The monomer gas that exits the evaporator condenses on the substrate as a liquid film and is subsequently polymerized by exposure to ultraviolet or electron beam radiation. Film thicknesses obtainable with the PML process range from a few tens of angstroms up to mils, with the limit largely imposed by the penetration depth of the cross-linking radiation employed. Film thickness uniformity better than ± 2% is readily achieved.

Approach

In this work, LEP materials were combined with PML web coating technology for the production of LEP and LEC thin film layers applicable to low-cost, wide-area lighting or display devices. The LEP devices that could conveniently be manufactured with this technology have been described under number 3 in the previous section. Two basic structures for the device depicted in Figure 1 are envisioned with LEP/PML processing: 1) the active electroluminescent layer is something like a bi-layer of TPD dispersed in an acrylate matrix and Alq dispersed in an acrylate matrix, or 2) both hole and transport molecules (like TPD and Alq) are dispersed in an ion conductive acrylate polymer electrolyte. Devices like 1) are called LEP devices while devices like 2) are labeled LEC devices.

The substrate used for the web was polyester. The LEP and LEC polymer layers were deposited with the PML process by flash evaporating a solution of acrylate/acrylic acid and either: 1) hole transporting TPD molecules, 2) electron transporting Alq molecules, or 3) a combination of both TPD and Alq with Li-Bistrifluoromethylsulfonyl imide as an electrolyte salt. Flash evaporation/ condensation of the solutions was onto a moving substrate and ultraviolet was employed as the curing agent.

Results

It was found that all of the LEP active molecules that we tried (TPD, Alq, Quinacridone, and all related compounds) were completely insoluble in the standard acrylate monomer mixtures. While trying to solve the solubility problem we discovered a completely new, and very general, technique that permits us to put any of these materials into an acrylate solution that can then be used in the PML flash evaporation process. With this new technique, we successfully PML flash evaporated acrylate solutions to produce the three MDP layers described above: 1) hole transporting TPD dispersions, 2) electron transporting Alq dispersions, or 3) dispersions of both TPD and Alq together with Li-Bistrifluoromethylsulfonyl imide as an electrolyte salt. Concentrations of up to 50%, by volume, of dispersed material in the matrix have been attained but the limit may be higher.

Conclusion

With the fabrication technique just described, a vacuum web coater would be capable of producing the entire light emitting polymer device in a single pass. Compared with current approaches using multistep, air-vacuum processes, the PML technique should be much more cost effective.

The generally applicable technique for producing PML compatible acrylate solutions, with typically totally acrylate insoluble materials, will greatly broaden the scope of the PML process in addition to permitting fabrication of PML-based LEP and LEC layers.

References

M. Aguiar, F.E. Karasz, and L. Akcelrud. 1995. *Macromolecules*, 28, 4598.

M. Aguiar, B. Hu, F.E. Karasz, and L. Akcelrud. 1996. *Macromolecules*, 29, 3161.

J.H. Burroughes, D.D.C. Bradley, A.R. Brown, R.N. Marks, K. Mackay, R.H. Friend, P.L. Burns, and A.B. Holmes. 1990. *Nature*, 347 539.

G. Gustafsson, G.M. Treacy, Y. Cao, F. Klavetter, N. Colaneri, and A.J. Heeger. 1993. *Synthetic Metals*, 55-57 4123.

J. Kido, K. Hongawa, K. Okuyama, and K. Nagai. 1993. *Appl. Phys. Lett.*, 63 2627.

J. Kido, K. Hongawa, M. Kohda, K. Nagai, and K. Okuyama. 1992. *Jpn. J. Appl. Phys.* 31 L960.

Polymer Handbook 3rd edn. 1989. Eds. J. Brandrup and E.H. Immergut, Wiley, New York.

C.W. Tang and S.A. Vanslyke. 1989. *Appl. Phys. Lett.*, 65 3610.

Mechanisms of Radiolytic Decomposition of Complex Nuclear Waste Forms

Thomas M. Orlando (Chemical Structure and Dynamics)
Keith Keefer (Interface and Processing Science)

Study Control Number: PN95054/1030

Project Description

The mechanisms of radiation-induced degradation of complex waste forms such as $NaNO_3$, soda-glass, and ZrO_2 were investigated. $NaNO_3$ is a primary constituent of the underground mixed (radioactive/chemical) waste tanks at the DOE Hanford Site in eastern Washington State, and it has been suggested this waste be vitrified into glass. Since Na removal will not be carried out prior to or during the vitrification process, glass compositions containing relatively large loadings of Na have been proposed as "final" waste forms. Zr-based alloys are commonly used as cladding for nuclear fuel rods and in various components in nuclear power plants, primarily because of the robust nature of the oxide that forms, which is generally highly resistant to corrosion. It is also present in the cladding of failed spent nuclear fuel rods which are currently in storage pools awaiting treatment and disposition. Zirconium oxide films break down under the extreme radiation conditions present in nuclear reactors or spent-fuel ponds, and the water present at the oxide interface can undergo efficient radiolysis. In fact, the low-energy secondary electrons generated in the material by the ionizing radiation (emitted by radioactive decay) leads to the degradation of all of the above-mentioned materials. However, the exact mechanisms and cross sections for damage are currently unknown. We have, therefore, conducted a set of controlled experiments to investigate the role of low-energy electronic excitations in the radiation damage of $NaNO_3$, soda-glass, and ZrO_2. The first year of the LDRD focused primarily on sodium-nitrate (Knutsen and Orlando 1996), the second on soda-glass (Knutsen et al. 1996), and the last year on zirconium oxides. This report summarizes much of the work we have completed on understanding radiation effects at ZrO_2 interfaces.

Our approach was to take well-characterized ZrO_2 surfaces and submit them to bombardment by a monochromatic beam of low-energy electrons or photons. Desorbing ions and neutrals were detected via quadrupole mass spectrometry and time-of-flight techniques. Information on the valence band electronic structure was also obtained via temperature and time-resolved laser-(213, 266, and 355 nm) and 500 eV electron-stimulated luminescence studies. Further information on the electronic structure was obtained (supported by a DOE, Basic Energy Sciences program on Interfacial Radiolysis Processes) using x-ray photoemission spectroscopy (XPS) at the national Synchrotron Light Source at Brookhaven National Laboratory.

Technical Accomplishments

Photon- and Electron-Stimulated Desorption of O^+ from Zirconium Oxide

Measurement of the O^+ desorption threshold and kinetic energy distribution, coupled with photoemission measurements of the electronic structure of the surface, enable the identification of the excitations that result in oxygen removal from a ZrO_2 surface. For both crystalline and amorphous ZrO_2, the O+ photon- and electron-stimulated desorption thresholds are at ~30 eV, corresponding to the removal of a Zr(4p) electron, and the ions have ~2 eV of kinetic energy. These findings are consistent with the Knotek-Feibelman (1972) mechanism for stimulated ion desorption from metal oxides, in which the ionization of a shallow metal cation core level, followed by interatomic Auger decay, leads to the formation and rapid ejection of O^+ ions from the surface.

Photon-Stimulated Desorption of Cations from Yttria-Stabilized Cubic $ZrO_2(100)$

The positive ion-yield resulting from the interaction of a pulsed 266-nm laser with yttria-stabilized cubic zirconia crystals was investigated. Although the photon energy (4.66 eV) is well below the nominal band-gap energy for ZrO_2 (5.0 to 5.5 eV), photon-stimulated ion desorption (PSD) of Y^+, Zr^+, YO^+, and ZrO^+ begins at about 2.5 MW/cm^2. We interpret this as the onset of laser ablation. The cation mass spectra resulting from the above threshold fluences (i.e., ~2.9 MW/cm^2), resembles that obtained via secondary-ion mass spectrometry (SIMS). The similarity between the laser ablation and SIMS data demonstrates the importance of surface electronic structure effects in photon-induced degradation of this material.

We suggest that the primary mechanism leading to (near threshold) laser ablation of yttria-stabilized cubic zirconia involves multi-hole localization as proposed by Itoh and

Nakayama (1982) to explain PSD from GaP(110) surfaces. In materials with weak electron-lattice coupling, such as semiconductors and some metal oxides, self-trapping of holes and excitons does not occur. Rather, localization of energy can involve the production of multiple electron-hole pairs (via a multiple photon excitation) followed by two-hole localization at surface defects. Two-hole localization can occur when the hole-hole coulomb repulsion energy (U) is less than the energy gained by lattice relaxation. These arguments are similar to the Anderson negative-U localization model for defects in the bulk (Anderson 1975). Desorption of ions occurs when at least two holes are localized in the same bond.

Laser-Stimulated Luminescence of Yttria-Stabilized Cubic Zirconia Crystals

The laser-stimulated luminescence (LSL) of yttria-doped (9.5 mole %) cubic zirconia (YSZ) is investigated at three wavelengths. We observe luminescence from the decay of three unique excited states, at 2.70, 2.27, and 2.10 eV following 213-, 266-, and 355-nm laser excitation, respectively. This is in good agreement with previously published data (Paje and Llopis 1993; PaiVerneker et al. 1989) in which continuous and 0.01-ms pulsed xenon lamp excitation was utilized. Each LSL band exhibits a different excited state lifetime. The emission kinetics for all of the luminescence bands are well-modeled by the equation $I = I_0(I+k\tau)^{-2}$, where I is the intensity and τ is the decay time. This type of kinetics occurs when the luminescence is produced by the ionization followed by recombination. However, 266- and 355-nm photons have insufficient energy to produce an electron-hole pair in cubic YSZ, which has a nominal band gap of approximately 5.0 to 5.5 eV. Photoelectron spectra of identical ZrO_2 (9.5% Y_2O_3) single crystals, which show that a weak density of occupied states extending 2 to 3 eV above the valence band and into the middle of the band gap, reconcile this apparent discrepancy. These gap states can easily be ionized by 266- and 355-nm laser light to produce free carriers. The temperature dependence of the maximum luminescence intensities is well approximated by Mott's equation, $I = I_0(1+Aexp(-Q/kT))^{-1}$, where Q is an effective activation energy and T is temperature. The luminescence decay kinetics differ significantly from the dependencies of the maximum intensities and can be approximated by the equation $\tau=\tau_0 exp(-T/T')$ where T is a constant. The difference between these decay modes is under further investigation.

References

P.W. Anderson. 1975. *Phys. Rev. Lett.* 34, 953.

P. Fiebelman and M. Knotek. 1972. *Phys. Rev. Lett.*

N. Itoh and T. Nakayama. 1982. *Phys. Lett. A92*, 471.

K. Knutsen, Y. Su, K. Keefer, and T.M. Orlando. 1996. *Proc. Am. Nucl. Soc. Progress in Hazardous Waste Cleanup*, 1, 616.

K. Knutsen and T.M. Orlando. 1996. *Surf. Sci.* 348, 143.

V.R. PaiVerneker, A.N. Petelin, F.J. Crowne, D.C. Nagle. 1989. *Phys. Rev.* B40, 8555.

S.E. Paje and J. Llopis. 1993. *J. Appl Physics* 57, 225.

Publications and Presentations

K. Knutsen and T.M. Orlando. 1997. *Phys Rev. B.* 55, 13246.

K. Knutsen and T.M. Orlando. "Low-Energy Electron- and Ultraviolet Photon-Stimulated Degradation of $NaNo_3$ Single Crystals." *Appl. Surf. Sci.* (in press).

D.P. Taylor, W.C. Simpson, K. Knutsen, M.A. Henderson, and T.M. Orlando. "Photon-Stimulated Desorption of Cations from Yttria-stabilized Cubic ZrO_2(100)." *Appl. Surf. Sci.* (in press).

W.C. Simpson, M.A. Henderson, and T.M. Orlando. "Low-Energy Electron-Stimulated Desorption of Yttria-stabilized ZrO_2(100) and H_2O/ZrO_2(100) Surfaces." *Surf. Sci.* (in preparation).

W.C. Simpson, W. Yei, J. Yarrmoff, and T.M. Orlando. "Photon-Stimulated Desorption and Photoemission Studies of Zirconium Oxide Surfaces." *Phys. Rev. B.* (in preparation).

N.G. Petrik, D.P. Taylor, W.C. Simpson, M.T. Sieger, and T.M. Orlando. "Laser-Stimulted Luminesence of Yttria-Stabilized Cubic Zirconia Crystals." *J. Appl. Phy.* (in preparation).

D.P. Taylor, K. Knutsen, W.C. Simpson, and T.M. Orlando. "Laser Ablation of Yttria-Stabilized Cubix ZrO_2(100):Ion and Neutral Yields." *J. Appl. Physics* (in preparation).

T.M. Orlando. 1997. "UV Photon- and Low-Energy (5-100 eV) Electron-Stimulated Processes at Environmental Interfaces." The 24th IEEE International Conference on Plasma Science, San Diego, California, May 19-22, invited.

T.M. Orlando. 1997. "A Comparison Between UV-Photon and Low-Energy electron-Stimulated Desorption Processes from Wide Band-Gap materials." The Fourth International Conference on laser Ablation, COLA '97, Monterey, California, July 21-25, invited.

D.P. Taylor, W.C. Simpson, K. Knutsen, M.A. Henderson, and T.M. Orlando. 1997. "Photon-Stimulated Desorption and Laser Ablation of Yttria-Stabilized $ZrO_2(100)$ Crystals." The Fourth International Conference on Laser Ablation, COLA '97, Monterey, California, July 21-15.

W.C. Simpson, W. Wang, J. Yarrmoff, and T.M. Orlando. 1997. "The Photon- and Electron-Stimulated Desorption of O^+ from Zirconium Oxide Surfaces." American Vacuum Society northwest Regional Meeting, Troutdale, Oregon, September 25-28.

N.G. Petrik, D.P. Taylor, W.C. Simpson, M.T. Sieger, and T.M. Orlando. 1997. "Laser-Stimulated Luminescence of Yttria-Stabilized Cubic Zirconia Crystals." American Vacuum Society Northwest Regional Meeting, Troutdale, Oregon, September 25-28.

Near Net Shape Forming of Resorbable and Implantable Devices

Beth L. Armstrong, Peter A. Smith, Lin Song,
Anna Gutowska, Greg W. Coffey (Material Sciences)

Study Control Number: PN96052/1119

Project Description

The overall goal of this project was twofold. The first objective was to continue to pursue the adaptation of PNNL's near net shape forming process for the fabrication of densified implants. Specifically, characterize the microstructure of the as-formed and densified components as a function of gelation properties. The second objective was to investigate new methods to fabricate resorbable implants. Specifically, utilize biocompatible gelling agents to fabricate and control porosity in biomaterials.

Technical Accomplishments

Both of the objectives required good mechanical performance of the products (i.e., microstructure) produced via the forming process. The near net shape forming process relies on rearrangement of the particles via shear deformation. In FY 1996, a processing-structure-property investigation was initiated to refine the near net shape forming process. The characterization of the processing behavior was obtained using rheological techniques; this approach provides information on deformation and the response to deformation of the precursor materials. The investigation of the processing-structure-property relationship was continued during FY 1997 to determine if the system (i.e., particle size, solids loadings) or the ceramic phase (zirconia, alumina, calcium phosphate) influences the gelation properties and the resulting fabricated microstructures.

Two types of experiments have been carried out to investigate the rheology of the polymer-ceramic system. The particulate phases examined during the experimentation were alumina, hydroxyapatite, tricalcium phosphate, and zirconia. Nontoxic and/or bio-benign, aqueous binder solutions were used. During FY 1996, the viscosity behavior as a function of solids loading in the precursor binder solutions was determined. These experiments indicated an asymptotic limit in the viscosity of the forming system. Viscosity is a transport property; it must be sufficiently low to facilitate suspension transfer to the mold. Beyond a specific volume loading of particulate, transport may be difficult and forming can become more challenging. In FY 1997, the morphology, particle size distribution, and surface areas of the ceramic phases were systematically changed to determine if the asymptotic viscosity limit could be controlled.

The second type of rheological experiments performed were dynamic oscillation tests. In FY 1996, the elastic and viscous responses to the application of a sinusoidal deformation were determined. This simulates the physical environment that the formulations are subjected to during forming. Observation of the elastic modulus and viscous modulus as a function of strain or frequency reveals the energy required to obtain microstructural rearrangement in the forming process. For strains and frequencies where the elastic modulus is greater than the viscous modulus, microstructural rearrangement is limited. In FY 1996, the components that were fabricated contained large flaws and had poor mechanical properties. Essentially, as the solids loading increased, the elastic component of the suspension increased in magnitude. As the elastic modulus increases, the suspensions become more difficult to deform and microstructural rearrangement was not obtained. In FY 1997, the balance between the rheological limitations and the final microstructure was further studied. Mixing techniques and mold technology were identified as opportunities for process improvements. Mechanical mixing was used during FY 1996 and did not provide adequate homogeneity of the binder-ceramic mixtures. In FY 1997, ball milling was used to achieve complete dispersion, minimize entrapped air, and remove solvent evaporation. The use of additives in the binder-ceramic solutions were also studied to improve ceramic solids loadings and increase mechanical integrity. Ultimately, the ceramic solids loadings were increased for the alumina and zirconia systems while maintaining low viscosities during forming. Improvements in mold design were made to reduce mold flaws and breakage during mold removal.

Lastly, three fabrication methods were investigated as feasible routes to produce porous, resorbable implant materials. Initial studies evaluated the feasibility of each method by fabricating baseline (nonporous) materials. The particulate phases examined were hydroxyapatite and tricalcium phosphate. As in the rheology experiments, nontoxic and/or bio-benign, aqueous binder solutions were used. In the baseline samples, the relationship between solids, loading, polymer content, and pore size was examined.

Publication and Presentation

B.L. Armstrong, L. Song, P.A. Smith, and G.W. Coffey. 1997. "Processing and Characterization of Biomaterials." Presented at and in *ASM Proceedings of the 30th Annual IMS Conference*, Seattle, Washington, July 20 - 23.

Thermoreversible Polymeric Gels

Anna Gutowska (Materials and Chemical Sciences)

Study Control Number: PN97102/1243

Project Description

The primary objective of this research is to develop a new drug delivery system based on stimuli-sensitive polymers for the chemo-embolization therapy that will enhance the efficacy and decrease the systemic toxic effects of chemo-therapy. Specifically, a new class of chemo-embolic materials will be developed and evaluated.

Technical Accomplishments

In recent years, transcatheter hepatic arterial chemo-embolization (TACE) has attracted attention as an effective therapy for unresectable malignant liver tumors. The aim of arterial chemo-embolization therapy is to increase the concentration of anticancer agents within the tumor and decrease the toxic systemic effects of chemotherapy. In clinical practice, TACE is most often performed using iodized oil (Lipiodol) and gelatin sponge (Gelfoam). To improve the efficacy of TACE, the research is continued on development of novel materials for chemo-embolization of the hepatic artery. Albumin microspheres and chitosan or chitin-treated albumin microspheres are examples of the currently studied new materials for chemo-embolization. The aim of this study is to develop and evaluate a new class of chemo-embolic materials. The expected advantages of our approach involve fast and effective embolization and easy incorporation of drugs by simple mixing.

In this study, the behavior of co-polymers with co-monomers was examined. The synthesized co-polymers were characterized by GPC, DSC, and NMR and the effect of co-polymer composition and molecular weight on gelation temperature and concentration was investigated.

Gelation properties of the co-polymers were affected by polymer composition and solution concentration. The feasibility of macromolecular release from the gels was investigated using a model macromolecule. The release followed the first order kinetics, with 50% of loaded protein released within 50 hours. The remaining protein was released with much slower rate within one week.

Presentations

A. Gutowska. 1996. "Thermoreversible polymer gels for chemo-embolization therapy of hepatocellular carcinoma." Presented at Biomedical Engineering Society 1996 Annual Fall Meeting, PennState, Pennsylvania, October.

A. Gutowska and A.A. Campbell. 1997. "Thermo-reversible polymeric gels for chemo-embolization therapy." Presented at Society for Biomaterials, New Orleans, May.

Molecular Science

Application of Mass Spectrometry to Life Science and Bioremediation Research

Richard D. Smith, Steve A. Hofstadler, Harold R. Udseth (Macromolecular Structure and Dynamics)

Study Control Number: PN95006/982

Project Description

This project was aimed at developing the basis for research in structural biology and health effects research related to the cellular level impacts of chemical and/or radiation exposure. It was also aimed at building the basis for much broader future efforts that would build upon and apply the accomplishments under DOE's human genome program to explicitly establish the linkages between the expression and modification of proteins and their protein-protein and protein-DNA interactions that result in the ultimate health effects. The basis for this will be the establishment of two new capabilities for comparing large arrays of cellular proteins from small cellular populations for changes in gene expression due to disease state, chemical/radiation exposure.

Technical Accomplishments

The complexity of biological processes involved in cell signaling, transcription, regulation, and responses to stresses requires new approaches to their understanding. Approaches are needed that not only aid in correlation of protein structure and function, but that also provide a "systems" level cellular characterization so that complex interactions and pathways can be studied. One desires to understand not only the interactions between genes, gene products (i.e., proteins) and their functions, but also to understand the complex linkages that determine system properties, such as those manifested as diseases. While methodologies are being developed for surveys at the RNA level, these approaches are less informative regarding the polypeptides actually expressed and their subsequent cellular processing, and provide no insights regarding post-translational modifications (such as the phosphorylation steps involved in signal transduction and glycosylation involved in cell surface recognition).

At present, proteome studies are based upon two-dimensional polyacrylamide gel electrophoresis (2D-PAGE), and the power of this approach, which allows as many as several thousand protein "spots" to be visualized, is well established. However, the 2D-PAGE technology is slow, labor intensive, cumbersome, precludes detection of subfemtomole quantities of proteins, and effectively inhibits many potentially rewarding lines of research. Protein identification from 2D-PAGE presently involves the separate extraction and analysis of each "spot," with the concomitant sensitivity disadvantages introduced by the additional sample handling and the need to first visualize the "spot" on the gel. The ability to monitor a large array of proteins and their modifications (i.e., the "proteome"), providing a detailed representation of complex interplay of biological processes, would prove enabling for achieving systems level understandings.

We are developing new methods for separations of large numbers of proteins from cellular samples coupled with mass spectrometric approaches that provide the large improvement in sensitivity and information gathering ability needed for proteome characterization. We will use capillary isoelectric focusing in microfabricated devices for obtaining rapid and high resolution separations based upon isoelectric points in conjunction with the information provided by Fourier transform ion cyclotron resonance (FTICR) mass spectrometry to construct "virtual two-dimensional gels" for proteome characterization in a manner that promises to be vastly more sensitive, informative, and faster than current technologies. Our plan is to also exploit novel "ion funnel" technology that can provide an approximate two orders of magnitude gain in sensitivity compared to the most sensitive mass spectrometer ion sources presently available, and which offer the potential to increase transfer efficiencies to close to 100%. In conjunction with high efficiency ion transfer optics, with the ability to mass select ions in transport or trapping and the ability to detect even single ions, the potential exists to make measurements even for proteins expressed at low to modest levels from single cells. We will use the world's highest magnetic field FTICR instrumentation constructed for the EMSL to provide high sensitivity and high resolution measurements for proteins extending to ~150 kDa size and implement new multi-trap FTICR methods that will greatly enhance sensitivity. Information obtained from multistage FTICR experiments will provide the basis for protein identification, along with partial sequence and information on the nature and site(s) of post-translational modifications. The new capability would enable, for example, high resolution "differential displays" of a substantial portion of the proteome, and

provide rapid and detailed views of how cellular systems respond to their environment.

Using advanced methods for collisional dissociation of ions in the trapped ion cell, a partial amino acid sequence was obtained from the injection of a population of 0.75 erythrocytes. These results demonstrate the methodology used for the generation of sequence information or information on the nature and sites of protein modifications. Additionally, the complexity of such high resolution tandem mass spectra clearly points to the need for development of advanced data visualization and interpretation schemes.

Selected ion accumulation (SIA), first demonstrated by us several years ago, involves application of a quadrupole excitation (QE) waveform in concert with ion injection and trapping and can enhance sensitivity since longer ion accumulation periods are possible without the normal losses due to expansion of magnetron radii from the presence of the gas added to facilitate trapping. Perhaps less obvious is the effectively extended dynamic range that can be achieved. We have shown that the effective dynamic range (as measured by the relative concentrations of analyte ions in solution) can be increased by several orders of magnitude by the sequential and selective removal of more abundant species with filtered or "colored" noise quadrupole excitation.

We have also initiated efforts to expand the flexibility, sensitivity, and dynamic range of FTICR. The dynamic range expansion approach as initially demonstrated was limited by the use of an FTICR cell arrangement that required that the pressure in the cell be rapidly changed between the quite different pressure regimes needed for quadrupole excitation and high resolution detection, and thus greatly reducing both the speed and over all efficiency (i.e., sensitivity) of the approach. Our plan is to eliminate the major ionic species to provide more "room" in the trap allowing low level species to be increased in abundance to an arbitrary extent, providing an effective increase in dynamic range and sensitivity.

Initial results have demonstrated the feasibility of efficient transfers of trapped ions. The use of our technology allows gains to be realized in terms of expanded structural information, increased sensitivity, and speed.

The full development of these capabilities would enable, for example, high resolution "differential displays" of a substantial portion of the proteome, and provide rapid and detailed views of how cellular systems respond to their environment.

Publications

Q. Wu, G.A. Anderson, H.R. Udseth, M.G. Sherman, S. Van Orden, R. Chen, S.A. Hofstadler, D.W. Mitchell, A.L. Rockwood, M.V. Gorshkov, and R.D. Smith. 1996. "A High Performance Low Magnetic Field Internal Electrospray Ionization-Fourier Transform Ion Cyclotron Resonance Mass Spectrometer." *J. Amer. Soc. Mass Spectrom.*, 7, 915-922.

D.W. Mitchell and R.D. Smith. 1996. "Prediction of a Space Charge Induced Upper Molecular Weight Limit Towards Achieving Unit Mass Resolution in FT-Ion Cyclotron Resonance Mass Spectrometry." *J. Mass Spectrom.*, 31, 771-790.

Q. Wu, X. Cheng, S.A. Hofstadler, and R.D. Smith. 1996. "Specific Metal-Oligonucleotide Binding Studied by High Resolution Tandem Mass Spectrometry." *J. Mass Spectrom.*, 31, 669-675.

L. Pasa-Tolic, G.A. Anderson, R.D. Smith, H.M. Brothers II, R. Spindler, and D.A. Tomalia. "Electrospray Ionization-Fourier Transform Ion Cyclotron Resonance Mass Spectrometric Characterization of High Molecular Mass Starburst Dendrimers." *Int. J. Mass Spec. Ion Proc.* (in press).

S.A. Hofstadler, R. Bakhtiar, and R.D. Smith. 1996. "Electrospray Ionization Mass Spectrometry. Part I. Instrumentation and Spectral Interpretation." *J. Chem. Ed.*, 73, A82-88.

P.J. Stang, B. Olenyuk, D.C. Muddiman, D.S. Wunschel, and R.D. Smith. "Transition Metal-Mediated Rational Design and Sefl-Assembly of Chiral, Nanoscale Supramolecular Polyhedra with Unique T-symmetry." *J. Am. Chem. Soc.* (in press).

M.V. Gorshkov, L. Pasa-Tolic, J.E. Bruce, G.A. Anderson, and R.D. Smith. 1997. "A New Dual Trap Design and its Applications in Electrospray Ionization FTICR Mass Spectrometry." *Anal. Chem.*, 69, 1307-1314.

D.W. Mitchell and R.D. Smith. "A Two-Dimensional Many-Particle Simulation of Trapped Ions." *Int. J. Mass Spectrom. Ion Proc.* (in press).

S.A. Hofstadler, J.C. Severs, R.D. Smith, F.D. Swanek, and A.G. Ewing. 1996. "A High Performance Fourier Transform Ion Cyclotron Resonance Mass Spectrometric Detection for Capillary Electrophoresis." *J. High Resol. Chromatogr.*, 19, 617-621.

R. D. Smith, J. E. Bruce, Q. Qu, and Q. P. Lei. 1997. "A New Mass Spectrometric Methods for the Study of Noncovalent Associations of Biopolymers." *Chem. Soc. Rev.*, 26, 191-202.

Catalytic Chemistry of Metal Oxides

Charles H.F. Peden (Interfacial and Processing Science)

Study Control Number: PN94012/902

Project Description

This project has been studying the chemistry and catalytic properties of metal-oxide materials. While the surface chemical properties of metal oxides impact an enormous number of environmental and energy problems and potential technological solutions, a general absence of detailed studies on well-characterized systems has prevented progress in developing a fundamental understanding in this area.

Transition metal oxides have found numerous applications as heterogeneous catalysts for industrially important processes, such as the selective oxidation, isomerization, and metathesis of hydrocarbons; photocatalytic oxidation of organics; and the selective catalytic reduction (SCR) of NOx. In spite of their importance, oxide catalytic materials and processes have received much less attention from a fundamental science point of view than have catalysis by metals. For this reason, we have initiated a project that includes fundamental studies of the catalytic properties of oxide materials. The following tasks were performed in FY 1997:

- surface analytical and high-pressure kinetics measurements on high-surface area catalysts and on model oxide substrates
- complementary spectroscopic measurements were made on both high-surface area materials and more structurally well-defined surfaces.

Technical Accomplishments

In the past year, we have performed the first studies of a photocatalytic reaction over a model, single crystal oxide surface in a unique high pressure catalytic reactor/ultrahigh vacuum surface science apparatus that was constructed under the auspices and funding of this project. In FY 1997, we measured the rate of the photocatalytic oxidation of a few hydrocarbon molecules over a TiO_2(110) model catalyst, including ethanol and propylene. These species were chosen because of the significant amount of literature that has addressed kinetics of photocatalyzed oxidation over titania powders. The latter studies raised a number of issues that are directly addressable by the model catalyst studies we are now capable of carrying out. In particular, the issue of "structure-sensitivity" (that is, the dependence of the reaction rate on the catalyst surface structure) is an important issue. As indicated below, the new apparatus available at PNNL for these studies is uniquely able to identify the origins of structure sensitivity in catalytic reactions.

During the first 2 years of this project, PNNL staff collaborated with Dr. David Belton of General Motors Research Labs. The research centered around understanding NO reduction over supported metal catalysts in contrast with the behavior of oxide catalysts.

In the collaborative studies, we examined the effect of surface structure on the NO-CO activity and selectivity by comparing the reactivity of Rh(100), Rh(110), and Rh(111) single crystal catalysts. These studies are motivated by many reports demonstrating that the selectivity for the two possible nitrogen containing products from NO reduction, N_2O and N_2, are dependent on Rh loading in supported catalysts. In previous years' LDRD reports, we described studies of the effects of temperature, NO conversion, and NO-CO ratio on the activity and selectivity of the NO-CO reaction at high (1 torr < P < 100 torr) pressures over two Rh single crystal surfaces [(111) and (110)]. We used the results to rationalize the behavior of realistic supported Rh catalysts for this important automobile exhaust catalytic reaction. While we found relatively small differences in the NO-CO activity over Rh(110) and Rh(111), large differences were evident between these surfaces with regard to their selectivities for the two competitive nitrogen-containing products, N_2O versus N_2. The more open Rh(110) surface tends to make significantly less N_2O than Rh(111) under virtually all conditions that we probed with these experiments. These results can be understood in terms of the relative surface coverages of adsorbed NO and N-atoms on the two surfaces under steady-state reaction conditions in that higher N coverages on the (110) surface favor N-atom recombination (N_2 formation) more than the NO+N reaction (N_2O formation) on Rh(110) relative to Rh(111). We tested these conclusions by making an indirect assessment of the state of the reactive surface with x-ray photoelectron spectroscopy (XPS). This technique can clearly distinguish between adsorbed nitrogen present as either molecular NO or as N-atoms formed by NO dissociation during reaction. For Rh(111), the spectrum

shows only a single N(1s) feature with a binding energy near 400.3 eV due to adsorbed NO. In contrast, the NO N(1s) feature on Rh(110), while present, is significantly smaller than another N(1s) feature at lower binding energy, 397.6 eV, due to adsorbed N-atoms. We also extended these studies to include kinetic experiments on the Rh(100) surface. This surface displays activity intermediate between the relatively rough (110) surface and smooth, close-packed (111) surface. FTIR studies were performed on the latter two surfaces in situ during high pressure reaction. While most of the ideas that rationalized our previous data were found to be mostly supported by the new FTIR results, we were able to identify a new and unexpected reaction intermediate that will now have to be included in the reaction model to explain the markedly different selectivity observed on this surface.

Publications and Presentations

C.H.F. Peden, G.S. Herman, I.Z. Ismagilov, M.A. Henderson, Y.-J. Kim, and S.A. Chambers. 1997. "The Growth, Structure and Surface Chemistry of Oxide Films as Model Catalysts." *Superficies y Vacio* (in press).

C.H.F. Peden, G.S. Herman, I.Z. Ismagilov, B.D. Kay, M.A. Henderson, Y.-J. Kim, and S.A. Chambers. "Model Catalyst Studies with Single Crystals and Epitaxial Thin Oxide Films." *Catal. Today* (in press).

C.H.F. Peden and P.D. Kaviratna. 1996. "Photocatalytic Destruction of Automobile Exhaust Emissions." 2nd International Conference on TiO2 Photocatalytic Treatment of Water and Air, Cincinnati, Ohio, October 27-29, invited.

C.H.F. Peden, G.S. Herman, I.Z. Ismagilov, M.A. Henderson, Y.-J. Kim, and S.A. Chambers. 1997. "The Growth, Structure and Surface Chemistry of Oxide Films as Model Catalysts." 2nd International Memorial G.K. Boreskov Conference, "Catalysis on the Eve of the XXI Century: Science and Engineering." Novosibirsk, Russian Federation, July 7-11, invited.

C.H.F. Peden, G.S. Herman, I.Z. Ismagilov, M.A. Henderson, Y.-J. Kim, and S.A. Chambers. 1997. "The Growth, Structure and Surface Chemistry of Oxide Films as Model Catalysts." 17th National Congress of the Mexican Surface Science and Vacuum Society, Mazatlan, Mexico, September 1-4, invited.

Colloid-Colloid Interactions: Forces and Dynamics

Donald R. Baer, Scott A. Lea (Interfacial and Processing Science)

Study Control Number: PN95016/992

Project Description

The objective of this project has been to measure forces between colloids in solution under conditions similar to those expected during the processing of waste tanks. Interparticle forces have a direct impact on the stability of colloids in solution and hence determine whether colloids flocculate or remain suspended and the degree of compaction of solids. Efforts at measuring these forces involved two different techniques: 1) using a force microscope for direct force measurements on single colloids, and 2) using an optical waveguide to determine the dynamic interaction fluorescently tagged colloids have with the surface of the waveguide. Because of limitations of the optical method, the major efforts have focused on the force measurements.

Technical Accomplishments

Force Measurement

The progress of this effort builds upon initial results which are summarized briefly before current progress is discussed. Progress was made during FY 1995 on silica, as a model system showed viability of the experiments. During this effort, a silica sphere was glued to a force microscope cantilever and the force distance curve was measured using scanning probe technology. Efforts on quantifying information from the data and defining limitations of the method and extending to the more relevant alumina surface were the focus of FY 1996 activities.

Initial measurements on the alumina surface showed a need to extend this capability to shorter separation distances and extend measurements to higher ionic strength. This work pushed the limits of the technology and required development of some alternate approaches for calibration and colloid mounting. During this year we started using stiffer probes and developed new methods for calibrating their stiffness. With the weaker probes, calibration of their stiffness was accomplished by attaching tungsten balls of known weight to the end of the cantilever and measuring the shift in the thermally excited natural resonant frequency. The thermally excited amplitude of the stiffer cantilevers are much too small to determine the resonant frequency and must be driven with a piezoelectric ceramic element. By doing so, however, the tungsten masses must be reversibly attached using a one-component epoxy. This new method produces linear calibration curves.

With these new probes, we have been able to make measurements on aluminum oxide systems that were not previously possible. The aluminum oxide surfaces had been prepared by sputtering aluminum in vacuum in the presence of oxygen so that 30 nm of aluminum oxide had deposited on a 2.6 micron silica sphere and on a freshly cleaved mica substrate. Conventional alumina microspheres are much too rough to correlate experimental data to theoretical predictions. We have been obtaining experimental force data between alumina surfaces at high ionic strengths and have begun to observe some data that are not adequately modeled by the Derjaguin, Landau, Verwey, and Overbeek theory and which we believe is indicative of hydration forces.

Equipment used in this LDRD project was moved to the EMSL, making progress more difficult during this past year. In spite of this difficulty (which limited staff and equipment availability), progress was made in three areas: experiments with the stiffer probes, development of a new model allowing measurements for different types of surfaces, and initial testing of a new surface forces apparatus.

A few sets of measurements were completed using the stiffer probes. An example of this work is shown in Figure 1 where the force curves are shown for alumina surface in a NaCl solution as the pH is altered. This figure shows dramatic changes in the force distance curve and the charge on the sample is altered. At the potential of zero charge (PZC at pH = 9) there is no electrostatic repulsion and attractions observed (negative values of Force/R). Only with the stiffer probes could the small repulsive and then attractive forces observed for the pH 7.4 curve be measured. This type of data allows measurement of the PZC (which can be measured by other means) and the force curves (which cannot be measured by any routine method). The ability of gathering this type of data allows effects of impurities and solvents on the PZC and force curve to be measured to assist prediction of aggregation and complex solutions.

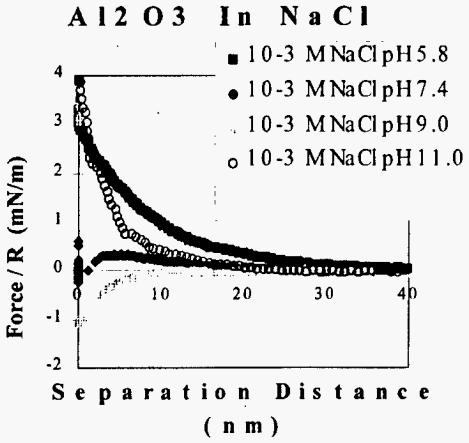

Figure 1. Force-distance curves between two alumina surfaces in 10^{-3} M NaCl solutions a different pH values.

An important part of the work has been relating force and solution models to the experimental data. Results to date involved fitting the force data obtained from identical surfaces to a Poisson-Boltzman model. Because this model is not valid for interactions between dissimilar surfaces, a linearized Derjaguins approximation model had been developed to include the interaction forces that arise when surfaces of different potential interact with each other. Due to the laboratory difficulties, we were unable to generate the data to allow application of the program, but use of the instrument to measure interaction forces between clay particles with different potentials on individual faces had been planned.

A surface force apparatus, which provides information that will complement the scanning force microscope, has been included as part of the EMSL project. Colloid interactions studies using the two different approaches to force measurement are planned as part of the colloid EMSP project. Some preliminary tests of the new apparatus of this instrument were undertaken.

Dynamical Interactions

The dynamical studies have demonstrated the ability of the optical measurement to produce the data. However, the results showed a combination of fundamental and experimental limitations to the information that could be obtained from the data. Therefore, starting in FY 1996 we focused our efforts on static colloidal force measurements using an atomic force microscope.

Computational Boron Chemistry

David A. Dixon (Theory, Modeling and Simulation)

Study Control Number: PN97026/1167

Project Description

The goal of this work was to model the liquid anhydrous hydrogen fluoride (LAHF) fluorinations of $\mathbf{1}^-$ and $\mathbf{2}^-$ to ascertain the factors that determine the site of fluorination and the regioselectivity of these reactions. Figure 1 shows the proposed mechanism for the fluorination reaction. The first step is protonation of a B-H vertex by HF (Step 1). The remaining F^- would then displace H_2 from the protonated vertex via an S_N2-like transition state (TS) to give the fluorinated product. The reaction was broken down into a number of steps including the removal of H_2 from the protonated vertex (Step 2) and the bonding of F^- to the now open vertex (Step 3).

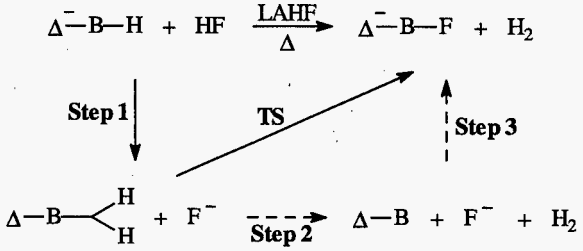

Figure 1. Proposed LAHF fluorination mechanism.

Calculations were done with the program DGauss 4.0. All of the molecular structures of interest were optimized at the local density functional theory (LDFT) level with the DZVP2 basis and the A1 density fitting basis. Second derivative calculations were done for each optimized structure to show minimums and to provide a zero-point energy correction to the total energy as well as other thermodynamic data. Vibrational frequencies were also calculated as an aid for experimental analysis. Final energies were calculated at the gradient-corrected level (non-local DFT) with the Becke exchange potential and the Perdew correlation potential (BP) at each optimized structure. To gain further insight into the LAHF fluorinations, detailed electronic population analyses and GIAO nuclear magnetic resonance calculations were done for many of the optimized structures.

Background

Boron-based compounds are important for neutron capture therapies as well as being important as separation agents for environmental remediation. In the latter context, tetraphenylborate (TBP) is being used in the in-tank precipitation process at SRP to separate Cs^+. Boron species may also prove to be useful complexing agents for a variety of metals. We have initiated a study with Professor Steven Strauss of Colorado State University on the fluorination of *closo*-carborane anions that will help us benchmark our ability to treat reactions of these compounds as well as investigate the design of new separation agents.

In the search for weakly coordinating anions, Strauss et al. have extensively studied the electrophilic fluorination of the carborane anions, $CB_{11}H_{12}^-$ ($\mathbf{1}^-$) and $CB_9H_{10}^-$ ($\mathbf{2}^-$) by liquid anhydrous hydrogen fluoride (LAHF) (Figures 2 and 3). Heating cesium salts of $\mathbf{1}^-$ and $\mathbf{2}^-$ in the presence of LAHF regioselectively fluorinates both anions. When $\mathbf{1}^-$ is fluorinated, the first fluorine is substituted on B12, the boron antipodal to carbon. Fluorination of the *closo*-deltahedral carborane anions $\mathbf{1}^-$ and $\mathbf{2}^-$ by HF is believed to proceed by a two-step process of protonation and then H_2/F^- substitution. Subsequent fluorinations occur on the lower belt boron atoms (B7-B11). This is usually explained in terms of the distribution of negative charge within the cluster. Being an electrophilic fluorinating agent, LAHF would be attracted to the most negatively charged site in the cluster, in this case the B12-H12 group. This is supported by cluster bonding theories as well as experimental observations. In contrast, when $\mathbf{2}^-$ is fluorinated, the first four substitutions occur on the lower belt (B6-B9) and the fifth fluorine then gets substituted on the antipodal boron (B10). This and other experimental evidence directly opposes the charge distribution argument used to explain the fluorination of $\mathbf{1}^-$.

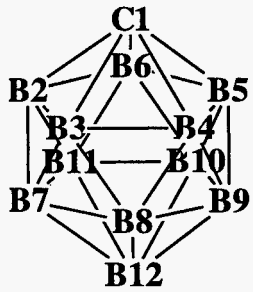

Figure 2. $CB_{11}H_{12}^-$ ($\mathbf{1}^-$).

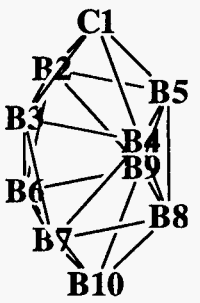

Figure 3. $CB_9H_{10}^-$(2⁻).

Technical Accomplishments

Table 1 shows the stepwise energies for the first and second fluorinations of $\mathbf{1}^-$. For both, Step 1 is the limiting factor determining which sites are fluorinated. The protonation of $\mathbf{1}^-$ is preferred at B12 over B2 and B6 by 12.4 and 3.4 kcal mol^{-1}, respectively, which would lead to the formation of 12-$CB_{11}H_{11}F^-$ ($\mathbf{3}^-$). This is confirmed by the observation that aqueous D^+ exchange occurs at a much greater rate at B12 than at B2 or B7. The protonation of $\mathbf{3}^-$ is favored at B7 over B2 by 8.4 kcal mol^{-1} which would lead to the formation of 7,12-$CB_{11}H_{10}F_2^-$ ($\mathbf{4}^-$). In both cases, this is experimentally observed product is the same as what is predicted.

The stepwise energies for the first and fifth fluorinations of $\mathbf{2}^-$ are outlined in Table 2. As before, Step 1 is restrictive for both $\mathbf{2}^-$ and 6,7,8,9-$CB_9H_6F_4^-$ ($\mathbf{5}^-$) but not completely for $\mathbf{2}^-$. Protonation of $\mathbf{2}^-$ is preferred at B6 by 15.5 and 1.2 kcal mol^{-1} over B2 and B10, respectively. This is consistent with the observation that aqueous D^+ exchange occurs at about the same rate at both B6 and B10. Therefore, Step 1 allows both 6-$CB_9H_9F^-$ ($\mathbf{6}^-$) and 10-$CB_9H_9F^-$ to be formed. Now Step 2 favors the removal of H_2 from B6 over B10 by 8.3 kcal mol^{-1} which then would lead to the formation of $\mathbf{6}^-$ as the preferred product, exactly as observed experimentally. Protonation of $\mathbf{4}^-$ is much easier at B10 over B2 by 23.7 kcal mol^{-1} which should lead to the formation of 6,7,8,9,10-$CB_9H_5F_5^-$ ($\mathbf{7}^-$). Experimentally, the reaction products are 2,6,7,8,9-$CB_9H_5F_5^-$ (92%) and $\mathbf{7}^-$ (8%). This is not what is predicted by theory but if we add the first two steps together (which will be validated by further experimentation) the 2 position is favored over the 10 position for fluorination by 4.6 kcal mol^{-1}.

Table 1. Stepwise energies for the LAHF fluorinations of $CB_{11}H_{12}^-$ ($\mathbf{1}^-$) and 12-$CB_{11}H_{11}F^-$ ($\mathbf{3}^-$) project description.

$CB_{11}H_{12}^- + HF \rightarrow$ x-$CB_{11}H_{11}F^-$	Step 1 (kcal mol^{-1})	Step 2 (kcal mol^{-1})	Step 3 (kcal mol^{-1})	Overall (kcal mol^{-1})
2	114.1 (12.4)	11.9 (0.0)	−149.4 (0.0)	−23.4 (0.0)
7	105.1 (3.4)	13.3 (1.4)	−140.9 (8.5)	−22.5 (0.9)
12	101.7 (0.0)	12.2 (0.3)	−137.1 (12.3)	−23.2 (0.2)
12-$CB_{11}H_{11}F^-$ + HF → x,12-$CB_{11}H_{10}F_2^-$	**Step 1 (kcal mol^{-1})**	**Step 2 (kcal mol^{-1})**	**Step 3 (kcal mol^{-1})**	**Overall (kcal mol^{-1})**
2	117.4 (8.4)	11.9 (0.0)	−152.4 (0.0)	−23.1 (0.0)
7	109.0 (0.0)	14.9 (3.0)	−145.3 (7.1)	−21.4 (1.7)

Table 2. Stepwise energies for the LAHF fluorinations of $CB_9H_{10}^-$ ($\mathbf{2}^-$) and 6,7,8,9-$CB_9H_6F_4^-$ ($\mathbf{5}^-$).

$CB_9H_{10}^- + HF \rightarrow$ x-$CB_9H_9F^-$	Step 1 (kcal mol^{-1})	Step 2 (kcal mol^{-1})	Step 3 (kcal mol^{-1})	Overall (kcal mol^{-1})
2	111.5 (15.5)	12.5 (0.0)	−148.0 (0.0)	−24.0 (0.0)
6	96.0 (0.0)	14.7 (2.2)	−132.6 (15.4)	−22.0 (2.0)
10	97.2 (0.0)	23.0 (10.5)	−143.4 (4.6)	−23.2 (0.8)
6,7,8,9-$CB_9H_6F_4^-$ + HF → x,6,7,8,9-$CB_9H_5F_5^-$	**Step 1 (kcal mol^{-1})**	**Step 2 (kcal mol^{-1})**	**Step 3 (kcal mol^{-1})**	**Overall (kcal mol^{-1})**
2	125.2 (23.7)	10.6 (0.0)	−158.9 (0.0)	−23.1 (0.0)
10	101.5 (0.0)	37.9 (27.3)	−157.9 (1.0)	−18.5 (4.6)

To further analyze the reasons behind the regioselectivity in the LAHF fluorinations, homolytic (Δ-B-H$^-$ + $\cdot CH_3$ _ Δ-B$\cdot^-$ + CH_4) and heterolytic (Δ-B-H$^-$ + CH_3^- _ Δ-B^{2-} + CH_4) bond strengths for **1**$^-$ and **2**$^-$ were also calculated. These results are given in Table 3. The heterolytic bond strengths are smallest for the B-H bond that gets fluorinated in both cases. The homolytic bond strengths for **1**$^-$ are too similar to draw any conclusions but the smallest for **2**$^-$ is also that for the B-H bond that gets fluorinated. This seems to correlate well with experiment. An alternate explanation for the regioselectivity may be that the weakest B-H bond is the onethat gets converted to a B-F moiety.

A general trend that can be seen throughout all of the data is the preference for the formation of kinetic products rather than the thermodynamically favored products. Confirmation comes from the appearance of the other possible monofluoro isomers when heating the cesium salts of **3**$^-$ and **6**$^-$. Energies of many different isomers of several fluorinated anions were calculated and compared to generate some general rules to determine the relative energies of different polyfluoro isomers of both **1**$^-$ and **2**$^-$:

1. define the base anion as 0.0 kcal mol^{-1}
2. add 99.0 kcal mol^{-1} for each fluorine
3. a fluorine in the lower belt adds an additional 2.0 kcal mol^{-1}
4. a fluorine in the antipodal position adds an additional 1.0 kcal mol^{-1}
5. add an additional 0.5 kcal mol^{-1} for each fluorine that has only one unique adjacent fluorine.

In general these rules work quite well for assigning stabilities among different polyfluoro isomers.

Table 4 shows the calculated ^{11}B, ^{12}C, and ^{19}F nuclear magnetic resonance chemical shifts for **1**$^-$, **2**$^-$, **3**$^-$, and **4**$^-$compared to the experimental chemical shifts. For all three nuclei, we can see there is a systematic difference between the calculated and experimental data (^{11}B 12.4 ppm; ^{12}C -3.8 ppm; ^{19}F 14.4 ppm).

Table 3. B-H bond strengths in $CB_{11}H_{12}^-$ (1$^-$) and $CB_9H_{10}^-$ (2$^-$).

$CB_{11}H_{12}^-$	Homolytic (kcal mol^{-1})	Heterolytic (kcal mol^{-1})	$CB_9H_{10}^-$	Homolytic (kcal mol^{-1})	Heterolytic (kcal mol^{-1})
B2-H2	-4.3 (0.7)	-166.0 (12.9)	**B2-H2**	-4.6 (2.5)	-168.6 (13.8)
B7-H7	-5.0 (0.0)	-174.1 (4.8)	**B6-H6**	-7.1 (0.0)	-182.4 (0.0)
B12-H12	-4.9 (0.1)	-178.9 (0.0)	**B10-H10**	-3.1 (4.0)	-172.6 (9.7)

Table 4. ^{11}B, ^{12}C, and ^{19}F nmr chemical shifts for 1$^-$, 2$^-$, 3$^-$, and 4$^-$.

Anion	Species	Calc.	Expt.	Diff.
$CB_{11}H_{12}^-$ (1$^-$)	C1	56.3	51.4	-4.9
	B2-B6	-26.8	-15.3	11.5
	B7-B11	-21.1	-12.4	8.7
	B12	-18.7	-6.0	12.7
$CB_9H_{10}^-$ (2$^-$)	C1	56.5	53.4	-3.1
	B2-B5	-31.4	-18.7	12.7
	B6-B9	-39.8	-24.2	15.6
	B10	18.0	30.6	12.6
12-$CB_{11}H_{11}F^-$ (3$^-$)	C1	40.2	36.1	-4.1
	B2-B6	-29.9	-18.8	11.1
	B7-B11	-22.9	-14.4	8.5
	B12	-0.5	14.3	14.8
	F12	-193.9	-190.4	3.5
6-$CB_9H_9F^-$ (4$^-$)	C1	51.4	48.5	-2.9
	B2,B3	-32.7	-20.6	12.1
	B4,B5	-25.1	-13.1	12.0
	B6	-8.1	4.4	12.5
	B7,B9	-33.2	-18.8	14.4
	B8	-47.7	-32.5	15.2
	B10	12.3	24.1	11.8
	F6	-256.7	-231.4	25.3

Development of a Whole Organ Perfusion System for Use in PBPK Modeling

Richard A. Corley (Chemical Dosimetry)
Charles Timchalk (Molecular Biosciences)

Study Control Number: PN97035/1176

Project Description

The objective of this project was to acquire, set up, and evaluate an isolated perfused liver organ system which can be used to assess the mode of action and metabolism of chemicals at the level of the whole, intact organ. The use of whole-organ perfusion systems provides a means to study the metabolism of chemicals in an isolated system that also maintains important features of cellular and organ structure. The isolated perfused organ system bridges between existing whole animal and in vitro metabolism technology and improves the Laboratory's ability to develop and validate physiologically based pharmacokinetic models (PBPK). These models are used to accurately simulate the internal dosimetry of chemicals and/or their toxic metabolites in animals and humans which is a key component of the Laboratory's PBPK-based real-time breath analysis system. In addition, the whole-organ perfusion system will have a direct application to other existing and planned research projects of importance to DOE that require accurate estimates of internal dosimetry of toxic chemicals.

Technical Accomplishments

Single-Pass Whole-Liver Perfusion Apparatus Setup

The single-pass perfusion apparatus (Figure 1) was obtained from Kent Scientific Corporation (Litchfield, Connecticut). The isolated liver is placed within the chamber and the portal and hepatic vein cannulas are connected to the perfusion system. The liver perfusion media is maintained within a heated (37°C) reservoir and the perfusate flow is set at approximately 2.5 mL/g liver per minute using a peristaltic pump to maintain a constant positive perfusion pressure. Physiological transducers for monitoring perfusion pressure, pO_2, pH, and temperature can be placed both upstream and downstream of the isolated liver for continual monitoring of liver function. The transducers are interfaced into an electronic data acquisition, storage, and reporting system (WorkBench® for Windows) for constant background data collection. The perfusate, which leaves the liver via the hepatic vein, is collected over time and analyzed based on the specifics of each experimental objective.

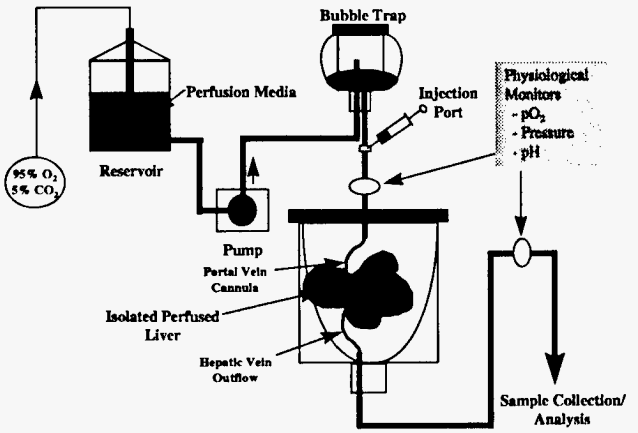

Figure 1. Single-pass liver perfusion apparatus.

Surgical Isolation of Rat Liver

A critical component for successfully conducting a perfusion experiment is the need to obtain viable whole liver as quickly as possible, avoiding conditions that result in anoxia and/or organ damage. All surgical procedures are conducted using aseptic techniques, and surgical instruments and related equipment are sterilized prior to the procedure. The donor rat is placed under general anesthesia [ip; ketamine (87 mg/kg): xylazine (13 mg/kg)] and a longitudinal midline incision is made from the pubis to the sternum. The inferior vena cava (anterior to the renal branch) and portal vein are isolated and loose ligatures are placed around these vessels. Heparin (100 IU) is administered via the vena cava to control for clotting and the vena cava is ligated anterior to the injection site. The portal vein is then cannulated (PE 100 tubing) and the liver is perfused with 2 to 3 mL of oxygenated perfusate. The chest cavity is opened and a second cannula (PE 200 tubing) is inserted into the inferior vena cava via the right atrium of the heart. Once the cannula is ligated, the liver is quickly removed from the animal and transferred to the perfusion chamber where the portal and hepatic vein cannulas are connected to the perfusion apparatus. It is also feasible to isolate and cannulate the hepatic bile duct, although that procedure was not attempted.

Preparation of Perfusion Medium

The choice of perfusion medium is critical, since differences in perfusion mediums are reported to contribute to significant variability in experimental results. The perfusion medium of first choice is whole rat blood; however, since a single-pass perfusion apparatus uses large volumes of perfusate, the use of whole rat blood is impractical. Therefore, a perfusate prepared from bovine blood was selected as a reasonable perfusion medium for this system. A local source for fresh bovine blood was identified. Once collected, the bovine blood is stored in a heparinized citrate buffer solution, which when refrigerated, is reported to maintain viability for up to 4 weeks. Immediately prior to conducting a perfusion experiment, the bovine erythrocytes are isolated from the bovine citrate blood by a series of centrifugation steps and the cells are repeatedly washed and then suspended in a heparinized Krebs-Ringers albumin solution. At this stage, the perfusion medium is transferred to the perfusion reservoir where it is oxygenated and warmed (37°C) prior to initiating the perfusion.

Whole-Liver Perfusion

Although validation studies with xenobiotics have yet to be conducted, the capability to isolate and perfuse viable rat liver in this system has been demonstrated. This technology is now available to support the development of PBPK models used in conjunction with the PBPK-based breath analysis system and for application to research problems of interest to the DOE.

Development of Dynamic Nuclear Polarization-Enhanced Capabilities for Applications in Environmental and Health-Related Research

Robert A. Wind (Macromolecular Structure and Dynamics)

Study Control Number: PN97031/1172

Project Description

In a collaborative project between Drs. R.A. Wind and P.D. Ellis of PNNL, and Professors R.J. Pugmire and D.M. Grant of the University of Utah, a special nuclear magnetic resonance (NMR) spectrometer is being constructed in which the NMR signals in specific materials can be enhanced by several orders of magnitude by dynamic nuclear polarization (DNP). The spectrometer will operate in an external magnetic field of 1.4 tesla and at variable temperatures at least in the range 120 to 350 K. It will be used to evaluate the possibilities of DNP-enhanced NMR in a variety of projects of environmental and health-related importance, to be carried out in collaboration with other scientists in and outside of PNNL. Examples of such projects are structural investigations of glasses and surfaces of catalysts used in waste remediation, flow and contaminant transport measurements on a micrometer scale, structural investigations of combustion engine deposits, chemical shift anisotropy measurements of rare nuclei such as ^{15}N in model compounds, studies of structures and dynamics in frozen bio-polymers, and DNP-NMR microscopic imaging and spectroscopy of live single cells, excised bones, and other biological compounds. Also, alternative, potentially more efficient, polarization transfer techniques will be examined, and the prospects of future high-field DNP-NMR, to be built at PNNL at a later date, will be considered. The 1.4 tesla DNP-NMR spectrometer will be constructed at the University of Utah, under the direction of Dr. Robert Wind.

Technical Accomplishments

This project started in late February 1997. Since then the following activities have been undertaken:

1. A 21-cm horizontal bore magnet and the necessary microwave equipment has been ordered. With the exception of a microwave traveling wave tube (TWT) amplifier, all instrumentation has arrived and was installed and tested. Also the NMR Chemagnetics console, to be used in this project, has been modified to accommodate low frequency DNP-NMR experiments.

2. Using 9 GHz microwave equipment, available at the University of Utah, initial experiments were carried out to optimize the efficiency of the DNP-NMR probe. It must be capable of handling relatively large (500 mg) samples. It was found that a circular horn antenna, a movable reflector, and a NMR coil with the same diameter as the horn, positioned with its axis parallel to that of the horn, gave the best results.

3. Using the results mentioned above, the first DNP-NMR probe was designed and built. This probe is capable of performing DNP-NMR on static samples in the temperature range of 120 to 350 K. This probe can also be used to perform c.w. EPR experiments at 40 GHz, and recently the first EPR measurements were carried out successfully. The EPR results are being used to further optimize the microwave efficiency of this probe. Also, the probe has been used successfully to detect ^{15}N NMR. It was found that acoustic ringing was not a serious problem, and that the probe NMR sensitivity was close to its optimal value.

4. Crystalline solids were doped with stable radicals using a melt-quench technique, and in a pilot study performed at the Wuhan Institute of Physics (PRC), it was established that large DNP enhancements (up to 300) can be obtained in these samples.

5. A method was developed to suppress unwanted background proton signals from proton-containing materials other than the sample of interest by almost 2 orders of magnitude. This technique will be applied in conjunction with proton DNP-NMR to obtain accurate values for the enhancement factors.

Publications and Presentations

R.J. Pugmire, M.S. Solum, R.A. Wind, and D.M. Grant. 1997. "^{15}N CPMAS NMR of the Argonne Premium coals." *Energy & Fuels*, 11, 491.

J.Z. Hu, J. Zhou, B. Yang, L. Li, J. Qiu, C. Ye, R.J. Pugmire, M.S. Solum, R.A. Wind, and D.M. Grant. "Dynamic Nuclear Polarization of Nitrogen-15 in Doped Benzamide." *Solid State NMR* (in press).

J.Z. Hu, C. Ye, R.J. Pugmire, M.S. Solum, R.A. Wind, and D.M. Grant. "^{13}C and ^{1}H NMR in melt/quenched-freezed doped benzofuran." (in preparation).

J.Z. Hu, B. Yang, R.A. Wind, D.M. Grant, R.J. Pugmire, and C. Ye. 1997. "Dynamic Nuclear Polarization in doped Benzamide and Dibenzofuran." Poster, 39th Rocky Mountain Conference, Denver, Colorado, August.

DNA Replication and Repair

Eric J. Ackerman (Environmental and Health Sciences)

Study Control Number: PN97039/1180

Project Description

DNA replication and repair are essential processes for life. Identifying the proteins involved and discerning their actions has implications for understanding basic life processes, defining the effects of environmental contaminants on human health, and exploiting novel organisms for remediation strategies.

Nearly 10% of all gene products are involved in DNA replication and DNA repair. The fundamental objective of this work is to understand the biochemical mechanisms of DNA repair and replication by studying these reactions in injected cells and in efficient extracts.

We developed the *Xenopus* system because *Xenopus* oocytes and extracts can repair 100% of the input DNA with no nonspecific incorporation on control substrate. The next best vertebrate extracts repair less than 2% of the substrate DNA. The higher sensitivity of the *Xenopus* system should permit identification and assignment f roles for proteins required in replication/repair. We have purified several proteins required for DNA repair and replication and prepared polyclonal antibodies to these proteins. Successfully reaching the milestones will result in a greater understanding of the molecular basis of several human diseases, including *Xeroderma pigmentosum* and perhaps even Alzheimer's. DNA replication and repair are essential processes for all life. Aside from the biomedical and therapeutic benefits, understanding replication and repair is essential for bioremediation of waste sites.

Background

We developed the *Xenopus* system for repair because *Xenopus* oocytes and extracts can repair 100% of the input DNA with no nonspecific incorporation on control substrate. The next best vertebrate extracts repair less than 2% of the substrate DNA. The higher sensitivity of the *Xenopus* system should permit identification and assignment of roles for proteins required in replication/ repair. We have purified several proteins required for DNA repair and replication and prepared polyclonal antibodies to these proteins. Successfully reaching the milestone will result in a greater understanding of the molecular basis of several human disease, including *Xeroderma pigmentosum* and perhaps even Alzheimer's. DNA replication and repair are essential processes for all life. Aside from the biomedical and therapeutic benefits, understanding replication and repair is essential for bioremediation of waste sites. No organism can survive hazardous environments such and waste sites without some mechanisms to alleviate damage to its DNA. Understanding these DNA repair mechanisms can enable the organisms to survive and perhaps remediate the site.

Technical Accomplishments

A key limitation of most DNA repair extracts is inefficient repair of substrate DNA with high background synthesis on undamaged control. Our *Xenopus* system overcomes these problems and can repair all of the input substrate with no incorporation on undamaged control. Furthermore, results obtained in our efficient nuclear extracts can be directly compared with results from injected cells to verify biological relevance. Defining the reaction requirements and roles of numerous proteins involved in DNA repair and replication is essential for understanding these processes.

The damage recognition process is one of the key aspects of DNA repair. We have purified the *Xenopus* damage recognition protein XPA. FY 1997 studies with the *Xenopus* XPA demonstrated an unexpectedly low affinity for damage lesions and suggested other proteins are required. (The NMR structural determination of a portion of the human XPA is being completed by Dr. Paul Ellis and colleagues in EMSL, and they began studying our full-length *Xenopus* XPA in early FY 1998.) We have raised polyclonal antibodies to our recombinant XPA protein, and we shall use both the protein and antibodies to search for proteins that interact with XPA. Our collaboration with Dr. Mick Smerdon (Washington State University) combines our *Xenopus* repair extracts with his randomly irradiated 5S nucleosome substrates to investigate repair. The same protein and antibodies will be useful for studying repair with defined substrates containing damage at defined sites with and without assembled nucleosomes. Understanding damage recognition may also be of widespread medical importance because the underlying cause of Alzheimer's disease may be a defect in nucleotide excision repair.

Preparing plasmid DNA substrates with damage at specific sites is complicated because it requires multiple steps with relatively low yields. In late FY 1997, we succeeded in producing several micrograms of plasmid containing a specific lesion at a defined site in the luciferase gene. We collaborated with a colleague at the National Institutes of Health to probe for defects in Alzheimer's cells in nucleotide excision repair using this plasmid, and related variants. The approach requires establishing a host cell reactivation assay of luciferase activity using oxidized DNA cleared of base-excision repair lesions with *E. coli* Nth enzyme and Fpg. The same substrates will also be used in our *Xenopus* extracts and cells.

Publications and Presentations

E.J. Ackerman, L.K. Koriazova, J.K. Saxena, and A.Y. Spoonde. "Nucleotide Excision Repair in Nuclear Extracts from Xenopus Oocytes. in DNA Repair Protocols." *Methods in Molecular Biology.* (in press).

Seminar for Department of Biochemistry, Washington State University, February 1997.

Presentation at DNA Repair Gordon Conference, February 4-9, 1997.

Eicosanoid Synthesis Following Exposure to Environmental Chemicals

Thomas J. Weber (Molecular Biosciences)

Study Control Number: PN97040/1181

Project Description

The objective of this project was to investigate the role of eicosanoid-related signaling in chemical-induced carcinogenesis. Eicosanoid biosynthesis is a rapid and highly sensitive response to chemical or physical stress. Eicosanoids elicit their biological effects via interaction with target eicosanoid receptors that are coupled to signal transduction cascades which are firmly associated with growth and differentiation programming. PNNL has invested considerable effort in defining the carcinogenic potential of environmental toxicants in the liver, and this organ is a logical place to initiate the proposed studies. The approach will be to determine basal and chemically induced eicosanoid synthetic profiles in mammalian cells. Although eicosanoid-mediated growth-regulation is the primary focus, in view of the prominent role eicosanoids play in differentiation, inflammation, and oxidative stress, this work will have broad implications for the Laboratory.

Technical Accomplishments

During this project, we examined the influence of eicosanoids on the growth behavior of isolated hepatocytes. Initial efforts assessed the influence of a stable prostaglandin E_2 (PGE_2) analog, 16,16-dimethyl PGE_2, on the growth behavior of isolated hepatocytes. Preliminary data indicate that 16,16-dimethyl PGE_2 may prevent apoptosis induced by serum-starvation. Subsequent studies will further evaluate the mechanisms for this response and evaluate the application of 16,16-dimethyl PGE_2-mediated cytoprotection against apoptosis induced by physiologically relevant agents. These studies are currently under way and we expect they will be completed in another LDRD project in FY 1998. In view of recent reports indicating that highly pure isolations of hepatocytes do not synthesize PGE_2, this suggests this autocoid is derived from neighboring cells. Future studies will address multiple cell systems to characterize basal and chemical-induced eicosanoid levels in the liver.

Experimental and Theoretical Study of Oxyanion Chemistry on Mineral Surfaces

Michael A. Henderson (Materials and Interfaces)
Stephen A. Joyce (Chemical Structure and Dynamics)
James R. Rustad (Environmental Dynamics and Simulation)

Study Control Number: PN96023/1090

Project Description

The adsorption, desorption, and diffusion of oxyanions on surfaces are important phenomena which occur during the transport of contaminants through soils. This project involves the application of experimental ultrahigh vacuum surface chemical and structural techniques combined with theoretical molecular mechanics to investigate the heterogeneous chemistry of oxyanions on mineral surfaces. Particular emphasis is placed on addressing the role of surface structure, both on the atomic and mesoscopic level, in the adsorption and subsequent chemistry of the adsorbed species. A number of candidate adsorbates are studied, including simple probe molecules such as water, alcohols, and organic acids, as well as more complex systems such as phosphates and chromates. Both ultrahigh vacuum surface science and geoscience are well-established disciplines with many common scientific interests; however, there has historically been limited overlap between the practitioners. This work brings together efforts from scientists in chemical physics, materials science and geochemistry.

Technical Accomplishments

In FY 1997, studies continued on both theoretical and experimental determinations of the structure and heterogeneous chemistry of the two low index, (001) and (012), surfaces of hematite. These two surfaces were chosen for a number of reasons. Both are fairly low-energy surfaces and are found on natural specimens. The different structures of the surfaces allows for a direct measure of the influence of cation coordination [threefold on the (001) and fivefold on the (012)]. Finally, we have observed that both surfaces reconstruct during vacuum annealing. This treatment presumably results in reduced iron sites (Fe^{3+} -> Fe^{2+}) and thus allows for a convenient way to study the role of charge state on the surface chemistry.

A strong coupling between theory and experiment occurred for the H_2O / α-Fe_2O_3(012)-1x1 system where both modeling/total energy calculations of the extent of dissociation and laboratory adsorption/desorption studies on a single crystal sample were performed. In addition, as described below, other studies included 1) beginning a series of quantum mechanical calculations on phosphate oxyanions to produce a model for phosphate which is consistent with our existing potentials for ferric oxide and water, 2) experimental studies of water interactions with the reconstructed α-Fe_2O_3(012)-2x1 surface, and 3) characterization of the surface structure of natural α-Fe_2O_3(001) surfaces.

The extent of water dissociation on hematite (012) was investigated through energy minimization calculations on a slab, three O-Fe-O-Fe-O layers thick, cut parallel to (012). Six neutral surface tautomers are possible within a single unit cell, but two pairs are symmetrically equivalent, leaving four unique tautomers. Two of these are 50% dissociated, one has no dissociation, and the other is completely dissociated. At the gamma point (every surface unit cell is exactly the same), complete dissociation is favored by about 0.9 J/m^2 over no dissociation, but 50% dissociation is favored over complete dissociation by about 0.1 J/m^2. This raised the question of whether there were other states away from the gamma point that were lower in energy than the 50% dissociated configuration. To explore this possibility, we constructed a supercell consisting of tilings of the six neutral cells in "a-b-a-b" and "a-b-b-b" patterns. For the "a-b-a-b" patterns, we also considered configurations involving a^{+1}-b^{-1}-a^{+1}-b^{-1}, meaning that we also considered supercells consisting of charged elementary cells, but combined them in such a way as to maintain a charge-neutral supercell. Energy minimizations were carried out on each of the 45 possible neutral supercells. These calculations included a stochastic searching procedure designed to locate low-energy proton configurations. These tilings allowed us to consider increments in dissociation at a finer scale of 12.5%. Taking the lowest-energy system at each of these increments, we find the set of values shown in Figure 1, with the minimum at 75% dissociation. We can perform a rough extrapolation by fitting the discrete set of points to a parabola which has a minimum at about 70%.

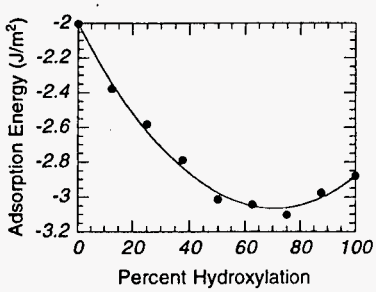

Figure 1. Calculated adsorption energies of water on the α-Fe_2O_3(012) surface as a function of the percent dissociated.

Quantum mechanical calculations were carried out on $H_4PO_4^+$, H_3PO_4, $H_2PO_4^-$, HPO_4^{2-}, and PO_4^{3-} at the NLDFT (B3LYP/6-311G**) level. A preliminary model for phosphate was produced, which mimics well the changes in P-O bond length as a function of the protonation state (these vary by about 25% from the median over the range of structures studied). Our model underestimates the successive deprotonation energies of $H_4PO_4^+$ by a remarkably uniform 20 kcal/mol. This is not unexpected since the dissociation energy of water at this level is about 25 kcal higher than the experimental value, to which our model is fitted.

Experimentally, we investigated the interaction of water with the fully oxidized and vacuum reduced surfaces of α-Fe_2O_3(012). When exposed to oxygen in ultrahigh vacuum at 800 K, the (012) surface of α-Fe_2O_3 forms a well-ordered (1x1) surface structure which we assign to the bulk terminated structure of the crystal. Water binds to this surface in one main desorption state evolving in TPD with classic first-order behavior at 350 K. The coverage of water in this peak is close to that of the surface density of Fe^{3+} sites expected for the (1x1) structure (approximately 7.3 x 10^{14} per cm^2). If the crystal is annealed at 950 K in ultrahigh vacuum, the (1x1) structure converts into a (2x1) structure based on LEED and STM which presumably possesses additional surface sites (Fe^{2+}) as a result of oxygen desorption. Water binds more strongly to this (2x1) surface, exhibiting a TPD state at about 410 K with non-first-order behavior; however, a considerably greater amount of water is also bound below 300 K. The total amount of water adsorbed on the (2x1) is about 10% greater than expected after removal of half the oxygen atoms in every other row of surface anion sites (approximately 9.1 x 10^{14} per cm^2).

The conversion of the (1x1) to (2x1) structure can be followed in TPD as a function of crystal preheating temperature, as shown in Figure 2. If the crystal temperature is maintained below 550 K, only (1x1)-like sites are present (the 350 K TPD peak). However, as the surface is preheated to progressively higher temperatures, the 350 K peak decreases and the 410 K peak appears and grows in intensity until the full (2x1) is formed. If the

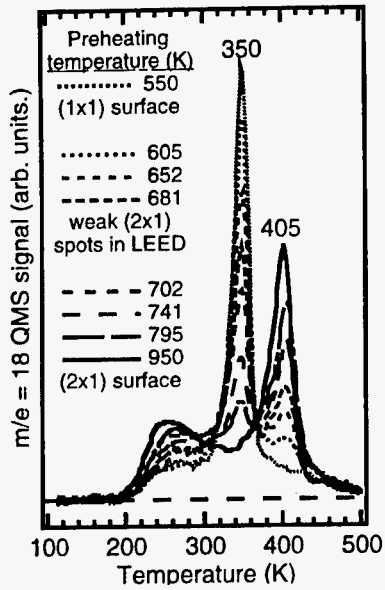

Figure 2. TPD of water from the (1x1) surface of α-Fe_2O_3(012) as a function of preheating temperature.

conversion is stopped halfway where there is an equal amount of the two TPD states and coverage dependent TPD experiments are performed, we observe that water fills the resulting (1x1) and (2x1) sites at the same rate. This result is counter to what would be expected based on thermodynamics, and suggests that the newly formed (2x1) domain sizes must be much larger than the diffusion length of water in the precursor state during adsorption and desorption. One obvious conclusion from this result is that reduced phases of iron oxides may form in nucleated patches as opposed to coalescence of random distributions of single reduced centers.

The surface structure of two different, natural α-Fe_2O_3(001) surfaces were examined using LEED and scanning tunneling microscopy. The surfaces were cleaned in vacuum by ion sputtering and oxidation at elevated temperatures. After repeated cleaning cycles, the surfaces were found to be clean by Auger electron spectroscopy. Hematite is a semiconductor with a ~3 eV bandgap and is intrinsically an insulator at room temperature. Often, however, either bulk oxygen vacancies or trace impurities act as electronic dopants, yielding samples with sufficient conductivity to allow for the use of electron-based surface analytical tools. For the first sample examined, the resistivity was found to be low enough for Auger and LEED studies to be performed, but too high for the STM. The first sample was annealed repeatedly in vacuum in an attempt to decrease the resistivity. Diffraction studies after this treatment reveals a complex surface reconstruction. Similar to the 2x1 reconstruction on the (012) surface, this is presumably due to oxygen loss and reduction of the iron leading to Fe^{2+} sites at the surface. The second sample had a low enough resistivity even for the STM, assumed to be

due to trace bulk impurities. To date, only the ideal bulk terminated 1x1 surface has been studied on this sample. A typical STM image is shown in Figure 3. Large flat terraces, some extending for thousands of angstroms, are observed. Well ordered, highly oriented steps are seen. By comparison with the diffraction measurements, we index the steps in the high symmetry <100> and <010> directions. The step densities are only on the order of a few percent of the surface, which compares quite favorably with the step densities of high-quality synthetic samples of metals and semiconductors. In addition to the step defects, several other extended defect structures are present. Emergent screw dislocations were commonly seen. A screw is present in the lower right corner of Figure 3

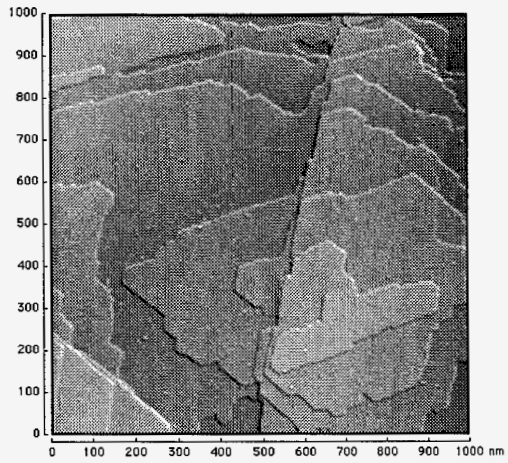

Figure 3. A 1000 nm x 1000 nm STM image of a natural α-Fe_2O_3(001) sample. Note the clear symmetry in the steps (120° kinks) and the screw defect emerging from the island in the lower right corner of the image.

(screws appear as steps emerging from an otherwise flat terrace). A low angle grain boundary was detected with LEED. Grain boundary and screw defects are common in natural samples, but due to their low densities, especially with respect to the steps, they are expected to play only a very small role in the surface chemistry.

Publications and Presentations

E. Wasserman, J.R. Rustad, A.R. Felmy, B.P. Hay, and J.W. Halley. 1997. "Ewald methods for polarizable surfaces with application to hydroxylation and hydrogen bonding on the (012) and (001) surfaces of α-Fe_2O_3." *Surface Science*, 385, 217.

E. Wasserman and J. Rustad. 1997. "Hydroxylation and Hydrogen Bonding on the (012) and (001) surfaces of α-Fe_2O_3." Northwest AVS meeting, Troutdale, Oregon.

Glass Structure, Chemistry and Stability

Keith D. Keefer (Interfacial and Processing Science)

Study Control Number: PN95036/1012

Project Description

The objective of this project is to define an experimentally observable scheme of silicate molecular speciation and formulate a statistical thermodynamic theory that permits the construction of phase diagrams for complex silicate liquids. By coupling a model of speciation with a thermodynamic theory, we are able to extract thermodynamic information from spectroscopic measurements and make predictions about features observed in spectra from thermodynamic data. The outcome is an extremely powerful description of the melting, phase separation, glass formation, and resistance to aqueous attack of complex, multicomponent silicate liquids, whose thermodynamic parameters can be determined from measurements on binary systems.

Technical Accomplishments

Our approach provides a rigorous thermodynamic treatment of silicate liquids in terms of the Lewis acidity of each of five silicate species that are categorized by only the number of bridging oxygens on each tetrahedron. This Lewis acidity is essentially the same for all silicate melts and independent of the type of network modifying oxides in the system. The Lewis basicity of the network modifier oxides that are dissolved in the melt are different and control the silicate speciation. The predictive power comes from the fact that the Lewis acid/base behavior, once established in one system or compositional range, should not differ much over a large quantitative and qualitative range of melt compositions.

One of the most important features of this theory is that the thermodynamic aspects describe the liquids behavior while the local chemical speciation provides a description of the short-range structure and chemical behavior at the molecular level. The longer-range polymeric structure can be treated with percolation theory and used to understand larger-scale melt behavior. For example, it appears that Q3 groups are much more likely to be hydrated than other species and so a large concentration of Q3 in a glass is likely an indicator of low chemical durability. But the ease of glass formation is due to the percolation of oxygen bridges. Systems with large amounts of Q3 will have the largest percolation threshold and be the easiest to quench to a glass. Using a lattice treatment of the statistical thermodynamics allows the percolation threshold of the silicate polymer and therefore glass formation to be predicted. The results of this study can be used to predict formulations that would have good glass forming qualities and still exhibit good chemical durability.

Publications

L.R. Corrales and K. D. Keefer. 1997. "Solubility limits of silicate melts." *J. Chem. Phys.* 106 (15).

K.D. Keefer and L.R. Corrales. "Phase separation in silicate melts: I. A perspective of lattice models, equilibrium theory, and associate models." (in preparation).

K.D. Keefer and L.R. Corrales. "Phase separation in silicate melts: II. The role of molar volume changes." (in preparation).

Glutathione Transferase Molecular Dynamics Simulation

Rick L. Ornstein (Environmental Technologies)

Study Control Number: PN96029/1096

Project Description

Glutathione S-tranferases (GSTs) play a key role in the detoxification of xenobiotics and in oxidative metabolism. In addition, GSTs have also been implicated in the development of resistance toward xenobiotics such as carcinogens, therapeutic agents, pesticides, and insecticides by cells and organisms ranging from humans to plants to bacteria. Tetrachlorohydroquinone reductive dehalogenase (TeCH-RD) has been isolated and purified by Dr. Luying Xun (WSU and PNNL). This enzyme is involved in the biodegradation pathway of pentachlorophenol. As part of a larger effort, Dr. Michael Kennedy and coworkers have been using solution NMR methods to solve the structure of this enzyme. TeCH-RD is a member of the important family of detoxifying enzymes called glutathione S-transferases. We are performing high-level quantum mechanics calculations to uncover the nature of the underlying fundamental mechanism of the GST family of enzymes, of which TeCH-RD is a member. In FY 1997, we completed a series of molecular dynamics simulations on a GST dimer with different bound reactants and products, and began to identify active site tight-binding regions of different chemical function groups that can be employed for rational drug design purposes.

Technical Accomplishments

Using high-level ab initio molecular orbital calculations, we identified the location and strength of the key mechanistic proton (involved in the first step of the chemical reaction) of the enzyme-glutathione binary complex, O---H---S. This was predicted to be near the phenolic oxygen, which is in agreement with experiments. However, the position of the proton can be manipulated by changing the acidity of the tyrosine.

In order to begin to understand the fundamental mechanism of this class of enzyme, we performed high-level ab initio molecular orbital methods to investigate the proton location in the deprotonated glutathione-GST binary complex and the strength of the hydrogen bond formed between the active site tyrosine residue and the thiol group of glutathione. The location of the key mechanistic proton of the enzyme-glutathione binary complex, O---H---S, was predicted to be near the phenolic oxygen, which is in agreement with experiments. However, the position of the proton can be manipulated by changing the acidity of the tyrosine. The hydrogen bonding between tyrosine and thiolate of glutathione is very strong. This work led to the prediction that in the Y6F (\Tyr->Phe) mutant, a water molecule replaces the function of the hydroxyl group of the active site tyrosine of the wild-type enzyme; several lines of evidence support this hypothesis.

The reaction mechanism of nucleophilic aromatic substitution of 1-chloro-2,4-dinitrobenzene by glutathione (as modeled by a thiomethoxide ion) in gas phase and in solution was elucidated using ab initio molecular orbital theory in combination with a continuum solvent model at the HF/6-31G*, HF/6-31+G**, and MP2/6-31+G** levels of theory. In the gas phase, the overall reaction occurs with little or no barrier. In aqueous solution, there is a large free energy barrier and C-S bond formation is predicted to be the rate-determining step, which is in agreement with experimental observation. In both gas phase and solution, the reaction is predicted to proceed via an intermediate (Meisenheimer complex); the minimum corresponding to this intermediate is very shallow on the free energy surface, and hence the intermediate may not be trapable. These results yield significant new information concerning the mode of action of GSTs and a related dehalogenase.

Publications and Presentations

Y.-J. Zheng and R.L. Ornstein. 1996. "Catalytic Role of the α-Carboxylate of the Glu Residue of Glutathione in Glutathione S-transferases." *J. Biomol. Struct. Dyn.* 14, 231-233.

Y.-J. Zheng and R.L. Ornstein. 1996. "An explanation of the single-turnover experiment of 4-chlorobenzoyl CoA dehalogenase." *Prot. Eng.* 9, 721-723.

Y.-J. Zheng and R.L. Ornstein. 1997. "Role of Active Site Tyrosine in Glutathione S-Transferase: Insights from a Theoretical Study on Model Systems. *J. Am. Chem. Soc.* 119, 1523-1528.

Y.-J. Zheng and R.L. Ornstein. 1997. "Mechanism of Nucleophilic Aromatic Substitution of 1-Chloro-2,4-dinitrobenzene by Glutathione in the Gas Phase and in Solution. Implications for the Mode of Action of Glutathione S-Transferases." *J. Am. Chem. Soc.* 119, 648-655.

Speaker at IBC Conf. on "Exploiting Enzyme Technol." San Diego, February 1997.

Speaker at Amer. Chem. Soc. in "Biocatalysis." San Francisco, April 1997.

Magnetic Resonance Spectroscopy Studies of Glasses, Minerals and Catalysts

Herman M. Cho (Macromolecular Structure and Dynamics)

Study Control Number: PN95052/1028

Project Description

The link between structure, dynamics, and macroscopic properties of certain inorganic solids is the focus of this project. The materials we are investigating include metal-supported catalysts, multi-component aluminoborosilicate glasses, and natural minerals associated with Hanford remediation science issues. An approach based on spectroscopy, primarily magnetic resonance and infrared, and analytical methods, is described.

Technical Accomplishments

Progress on Multicomponent Glasses

The following simulants of vitrified low-level radioactive waste forms, with the approximate composition $yP2O5$-$(0.034)SO_3$-$(1.098)B_2O_3$-$(8.030)SiO_2$-Al_2O_3-$(2.741)Na_2O$ (where $0.071 \leq y \leq 0.581$), have been studied by ^{31}P magic angle spinning (MAS) nuclear magnetic resonance (NMR) to determine the dominant modes of phosphorus incorporation in these materials, both inside and outside the glass network. Based on analyses of current waste contents and projections of probable pretreatment scenarios, these compositions are representative of the low-level nuclear waste glasses that will be produced by DOE at the Hanford Site. Several distinct environments have been identified, with some of the nearest neighbor cations of phosphorus sites inferred by manipulating the ^{11}B, ^{27}Al, or ^{23}Na resonances together with the ^{31}P resonance in double resonance NMR experiments (see Figure 1). Combined with numerical deconvolution of the ^{31}P MAS NMR spectra, concentrations of the various phosphorus-containing species have been estimated from these results, and the partitioning of phosphorus in the glass has been deduced. These experiments and others also reveal the existence and identities of separate ortho- and pyrophosphate phases in the glass.

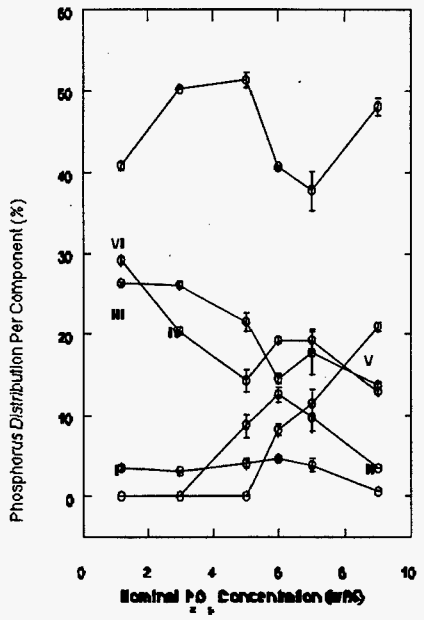

Figure 1. Percentage of total integrated ^{31}P NMR signal contained in each glass component as a function of total P_2O_5 concentration. Six distinct phosphorus environments have been found in this series of glasses. The standard deviation of multiple measurements is shown in the error bars.

Progress on Sulfated Zirconia Catalysts

A series of sulfate-promoted ZrO_2 solid acid catalysts samples were prepared, each sample differing only in the pH of the sulfuric acid soaking step of the synthesis procedure. Fourier-transform infrared (FTIR) spectra and thermal weight-loss measurements (as measured by thermal gravimetric analysis [TGA]) indicate that the pH of the sulfuric acid soaking solution influences the number of surface proton sites (see Figure 2). The activity of sulfate-promoted ZrO_2 in catalyzing the isomerization of n-butane to iso-butane at 220°C and the surface area of the calcined catalyst are found to depend on the soaking solution pH, with maximum surface areas and activities observed between pH 6 and 9. Proton NMR chemical shifts measured using combined rotation and multiple pulse spectroscopy indicate that the sulfating step produces proton species that are more acidic than proton sites on the non-sulfated support. The proton NMR spectra of these samples consist of at least two overlapped, but distinct, resonances that can be separated on the basis of differing spin-lattice (T_1) relaxation times. On the basis of a comparison of the experimental spectra with a series of simulated spectra, the long T_1 component has been

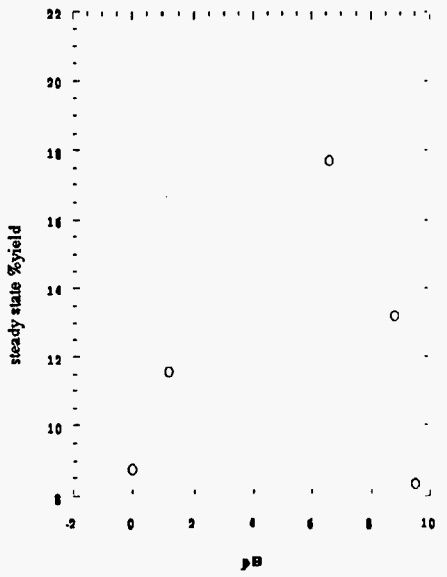

Figure 2. Steady-state yield as a function of sulfating solution pH of the SO_4/ZrO_2 catalysts for the isomerization of n-butane to iso-butane at 220°C.

assigned to a discrete three- or four-proton site that includes one water molecule, and the short T_1 component to an ill-defined cluster of protons. Variable-temperature NMR line shape data also suggest that the protons are in rapid motion on the sulfate-promoted zirconium oxide surface.

Progress on Mineral Studies

A series of hydrotalcite-like materials $[Mg_{1-x}Al_x(OH)_2A_yB_{1-y})_{3/2x}nH_sO$; $A=CO_3^{2-}$ and $B=p\text{-}C_6H_4COO^{2-}$] were synthesized at pH 10, 8.5, 7.5, and 7.0 with carbonate and terephthalate (TA) anions as charge balancing interlayer species. The dynamics of the anions were investigated by ^{13}C and ^{2}H variable temperature solid-state NMR methods. The terephthalate anions were found to undergo rotational diffusion about their C_2 axis in the temperature range $200\ K < T < 350\ K$ for orientations both perpendicular and parallel to the hydroxide layer sheet. Evidence for both small angle librational motion of the C_2 axis and for a distribution of motional rates was discovered. The correlation time at room temperature depends on layer charge and interlayer spacing, with the width of the distribution depending on the diorder of the 14.2 Å perpendicular phase.

Progress on New NMR Methods

The standard coherent averaging theory treatment of the resonance offset interaction was compared to exact calculations for several multiple-pulse homonuclear decoupling sequences. Significant differences between coherent averaging theory approximations and exact results were revealed by this comparison, even for idealized conditions. The origin of this disagreement was shown to be the comparatively large higher order terms in the Magnus expansion of the toggling frame resonance offset Hamiltonian. A different interaction representation was proposed for the analysis of multiple-pulse sequences consisting of solid-echo pulse groups. The resonance offset is included as part of the main Hamiltonian in this interaction representation, and is treated exactly in calculations of dynamics rather than by an approximation. This interaction representation is better suited for quantitative modeling of the off-resonance performance and dynamics of this class of sequences. We have used the insights obtained from this investigation to derive a qualitatively new type of decoupling sequence, and evaluate the performance and advantages of this sequence with both simulations and experimental tests.

Publications and Presentations

C. Rong, H. Li, P. Hrma, and H. Cho. 1996. "Spectroscopic Investigations of Simulated Low-Level Nuclear Waste Glasses." *Ceram. Trans.*, ed. by V. Jain and D. Peeler, *Amer. Ceram. Soc.*, Columbus, Ohio, 551.

C. Rong, K.C. Wong-Moon, H. Li, P. Hrma, and H. Cho. "Solid-State NMR Investigation of Phosphorus in Aluminoborosilicate Glasses." *J. NonCryst. Solids* (in press).

D.F. Stec, R.S. Maxwell, and H. Cho. "Protonated Sites on Sulfate-Promoted Zirconium Oxide Catalysts: A Fourier Transform IR, Thermal Analysis, and Solid-State ^{1}H NMR Study." *J. Catalysis* (in press).

H. Cho. "Multiple-Pulse Homonuclear Decoupling in Solid-State NMR Spectroscopy: A Revised Coherent Averaging Theory Analysis." *J. Chem. Phys.* (to be submitted).

T. Schaller, C. Rong, M. Toplis, and H. Cho. "TRAPDOR NMR Investigations of Phosphorus Containing Aluminosilicate Glasses." *J. NonCryst. Solids* (to be submitted).

D.F. Stec, R.S. Maxwell, and H. Cho. "Quantification of Aluminum Sites in Aluminas by ^{27}Al Solid State NMR." (in preparation).

R. Maxwell, R.K. Kukkadapu, J.E. Amonette, and H. Cho. "C and H Solid State NMR Investigation of Carbonate and Terephthalate Anion Dynamics in Mixed Metal Hydrotalcite-Like Materials." (in preparation).

R.K. Kukkadapu, M.S. Witkowski, R.S. Maxwell, H.M. Cho, and J.E. Amonette. "Manipulation of pH during Synthesis of Hydrotalcite-like Compounds: Effect on Carbonate Content and Layer Charge." (in preparation).

R.K. Kukkadapu, R.S. Maxwell, M.S. Witkowski, and J.E. Amonette. 1997. "Interlayer-Anion Orientation in a Mixed Terephthalate-Carbonate Hydrotalcite-Like Compound." Invited talk, 11th International Clay Conference, Clay Minerals Society, Ottawa, Canada, June.

R.K. Kukkadapu, R.S. Maxwell, M.S. Witkowski, and J.E. Amonette. 1997. "Coherent Averaging Theory and Chemical Shift Measurements: How Good Are the Approximations?" Invited talk, 39th Rocky Mountain Conference on Analytical Chemistry, Denver, Colorado, August.

R.K. Kukkadapu, R.S. Maxwell, M.S. Witkowski, and J.E. Amonette. 1997. "Increasing Sensitivity, Bandwidth, and Resolution in Multiple-Pulse Experiments." Invited talk, 8th Annual Chemagnetics Solid State NMR Workshop, Estes Park, Colorado, August.

C. Rong, K.C. Wong-Moon, H. Li, and P. Hrma. 1997. "A Revised Coherent Averaging Theory Analysis of Multiple-Pulse Homonuclear Decoupling Sequences." Thirty-Eighth Experimental Nuclear Magnetic Resonance Conference, Orlando, Florida, March. Poster presentation.

C. Rong, K.C. Wong-Moon, H. Li, and P. Hrma. 1997. "Structural Investigations of Simulated Low-Level Nuclear Waste Glasses Using Solid State NMR." Thirty-Eighth Experimental Nuclear Magnetic Resonance Conference, Orlando, Florida, March. Poster presentation.

R. Maxwell, R.K. Kukkadapu, M.S. Witkowski, and J.E. Amonette. 1997. "Interlayer-Anion Orientation and Dynamics in a Mixed Terephthalate-Carbonate Hydrotalcite-Like Compound." Thirty-Eighth Experimental Nuclear Magnetic Resonance Conference, Orlando, Florida, March. Poster presentation.

Mechanisms of Heterogeneous Electron-Transfer Reactions at Fe-Bearing Mineral Surfaces

James E. Amonette (Environmental Dynamics and Simulation)

Study Control Number: PN97069/1210

Project Description

The focus of this project was to develop the capability to perform time-resolved synchrotron-Mössbauer spectroscopy for the study of rates and mechanisms of electron-transfer reactions occurring at the surfaces of Fe-bearing minerals in contact with aqueous solutions. These reactions are integral to the geochemistry and biogeochemistry of natural water systems and to the chemical dynamics of inorganic and organic contaminants. Synchrotron-Mössbauer spectroscopy is a new technique that allows unprecedented time resolution for the collection of Mössbauer data. The project was funded in the last quarter of the fiscal year and consisted of the design and fabrication of a flow-through cell, synthesis of ^{57}Fe-enriched mineral specimens, and an initial test run at the Advanced Photon Source (APS) during the last week of the fiscal year.

Technical Accomplishments

Conventional Mössbauer spectroscopy is not well-suited to kinetic studies due to the long data collection period required (typically several hours to days). An entirely new approach to Mössbauer spectroscopy (Alp et al. 1995) has emerged with the opening of the APS, a high-brilliance third-generation hard x-ray synchrotron facility. This approach relies on pulsed monochromatic (bandwidth ca. 0.1 meV) x-rays as an excitational source, which monitors the intensity of the Mössbauer resonance in the time domain rather than in the energy domain, eliminates the high background associated with the conventional approach to maximize signal-to-noise, and thereby allows collection of complete Mössbauer spectra in periods of seconds or minutes rather than hours or days. Our approach was to collaborate with the team at the APS led by E.E. Alp to demonstrate the potential of this new technique for kinetic studies of Fe redox reactions in solids.

We designed and fabricated a flow-through cell constructed from polyetheretherketone (PEEK) that would allow collection of Mössbauer spectra during the course of a heterogeneous electron-transfer reaction involving Fe in a solid phase and a gaseous or aqueous reacting fluid. This cell (Figure 1) consisted of 1) an internal specimen holder that retained the solid phase while allowing contact with the solution or gaseous phase in which it was immersed by means of two porous semipermeable membranes, and 2) an external reaction vessel equipped with ports for introduction of a reaction solution and with windows for optical access. The specimen holder was held in the reaction vessel and bathed in the reaction solution, which entered and left the cell through four ports connected to supply and receiving reservoirs using standard liquid-chromatography hardware. Optical access to the reaction chamber and specimen holder was provided by means of an optical tunnel aligned with the incident x-ray beam and sealed by four thin polymer-film windows to retain the fluid and prevent interactions with atmospheric constituents.

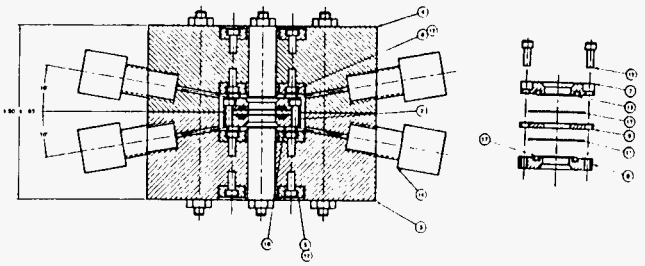

Figure 1. Cross section of reaction chamber with specimen holder (left) and details of specimen holder (right) designed for synchrotron-Mössbauer kinetic experiments.

To ensure that the highest time resolution possible could be obtained in our trial run with the cell, we prepared specimens that were enriched in ^{57}Fe. Due to the high cost of this isotope (ca. $14/mg) we were able to purchase only 400 mg of Fe(m) enriched to 92.4% with the ^{57}Fe isotope. We prepared the $Fe(NO_3)_3$ hydrate by dissolution of the metal in hot 48% HNO_3 and crystallization at 4°C. This salt was then used with $Mg(NO_3)_2$, $Al(NO_3)_3$, NaOH, and either Na-terephthalate or Na_2CO_3 to synthesize a series of pyroaurite-like compounds that differed in layer charge, octahedral-sheet composition, and nature of the interlayer anion suite following the method of Kukkadapu et al. (1997). For our initial experiment, we selected a terephthalate-pyroaurite having a Mg:Fe ratio of 3 [i.e., $Mg_3Fe(OH)_8(TA)_{0.5}\cdot 2H_2O$, where TA refers to terephthalate]. This compound was expected to exhibit rapid redox kinetics when exposed to an aqueous reductant because of the open gallery (about 0.35 nm) between the hydroxide layers maintained by the interlayer terephthalate ions.

We were fortunate to obtain 3 days of beamtime at the Advanced Photon Source during the last week of September; in part because of the short notice, and in part because the synchrotron needed to be operated in singlet filling mode with bunches spaced every 150 ns rather than the customary triplet mode with bunches more closely spaced in time. The experiment was conducted on the insertion-device beamline at Sector 3, which is operated by Dr. Alp's group in the Synchrotron Radiation Instrumentation Collaborative Access Team (SRI-CAT). Monochromatic synchrotron radiation centered at the ^{57}Fe Mössbauer resonance near 14.41 keV and having a band pass of approximately 0.1 meV was provided by two sets of Si-crystal double monochromators, the second of which was cut and oriented to provide back reflections at angles nearly parallel with the surface of the crystals (i.e., 2θ angles approaching 180°). Most of the beam time was spent refining the specimen-packing procedure and tweaking the monochromator to find and maintain the incident beam energy at the resonance value. Once these factors were controlled, a single experiment involving the in situ reduction of Fe in the TA-pyroaurite specimen [about 6 mg(^{57}Fe) cm^{-2}] was performed. Background spectra of the specimen in the oxidized state were collected before and after wetting with water. The reaction chamber was then filled with a solution containing 0.1 M $S_2O_4^{2-}$ as the reductant and 0.4 M CO_3^{2-} as a pH buffer and a series of Mössbauer spectra collected at 5- or 10-minute intervals for the next 2.4 hours. During this period, the reducing solution inside the reaction chamber was refreshed several times.

The results of this experiment (Figure 2) show a progressive evolution of the time-domain spectrum, with most of the change occurring in the first 90 minutes. In a qualitative sense, the quantum-beat spacing (i.e., the intervals between the successive valleys in the time-domain spectrum) is inversely proportional to the quadrupole splitting of the ^{57}Fe nuclear states. Thus, as the Fe(III) in the pyroaurite is reduced to Fe(II), the quantum-beat spacing decreases and quadrupole splitting increases. Measurements of the quadrupole splitting values by conventional Mössbauer spectroscopy in our laboratory at EMSL yielded values of about 0.65 mm s^{-1} for the oxidized form of TA-pyroaurite and 2.1 mm s^{-1} for the reduced form, in agreement with the observed synchrotron data.

In collaboration with Dr. Alp, we are in the process of quantitatively analyzing the synchrotron spectra. A second run is planned in early February 1998 in which we will follow the changes in the pyroaurite through a complete reduction/oxidation cycle. The results of these first known kinetic experiments with synchrotron-Mössbauer spectroscopy will be published in the peer-reviewed literature.

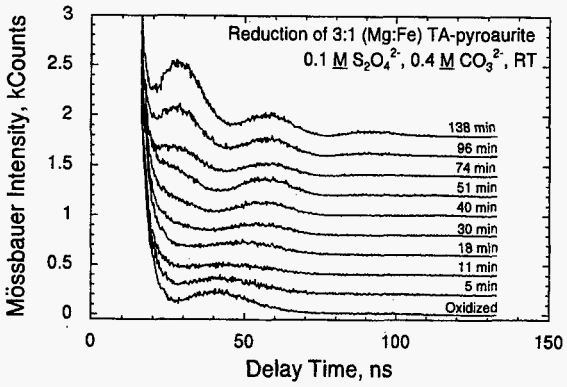

Figure 2. Synchrotron-Mössbauer spectra for oxidized TA-pyroaurite and for the same specimen at various stages during the 2.4 hour treatment by a buffered dithionite solution.

Acknowledgments

Much of the work in the project was performed by R.K. Kukkadapu (AWU postdoctoral fellow). We gratefully acknowledge the collaboration with E.E. Alp, W. Sturhahn, T. Toellner, and other members of the SRI-CAT at APS.

References

E.E. Alp, W. Sturhahn, and T. Toellner. 1995. "Synchrotron Mössbauer Spectroscopy of Powder Samples." *Nucl. Instrum. Meth. Phys. Res. B* 97:526-529.

R.K. Kukkadapu, M.S. Witkowski, and J.E. Amonette. 1997. "Synthesis of a Low-Carbonate High-Charge Hydrotalcite-Like Compound at Ambient Pressure and Atmosphere." *Chem. Mater.* 9:417-419.

Molecular Modeling of Bacterial Lipopolysaccharide/Amino Acid Binding in Solution and to Mineral Surfaces

Andrew R. Felmy, James R. Rustad, David A. Dixon, James K. Frederickson (Environmental and Health Sciences)

Study Control Number: PN97077/1218

Project Description

This project was tasked to develop a molecular-based modeling capability (including ab initio electronic structure molecular orbital and density functional theory calculations, molecular dynamics simulations, and thermodynamic modeling) of lipopolysaccharides functional groups present on gram-negative bacterial surfaces. This will form the foundation of theoretical modeling at PNNL needed to predict the effects of pH and bacterial surface structure on the development of bacterial surface charge, the binding of cations to microbial surfaces, and on the binding of lipopolysaccharides functional groups to specific sites on mineral surfaces.

Technical Accomplishments

Funding was available for this project for only a few weeks at the end of FY 1997. Initial emphasis was placed on conducting a complete literature review of the subject area. This literature review included studies on the surface chemistry, molecular structure, metal binding, and surface charging properties of the microbial surface. Based upon the results of this literature review, a preliminary charging model of the microbial surface was developed using estimated values for the metal binding and protonation constants of the carboxylic acid, phosphate, and amine groups on the microbial surface. This model was then compared to the available literature data on the charging of microbial surfaces and found to be only qualitatively correct because the local molecular structure at the binding sites was not taken into account. Molecular modeling calculations (using density functional theory) were outlined to help determine or estimate the effects of local molecular structure on the metal binding and protonation (i.e., charge development).

It was also determined that very little experimental data exist on the surface charging and metal binding for important gram-negative bacteria of potential importance to DOE in bioremediation efforts. Such data are needed to develop and test molecular models of the bacterial metal binding and surface charge development. Such information is important because surface charge development is a key factor in determining the mobility of bacteria in subsurface systems.

Information gained from these initial few weeks of effort resulted in the project being rescoped and retitled as a new project in FY 1998.

Near Field Optical Microscopy of Dehalogenase Electron Transport

X. Sunney Xie (Chemicial Structure and Dynamics)
Luying Xun (Environmental Microbiology, Washington State University)

Study Control Number: PN96053/1120

Project Description

We are applying the new capability of single-molecule spectroscopy to a newly identified and isolated dehalogenase system to gain a molecular-level understanding of dehalogenation.

Recent advances in fluorescence microscopy, including those made at PNNL, have made it possible to image single molecules in ambient and aqueous environments. Single-molecule spectroscopy at room temperature has recently been demonstrated, allowing the determination of both the locations and chemical identities of single molecules. Using state-of-the-art microscopes developed at PNNL, we have conducted single-molecule spectroscopy in real time, which enables us to directly observe and study chemical reactions such as electron transfers of individual molecules (Lu and Xie 1997a, b).

Many chlorinated hydrocarbon compounds can be degraded by microorganisms. Many enzymes involved in these processes are flavin-proteins. For example, pentachlorophenol 4-monooxygenase (PCP-Mo) and chlorophenol 4-monooxygenase catalyze chlorophenol hydroxylation; both contain flavin mononucleotide as the prosthetic group. Nitrilotriacetate (NTA) monooxygenase uses NTA-metal complexes as substrate, while EDTA monooxygenase degrades both NTA- and EDTA-metal complexes; both contain flavin mononucleotide as the prosthetic group. The purification, properties, and kinetics of these enzyme reactions, and the cloning and sequencing of the corresponding genes have been recently documented in a series of publications (Xun and Orser 1991; Xun 1992a, b).

Technical Accomplishments

Flavin proteins have strong natural fluorescence. During enzymatic reaction, the flavin is first reduced by NADH or NADPH, and then the reduced flavin will activate molecular oxygen to attach the substrate. As an example, for PCP-Mo, the substrates are chlorinated phenols, and the oxidized form of flavin mononucleotide is fluorescent, whereas the reduced form is not. As the enzymatic activities take place on a single protein, the fluorescence from the flavin mononucleotide will be turned on and off.

By monitoring the fluorescence of single flavin, we can directly monitor the catalytic cycles of the single enzyme in real time, each corresponding to a single chlorine-carbon bond breakage. Such experiments will provide unprecedented information regarding detailed kinetics, reaction intermediates, and mechanisms of the enzymatic reactions, free from complications arising from conventional experiments done on a large ensemble of molecules. The impact of these experiments to molecular-level understanding of dehalogenation cannot be underestimated. The fundamental knowledge will be useful for the selection, design, and refinement of bioremediation processes.

Our initial results have clearly demonstrated the feasibility of the proposed studies. Using a confocal microscope, we have imaged single pentachlorophenol 4-monooxygenase embedded in an agrose gel with good signals. We have demonstrated the real-time observation of enzymatic reactions of single flavin proteins such cholesterol oxidase and glucose oxidase. The work is featured in a news article in *Science* magazine (Service 1997).

References

H.P. Lu and X. Xie. 1997a. "Single-molecule kinetics of interfacial electron transfer temperature." *J. Phys. Chem.* 101, 2753.

H.P. Lu and X. Xie. 1997b. "Single-molecule spectral fluctuations at room temperature." *Nature* 385, 143.

R. Service. 1997. "Chemists explore the power of one." *Science* 276, 1027.

L. Xun and C.S. Orser. 1991. "Purification and properties of pentachlorophenol hydroxylase, a flavoprotein from Flavobacterium sp. strin ATCC 39723." *J. Bacteriol.* 173, 4447-4453.

L. Xun, E. Topp, and C.S. Orser. 1992a. "Confirmation of oxidative dehalogenation of pentachlorophenol by a flavobacterium pentachlorophenol hydroxylase." *J. Bacteriol.* 174, 5745-5747.

L. Xun, E. Topp, and C.S. Orser. 1992b. "Diverse substrate range of a Flavobacterium pentachlorophenol hydroxylase and reaction stoichiometries." *J. Bacteriol.* 174, 2898-1902.

Presentations

S. Xie. 1997. Gordon Conference on Molecular Electronic Spectroscopy and Dynamics, Oxford, United Kingdom, Invited talk, August 3 - September 5.

P. Lu. 1997. ACS meeting, Invited talk, San Francisco, California.

S. Xie. 1997. AAAS/AMSIE '97, Invited talk, Seattle, Washington, February 14-18.

Near Field Spectrographic Mapping and Manipulation of Enzymatic Reactions in Biological Membranes

X. Sunney Xie (Chemical Structure and Dynamics)
Randy X. Bian (Atmospheric Sciences)

Study Control Number: PN96051/1118

Project Description

Optical trapping by highly focused laser beams has been extensively used for the manipulation of submicron-size particles such as biological structures (Ashkin and Dziedzic 1987). Conventional optical tweezers rely on the field gradients near the focus of a laser beam, which give rise to a trapping force toward the focus. The trapping volume of these tweezers is diffraction limited. Near-field optical microscopy enables optical measurements at a dimension beyond the diffraction limit. With near-field microscopy, it is now possible to optically monitor chemical changes of single biomolecules. We have started an effort to extend the near-field approach to high-resolution optical tweezers (Novotny et al. 1997), with the aim of manipulation and control of biomolecules in an aqueous environment at the nanometer scale.

Technical Accomplishments

We have performed a rigorous electromagnetic analysis for the field enhancement. To solve Maxwell's equations in the specific geometry of the tip and its environment, we employed the multiple multipole method (Novotny et al. 1997).

We also performed a rigorous calculation of trapping force at different center positions of the particle using the Maxwell stress tensor (Novotny et al. 1997). The calculations demonstrate the feasibility for trapping on a nanometer scale with a moderate power level.

A practical concern is heating of the tip, which could damage the sample and induce convection at the tip surface. A finite-difference time-domain method was employed to simulate the steady-state temperature distribution around the tip. For 65 $mW/\mu m^2$ of illuminating intensity, the maximum temperature rise at the surface of the tip was 6.5 K (Novotny et al. 1997). This result indicated that the temperature rise induced by heating is minimal for the intensity level required for stable trapping.

In our optical trapping scheme, a tip is brought to the focus of an illuminating beam where a particle has been trapped by the conventional means. The particle is then trapped in the near-field zone of the tip. The trapped particle can be released by turning off the illumination. Experimental realization of this scheme is under way. The scheme has the potential for nanometric manipulation of individual biomolecules in their aqueous environment and control of their chemical activities.

References

A. Ashkin and J.M. Dziedzic. 1987. *Science* 235, 1517.

L. Novotny, R.X. Bian, and X.S. Xie. 1997. "Theory of Nanometric Optical Tweezers." *Phys. Rev. Lett.* 79, 645.

Publications and Presentations

E.J. Sanchez, L. Novotny, G.R. Holtom, and X.S. Xie. 1997. "Room-Temperature Fluorescence Imaging and Spectroscopy of Single Molecules by Two-Photon Excitation." *J. Phys. Chem.* A 101, 7019-7023.

L. Novotny, E.J. Sanchez, and X.S. Xie. "Near-Field Optical Imaging Using Metal Tips Illuminated by Higher-Order Hermite-Gaussian Beams." *Ultramicroscopy* (submitted).

E.J. Sanchez, L. Novotny, and X.S. Xie. 1997. "Fluorescence Imaging of Single Molecules and Photosynthetic Membranes with Two-Photon Excitation." 213th American Chemical Society National Meeting, San Francisco, April 13-17.

L. Novotny, E.J. Sanchez, and X.S. Xie. 1997. "Is Near-Field Fluorescence Imaging with 10-nm Resolution Possible?" Fourth International Conference on Near-Field Optics, Jerusalem, Israel, February 9-13.

NMR Studies of Proteins

David F. Lowry (Macromolecular Structure and Dynamics)

Study Control Number: PN95063/1039

Project Description

High resolution NMR structure determination of medium sized proteins (10 to 30 kDa) is now routine. One of the current challenges for biological NMR spectroscopy is structure determination of protein complexes. Our goal is to identify strongly interacting proteins, and after solving the structures of these proteins, try to solve the structure of their complex.

Replication Protein A (RPA) has been the major focus of this project. RPA is involved in all aspects of DNA metabolism, but we were initially interested in RPA's role in recombination repair. Subsequently, new information suggests that other prokaryotic single-stranded DNA binding proteins can substitute for RPA in human recombination repair. Marc Wold, University of Iowa, has recently shown that RPA acts in replication by stimulating DNA-polα catalytic activity and processivity. This stimulation is specific and therefore compelling for the study of protein-protein interaction.

Technical Accomplishments

A human cell must faithfully replicate its DNA before it divides and passes on the copy of its DNA to daughter cells. High fidelity in the copy DNA is achieved by a complex and not fully understood coordination among cellular repair, replication, and cell cycle control machinery. Before cell division can occur, the cell must pause in its cell cycle, check the integrity of its DNA, and if necessary, repair the DNA. It is almost certain that in order to effect the coordination of replication, repair, and cell cycle, some proteins will function in all three processes. Replication Protein A is a heterotrimeric single-stranded DNA binding protein necessary for replication. RPA appears to have also been co-opted for most types of DNA repair and for cell cycle checkpoint control.

We have been working for some time in collaboration with Marc Wold (University of Iowa) to dissect the structure and function of the individual subunits and domains of RPA. Here we describe our efforts toward understanding the mechanism of RPA stimulation of DNA-polα catalytic activity. Wold's laboratory has isolated this function of RPA to the N-terminal domain of the 70 kDa subunit of RPA (RPA70). A first step toward understanding protein-protein interaction is to determine structures of the individual proteins. We have made considerable progress on this N-terminal domain of RPA70. We used traditional methods to isotope label and purify large quantities of RPA70-D169. We also used traditional three-dimensional heteronuclear 13C-15N-1H NMR techniques to obtain residue specific assignments and secondary structure of the protein (Figure 1).

RPA70Δ169: D. Lowry(EMSL) & M. Wold(U. Iowa)

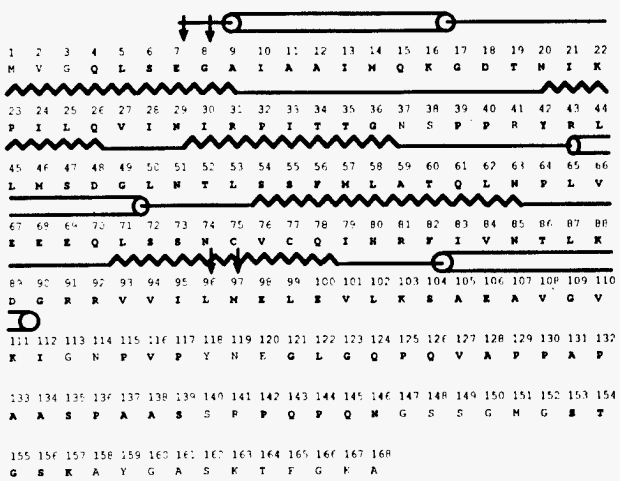

Figure 1. Secondary structure of RPA70-Δ169. The type of secondary structure is shown at the top of each row: cylinders are α-helices; zig-zags are β-strands; lines are either tight turns or loops; random coil regions are left blank. The next line of each row shows the residue number and the last line of each row gives the one-letter amino acid code for that residue number. Assigned residues are in boldface. The arrows indicate the position of yeast lethal mutations mapped onto the human RPA sequence; note that all these mutations map to the globular part of this domain.

We have made a couple of interesting conclusions based on our secondary structure of this fragment of RPA. First, we note that the fragment is globular only up to amino acid 112. The rest of the fragment is random coil and possibly a flexible linker to the next domain. A possibility is that truncation at residue 169 destabilizes any structure that this C-terminal region may have had in the intact RPA. We feel this is not the case for several reasons: the stimulation of polα was mapped to the globular part of RPA70-Δ169- amino acids 1-112, and it is difficult to understand how a completely random structure could

exhibit a specific modulation of the function of another protein; this domain of RPA was first discovered by protease mapping so the region near residue 168 is likely unstructured; the homology with RPA from other eukaryotes is not high in the C-terminus of this fragment. There are no lethal mutants mapped to this region, they all map to within the globular region. We therefore adopt the interpretation that this C-terminal region is an unstructured linker to the next domain—the first single-stranded DNA binding domain.

Our second conclusion concerns the β-sheet regions. The β-sheets of this domain are not canonical, i.e., there are four beta bulges in this domain. In fact, two yeast lethal mutants map to one of the four bulges. We conclude that this particular β-bulge is a particularly important structural element for protein interaction.

Protein DNA Complexes: Dynamics and Design

Rick L. Ornstein (Environmental Technologies)

Study Control Number: PN95069/1045

Project Description

A quantitative understanding of health risks, particularly from cancer, will play a major role in establishing cleanup standards and priorities. Due to the lack of fundamental understanding, present standards are very conservative. Substantial cost savings in terms of remediation, as well as improving worker and public health protection would result from better methods to deal with the risk issue. Accurate cancer risk assessment requires a thorough mechanistic understanding of the molecular processes in the cell that occur after exposure to chemicals or to radiation. Damage to DNA is thought to be a critical step in initiating tumor growth. A critical need in understanding fundamental mechanisms of damage to DNA is to gain insight into how proteins recognize their appropriate interaction with DNA. This will provide us with fundamental mechanistic understanding of the processes of biomacromolecular recognition. Protein-DNA recognition, for instance, is crucial to proper DNA replication fidelity, repair of DNA damage, regulation of transcription, and related processes. There is actually little understanding of the underlying dynamic interactions that govern protein-DNA recognition. This project has focused on predicting the underlying interactions, both static and dynamic, by using modern computational chemistry methods including ab initio electronic structure theory and molecular dynamics with classical force fields.

Technical Accomplishments

Using AMBER 4.1 with the particle mesh ewald (PME) method is essential for studying isolated DNA, without imposing artificial structural constraints. On the other hand, using this method for DNA presents significant new questions. We completed our study of the influence of box size. This is an important issue with respect to reducing crystal lattice effects and computational cost. We simulated a single DNA dodecamer sequence in boxes that effectively had a minimum 5, 10, or 15 Å layer of water around the DNA. Whereas only the two larger box simulations produced converging results, the middle box size appears to be the best choice for combined quality and efficiency. Second, we completed studies on the effect of starting conditions on the curvature of DNA.

If we are to depend on the simulation results to compare inherent differences in curvature of DNAs with different sequence, then we must first estimate the uncertainty in the simulated value due to statistical and methodological effects. We compared the curvature resulting from three different starting conditions for runs of 1500 ps each and the result from the first and second half of a single 3000 ps simulation. There appears to be adequate uniformity in these simulations; thus, single simulations of different sequences can be meaningfully compared for intrinsic sequence-dependent structure-dynamic differences.

An important part of protein recognition is the ability of protein side chains and DNA base pairs to form weak hydrogen bonds. Ab initio calculations have been initiated to look at weak hydrogen bond interactions, especially for C-H bonds. Such interactions, although weak, are numerous and may have a larger impact in controlling binding energies and specificity than previously thought. We compared the potential energy surfaces for hydrogen bonding between an oxygen acceptor of water with N-H and C-H donors of imidazole using ab initio molecular orbital methods at the MP2/6-31++G(2d,2p) level of theory. We find the C-H...O interactions of imidazole with water to be indicative of hydrogen bonding interactions, albeit significantly weaker than the N-H...O interaction, but significantly stronger than just van der Waals interactions. The high level ab initio potential energy surfaces are compared to those computed with available AMBER force fields and indicate that the C-H...O interaction is underestimated by conventional force fields. A simple correction for the AMBER force field is proposed and is expected to yield significantly improved intramolecular packing and dynamics of regions containing histidine residues. The purine bases allow for similar C-H...O and C-H...N interactions; these are currently being studied.

In FY 1997, we completed molecular dynamics simulations (using AMBER 4.1) on TATA-box DNA sequences aimed at the evaluation of intrinsic deformability and propensity for deformation (bending and kinking) of the various related sequences. The intrinsic properties of such sequences may be critical for specificity of the interaction with key regulatory proteins, since DNA is very highly deformed when bound to TATA-box binding protein (TBP). Based on molecular dynamics simulations of

1500 to 3000 ps each (using AMBER 4.1) for three strong binding TATA sequence dodecamers and one weak binding, but related sequence, it appears that the intrinsic curvature and deformability of DNA plays a significant role in the TBP-DNA complexation process.

Publications

O. Norberto de Souza and R.L. Ornstein. 1997. "Effect of Warmup Protocol and Sampling Time on Convergence of Molecular Dynamics Simulations of a DNA Dodecamer Using AMBER 4.1 and Particle-Mesh Ewald Method." *J. Biomolec. Struct. Dyn.* 14, 607-611.

O. Norberto de Souza and R.L. Ornstein. 1997. "On the effect of periodic box dimensions on the structure and dynamics of DNA oligonucleotides in aqueous molecular dynamics simulations with Particle Mesh Ewald method." *Biophys. J.* 27, 2395-2397.

R.L. Ornstein and Y.J. Zheng. 1997. "Ab Initio Quantum Mechanics Analysis of Imidazole C-H...O Water Hydrogen Bonding and a Molecular Mechanics Forcefield Correction." *J. Biomolec. Struct. Dyn.* 14, 657-665.

O. Norberto de Souza and R.L. Ornstein. "Inherent Curvature of TATA Box DNAs: A Molecular Dynamics Simulation Study of Wild-Type and A/T Mutants." (submitted).

Rational Redesign of Warfare Nerve Agent Degrading Enzyme: Phosphotriesterase

Rick L. Ornstein (Environmental Technologies)
David A. Nelson (Material Sciences)

Study Control Number: PN97090/1231

Project Description

The purpose of this project is to employ a coupled experiment-simulation (theory) approach for rational redesign of phosphotriesterase (PTT); the only known enzyme that will degrade many neurotoxin warfare agents. This enzyme, however, operates at a greatly reduced level of efficiency on key warfare agents than on more biologically relevant compounds. In addition, the enzyme is likely to be of even more limited use under field conditions. A rational redesign program is capable of leading to a series of highly specific PTT analogues with greatly improved degradation of warfare neurotoxins. In addition, it is now also possible to further redesign the enzyme analogues for improved functionality and stability under field conditions. The preliminary simulations not only lead to essential fundamental knowledge needed for rational redesign, but also permit greater safety since actual experiments with the neurotoxins can be reduced in number and scope.

Background

Phosphotriesterase from *Pseudomonas diminuta* and *Flavobacterium sp.* catalyzes the hydrolysis of a broad spectrum of organophosphate neurotoxins by P-O, P-F, and/or P-CN bond hydrolysis (Dave et al. 1993; Dumas et al. 1989a,b; 1990; Caldwell et al. 1991; Ashani et al. 1991). Although chemical warfare agents, such as soman, sarin, and tabun can be hydrolyzed by PTT, hydrolysis of other organophosphates can occur at far greater rates (Dumas et al. 1990; Ashani et al. 1991). Whereas the three-dimensional x-ray crystal structure of the apoenzyme (without bound metal ions, Benning et al. 1994) and the holoenzyme (with bound metal ions, Benning et al. 1995) have been determined, "it may be possible in the future to design various enzymes with high specificities for sarin, soman, or other related compounds" (Benning et al. 1994). We propose a coupled experiment-computation (theory) approach for rational design of PTT, in order to develop a series of highly specific PTT analogues for improved degradation of warfare neurotoxins.

The most comprehensive analysis of any enzyme studied by crystal structure analysis is that for T4 lysozyme. The structure for this enzyme has been solved in 25 different crystal forms and clearly demonstrates the large impact that crystal packing forces can have on enzyme structure and dynamics (Zhang et al. 1995). Having anticipated such an outcome, we have performed simulations on several proteins, starting from the crystal structure, under solution conditions that would avoid crystal packing effects. Our simulations indicate that crystal packing forces can partially close the active site of an enzyme (Paulsen and Ornstein 1995; Arnold and Ornstein 1997a), or have the opposite effect (Miaskiewicz and Ornstein 1996; Arnold and Ornstein 1997b). The nature of the effect, if any, due to the crystal packing, appears to be dependent on intermolecular interactions that are not present in solution. State-of-the-art molecular dynamics simulations permits one to gain a "relaxed" view of the structure and dynamics of an enzyme, in the absence of crystal packing forces. Such molecular information is an essential component of gaining a fundamental understanding of the structure-function-dynamic relationships for an enzyme and the required fundamental knowledge for subsequent rational redesign (Ornstein 1994; Paulsen et al. 1996).

The use of PTT under field conditions will likely require nonbiological conditions, such as nonaqueous solvents and lower temperatures. Although most enzymes have evolved for stability and function in an aqueous environment, advantages of carrying out enzymatic reactions in nonaqueous environments have been identified. These include higher solubility of substrate in organic solvent, increased thermostability of enzymes (Zaks and Klibanov 1984), altered substrate specificity (Zaks and Klibanov 1986, 1988; Gololobov et al. 1992; Tawaki and Klibanov 1992) and regiospecificity (Riva et al. 1988; Rubio et al. 1991), easy enzyme recovery from organic solvent, and the ability to carry out reactions which are impossible in water due to either kinetic or thermodynamic reasons (Klibanov 1986). To obtain a mechanistic understanding and to predict the effect of different solvent environments, it is essential to uncover fundamental structure-function-dynamics relationships of an enzyme in a range of solvents. With this in mind, we have recently performed molecular dynamics simulations on the protease enzyme subtilisin in a wide range of different solvents (Zheng and Ornstein 1996a,b,c). We, therefore, plan to perform similar molecular dynamics simulations on PTT in different

chemical environments, in order to measure and understand the molecular basis for critical structural and dynamic perturbations caused by each environment. It should then be possible to predict and test for mutant enzymes that exhibit improved structural and functional characteristics in relevant solvents.

Most of the described enzymes from cold-adapted organisms have evolved different fundamental processes then their counterparts from warm-temperature species; thus, enzymes from ectothermic organisms have a lower energy of activation (Low and Somero 1974). It is thought that low-temperature efficiency is due to increased flexibility of the enzyme (Low and Somero 1974; Asgeirsson et al. 1989), and the increased flexibility will in turn be at the cost of stability (Heimstad et al. 1995). Increased molecular flexibility may be caused by a reduction in the number of stabilizing intramolecular interactions, while the opposite would hold for increasing the specificity. Crystal structures are currently available for homologous enzymes from cold-adapted and warm- or hot-adapted organisms (for instance see Smalas et al. 1994); thus making it possible to uncover the fundamental basis for temperature-dependence and subsequent low-temperature optimization of PTT by a rational redesign approach.

Technical Accomplishments

Following are accomplishments for FY 1997:

- completed a thorough literature search of both DoD and all other significant publicly accessible databases, in order to become better acquainted with the status and need for improved PTTs (previously delivered to Hal Undem)
- established a formal collaboration with Professor James Wild of Texas A&M University, whose laboratory is pioneering basic and applied studies on the use of PTTs for CW catalysis
- took preliminary steps toward the modeling and simulation of PTT from the available x-ray crystal structures.

References

G.E. Arnold and R.L. Ornstein. 1997a. *Biopolymers* 41:533-544.

G.E. Arnold and R.L. Ornstein. 1997b. In: *Biomacromolecules from 3-D Structure to Applications*, ed. R.L. Ornstein, pp. 215-230, ed. R.L. Ornstein, Battelle Press, Columbus, Ohio.

B. Asgeirsson, J.W. Fox, and J.B. Bjarnason. 1989. *Eur. J. Biochem.* 180:85-94.

Y. Ashani, N. Rothschild, Y. Segall, S. Levanon, and L. Raveh. 1991. *Life Sci.* 49:367-374.

M.M. Benning, J.M.Kuo, F.M. Raushel, and H.M. Holden. 1994. *Biochemistry* 33:15001-15007.

M.M. Benning, J.M. Kuo, F.M. Raushel, and H.M. Holden. 1995. *Biochemistry* 34:7973-7978.

S.R. Caldwell, J.R. Newcomb, K.A. Schlecht, and F.M. Raushel. 1991. *Biochemistry* 30:7438-7444.

K.I. Dave, C.E. Miller, and J.R. Wild. 1993. *Chem.-Biol. Interactions* 87:55-68.

D.P. Dumas, S.R. Caldwell, J.R. Wild, and F.M. Raushel. 1989. *J. Biol. Chem.* 264:19659-19665.

D.P. Dumas, J.R. Wild, and F.M. Raushel. 1989. *Biotech. Appl. Biochem.* 11:235-243.

D.P. Dumas, H.D. Durst, W.G. Landis, F.M. Raushel, and J.R. Wild. 1990. *Arch. Biochem. Biophys.* 277:155-159.

M.Y. Gololobov, T.L. Voyushina, V.M. Stepanov, and P. Adlercreutz. 1992. *FEBS Lett.* 307:309-312.

E.W. Heimstad, L.K. Hanse, and A.O. Smalas. 1995. *Prot. Eng.* 8:379-388.

A.M. Klibanov. 1986. *CHEMTECH* 16:354-359.

P.S. Low and G.N. Somero. 1974. *Comp. Biochem. Physiol.* 49B:307-312.

K. Miaskiewicz and R.L. Ornstein. 1996. *J. Biomolec. Struct. Dyn.* 13:593-600.

R.L. Ornstein. 1994. In *Structural Biology: State of the Art 1993*, eds., R.H. Sarma and M.H. Sarma, vol. 1, pp. 59-76, Adenine Press, Albany, New York.

M.D. Paulsen, J.I. Manchester, and R.L. Ornstein. 1996. *Meth. Enzymol.* 272:347-357.

M.D. Paulsen and R.L. Ornstein. 1995. *Proteins* 21:237-243.

S. Riva, J. Chopineau, A.P.G. Kieboom, and A.M. Klibanov. 1988. *J. Am. Chem. Soc.* 110:584-589.

E. Rubio, A. Fernandez-Mayorales, and A.M. Klibanov. 1991. *J. Am. Chem. Soc.* 113:695-696.

S. Tawaki and A.M. Klibanov. 1992. *J. Am. Chem. Soc.* 114:1882-1884.

F. Yang, J.R. Wild, and A.J. Russell. 1995. *Biotechnol. Prog.* 11:471-4.

A. Zaks and A.M. Klibanov. 1984. *Science* 224:1249-1251.

A. Zaks and A.M. Klibanov. 1986. *J. Am. Chem. Soc.* 108:2767-2768.

A. Zaks and A.M. Klibanov. 1988. *J. Biol. Chem.* 263:3194-3201.

X.-J. Zhang, J.A. Wozniak, and B.W. Matthews. 1995. *J. Mol. Biol.* 250:527-552.

Y.-J. Zheng and R.L. Ornstein. 1996a. *Biopolymers* 38:791-799.

Y.-J. Zheng and R.L. Ornstein. 1996b. *J. Am. Chem. Soc.* 118:4175-4180.

Y.-J. Zheng and R.L. Ornstein. 1996c. *Prot. Eng.* 9:485-492.

Spectroelectrochemistry

John L. Daschbach (Interfacial and Processing Science)

Study Control Number: PN95078/1054

Project Description

The purpose of this project is to study electrified interfaces, using a combination of electrochemical and optical techniques, in an effort to understand solid/liquid and liquid/liquid interfaces, especially those relevant to waste and remediation problems. A principal goal of this project was to develop the capability to perform a wide variety of spectroelectrochemical techniques with a specific focus on nonlinear optical techniques.

Technical Accomplishments

There were three areas of accomplishment during FY 1997. The first was the continuation of studies on well-defined and defected TiO_2. The second was the continuation of the construction of a picosecond tunable infrared source for vibrational sum frequency generation studies of interfaces. The third was the development of computational machinery to handle complicated reaction-diffusion problems at interfaces. A wide range of problems at interfaces can be understood only by explicitly treating both reaction and diffusion. We have developed a technique that allows the treatment of arbitrarily complicated interfacial kinetic schemes with the traditional ordinary differential equation mechanism including diffusion over short spacial scales coupled to a spatially adapted partial differential equation treatment of diffusion over semi-infinite spacial scales.

The role of surface defects on the observed electrochemical response of TiO_2 is not well understood. For example, deviations from ideal capacitive behavior, in the Mott-Schottky sense, have been attributed to both surface states and nonuniform doping. Electrical and electrochemical defects have been studied by preparing single crystal samples in ultrahigh vacuum conditions and introducing surface defects in a controlled manner prior to transfer to an electrochemical cell. We investigated the controlled potential interaction of surface defects with an electrolyte in an effort to understand the role and fate of these defects in different electrochemical environments. Both x-ray photoelectron spectroscopy and electrical measurements have been made on several samples prepared in somewhat different ways.

Samples were prepared by fully oxidizing the surface of bulk reduced TiO_2 (110) and then introducing defects. The quality of the "defect-free" or "ideal" surface was monitored by comparison of Ti~2p x-ray photoelectron spectroscopy spectrum with a reference spectrum. After preparation of an "ideal" surface, defects are introduced by sputtering with 1 to 4~keV Ar^+. Transfer to a ultrahigh vacuum compatible electrochemical cell is accomplished under a nitrogen atmosphere. Samples are transferred to electrolyte and held under potential control.

One example is behavior for a 10-minute exposure in 0.1 N H_2SO_4. Samples potentiostated near flatband (-0.7 V versus SCE) and 800 mV positive of this (0.1 V versus SCE) were examined. Ti~2p x-ray photoelectron spectroscopy spectra taken after emersion show a surface electronic structure largely restored to the defect-free condition but with a clear lower oxidation state shoulder on the Ti~2p~3/2 peak. This peak is significantly more prominent for the sample held at 0.1~V. It is clear that the healing (oxidation) of these surface defects is potential-dependent in a manner consistent with the potential of the surface with respect to flatband. It is also evident that with this high degree of surface defects, short exposure to electrolyte does not completely heal the defects (within the surface sensitivity of x-ray photoelectron spectroscopy [~5 nm]). Measurements taken using UPS, which senses less depth of material, suggest that the surface region of the specimen is healed of defects and the remaining defects are subsurface.

"Ideal" and "defected" surfaces, transferred from vacuum, exhibit hysteresis in the capacitive behavior under potential cycling. In all cases, the samples exhibit lower capacitance when cycling from depletion toward flatband compared to the opposite scan direction. In the case of "ideal" surfaces, a single reduction in the space charge carrier density is observed upon biasing samples well positive of flatband. Subsequently, there is a linear decrease in measured space charge capacitance with time independent of applied bias. This is consistent with a diffusion limited reduction of doping defects (oxygen vacancies) with subsequent oxidation at the surface. The initial reduction is most likely due to oxidation of shallow subsurface defects remaining after the annealing process (using electron beam heating). The defected surface exhibits both potential-dependent and potential-independent reductions in carrier density. The potential dependence has two components which have been studied by a series of stepped potential measurements monitoring the capacitance versus time. The reduction in carrier density as a function of the degree of anodic

polarization relative to flatband may be considered as a field-dependent migration of defects in the space charge region. The depth of the space charge region varies as a function of carrier density and applied bias. Consistent with the initial oxidation of subsurface defects on "ideal" crystals, these defects are annealed out under electrochemical control. Mott-Schottky analysis after removal of the field dependent response may be modeled using a two-layer system in which the top layer has a lower carrier density than the bulk. The depth of the top layer for 2 KeV Ar^+ sputtering is ~7 nm, consistent with angle-resolved x-ray photoelectron diffraction work at slightly lower energy.

The tunable infrared laser system under development is an extension of the Shen design. The first stage has a pair of BBO crystals which are double passed with a 532 nm pump. A combination of angle tuning and a diffraction grating for the signal retroreflection yield a seed for the second stage with a line width of 2 to 4 wave numbers. The second stage has a pair of potassium niobate crystals which are angle tuned and pumped at 1064 nm. Currently the output of the second stage has a pulse energy of above 200 μJ at 3600 cm^{-1} (perhaps attenuated a bit by some atmospheric water absorption), rising to above 400 μJ at 3000 cm^{-1}, plateau to about 2700 cm^{-1}, then starting to fall again to over 100 J at 2200 cm^{-1}, and reaching a cutoff at 2000 cm^{-1}. In the past year we have repaired a persistent power loss problem with the pump laser, rebuilt the optical layout with more robust components, and redesigned portions of the system for ease of use as a multi-user collaborative research tool.

The computational machinery developed for reaction diffusion problems combines treatment of local kinetics and diffusion with an ordinary differential equation approach with a partial differential equation approach for long-range diffusion. Both are standard approaches. On time scales comparable to the diffusion length, one end of the ordinary differential equation matrix has an improper boundary condition while at all times the other end of the partial differential equation matrix has an improper boundary condition. At each time step, chosen to limit the propagation of end effects, the two systems are interpolated together in alternate directions. This same approach is applied to a geometrically expanding spacial grid in the partial differential equation system. By using ordinary differential equations to treat the interface, we have a system which allows arbitrary complexity in the description of the kinetics and any observables derived from such a treatment, circumventing a limitation in the traditional approach to treating boundary conditions in partial differential equation diffusion problems. We have applied this approach to two interfacial problems. One is the kinetics of water adsorption and desorption at MgO(100) surfaces, and the other is transport of small molecules across the liquid/vapor interface. In the first case, extended exposure of MgO(100) to a molecular beam of water above the desorption temperature led to the uptake of multiple monolayers of water in the form of a near surface hydroxide. Subsequent temperature programmed desorption of water from this surface exhibits a very broad high temperature tail which we have modeled and shown to be due to surface-defect mediated hydroxylation with diffusion into the MgO bulk. The transport of small molecules has been studied using kinetic parameters derived from molecular dynamics calculations and includes explicit treatment of diffusion in both the vapor and liquid phases. Results of this work have led to a better understanding and interpretation of laboratory experiments.

Presentations

J.L. Daschbach, L.Q. Wang, M.H. Engelhard, and D.R. Baer. 1996. "Electrochemical Healing of Surface and Subsurface Defects in TiO2." American Vacuum Society, National Meeting, Philadelphia, Pennsylvania, October 14-18.

R.S. Taylor, D.S. Karpovich, J.L. Daschbach, B.C. Garrett, and D. Ray. 1997. "Transport of Small Molecules Across the Liquid/Vapor Interface of Water." American Chemical Society, 214th National Meeting, Las Vegas, Nevada, September 7-11.

J.L. Daschbach, M. J. Stirniman, R.S. Smith, S.A. Joyce, and B.D. Kay. 1998. "Kinetics of Water Adsorption, Desorption, and Hydroxylation on MgO(100)." Invited talk; American Chemical Society, 215th National Meeting, Dallas, Texas, March 29 - April 2.

X-Ray Adsorption Fine Structure

Steven M. Heald (Environmental and Molecular Sciences)

Study Control Number: PN94086/976

Project Description

This project supports the Pacific Northwest Consortium Collaborative Access Team (PNC-CAT) in the creation of an advanced x-ray microprobe and other advanced x-ray absorption fine structure (XAFS) capabilities. We have worked on the beamline design, optics, and special software needed for an insertion device and bending magnet beam line with x-ray microprobe and spectroscopic capabilities. The intent of this research is to push x-ray methods to new realms of spatial resolution and to apply other advanced x-ray methods to applied problems. This effort involves both support of the PNC-CAT in the development of these capabilities at the Advance Photon Source and the use of these methods on environmental research problems.

Technical Accomplishments

Although x-ray methods have proven extremely important in the analysis of a wide variety of environmental, chemical and materials problems, the information that can be obtained is limited by both the intensity of the radiation and the size of the beam that can be produced. PNNL has joined with several Northwest institutions to form a consortium (PNC-CAT) for the development of an unique focused beam capability at the Advanced Photon Source (APS). The PNC-CAT has been approved by the APS, the beam lines have been subjected to three rounds of design review, and beamline construction is in progress. In addition to these designs, software specifications need to be prepared, and different experimental approaches must be developed for the different specimen types of interest to environmental research.

In FY 1997, construction and commissioning of the beamlines continued. A major milestone was reached when monochromatic x-rays were obtained in the first optical enclosure of the insertion device beamline. This is an important step, since we can now begin commissioning our beamline optics and experimental setups. Initial studies have concentrated on commissioning the capillary based x-ray microprobe, and the x-ray monochromator. Using capillaries previously characterized at the NSLS we have seen the expected increase in flux, and now have more than 10^9 photons/sec/micron^2. Various test images have been obtained to characterize our capabilities and to debug the control software. Additionally, new capillaries have been tested which give a spatial resolution down to 0.5 micron. This is the type of resolution that we will need for many of the planned PNNL experiments. The efficiency of this capillary is still below expectations, but we expect that better mounting will improve this.

Initial EXAFS experiments have demonstrated the basic soundness of the monochromator design and identified some areas which can be improved. Based on these tests, we have designed an improved second crystal translation stage. When this is installed in October, the beamline should be capable of providing high quality spectroscopy, including quick scanning capability. Implementing EXAFS capabilities on the insertion device beamline requires a coordinated scanning of the undulator radiation source and the monochromator. We were one of the first APS CATs to successfully implement this capability.

We expect the main components of the insertion device beamline to be in place in January 1998. Accordingly, our design efforts have been switching to the experimental support equipment. Through non-LDRD funding, we have begun procurement of an advanced multielement Ge detector. This will allow experiments such as dilute fluorescence XAFS, trace element analysis, and elementally sensitive imaging. Another important facility which is under construction is a ultrahigh vacuum chamber capable of surface XAFS, x-ray standing wave, and x-ray reflectivity. This will eventually be upgraded to full MBE and surface diffraction capabilities. Both of these capabilities will be essential for the types of experiments proposed by PNNL personnel. To take optimum advantage of the high fluxes at the APS, we are also exploring alternative fluorescence detectors, such as Si drift detectors and avalanche photodiodes.

Publications and Presentations

S.M. Heald, D.L. Brewe, K.H. Kim, F.C. Brown, B. Barg, and E.A. Stern. 1996. "Capillary concentrators for synchrotron radiation beamlines." *Optics for High-Brightness Synchrotron Radiation Beamlines II.* L.E. Berman and J. Arthur, Eds., Proc. SPIE 2856, 36.

S.M. Heald, D.L. Brewe, B. Barg, K.H. Kim, F.C. Brown, and E.A. Stern. 1997. "Micro-XAS using tapered capillary concentrating optics." Proc. XAFS IX, 9th Int. Conf. on XAFS, *J. de Phys.* IV 7, colloq C2, 297.

S.M. Heald. 1996. "Microbeams and Micro-XAFS Using Tapered Capillary X-ray Concentrators." 1996 SRRC Users Meeting, Hsinchu, Taiwan, November 13-14.

D.L. Brewe, S.M. Heald, W. Barg, F.C. Brown, K. H. Kim, E.A. Stern. 1997. "MicroXAFS Using Tapered Capillary X-Ray Concentrators." Annual Meeting of the American Crystallographic Association, St. Louis, July.

F.C. Brown, A. Frenkel, S.M. Heald, K.H. Kim, Y. Nishihata, and E.A. Stern. 1997. "A Microfocus X-ray Beamline for the Advanced Photon Source Using Elliptical Mirrors at Grazing Incidence." Int. Conf. on Synchrotron Radiation Instrumentation, Himeji, Japan, August.

Nuclear Science and Engineering

Silicon-Based Beta Sensor for Onsite Inspection

Sonya M. Bowyer, Theodore W. Bowyer
(National Security Division/Radiological and Chemical Sciences)

Study Control Number: PN97096/1237

Project Description

The recent signing of the Comprehensive Test Ban Treaty by President Clinton and more than 50 nations has brought a push to develop technologies related to on-site inspection (OSI) of suspected nuclear test sites. Even though terms of on-site inspection for the CTBT have been preliminarily set in the CTBT treaty document, specific technologies do not yet exist to measure some of the signatures expected on site after an underground nuclear detonation. One of the most useful signatures expected in prompt venting of a nuclear test is ^{89}Sr (half-life = 50.5 day), formed by decay of ^{89}Kr (half-life = 3.15 minute) which may be one of the only gases vented near an underground detonation. Determination of high levels of ^{89}Sr could allow OSI inspectors to localize probable vent locations so that sophisticated drilling and radionuclide measurements could be made.

The objective of this project is to develop a miniature silicon microstrip-based high-energy beta sensor for detecting abnormally high levels of ^{89}Sr. The detection principles that will be employed are similar to those used for successful scintillating fiber technology invented and developed at PNNL. The silicon-based beta sensor will be extremely compact, lightweight, battery operated, rugged, and capable of measuring levels of ^{89}Sr indicative of ^{89}Kr fallout within a few minutes. This technology has advantages for on-site inspection because of its low power use, high efficiency, simple electronics, light weight, degree of specificity, and compact design.

Technical Accomplishments

On-site inspection of sites suspected of nuclear detonations requires sensitive field instrumentation for detecting and analyzing soil samples. The current state of the art for beta detection involves the use of scintillating plastic fibers. These fibers are used to detect the high-energy betas and discriminate against background gammas by requiring a coincidence between multiple layers of fiber. Though successful, there are a number of disadvantages in using fibers that are mitigated against by using silicon wafers instead. The pursuit of this detection method is now viable since commercially available, large-area, high-purity silicon wafers now exist that allow for this layered beta detection technique. However, it was unknown whether these detectors could be adapted to provide the desired high resolution for on-site inspection applications.

During FY 1997, we designed, constructed, and tested a prototype silicon beta spectrometer in a stacked configuration capable of detecting betas from high-energy beta emitters.

The design of the detector system included a Monte Carlo simulation of several detector configurations, so that optimal detector thickness could be determined before purchasing the multiple detectors that would be positioned in a stacked configuration. Figure 1 shows the basic stack configuration in which the detectors were arranged.

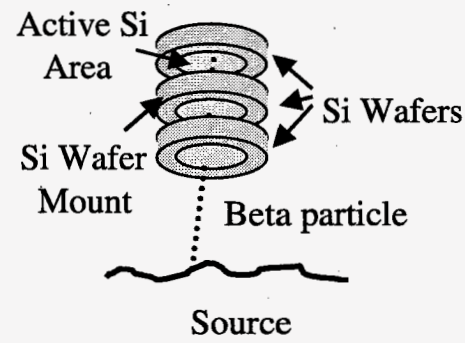

Figure 1. Schematic of silicon detector arrangement in a stack.

Since the energy deposited per wafer is quite close to expected noise-energy equivalent signal for wafers of thickness less than 500 microns, we decided that wafers of at least this thickness should be used. Detectors of both 500 microns and 1 millimeter were used in this project.

Figure 2 shows a plot of the energy distribution expected in a silicon detector which requires a coincidence beta signal (i.e., energy loss above a certain threshold) in the detector closest to the source. This plot demonstrates the success of noise reduction and increased sensitivity via the coincidence requirement.

This project also necessitated development of a graphics-based data acquisition and display system for readout of the detector system. The graphics-based data acquisition system was based on the LabView™ graphical

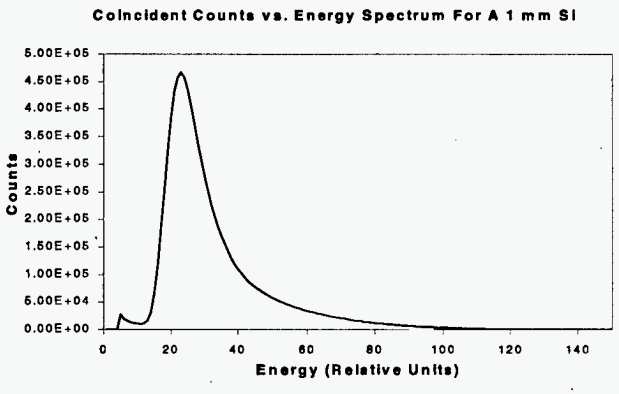

Figure 2. Energy distribution plot requiring coincidence.

programming interface, National Instruments^{TM} digital input-output boards, and Canberra 8713 analog-to-digital converters (ADCs). This system allowed for two-dimensional energy-energy correlation data collection and display. This system allowed for complex software triggering and data routing normally only possible through complicated programming or sophisticated hardware-computer interfaces (e.g., CAMAC or VME).

After the design was completed, we purchased the electronics necessary for readout of the silicon wafers and assembled the electronics necessary for simultaneous readout of three silicon wafers. Most of the electronics needed for this readout system was borrowed from the in-house supply and/or existing programs. The detector system, electronics, and software were setup, tuned, and tested using a ^{90}Sr based source.

Of particular interest to analyze are acquired energy-energy correlation plots for the silicon detector system. These plots are usually constructed with the vertical axis as the total energy deposited in the silicon stack and the horizontal axis as the energy deposited in a particular silicon wafer. We are currently examining these plots in order to fully understand and determine the achievable sensitivity of the detector system. At present, there is no evidence of cosmic-ray interference in this spectrum, consistent with the design specifications.

We were pleased to find that the noise levels and geometric contributions to the energy spread in the wafers were small enough to achieve good energy resolution in the individual silicon wafers. We also found that the wafers were quite stable—no significant energy shifts were observed after running continuously for several days.

During the course of investigation of the stacked silicon configuration, we concluded that adding the capability of gamma energy determination would greatly enhance the flexibility of this system. This in situ beta-gamma coincidence spectrometer would have a large advantage over single gamma-ray spectrometry, since some isotopes would have greatly reduced background interferences when detection of a beta and gamma in coincidence was required.

Process Science and Engineering

Advanced Biotreatment for Industrial and Municipal Wastewater

Rodney S. Skeen, Jianwei Gao (Bioprocessing)

Study Control Number: PN97007/1148

Project Description

The objective of this project was to develop a rationally designed biomass support matrix that could be coupled with an attached growth reactor system and an efficient aerator to create an advanced biotreatment process that would replace activated sludge. If successful, this new biotreatment process could reduce biosolids production by up to 90%. In addition, it would dramatically improve process tolerance to shock loadings and increase treatment capacities by at least fourfold.

Technical Accomplishments

Several types of support material were evaluated for use in an attached growth wastewater treatment reactor. These supports include high silica foaming glass and polymer nets. Mass transfer analysis for oxygen and nutrients showed that the foaming glass materials have too large a mass transfer resistance due to channel clogging. In contrast, the polymer netting was predicted to have minimal mass transfer limitations at the biofilm thickness required to achieve the desired loadings. Theoretical analysis revealed that the optimal netting material would have an average fiber diameter of 0.1 mm and a pore opening of 0.4 mm.

A commercially available polypropylene net was chosen to evaluate the theoretical predictions. This material had a porosity of 0.70, a fiber diameter of 0.4 mm, and a pore diameter of 1 mm. Tests were conducted using a 2.6 L continuous bioreactor to evaluate the ability of the sample netting to maintain attached biomass in a high shear environment. Synthetic wastewater was fed to the reactor at 10 mL/min (residence time of 4.3 hours). The waste stream was composed of 0.75 g/L glucose, 1 g/L yeast extract, and 0.5 g/L ammonium chloride dissolved in deionized water. The reactor contained 1.1% (volume net/volume reactor) of netting material. Agitation and aeration was achieved using a sparge stone and injecting air at a high rate.

Results from this test indicated that an average biofilm thickness of 0.65 mm could be maintained. This thickness is above the target of a 0.20 mm required to meet the desired performance objectives. Finally, it was observed that material with a rougher surface provided more rapid initial biomass attachment, but did not affect the steady-state level of biomass attached to the packing material.

The potential cost benefits of using an attached growth reactor system over a conventional wastewater treatment system were also evaluated. Comparison of the designs for a conventional extended aeration system with an attached growth process shows that, at all three design flow rates (0.1, 0.5, and 1.0 million gallons per day [MGD]), both reactor systems can achieve similar effluent water characteristics. However, the attached growth process has two distinct advantages. First, less solids handling is required since biomass recycle is not needed to maintain high biomass concentrations. Second, the combined volumes for the reactor and clarifier for the attached growth system is less than half that required for a conventional system. These differences result in an annualized cost savings of 18%, 11%, and 9% for a 0.1, 0.5, 1.0 MGD attached growth plant, respectively. This cost savings includes both annualized capital cost and the yearly operating costs. In all cases, approximately 50% of the savings is capital cost and 50% is operating cost.

Advanced Technologies for Selective Anion Separation

Johanes H. Sukamto, Anthony J. Peurrung (Process Technology)

Study Control Number: PN97009/1150

Project Description

The objective of this project is to develop new, advanced technologies for selective and efficient anion separation. Two specific technologies were examined: oscillatory-fields based processes (enhanced diffusion) and electrically switched ion exchange (ESIX).

- Oscillatory-Fields Based Separation Processes. Recent work has demonstrated that transport rates can be increased by several orders of magnitude or more via a process known as "enhanced diffusion," where an oscillatory velocity field is used in conjunction with diffusion processes in the direction orthogonal to the velocity field. We intend to explore and expand the application of this novel technology to anion separation. To this end, design equations to determine the viability of separation processes that use oscillatory fields will be derived.

- ESIX-Based Separation Processes. ESIX is a technology that is currently being developed at PNNL for the removal of radioactive cesium. It produces less secondary waste than conventional ion exchange. Since the candidate materials will be different than those that have been used for cation separations, there is a need to define the functional requirements of the candidate materials. That is, evaluation of the viability of ESIX as a viable technology deployment vehicle and design of equations for the ESIX process given in terms of the material properties are required. Relevant figures of merit as well as relevant material parameters will be defined.

Technical Accomplishments

Enhanced Diffusion

The design of separation systems based on enhanced diffusion have been studied. Three figures of merit have been determined to be relevant for comparing enhanced diffusion systems to conventional separation systems: 1) achievable separation or, equivalently, overall separation factor based on the input and output of the system; 2) yield per unit power consumed; and 3) device size and complexity.

Enhanced diffusion is a physical phenomenon that greatly elevates the effective diffusion constant in a region of space. A separations system is constructed by imposing a net flow in the direction opposite to the desired diffusional flux. This flow, called counterflow, retards all fluxes but preferentially retards those species with lower enhanced diffusion constants, leading to substantial enrichments.

Prior to evaluation of any of the figures of merit stated above, the exact values of the enhanced diffusion constants based solely on the flow configuration must be calculated for the chosen species. The enhanced diffusion constants for roughly a dozen distinct flow geometries have been calculated.

Experimental verification of the design equation for a conventional enhanced diffusion system has been completed. The separation between KNO_3 and K_2SO_4 was the initial target. The initial experimental results support the theory and as more experimental data is collected, verification of the other enhanced diffusion systems will be carried out.

Electrically Switched Ion Exchange

A complete model description of an ESIX system requires the use of a volume-averaging technique similar to that outlined by de Vidts and White (1997), but specialized to systems where selectivity must be accounted for. In this technique, a consistent set of transport equations is derived using averages of quantities such as solution and solid phase concentrations, solution and solid phase potentials, and the average convective velocity within the pores. The objective in FY 1997 was to examine the limiting cases of the general description. The two limiting cases considered were 1) transport limitations within the ESIX film, and 2) transport limitation in the solution. Of particular interest are the implications that these limitations have on the performance of ESIX systems as compared to other separation systems. In comparing ESIX to traditional separation systems, such as conventional ion exchange and solvent extraction, the two figures of merit that should be examined are 1) processing rate/capacity, and 2) electrical power requirement. These two figures of merit were chosen because they can be used directly to estimate the capital and operating costs, which in turn can be compared to more traditional separation techniques.

The best achievable separation is one where transport in the liquid phase is the rate-limiting step. At this limit, the only relevant characteristic of the separating agent is the separation factor, and the higher it is, the better the separation system is. To quantify the processing rate/capacity, the traditional convective diffusion equation was solved using a commercial finite element package, PDEase®. Two different forms of driving forced were used: 1) bimolecular, and 2) Freundlich type adsorption for very low concentrations of contaminants. Numerical solutions were required since available analytical solutions that account for dispersion are only applicable to infinitely long columns, and dispersion effects are usually more pronounced for short columns. ESIX columns are necessarily short since long columns, as used in conventional ion exchange, lead to highly nonuniform potential distribution (Newman 1991).

In summary, two limiting cases of ESIX systems have been examined with the model. For each case, methodologies to determine 1) processing rate/capacity, and 2) electrical power requirement have been established.

The required material properties have been identified, but the range of values has not been established.

References

de Vidts and White. 1997. "Governing Equations for Transport in Porous Electrodes." *Journal of the Electrochemical Society*, 144:1343.

J.S. Newman. 1991. *Electrochemical Systems*. 2nd Edition, Prentice-Hall, New York.

Publications and Presentations

A.J. Peurrung, S.R. Billingsley, L.M. Peurrung, J.H. Sukamto, and M.D. Tinkle. "Design of an Enhanced Diffusion Separator using Steady, Buoyancy-Driven Flo." *AIChE Journal* (to be submitted).

A.K. Savineau, J.H. Sukamto, A.J. Peurrung, S.R. Billingsley, L.M. Peurrung, and M.D. Tinkle. "Separation of KNO3 and K2SO4 using Enhanced Diffusion." (in preparation).

J.H. Sukamto, R.J. Orth, S.D. Rassat, M.A. Lilga, and R.T. Hallen. 1997. "Separations using Electroactive Materials for DOE Applications." Presented at the 192nd Meeting of the Electrochemical Society, Inc. and the 48th Annual Meeting of the International Society of Electrochemistry, September.

Biological Catalysis and Processes for Chemical Synthesis

Michael J. Truex (Environmental Technologies)

Study Control Number: PN97018/1159

Project Description

Oxioreductase enzyme systems may be of use in chemical synthesis reactions. This type of enzyme system may include combinations of oxygenase and dehydrogenase enzymes which are cofactor-requiring enzymes. Many oxygenases also require molecular oxygen. The combined need for providing both cofactor and molecular oxygen is beyond what is currently applied in enzyme processing. Additionally, for chemical synthesis, mass transfer limitations in reactions involving organic feed stock may be a key factor in the process cost effectiveness. This project was focused on addressing these technical gaps related to application of oxioreductase systems to partial oxidations for chemical synthesis.

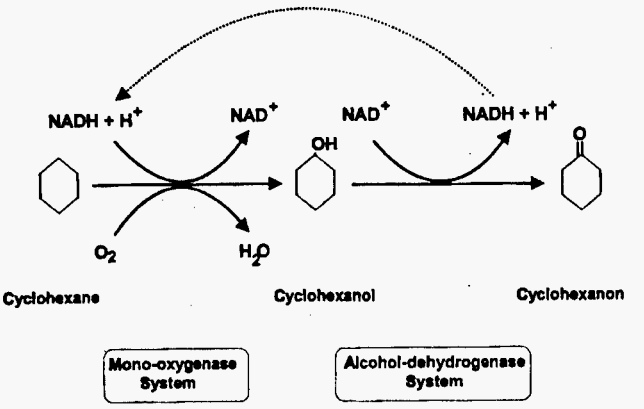

Figure 1. Enzymatic production of cyclohexanone with NADH recycling.

Background

Monooxygenases are heme-containing compounds that catalyze the incorporation of a single oxygen atom into a variety of chemicals that can include drugs, pesticides, carcinogens, and hydrocarbons. With hydrocarbons, the introduction of an oxygen atom (from molecular oxygen) causes hydroxylation to form an alcohol, while the remaining oxygen atom is reduced to form water. The energy required for the hydroxylation is supplied by reducing equivalents from NADH which are shuttled through a flavoprotein. Although some monooxygenases have variable and overlapping substrate specificities, when compared to current alkane oxidation catalysts, enzyme systems have the capability to provide very controlled and selective chemical oxidations.

As applied to the chemical process industry, the monooxygenase enzyme would perform the specific oxidation of cyclohexane to cyclohexanol which is subsequently converted to cyclohexanone by alcohol dehydrogenase as illustrated in Figure 1.

While enzymes have been demonstrated to perform the chemical conversion of cyclohexane to cyclohexanol, a number of issues must be overcome before these enzyme systems can become cost-competitive in the marketplace. These issues include the following:

- Recycling and regeneration of NAD (or other hydrogen carrier). One potential method for recycling of this compound is through further enzymatic conversions of cyclohexanol that regenerate reducing power. As can be seen in Figure 1, NADH is produced during the conversion of cyclohexanol to cyclohexanone. Consequently, this two-step enzymatic process is an ideal candidate for NADH recycling, since the NADH that is used in the first reaction is regenerated in the second.

- Effective enzyme immobilization with minimal loss of activity. An immobilization matrix will be required for the monooxygenase and alcohol dehydrogenase enzymes and flavoproteins in continuous-flow applications. It will be necessary to immobilize the enzyme through binding of some of its functional groups in a way that does not interfere with the active site on the enzyme. In addition, the matrix must be compatible with delivery and recycle of reducing equivalents and functioning of the flavoprotein to drive enzymatic conversions.

Reaction kinetics as defined by the enzyme reaction and limitations imposed by the low solubility of cyclohexane must be quantified in context of the above two issues. These processing parameters can then be used as a basis for development of the bioreactor configuration (e.g., hollow fiber, membrane), operating conditions (e.g., temperature, pressure, and use of surfactants), and final product separations (based on conversion efficiencies).

Technical Accomplishments

This project investigated the feasibility of bioprocessing for replacing a conventional chemical synthesis route. The technical goals of the project include investigating key factors in enzyme bioprocessing for the conversion of cyclohexane to cyclohexanol. These factors include

- methods for recycling and regenerating electrochemical reducing species
- defining requirements for enzyme immobilization and testing immobilization techniques
- establishing reaction kinetics for processing conditions (e.g., immobilized enzyme) where kinetic information is not available in the literature.

In FY 1997, we identified a model oxioreductase enzyme system that can be used to test concepts in the area of enzyme-catalyzed chemical synthesis. The partial oxidation of cyclohexane to cyclohexanone was selected as a test system. For testing purposes, horse-liver alcohol dehydrogenase was used to examine the kinetics of dehydrogenase systems. Batch kinetic testing was completed to quantify the conversion as a function of enzyme concentration and feedstock concentration.

We also developed a conceptual reactor design for use with the model enzyme system. Reactor designs were evaluated with respect to estimated mass transfer rates coupled with the enzyme system kinetics. The designs evaluated were for a three-phase system: feedstock, enzyme solution (aqueous), and gas phase (oxygen). The reactor configuration selected was a dual-membrane reactor. This type of reactor may provide sufficient mass transfer rates of reactants and products. Key factors in the mass transfer rates are the membrane properties and thickness and the surface area to volume ratio. Based on these requirements, we determined that some of the reactor concepts being developed within the microtechnology initiative may be suitable for enzyme processing.

Testing microtechnology reactors to determine the mass transfer rates for cyclohexane into water were performed. Difficulties with the membrane configuration caused inconclusive results. Further testing in FY 1998 will continue to address the mass transfer issues with these reactors.

Catalytic Hydrothermal Reductions

Douglas C. Elliott, Yong Wang, John G. Frye (Chemical Process Development)
Scott Elder, John Darab (Materials Science)

Study Control Number: PN97022/1163

Project Description

The ultimate success of all pressurized aqueous catalytic conversion processes depends on the ability to develop robust catalysts and supported catalysts that can withstand aggressive hydrothermal reaction conditions. A new class of robust materials were investigated for use as aqueous catalyst supports. In addition, newly emerging schemes for the formation of ordered structures were used to synthesize "next generation" supports for noble and base metal catalysts. Using powder synthesis and ceramic forming techniques unique to PNNL, supports were synthesized with the required surface area, porosity, mechanical integrity, and chemical stability necessary for this application. Other high-surface area materials were also investigated as supports for catalysts for aqueous phase processing. These catalytic formulations were tested in model reactions to determine stability of the active metal sites and the resulting catalyst activity in the aqueous processing environment. Surface analysis techniques were used to evaluate mechanisms of catalyst degradation as well as catalytic reduction. Models of useful catalytic materials will be developed based on these materials and analysis.

Technical Accomplishments

The focus of this effort has been to synthesize high surface area (preferably >100 m^2/g) solid-state materials with suitable hydrothermal stability for use as catalyst supports. High surface area materials for catalyst supports are desirable because as surface area of the support increases, the concentration of supported active metal catalyst can increase while maintaining sufficient dispersion of the metal. Thus, a given volume of support with catalyst has increased activity. These catalytic materials will be useful in new technologies being developed for synthesis of chemicals from renewable biomass sources. The new technologies are typically water-based, avoiding the use of organic solvents, but requiring new formulations for catalysts which can withstand degradation in water.

Based on our experience in chemical process development using catalysts in water-based systems, we have been able to survey a range of materials for compatibility with water at reaction conditions. With this information in hand and our knowledge of materials properties, we have been able to identify several areas of new materials development which have potential for breakthroughs in this technology.

The catalyst testing has been the evaluation of physical and chemical stabilities of the potentially promising catalysts or catalyst supports under aqueous processing conditions. Typically, catalytic materials were tested in deionized water at 200 to 350°C and 1900 psi H_2 for 70 to 400 hours. Materials being tested included novel supports developed at PNNL, supported base- and precious-metal hydrogenation catalysts on a premium Engelhard amorphous carbon, a commercial catalyst from Calsicat, and a catalyst from BASF.

Oxynitrides and Mesoporous Materials

We began by considering TiO_xN_{1-x} ($0 < x < 1$, depending on reaction conditions) as a catalyst support for two reasons: 1) it can be synthesized from TiO_2 using a unique synthetic process at relatively low temperatures (as low as 625°C) so we expected to maintain higher surface areas, and 2) transition metal nitrides in general are considered to be refractory—stable at high temperatures and in acidic and basic conditions. We synthesized and hydrothermally tested a variety of TiO_xN_{1-x} samples to assess their hydrothermal stability. The general conclusion from these reactions is that the TiO_xN_{1-x} (surface areas >75 m^2/g) materials we investigated were not stable under the hydrothermal conditions used in processing.

The structural arrangement of a mesoporous inorganic material is a result of the templating influence of surfactant micelles. Surfactant molecules consist of both hydrophobic and hydrophilic chemical units, which permit them to organize into supramolecular micellar arrays as a function of solvent type and concentration. These micellar arrays act as templating meso-units in which small, inorganic building blocks (titania or zirconia) are deposited, producing an inorganic network organized about surfactant templates. A completely inorganic network, with pores resembling the surfactant micelle shape and size, may result upon removal of the surfactant template. These porous (20 Å < pore diameter <100 Å) titania and zirconia materials have surface areas ranging from 150 to 260 m^2/g and are obvious candidates as catalyst supports. Our initial results from the hydrothermal experiments on mesoporous materials are encouraging.

RTDS Zirconia

The second area delineated for this project was to use PNNL's patented Rapid Thermal Decomposition of precursors in Solution (RTDS) process for production of zirconia powders. The task was defined as 1) prepare experimental quantities of nano-crystalline, high surface area zirconia preferably of the monoclinic phase; 2) prepare high surface area, high crush strength pellets from these powders for use as catalyst supports; 3) characterize these materials in terms of phase, crystallite diameter, and surface area; and 4) provide these materials for testing under catalytic reaction conditions.

Using the methods typically outlined in the RTDS patent, zirconia materials were synthesized. Cylindrical pellets were pressed from several of the RTDS powders and sintered at different temperatures in order to achieve some level of pellet crush strength (which also, inevitably causes a decrease in the surface area).

Carbon Supports

Amorphous carbon has high surface area and unusual inertness, but carbon also lacks interaction with metals. Our TEM results show that base and precious metals have different stabilities under aqueous processing conditions. A surface science approach was attempted to explain these phenomena. However, hidden metal particles inside the pores and the unclean surface of the amorphous carbon inhibit the application of, for example, EELS, STM, and AFM and interpretation of the interactions between metal and carbon. A highly oriented pyrolitic graphite has been ordered and will be used to model the carbon-supported metal catalysts. The flat and clean surface of pyrolitic graphite, as well as its electrically conducting characteristic will not only allow the application of EELS, STM, and AFM, but will also enhance the resolutions in techniques such as XPS, SIMS, and AES.

Commercial Supports

The Calsicat Ni/Kieselghr catalyst (#69F-095A) was evaluated for aqueous processing use on the recommendation of the manufacturer. It underwent a dramatic reduction in BET surface area from 192 to 93 m^2/g in 64 hours of aqueous processing as a result of the solubility of the aluminosilicate structures in the mineral support.

A BASF catalyst formulation was tested for stability in an aqueous processing system. It is a proprietary formulation developed in our laboratory. The catalyst was tested at 350°C in a reforming/methane synthesis reaction.

Summary

In total, these results show good progress on several fronts for developing capabilities as well as actual new materials for aqueous phase processing catalysts. The oxynitrides have been investigated and proved uninteresting from a catalytic material point of view and, therefore, have been abandoned. Ordered materials, a subject for the second year of this LDRD project was initiated this year and is well under way with interesting results. A novel catalyst synthesis method has produced materials which may be of interest, but further optimization through process modifications is planned to maintain the exceptional material properties of the initial product. Investigations continue in order to better understand the interaction of the catalytic metal with a carbon support surface. Communication with commercial catalyst producers remains a key ingredient in our strategy for catalyst material development.

Catalytic Upgrading of C_5 Feedstocks to Ethylene and Propylene Glycols

Douglas C. Elliott, Yong Wang, John G. Frye (Chemical Process Development)

Study Control Number: PN97023/1164

Project Description

The objective of this project was to develop capabilities and technologies for the conversion of pentose sugars (C_5) to value-added products. Primary products from the conversion of pentose sugars are ethylene and propylene glycols. In this project, we developed processing methods for the production of commodity chemicals from C_5 feedstocks. The work focused on catalytic hydrogenation and hydrogenolysis for the production of glycols. Chemical analytical methods were developed in order to adequately evaluate the processing experiments. Preliminary economics of the process were also determined for the process.

Technical Accomplishments

Semi-batch reactor tests were performed with different candidate catalysts using both xylitol and arabinotol, C_5 sugar alcohols (monomer pentahydroxypentanes) which are derived from biomass C_5 structures. These results have suggested the uniformity of the processing using either feedstock, i.e., nearly identical product mixtures were formed at essentially the same rates for either feedstock. Therefore, complex feeds derived from biomass containing mixtures of C_5 sugars should not add any significant complexity to the process. We have tested both C_5 sugar alcohols with a commercial nickel metal catalyst and a PNNL-developed, stabilized nickel metal catalyst to develop a baseline activity and then proceeded to promoted nickel metal catalysts and precious metal catalysts.

The results with the alternative catalysts suggest that a range of products can be produced from C_5 sugar alcohols under hydrogenolysis conditions. Tests with promoted nickel catalysts showed good activities for polyol production. Total conversion of xylitol was achieved with 77% yield of glycols and less than 1% gas formation. Attempts to reduce the activity of certain catalysts in this environment were unsuccessful in that the major product remained methane with limited production of polyols. Tests with other materials showed little activity at these processing conditions.

We have been developing our analytical methods to better quantify feed and products in the aqueous hydrogenolysis of C_5 sugar alcohols. We tested gas chromatography with flame ionization and mass selective detectors, ion chromatography with a pulsed amperometric detector method, and ^{13}C nuclear magnetic resonance spectrometry. We have coordinated our analytical needs with the new instrumentation coming on line in the EMSL, providing samples for use in start-up and test-out of the equipment and operator training.

The economic model for polyols production developed at International Polyol Chemicals, Inc., was modified from its original C_6 application to address the economics of C_5 processing. Based on this model, an internal rate of return of 47% is predicted. This is a preliminary number that indicates only what is possible with further development to prove out the steps for utilization of C_5 sugars. The model assumes the use of crude hemicellulosic feedstocks (corn fiber, wood pulping byproduct, bagasse) with "dirty" hydrogenolysis to directly produce a polyol stream from which the final products can be recovered.

Characterization of Rapid Dechlorinators: Remediation of DNAPL

Brian S. Hooker (Process Technology)
Margaret F. Romine (Earth Systems Science)
Rodney S. Skeen (Atmospheric Sciences), Jianwei Gao (Environmental and Health Services)

Study Control Number: PN95015/991

Project Description

The objective of this research was to determine the potential for NAPL biodegradation using microorganisms that derive energy from reductive dechlorination. The research included isolation and phylogenetic identification of bacteria in pure culture and consortia, and characterization of enzymatic pathways for dehalogenation. Results provided the basic understanding of organisms that derive energy from dechlorination that is needed to identify and develop strategies for in situ NAPL bioremediation.

Technical Accomplishments

Anaerobic microcosms of subsurface soils from four locations were used to investigate the separate effects of several electron donors on tetrachloroethylene (PCE) dechlorination activity. The substrates tested were methanol, formate, lactate, acetate, and sucrose. Various levels of sulfate reducing, acetogenic, fermentative, and methanogenic activity were observed in all sediments. Tetrachloroethylene dechlorination was detected in all microcosms, but the amount of dehalogenation varied by several orders of magnitude. Trichloroethylene was the primary dehalogenation product, however, small amounts of cis-1,2-dichloroethylene, 1,1-dichloroethylene, and vinyl chloride were also detected in several microcosms. Lactate-amended microcosms showed large amounts of dehalogenation in three of the four sediments. One of the two sediments which showed positive activity with lactate also had large amounts of dehalogenation with methanol. Sucrose, formate, and acetate also stimulated large amounts of dehalogenation in one sediment that showed activity with lactate. Amendment with formate, acetate, or sucrose resulted in only slight dehalogenation in the other three sediments. Elevated levels of dehalogenation were not consistently associated with any observable anaerobic metabolisms (sulfate reduction, acetogenesis, fermentation, or methanogensis). The lactate amended cultures for two of the three sediments that showed high levels for dehalogenation were subdivided and incubated with lactate and PCE, TCE, cis-DCE, or VC. PCE and TCE were rapidly converted to TCE and cis-DCE, respectively. Neither DCE nor VC was dehalogenated. However, PCE was converted to ethylene in one sediment which was incubated with lactate, yeast extract, and vitamin B_{12}. Unfortunately, this condition was tested with only the one sediment, and further work is needed to determine if these additives will have a similar effect on the other cultures. These results suggest that lactate may be an appropriate substrate for screening sediments for PCE or TCE dehalogenation activity, but that the microbial response is not sufficient for complete in situ bioremediation. However, other cofactors may aid in stimulating the complete dehalogenation of PCE to ethylene.

Analysis of the rate of PCE and TCE dehalogenation in the sediment microcosms that showed high levels of dehalogenation products revealed similarities between all sediments. A detailed study of the Victoria activity revealed that dehalogenation rates were more similar to the Cornell culture (DiStefano et al. 1991) than to rates measured for methanogens, or a methanol-enriched sediment culture (Skeen et al. 1995; Fathepure et al. 1987). This may suggest that these sediments contain a highly efficient dehalogenation activity similar to the Cornell culture. This assertion is further supported by the fact that an average of 3% of added reducing equivalents could be diverted to dehalogenation in tests which were conducted using PCE-saturated hexadecane as a constant source of PCE during incubation. However, further evidence is needed to confirm this premise.

Publications and Presentations

J. Gao, R.S. Skeen, B.S. Hooker, and R.D. Quesenberry. 1997. "Effects of Several Substrates on Tetrachloroethylene Dechlorination in Anaerobic Soil Microcosms." *Water Research*, 31, 2479-2486.

J. Gao, R.S. Skeen, and B.S. Hooker. 1997. "Carbohydrate Induced Biodegradation of Cis-dichloroethylene and Vinyl Chloride under Aerobic Conditions." *Biotechnol. Bioeng* (submitted).

R.S. Skeen, J. Gao, B.S. Hooker, and R.D. Quesenberry. 1996. *Characterization of Anaerobic Chloroethene-Dehalogenating Activity in Several Subsurface Sediments.* PNNL-11417, Pacific Northwest National Laboratory, Richland, Washington.

R.S. Skeen, J. Gao, and B.S. Hooker. 1997. "Process Scale-up Considerations for In Situ Reductive Dechlorination of Chloroethenes." Paper presented at the 1997 In Situ and On Site Bioremediation Conference, New Orleans, Louisiana, April 28 - May 1.

R.S. Skeen. 1996. "Screening of Indigenous Potential For Complete In Situ Destruction of Tetrachloroethene." Paper presented at the 1996 International Business Communications Natural Attenuation Conference, Annapolis, Maryland, December 5-6.

Chemical Process and Reactor Modeling for Innovative Conversion

Annalee Y. Tonkovich, Eric A. Daymo (Process Technology)

Study Control Number: PN96009/1076

Project Description

The objectives of this project were to 1) develop and validate an experimentally realistic model of the membrane reactor, and 2) verify the electrical discharge model as a major step in the creation of a practical tool for scale-up design and performance prediction for a non-equilibrium plasma conversion process.

Technical Accomplishments

In FY 1997, work continued on the development of one-, two-, and three-dimensional membrane reactor models. These models were constructed as tools for screening applicable reaction systems and selecting operating conditions where the membrane reactor would outperform a conventional plug flow reactor. Propane partial oxidation data were used to validate the one-dimensional membrane reactor model, but the model only qualitatively matched the experimental trends. It was postulated that radial concentration gradients within the reactor, due perhaps to a fast reaction between oxygen and hydrocarbon at the membrane wall where oxygen is introduced, could explain why the one-dimensional model did not quantitatively predict the experimental data at all conditions.

As a result, two- and three-dimensional models were constructed with TEMPEST, but these models only predicted the flow field. Even though no reactive flow solutions were obtained because of numerical complications, two- and three-dimensional TEMPEST models did provide a better understanding of flow patterns in the reactor.

Although the one-dimensional membrane reactor model only qualitatively predicted selectivity and conversion trends for the partial oxidation of propane, this model was well suited to explore and explain the operating envelope (kinetics, hydrocarbon: oxygen feed ratio, and residence time) where the membrane reactor outperforms the plug flow reactor for generic partial oxidation networks. For a pseudo-homogeneous generic partial oxidation reaction network, the one-dimensional model predicted that a membrane reactor will outperform a plug flow reactor at low residence times. The same model predicted that a membrane reactor will outperform a plug flow reactor at longer residence times for a similar heterogeneous generic partial oxidation reaction network. Thus, the one-dimensional model suggests that regime where the membrane reactor outperforms the plug flow reactor fundamentally depends on the kinetics of the reaction network.

Presentation

A.Y. Tonkovich. 1996. "Inorganic Membrane Reactors for Partial Oxidation Reactions: Mathematical Validation of Experimental Results." 1996 American Institute of Chemical Engineers National Meeting, Chicago, Illinois.

Controlled Oxidation Reactions of Organics by a Unique Gas Phase Corona Heterogeneous Reactor System

Gary B. Josephson, David A. Dixon (Process Technology)

Study Control Number: PN97027/1168

Project Description

PNNL has unique capabilities in reactor design, surface analysis, and experimental and computational analysis of gas phase processes. This project integrated these capabilities to develop new processes aimed at controlled, partial oxidation of alkanes and alkenes. Partial oxidation reactions are an economically important class of gas phase reactions which appear promising for plasma reaction. This project investigated the reaction mechanisms, as well as the means to control oxidation reactions on the surfaces of a packed bed in a plasma reactor. We initially focused on the production of phenol and propylene oxide as initial targets. This project investigated the oxidation reactions and mechanisms of propene and benzene oxidation in a plasma reactor. The investigation specifically focused on surface reactions and on how to control surface reactions to significantly improve the reaction efficiency, minimize complete oxidation and the formation of byproducts, and reduce power requirements.

The ultimate objective of the proposed effort was to demonstrate the use of gas phase plasma reactors combined with heterogeneous catalysts in a real reactor configuration as an economically viable process for controlled oxidation of alkanes. The initial effort focused on the synthesis of propylene oxide and phenol from the respective starting materials propylene and benzene.

Phenol and propylene oxide were the initial targets and focus. Improvements in their synthesis would provide a significant impact as they are among the top 50 chemicals produced. In addition, the detailed investigation of the reaction mechanisms and surface reactions of the oxidation of propylene and benzene provides a basis for what may be an entire new branch of heterogeneous catalysis. Such a fundamental understanding will be highly relevant for the broad class of partial oxidation reactions. It will also be relevant to other organic and inorganic syntheses that could use the unique high-energy, highly reactive species which only a plasma can provide under controlled conditions as compared to thermal systems.

Background

Controlled oxidation of alkanes is one of the intermediates for further synthetic changes. For example, cyclohexane is presently oxidized to adipic acid, a key monomer for nylon synthesis by a complex, difficult-to-control process.

In order to develop new industrial-strength processes that are more energy efficient and produce less waste, new types of technologies need to be developed. One such technology which has been developed at PNNL is the gas phase corona reactor (GPCR). Previous research at PNNL has determined that the packing materials in the GPCR can significantly affect the reaction products and energy requirements. Investigations to understand and take advantage of these reactions continues for treatment of VOCs, an environmental remediation use. The phenomena of improved reaction rates in a gas phase plasma raises the potential of using a non-equilibrium plasma for chemical synthesis reactions. Significant plasma research has been conducted over the years investigating the possibilities of plasma-driven chemical reactor systems. Only ozone formation has to-date proven economic. It is generally recognized that plasma reactions feature the advantage of producing high energy active species which can produce different reaction pathways than available through traditional thermal activation. However, the reaction pathways have so far not been controllable and have consumed too much power. In part, this is because of the highly "effective" temperature present in the plasma.

Most plasma synthesis research has been considered to be gas phase homogeneous chemistry or uncontrolled unidentified surface reactions on reactor walls. There has been some work in the CVD area based on combining surface and gas phase reactions to control surface growth on a specific substrate. The typical plasma synthesis approach is similar to improving the yield for a synthesis reaction simply by heating up the reaction vessel. Very poor yields and little control of the products and stereochemistry are generally achieved by such a process. Heterogeneous catalysts based on reactions on surfaces has been a fundamental scientific and engineering tool that has been used to make enormous improvements in yield, to control byproduct formation, and to minimize energy requirement for both gas-phase and liquid-phase synthesis reactions. Can similar improvements and advances be made with heterogeneous reactions in a plasma activated system? The use of the surface catalyst material is to lower

the effective temperature of the plasma to gain increased control of the reaction in order to minimize complete oxidation and to lower the energy requirements of the process.

Technical Accomplishments

During this project the formation of propylene oxide from propylene using a heterogeneous non-thermal plasma reactor was demonstrated. Propylene gas (at approximately 3000 ppm) was fed into a GPCR. The product gases were analyzed by GC/FID and GC/MS.

Figure 1 shows that propylene oxide was formed with a selectivity of up to 20% with the best performance occurring at 10 watts of reactor power input and a high oxygen ration, 50:1:: O2:propylene.

In addition to propylene oxide, other identified reaction products were acetaldehyde, propionaldehyde, and acetone. Acetone and propionaldehyde are likely formed from propylene oxide and are a sink in the reaction path. Acetaldehyde is formed from cleavage of the propylene oxide and is probably formed in conjunction with carbon monoxide or carbon dioxide.

The results of this work established a range of reaction conditions and established analytical procedures for a continuation of this investigation in FY 1998.

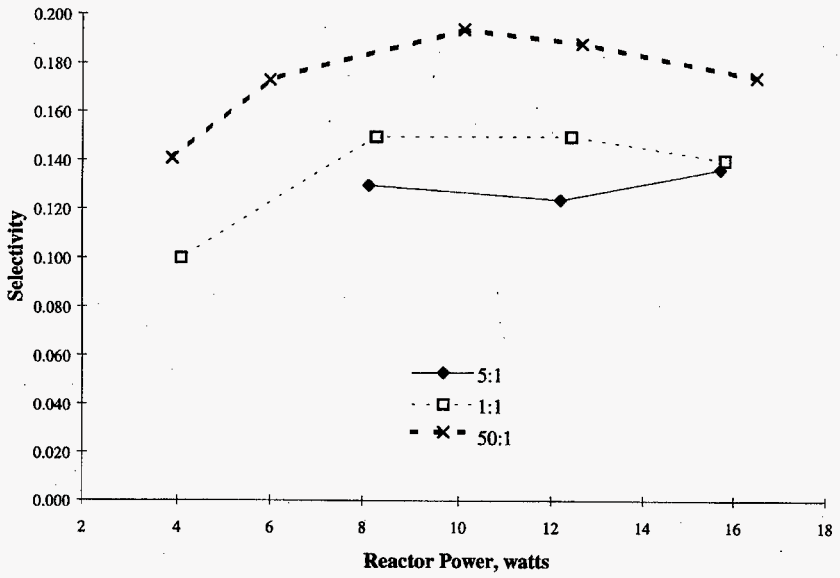

Figure 1. Selectivity for propylene oxide conversion versus reactor power for different oxygen:fuel ratios.

Cost Indexed Process Design Heuristics

Robert S. Butner (Environmental Policy and Planning)

Study Control Number: PN97028/1169

Project Description

The key technical objectives of this work were to 1) identify alternative approaches to discriminating between competing design heuristics, specifically those that are keyed to project cost and other attributes which reflect the engineering feasibility of the design approach; and 2) evaluate selected alternatives for their utility in the Process Heuristic Review for Environmental Design (PHRED) tool. Because of the strong overlap in research interests related to design heuristics, the first step was to meet with staff at DuPont to evaluate the cost-indexed design rules (being developed at DuPont Chemical). Other approaches to heuristic design (including those being evaluated by Dr. David William Pennington at the U.S. EPA Office of Research and Development) also were evaluated. These alternative design heuristics were combined with unit operations-based design rules being developed by PNNL. The resulting heuristics will be incorporated into a software tool that is being designed to help engineers make pollution prevention choices in early stages of chemical process design. The expected result is a significant improvement in the usefulness of the heuristic methods currently being investigated, along with substantial industrial input into the development process.

Technical Accomplishments

A project at PNNL has focused on an environmental process design framework known as Process Heuristic Review for Environmental Design (PHRED). PHRED is intended as a design review process that can be used at all stages of process design to provide guidance regarding conceptual design, equipment selection, equipment specification, control system and piping design, and even the design of ancillary facilities such as storm water collection systems and control rooms. PHRED is being implemented in a rule-based expert system shell, which permits the system to rank the applicable heuristics according to information about the process.

Currently, the decision techniques focus exclusively on the application of unit-operation based heuristics; that is, the selection of design "rules" is based almost entirely on the presence or absence of specific unit operations or pieces of equipment. While such methods have the advantage of being easily generalized to a wide range of processes, they often do not provide sufficient recognition of important design criteria such as cost, ease of implementation, and technical risk. In particular, the design heuristics do not make use of process cost data or treatment cost "rule of thumb" data because these have been difficult to obtain for the target industries (chemicals, petrochemicals, and pharmaceuticals). PNNL has become aware of several alternatives to unit-operation based heuristics, including cost-indexed decision rules/heuristics being developed by the Corporate Environment and Process Safety group at DuPont. Both teams feel that there is significant opportunity to improve the reliability of the heuristic methods by combining cost data and basic process phenomena.

Accomplishments during FY 1997 include the following:

Significant progress was made on tasks 1 (literature review) and 2 (identification/evaluation of applicable approaches to discriminating between design heuristics). We were unable to make significant progress on task 3 (integration of these approaches into existing knowledge base) due to the higher than anticipated data requirements of the cost-indexed approach used by DuPont. Specific accomplishments are described below:

1. Conducted a review of several approaches to discriminating between design heuristics in chemical process design, and related methods used in product-oriented design. This included a review of the chemical engineering literature and review of the literature related to the application of cognitive methods to design in general. Based on this review, we elected to conduct more detailed evaluation of two methods: 1) the cost-indexed design heuristic method being developed by Ken Mulholland et al. at DuPont; and 2) the "root-cause" approach described in a doctoral dissertation by Dr. David William Pennington, currently employed as a post-doctoral investigator by the EPA-ORD.

2. Visited the two groups (DuPont and EPA) to further evaluate these methods. The discussions covered data requirements, overall decision structure, and compatibility with PHRED. During each visit, the principal investigator presented a short technical synopsis of our current approach to heuristic design.

Based on these visits, we arrived at the following conclusions:

1. The cost-indexed heuristic approach, while potentially valuable as a primary discriminator between equally relevant process-based heuristics (including unit operation or root-cause), requires frequent update of cost indices, and may be company-specific in its implementation. While this approach would significantly increase the value of the design tool to specific industry users, it does not appear feasible to implement in a generic fashion. This would be a good subject of later CRADA-based work, but was not implemented at this time.

2. The root-cause based approach appears to have promise as well, but currently there is an insufficient experience base in the published literature to support the extensive development of such heuristics. While Dr. Pennington has developed a prototype knowledge-based system containing a useful number of design rules, large differences in the knowledge bases used by the two systems make it impossible to integrate the two approaches under the initial funding.

3. Through discussions with DuPont, we determined that a distributed knowledge-base approach to documenting various heuristics should be considered in any future development of PHRED-like tools. This would permit individual companies to have an opportunity to customize the knowledge base and dramatically increase the applicability of the tool.

Development and Testing of Microchemical Separations

Ward E. TeGrotenhuis (Process Technology)

Study Control Number: PN97031/1172

Project Description

The objectives of this project are to develop a flexible architecture for microchemical separations, understand the importance of system parameters, establish capabilities for fabricating components and devices, determine device performance in a laboratory test apparatus with a simple test system, and evaluate performance against theoretical prediction.

Microchemical separations systems offer a flexible platform in which to perform waste treatment and chemical processing. As envisioned, these systems will consist of separations hardware that will have a much higher throughput per unit of equipment volume than conventional chemical separations equipment. In addition, the reduced equipment size and enhanced mass transport can improve energy efficiency and reduce capital and operating costs over conventional chemical processes. Several application areas have been identified including: tank waste disposal and environmental restoration activities, developing technologies with greater energy efficiency, and point-of-use manufacturing of toxic and hazardous chemicals.

The initial effort for microchemical separations is a contactor to be used for solvent extraction. In the future, this can be adopted for other separations, such as gas absorption, membrane separations, and facilitated transport. Microchemical separations technologies are expected to achieve 1) higher throughput per unit system volume, 2) flexible and agile manufacturing, 3) increased ease of distributed processing, and 4) short contact times to exploit kinetic effects and enhance separations.

Technical Accomplishments

An architecture was developed in FY 1997 for solvent extraction, which can also serve for other microchemical separations technologies in the future. The architecture allows for versatile contacting of uniform thin films of two or more immiscible liquids in co-current or countercurrent flow directions. Devices have been operated with channel heights ranging from 100 μm to 500 μm. The architecture is easily scalable to higher throughputs by adding channels.

One technical challenge in making the microcontactors operate is preventing breakthrough (convective flow) of the fluids through the contactor plate. The breakthrough pressure, the maximum allowable pressure drop across the plate, is dependent on the maximum pore size, r_p, the interfacial tension, γ, and the contact angle, θ (wettability) according to the relationship,

$$\Delta P = \frac{2\gamma \cos(\theta)}{r_p} \qquad (1)$$

for round holes. Figure 1 illustrates the relationship for a nonwetting fluid. The other parameter that has been adjusted in this work is wettability by applying coatings.

Experiments were performed with membranes fabricated as part of this project, as well as with commercially available polymeric membranes for comparison.

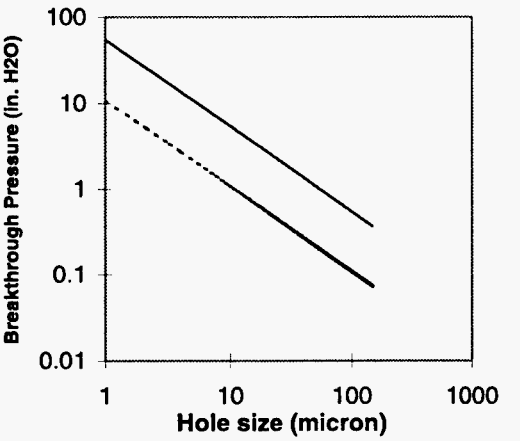

Figure 1. Breakthrough pressure round holes as a function of maximum hole size for interfacial tensions of 50 dyne/cm (—) and 10 dyne/cm (- - -). One fluid is assumed to be nonwetting giving a contact angle of zero.

Figure 2 illustrates how cyclohexane concentration in the effluent water stream agrees with numerical finite difference solutions of the convective-diffusion equation for different channel heights and flow rates. Results are shown for both the commercial membrane and a micro-machined membrane.

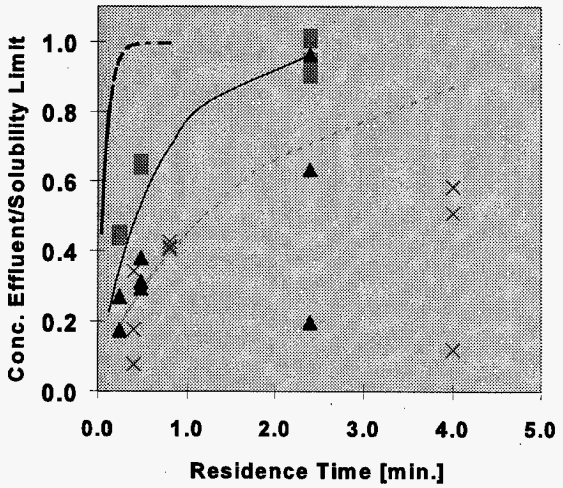

Figure 2. Cyclohexane concentration in water after contacting liquid cyclohexane in a microchemical contactor as a function of residence time for 300 micron channels using a micromachined contactor (■) and a commercial membrane (▲), and for 500 micron channels using a commercial membrane (X). Lines indicate numerical solution to the convective-diffusion equation for 100 micron channels (- - —), for 300 micron channels (——), and 500 micron channels (- - -).

In general, the agreement is very good at higher flows and shorter residence times. The possibility of cyclohexane vaporization losses during sample collection and system leaks increases at longer residence times. The micro-machined membrane performed comparably but not as well, most likely due to lower porosity and shorter active area for transport. Figure 2 also illustrates the importance of minimizing the film thicknesses in microchemical separations devices. Whereas, 300 to 500 micron channels require residence times of minutes for effective mass transfer, a 100 micron channel theoretically requires less than a minute.

Continued developments in contactor plate fabrication and testing are anticipated, including increased hole density (porosity) and decreased hole size, which will begin to realize the potential of the technology.

Publications and Presentations

W.E. TeGrotenhuis, R. Cameron, M.G. Butcher, P.M. Martin, and R.S. Wegeng. "Micro Channel Devices for Efficient Contacting of Liquids in Solvent Extraction." Presented at the 10th Symposium on Separation Science and Technology for Energy Applications, Gatlinburg, Tennessee, October, and to appear in *Separation Science and Technology*.

D.W. Matson, P.M. Martin, W.D. Bennett, D.C. Stewart, and J.W. Johnston. 1997. "Laser Micromachined Microchannel Solvent Separator." Presented at SPIE Conference on Micromachining and Microfabrication, Vol. 3223, Austin, Texas, September, and to appear in the proceedings.

Enhanced Mixing for Supercritical Fluid Oxidation - Phase Separations

Fadel F. Erian, David P. Pfund (Analytic Sciences and Engineering)

Study Control Number: PN94067/957

Project Description

The supercritical water oxidation process has great potential for use in the pretreatment of mixed wastes. The solubilities of organic compounds in supercritical water are enhanced, and those of inorganics are reduced relative to ambient water. Thus, the use of this solvent offers the possibility of simultaneously oxidizing organic and separating inorganic wastes. In addition, aggregation of solute and solvent molecules occurs which causes solubilities, and sometimes reaction rates, to be strong functions of pressure as well as temperature. Thus, control of pressure provides an additional way of manipulating the reaction. In a process that uses this chemistry, three conditions need to be fulfilled:

1. contaminants must be desorbed from the solid matrix into the supercritical solvent

2. oxidant and contaminant loaded solvent must be combined

3. fine, uniform suspension of solids must be maintained.

The last condition is necessary to allow the development of a continuous, steady-state process which allows no build-up of solids or reaction products. A continuous process is more desirable than a batch process in most cases involving large throughput because of the lower equipment cost and/or higher stream factor of the continuous process. A technology of mixing in supercritical fluid systems needs to be developed to meet these conditions. Due to the harsh environment of supercritical water, 374°C and 218 bar, extensive turbulence measurements in supercritical water would be difficult and prohibitively expensive. A valuable and practical supercritical fluid simulant used in this system was carbon dioxide.

The aim was to utilize turbulence and "chaos" to enhance mixing in vessels whose geometries are suited for a variety of industrial processes. In particular, we hoped to test the enhancement of hydrodynamically induced mixing between a supercritical fluid and an oxidant, as they are introduced independently into a specially designed observation vessel. The internals of the vessel are changeable and are designed (but could be changed as necessary) to enhance turbulent mixing. The mean velocity field was determined by particle image velocimetry, the turbulence field by laser-doppler velocimetry, and the degree of mixing was characterized by fluorescence spectroscopy. A test view cell was designed and constructed during FY 1996. The moving fluid—supercritical carbon dioxide, was examined through a series of vertical windows that are slotted on both sides of the vessel. Ultraviolet sheets of visible laser light penetrate these slots normal to the flow direction, allowing an end view camera at the end of the vessel to capture cross-sectional mixing patterns and other phenomena.

Technical Accomplishments

The extent of mixing of contaminant and oxidant streams will be determined using fluorescence spectroscopy. A fluorescent probe molecule will be dissolved in the carbon dioxide—a probe whose fluorescence is quenched by oxygen. A vertical sheet of light from an ultraviolet-enhanced argon ion laser will be used to excite the probe, thus providing a luminous cross section of the fluid. The cross section of the fluid will be viewed at right angle to the laser beam with a CCD-based camera. The second stream containing oxygen will be mixed with the carbon dioxide stream so that the oxygen can react with the probe and quench its fluorescence. Uniform, low fluorescence across the flow path will indicate good mixing between the carbon dioxide and oxygen streams.

Work Completed Prior to FY 1997

The requirements for the CO_2 fluid flow loop have been identified and the process design completed for an operating range which spans 0 to 5 gpm capacity, pressures between 300 and 2400 psig, and temperatures which can vary from ambient to 140°F. A high-pressure CO_2 pump, several heat exchangers, and all the necessary control valves, monitoring instrumentation, and process vessels were purchased.

Estimates were made of the expected luminescence from the experiment. From these estimates, specifications for the laser and the CCD camera were determined. The laser

system, laser optics, and the optical mounts were acquired. Several candidate probe species have been selected for batch tests and the necessary chemicals and equipment for such tests were acquired. Flow rates, temperatures, and pressures of oxygen and carbon dioxide were determined and equipment sizing was achieved. Contacts were made with Laboratory safety personnel to development the procedures for safe operation of the laser and of the high pressure oxygen system.

We have been able to acquire suitable laboratory space in the PDL-W high bay building. Utilities such as water, compressed air, and electrical power had to be brought to the location of the planned experimental facilities.

Based on the planned experimental program, a process design was completed for the pipe loop. An engineering firm was contracted to produce mechanical and electrical designs based on the supplied process design. Partial fabrication of the pipe loop facility has been carried out. This includes the structural fabrication of the support skids and most of the CO_2 system piping assembly. The control system software (Labview) is 90% complete.

Model development for turbulent mixing in supercritical fluids was started and some initial models have been derived based on dimensional reasoning. On the equipment side, funding limitations resulted in the partial completion of the CO_2 circuit and the postponement of the construction of the O_2 circuit. These changes necessitated some redesign of the CO_2 circuit to allow for a separate stream to be diverted from the single CO_2 source (pump outlet) thus bypassing the main stream. This separate CO_2 stream will be marked with color or fluorescing particles then injected back into the main stream within the test view cell. Sufficient pressure difference must be maintained in order to allow a jet-like flow to be introduced into the main stream. This scheme will allow us to obtain some preliminary mixing data by imaging the fluorescing particles during the jet mixing with the main stream, in the absence of O_2 as the separate and different fluid. Completed items are listed below.

1. CO_2 Section of the Flow Loop—Two code stamped pressure vessels for the CO_2 circuit have been fabricated and assembled into the flow loop. The redesign of the CO_2 circuit has been completed and all of the necessary piping, fittings, and valves required to complete the assembly of the redesigned circuit have been purchased.

2. High Pressure Test View Cell—Detailed process and mechanical design of the test view cell, which is the main test section of this facility, its fabrication, delivery, and the building of a suitable support stand have been completed successfully. This has been a major task which was done well and on time.

3. Setting and Testing of the Laser System—The laser system has been set, tested, and debugged. However, to test the fluorescent probes, actual CO_2 circulation is required. The optical system needs some additional components to work optimally.

4. Briefing Manual—A detailed design and operation manual has been started. This extensive document, when completed, will be indispensable for anyone who may, in the future, wish to use and operate this facility.

Work Completed in FY 1997

The following tasks were completed in FY 1997:

1. CO_2 Source to Test View Cell Connections—The processed CO_2 source from the skid was connected to the test view cell through two paths. One for the large capacity main flow and the second for the jet stream that contains the fluorescing particles. The jet stream can be introduced into the test view cell axially from its end flange, or diametrically from four different axial locations along the top of the high-pressure test view cell. Selecting particular inlet paths for the main flow, for the jet stream, and an exit path for the combined streams was achieved by a set of strategically located on/off valves.

2. Monitoring and Control Systems—Piping for the instrument air was installed and all control valves were connected to the compressed air source and were made operational. Also all monitoring instrumentation was powered, wired, and connected to input terminals at the analog-to-digital converter. The control system software (Labview) is 100% complete. A clear step-by-step procedure manual for the use of the Labview process control program has been written, reviewed, and archived (should be suitable for current and/or new future users of the system). The manual includes a description of the modules, data structure, inputs including guesses for the initial constants, outputs of the control system for the flow loop in preparation of a shake down test, and other useful features.

3. Optical System—All remaining components of the optical system have been acquired. The assembly and testing of the laser system and the associated optics including the newly purchased ten Sapphire windows and ten Pyrex windows have been completed. A laser beam containment housing has been designed to be built according to laser permit specifications for safety considerations. Very thin sheets of ultraviolet laser light can now be generated and introduced into the test view cell through the side slots.

4. Reports—A comprehensive report was written that contains a) the final design package which includes all system modifications, all the associated drawings, and the supporting software, and b) the Safe Operating Procedure manual for the supercritical fluid flow loop.

5. Material Acquisition—A small amount of additional funding was made available near the end of the fiscal year which allowed the purchase of nearly all the needed hardware to construct the O_2 piping.

Extension of Acid Hydrolysis for the Minimization of Biosludge

Andrew J. Schmidt, Rick J. Orth, Alan H. Zacher (Chemical Process Technologies)

Study Control Number: PN97043/1184

Project Description

The disposition of biosolids wastes has become a global problem of epic proportions. Biosolids wastes are generated from virtually all manufacturing industries and municipalities. The biotreatment of wastewater from both domestic and industrial sources is very effective in removing soluble organics. However the handling and subsequent disposal of biosludge resulting from the wastewater treatment plants is a difficult and costly part of the entire process. Biosludge, which is mostly water, has typically been disposed of in landfills, land farmed, or treated by incineration. As landfill space becomes limited and incineration becomes publicly unacceptable, alternative options for disposal/minimization of biosludge are being sought. Tests at PNNL with an acid hydrolysis process have demonstrated that the amount of biosolids requiring disposal may be reduced by as much as 90%.

This project will explore enhancements and alternatives to acid hydrolysis for minimization of biosolids. If acid addition could be eliminated or minimized, both capital and operating costs for the process could be decreased. With no acid, cheaper materials of construction could be used. Decreasing the operating temperature and pressure would also significantly reduce costs and perhaps allow for a simpler and safer system design. If costs are sufficiently reduced, this process could potentially become cost-effective for industrial and municipal wastewater treatment plants.

Technical Accomplishments

During FY 1997, a set of four sludges were assembled from various wastewater treatment facilities from across the nation. This included three biosludges and one API sludge that was obtained from a local refinery for oil/water emulsion breakdown testing. We subjected the biosludge materials to preliminary examination and handling, and developed screening criteria based upon expected processing capabilities of the standard wastewater treatment facility. Through this, we developed a standard testing regime designed to quickly screen process materials to determine the applicability of acid hydrolysis testing, and to examine the efficacy of treated materials.

Initially, rapid depressurization was identified as a potential tool for further dewatering of biosludge materials in conjunction with hydrolysis. However, recent experience in other sludge processing projects indicated that this process tended to lower the filterability of treated sludges, perhaps by reducing the particle size distribution and more quickly blinding the filters used in the solid/liquid separation. Thus, this process was not pursued at this time.

Biosludge No. 3 examined the use of low-toxicity metal catalysts. It was suspected that small dosages of metal ions could enhance the dewatering of the sludges under hydrolysis conditions. Testing indicated that metal catalyst alone was not sufficient for significant biosludge dewatering under hydrolysis conditions. It appeared that the addition of the metal catalyst to hydrothermal processing enhanced the ability of the sludge to retain water during filtration. Further testing with metal catalysts in conjunction with acids may be necessary to develop this idea.

We performed three tests with H_2O_2 on biosludge No. 2 with poor results. Use of H_2O_2 increased the filtered cake possibly due to particle size reduction. Thus, we elected to examine the effects of an oxidizing acid versus a much less oxidizing one. The results showed that the use of oxidizing acid may be breaking down organics within the sludge and releasing CO_2 in the offgas.

Results from the treated stream from hydrolysis with various acid tests yielded some interesting application points. Although certain acids were shown to be successful, residual acid was present in the treated stream, resulting in a possible low pH problem for downstream processing of the effluent, but with negligible offgas produced. Other acid testing, which was also shown to be successful at biosludge dewatering, yielded measurably less residual acid in the hydrolysis product stream while producing offgas. This suggests that in certain cases, the acid is partially oxidizing the organics in the biosludge and potentially breaking them down into smaller products. Our testing indicated that under certain conditions, the biosludge would agglomerate and form a slurry that was appreciably more difficult to separate after hydrolysis.

Conditions that could decrease filterability of the biosludges were noted as part of the experimental program. This reiterated the importance of developing and maintaining a database of biosludge types and sources along with successful acid hydrolysis dewatering approaches for each type.

An API refinery sludge was obtained for hydrolysis testing with a stable oil/water emulsion layer. This material was subjected to hydrolysis testing, however, testing yielded no significant reduction in the emulsion layer.

Presentations

R.J. Orth, A.J. Schmidt, and A.H. Zacher. 1997. "Receiving Water Baseline Metals Study and Biosludge Reuse/Minimization Options Evaluation." 1997 DOE National Petroleum Review Meeting, June 20, and WSPA, July 30.

R.J. Orth, A.J. Schmidt, and A.H. Zacher. 1997. "Acid Hydrolysis Results- Radford Wastewater Treatment Plant Biosludge." Radford Army Ammunition Plant, July.

Feasibility of Membrane-Plasma Reactor for Partial Oxidation

William O. Heath, Gary B. Josephson
Kenneth G. Rappe, and Annalee Y. Tonkovich (Environmental Technologies)

Study Control Number: PN97044/1185

Project Description

We investigated partial oxidation reactions in a gas-phase corona reactor (GPCR) for converting an alkane into an alcohol and a ketone. The GPCR technology uses gaseous electrical discharges (corona) in a packed bed of dielectric pellets to form a nonthermal plasma. A variety of active species are generated at low temperatures (typically below 100°C) within the plasma, including ions, radicals, and free electrons that are capable of initiating chemical reactions.

For this study, we used cyclohexane (C_6H_{12}) as the substrate for conversion to cyclohexanol ($C_6H_{10}OH$) and cyclohexanone ($C_6H_{10}O$). These compounds are used industrially (Tonkovich and Gerber 1995) to produce caprolactam and adipic acid, which are the principal feedstocks for nylon 6 and nylon 6/6. The partial oxidation of cyclohexane is presently conducted on a commercial scale using a liquid-phase process (Silva et al. 1991). In this process, reactions are typically carried out with soluble metal catalysts like organic cobalt (III) complexes (Chavez et al. 1996) with organic peroxides added as oxidants. Yields are low,[(a)] on the order of 2% to 5% to maintain high product selectivity. The primary driver for developing new synthesis routes is to increase yields to lower the cost of production (Cookson 1997).

Several groups have investigated nonthermal plasmas for driving synthesis reactions, including the conversion of cyclohexane to other products. These include the formation of alkyl amines (Zakharov-Nartsissov and Pilyugina 1969; Burleson and Yates 1970) from cyclohexane in the presence of ammonia, and bisnitrosocyclohexane and cyclohexanone oxime (Wagenknecht 1971) in the presence of nitric oxide. All of these studies were conducted using a silent discharge plasma (SDP), commonly used in ozone synthesis (Elliasson and Kogelschatz 1991). The GPCR differs from an SDP in that the discharge space in a GPCR is filled with dielectric pellets. The pellets amplify the electric field, enabling a volume filling plasma at large electrode spacings, and can influence reaction kinetics and presumably pathways through surface-mediated catalytic and sorption effects (Heath et al. 1994).

(a) Personal communication with A.K. Uriarte, Fibers Business Unit, Monsanto.

The partial oxidation of cyclohexane in a nonthermal plasma was studied extensively by Inoue et al. in the late 1950s using an SDP device with air as the oxygen source (Inoue and Sugino 1957). They reported molar yields of the combined product (cyclohexanol and cyclohexanone) up to 50% at an energy requirement of 26 kWhr/kg. Their work showed that the reactions are probably initiated by atomic oxygen formed in the discharge via dissociative electron impact. The overall reaction then proceeds by chain propagation and termination to form the ketone and alcohol products (Inoue 1954):

Initiation:

$$O_2 + e^- \rightarrow O + O + e^-$$

Propagation:

$$RH + O(+M) \rightarrow R\bullet + OH(+M)$$
$$RH + OH(+M) \rightarrow R\bullet + H_2O(+M)$$
$$R\bullet + O_2 \rightarrow ROO\bullet$$
$$ROO + RH \rightarrow ROOH + R\bullet$$

Termination:

$$O + O_2(+M) \rightarrow O_3(+M)$$
$$O + O(+M) \rightarrow O_2(+M)$$
$$2ROO\bullet \rightarrow ROH + RO + O_2$$

where R represents an alkane and M is a third body. The final products are thought to be formed via the Russell mechanism (Khursan et al. 1991). In this mechanism, two diperoxide radicals (ROO•) combine to form the cyclic tetroxide (ROOOOR) which decomposes to form the alcohol and ketone.

Technical Accomplishments

All experiments were performed using a small corona reactor as illustrated in Figure 1. The reactor consisted of a 25-mm quartz tube with a 1.5-mm wall thickness. A concentric 3-mm stainless steel rod served as the electrode connected to a 20-kV, variable frequency (60 to 600 Hz) alternating current power supply. A metal screen attached to the exterior of the quartz tube served as the ground electrode. For all tests, the length of the grounded outer

surface was fixed at 130 mm, establishing a reactor volume of 50 cm^3. Electrical power deposited within the reactor was measured using Lissajois figures (Manley 1944). For all tests, the power ranged from 3 to 10 W at applied voltages from 4 to 7 kV at 400 Hz.

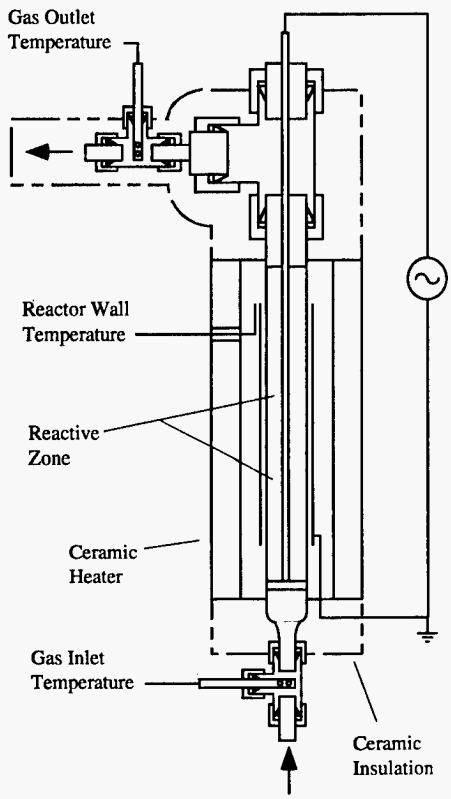

Figure 1. Reactor used for experiments.

The reactor was placed inside a ceramic oven to control the wall temperature and insulated to minimize heat losses. Fiber-optic probes were used to measure the temperature of the gas entering and exiting the reactor and the exterior reactor wall (near the top of the ground screen). The inlet and outlet gas temperatures were used to estimate the average temperature of the gas within the reactive zone (the reaction temperature).

All of the experiments were performed using a feed stream of cyclohexane at 3200 to 4500 ppmv in argon, with oxygen added in a molar ratio ranging from 1:1 to 1:10 (oxygen:cyclohexane). Mass flow controllers were used to adjust the flows of the test gases (argon, oxygen, and a mixture of cyclohexane-in-argon), and the total flow of the resulting feed gas into the bottom of the reactor. Cyclohexane vapor was introduced by bubbling argon through cyclohexane liquid. Feed rates varied from 0.4 to 10 slpm, corresponding to apparent residence times (reactor volume divided by flow) of 0.3 to 7.4 seconds. For all experiments, the reactor was operated at a pressure of 700 to 800 torr.

The gas streams entering and exiting the reactor were analyzed using an HP 5890 Series II gas chromatograph operated with a flame ionization detector (FID) and an HP 5970 mass spectrometer (MS). The FID was used to quantify cyclohexane, cyclohexanol, and cyclohexanone and the MS was used to quantify carbon dioxide and oxygen. All separations were achieved using a J&W 30-m DB Wax column with a 0.32-mm inside diameter. Stream compositions were sampled on-line using heated sample lines at a temperature of 50°C.

Figure 2 is a chromatogram showing the FID signal versus time for a typical sample of the reactor effluent during testing. As shown, the only major product peaks corresponded to cyclohexanone and cyclohexanol. Other minor peaks were assigned to cyclohexene (C_6H_{10}), pentenal ($C_5H_{10}O$), hexanal ($C_6H_{12}O$), 1,4- hexadiene (C_6H_{10}), and 2-cyclohexen-1-one (C_6H_8O) based on matching their fragmentation patterns to library compounds using the MS. Conversions and yields were determined on a molar basis (with concentrations in ppmv):

$$\%\ conversion = \frac{(C_6H_{12})_{in} - (C_6H_{12})_{out}}{(C_6H_{12})_{in}}\ 100$$

$$\%\ yield = \frac{(C_6H_{10}OH)_{out} + (C_6H_{10}O)_{out}}{(C_6H_{12})_{in}}\ 100$$

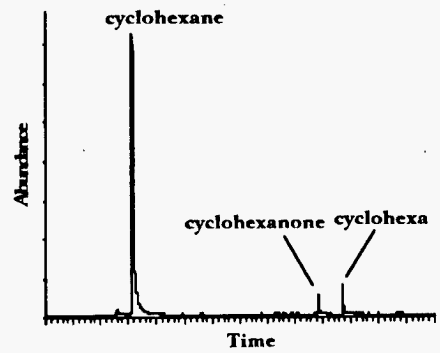

Figure 2. Typical effluent chromatogram.

Initial experiments were performed using 2-mm soda glass beads as the reactor packing to investigate the effect of oxygen ratio, reactor power, and flow rate on product yields. The results are plotted in Figure 3, as product yield versus energy density (in J/L) and oxygen ratio. The energy density is calculated as the reactor power divided by the feed flow rate, and is a measure of the total electrical energy dose per volume of feed gas. We found that yields were controlled by the energy density rather than power or

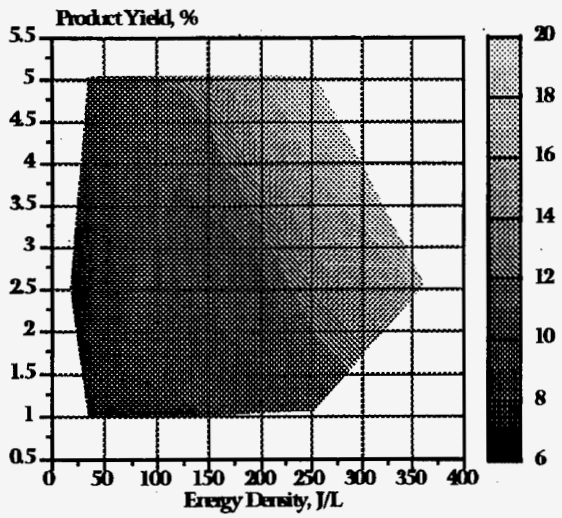

Figure 3. Yields on soda glass as a function of energy density and oxygen ratio.

flow rate individually. In these experiments, the total product yield varied from 6% to 20%, with the highest yields occurring at a 5:1 oxygen ratio and at energy densities from 250 to 350 J/L, both representing the upper ranges of those parameters. During these initial experiments, the reactor was operated without the ceramic oven. The reaction temperature (average of inlet and outlet gas temperatures) ranged from 25 to 30°C and the reactor wall from 40 to 70°C.

A second set of experiments was performed using the same soda glass packing to evaluate the effect of reaction temperature and reactor wall temperature (controlled using the ceramic oven) on product yields. These experiments were performed at an energy density of 85 J/L, a 2.5:1 oxygen ratio, and a reactor residence time of 0.7 second. The results are plotted in Figure 4 as product yield at two wall temperatures (100°C and 180°C) versus reaction temperature. Two data points from the initial experiments (without the oven) are also shown at a wall temperature of 50°C.

The data in Figure 4 show that the highest yields were produced at the lowest reaction temperatures. However, at constant reaction temperature, yields were found to increase as the wall temperature of the reactor was raised. We suspect that higher wall temperatures promoted more effective removal of cyclohexanol and cyclohexanone from the reactor because of their low volatilities (respective boiling points at 161 and 156°C) relative to cyclohexane (boiling point at 80.7°C). During these experiments, the temperature of the sample lines was raised to 120°C.

A third set of experiments was performed using cobalt (III) acetate deposited at 5 wt% on 3-mm gamma alumina beads as the reactor packing. Cobalt (III) is thought to act by stabilizing the tetroxide (Chavez et al. 1996).

In these experiments, the oxygen ratio was extended to a level of 10:1 and energy densities to 800 J/L. The results are summarized in the area plot in Figure 5. As shown, product yields increased to 40% during these experiments.

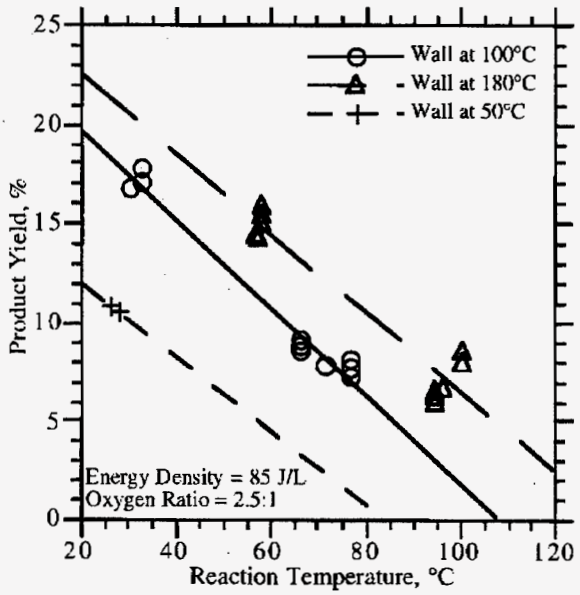

Figure 4. Effect of temperature on yield.

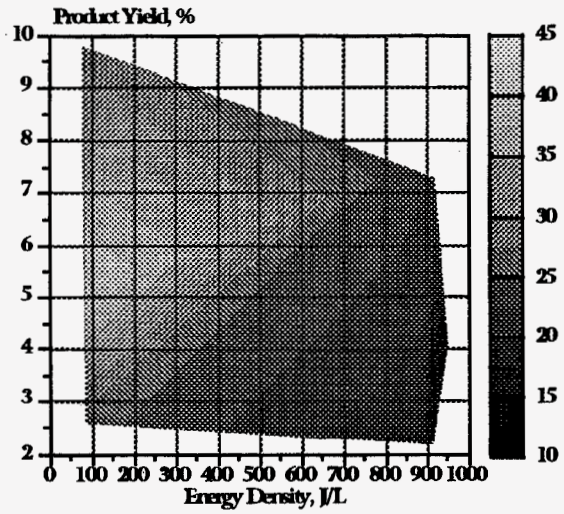

Figure 5. Yields on cobalt catalyst as a function of energy density and oxygen ratio.

An optimum oxygen ratio was finally observed, evidently between 4:1 and 7:1. This is illustrated in Figure 6 by plots of product yields versus oxygen ratio at a fixed energy density (85 J/L), reaction temperature (95°C), and wall temperature (110°C). Evidence for an optimum in energy density was also observed in that yields became greatly reduced at energy densities beyond 700 J/L. However, insufficient data in the range between 100 and 700 J/L

prevented an optimum energy density from being identified. Selected data from our experiments with both reactor packings are presented in Table 1.

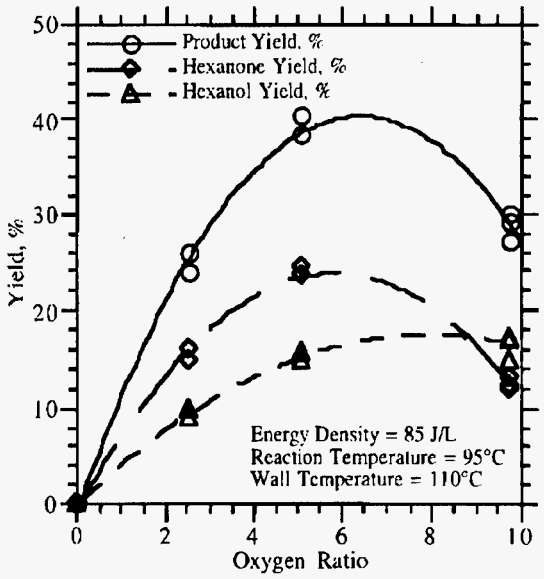

Figure 6. Effect of oxygen ratio on component yields at low energy on a cobalt catalyst.

Although yields during experiments with the cobalt (III) catalyst were high, we would surmise that the reaction conditions during those experiments were far from optimal. Data obtained using the soda glass beads suggest that higher yields would have been obtained by operating at lower reaction temperatures. (In Figure 4, yields were significantly higher at 30°C than at 95°C). Likewise, the data in Figure 3 suggest that yields would have been higher at an intermediate energy density of 250 to 350 J/L. It may thus be possible to increase yields under more optimum conditions, perhaps reaching the 50% yields reported by Inoue et al.

Conclusions and Recommendations

This project demonstrated the partial oxidation of an alkane in relatively high yields using a nonthermal plasma. We found that yields depended on a variety of experimental conditions, including power, flow, temperature, and oxygen ratio, as well as on the packing material used to support the plasma. In terms of energy requirement, we observed product yields on the order of 5 kWhr/kg, or roughly $0.10 per pound at an electrical unit cost of $0.05/kWhr. In addition to higher single-pass yields, this study showed that cyclohexane conversion can be accomplished in the gas phase for potentially simpler and less expensive separation of the products as liquids, and can use oxygen as a more cost-effective oxidant source than the organic peroxides or hydrogen peroxide now used in commercial liquid-phase processes.

Further work will be required to perform a mass balance on the reaction so as to rule out accumulation effects on product yields. We would also recommend additional experiments to determine whether the cobalt (or other catalyst) would require regeneration, to better identify conditions for optimum product and energy yields, to evaluate air and possibly other oxygen sources, and to probe scaling parameters.

Table 1. Summary of selected experimental data.

packing material	soda glass						cobalt on alumina			
cyclohexane inlet (ppm)	3470	3190	3316	3316	3286	3180	3219	3200	4542	3302
oxygen molar ratio	0.97	1.05	2.54	5.01	2.60	2.60	2.56	5.11	7.28	9.78
feed rate (slpm)	4.20	1.43	10.07	10.15	4.12	4.28	4.70	4.70	4.69	4.69
residence time (s)	0.71	2.08	0.29	0.29	0.72	0.69	0.63	0.63	0.63	0.63
reactor power (W)	3.05	6.04	9.41	5.97	5.94	5.91	6.07	6.2	6.17	5.85
energy density (J/L)	43.5	253.9	56.1	35.3	86.4	82.8	85.1	88.5	795.8	82.0
reaction temperature (°C)	25.2	25.9	31.6	27.9	32.8	100.4	96.4	96.3	64.6	93.5
wall temperature (°C)	37.5	57.3	50.9	41.8	86.1	187.6	109.7	110.9	130.7	111.6
cyclohexane (ppm)	2280	1458	1567	1985	2256	2252	2328	2241	441	2045
cyclohexanone (ppm)	94.4	57.6	38.0	103.4	185	89.7	519	782	672	391
cyclohexanol (ppm)	183.0	265.0	244.0	242.1	400	184	314	507	444	570
total conversion (%)	17.0	54.4	52.7	40.1	31.3	29.2	27.7	30.0	90.3	38.1
molar product yield (%)	8.0	10.1	8.5	10.4	17.8	8.6	25.9	40.3	24.6	29.1
energy yield (kwhr/kg)	9.8	49.1	12.4	6.4	9.2	18.9	6.4	4.3	44.9	5.4

References

J.C. Burleson and W.F. Yates. 1970. Manufacture of Alkyl Amines using a Silent Electric Discharge. U.S. Patent No. 3,518,178.

F.A. Chavez, C.V. Nguyen, M.M. Olmstead, and P.K. Mascharak. 1996. "Synthesis, Properties, and Structure of a Stable Cobalt (III) Alkyl Peroxide Complex and Its Role in the Oxidation of Cyclohexane." *Inorg. Chem.* Vol. 35, 6282-6291.

C. Cookson. 1997. "R&D--Combining Brainpower." *Chemical Week*, September 24, pp. 11-12.

B. Elliasson and U. Kogelschatz. 1991. "Modelling and Applications of Silent Discharge Plasmas." IEEE Transactions on Plasma Science, Vol. 19, No. 2, pp. 309-323.

W.O. Heath, S.E. Barlow, T.M. Bergsman, D.E. Lessor, T. Orlando, A. Peurrung, and R.R. Shah. 1994. "Development and Analysis of High-Energy Corona Process for Air Purification." PNL-SA-24432 S. Pacific Northwest Laboratory, Richland, Washington.

E. Inoue. 1954. "Reaction Mechanism of Slow Oxidation of Hydrocarbons by Silent Electric Discharge (Part 1) Main Oxidation Process of Cyclohexane." *J. Electrochem. Soc.*, Japan Vol. 22.

E. Inoue and K. Sugino. 1957. "Preparation of a Mixture of Cyclohexanol and Cyclohexanone from Cyclohexane and Air by Silent Electrical Discharge--a Large Scale Experiment Using a Pre-pilot Plant." *J. Electrochem. Soc.*, Japan Vol. 25, No. 2, E 16.

S.L. Khursan, V.S. Martem'yanov, and E.T. Denisov. 1991. "Mechanism of the Recombination of Peroxyl Radicals." *Kinetics and Catalysis* Vol. 31, No. 5 pt. 1, pp. 899-907.

T.C. Manley. 1944. "The Electrical Characteristics of the Ozonator Discharge." *Trans. Electrochem. Soc.*, Vol. 84, pp. 83-96.

L.J. Silva, M.A. Lilga, D.M. Camaioni, and L.J. Snowden. 1991. *Preliminary Economic Evaluation of the Alkox Process*. PNL-7807. Pacific Northwest Laboratory, Richland, Washington.

A.Y. Tonkovich and M.A. Gerber. 1995. *The Top 50 Commodity Chemicals: Impact of Catalytic Process Limitations on Energy, Environment, and Economics.* PNL-10684. Pacific Northwest Laboratory, Richland, Washington.

J.H. Wagenknecht. 1971. "Formation of Bisnitrosocyclohexane and Cyclohexanone Oxime by Silent Electric Discharge." *Ind. Eng. Chem. Prod. Res. Develop.*, Vol. 10, No. 2, 1971.

O.I. Zakharov-Nartsissov and N.G. Pilyugina. 1969. "The Reaction of Benzene, Toluene, Cyclohexane, and Cyclohexene with Ammonia in a Barrier Discharge." *Khimiya Vysokikh Energii*, Vol. 3, No. 3, pp. 267-268.

"Glow Discharge Plasma" Process

Gary B. Josephson (Process Technology)

Study Control Number: PN97047/1188

Project Description

Glow discharge plasma treatment of contaminants in wastewater is a nonthermal treatment process that has been shown in the laboratory to be effective on oxidizable materials, as well as materials which are not generally considered to oxidize. This project enabled the first step from the laboratory to actual practice by designing and constructing a first-of-a-kind continuous reactor that can be used to establish performance of this technology on particular contaminants and contaminant streams.

The objective of this project was to expand upon the proof-of-principle demonstrated in 1996 on another project, so that a small continuous flow glow discharge reactor could be designed and built to demonstrate the feasibility of a continuous process.

Background

Glow discharge plasma treatment of contaminants in wastewater is a nonthermal treatment process that has been shown to be effective on oxidizable materials as well as materials that are not generally considered oxidizable. Further development of the technology has been hindered by two significant knowledge gaps: 1) a method to scale up the technology from a laboratory phenomenon to a viable continuous process, and 2) the performance of any such scaleable process compared to existing technologies (initial laboratory results would need to be established). This project addressed the first of the principal knowledge gaps and enables addressing the second gap.

Earlier work at PNNL had demonstrated that high-voltage (1500 to 4000 V) alternating-current power could be applied to a quartz dielectric to form an electrical glow discharge. The discharge appeared similar to the glow discharge from a metal point electrode with direct-current voltage but could cover a larger area. This project extended that previous observation to design a prototype based upon a large-area, alternating-current glow discharge.

Technical Accomplishments

An operational glow discharge plasma prototype unit was designed and built, and initial performance tests on penta-chlorophenol were completed. A process model was developed to predict the performance of the unit. Results of the model compared favorably with the experimental data on pentachlorophenol.

The prototype unit is based upon a falling-film design to most closely approximate plug flow. Pictures of the unit, electrode assembly, and plasma in operation are shown in Figures 1, 2, and 3, respectively. Data from the initial performance tests are contained in Table 1. Figure 4 contains a plot of results from the process model for destruction of pentachlorophenol.

Based on this project, a viable scale-up method to apply glow discharge plasma in a continuous process has been demonstrated in a prototype apparatus. A process model based upon reaction kinetics and mass transfer can be used to estimate system performance. Several areas of further investigation have been identified, which can enhance the performance and improve the technology.

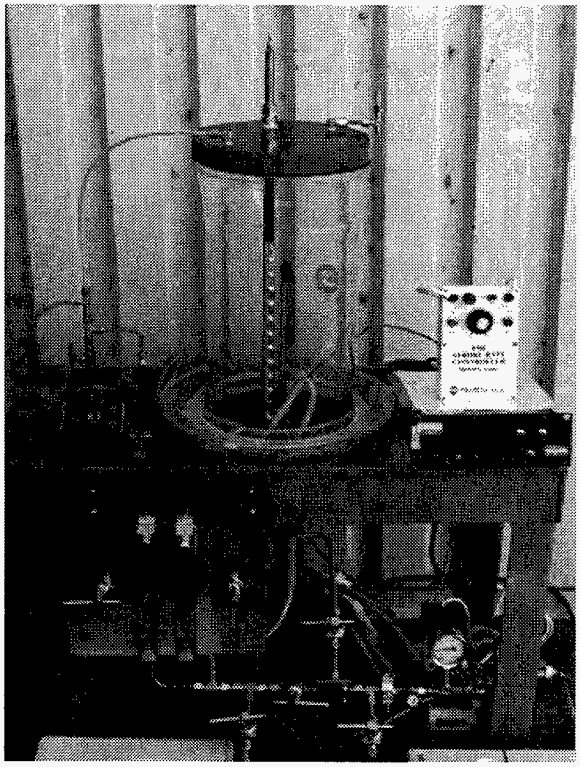

Figure 1. Glow discharge prototype falling-film reactor.

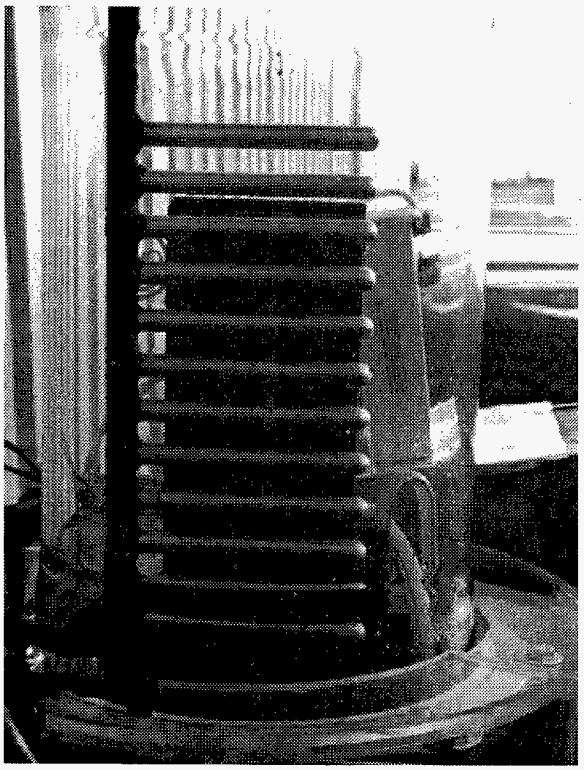

Figure 2. Electrode assembly.

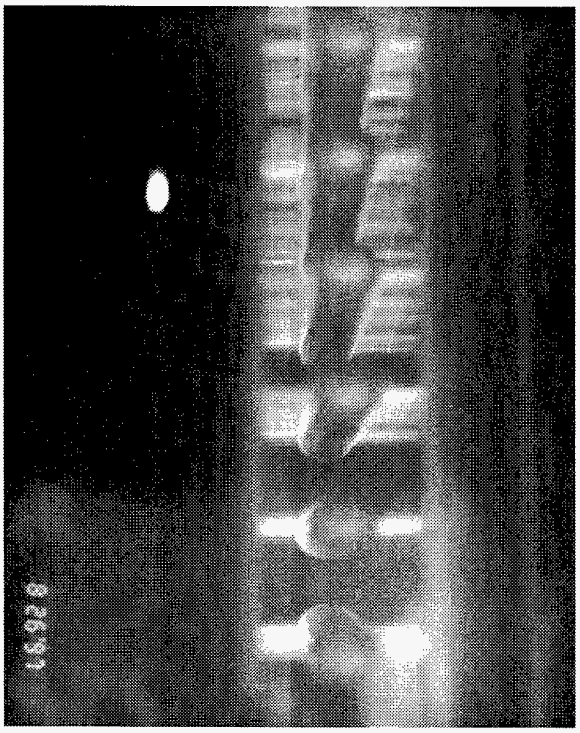

Figure 3. Glow discharge plasma.

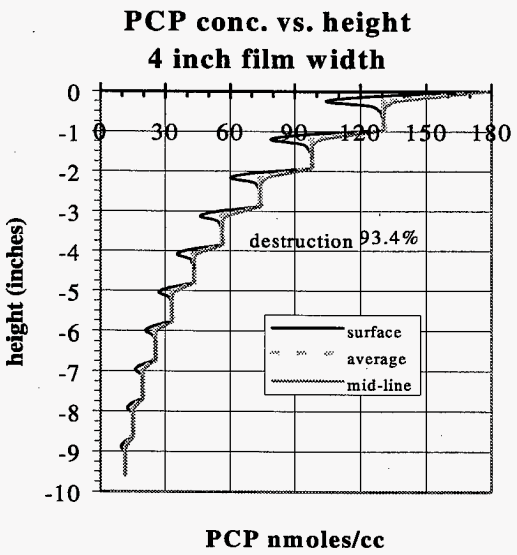

Figure 4. Process model plot of reactor performance.

Table 1. PCP tests on continuous prototype reactor.

Flow gals/hr	Pressure mm Hg	Hz	Current mA	Voltage kV	Power watts	PCP ppm	PCP destruct	kWh/ 1000 gals	Power $/1000 gals	Predicted Two-stage Destruction	Two-stage Power $/1000 gals
						initial 50.6					
1.9	41	467	5.1	3.2	11.4	19.3	0.62	5.9	$0.35	0.92	$0.71
1.1	36	466	5.2	3.1	10.9	18.6	0.63	9.9	$0.59	0.95	$1.19
0.55	37	467	5.2	3.2	10.9	13.4	0.73	19.8	$1.19	0.98	$2.37
						initial 18.2					
0.96	38	467	2.6	3.8	6.8	3.7	0.80	7.0	$0.42	0.99	$0.85
0.55	38	466	2.6	3.8	6.8	2.7	0.85	12.3	$0.74	1.00	$1.48
0.28	38	466	2.6	3.8	6.8	1.4	0.92	24.7	$1.48	1.00	$2.96
						@ 6 cents/kWh					

Hydrocarbon Processing with Microsystems

Annalee Y. Tonkovich, Charles J. Call (Environmental Technologies)

Study Control Number: PN97050/1191

Project Description

This project aims at developing and demonstrating integrated chemical process systems built on PNNL's microchannel technology. A key objective is to demonstrate the capability to fabricate and operate catalytic micromachined reactors and to integrate the reactor into a complete chemical process system consisting of separation, recycle, and monitoring and control. The target process is the production of hydrogen from methane. Components for these systems will be investigated and selectively developed for integration into a system.

Our objective is to demonstrate a chemical process system with integral reactor, product separation, and reactant recycle. The goal is to demonstrate a system that can be easily and cost-competitively scaled up. In FY 1997 we developed and demonstrated the fabrication of several components for such a system. Two systems under investigation are a methanol synthesis pant and a hydrocarbon to hydrogen gas conversion system. The chemistry employed by these systems has significant thermicity, and as such, selectivity and per-pass yields can be significantly improved with integrated microchannel heat exchangers. Micromachined reactors, heat exchangers, pumps, and valves are to be integrated into complete systems.

Background

Many industrially important reactions are carried out in packed catalyst beds in pressure vessels. The mechanical strength requirements of a reactor vessel are proportional to its diameter. Thus, a large (macro-sized) vessel requires more metal per unit of interior reactor volume. An array of microchannels assembled in the sheet architecture will require less metal per unit of processing. Additionally, thermal integration is readily achieved with microsystems, and demonstrated recently by PNNL in the performance of its contract with DARPA on an integrated microchannel combustor/evaporator. Thermal integration reduces the environmental impact of the technology, lowers operating costs, and improves product yields.

Technical Accomplishments

Scoping work was performed to evaluate partial oxidation reactions in microchemical reactors based on the concept of millisecond residence times. An attractive catalyst system was found to promote the production of synthesis gas (CO and H_2) from methane with high yields. An experimental methane conversion greater than 60%, a hydrogen selectivity near 50%, and a CO selectivity greater than 70% were obtained in an existing low temperature (~ 700°C) reactor system using a powder Rh-based catalyst. Performance trends were observed to increase with increasing temperature up to the reactor operating limit (700°C) (see Figures 1 and 2). Nonequilibrium chemistry is achieved in the microreactor even at low temperatures. Thermodynamics predict that coking will dominate the conversion products, but coke formation is slow relative to the fast initial synthesis gas production reactions and was not observed in the microreactor.

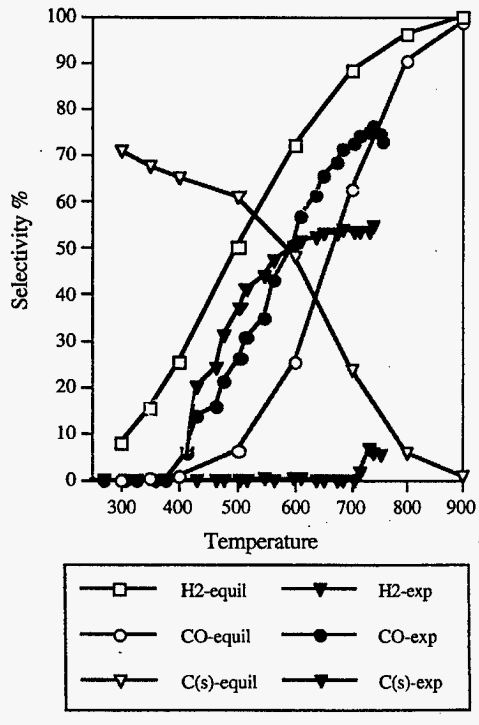

Figure 1. Methane partial oxidation to synthesis gas in a microchannel reactor: experimental versus equilibrium product selectivities.

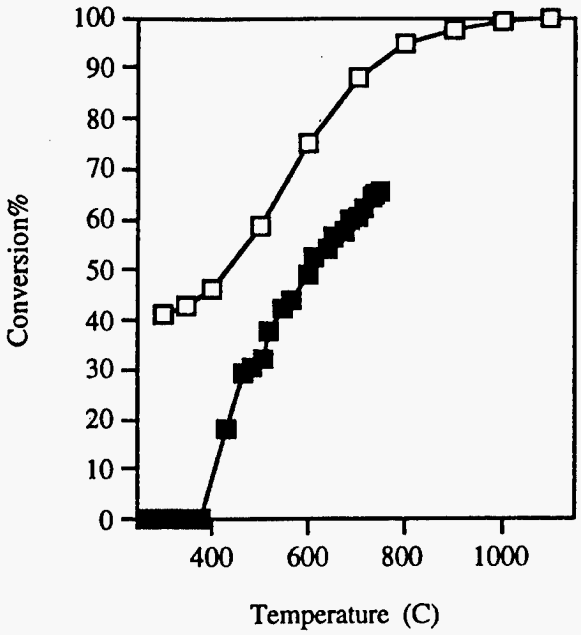

Figure 2. Methane partial oxidation to synthesis gas in a microchannel reactor: experimental versus equilibrium methane conversion.

Methanol decomposition and partial oxidation to synthesis gas were investigated. Coking is always observed on the Rh/Al_2O_3 catalyst during thermal decomposition, but can be retarded in the presence of 8 to 10 mol% O_2. Stable operation is observed for over 8 hours of testing. Initial microreactor experiments showed hydrogen yields near 52%. Additional catalyst investigations on new materials and fabrication methods showed the feasibility of achieving greater than 90% H_2 yields. Catalytic powders were used for all microreactor tests; powders and pellets promote unwanted series reactions (including combustion) inside the hot porous pellets.

Presentation

C.J. Call, A.Y. Tonkovich, M. Powell, and R. Wegeng. 1997. "Partial oxidation of methanol in a microreactor." Engineering Foundation Reactor Engineering for Sustainable Processes and Products conference held in Banff, Canada.

Integration of Advanced Technologies for Selective Anion Separation

Richard T. Hallen (Environmental Technologies)

Study Control Number: PN97058/1199

Project Description

This project performed the evaluation of advanced technologies for the separation of anions from process and wastewater streams. Specific target anions were identified and performance criteria determined to maximize the potential for deployment of the newly developed technologies. This included definition of specific product streams, compositions of target and competing ions, volumes/flow rates to be processed, process economics, and potential integration points within existing processes. This project provided process modeling capabilities for evaluation of various separations schemes and comparison to conventional technologies such as ion exchange. The result was the development of the most appropriate separation technology for the need.

Technical Accomplishments

Separation of anions from aqueous streams is a broad need across the DOE complex. Many of the anions, such as nitrate, are also a concern for agriculture and industry. PNNL staff worked together to collect waste stream composition data from DOE and industrial sources. DOE documentation, information from the Chemical Industry Environmental Technology Projects and the Center for Waste Reduction Technologies, and industrial site visits provided data to support the need for new and improved separation technologies for nitrate separation. A major industrial driver is the addition of nitrate to EPA's SARA list of reportable chemicals in 1995. Nitrate was 65% of the reported new water releases and most significant for the 28xx standard industry code (chemicals and allied products). A white paper focusing specifically on nitrate was prepared. The major competing technology for nitrate separation is ion exchange, which is currently not economically attractive because of low selectivity and production of secondary wastes.

SAMMS (Self-Assembled Monolayers on Mesoporous Supports) and ESIX (Electrically Switched Ion Exchange) are two new technologies developed at PNNL which were examined for selective separation of anions from aqueous streams. The major advantage is high selectivity obtainable by these technologies. Both technologies obtain selectivity through the careful selection of the separating material and/or immobilization of the correct functional group. The deployment and operation of these technologies are most similar to conventional ion exchange. The performance of these technologies can be modeled by conventional ion exchange theory and the models used for process scale-up.

Typical environmental separations require high selectivity because of low target ion concentration and the presence of competing ions. This is in contrast to many industrial process streams. Selectivity is not as great an issue as with environmental contaminates, and universal, high capacity separating agents are needed, preferably with higher capacity than conventional, cross-linked polystyrene ion exchange resins. For example, nitrate contamination in groundwater is usually around 50 ppm and nitrate concentration in industrial waste is in the percent range, 3% in wastewater from aniline manufacture. Both SAMMS and ESIX have upper limits for the economic removal of target ions. This is similar for conventional ion exchange, and is specific to the composition of the waste stream. The limit is generally in the hundreds of parts per million but there are special conditions which favor deployment for higher concentrated streams.

An economic evaluation of ESIX for application to removal of chloride from the electrostatic precipitator ash in a pulp and paper mill shows the need for cheaper electrode materials, such as carbon felt, and higher unit volume capacity. This is due to the large volume of high chloride material requiring treatment. At high concentration of contaminant, cycle times become too short to be practical or electrode surface area becomes too large (costly). The advantages of ESIX over conventional electrodialysis are primarily due to the increased selectivity, energy requirements are near equivalent on a basis of total deionization, 0.9 kWh/kg salt removed (as NaCl). Separation of radioactive elements (such as pertechnetate) using ESIX is attractive because of the high selectivity, low concentration in the waste stream, and reduction in secondary wastes.

Process modeling for evaluating separation technologies was obtained. This is needed to integrate and compare processing options and new separation technologies. Two commercial software packages were evaluated and final selection was completed.

Isolation and Use of Extremophilic Bacteria for the Treatment of High Nitrate and Sulfate Containing Wastes

Brent M. Peyton, Michael J. Truex, Melanie Mormile (Bioprocessing)
Margaret F. Romine (Environmental Microbiology)

Study Control Number: PN95049/1025

Project Description

The objective of this study was to develop a bioprocessing capability using extremophilic microorganisms for treating and reducing high nitrate and/or sulfate concentrations in industrial wastes. Tasks included enrichment, purification, and identification of extremophiles, and characterization of growth and metabolic capabilities and reaction kinetics in support of design and testing of bench- and pilot-scale biological treatment processes.

Technical Accomplishments

The development of the bioprocess for nitrate and sulfate degradation under harsh conditions included the isolation of extremophilic microorganisms, determining bioprocessing parameters, and demonstrating the bioprocess.

Two approaches were employed to obtain cultures of nitrate- and sulfate-reducing bacteria that can function under conditions of extreme pH and salinity. Bacterial strains having the desired properties were obtained through local, national, and international collaborative relationships. For example, halophilic nitrate-reducing bacteria were obtained from the University of Nevada at Las Vegas, Brookhaven National Laboratory, and from Northern Illinois University. Additionally, a halophilic sulfate-reducing bacterium was received from the University of Aarhus, Denmark. In addition to obtaining pure cultures, environmental samples from high saline and alkali environments were requested from researchers working with these systems. Environmental samples from evaporation ponds in Australia, the Great Salt Plains of Oklahoma, and the Dead Sea in Israel were requested and received. Samples were also collected from the Soap Lake area of Washington State. The environmental samples collected were enriched for consortia possessing desired traits, such as, denitrification ability at pH 9 and 25% salt concentration. Moreover, isolates were obtained from enrichment cultures that depleted both nitrate and nitrite. From the enrichments from the Soap Lake area, a total of 35 bacterial strains were isolated that can reduce nitrate. In addition, a mixed culture with sulfate-reducing activity at 25% salts was enriched from the Great Salt Plains.

One of the denitrifying strains, isolate 4a, was selected for 16s rDNA analysis and phenotypic characterization based on its ability to reduce both nitrate and nitrite at high salt concentrations and pH values. This isolate has been identified as a unique organism by its 16s RNA sequence when compared to other sequences deposited in the NCBI database. Isolate 4a is a squat rod-shape with an optimum temperature for growth at 40°C and growth possible at temperatures between 4°C and 50°C. The optimum pH for growth was 9.0 to 9.5 with growth occurring between pH 6 to 11. It was determined that isolate 4a can grow at NaCl concentrations of 0.2 to 4.5 M with optimum growth occurring at 1.5 M. Isolate 4a could grow with acetate, n-acetyl-D-glucosamine, ethanol, D(-) fructose, D(+) glucosamine, D-glucose, glycerol, lactate, maltose, pyruvate, sucrose, and yeast extract as carbon and electron donor sources. However, isolate 4a was unable to ferment glucose. Isolate 4a clustered phylogenetically within the gamma subclass of the *Proteobacteria* and is closely related to other alkaliphilic members of the *Halomonas-Deleya* branch. Isolate 4a has been tentatively named *Halomonas campusalis.*

While characterizing and determining the phylogeny of the isolated organisms is important, the collection of cultures was based on functional capability at various pH and salt conditions. The goal was to have the ability to select cultures for inoculation that meet treatment needs based on waste stream characteristics. Bioprocess demonstration tests were conducted on the nitrate reducing isolate 4a to quantify important parameters, such as the maximum specific growth rate, half-saturation coefficient, and biomass yield, for use in engineering design for the construction and operation of a bench-scale bioreactor process. Tests were run in batch culture.

Biological treatment of model ion exchange regeneration fluids and DOE tank wastes served as the target to help drive the research toward useful application and develop capabilities in this technical area of research. Ion exchange regeneration produces a brine containing high concentrations of nitrate and sulfate that is difficult and expensive to dispose and potentially can cause problems in downstream processing.

Nitrate-Reduction Kinetics

Previously, a nitrate-reducing consortium at a pH of 8.5 and 10% salinity, maintained in a continuous bioreactor, was able to reduce 520 mg/L nitrate to effluent concentrations of nitrate and nitrite of 17 and 10 mg/L, respectively with a non-optimized reactor residence time of 6 days. Batch cultures of nitrate-reducing bacteria from the Dead Sea at pH 7 and 25% salinity were able to reduce nitrate at a rate of 2.5 mg nitrate per milligram protein per day. These cultures were also able to reduce the resulting nitrite. While these rates are lower than typical mesophilic denitrification rates, mesophilic cultures cannot denitrify under these high salt conditions. However, the specific nitrate reduction rates obtained with isolate 4a at 12.5% NaCl and pH 9.0 compare favorably with those obtained with mesophilic bacteria. After growth under anaerobic conditions with nitrate as an electron acceptor, isolate 4a had specific nitrate reduction rates of 5.6 to 10.0 (mg NO_3—N(mg biomass day)$^{-1}$). Tests were run to determine denitrification rates as a function of various carbon sources. Figure 1 demonstrates nitrate reduction with lactate as the sole carbon source.

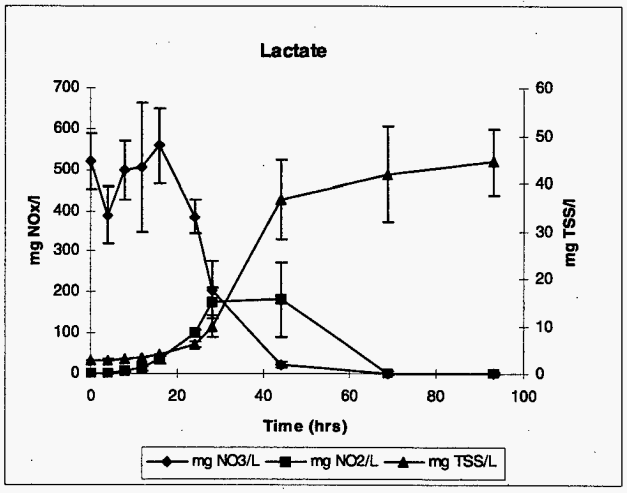

Figure 1. Nitrate reduction with lactate as the sole carbon source.

As regulations continue to tighten and landfills reach capacity, reducing biomass yield and sludge production will have a significant cost impact on industrial wastewater treatment systems. In addition to acquiring microorganisms that can treat high sulfate or nitrate containing wastewater, we have begun to investigate the potential for microbes to treat highly alkaline wastewater. A consortium that grows at pH 10 was enriched from samples obtained from Soap Lake. The objective of this work was to determine if organisms that thrive under extreme conditions would produce significantly less biomass than mesophilic bacteria. Industrial follow-on funding has been awarded to PNNL and WSU to pursue this research path.

Publications and Presentations

M.R. Mormile and B.M. Peyton. 1997. "Use of halophilic denitrifying bacteria for nitrate removal in high-salt solutions." Poster Presentation. *In Situ and On-Site Bioremediation Symposium Proceedings*, New Orleans, Louisiana, Battelle Press, 4(5), p. 265.

M.R. Mormile, M.F. Romine, and B.M. Peyton. 1997. "Use of halotolerant, alkaliphilic bacteria for nitrate removal in high-salt wastes." Poster Presentation. Gordon Research Conference on Applied and Environmental Microbiology. Newport, Rhode Island, August 17-22.

M.R. Mormile and B.M. Peyton. 1997. "Biological treatment of nitrate from ion exchange regeneration fluids." Invited Presentation. National Ground Water Association Convention and Exposition. Las Vegas, Nevada, September 4-6.

Lattice-Boltzmann Simulation of Microfluid Systems

David R. Rector, Judith M. Cuta (Environmental Technologies)

Study Control Number: PN97063/1204

Project Description

Lattice-Boltzmann simulation has the potential to model complex fluid dynamics problems in a size range that is currently not amenable to conventional simulation methods, and that is critically important to the development of compact energy and chemical systems. Therefore, we are developing a lattice-Boltzmann simulation code which takes into account microscale surface interactions that can strongly affect physical and chemical properties of the fluid, therefore substantially influencing heat, mass, and momentum transport in microfluidic systems. This code is based on the lattice-Boltzmann approach, which has the virtue of being applicable to a wide range of flow fields, including the representation of phase interfaces (e.g., solid-liquid, solid-gas, liquid-liquid, and liquid-gas interfaces). We will apply this simulation code to model a series of microfluid systems. The results will be used to characterize the importance of such parameters as wall surface effects, wettability, and phase interfaces on the fluid flow behavior of these systems.

Technical Accomplishments

This project is a three-year effort. The original schedule called for the completion of the base lattice-Boltzmann computer program in FY 1997, with the addition of fluid-fluid and fluid-solid interaction terms in FY 1998 and FY 1999. We completed the base program on schedule and have also made significant progress in incorporating the interaction terms during this fiscal year.

In the lattice-Boltzmann method, space is divided into a regular lattice. Each lattice point has an assigned set of velocity vectors with specified magnitudes and directions connecting the lattice point to neighboring lattice points. The total velocity and fluid density is defined by specifying the amount of fluid associated with each of the velocity vectors. The fluid distribution function evolves at each time step through a two-step procedure. The first step is to advance the fluid particles to the next lattice site along their directions of motion. The second step is to simulate particle collisions by relaxing the distribution toward an equilibrium distribution using a linear relaxation parameter. If the interaction rules are correctly designed to satisfy mass and momentum conservation, the result is a second-order solution of the Navier-Stokes equations.

A base lattice-Boltzmann computer program was developed during FY 1997. Features of the program include

- two- and three-dimensional modeling capability
- flexible geometry input which allows the specification of solid lattice sites. (The program automatically implements the solid boundary conditions based on the local geometry. This is especially useful for complex geometries.)
- multicomponent capability (which includes convection and diffusion)
- graphics output for visualization of program results (based on the Silicon Graphics AVS system).

Modeling a wide range of fluid systems requires a variety of flow boundary conditions. The boundary conditions currently available in the lattice-Boltzmann program include

- specified velocity or flow rate
- specified pressure
- stationary solid surfaces
- moving solid surfaces (shearing motion)
- periodic boundary.

One major advantage of the lattice-Boltzmann method is the ability to incorporate interaction potential terms into the equations of motion. A preliminary version of a lattice-Boltzmann program with both fluid-fluid and fluid-solid interaction potentials has been developed. A fluid-fluid interparticle potential is used to incorporate a non-ideal equation-of-state which represents both liquid and vapor phases. This allows a first-order phase transition to occur, forming individual bubbles or droplets (represented by hundreds of lattice points) which are free to move through the lattice grid. Using these interaction terms, liquid droplets have been simulated which are in equilibrium with the surrounding vapor. The interfacial region, where the fluid density transitions from liquid to vapor values, is usually only a couple of lattice sites in thickness and has an associated surface tension. A similar approach has also been demonstrated for simulating immiscible fluids. A fluid-solid interparticle potential is used to incorporate an external chemical potential that is a function of the material properties of the solid boundary. These terms are used to represent the wettability or non-wettability of a solid surface.

Ligand Design and Testing in Support of Metal Ion Separations

Brian M. Rapko (Process Chemistry)

Study Control Number: PN96040/107

Project Description

Research was performed into the synthesis, characterization, and coordination chemistry of novel, polydentate ligands for f-element complexation. In FY 1996, work focused on a compound containing both phosphine oxide and pyridine N-oxide functionality. In FY 1997, the focus shifted to new compounds containing mixed pyridine N-oxide/amide functionality.

Technical Accomplishments

Separation needs for a variety of metal ion species, with greatly different chemical properties, have been targeted for treatment across the DOE complex. These include toxic metals (Ag, As, Ba, Cd, Cr, Hg, Pb, and Se), actinides (U, Np, Pu, Am), noble metals (Pd, Pt, Rh), and other radionuclides (Cs, Sr, Ra, Tc). These metal contaminants occur in a number of matrices including concentrated chemical processing wastes (e.g., Hanford underground storage tanks), decommissioned reactors and equipment, soils, and groundwater.

Organic ligands with metal ion specificity are critical components in the development of selective solvent extraction and ion exchange processes. To be able to respond to the challenges in metal separations, it is crucial to continue developing capabilities in fundamental and applied metal-ligand chemistry. Key focus areas include ligand design, ligand synthesis and fabrication into engineered forms, the structural characterization of the ligand and its metal complexes, thermodynamics, and kinetics of metal ion complexation, and process optimization.

During FY 1997, work progressed along two fronts. The first involved elaborating on the research performed during FY 1996 to reach a point where the research could be published in peer reviewed journals and presented in open scientific forums. In addition, work began on the study of a new compound in which phosphine oxide functionality in the compound previously studied would be replaced with an amide, yielding a potential extractant which could now be incinerated after use to form only gaseous products and so generated no secondary wastes requiring long-term storage.

With regard to completing work in FY 1996 and the efforts devoted toward disseminating these research results, two public presentations were made and one manuscript was submitted and accepted for publication.

With regard to preparing a C, H, and N analogue to the 2,6-bis[(Diphenylphosphine oxide)methyl] pyridine N-oxide molecule studied in FY 1996, work was frustrated by the inability to isolate the needed precursor in this multistep synthesis, pyridine 2,6-diacetic acid. Eventually in situ conversion of the diacid to the di-methyl ester allowed isolation and purification of a suitable precursor to convert to the amide. Unfortunately, the methyl ester is sufficiently unreactive that all attempts to prepare the 2,6-bis[(Diphenyl amide)methyl] pyridine were unsuccessful. However, dihexylamine proved sufficiently nucleophilic that reaction of the methyl ester was successful and allowed the eventual preparation of 2,6-bis[(Dihexylamido)methyl] pyridine N-oxide. At this point resources were exhausted and experimental work was discontinued.

Publications and Presentations

L. Rao, Y. Xia, P.F. Martin, and B.M. Rapko. "Synergistic Extraction of Eu(III) and Am(III) by Thenoyltrifluoroacetone and Neutral Donor Extractants: (Carbamoylmethyl)phosphine oxide and 2,6-bis[(Diphenylphosphino)methyl]pyridine N,P,P-Trioxide." *Solvent Extraction and Ion Exchange* (accepted).

B.M. Rapko. 1997. "Extraction of f-Elements by Phosphine Oxide/Pyridine N-Oxide Ligands." Presented at the 213th American Chemical Society National Meeting, San Francisco, California, April 13-17.

L. Rao, Y. Xia, B.M. Rapko, P.F. Martin. 1997. "Synergistic Extraction of Eu(III) and Am(III) by Thenoyltrifluoroacetone and Neutral Donor Extractants." Presented at the 21st Annual Actinide Separations Conference, Aiken, South Carolina, June 23-26.

Micromachined Electrokinetic Converter for the Treatment of Tank Wastes

Joseph G. Birmingham, Johanes H. Sukamto, Charles J. Call
Robert S. Wegeng, Dean E. Kurath (Environmental Technologies)

Study Control Number: PN97073/1214

Project Description

The use of a micromachined electrokinetic converter (MEC) with a moving ion-exchange membrane to remove cesium and other compounds was the focus of this project. The MEC pulls a strip of an ion exchange membrane through microchannels where it selectively removes cesium and transports it to a regeneration sheet via pulleys. The membrane is pulled through the regeneration micromachined sheet where the cesium is exchanged and the replenished ion-exchange material is returned to treat the tank waste. The pumping of the liquid is accomplished electrokinetically taking advantage of the conductive nature of the material and evidence exists for the augmentation of separation of certain materials under these conditions (Angrist 1982). Although electrokinetic pumping fails for highly conductive solutions, this Debye shielding effect is mimimized due to the small distances between the electrodes of the electrochemical cell and the membrane material. Both the electrokinetic pumping and the entrainment of liquid by the membrane material will serve to move tank waste material through the MEC. The anticipation of the successful incorporation of cobalt dicarbollide (or similar derivatives) into polymers to produce a material with the benefits of conventional ion-exchange resins facilitates the development of the MEC system (Mason and Kinkead 1994). This MEC system is configured in a similar fashion to a Van De Graff generator where the objective is to transport cesium and other compounds instead of electrical charges.

The electrokinetic methods involve the separation of compounds wherein the current is carried by the separating species. Thus, charged species are moved through a fluid phase preferentially. Several researchers have been exploring the removal of heavy metals, including radionuclides from groundwater, by electrokinetic methods. An electrokinetic converter imposes an electric field upon a flowing fluid in a fine capillary tube (or for a microchannel) and electrical power is directly converted into pumping power. One of the theories used to explain the electrokinetic effects in a fluid electrolyte is the selective ion absorption on the tube wall which results in a net charge density in the bulk fluid (Angrist 1982). This phenomena could be utilized for the selective ion removal of cesium from a stream laden with sodium. Surprisingly, it is predicted that the conductivity of sodium augments the pumping rate. At first glance, the electrokinetic pumping should not be effective due to the highly conductive nature of the tank waste. The shielding of the charges described as the Debye effect should be minimized due to the proximity of the electrodes of the electrochemical cell and the membrane material being pulled through the MEC system. Consequently, the sodium reduces the pressure drop in the microchannel. It should be understood that the pumping of tank waste through the MEC is augmented by the electrokinetic effect and the entrainment of the tank waste by the moving membrane. In summation, the electrical driving force combines with a chemical driving force to synergistic separate compounds uniquely in a micromachined electrokinetic converter.

The selection of the ion-exchange material will be crucial. The membrane materials that are usually considered for cesium removal are brittle. Researchers at Los Alamos (Mason and Kinkead 1994) are incorporating cobalt dicarbollide (or its similar derivatives) into polymers to produce the benefits of conventional ion-exchange resins. Cobalt dicarbollide has been grafted onto a variety of polymers, including polystyrene and polybenzimidole (PBI). The development of appropriate polymeric materials suitable for this belt approach encourages the development of the MEC.

One concern with the microchannel approach is the possibility of clogging or occluding the passageways. Upstream from the MEC, a dielectric filter will be placed (Acar and Alshawabkeh 1993). A dielectric filter places a high voltage electric field upon a bed packed with a dielectric packing. The dielectric filter removes submicron particulate from a flowing fluid. The filter is easily cleaned by turning off the field and backflushing. The effectiveness of the filter is directly related to the dielectric constant of the packing in the liquid phase. Materials such as titanates that have a higher dielectric constant would have an advantage.

Technical Accomplishments

The objective of the work was to design, fabricate, and test a micromachined electrokinetic converter (MEC) system for the removal of cesium and other materials using a belt system of ion-exchange materials. The Hanford waste (with the large particulates removed) would be passed through microchannels where an ion-exchange membrane material would be pulled through the MEC system. The cesium would be selectively removed and the ion-exchange material would be regenerated in the sheet above (Mason and Kinkead 1994). This simple pulley system would maintain recirculation rates that are dictated by the amount of cesium found in the effluent of the Hanford wastes and is shown in Figure 1.

The scope of this project is to quickly bring the MEC system to a testing condition. The first year will involve the design and fabrication of the MEC, and the selection of ion-exchange materials for the cesium removal. The design of the MEC must allow the electrokinetic pumping capability to be realized.

The primary tasks completed in FY 1997 included the following:

- *Design of the MEC.* The microchannels were selected to allow the passage of an ion exchange membranes. The electrodes were configured to test the electrodeposition, precipitation, and ion exchange techniques for the retention of cesium.

- *Fabrication of the MEC.* The vacuum deposition techniques used for the microplasma reactor fabrication were applied to the micromachined electrokinetic converter. A singular test unit was made to test the initial ion exchange materials.

- *Test Stand Fabrication.* The test stand was designed to accommodate the hot cell requirements. The efficiency of the removal of cesium was determined by ICP and sample collection was designed into the test apparatus. At this point, the project funding was canceled. Initital testing of the MEC, which was the next step, was not accomplished.

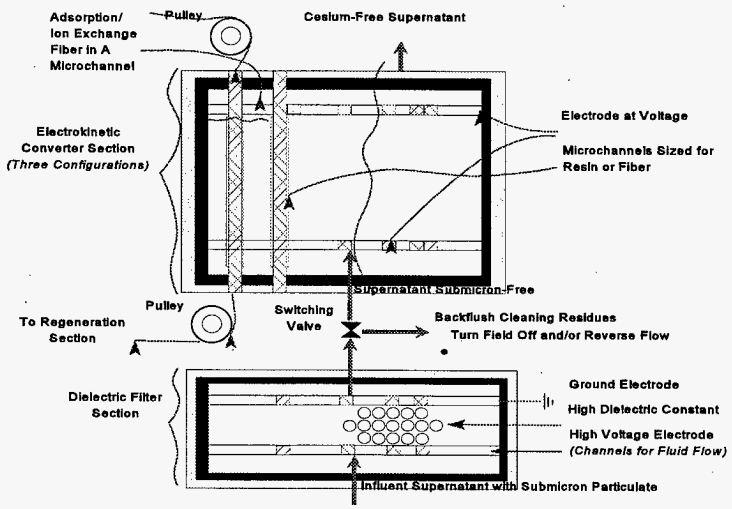

Figure 1. Micromachined electrokinetic convertor system schematic.

References

Y.B. Acar and A.N. Alshawabkeh. 1993. "Principles of Electrokinetic Remediation." *Envir. Sci. Technol.*, 27 #13.

S.A. Angrist. 1982. *Direct Energy Conversion*, 4th ed. Allyn & Bacon, Boston.

C.F.V. Mason and S.A. Kinkead. 1994. *Cobalt (III) Dicarbollide. Developments in the Chemistry and Process Design for this Potential Cs-137 and Sr-90 Waste Extraction Agent Since 1989.* LA-UR-94-51, Los Alamos National Laboratory, Los Alamos, New Mexico.

Micromachined Fuel Cell Systems

Gautam Pillay, Joseph G. Birmingham (Process Technology)

Study Control Number: PN96047/1114

Project Description

The focus of this effort has been to design and test a micromachined device that will be used for detection and analysis of specific components of high-level waste off-gases and gases present in the head spaces of underground storage tanks. These gases include hydrogen, ammonia, and trace organics. The objective is to produce a compact gas analysis system that can detect these gases from approximately 10 ppm to 30,000 ppm. In FY 1997, efforts focused on studying the feasibility of using an ammonia fuel cell as an ammonia sensor and a compact power generator (10 W). All data presented below were obtained using an alkaline fuel cell.

Technical Accomplishments

A compact alkaline fuel cell fuel cell was constructed. The projected area of each electrode was 21 mm^2. Commercial gas diffusion electrodes loaded with platinum (0.40 to 0.50 mg/cm^2) were used (Electrosynthesis Company Incorporated). Both the anode and the cathode were made of the same material. A schematic of the alkaline fuel cell is shown in Figure 1.

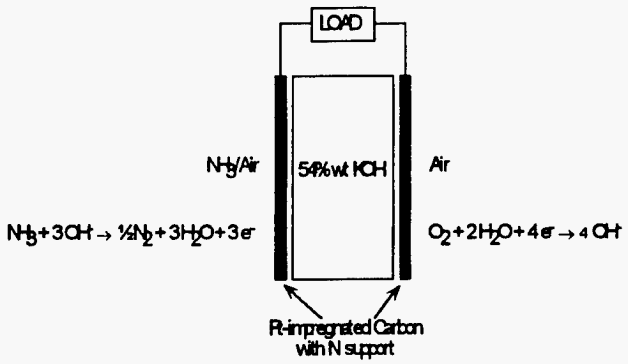

Figure 1. Schematic of alkaline fuel cell.

The difference in the Gibbs free energy of the two reactions shown results in the passage of current through and a potential difference across the load resistance. The measured current, voltage, or power is the basis for using the alkaline fuel cell as an ammonia sensor. The relevant parameters to consider in assessing the feasibility of the alkaline fuel cell as an NH_3 sensor are

- flow rate of air in the air side
- flow rate of the gas in the NH_3/air side
- the concentration of NH_3
- the temperature
- the value of the load resistance.

For this project, the air and gas flow rates were fixed at 80 mL/min since this was the maximum flow rate for the gas mixing system used. Slower flow rates are expected to reduce performance. For the duration of typical experiments carried out for this project, the operating temperature was found to remain relatively constant. It should be noted, however, for long-term operation of the sensor, the ability to control the temperature is potentially important. The two remaining parameters are the NH_3 concentration and the load resistance value. The effects of these two parameters on the signal strength, response time, and recovery time were examined.

NH_3 concentration in the range of 100 to 30,000 ppm was used. Lower NH_3 concentration resulted in signals that were not distinguishable from the background noise. The load resistance used was in the range of 100 to 4,700 ohms. In Figure 2, the effect of the load resistance value is shown for an inlet NH_3 concentration of 1000 ppm. The data shown clearly suggest that a higher load resistance leads to higher sensitivity. The signal strength for different inlet NH_3 concentrations is shown in Figure 3. As expected, larger signals are observed for higher NH_3 concentrations. Finally, the effects of the load resistance value on the respond and recovery times are shown in Figure 4. The results clearly show that lower load resistance values lead to faster respond and recovery times. In summary, higher NH_3 concentrations lead to larger signals; for a fixed NH_3 concentration, a larger load resistance leads to a higher signal (i.e., higher signal-to-noise ratio), but it also leads to longer respond and recovery times.

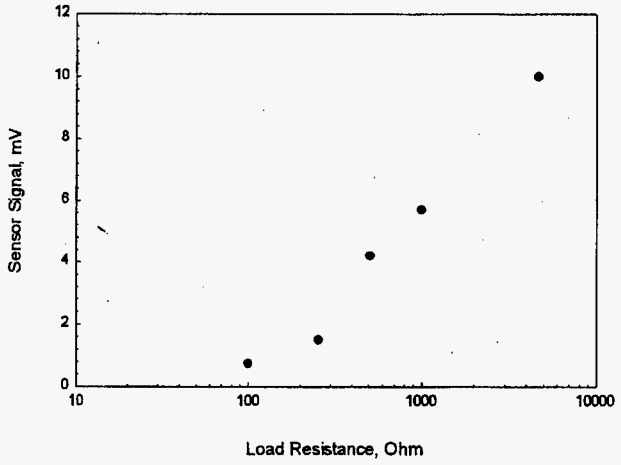

Figure 2. Sensor signal for various load resistances for 1,000 ppm NH_3.

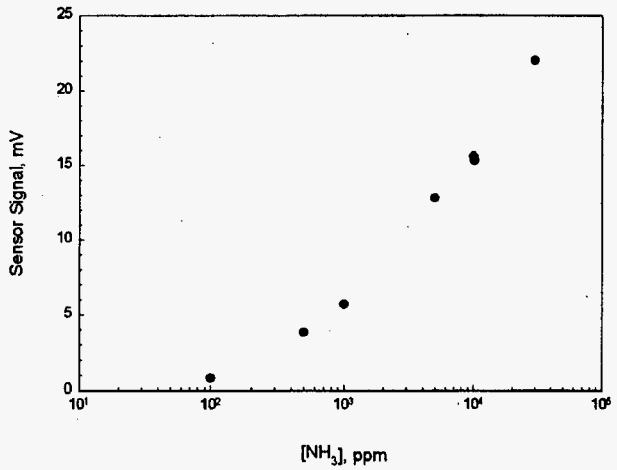

Figure 3. Sensor signal for various NH_3 concentrations using 1 k-ohm load.

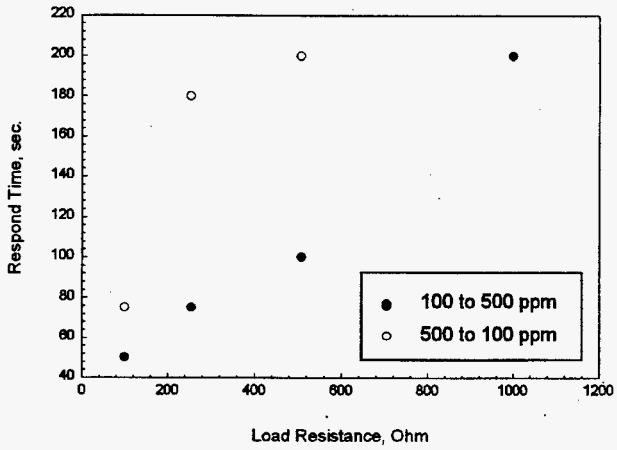

Figure 4. Respond time for various load resistances with concentration switching between two values.

Mixed Waste Treatment with Iron Reducing Bacteria

Michael J. Truex (Process Technology)

Study Control Number: PN96049/1116

Project Description

The goal of this project is to examine the use of sulfate reducing bacteria for combined treatment of metals/radionuclides and chlorinated organics. The work is based on the premise that through hydrogen sulfide produced by the bacteria or through direct reduction via the sulfate reducing bacteria electron transport system, metals and radionuclides can be immobilized in sediments such that remobilization occurs at a slow rate. If the rate of remobilization is slow enough, then immobilization may be accepted as a technique for in situ treatment of some metals and radionuclides. Further, the ability to dechlorinate contaminants such as PCE during or subsequent to metals/radionuclide immobilization is possible under the anaerobic conditions created during metals immobilization. Thus, mixed plumes may be treatable in situ under sulfate reduction conditions. Experiments consist of microcosm tests to examine the stability of immobilized metals, the ability to induce PCE dechlorination during or subsequent to metals immobilization, and to determine the role of specific sediment minerals in these processes.

Technical Accomplishments

To date, microcosm tests have been conducted to examine precipitation of copper and dechlorination of PCE under sulfate reduction conditions. Sediments and growth media were sealed in serum bottles and spiked with 100 ppm copper and 1 ppm PCE. Sulfate reduction was successfully induced resulting in the precipitation of copper within 20 days. Subsequent sampling over the next 6 months showed a decrease in PCE concentration and an increase in TCE and DCE concentrations relative to controls. TCE and DCE are microbial dechlorination intermediates for PCE.

The stability of the precipitated copper was examined in selected treatments by resuspending the sediments in aerated distilled water to create a concentration driving force for partitioning of copper back to the dissolved phase and to provide an oxidizing environment to challenge the sulfide materials in the sediments. In these tests, some sulfide was oxidized and appeared in the aqueous phase as sulfate. The amount of sulfide oxidized was much less than the amount in the sediment and only a small portion of the available oxygen was consumed. The rate of sulfide oxidation decreased to one-tenth of the initial rate after about 2 months. No copper (always below detection limits) was released into the water. In comparison, controls without SRB-induced precipitation quickly released copper back into the aqueous phase.

The results of this study suggest that under sulfate reduction conditions, the sulfide precipitates form in such a way that the metal is tightly held within the precipitate and the sulfide materials are resistant to oxidation. Additionally, it was shown that the conditions used to precipitate metals are conducive to subsequent PCE dechlorination.

Molecular Design of Agents for Selective Anion Separation

Gregg J. Lumetta, Bruce J. Palmer, S. A. Bryan, Glen E. Fryxell, Timothy L. Hubler, John H. Sukamto (Environmental Technologies)

Study Control Number: PN97075/1216

Project Description

The objective of this project is to design molecular species that are capable of selectively binding specific anions. A concerted, theoretical/experimental approach has been adopted to achieve this objective. To avoid an empirical "shotgun" approach to design anion separating agents, molecular modeling is being used to examine structures and help screen potential (anion separations) agents. Using the modeling results and information from the literature as a guide, specific anion separation agents were chosen for synthesis and testing. To focus these studies, a basis set of anions was chosen; this consisted of chloride, nitrate, chromate, and perrhenate. These represent spherical (chloride), trigonal planar (nitrate), and tetrahedral geometries (chromate and perrhenate). Except for chloride, all of these anions are of concern from an environmental standpoint. Perrhenate was chosen as a nonradioactive surrogate for pertechnetate. Because it is often present as a competing ion, sulfate was considered as well.

Technical Accomplishments

Modeling of potential anion ligands has primarily been restricted to examining the three-dimensional structure of ligands in the gas phase. The AMBER molecular simulation package has been used for the modeling. Most of the parameters for the molecular potential functions have been obtained from the PARM91 force field. Because this force field was primarily designed to model proteins, it had to be supplemented to handle all the ligands investigated as part of this task. The anion potentials were obtained from the literature and most of the other parameters were obtained by mapping the values from bonds or angles with similar properties to the bonds and angles that were not already represented in the PARM91 force field. For a few terms in the potentials, the parameters were developed from scratch based on experimental numbers or values obtained from electronic structure calculations. Partial charges for the atoms were developed by comparing structures in the ligands to amino acids for which partial charge distributions have already been developed. The ligand force fields developed using this approach are crude but are expected to be good enough to accurately represent three-dimensional structures and to pick out large changes in the energetics of the system.

The strategy for modeling was to look for compounds with a charged site or sites that would be electrically neutral when forming the complex with the anion and that formed numerous hydrogen bonding contacts with the anion. Restricting the size of the binding site using steric effects was also investigated. Over 30 compounds have been examined. The minimum energy structures of these compounds in the presence of anions were computed. These structures were then examined to see if the anions were forming a large number of contacts with potential anchor points and to see if a large amount of strain or distortion of the binding site appeared to be associated with forming the anion-ligand complex. Several of the compounds gave structures for the ligand-anion complex that appeared to be promising, these compounds were then synthesized in the lab for further study.

The synthesis efforts focused on making the appropriately functionalized macrocycles that modeling suggested would bind anions of specific shape and charge. Incorporation of a method for switching the anion-binding capability on and off also is desired. The synthesis of nine functionalized macrocycles was completed this year. The crystal structure of one has been determined and matches quite well to the predicted structure.

The functionalized macrocyclic compounds were examined experimentally to determine the extent to which anions bind to the potential anion separating agents. Cyclic voltametry was used to probe anion binding to the organometallic derivatives. Potentiometry and solution conductivity were used to evaluated anion binding to the amine derivatives.

Electrochemical studies were performed using an EG&G 273A potentiostat/galvanostat control using the EG&G 270 software. The reference electrode used was an SCE. Both the working and counter electrodes were platinum. The potential was scanned between -200 mV (SCE) and 1300 mV (SCE) at 100 mV/sec. Since the length of the Pt working electrode immersed in the solution was not easily

controlled, the absolute current magnitude cannot be used for quantitative comparison. Dichloromethane solvent with 0.1 M tetrabutylammonium tetrafluoroborate (TBAT) as the supporting electrolyte was used for all experiments. The nitrate source was 0.1 M tetrabutylammonium nitrate (TBAN) and the chloride source was 0.1 M tetrabutylammonium chloride (TBAC). The concentrations of anion agent were 0.001 M.

Comparison of the anion agent CV with the background CVs clearly show the distinct oxidation and reduction peaks of the functional group. Since the reduced form of functional group compound should be less dependent on the identity of anions in solutions, attention was focused on the cathodic peak. The CV results suggest that the selectivity compounds examined are in the order of $Cl^- > NO_3^- > BF_4^-$. This was confirmed by other studies.

Potentiometry is a classic method for probing pH-sensitive reactions. Combination pH electrodes are generally used for this purpose. Because some of the macrocyclic compounds developed are expected to have limited aqueous solubility, a nonaqueous solvent is required for these studies. This presented some complications in experimental design. Initially, acetonitrile was chosen as the solvent. The Ross® combination pH electrode used in this study responded adequately to changes in $[H^+]$, but the response was erratic. The erratic response was traced to the fact that the electrode filling solution was being transported across the ceramic reference junction into the reaction mixture. This problem was vitiated by using a 50:50 (vol:vol) mixture of acetonitrile and water as solvent. Initial screening of this method was done using a noncyclic analog of the compounds to be tested. The results indicated that potentiometry should be a useful method for determining anion selectivities for these compounds.

As an alternative, solution conductivity is also being investigated as a method to determine anion binding constants. For these measurements, a series of RNH_3X (RNH_2 = p-toluidine, and $X = Cl^-$ or NO_3^-) solutions were prepared in acetonitrile/water (9:1). These solutions were prepared by mixing one molar equivalent of HX with p-toluidine in acetonitrile and adding enough water to give 10% water in the solution. The specific conductance (L) of each solution was measured at 25 °C. The specific conductance values were converted to equivalent conductance (Λ) values by applying the formula $\Lambda = 1000*L/c$, where c is the total concentration of p-toluidine. Plotting Λ versus the square root of c, and extrapolating to c = 0, yields the molar conductance Λ_0. For sufficiently dilute solutions, the degree of dissociation is given by $\alpha = \Lambda/\Lambda_0$, and the equilibrium constant for the dissociation reaction in terms of concentration is defined as

$$Kc = c \cdot \alpha^2/(1-\alpha)$$

To get the true thermodynamic equilibrium constant, K_c is plotted against the square root of $\alpha \cdot c$, and the resulting plot is extrapolated to infinite dilution to yield the thermodynamic equilibrium constant. Again, initial screening of this method was done using a noncyclic analog of the compounds to be tested. The results indicated that conductivity should be a useful method for determining anion selectivities. This technique will be evaluated further with other functional groups.

Novel Photocatalytic Reactor Technology

Charles J. Call, Gita Golcar (Chemical Separation and Slurry Process)
John H. Sukamto, Joseph G. Birmingham (Electrical and Chemical Process)

Study Control Number: PN97081/1222

Project Description

Novel reactor design and fabrication processes are required to improve the economic viability of photoelectrochemical oxidations of organic pollutants dissolved in water. Further, photoelectrocatalysis has not been exploited for its potential for reduction of pollutants, such as chlorinated solvents. Also, synthesis of value-added chemicals from waste or feedstocks via photoelectrocatalysis (via partial oxidation or reduction) in very short residence time reactors has not been investigated. This work focused on the demonstration of reactor designs that are capable of achieving efficient photon use, compactness, uniform photon distribution, and short residence time. The research initially focused on oxidation and reduction of trichloroethylene (TCE), a compound that occurs frequently in wastewater streams in numerous industries and in groundwater at DOE sites including Hanford.

Our objective was to develop a novel reactor design/ architecture for photoelectrochemical processing. This reactor technology addresses the three critical problems that currently plague existing technology: cost-competitive scale-up, catalyst materials stability, and quantum efficiency. Quantum efficiency is a measure of the percentage of useful reactions that result from a given number of photons. The new technology resolves these issues through the development of an alternative configuration—the "sheet" architecture. This technology is readily scalable and provides for uniform light distribution. Photons can be generated at an acceptably low cost (5 cents/mol), but typical quantum efficiencies for existing reactors are 10^{-2} to 10^{-4}. The project addressed low-cost fabrication in concert with existing fabrication research capabilities and efforts at PNNL. We investigated photoelectrochemical reaction kinetics, catalysts, and reactor designs that accommodate integral light distribution. Initial work was on destruction of trichloroethylene. The scope of this research included the development of hardware and models for photon transport in waveguides and photoelectrochemical kinetics. We expected to leverage PNNL capabilities in photocatalysis and reaction mechanisms, but the project focused on advanced reactor engineering. Our microchannel photocatalytic reactor capabilities are unique to the world in that they leverage the significant investments being made in microchemical systems technology.

Background

The photocatalytic oxidation of organic contaminants is a simple, low-cost, fast, and environmentally friendly process that has attracted the interest of many research groups around the world in the last 10 years (Ollis et al. 1993). This process involves the illumination of catalytic particles with near ultraviolet light that promotes photo excitation of valence band electrons and holes. These electrons and holes migrate to the surface of the catalytic particles and participate in reduction/oxidation (redox) reaction with adsorbed species. Highly reactive hydroxyl radicals (•OH) are produced from these redox reactions that are responsible for the oxidation and, in some cases, the mineralization (complete oxidation to CO_2 and HCL) of the organic species. Among all semiconductors that have been used for the photocatalytic oxidation of organic pollutants, the anatase phase of titanium dioxide is the most effective for its catalytic activity and stability.

Commercial applications of waste processing using full-scale photocatalytic reactors are unknown. The published studies thus far involve laboratory and bench-scale systems. These reactor architectures cannot be scaled-up to a cost-competitive industrial waste treatment option. NREL has been active in photocatalyst reactor development and has focused on larger, solar-driven technology. The commercial state of the art in photocatalysis of liquids is to implement a slurry of nanoscale TiO_2. This approach creates a significant colloids separations problem to recover the catalyst from the processed stream, and consequently, this technology has not drawn significant commercial interest.

Technical Accomplishments

During FY 1997 the photocatalytic reactor device was designed and fabricated. A coating procedure to bind TiO_2 to the reactor surface using heat treatment was developed. The reactor surface was coated with TiO_2.

Initial benchmarking experiments to study the degradation of a TCE/water solution at the concentrations of 1300 and 500 ppm (4.6 and 0.2 moles/L) were completed. The preliminary result at a flow rate of 1 cc/min is presented in Table 1.

Table 1. Preliminary performance results.

Initial TCE concentration (ppm):
1300 ppm (4.68 moles /L) and 500 ppm (0.21 moles /L)
Final concentration after circulation of 3 reactor volumes:
3.55E-05 moles/L and 1.62E-06 moles/L

Novel Small-Scale Membrane Reactor Fuel Processor Technology

John L. Cox, Dean W. Matson (Process Technology)

Study Control Number: PN97082/1223

Project Description

Membrane reactors offer the potential of an efficient and cost-effective fuel processor for hydrogen production. This project will demonstrate PNNL's membrane reactor concept in conjunction with a fuel cell developed by Washington Water Power.

Fabrication methods for hydrogen permselective (supported Pd-Ag) tubular membranes will be demonstrated for eventual use in PEM fuel processors. The membrane is critical to produce the ultrahigh purity hydrogen required for PEM fuel cells, which are poisoned by carbon monoxide. The proposed membrane reactor fuel processor concept offers the opportunity to achieve large hydrogen production rates from methane and steam while also reaching high hydrogen purities in a single-stage and economically viable process. The purpose of the proposed work is to fabricate membrane tubes, either Pd-Ay alloy or coated ceramic, install and test them on an existing bench-scale reactor, then ship the reactor to SIRTI where Washington Water Power and Washington State University will test the system with their PEM fuel cell.

Background

The Pd-alloy membranes separate hydrogen as it is produced from the methane reforming and subsequent water gas shift reactions to overcome reaction equilibration. Traditional technologies require multiple and costly processing steps to overcome thermodynamic limitations. Previous work by Thomson et al. at Washington State University has demonstrated a promising membrane fabrication technique on planar disks that includes a 1 to 10 μm thick surface smoothing layer of γ-alumina followed by a 5 to 10 μm Pd-alloy coating. Fabrication of tubes using this technique is the key to the economy of a membrane reactor fuel processor. Such a fuel processor could be linked to small PEM fuel cells to provide electricity for commercial and residential applications.

Technical Accomplishments

A meeting was held with Dr. Thomson of Washington State University and representatives of SIRTI and Washington Water Power to develop the design considerations for the bench-scale fuel processor system to be coupled with the PEM fuel cell at SIRTI. Based on data presented by Washington State University, there did not appear to be sufficient information to design the membrane based on the coating Pd on alumina tubes. A decision was made to fabricate the membrane for the fuel processor from Pd alloy using commercially available 1/8-inch outside diameter tubing. Hydrogen flux requirements for the bench-scale fuel processor were defined to meet the requirements of the fuel cell.

A fuel processor design was developed based on a bundle of Pd alloy tubes submerged in a bed of reforming catalyst. Palladium membrane tubes were obtained from Johnson-Mathey and were manifolded together. Approximately 30 1/8-inch outside diameter tubes were welded to a common nickel header plate. Gas leak tests were conducted at room temperature in nitrogen to assess the quality of the metal joining. Numerous leaks were observed. The pinholes on the tubes on the exterior of the tube bundle were readily repaired. It was not feasible to repair the pinholes on the inside of the tube bundle without first severing the external tubes. An improved metal joining protocol is required. Because of the difficulties in fabricating the tube bundle, the bench-scale demonstration of the reformer was not completed. A fuel processor based on a membrane reactor still appears feasible, however improved techniques for fabrication of the membrane tube bundle will be required.

Plasma Spray Coating of Small Diameter Tubes with Aluminum

Glenn W. Hollenberg (Environmental Technologies)

Study Control Number: PN97084/1225

Project Description

The objective of this study was to identify viable techniques for coating the inside diameter of small stainless steel tubes with aluminum in preparation for aluminizing. Aluminized coatings possess unique properties which have demonstrated value in a variety of applications: abrasion resistance, corrosion resistance, and low hydrogen permeability. These properties should make aluminide coated, small-diameter tubes useful in nuclear power plants, heat exchangers, and chemical process tubing.

Technical Accomplishments

Aluminide barriers are typically applied by either the packed bed process (turbine blades) or the molten aluminum dipping process (mufflers). But neither of these processes are highly compatible with small-diameter tubes. A variety of commercially available metallurgical processes were explored in order to provide viable candidates for subsequent developmental activities.

Several processes were examined but were not attempted during this project. Sputtering was considered too slow to achieve robust coating depths. In addition, the Crook's region would probably block any deposition from occurring in small-diameter tubes. Metal inert gas welding was considered, but welding engineers discouraged further pursuit on the basis of instability of the arc within a small-diameter tube.

Induction-heated physical vapor deposition was unsuccessfully attempted. At low temperatures there were susceptor materials which permit a central rod to be heated within the less magnetic stainless steel. However, none of these susceptor materials retained this advantage above their Curie point. Hence, temperatures consistent with physical vapor deposition were not achieved.

Plasma spray coating has been used to put aluminizing coatings on the exterior of components. Attempts at a vendor site to coat the inside diameter of these tubes indicated that arc stability plagues the process. Highly inhomogeneous coatings and even some cracking resulted from these attempts.

Electro spark deposition consists of a contact electrode made from aluminum which is pulsed by an electrical power source. Unlike welding, the pulsed arc is much more controllable and a spot of aluminum is transferred to the stainless steel surface. By circumferential and axial translation it is possible to coat the complete interior of the tube. Although only 3-foot sections were done in this study, one of the electrodes was 10-foot long indicating how easily this process can be scaled. Homogeneous single-pass coatings of up to 0.002 inch were readily obtained. Attempts to deposit a second layer on the first ended with cracking of the second layer.

Resistance-heated physical vapor deposition is the standard process used for aluminum coating of mirrors. Insertion of a central resistance heater down the tube with aluminum on it provided a very homogeneous coating to the inside surface of up to 18-inch long tubes. However, the molten aluminum tended to flow down the heater and cause short circuiting. Coating layers of up to 0.004 inch were obtained, although thicker coatings should be easily achieved. For very long tubes, even small bowing of the tube or heater would result in short circuits.

In conclusion, resistance-heated physical vapor deposition resulted in the most homogeneous coatings. However, the technique is plagued by short circuiting of the heater element. Electro spark deposition resulted in good coating characteristics but only up to 0.002 inch in the present investigation.

Production of Medical Isotopes Using Microtechnology

Dean E. Kurath, Wesley E. Lawrence, Lane A. Bray, Yuehe Lin (Environmental Technologies)

Study Control Number: PN97088/1229

Project Description

The objectives of this project were to demonstrate an alternative separations technology for the production of purified ^{213}Bi for medical isotope applications, and to develop a prototypical medical isotope generator design based on this technology. The electrochemical process for purifying bismuth was demonstrated using nonradioactive bismuth. The process was monitored with a quartz crystal microbalance that can detect less than microgram quantities of material. A prototypical design for a generator based on technology was developed using commercially available and in-house manufactured micro unit operations.

Technical Accomplishments

The use of short-lived radioisotopes is currently being investigated for the treatment of cancer. These isotopes are linked to antibodies that recognize certain cancer cells when injected. Using this technology, radionuclides can be delivered directly to the cancer cells with a minimum amount of damage to surrounding tissue. The radioisotope ^{213}Bi is currently in clinical trials at the Memorial Sloan Kettering institute for the treatment of acute myelogenous leukemia.

The ^{213}Bi (47m half-life) is obtained by separation and purification from a ^{225}Ra/^{225}Ac source or "cow." The short half-life of the ^{213}Bi requires that the separation/ purification and reaction with the antibodies be performed as fast as possible in order to minimize product loss due to radioactive decay. FDA requirements dictate the process be sterile and that the product meet stringent purity requirements. The existing technology for the production of ^{213}Bi uses an organic ion exchange resin for separation from the "cow" and may have a limited lifetime due to the intense alpha radiation.

This project involved the testing of an alternative separations process for ^{213}Bi from a ^{225}Ra/^{225}Ac "cow" using an electrochemical process as a microchemical separations method. The application of microchemical chemistry is expected to provide rapid separation of the medical isotopes, thereby reducing losses due to the short half-lives. The development of small, inexpensive disposable separations units has the potential to make it easier to meet the FDA requirements for sterility. The use of an electrochemical process enables the development of an "organic-free" design which is expected to be radiation resistant.

The feasibility of the electrochemical separations method was demonstrated with nonradioactive solutions. This approach was used to avoid the expense of working with radioactive materials and to eliminate dose to workers. Since the nonradioactive analytical techniques are not sensitive enough to detect quantities that would be encountered in an actual process, process rates were monitored at several concentrations and the results extrapolated to dilute solutions.

These data were used to develop a prototypical design for a small microelectrochemical ^{213}Bi generator (Figure 1). The system includes three sample reservoirs, one for the "cow" solution, one for the rinse, and another for the elution solution. If the rinse and elution solutions are the same, then only two reservoirs would be needed. Two electronically controlled micro valves and a micropump would be used for microfluidic control. Solution reservoirs, valves, pumps, electrochemical cell and fluid connections would be integrated on one layer. Electronic connections and the electronic controller would be integrated on the bottom layer, providing a small compact and portable medical isotope generator suitable for bedside use.

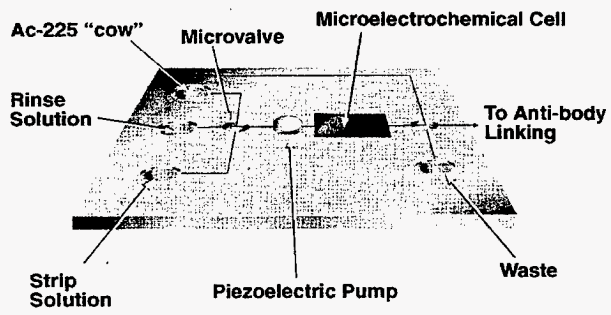

Figure 1. Microelectrochemical ^{213}Bi medical isotope generator.

Real-Time Tomographic Ultrasonic Velocimetry and Densitometry

Alireza Shekarriz (Fluid Dynamics)
David M. Sheen (Imaging/NDE)

Study Control Number: PN97091/1232

Project Description

The main scope of this work was to develop a novel tomographic ultrasonic technique to obtain the real-time distribution of acoustic velocity and flow velocity. The goal was to obtain real-time rheology and solids concentration within a solid-liquid suspension flowing in a pipeline. To nonintrusively obtain the rheology of the fluid flowing in a pipe, an accurate measurement of local shear rate distribution was developed. This data is also used to yield the profile of solids concentration. In addition, the volumetric flow rate was determined from integration of the velocity profile. From the knowledge of the concentration profile, the mass flow rate can also be determined.

Technical Accomplishments

A fully developed flow in a circular pipe was generated using the appropriate hydraulic system. The velocity profile for this particular condition, if the flow is laminar and Newtonian, would be parabolic. The processed signal was then converted into a velocity profile. Figure 1 is the reduced data for a solution of propylene glycol, which is Newtonian, at a Reynolds number of ~400. Thus, the flow is laminar and fully developed. Clearly, the velocity profile is parabolic, as expected. Comparison of these results against laser Doppler measurements showed very close agreements.

Similar results were obtained for the flow of Carbopol solution, which is a pseudoplastic fluid with a behavior index of n=0.47. The results are shown in Figure 2. With such high level of shear thinning behavior, the velocity profile commonly shows a plug-like regime in the core. Figure 2 clearly shows such behavior. Indeed, it was observed that at lower velocities the size of the plug increases in the radial direction, as is reported by other investigators. Therefore, qualitatively, we believe the measurements are providing the correct results. Further tests were performed to investigate the uncertainty obtained in the measurements.

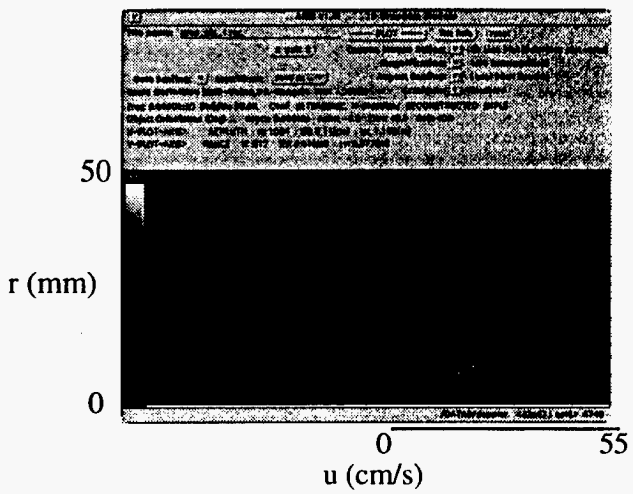

Figure 1. Probability density function of velocity profile for Newtonian flow.

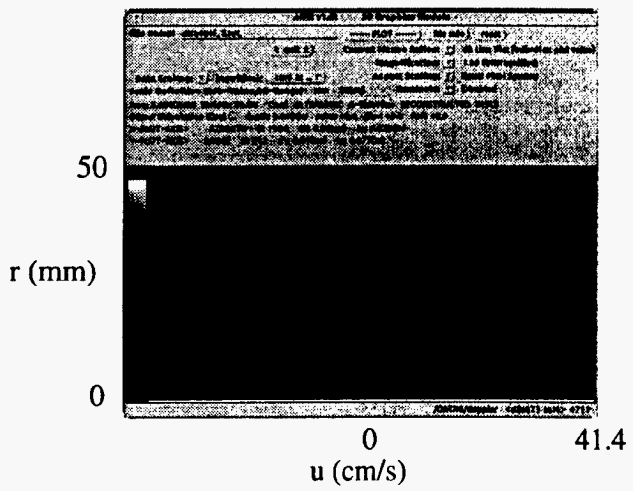

Figure 2. Probability density function of velocity profile for non-Newtonian flow.

Figure 3 is a plot of the center chord velocity profile measured using the current approach versus the theoretical prediction using an analytic solution for a power-law fluid shown below.

$$v(r) = \frac{Q(3n + 1)}{\pi R^2(n + 1)} \left[1 - (r/R)^{\frac{(n+1)}{n}}\right] \qquad (1)$$

where v is the axial velocity, Q is the volumetric flow rate in the pipe, R is the radius, and n is the behavior index of the pseudoplastic fluid. Substitution of the flow rate measured (367 ± 15 mL/s), radius of the pipe (27 mm), and the behavior index of the fluid obtained from rheological measurements (0.47) results in the following relation:

$$v(r) = 26.3 \left[1 - (r / 2.7)^{3.13}\right] \qquad (2)$$

where the velocity is in cm/s and r is in cm. Using this relationship, the analytic results, shown as a solid line on Figure 3, closely matches the experimental results obtained with our technique. Further, when the profiles of velocity measurements are numerically integrated over the cross-section of the pipe, we find less than 3% deviation from the flow meter measurements is found.

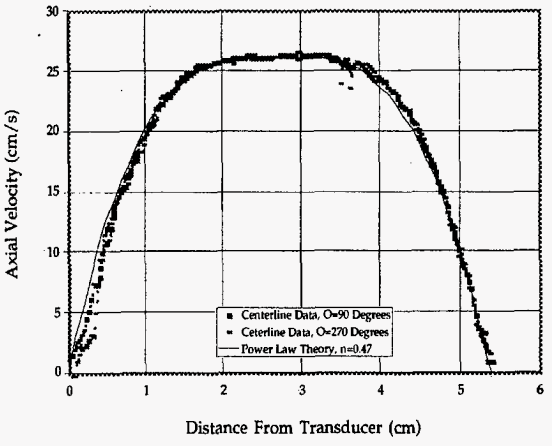

Figure 3. Measured velocity distributions versus theoretical predictions.

Recycling Heavy Metal Process Streams: Biogenic Sulfide Precipitation

Michael J. Truex, James J. Toth (Process Technologies)

Study Control Number: PN97092/1233

Project Description

Many wastewater streams, particularly in the electroplating and electronics industries, are characterized by the presence of heavy metals and substantial concentrations of sulfate. We are developing a biological process that uses this sulfate to remove heavy metals. Sulfate-reducing bacteria (SRB) produce H_2S, which can precipitate such metals as copper, cadmium, zinc, nickel, tin, and chromium, even in the presence of strong chelators like EDTA. The result is a metal sulfide precipitate from which metals can be recovered and metal-free water that can be recycled back into the process. On-site recycle of process rinse and etching solutions has the potential to boost production capacity and reduce operating expenses.

Metal sulfide precipitation has been previously examined as an alternative to conventional metal precipitation technology that uses hydroxide- or carbonate-based chemistry. Microbially generated H_2S resulting from the reduction of sulfate has lower reagent costs than the use of sodium sulfide or ferrous sulfide. Also, in contrast to these other sulfide delivery systems, H_2S contributes to the desired acidic nature of the process stream and is "clean" in that it does not increase that amount of total dissolved solids in the process stream. Thus, the process stream can be reused without costly filtration or other major treatment and retains characteristics such as acidity and organic constituents that are required for the manufacturing operation. Preliminary cost estimates suggest that the bioprocess will be cost competitive.

Technical Accomplishments

A sulfate reducing bioreactor was designed and operated. Tests were performed to quantify the kinetics of the sulfate reduction/sulfide production. The reactor was operated for approximately 4 months. The impact of variations in the operating parameters on the sulfate reduction/sulfide production kinetics were determined.

The microbial inoculum used for the bioreactor was obtained from a bioreactor that had been operated for several years by researchers at another institution. The kinetics of sulfate reduction from this consortium of organisms was found to be much superior to the kinetics of organisms obtained in preliminary experiments using both sediment enrichments and sewage sludge enrichments.

The testing was successful in demonstrating that the bioreactor could be operated to produce hydrogen sulfide for use in precipitating heavy metals.

Separation via "Enhanced Diffusion"

Anthony J. Peurrung (National Security)
Steven R. Billingsley, Loni M. Peurrung, Johannes H. Sukamto (Environmental Technologies)
Mark D. Tinkle (Environmental and Health Sciences)

Study Control Number: PN97094/1235

Project Description

The general objective of this project was to establish the utility of enhanced diffusion technology by investigating the engineering design of separations systems based on this technique. A large number of possible strategies for the design and construction of enhanced diffusion-based separations systems are known. Work focused initially on learning to quantifiably assess the performance of various design approaches. Subsequently, a detailed engineering design was completed for two of the most attractive designs, and one was constructed for later evaluation.

Enhanced diffusion arises from the random diffusive motion of molecules in the direction transverse to a flow in the presence of shear. Consider the motion of molecules within an oscillating Poiseuille flow inside a hollow tube. Molecules "sample" flow with widely disparate velocities as they diffuse into and out of the strong central flow and as the flow itself oscillates with time. The resulting complex motion involves large random movements in the flow direction described by the term enhanced diffusion. This process must be "tuned" for species of a particular mass; only those molecules that typically diffuse across the tube diameter in a time that roughly equals the flow oscillation time undergo the maximum enhanced diffusion. Heavier and lighter molecules undergo enhanced diffusion that is considerably less rapid. Typically, enhanced diffusion requires flow channel sizes of about 0.1 cm and oscillation frequencies on the order of 1 Hz.

A separations system can be constructed that exploits enhanced diffusion by using "counterflow," a deliberate net fluid flow applied in the direction opposite to the desired diffusional flux. Although this counterflow retards the motion of all diffusing species, those species for which enhanced diffusion is optimized receive the least retardation. In this way, a "filter" can be constructed with a yield and selectivity that can be controlled by a simple variation of the counterflow strength.

Technical Accomplishments

This project supported several areas of investigation in order to permit the design of a successful enhanced diffusion-based separations system. Among the topics investigated were power consumption, dissolution effects, staging, scale-up, and design complexity. Several of these issues are briefly discussed below.

The power consumed (P) per unit of product yield (Y) is an important measure of the operational cost of an enhanced diffusion system. Power is expended primarily in the process of vaporizing and condensing the carrier fluid. Assuming that the carrier fluid is used equally to apply a "counterflow" to the diffusion region and to "flush" the output reservoir, the power-to-yield ratio is given by

$$\frac{P}{Y} = \frac{\Delta H_{vap}}{\rho_C c_0}[2e^{(LV_C/D_1)} - 1]$$

where ΔH_{vap} is the specific heat of vaporization of the carrier fluid and ρ_C is its gas-phase density, and c_0 is the source concentration of the species of interest. The diffusion region has length L, counterflow velocity V_C, and diffusion constants D_1 and D_2 for the two species to be separated. Notably, this product efficiency is completely fixed once the species to be separated are chosen and an enrichment is specified.

Careful consideration was given to the consequences of dissolution of the desired product in the carrier fluid. It must be remembered that enhanced diffusion can separate one species from another but results ultimately in a product that is relatively dilute in the carrier gas stream. If the necessary subsequent separation of the product from the carrier fluid is arduous, the overall method will lose utility. It was found that separation of the product does not normally present a problem unless very high enrichments per stage are desired or unless the products are highly soluble in the carrier fluid. .

The use of multiple stages was found to allow design of an enhanced diffusion system with greatly improved yield for a particular enrichment. A schematic diagram of one of a series of enhanced diffusion stages is shown in Figure 1. A computer program that numerically calculates the yield and enrichment for a multistage design has been written. The predictions of this computer model were found to be in agreement with simpler, but analytically tractable, theoretical models.

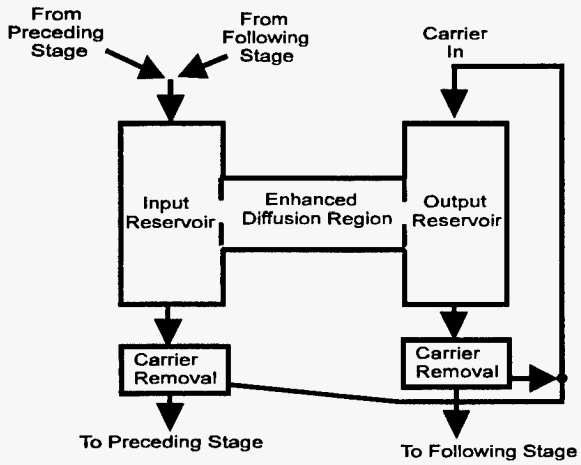

Figure 1. Block diagram of one of a series of enhanced diffusion stages in a separations system.

Two approaches were ultimately selected for detailed design on the basis of scalability and minimum complexity. Although the product efficiency is nearly independent of design method, various designs differ greatly in their achievable yield for an apparatus of a given size. It is this "scalability" criterion that strongly favors the enhanced diffusion-based systems over the much older counterflow separations systems that use conventional diffusion.

Our approach was found to lead to exceptionally high diffusion constants and thus to a separations system with exceptionally high capacity.

The second design considered achieves moderate performance but is extraordinarily simple and thus may be well suited for several separations applications. A detailed study of this design was completed and has been submitted for publication in *AIChE Journal.*

Publication

A.J. Peurrung, S.R. Billingsley, L.M. Peurrung, J.H. Sukamto, and M.D. Tinkle. "Design of an Enhanced Diffusion Separator using Steady, Buoyancy-Driven Flow." *AIChE Journal* (submitted).

Spray Coating Supercritical Carbon Dioxide to Eliminate or Reduce VOC Emissions

Max R. Phelps, John L. Fulton, George S. Deverman (Process Technology)

Study Control Number: PN97097/1238

Project Description

The principal objective of the project was to test and develop a spray coating process using supercritical carbon dioxide which can be applied by spray application without the use of volatile organic compounds (VOCs) or other hazardous air pollutants.

We planned to identify and characterize a low-cost, environmentally friendly, and efficient process that can be adapted for use by industry to eliminate the need for VOCs and other hazardous air pollutants in spray coating processes while meeting the standards for a quality product.

Background

Amendments to the Clean Air Act have mandated the substantial reduction or elimination of VOC emissions in a wide range of processes, including spray coating applications. Several alternatives to existing spray coating technologies either have been or are currently being developed in response to this need. All of these alternative processes have been developed around altering or reformulating existing coatings mixtures to enable application with little or no VOC solvent emissions. As a general rule, these alterations have resulted in inferior coating performance while substantially increasing the cost and amount of energy required to apply the new coating materials. For a significant portion of the metals and wood coating industries, the available new alternatives do not provide coatings or processes that satisfy existing needs.

Supercritical spray coating has been successfully used to demonstrate the application of uniform, no-VOC alkyd resins and low-VOC polyurethane coatings onto a variety of substrates. Additional tests were performed to successfully apply solvent-reduced paints onto paper substrates, but no testing has yet been performed to verify coatings quality. Current supercritical processes used by government and industry use alternative coatings formulations to make their processes tenable. These coatings have been deemed inferior for most needs.

Solvent alternatives based on the use of supercritical carbon dioxide offer a rapidly growing set of solutions to pollution prevention problems in industry. Existing alternatives are not sufficient as replacements for VOCs in spray coating industries.

Researchers at PNNL have an extensive background in the development of supercritical carbon dioxide-based technologies. The intent of this project is to combine recent developments to develop a unique and novel process for meeting government and industrial spray coating needs.

Technical Accomplishments

A significant portion of the project funding was used to identify various urethane/polyurethane coating requirements currently used by industry and government. Based on those results, we contacted several suppliers of polyurethane type coating formulations and acquired potential mixtures for further development.

Every formulation contained volatile organic solvents. The purpose for development of this technology is to eliminate volatile organics from the coating formulation. Our only alternative was to attempt solubilization of the basic urethane monomer and the accelerator in a supercritical solution.

We found that urethane as the monomer is soluble in carbon dioxide. The icocyanate binder that promotes polymerization is also soluble in carbon dioxide.

Since ending the project we found that there is an environmentally safe alternative to icocyanate for the binder in polyurethane films.

Stabilized Native Enzymes and Chemical Treatment for Conversion of Organic Chemicals from Biomass

Steven C. Goheen, James A. Campbell, Manish M. Shah, James A. Franz (Chemical Sciences)
Richard J. Orth, Andrew J. Schmid (Chemical Processing)
Rick L. Ornstein (Environmental Molecular Sciences)

Study Control Number: PN97098/1239

Project Description

This project develops and examines new technologies for converting biomass to new chemical products. The technologies include both chemical and biochemical processes. The immediate goal is to develop processes for converting corn fiber, a low-cost feedstock, to high-value chemicals. When successful, this capability can be transferred to other biomass feedstock of similar composition.

During FY 1997 four principal investigator teams supported this project. The teams supported chemical treatment, enzyme processing, enzyme modeling, and analytical methods development and analysis. The common goal has been to produce simple sugars from corn fiber. We have shown this can be done. The primary degradation products have been identified by nuclear magnetic resonance (NMR), liquid chromatography (LC), and chemical derivatization in combination with gas chromatography/mass spectrometry (GC/MS). Progress in detection, characterization, and quantification of oligomeric intermediate hydrolysis products has been achieved, important for measurement of selective early product forming steps in enzymatic conversion.

Background

Numerous low molecular weight hydrolysis intermediates are produced during acid hydrolysis. Categories of structures of these materials have been established. While the precise structure of oligomeric products is difficult to determine, statistical spectroscopic (^{13}C NMR) and chromatographic methods have been identified to characterize the conversion of oligomers by hydrolytic or enzymatic procedures.

Technical Accomplishments

Chemical Treatment

This task has evaluated how process conditions affect reaction products. Chemical treatment may produce feedstock for enzyme and/or catalytic processing. Products of this process are liquid hydrolysate and filter cake. Corn fiber contained approximately 13% crude protein, 15% ADF (the portion of the cell wall containing cellulose and lignin), and 57% NDF (the portion of the cell wall containing cellulose, lignin, and hemicellulose). If the hemicellulose content was about 42% (NDF - ADF) and only hemicellulose was solubilized, then approximately 40% of the original corn fiber could be solubilized. These issues will be examined in FY 1998.

Enzyme Processing

Xylan from oat spelt was used to mimic corn fiber xylan. Xylan from corn fiber is not available commercially, but should have structure comparable to oat spelt xylan. Both oat spelt xylan and corn fiber xylan are insoluble carbohydrates. Research to date suggests that xylan can be converted to xylose by an enzyme from a variety of sources. Mass spectrometric and liquid chromatography analysis has confirmed that xylose is the major product. The attack of different enzymes on two different types of xylan was tested. Interestingly, both xylans were degraded by enzymes from different sources. However, the extent of the conversion varied. The stability of one variety of enzyme capable of transforming oat spelt xylan was tested. Further experiments are under way to produce xylan from corn fiber.

Enzyme Modeling

In FY 1997, the enzyme modeling task progressed in four areas. In the first area, we assessed relevant, potential targeted enzymes with available x-ray crystal three-dimensional structures and performed sequence alignments. In the second area, we assessed potential cross-linking agents with respect to availability of x-ray crystal three-dimensional protein structures and their suitability for chemical cross-linking. We completed several high-level quantum calculations examining the effect of some different small amino acid side-chain functional groups on disulfide-bridge stability. Quantum calculations examining the larger side-chain disulfide-bridge calculations are in progress. We began to design and construct a computer program to search for potential disulfide-bridge sites within any protein with available x-ray crystal three-dimensional structure.

Analytical Methods

Analytical support has been instrumental in providing information to optimize our processes. We developed liquid chromatography, GC/MS, and methods to provide semi-quantitative and quantitation information. This information was used to optimize the process for the production of specific analytes.

The ^{13}C NMR method for characterization and semi-quantitation of soluble oligomers was developed using the anomeric linkage carbons of polysaccharides. The carbon linking two glucose or comparable units is in the region 98 to 106 ppm. Analyzing this region of the hydrolysate samples provided a method for estimating intermediate oligomer concentrations.

Analysis of hydrolysate solutions revealed a variation of xylose, arabinose, and oligomer formation and aldehyde formation.

Superstructural Assembly of Materials for Selective Anion Separation

Jun Liu, Glen E. Fryxell, John H. Sukamto, X. Feng
(Materials and Chemical Sciences)

Study Control Number: PN97101/1242

Project Description

The focus of this project is on the structural assembly of anion separation materials/membranes based on molecular separating agents developed at PNNL. In order to enhance anion exchange properties, novel self-assembly and electrochemical processes are being used to tailor the properties of the anion exchange materials on the molecular, nanometer, and micrometer levels. Anion selectivity will be enhanced by optimizing molecular recognition, size-limited dynamic diffusion, and electrostatic binding.

Technical Accomplishments

This project has examined new separation materials prepared using self-assembled monolayers (SAMs) technology for attaching separating agents (functional groups) to mesoporous materials. This is illustrated in Figure 1. A wide range of reaction conditions have been explored for attaching the functional molecules to the mesoporous support. Currently, we can systematically vary the population densities of functional groups on the mesoporous materials from 10% up to 100% of the full surface coverage with 100% yield, which means no excess molecules are used in the reaction and all the molecules end up in the monolayers.

Compared with SAMs on flat substrate, it is more difficult to attach organic monolayers to mesoporous supports. The functional molecules must be able to access the interior surface of the pore channels (a few nanometers wide), and must not hydrolyze and condense with themselves prematurely. The population density and the quality of the functionalized monolayers on the mesoporous materials are also important factors.

Systematic change in the charged site was evaluated for anion selectivity. Simple quarternary amine compounds were used to evaluate the synthesis conditions and the factors for anion selectivity.

Agents for selective anion separation can be assembled into separating materials. Model compounds were chosen for initial studies as the molecular design activities at PNNL

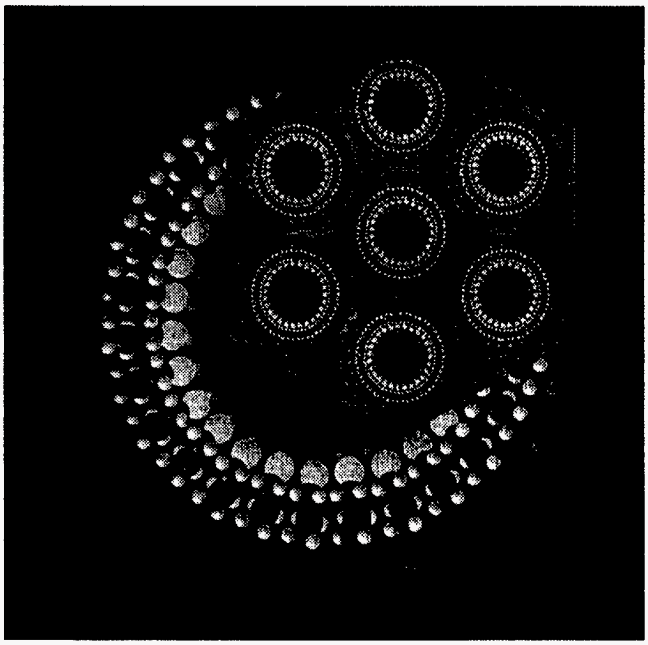

Figure 1. Illustration showing the assembly of separating agents in the pores organized in the pores of mesoporous materials.

examine potentially more selective analogs. Films were deposited on electrodes. The selectivity of the films for ReO_4^- (surrogate for TcO_4^-) in the presence of high NO_3^- concentration was investigated using cyclic voltametry. Cyclic voltametry can provide early screening information to determine the economic feasibility of the separation process. From the data, a number of processing issues can be evaluated: 1) selectivity, 2) stability, and 3) capacity. All three issues have been addressed to some degree for the model film.

Publications and Presentations

J. Liu. "Hybrid Mesoporous Materials with Functionalized Monolayers." Invited article in *Advanced Materials* (submitted).

J. Liu. 1997. "Heavy Metal Separation by Functionalized Mesoporous Materials." Presented at Annual ACS Meeting, invited talk, Las Vegas, September 7-12.

Risk and Safety Analysis

Cell and Tumor Growth Kinetics

Robert A. Wind (Chemical Structure and Dynamics)
Lyle B. Sasser (Molecular Biosciences)

Study Control Number: PN95013/989

Project Description

The purpose of this project was to develop experimental data that would allow descriptions of changes in cell division and tumor growth induced by the active metabolites of chlorinated hydrocarbon solvents widely distributed in DOE sites. Recent data indicate that these metabolites act by four distinct modes of action. Obtaining quantitative data on how each of these modes of action influences tumor growth and progression is critical to the development of alternative methods for estimating cancer risk at low exposures found in the environment. Specifically, data were to be developed that would allow more realistic non-linear dose-response relationships for non-genotoxic carcinogens. For this study, hepatic cancer induced by dichloroacetate (DCA) was studied in the B6C3F1 male mouse to investigate the hypothesis that these chemicals selectively stimulate the growth of intermediate cell populations that make up the hyperplastic nodules. The aim of this project was to evaluate the use of high-field, in vivo magnetic resonance imaging techniques for following the progression of initiated cells into hepatic tumors in mice. Magnetic resonance imaging is completely noninvasive and nondestructive, therefore, animals do not have to be periodically sacrificed to obtain kinetic data. Moreover, because specific lesions in individual animals can be followed, animal-to-animal variability is eliminated; thereby, improving statistics. In principle, this means that relatively few animals need to be examined in order to get statistically valid results, and an imaging based approach can be used for acquiring the kinetic data needed for developing models describing the toxicodynamics effects of different chemicals.

Technical Accomplishments

In FY 1997, in vivo magnetic resonance imaging was to be used for following the growth, and possibly the regression, of chemically induced hepatic lesions in live mice. After the successful pilot study in FY 1996 in which 94% of lesions induced by chronic exposure to dichloroacetate (DCA) were detected, the focus in FY 1997 was on whether initiation with vinyl carbomate could be employed to significantly increase tumor multiplicity; thereby, reducing the number of animals needed for statistically relevant data.

In anticipation of the demands associated with following 20+ initiated animals, imaging capabilities were first extended to a 300 MHz imaging system. This was necessary since the 500 MHz system used in last year's pilot study was heavily used by other projects, and therefore, unavailable for frequent mouse-imaging activities. Surprisingly, observed signal-to-noise ratios in images acquired at 300 MHz were better than previously observed at 500 MHz. Since imaging coils with the same efficiency (B_1/I) were used at both frequencies, this result could only be explained if radio-frequency induced sample losses at 500 MHz were roughly a factor of 7 larger than those at 300 MHz. Importantly, this would significantly diminish the relative signal-to-noise advantage normally expected from the larger equilibrium magnetization.

As a result of organizational changes in the inhalation toxicology group (LSL II), key components needed for a respiratory triggering system were no longer available. During the FY 1996 effort, respiratory triggering was shown to significantly reduce respiratory-induced image degradation. It was also shown that high quality images could be acquired in a shorter amount of time with respiratory triggering; thereby, increasing overall animal throughput. Moreover, with triggering, the contrast of smaller lesions around 1 mm in diameter improved because motion-induced blur was significantly reduced. As a result of these benefits, respiratory triggering was judged to be essential for planned experiments. However, without the computer based pulmonary analysis system from the inhalation toxicology group, a self-contained, digital-to-analog triggering circuit had to be designed, built, and tested. Fortunately, this proved to be as effective as the borrowed equipment previously used in the original configuration of the triggering system.

Shortly after imaging capabilities were extended to the 300 MHz system, two small groups of mice were imaged after 30 weeks of chronic exposure to 2 g/L of DCA. One group was initiated with vinyl carbomate, and the other with diethylnitrosamine (DENA). Importantly, all mice were treated with DCA for two months longer than a larger vinyl carbomate-initiated population that would ultimately be the main focus of the project. In this context, valuable information about the stage of lesion progression after 30 weeks of DCA exposure was gained. This was essential

for scheduling imaging experiments for the larger group of vinyl carbomate-initiated mice; particularly, if lesions were to be detected at an early enough stage when regression was thought to be more likely to occur upon cessation of DCA-treatment.

In both the vinyl carbomate- and DENA-initiated animals, lesions with diameters ranging between 1 to 8 mm were readily detected. Moreover, tumor multiplicity indeed appeared to be significantly higher; particularly, if compared to mice exposed to DCA for the same duration but not treated with an initiator. Unfortunately, upon necropsy, it became apparent that a high number of lesions in the magnetic resonance-observable size range were not seen with imaging. Low detection sensitivity in initiated mice was unexpected; especially, given previous results acquired at 500 MHz with non-initiated mice (see Table 1).

Table 1. Magnetic resonance-detection sensitivity for different initiation-promotion protocols.

VC + DCA (n=5)	DENA + DCA (n=4)	*DCA-Only (n=14)
35%	33%	94%

***Non-initiated mice previously measured at 500 MHz in last year's pilot study.**

To understand why low detection sensitivities were observed, a comparative study was undertaken in which four vinyl carbomate-initiated animals were imaged at both 300 and 500 MHz. With all other experimental parameters identical, this study was meant simply to test whether detection sensitivities observed at 300 MHz were somehow lowered by either unknown hardware problems and/or field-dependent liver-lesion contrast. Importantly, with the exception of a constant frequency artifact seen in 300 MHz images, no significant difference in overall image quality was observed (see Figure 1). Moreover, liver-lesion contrast was largely field-independent. As a result of these findings, it was concluded that relatively low detection sensitivities observed in initiated mice was not attributable to imaging at a lower frequency.

To determine whether initiation with vinyl carbomate had influenced the detection sensitivity by changing the imaging characteristics of non-involved liver tissue, the NMR properties of tissue-water were measured in vivo as a function of treatment. In each treatment group, water in non-involved liver tissue was characterized in terms of both its relaxation times (T_1,T_2) and molecular mobility (D - diffusion coefficient). In addition, images were acquired under identical experimental conditions. As shown in Table 2, no significant differences were seen in either water mobility or NMR relaxation. This meant that any

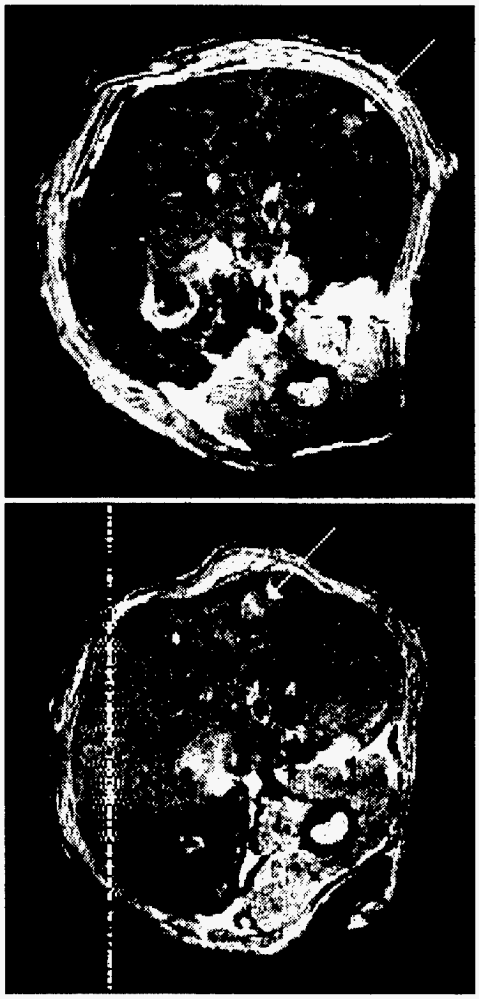

Figure 1. Images of the same vinyl carbomate-initiated mouse acquired at 500 (top) and 300 MHz (bottom). The 300 MHz image was acquired 6 days after the 500 MHz image. In both cases, a lesion is visible (arrows) and liver-lesion contrast is comparable - 3.9 and 4.7 respectively for top and bottom. Note increased lesion size after six days.

Table 2. NMR parameters for water in noninvolved liver tissue. Control mice (n=5) were not initiated and received pure drinking water for 36 weeks. Vinyl carbomate-only mice (n=5) were initiated with vinyl carbomate and received pure drinking water for 36 weeks. DCA-only mice (n=5) were not initiated and received 2 g/L of DCA in their drinking water for 36 weeks. Vinyl carbomate+DCA mice (n=3) were initiated with vinyl carbomate and received 2 g/L of DCA in their drinking water for 36 weeks. Note that relaxation times are given in seconds and diffusion coefficients given in 10^{-5} cm^2/sec.

Group	T_1	T_2	D
Control	1.39±0.17	17.8±1.7	1.2±0.1
VC-Only	1.42±0.17	17.0±2.8	1.6±0.2
DCA-Only	1.57±0.14	16.4±1.4	1.5±0.3
VC+DCA	1.60±0.10	16.5±1.8	N.A.

treatment-dependent changes in the NMR properties could only be manifest as relative differences in overall water content.

Although this possibility still has to be checked through direct analysis of acquired images, differences in water content are likely to be marginal since the parameters summarized in Table 2 are also highly sensitive to overall water content. Moreover, since little variation in liver-lesion contrast was observed for DCA-induced lesions ranging from hyperplastic foci to hepatocellular carcinoma, marginal differences in water content would not likely explain why some lesions were seen and others were not. A more plausible explanation, therefore, seems to be that the initiator-promoter combination itself results in a broader spectrum of lesion phenotypes than DCA alone, importantly, some of which are not observable with magnetic resonance imaging. This possibility is currently being tested through an immuno-histological comparison of detected and undetected lesions in vinyl carbomate-initiated mice.

Despite relatively low detection sensitivity in vinyl carbomate-initiated mice, some growth data was acquired. One particularly nice example is shown in Figure 2 where the volume of a single lesion was successfully followed over a 13-day period. During this time, the diameter of the lesion increased from 1.3 to 3.2 mm. Unfortunately, the mouse died in its cage after imaging on the 13th day. Although this particular death was unusual in that it did not occur during imaging, over the year, death did occur during imaging in 20% of all the animals. At the present time, these deaths are known to be an entirely avoidable and a result of suffocation (see Figure 3).

Unfortunately, as already indicated, much of the effort in FY 1997 was devoted to understanding why low detection sensitivities were observed in initiated mice.

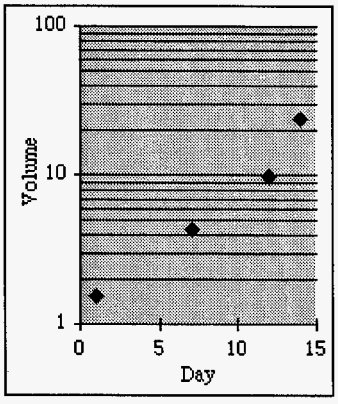

Figure 2. Magnetic resonance-measured growth kinetics for a single lesion in a DCA-exposed mouse initiated with vinyl carbomate (same mouse as shown in Figure 1). Measured volume is plotted in cubic millimeters.

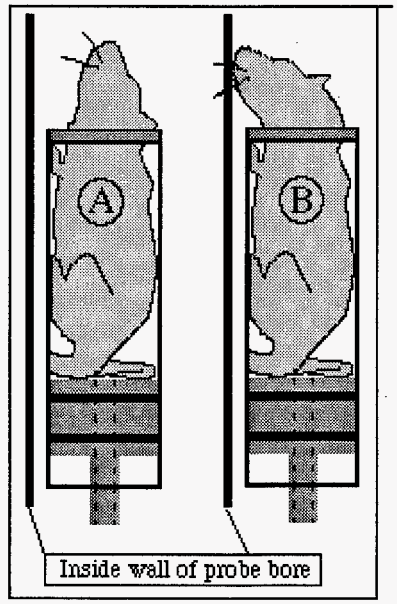

Figure 3. Suffocation occurs when the animal is positioned improperly inside the plethysmograph used for monitoring respiration. When properly positioned, the head of the animal points up when the plethysmograph is held vertical (A). Under these circumstances, air inside the imaging probe can freely circulate around the animal's nose. When the animal is improperly positioned (B), the head falls forward and fresh air is prevented from circulating around the nose. Improper positioning is a direct result of pushing the bottom plunger assembly too far into the plethysmographic body tube; thereby, forcing the mouse's head to extend too far through the latex collar gasket. When positioned improperly, the animal's nose can form a tight seal against the flat, inner surface of the probe bore. Because the animal is anesthetized, it cannot move and suffocation occurs rapidly either through the lack of oxygen (hypoxia) or because carbon dioxide levels build up (hypercarbia) in the dead space formed between the inside wall of the probe bore and the animal's nose. Importantly, when positioned improperly, no amount of air flow will save the animal - death is inevitable. Conversely, with careful attention, the majority of animal deaths can be avoided.

Consequently, little growth data was actually acquired. Moreover, with few small lesions actually detected in vinyl carbomate-initiated mice, only a handful of mice were removed from DCA-treatment to test whether regression would occur. Importantly, mice removed from treatment were done so at a much later stage than originally planned and, not surprisingly, no regression was observed. The only noteworthy data from the limited number of regression experiments was one lesion that seemed to "disappear" completely only 2 days after suspension of DCA treatment. However, initial excitement faded rapidly; particularly, when at necropsy, the lesion was found with no change in size. This finding suggested that changes in the NMR properties might occur before regression; thereby, significantly confounding efforts to observe regression.

In the end, the initiation-promoter protocol proved highly problematic. On the other hand, DCA-only exposure looks much more promising. However, more work on a larger

group of DCA-exposed animals is needed to clearly establish that growth and regression can be observed consistently.

Publications and Presentations

K.M. Minard, R.J. Bull, A.J. Stauber, and R.A. Wind. 1997. "*In vivo* MR Imaging Study of DCA-Induced Hepatic Lesions in Male B6C3F1 Mice." In *Proceedings, ISMRM 5th Scientific Meeting*, Vancouver, BC, Canada, p. 938.

K.M. Minard and R.A. Wind. "Practical Consequences of RF-induced Sample Losses in Microimaging Studies of Laboratory Mice." *J. Magn. Res. Imaging* (to be submitted)

K.M. Minard, R.A. Wind, and R.L. Phelps. 1997. "A Plethysmographic Approach for Routine Respiratory Gated MR Imaging of Live Mice in a High-Field, Vertical Bore Magnet." in *Proceedings ISMRM 5th Scientific Meeting*, Vancouver, BC, Canada, p. 1906.

K.M. Minard, R.A. Wind, and R.L. Phelps. "A Compact Respiratory Triggering Device for Routine Microimaging of Laboratory Mice." *J. Magn. Res. Imaging* (to be submitted).

R.A. Wind. 1997. "In vivo and in vitro NMR microscopy." (invited seminar) M.I.T., Boston, February 13.

Cell Signaling Mechanisms

Brian D. Thrall (Molecular Biosciences)

Study Control Number: PN95014/990

Project Description

Cellular signaling pathways that regulate cell growth and cell death are important to a number of disease processes associated with exposure to environmental contaminants. In particular, deregulation of signaling pathways that balance cell growth and death is becoming a recognized mechanism by which nongenotoxic carcinogens may promote cancer. This project focused on understanding whether the mitogen-activated protein kinase (MAPK) pathways regulate the growth and death of hepatocytes. Furthermore, we focused our studies on determining the potential role that environmental contaminants, which induce liver cancer in rodents, play in altering the regulation of the MAPK pathway.

Technical Accomplishments

Mitogen-activated protein kinase pathways involve a cascade of proteins whose function is to transmit extracellular signals to the nucleus where alterations in gene regulation result in cellular responses. The most extensively characterized MAPK proteins include the 44 and 42 kD extracellular signal-regulated kinases (ERK1 and ERK2), which are phosphorylated and activated by the MEK (MAPK kinase) family of kinases. A major effector of MEK activation is the product of the raf-1 oncogene, a 74 kD kinase which interacts at the cell membrane with GTP-bound Ras proteins. Upstream mediators of Ras activation include a number of tyrosine kinase growth factor receptors, G proteins, as well as protein kinase C. The importance of the ERK pathway in disease processes is highlighted by the oncogenic nature of the proteins involved. For example, Ras, Raf, and MEK have all been demonstrated to have oncogenic potential. In addition, activation of ERK proteins by phosphorylation is associated with a variety of cellular responses, including stimulation of cell replication, differentiation, and inhibition of programmed cell death (Seger and Krebs 1995; Xia et al. 1995). A major function of liver growth factors, such as insulin and epidermal growth factor, is mediated through activation of the ERK pathway. Since tumor promoters disrupt the balance between cell growth and cell death regulated by these growth factors, it is possible that these promoters modulate the ERK pathway.

Carcinogenic metabolites produced from exposure of rodents to halogenated solvents, such as trichloroethylene and tetrachloroethylene include trichloroacetate (TCA) and dichloroacetate (DCA). Trichloroacetate belongs to a class of rodent liver carcinogens known as peroxisome proliferators, due to the effect these chemicals have on peroxisome synthesis and fatty acid oxidation pathways. Dichloroacetate is also a peroxisome proliferator, although it is less potent in this regard as compared to trichloroacetate. It has become well documented that the carcinogenic activity of peroxisome proliferators is due to their ability to stimulate cell division and concurrently inhibit programmed cell death (apoptosis) (Roberts et al. 1997). Studies conducted in our laboratory have confirmed that peroxisome proliferators and metabolites of trichloroethylene suppress apoptosis in isolated hepatocytes (data not shown). Phosphorylation of ERK and activation of the ERK pathway is associated with both increased cell division and suppression of apoptosis (Xia et al. 1995). Therefore, we have conducted studies to determine whether trichloroacetate and related liver carcinogens affect the ERK pathway. As is shown in Figure 1, exposure of primary hepatocytes isolated from male B6C3F1 mice to trichloroacetate results in a dose-dependent increase in phosphorylation of the ERK2 protein. Similar results have been obtained with dichloroacetate and other peroxisome proliferators (data not shown). Of particular importance is that the increase in ERK2 phosphorylation occurs at concentrations of trichloroacetate which are well within the range of trichloroacetate levels produced by exposure of

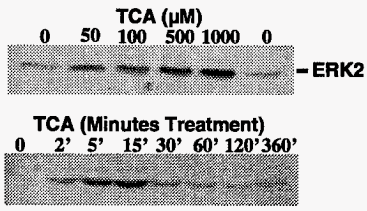

Figure 1. Effect of TCA on phosphorylation of ERK2 in mouse hepatocytes. Hepatocytes isolated from male B6C3F1 mice were treated with TCA, and total protein lysates were used to measure phosphorylation of ERK2 by western blot analysis using an antibody specific for phosphorylated ERK2. The upper panel shows the response at varying concentrations of TCA and the lower panel shows the time course using 1 mM TCA.

mice to carcinogenic doses of either trichloroacetate, trichloroethylene, or tetrachloroethylene. The effect of trichloroacetate on ERK phosphorylation is also rapid, occurring within 2 minutes after exposure (Figure 1).

The time course for ERK2 phosphorylation by trichloroacetate is very similar to that produced by endogenous growth factors, such as insulin and epidermal growth factor (data not shown). Additional studies have demonstrated that ERK2 is not only phosphorylated after trichloroacetate exposure, but that the kinase activity of ERK2 is activated (data not shown).

Since our experiments have indicated that trichloroacetate and other peroxisome proliferators not only activate the ERK pathway but also suppress apoptosis, we investigated whether ERK phosphorylation plays a role in regulating apoptosis in mouse hepatocytes. We have found that the flavonoid and putative anticarcinogen, apigenin, is an efficient inhibitor of ERK phosphorylation. Pretreatment with apigenin blocks ERK2 phosphorylation stimulated by the hepatic growth factor insulin (not shown). Furthermore, exposure of hepatocytes to 25 μM apigenin for 1 hour is sufficient to reduce endogenous phosphorylated ERK levels to a nondeductible level (Figure 2). Interestingly, exposure of hepatocytes to apigenin also stimulates apoptosis (Figure 2, bottom panel). At concentrations of apigenin which sufficiently reduce ERK2 phosphorylation, an significant increase in the proportion of hepatocytes which die by apoptosis are observed. We have found similar results in other cell types and using a different inhibitor of ERK phosphorylation, PD98059 (data not shown).

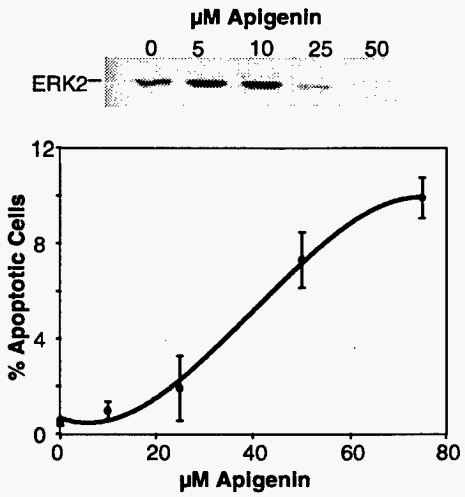

Figure 2. Apigenin inhibits ERK2 phosphorylation and stimulates hepatocellular apoptosis. Panel A) Effects of varying concentrations of apigenin on ERK2 phosphorylation in isolated hepatocytes after 1 hour exposure. Panel B) Effects of apigenin on apoptosis in hepatocyte monolayers treated for 48 hours with varying concentrations of apigenin. Apoptosis was measured by fluorescent microscopy by staining with Hoecsht 33258 dye and scoring the number of cells with condensed nuclei.

It is known that growth factors which act by stimulating ERK2 phosphorylation, including insulin-like growth factors, suppress apoptosis in hepatocytes (Tanaka and Wands 1996; Kummer et al. 1997). Consistent with a previous study in neuronal cells (Xia et al. 1995), our results suggest that sufficient levels of phosphorylated ERK2 are necessary to maintain the viability of hepatocytes. In additional experiments, we have shown that these inhibitors of ERK2 phosphorylation also block hepatocyte division stimulated by epidermal growth factor (data not shown). Thus, the level of ERK2 phosphorylation is important to maintaining the balance between cell growth and death in hepatocytes, and a possible mechanism by which liver carcinogens act is by altering this balance through stimulating the ERK2 pathway. Ultimately, these studies will provide a molecular rationale for how these signaling pathways regulate cell growth and death, and will allow us to more closely define the dose-response relationships by which nongenotoxic carcinogens disrupt regulation of these processes.

References

J.L. Kummer, P.K. Rao, and K.A. Heidenreich. 1997. "Apoptosis induced by withdrawal of trophic factors is mediated by p38 mitogen-activated protein kinase." *J Biol Chem* 272:20490-20494.

R.A. Roberts, D.W. Nebert, J.A. Hickman, J.H. Richburg, and T.L. Goldsworthy. 1997. "Pertubation of the mitosis/apoptosis balance: a fundamental mechanism in toxicology." *Fund Appl Toxicol* 38:107-115.

R. Seger and E.G. Krebs. 1995. "The MAPK signaling cascade." *FASEB J* 9:726-735.

S. Tanaka and J.R. Wands. 1996. "Insulin receptor substrate 1 overexpression in human hepatocellular carcinoma cells prevents transforming growth factor β1-induced apoptosis." *Cancer Res* 56:3391-3394.

Z. Xia, M. Dickens, J. Raingeaud, R.J. Davis, and M.E. Greenberg. 1995. "Opposing effects of ERK and JNK-p38 MAP kinases on apoptosis." *Science* 270:1326-1331.

Publications and Presentations

A.J. Stauber, R.J. Bull, and B.D. Thrall. 1997. "Dichloroacetate and trichloroacetate promote clonal expansion of initiated phenotypes in mouse hepatocytes in vitro." Conference on "Mechanisms of Susceptibility to Mouse Liver Carcinogenesis," Chapel Hill, North Carolina, September 8-10.

J. Kato-Weinstein, B.D. Thrall, and R.J. Bull. 1997. "Alterations in carbohydrate metabolism with haloacetate treatment." *PANWAT* 14, 15.

G.A. Orner, L.C. Stillwell, R.S. Cheng, L.B. Sasser, R.J. Bull, and B.D. Thrall. 1997. "Comparison of H-ras mutation spectra in tumors of trichloroacetate and dichloroacetate-treated B6C3F1 mice." *PANWAT* 14, 29.

M.K. Lingohr, B.D. Thrall, and R.J. Bull. 1997. "Dichloroacetate (dichloroacetate) modulates the insulin signaling pathway in mouse liver cells." *PANWAT* 14, 34.

Comparative Metabolism and Pharmacokinetics

Irvin R. Schultz (Molecular Biosciences)

Study Control Number: PN95019/995

Project Description

This project examined the metabolism and toxicokinetics of the chloroacetic acids in rats and mice as they are formed in the metabolism of trichloroethylene. We later expanded this effort to include specific bromo- and mixed bromo-chloroacetic acids which were used as tools to better understand the metabolism of haloacetic acids in rodents and humans. While di- and tri-haloacetic acids are similar chemically, they induce liver tumors by very different mechanisms (see cell signaling project). The metabolism of dichloroacetic acid (DCA) is very rapid while that of trichloroacetic acid (TCA) is slow. There is substantial interspecies differences in the elimination of DCA which was also previously shown to be affected by prior exposures. These variables have a dramatic impact on haloacid kinetics and make it difficult to accurately estimate chemical dosimetry in humans from solvent exposure. Therefore, knowledge regarding the disposition and metabolism of DCA and the role of tri- to di-haloacid formation in increasing the dosimetry of di-haloacids is needed. During FY 1997, this project focused on obtaining a better understanding of the nature of holoacid metabolism and worked toward development of a kinetic model which can be used to predict dosimetry.

Technical Accomplishments

During FY 1997, we investigated the interspecies differences in the blood elimination and liver metabolism of DCA and other haloacids, and the effects of prior exposure to TCA and DCA and other di-haloacids on the disposition of DCA. Our experimental approach was to expose groups of mice and rats to DCA or TCA in their drinking water followed by intravenous injections or oral dosing of a haloacid and measurement of the subsequent blood concentration-time profile. A toxicokinetic analysis was performed on these profiles which provided a quantitative interpretation of the effects of pretreatment. The in vitro liver metabolism of these haloacids was also characterized using tissue homogenates from mice and rats (control and pretreated), and dogs and humans. An initial PBPK model was developed for di- and tri-haloacetates in the F344 rat which is anticipated to be used for correlating chemical dosimetry and biological effects of haloacids in mice and rats and allow subsequent extrapolation to humans.

In Table 1, we summarize our toxicokinetic results in mice (a similar study was performed in rats, but the data is not shown). All blood concentration-time profiles for haloacetates from either naive or pretreated mice exhibited a mono-exponential decline and were analyzed using a one-compartment pharmacokinetic model. The comparative elimination of the four haloacetates in naive mice was similar to rats with the tri-haloacetates having longer half-life ($t_{1/2}$) and decreased total body clearance compared to the di-haloacetates. Also notable was the similarity in distribution volumes (a measure of the extravascular distribution) among the haloacetates. The effect of pretreatment on the pharmacokinetic parameters varied between the tri-haloacetates and di-haloacetates. Pretreatment had only a small effect on TCA elimination but had a dramatic effect on the di-haloacetates (DCA and DBA) where the $t_{1/2}$ increased due to a decrease in total body clearance.

In Vitro Metabolism of HAs

In Figure 1 we summarize some of our work with liver homogenates. Mice metabolized DCA more rapidly than other species, and the interspecies differences in the metabolism of DCA ([rapid] mice > rat > human > dog [slow]) appears to correlate with published differences in the elimination of DCA. These results indicate that the primary determinant of DCA exposure is the extent of metabolism.

PBPK Modeling of DCA and BDCA in the F344 Rat

Figure 2 shows a schematic outline of the PBPK model developed and designed to predict the elimination of BDCA and the formation of DCA after intravenous injection of BDCA. This model was also used to predict DCA metabolism and liver dosimetry after oral dosing. The model has individual tissue compartments for organs involved in elimination (liver and kidney) and lumped tissue compartments for remaining tissues which are divided into poorly (muscle) and richly perfused tissues. The model was parameterized for DCA and BDCA in rats using metabolism parameters estimated from intravenous dosing studies and the in vitro metabolism studies shown in Figure 1. The observed and predicted values are shown in Figure 3. Observed values for the liver concentrations of DCA in control and pretreated rats were obtained from a previous study. In general, the model did an adequate job

Table 1. Toxicokinetic parameters for haloacids after intravenous injection (100 mg/Kg).

Haloacid[a,b] (pre-treatment)	$AUC_{0-\infty}$ (μg ml hr)	Distribution volume (ml kg^{-1})	C_{max} (μg ml^{-1})	t½ (hr)	Total clearance (ml hr^{-1} kg^{-1})
TCA	2190 ± 772	577 ± 81	176 ± 27	9.3 ± 2.3	56.1 ± 36
(TCA)-TCA	2963 ± 1024	483 ± 102	214 ±41	9.4 ± 1.7	37.2 ± 12
(DCA)-TCA	2977 ± 510	521 ± 31	192 ± 12	10.7 ± 2	33.6 ± 5.6
BDCA	473 ± 77	998.1 ± 98	100 ± 10	3.3 ± .7	211 ± 35
(DCA)-BDCA	192 ± 23	909.0 ± 84	110 ± 10	1.2 ± .2	518 ± 62
DCA	81.8 ± 9	570.8 ± 87	175 ± 27	0.32 ± .05	1221 ± 134
(DCA)-DCA	222 ± 33	487.5 ± 66	205 ± 28	0.75 ± .14	449 ± 67
DBA	53.3 ± 6.6	861.5 ± 47	123 ± 21	0.32 ± .03	1988 ± 245
(DBA)-DBA	149 ± 16	615.7 ± 85	167 ± 23	0.61 ± .01	616 ± 85
(DCA)-DBA	305 ± 14	254.9 ± 16	392 ± 24	0.53 ± .04	327 ± 5

(a) Sample size: n=6 for TCA, DCA and DBA; n=2 for BDCA.
(b) DBA = di-bromo acetic acid; BDCA = bromo-di-chloro acetic acid.

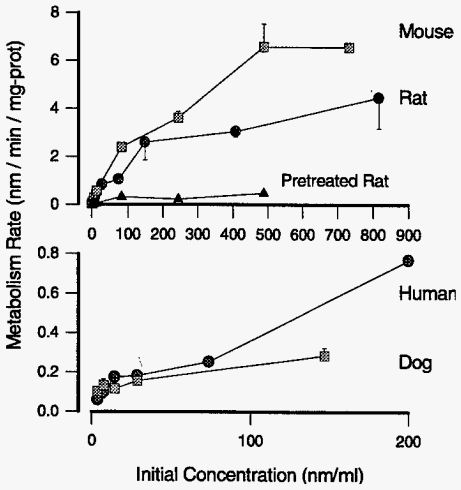

Figure 1. Initial metabolism of DCA in liver S9 fractions isolated from mice, rat, human, and beagle dogs.

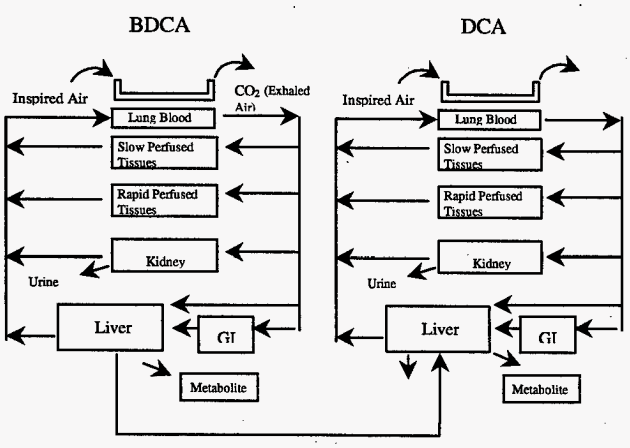

Figure 2. Schematic representation of PBPK model.

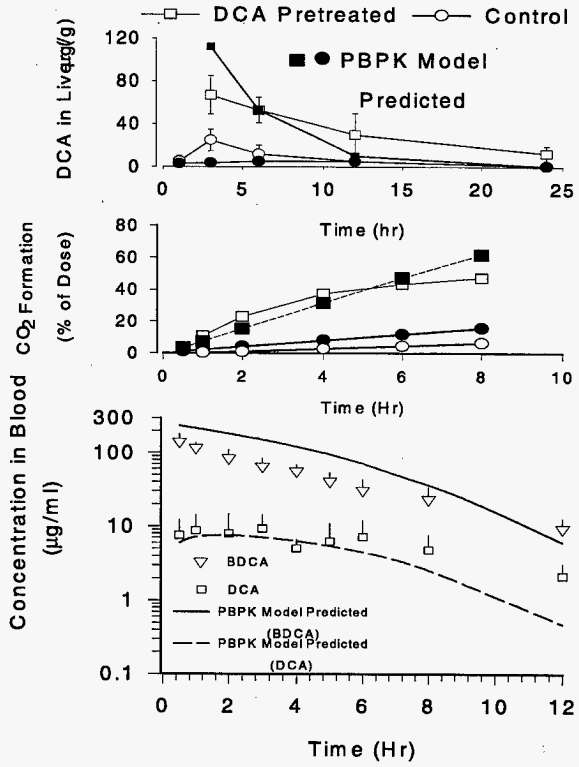

Figure 3. PBPK model predictions in F344 rats. Top panel shows DCA levels in rat liver and the middle panel shows CO_2 formed after a gavage dose of DCA. Bottom panel shows blood elimination of BDCA and DCA formed after intravenous dose of BDCA.

of describing the observed data and appears to be a useful model for further development to allow prediction of the dosimetry of haloacids in humans.

Publications and Presentations

A. Gonzalez-Leon, I.R. Schultz, G. Xu, and R.J. Bull. 1997. "Pharmacokinetics and metabolism of dichloroacetate in the F344 rat after prior administration in drinking water." *Toxicology and Applied Pharamacology* 146:189-196.

E.A. Austin and R.J. Bull. 1997. "Effect of pretreatment with dichloroacetate or trichloroacetate on the metabolism of BDCA." *J. Toxicol Environ Health* 52:367-383.

I. R. Schultz, G. Xu, A. Gonzalez-Leon, and R. J. Bull. 1997. "Interspecies differences in the toxicokinetics and metabolism of bromodichloroacetate in F344 rats and B6C3F1 mice." Annual Meeting of the Society of Toxicology, March.

Development of Risk Modules for the RT3D Bioremediation Code

T. Prabhakar Clement (Bioprocessing)

Study Control Number: PN97033/1174

Project Description

Presently, almost all subsurface clean-up activities are targeted at remediating contaminated groundwater to drinking water standards, ignoring the natural assimilative capacity of aquifer formations. A recent survey of over 1000 fuel hydrocarbon plumes by the Lawrence Livermore National Laboratory has found that most aquifer formations posses the intrinsic potential to naturally biodegrade hydrocarbon plumes. The natural attenuation protocol published by the Air Force Center for Environmental Excellence has several documented evidences for intrinsic BTEX plume degradation in saturated aquifers via various terminal electron accepting processes under both aerobic and anaerobic conditions. A similar study is also under progress to document cases for chlorinated solvent plumes. These studies, together with recent understanding of natural subsurface biological decay processes, have demonstrated that the long-term risk levels posed by subsurface contaminant plumes are, in general, smaller than previously expected levels. Hence, a risk-based clean-up strategy that account for all natural attenuation processes while evaluating the future risks posed by the plume, will be the most pragmatic strategy for cleanup decision making. Although available historic plume monitoring data can support such a decision making process, further use of the data within a modeling framework to assess future risks will not only expedite site closures but also help understand and manage potential risks posed by migrating plumes. To develop a risk-based modeling framework for analyzing naturally degrading subsurface plumes, one would need: 1) a simulation tool for predicting biologically reactive multi-species transport in saturated, three-dimensional porous media; and 2) a comprehensive environmental assessment tool for evaluating potential risks.

The objective of this project was to integrate RT3D (a three-dimensional reactive groundwater transport computer model) with MEPAS to develop an integrated groundwater risk assessment tool. The integrated product will be a useful tool for evaluating risk-based remediation alternatives, and for setting-up monitoring goals for naturally degrading groundwater plumes. The tool can also be directly used for evaluating site-specific present/future risks posed by the migrating groundwater plumes contaminated with common chemicals such as BTEX and/or chlorinated solvent plumes. Based on the estimated risk levels, future monitoring and active remediation tasks can be planned.

Technical Accomplishments

In this work, we have developed an approach for obtaining risk and hazard quotient information based on a risk calculation done in MEPAS. The risk values are linked to RT3D to provide "risk maps" for RT3D simulations.

In this project we linked the groundwater model RT3D with the FRAMES User Interface (FUI), and thus indirectly with MEPAS. MEPAS is currently being integrated into FUI. The FUI provides two main functions: 1) a graphical user interface (compared to the DOS-based user interface in MEPAS) that makes the program more user-friendly and conceptually easier to understand, and 2) more flexibility for the user by allowing the user to choose from a number of computational models for performing various components of fate/transport/risk calculations.

In the planning stages it was determined that the best method for integrating the FUI and RT3D would be by using unit risk factors. The unit risk factor approach is a methodology developed by Strenge and Chamberlin (Strenge and Chamberlin, 1994, PNL-10190). In this approach, a unit concentration (e.g., 1 mg/L) is used in the risk calculations. This results from the unit risk factor approach that can be applied regardless of the transport calculations involved. The unit risk factor is used as a multiplier that is scaled by the actual concentration. For example, if a MEPAS calculation returns a unit risk factor of $1.15 \cdot 10^{-5}$ (in units of cancer incidence) for carbon tetrachloride, and if a separate transport calculation determines that the carbon tetrachloride concentration at the point of interest is 15 mg/L, then the risk at the point of interest is $(1.15 \cdot 10^{-5}) \cdot (15) = 1.725 \cdot 10^{-4}$ (in units of cancer incidence).

The way the FUI is currently set up, it would have involved an enormous amount of data entry for the user to get risk information, and/or a large code development effort to implement a multi-concentration risk calculation model. Thus, the unit risk factor approach was selected to be the best way to obtain the desired information with minimum change to FUI.

A "known concentration" saturated zone model was developed for use in the FUI. This model is run instead of a saturated zone model, such as the MEPAS saturated zone model, with a unit input concentration (e.g., 1 mg/L). MEPAS models are then used for estimating the exposure and health impacts portions of the risk calculation. The known concentration saturated zone model allows the source and saturated zone transport modeling to be circumvented; RT3D fulfills these functions as an independent code (i.e., outside FUI). The known concentration module interface was created in FUI specifically for this project.

The link between the FUI and RT3D is established via a FUI output file. Since FUI has a specific output file format, an interfacing code was developed to link FUI output with RT3D. This included codes to read and track the outputs and to properly apply the unit risk factors to the RT3D results. An output file was used as the link between the FUI and RT3D because 1) this avoids creation of a new user interface and 2) the unit risk factors transferred via the output file may be applicable for many scenarios. For example, the user may choose exposure and health impacts options that can be applied at a variety of sites so that the FUI only needs to be run to generate a set of unit risk factors for those conditions and the contaminants of interest. The output file can then be saved, and future RT3D simulations need only access the FUI output file instead of re-running the risk calculations. However, should the exposure and/or health impacts options change, FUI needs to be re-run to calculate unit risk factors for the new conditions. FUI-derived unit risk factors calculated for typical contaminants of interest during chlorinated solvent bioremediation are listed in Table 1.

This FUI/RT3D link will be used in future projects to demonstrate our capabilities to potential clients, and to perform risk estimates for actual remediation projects. As part of this DOE project, the FUI/RT3D link will be used to provide modeling support for the natural attenuation studies conducted by the Remediation Technologies Development Forum (RTDF). The RTDF is currently conducting field tests at the Dover Air Force Base to study the natural attenuation of chlorinated solvents (primarily TCE). RT3D was chosen be the primary simulation tool for modeling the natural attenuation processes at this study site. The FUI/RT3D link will enable the RTDF modelers to estimate the time-variant risks posed by the naturally degrading TCE plume.

This LDRD project has also produced a research idea on how to apply Risk Based Corrective Action (RBCA) methods at chlorinated solvent sites using the FUI/RT3D link. RBCA is a protocol to evaluate the need for and extent of corrective action at a contamination site. RBCA analysis may indicate that as little as a series of monitoring wells will suffice as the corrective action at a site or that a full-blown RI/FS and remedial action are required. A RBCA protocol has been adopted by the American Society for Testing and Materials (ASTM E-1739-95, 1995) and other similar protocols have been developed by other agencies. However, the majority of the work is related to petroleum hydrocarbon contamination. A similar protocol is needed for chlorinated solvent contamination. However, the RBCA protocol for chlorinated solvents will be significantly different because chlorinated solvents are biodegraded in a different manner and they can also produce toxic daughter products.

Table 1. Unit risk and hazard index[a] values for common contaminants.

Exposure Pathway --> Exposure Route --> Contaminant	water ingestion	showering dermal	showering ingestion	beef ingestion	milk ingestion	showering inhalation		
Carbon Tetrachloride	5.300 E-05	1.150 E-05	2.650 E-07	3.430 E-09	7.490 E-09	1.420 E-04	2.068 E-04	--
Chloroform	2.490 E-06	2.490 E-06	1.240 E-08	3.490 E-11	7.560 E-11	2.170 E-04	2.220 E-04	--
Tetrachloroethylene (PCE)	2.860	1.130 E+01	1.430 E-02	1.880 E-04	3.740 E-04	4.820 E-06	4.820 E-06	14.175
Trichloroethylene (TCE)	4.490 E-06	8.680 E-06	2.240 E-08	1.650 E-10	3.500 E-10	3.480 E-05	4.799 E-05	--
1,1 Dichloroethylene	2.450 E-04	2.590 E-05	1.220 E-06	2.480 E-09	5.470 E-09	4.820 E-04	7.541 E-04	--
1,2 Dichloroethylene	1.430	9.450 E-02	7.150 E-03	7.050 E-07	1.420 E-06	9.350 E+00	--	10.882
Vinyl Chloride	7.750 E-04	2.930 E-05	3.880 E-06	2.700 E-09	6.020 E-09	7.770 E-04	1.585 E-03	--

(a) Hazard index values are indicated by the gray shading.

Direct and Indirect Genotoxic Mechanisms

David L. Springer (Molecular Biosciences)

Study Control Number: PN93127/845

Project Description

Carbon tetrachloride, a major contaminant at several DOE sites, is known to produce hepatic tumors in laboratory animals. Although the precise molecular mechanisms responsible for the carcinogenic response is unclear, CCl_4 does not appear to produce tumors through genotoxic mechanisms but rather by causing cytotoxicity followed by compensatory cell replication. Thus, an understanding of the molecular events produced by CCl_4 and comparison of these changes in laboratory animals and human tissues will contribute to improved health risk estimates.

Background

Halogenated hydrocarbons are metabolized to reactive intermediates by the mixed-function monooxygenase enzyme system (Kalf et al. 1987). For CCl_4, the reactive intermediates are trichloromethyl radical and its corresponding peroxy radical (Tomasi et al. 1987); these radicals are capable of damaging proteins, lipids, and DNA; altering gene expression; and producing lipid peroxidation which damages membranes. Metabolism of CCl_4 occurs via homolytic cleavage of the carbon-chlorine bond. Unequivocal evidence for the production of the trichloromethyl free radical was obtained using isolated rat hepatocytes and spin traps. This enzymatically catalyzed reaction involves a complex between CCl_4 and cytochrome P450 (Fe^{2+}). The free radical can either be released from the P450 complex or be converted by a one-electron reduction to the Fe^{3+} trichloromethyl radical complex. When the radical is released from the P450 complex, a significant amount reacts in the vicinity of the P450 active site forming covalent modifications with the P450 heme moiety; another portion binds to nearby phospholipids. The free radical can also abstract a proton to form chloroform or, after further reduction to form the ferrodichlorocarbene complex, it may hydrolyze to yield carbon monoxide and hydrochloric acid. The trichloromethyl radical can also react with oxygen (O_2) to form phosgene. Upon completion of this reaction, the cytochrome P450 will either have been inactivated by covalent modification or is again available to react with another molecule of CCl_4.

The mixed-function monooxygenase enzyme P4503E1 is believed to be the predominant cytochrome P450 isoform responsible for conversion of CCl_4 to reactive intermediates (Tierney et al. 1992), although members of the CYP2B family may also participate (Gruebele et al. 1996). Early studies (Head et al. 1981) demonstrated that phenobarbital treatment increased the metabolism and hepatotoxicity of CCl_4, suggesting that P4502B isoforms were involved in conversion of CCl_4 to reactive intermediates. Subsequent studies have shown that ethanol and pyridine, which are potent inducers of P4502E1 produce substantial increases in CCl_4 toxicity. Conversely, N-acetylcysteine, which inhibits P4502E1, both protect against CCl_4 toxicity (Kalf et al. 1987). Together this information provides a strong case for the involvement of P4502E1 and 2B isoforms in CCl_4 toxicity.

Technical Accomplishments

During the course of this project we began studies to determine the relationship between cytotoxicity, cell proliferation, and mixed-function monooxygenase activities. The results indicate that the rats and mice respond very differently to single versus multiple doses of CCl_4 suggesting that the species differences have significant influence on the degree of cytotoxicity and possibly the carcinogenic response. The disparity in sensitivity between rats and mice to CCl_4 is attributable to differences in metabolism. Prior studies have shown that treatment of animals with CCl_4 results in decreased mixed-function monooxygenase activity and that a small but significant portion of the reactive intermediates (presumably the trichloromethyl radical) binds to the heme moiety of cytochrome P450. This covalent modification permanently inactivates the P450 and marks the protein for proteolytic degradation.

Both Western blots and enzymatic activity measurements suggest that the differences in sensitivity to CCl_4 between rats and mice is at least partially due to mixed-function monooxygenases activity. This is supported by the observation that in the mouse nearly all of the P4502E1 is knocked out by CCl_4 whereas in rats this isoform retains at least half of its activity. Since there is only one known pathway for CCl_4 metabolism which involves formation of the trichloromethyl radical, these data suggest that irrespective of the isoform involved differences in toxicity are attributable to the rate of production of the reactive intermediate. Further this suggests that the species differences are attributable to the affinity and/or kinetic

parameters (Km and Vmax) of the specific isoform. Lack of this type of information represents a major gap in our understanding of CCl_4 cytotoxicity, cell replication, and the contribution of these processes to the carcinogenic response. Ongoing DOE funded research is providing information that will improve the human health risk estimates for CCl_4.

References

A. Gruebele, K. Zawaski, D. Kaplan, and R.F. Novak. 1996. "Cytochrome P4502E1 and cytochrome P4502E1/2B2-catalyzed carbon tetrachloride metabolism." *Drug Metab. Disposit.* 24:15-22.

B. Head, D.E. Moody, C.H. Woo, and E.A. Smuckler. 1981. "Alterations of specific forms of cytochrome P450 in rat liver during acute carbon tetrachloride intoxication." *Toxicol. Appl. Pharmacol.* 61:286-295.

G.F. Kalf, G.B. Post, and R. Snyder. 1987. "Solvent toxicology: Recent advances in the toxicology of benzene, the glycol ethers and carbon tetrachloride." *Ann. Rev. Pharmacol. Toxicol.* 27:399-427.

D. Tierney, A.L. Haas, and D.R. Koop. 1992. "Degradation of cytochrome P450 2E1: Selective loss after labilization of the enzyme." *Archives Biochem. Biophys.* 293:9-16.

A. Tomasi, E. Albano, S. Banni, B. Botti, F. Corongiu, M.A. Dessi, A. Iannone, V.Vannini, and M.U. Dianzani. 1987. "Free-radical metabolism of carbon tetrachloride in rat liver mitochondria." *Biochem. J.* 246:313-317.

Enhanced Windows Version of MEPAS

John W. Buck (Strategic Environmental Management)

Study Control Number: PN97042/1183

Project Description

The objective of this LDRD project was to develop a state-of-the-art framework and user interface to allow separately developed DOE environmental models to be linked to meet the continuing needs of DOE-HQ, DOE field offices, and other government agencies. This project developed a proof-of-principle framework and user interface that incorporated the Multimedia Environmental Pollutant Assessment System (MEPAS). The following items were key research efforts in this project:

- research and develop input/output specifications for the framework system to incorporate MEPAS models
- develop pre- and post-processors to fit into file specifications defined
- apply state of science on-line help and engineering judgment database to the system
- link model inputs/outputs to display and presentation software to provide pre-defined or user-defined graphics, tables, and charts.

Technical Accomplishments

MEPAS was separated into seven physical-based object-oriented modules to fit under a new Windows-based user interface. These physical-based modules are Source-Term, Atmospheric, Vadose Zone, Saturated Zone, Exposure, Intake, and Impact modules. A module is defined as a model, a user interface, and associated pre- and post-processes. Each module has a module user interface developed that allows the user to input data for the specific model.

File and data specifications were developed that allow each module to interact with the other modules by defining boundary conditions. Pre- and post-processors were developed where needed to allow the different modules to meet the file and data specifications associated with other modules. The specifications that allowed the different modules to communicate without having to modify the current existing model were developed for the MEPAS modules as a proof of principle, but they were developed to be generic to allow other modeling systems, like GENII, RAAS, and other DOE environmental models to operate under the framework user interface.

On-line help was also developed for the MEPAS modules using generic specifications and formats to allow other software packages to link their help into the system. One format allows the help information to be viewed, printed, or linked to a web page. This minimizes the maintenance and quality control of the help files.

Another key element to the framework system developed for DOE environmental assessment software is a graphical display system to provide intermediate and final results. Instead of developing software to produce these graphical results, which already exist, Micosoft Excel was selected as the proof of principle for this effort. Graphical viewers associated with the framework and MEPAS modules were developed to link to the Excel software package. The linkages were developed to allow other environmental software packages to interface with the graphical viewers. Tables and charts were not included at this time but the general design and conceptual development for these products were investigated.

The final product of this LDRD effort is an operational prototype of a new framework system that has integrated the MEPAS modules into it. On-line help and graphical viewers were added to the system to make the housed environmental software easier to use and display results. This new framework system can be used for much of the current environmental modeling software that has been developed for the DOE, as well as Environmental Protection Agency and Nuclear Regulatory Commission associated packages.

Integrated Contaminant-Based Ecological Risk Assessment Methodology

Gene Whelan, Karl J. Castleton, Gariann M. Gelston, Mitch A. Pelton, Bonnie L. Hoopes, Ronald N. Kickert, Mark S. Wigmosta, Charles A. Brandt, Terri B. Miley, Michael J. Scott (Environmental Technology)

Study Control Number: PN97055/1196

Project Description

The overall goal of this project was to develop a quantitative, ecological-risk, decision-support framework that is coupled to a state-of-the-art, PC- and physics-based, multimedia model.

Over the past 15 years, intermedia (multimedia) models have been developed that address the release of contaminants into the environment, contaminant migration and fate in various environmental media (e.g., groundwater, surface water, air, and overland), movement through the food chain, exposure to various sensitive receptors, and the carcinogenic and noncarcinogenic health impacts associated with the exposure. These multimedia approaches have primarily focused on human-health impacts from radiological and chemical contaminants. One of the most important components that has been omitted is the impact to the environment from contamination that has been or may be released into the environment (i.e., past-practice waste sites and active releases, respectively). Currently, there is no platform and comprehensive, quantitative, ecological-risk approach, which assesses impacts to specific organisms from specific contaminant exposures that is compatible with human-health-risk assessments. By establishing a computer platform for integrated, holistic, ecological assessments, decision-support analyses will be greatly enhanced and the implementation of preliminary assessments would be greatly simplified. The focus of such a tool is to be able to provide enough information to the decision makers so they can make cost-effective and timely decisions.

Specific objectives of this effort include

- link Frequency of Analysis (FRAN) and the Multimedia Environmental Pollutant Assessment System (MEPAS)
- investigate the development of a database for application of FRAN in the aquatic environment
- identify data and input/output specifications to link the Health and Ecological Risk Management and Evaluation System (HERMES) with MEPAS, FRAN, and Framework for Risk Analysis in Multimedia Environmental Systems (FRAMES)
- initiate linkages of a Columbia River Comprehensive Impact Assessment (CRCIA)-based, food-web model to the other five PNNL tools as a platform for users to access the more robust, food-web model for ecological assessments.

Background

At many DOE installations, ecological-risk assessments must be performed. Because of restricted access to these installations, there may essentially be no human-health impact, but this does not mean that the environment is free of contamination. The degree of environmental degradation still needs to be assessed for both pre- and post-remediation conditions. Currently, PNNL is involved with the development and implementation of a number of multimedia-related tools to help DOE assess its alternatives in the decision-making process. Following is a list of the tools:

1. MEPAS uniquely integrates the 1) release contaminants from a source; 2) transport and fate of contaminants through a multimedia environment; 3) exposure to human receptors through inhalation, ingestion, dermal contact, and external dose; and 4) health impacts by providing a) temporally and spatially varying concentrations in soil, groundwater, surface water, and air, and b) human-health risks due to exposure through these media. MEPAS is a fully integrated, holistic, operational, PC- and physics-based model, containing direct linkages to a 550-contaminant database and Latin-Hypercube, sampling-based, Monte-Carlo sensitivity/uncertainty analysis module.
2. The Remedial Action Assessment System (RAAS) assesses remedial alternatives for waste cleanup and cleanup costs.
3. The FRequency ANalysis of COncentration (FRANCO) model was developed for regulatory and compliance purposes and is a statistical package that 1) correlates duration of exposure to contaminant levels to help determine the impacts of the exposure to organisms and 2) bridges the gap between simulated chemical modeling and ecological-risk assessment data that are available

from laboratory studies. The FRANCO statistical analysis accommodates different organisms as they relate to different contaminants, resulting in a flexible and versatile tool. There is no reason why the FRANCO-type analysis cannot be extended to provide three-dimensional risk isopleths for non-aquatic wildlife.

4. The proof-of-principle HERMES is being developed to investigate ecological risk habitat susceptibility by accounting for regulatory requirements associated with mitigation activities, including cost, using a GIS platform. HERMES has also been linked to Hanford's Biological Resource MAPping (BRMAP) database.

5. An ecological model is being developed as part of CRCIA and will be a convoluted, ecological, food-web approach that will address impacts to organisms associated with aquatic and riparian zones for multiple contaminants at multiple locations.

6. DOE-HQ (EM-40) and EPA (Athens and HQ) are co-sponsoring and co-funding PNNL in the development of an object-oriented Framework (FRAMES) from which these organizations would be able to access environmental-assessment tools like those described in items 1 through 5.

These six tools cover contaminant transport, risk to humans, cleanup strategies and cost, habitat susceptibility and cost, and ecological risk to organisms. They also represent many of the assessment components required in a regulatory, compliance, and planning setting and provide a platform from which DOE and EPA can access these tools. These six tools represent the basic platform/foundation for performing holistic, integrated, quantitative, human-health-risk and wildlife- and aquatic-ecological-risk assessments. The basis of this effort centers on coupling GIS technology, temporally and spacially varying changes in environmental contaminant concentrations, and concentration versus duration-of-exposure data to statistically assess the impacts to a variety of organisms. A fully integrated, holistic, multimedia approach is required because contamination can enter the ecosystem at different locations with varying strengths through the air, groundwater, and surface water.

Technical Accomplishments

A new version of the FRANCO model, called FRAN, was developed, which is more versatile and comprehensive than the FRANCO model that was originally developed for EPA in the 1980s. FRAN was linked to MEPAS and to FRAMES. A user-friendly interface was developed, and as a proof of principle, a quantitative ecological-risk assessment of the aquatic environment was demonstrated. A simple database structure for the example test case was developed and initially populated with the aquatic toxicological information used in the demonstration. It was determined though that a separate ecological database would have to be developed to support not only FRAN but also any linkages with FRAMES, MEPAS, HERMES, and CRCIA. Specification for linkages to the CRCIA and HERMES-GIS systems were investigated and documented. Data specifications and input/output specifications have been proposed to help ensure a smooth and transparent connection.

Publications

G. Whelan, G.M. Gelston, M.A. Pelton, K.J. Castleton, and M.S. Wigmosta. 1997. "Multimedia Ecological Risk Assessment Integrating FRAMES, MEPAS, and FRAN." Risk Analysis (to be submitted).

R.N. Kickert and G. Whelan. 1997. *Food-Web Module Input, Output, and Data-Specification Linkages to the Framework for Risk Analysis in Multimedia Environmental Systems (FRAMES).* Pacific Northwest National Laboratory, Richland, Washington (position paper).

T.B. Miley and G. Whelan. 1997. *HERMES Module Input, Output, and Data-Specification Linkages to the Framework for Risk Analysis in Multimedia Environmental Systems (FRAMES).* Pacific Northwest National Laboratory, Richland, Washington (in preparation).

Integrated Environmental Decision Support Tool

Michael R. Sackschewsky (Water and Land Resources)

Study Control Number: PN96038/1105

Project Description

Decisions facing DOE regarding environmental restoration and management require the balancing of multiple objectives and impacts (dimensions) over a variety of temporal and spatial scales. Many types of environmental data have been collected for the Hanford Site and the Columbia River over the last 50 years. However, the data have not been successfully organized and integrated to provide a concise description of the current site environment that can be used to evaluate impacts of different land uses and remediation and restoration options on subareas of the site, let alone the site as a whole. The objective of this project was to develop the framework, computer structure, and module linkages of an environmental decision support tool that could be used for site evaluation and selection. The tool summarizes and compares ecological effects and the costs of alternative actions and land uses, and is adaptable to different geographic settings. Ultimately, the tool can be modified to incorporate additional decision dimensions such as various other types of risk (cultural, public health, and safety) and monetary factors such as engineering costs.

Technical Accomplishments

We have developed an environmental decision support tool that provides quantitative estimates of ecological resources within various portions of the Hanford Site. The tool enables the user to select one or more areas where a proposed project will be placed, and then provides the user with a GIS representation of the vegetative cover classes found within that area, and an estimate of the quantity of each cover class in hectares. The tool identifies mitigable habitats within the selected area, determines if the amount of mitigable habitat is greater than a predetermined mitigation threshold, and provides an estimate of the mitigation costs for those habitats if compensatory mitigation is required. Additionally, the model estimates the population sizes within the selected areas for a selected group of indicator species and assigns a monetary value to these populations. The tool can also calculate the volume of material to be removed (if the proposed project is an excavation) and automatically determines the landfill area requirements for that material. The ecological effects and mitigation requirements of alternative landfill locations can then be evaluated.

The tool uses the existing HGIS database (maintained by Bechtel Hanford Inc.) but can be readily applied to any other location with GIS-based habitat information. The rules for estimating mitigation costs and species population sizes and values are readily manipulated by the user. Therefore, the output can be tailored to the specific setting and decisions being addressed.

An example of the output and utility of this decision support tool is provided in Figure 1. In this example, the user has identified three areas that will be excavated for environmental clean-up (cross hatched areas). The decision support tool determined that the selected areas encompass a total of 9.48 ha, and of this 2.66 ha are considered mitigable. The cost of replacing the mitigable habitat is estimated to be just under $30K. The value for the species within the selected areas is estimated to be approximately $7.8K, and the total ecological value of the selected areas is estimated to be approximately $37.5K.

Presentation

M.R. Sackschewsky, T.K. O'Neil, S. Tzemos, M.J. Scott, C.A. Brandt, and P.G. Doctor. 1996. "Integrated Environmental Decision Support Tool Based on GIS Technology." Society for Environmental Toxicology and Chemistry, November.

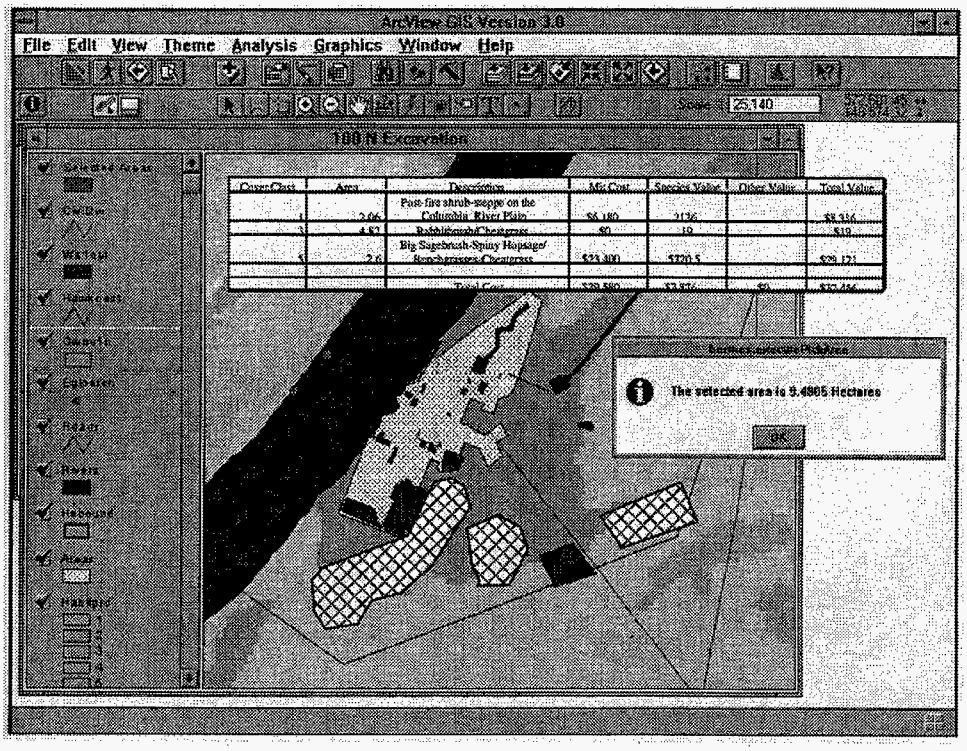

Figure 1. Output and utility of this decision support tool.

Technical Analysis and Integration of Health Effects Data

Richard J. Bull (Molecular Biosciences)

Study Control Number: PN95083/1059

Project Description

This research concentrated on three modes of action by which a chemical might act to influence tumor development in experimental animals. Mode of action is differentiated from mechanism of action in that much less experimental information is needed to identify a mode of action than a mechanism of action. By definition, a mechanism of action includes the description of all events pertinent to the pathological condition that is produced. Thus, one would have to begin with the molecular interactions (frequently more than one) into which a chemical enters to initiate the pathological process. The details of how that molecular event becomes translated into a toxicological response requires experimental detail at the cellular, tissue, and whole organism level to be established as a mechanism of action. The mode of action deals primarily with events at the cellular level that can be articulated as accounting for the chemical's specificity for a particular tissue. This descriptive data serves two purposes, one that allows the actual toxicological response to be modeled at the whole animal level and the other to serve to identify a course of action for determining the mechanism of action. Knowledge of the mechanism of action ultimately must come into play when the question of low-dose extrapolation of data is raised.

Research has included four major modes of action that are known to play roles in chemical carcinogenesis and how they impact risk assessment through models. Three of these modes do not involve chemically induced mutations: 1) killing of normal cells, 2) selectively stimulating growth of clones of cells initiated for cancer, and 3) preventing apoptosis of damaged cells leading to replication and eventual stabilization of a malignant phenotype. During this project, we made significant progress in identifying modes of action of chemicals fitting into the second and third groups that induce liver cancer. Because of resource limitations, it was necessary to curtail efforts related to the impact of killing of normal cells on growth of pre-initiated cells. It was also intended to explore mathematical models for these modes of action based upon imaging data of tumor growth and regression based upon MRI data.

Demonstration of consistent and predictable outcomes when chemicals that act through the same or different modes of action are tested together provides the basis for predicting interactions from the data available on individual chemicals.

Technical Accomplishments

The overall project has focused upon how metabolites of trichloroethylene induce liver cancer and to develop technical input to the application of EPA's new cancer risk assessment guidelines.

A unique finding arising from this project and related efforts was the implication of the insulin-signaling pathway in liver tumor induction by dichloroacetate (DCA), an important metabolite of trichloroethylene and other chlorinated solvents. The various figures designate a series of proteins that are involved in the insulin signaling pathway, beginning with the membrane receptor and ending with the extracellular receptor activated kinases (ERK) (see Figure 1) The key steps modified by DCA are hypothetical at this time. Changes identified with DCA treatment in normal cells or tumors induced by DCA are marked with broader arrows. The key observations are that cell division in normal cells has been suppressed and this is associated with a decrease in serum insulin concentrations and evidence of increased activity of protein kinase A (PKA). These data indicate a down-regulation of the insulin-stimulated pathway within normal cells. On the other hand, the tumors induced by DCA have increased sensitivity to insulin (indicated by a higher expression of the insulin receptor) and no evidence of down regulation by PKA. Since insulin is mitogenic in liver cells, this could well be the mechanism that causes tumors to grow so rapidly. To our knowledge this is the first time that this pathway has been implicated in carcinogenic responses to environmental agents. The figure provides a abridged version of this pathway and identifies those points that appear important in causing the net growth of pre-initiated cells in the liver.

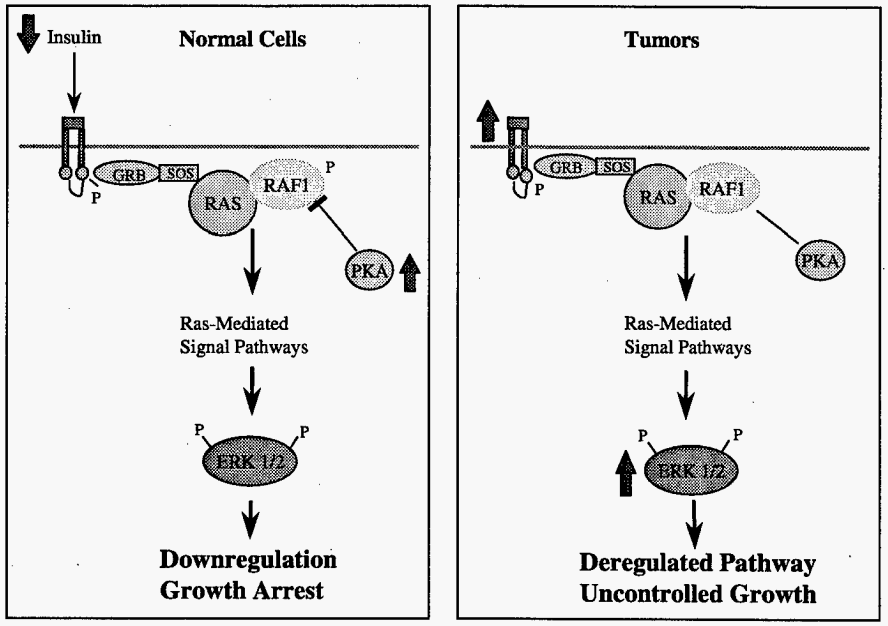

Figure 1. Potential mechanism for selection of preexisting tumor cells by DCA (broader arrows indicate changes in normal cells with DCA treatment or in tumors induced by DCA).

Major accomplishments include the following:

- The efforts from three separate projects (i.e., the cell and tumor growth kinetics, the cell signaling task, and the metabolism and pharmacokinetic projects) provide for comparing data on tumor imaging with cellular phenotype and replicative activity of cells within DCA and TCA-induced lesions.
- Championed the mode of action approach as a means of improving the classification of chemicals for risk assessment purposes to DOE.
- Developed an experimental approach for validating low dose extrapolation with mixtures of chemicals based upon the modes of action of the individual constituents of the mixture.
- Developed a small nucleus of activities in cell signaling mechanisms.

Publications and Presentations

R.J. Bull, B.D. Thrall, L.B. Sasser, and J.H. Miller. Mechanisms involved in trichloroethylene induced liver cancer: Importance to Environmental Clean-up. Funded by Environmental Management Science Program.

Toxicodynamic Modeling

John H. Miller (Molecular Biosciences)

Study Control Number: PN96070/1137

Project Description

The objective of this project is to develop and test biologically based risk assessment models that specifically consider the effects of carcinogens on cell division and death rates. These models will play a major role in the reevaluation of cancer risks from contaminants frequently found at DOE cleanup sites under new EPA guidelines that allow alternatives to linear risk extrapolation for nongenotoxic carcinogens.

Technical Accomplishments

The two-stage model of carcinogenesis (Moolgavkar 1986) is widely accepted in biologically based risk assessment. It assumes that cancer results from two rare cellular events usually considered to be somatic mutations. The first event produces an "initiated" cell with a growth advantage over surrounding cells. With time, a clone of initiated cells develops, which increases the probability of a second event leading to total abrogation of growth control. Agents that can induce one or both of these cellular transitions are called "genotoxic." Nongenotoxic carcinogens cause the early appearance of tumors by stimulating the growth of initiated cells.

Clones of initiated cells do not grow at a constant rate. Their initially rapid growth is slowed as they reach a size limitation of about 1 mm at which oxygen and nutrients can no longer diffuse throughout the clonal mass. The gradual decrease in growth rate can be due to either initiated cells becoming quiescent (i.e., they cease to pass through the cell cycle and both division and death rates go to zero) or cells continue to divide but die at an equal rate. Evidence exists to support both mechanisms; hence, we compared models of tumor promotion based on the two mechanisms with the aim of finding distinguishing characteristics that are observable.

Luebeck and Moolgavkar (1991) modeled the appearance of quiescent cells by coupling an exponential decrease in growth rate (division minus death rate) with the assumption of a constant ratio of division and death rates. A recent study of cell division and death during both early and late stages of rat-liver cancer (Kong and Ringer 1996) indicated that cell replication rates remain high throughout tumor development; nevertheless, growth rates decrease in the later stages because cellular death rates are almost equal to replication rates. Hence, Kong and Ringer speculate that suppression of apoptosis (i.e., programmed cell death) may be responsible for clonal expansion of initiated cells.

Clonal expansion due to suppressed apoptosis was modeled by expressing the rates of cell division and death as λa and λb, where λ is the rate of cell cycling, a is the probability that a cell cycle terminates in division, and b is the probability that apoptosis terminates the cycle. Since the probability of other outcomes, such as malignant transformation, is small, a + b is approximately unity. Hence, the net growth rate can be determined from the time dependence of the probability that apoptosis is the outcome of a cell cycle. A model in which this probability varies from 0 to 0.5 is obtained by assuming

$$2b = 1\ B \exp\left[-(t-t_0)/\tau\right] \qquad (1)$$

where t_0 is the time of initiation and τ is the relaxation time for rapid growth of initiated cells.

Computer simulations of clonal expansion due to suppresed apoptosis were performed with help from Kevin Anderson in PNNL's Statistics Group. Due to extinction (i.e., random birth-death processes resulting in no survivors), the number of clones that reach the upper limit on size is less than the number of primary initiated cells. For comparison with the Luebeck and Moolgavkar model of clonal expansion, we chose values of the parameters of both models that gave approximately the same number of 1-mm sized clones. In the suppressed-apoptosis model, the probability of extinction approached its upper limit of unity much slower than the Luebeck and Moolgavkar model reached its limit of 0.95; hence, small non-extinct clones may persist for a long time after balance has been restored between birth and death rates. The persistence of small non-extinct clones may be a characteristic of clonal expansion due to suppressed apoptosis that can be observed by measuring lesion size distributions when animals are sacrificed.

Regardless of the details of the model, the size of non-extinct clones at any time t after initiation can be expressed as

$$P_m = (S/N)(1-S/N)^{m-1} \qquad (2)$$

where S(t) is the probability that a clone has survived extinction and N(t) is the mean number of cells in non-extinct clones. In both the suppressed-apoptosis and Luebeck and Moolgavkar models, N(t) approaches a finite limit related to the upper limit on the size of a clone discussed above. At times sufficiently long that N(t) has reached this limit, S(t) is still much larger in the suppressed-apoptosis model than in the Luebeck and Moolgavkar model. Equation (2) shows that this difference in clone-survival probability will result in a difference in the clone-size distribution. Figure 1 compares these distributions when the ratio of death rates to division rates is 0.95 in the Luebeck and Moolgavkar model.

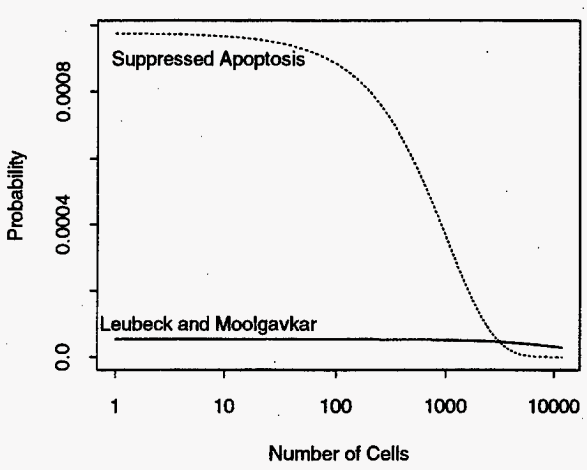

Figure 1. Nonextinct clone size distributions.

References

Kong and Ringer. 1996. *Cancer Letters* 105:241-248.

Luebeck and Moolgavkar. 1991. *Risk Analysis* 11:149-157.

Moolgavkar. 1986. *Ann. Rev. Public Health* 7:151-169.

Socio-Technical Systems Analysis

Life Cycle Assessment Design Tools

Kenneth K. Humphreys, Devin E. Terry, Tamara S. Stewart (Energy)

Study Control Number: PN97064/1205

Project Description

This project created the framework for a software tool and associated methods that will help technology developers evaluate the full life-cycle energy, environmental, and economic impacts associated with new products and processes. Using the improved level of information that the tool provides, product developers, chemical process engineers, and other technology developers will be able to identify energy efficiency and environmental improvement opportunities early in the technology development activity, when improvements can be feasibly incorporated. Technology developers will thus be able to reduce the likelihood that newly developed technologies will later require energy efficiency upgrades or end-of-the-pipe treatment to deal with environmental problems.

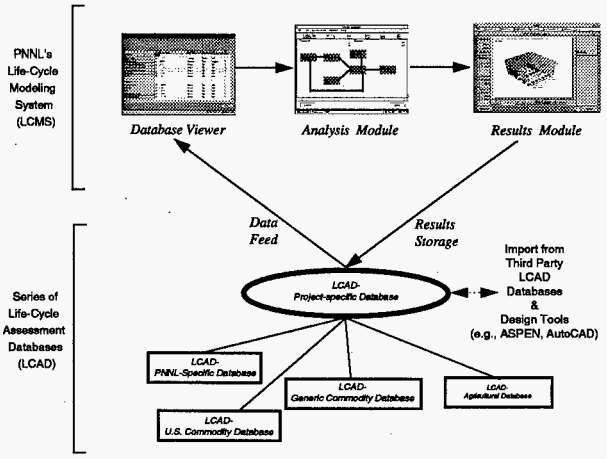

Figure 1. Software-based elements of the platform.

Technical Accomplishments

During FY 1997, LDRD funding was used to develop the overall framework for this project and fund the development of several basic proof-of-concept activities. Specifically, FY 1997 efforts addressed four areas: 1) identifying the technical hurdles and system components that were required to complete the project, 2) developing computational methods and data storage structures to support the modeling of industrial processes, 3) developing algorithms and a computer-user interface to facilitate data and results interpretation, and 4) creating several application examples. For each of the above four activities, the LDRD work was brought to a sufficient state of completion.

In the first task, major elements were identified and their functionality defined. The elements included 1) a software-based database viewer; 2) a software-based analysis module; 3) a software-based results interpretation module; 4) data exchange linkages with U.S. and international energy/environmental databases offered by universities, government agencies, and other parties; 5) linkages to conventional design tools (e.g., ASPEN and AutoCAD); and 6) a codified assessment process to be used in tandem with the tools. Figure 1 graphically depicts elements 1 through 5.

The first three elements, which are shown at the top of Figure 1, allow a technology developer or analyst to define the characteristics of a technology and subsequently generate life-cycle energy, environmental, and economic profiles for that technology. For example, a chemical engineer developing a biomass-based chemical process can specify the basic inputs and products associated with the process, and the software will generate profiles of all energy consumption and environmental releases that are associated with extracting, transporting, and preprocessing the energy and material feedstocks to the chemical process. As the engineer changes various raw material feeds or process energy sources, changes in the life-cycle energy and environmental profiles of the process can be observed. By making intelligent raw material and energy source choices, the life-cycle energy efficiency can be improved and the life-cycle environmental impact can be reduced.

In FY 1996, under a different project, considerable LDRD effort was invested in developing improved computational methods and data storage structure to support process modeling. The improved methods allow intuitive technology/process definitions (see Figure 2). A user simply specifies all inputs (e.g., raw materials or energy) and outputs (emissions and products) associated with a technology. To ensure the acceptance with the global

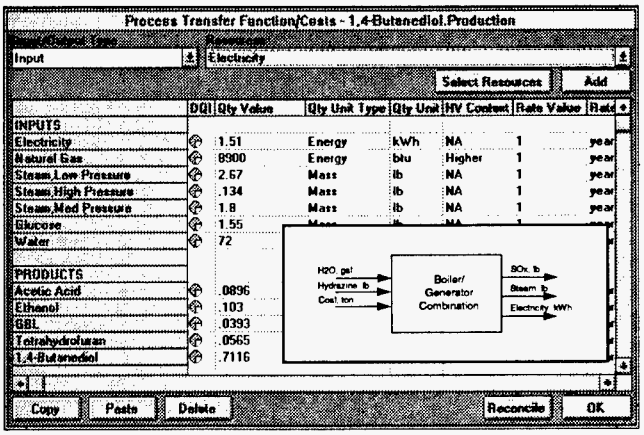

Figure 2. Process model representation.

technical peer community, the software is designed to deal with a wide range of units, heating value bases, approaches to defining input/output variables, and nomenclature. The computational approach that underpins this modeling capability reduces all input data to a set of mathematical vectors that are archived as a reusable module in the underlying Life-Cycle Assessment Database (LCAD).

The LCAD data structure was originally developed under a previous DOE-funded effort and has been modified to support this concept. Part of this expansion includes the concept of having multiple databases networked together, rather than a single stand-alone database. While the network concept itself is not novel, the practical aspects of numerous organizations from around the globe (universities, government agencies, and companies) sharing data are a tremendously complicated information technology challenge, as all the involved parties have their own technical perspectives, use different nomenclature, and otherwise have different conventions. Over a dozen organizations from various countries have expressed interest in participating in the data exchange network when fully developed.

The supporting codified assessment process (i.e., the last project element) that will be used in tandem with the software tools has been fairly well developed. It is based on formal life-cycle assessment methods previously developed by PNNL for DOE, DoD, EPA, and private industry, as well as methods that are emerging as part of the ISO14000 standards setting process.

Presentation

K.K. Humphreys. 1997. "Application of Life-Cycle Design Tools to Material Systems." Keynote Presentation: 2nd Annual NIST Conference on Computer-Integrated Knowledge Systems for Materials & Systems, September.

Management of International Environmental Treaties in Support of Environmental Security

Glenna S. Shields, Gordon R. Bilyard, Larry A. Bagaasen (Environmental Management)

Study Control Number: PN97068/1209

Project Description

We developed a process model that provides a framework for examining the activities that surround the evolution of international environmental agreements and treaties. The framework is divided into three segments, which encompass the sequence of activities through which environmental problems are recognized and collectively addressed within the international community. This model was based on literature review and personal interviews with individuals involved in various aspects of the international and treaty process.

Technical Accomplishments

We identified three segments representing phases of the environmental treaty development process—initiation, negotiation and entry into force, and implementation and verification—and the transitions between them. The framework is an "ideal" process for identifying, characterizing, and solving environmental problems that cross national boundaries (see Figure 1).

The framework is built around four basic elements—the environmental landscape, the environmental baseline, the environmental problem, and solutions to the problem. We defined the landscape as the abiotic and biotic resources and the ecological processes and functions exhibited among those resources. Two major concepts that are integral to this framework are the degree of adequacy with which the environmental baseline is described, and the type(s) and severity of the risk(s) associated with the environmental. Overlying and influencing the entire process are the "national perspectives" of affected countries. The term "national perspective" is used to represent the collective influence of the cultural, economic, political, military, and social forces that shape a nation's perception of and tolerance for environmental risk.

Figure 2 provides a detailed flowchart of the first segment, the initiation phase. This segment pertains to the existing environment. During this phase environmental problems and associated risks are recognized, characterized, and brought to the attention of the international community. The product of this phase is a validated, or agreed-upon, environmental issue.

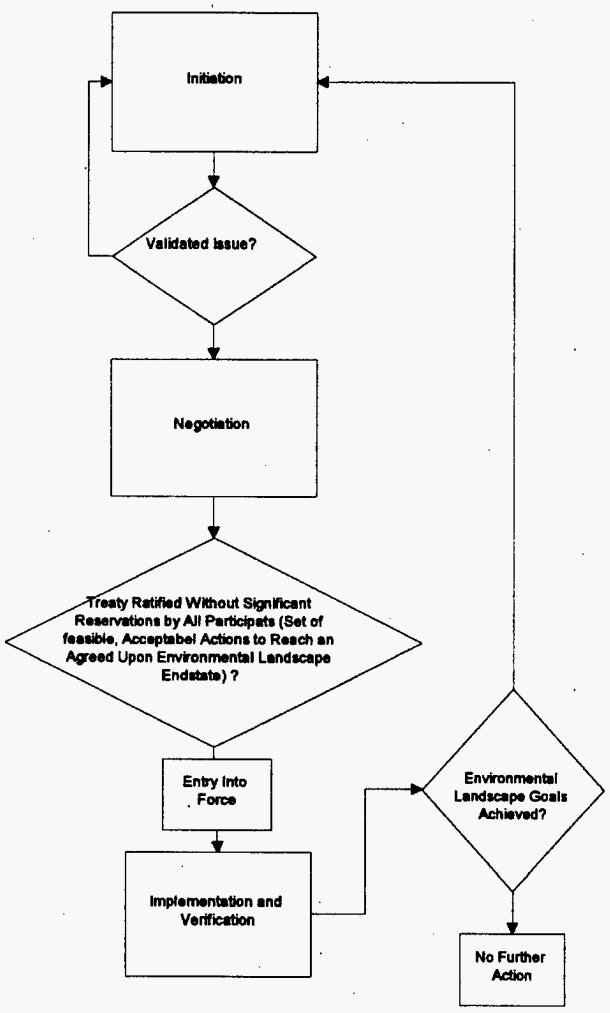

Figure 1. Overview.

Figure 3 illustrates the components of the second segment, negotiation and entry into force. The second segment pertains to the development of consensus on the desired future condition of the affected environmental landscape and the means for attaining that state. During this phase, potential solutions are identified and then tested for technical feasibility as well as acceptability to potential signatories through informal negotiations and scientific inquiry. Formal negotiations produce the final treaty, and ratification by signature nations concludes the activities in this phase by bringing the agreement into force.

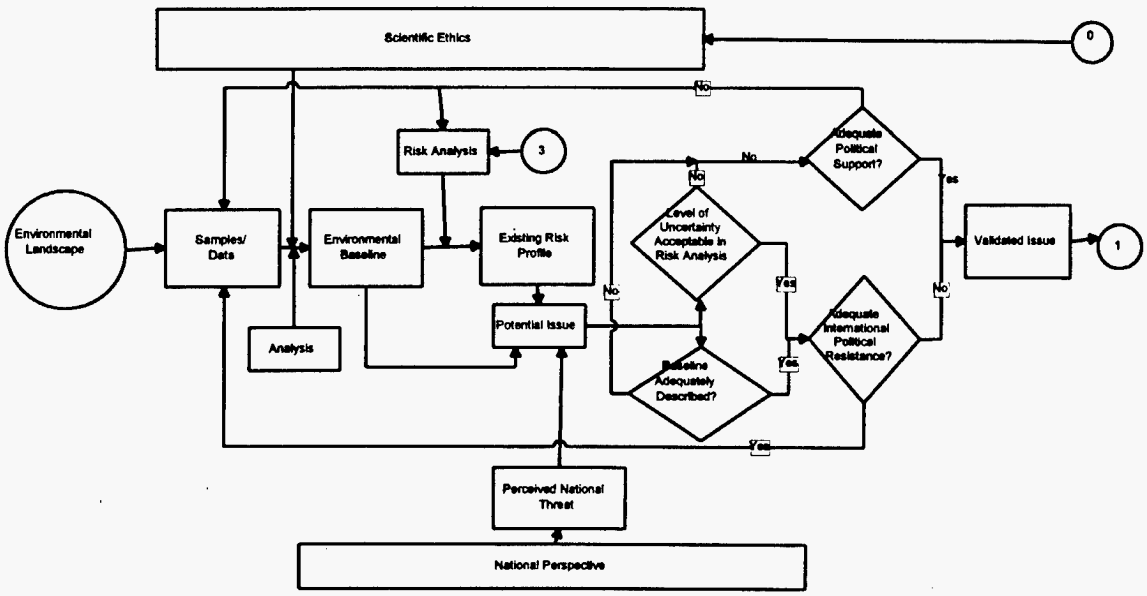

Figure 2. Initiation.

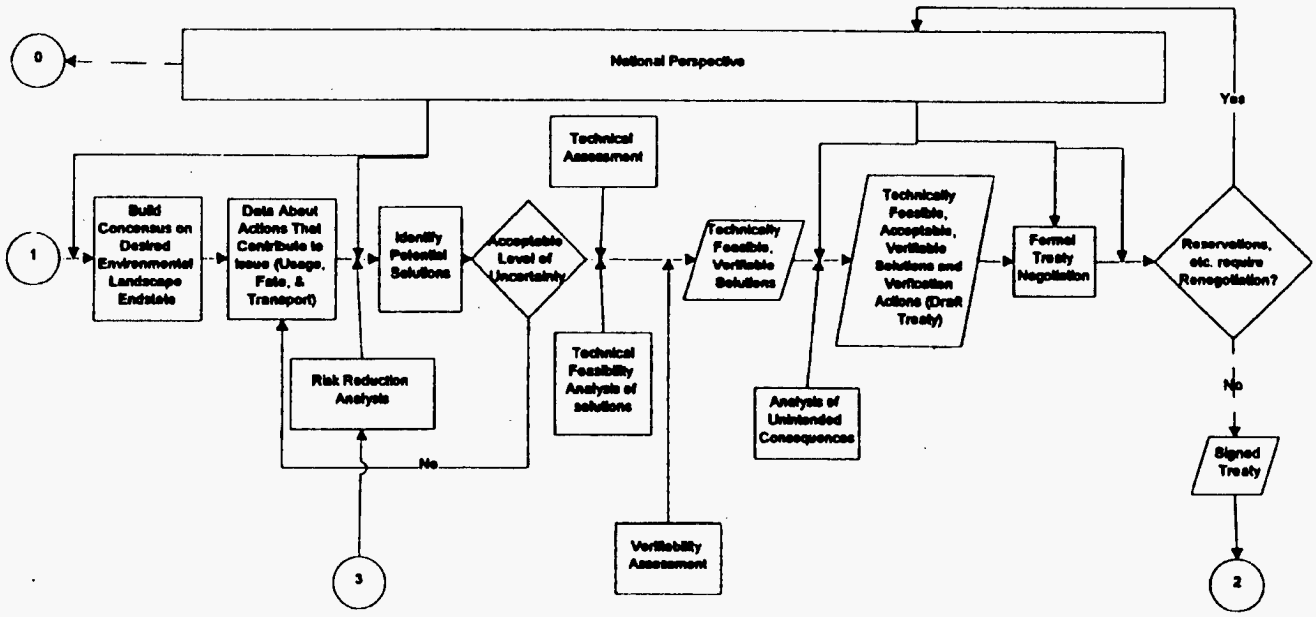

Figure 3. Negotiation and entry into force.

The third segment, shown in Figure 4, pertains to implementing the agreed upon solutions, monitoring their effectiveness in achieving the desired environmental end state, and verifying the adherence of signatories to stipulations of the treaty. Implementation of the solutions involves deployment of technologies that can mitigate environmental problems and reduce the associated environmental risks. This calls for the development and deployment of monitoring and verification technologies to ensure cooperative threat avoidance and identification.

The framework is highly flexible, and is intended to be applied to a broad range of environmental challenges facing the international community. It can be applied to cross border environmental problems that involve two or more member nations, to entire regions, or to global environmental problems. In addition, it can be used by individuals and organizations to explore the activities and processes that collectively result in the development of international environmental agreements. A brief review of several of the existing treaties showed that the treaty documents were generally quite broad and did not help identify technology development opportunities. However, supporting documents developed by committees at various stages in the treaty process contained more pertinent information.

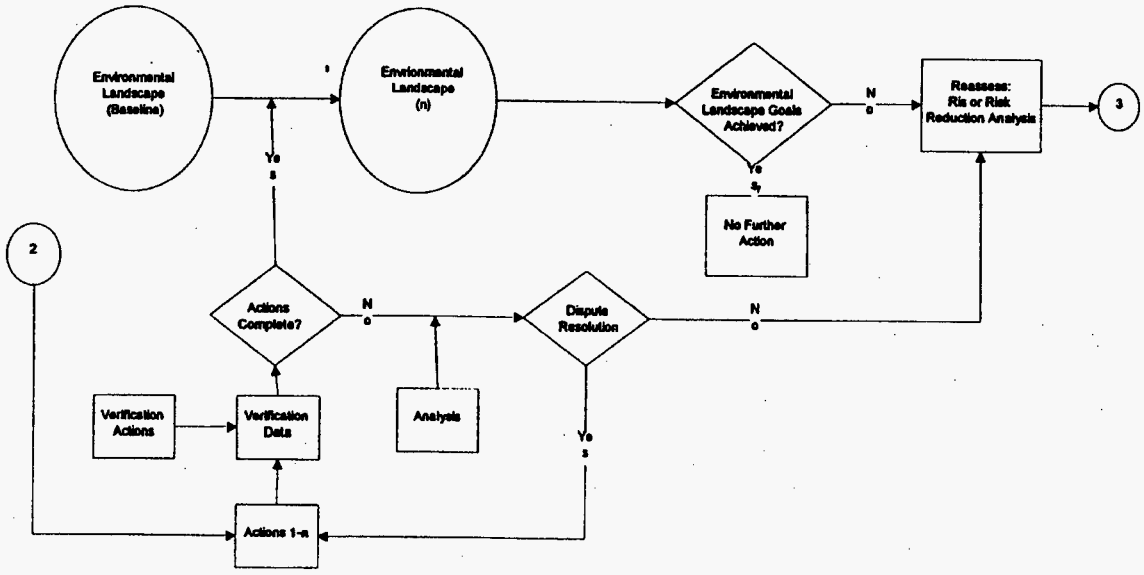

Figure 4. Implementation and verification.

The Montreal Protocol serves as a model for how future environmental treaties are likely to be structured. We examined the Montreal Protocol environmental agreements, and the reports supplied by the associated technology and economics panels to identify the types of technology development needs that emerge during the functioning of these kinds of panels. In addition, although many of the technology innovations required to meet this specific set of agreements have previously been addressed, it nonetheless and indicates the stage in the treaty process where technology development questions will be taken up.

A specific example is provided by the technology assessment panel. The panel established options committees that examined improved conservation and recovery practices, alternate solvents with lower ozone depleting characteristics, and alternate methods that did not require solvents. CFC and Halon banking and destruction issues were specifically examined and required the development of new technologies. Disposal technologies for CFC-containing products, such as closed cell foam products, that have reached the end of their useful life were also addressed. (The committees also operated in the policy realm in setting up such as an essential use program that exempted current critical uses.)

In addition to technological innovations required to deal directly with environmental problems, means for monitoring the impact of these technologies and verifying compliance with treaty provisions would also require that new technologies be developed. Environmental treaties generally do not specify any type of verification process and rely largely on voluntary efforts for compliance. However, the economic advantages gained by not complying with environmental treaty agreements may interfere with voluntary compliance. The large expansion of contraband CFCs that are currently entering the U.S. is an example of the effects of economic incentives interfering with the goals of an environmental treaty. There is considerable debate at this time as to the desirability (and feasibility) of moving toward more structured monitoring and verification processes. If consensus builds for more stringent verification, considerable research and development efforts would be required.

Navigating Obstacles to Environmental Technology Deployment Using Environmental Management Systems (EMS)

Jean E. Shorett (Systems and Risk Management)

Study Control Number: PN97079/1220

Project Description

The purpose of this project was to better understand the role that the International Organization for Standardization Environmental Management System Standard (ISO 14001) can play in better integrating technology development and deployment, and easing the nontechnical barriers to the deployment of new science and technology at DOE sites. In this project, we conducted analyses and developed tools that can be used across the complex to address the organizational and institutional factors influencing technology deployment and implementation.

Background

It is widely recognized that breakthroughs in science and technology are central to DOE's plans for environmental restoration. In addition to scientific and engineering challenges, breakthroughs require integration with a site operator's management system. At Hanford and DOE generally, that can include an assortment of jurisdictional, regulatory, stakeholder, liability, and contractual obstacles that must be navigated using uncertain understanding and tools. And each application starts from scratch—producing glacial progress, great uncertainty, and often inconsistent results for the same technology at the same site and across sites.

Fortunately, things are beginning to change. DOE is actively considering a new approach to environmental management systems—ISO 14001 (International Organization for Standardization Environmental Management System Standard). At RL, Section SM7.1 of Fluor's new contract requires "implementation of an EMS consistent with the principles of ISO 14000." Assistant Secretary Alm told EM staff that ISO 14001 should be adopted. EM-40 is linking ISO 14001 with their management action process. And more broadly, DOE-EH/HQ is preparing an EMS Policy Statement for the Secretary's signature, encouraging use of EMSs across the Complex.

While an EMS approach can have many benefits, a major element is easing the deployment of new technologies. If this were better understood, it could lead to more effective approaches to technology development, managing obstacles more effectively—and therefore cheaper, faster, and easier to navigate. Adopting an EMS-based approach can provide a consistent framework for operations. Sites, activities, and technologies could vary, but the management framework would remain predictable. With this framework, needed information and actions also become more predictable. This allows easier integration with the sites' management structures. Many new technologies need flexible regulatory interpretations.

Of the first seven Project XL efforts (EPA's regulatory flexibility program), three were based on an Ems approach. For example, Lucent Technologies (formerly AT&T Microelectronics) proposed flexibility in NPDES permitting. Their product cycle is 18 months; their permits run for 5 years. This required constant, expensive, time-consuming revisions that blew schedules and lost market share. Their Project XL proposal used ISO 14001 as the framework for negotiating performance-based discharge levels. This will allow Lucent to change the manufacturing mix without renegotiating permits—making the path much smoother for new products. The Project XL efforts are still under way but point to the leverage the ISO standard can have in streamlining, standardizing, and simplifying the path for new technologies. For DOE sites, a more predictable path could well be pivotal in expanding use of new environmental technologies.

If we gain a better understanding of how an EMS-based approach can be used in deploying new technologies, we can amplify the value of science and engineering breakthroughs. Similarly, it can reduce uncertainty and ease the use of new technology. The Laboratory is recognized as a leader in developing environmental technology and as DOE's leading laboratory on ISO 14001. The timing is right to harness these two strengths.

Technical Accomplishments

The DOE Office of Science and Technology "stage-gate" model for technology development and deployment includes both engineering and non-engineering activities important to successful development and deployment of new environmental technologies at DOE sites. A strength of this model is that it specifies kinds of activities that need to be completed, by whom, and in what sequence to proceed along the path from idea to technology deployment. However, it fails to provide a system or

context for doing in a time- and cost-effective manner. For engineering activities, the lack of a system is less of an issue because effort focuses on technical and scientific concerns. For non-engineering activities, however, the lack of a system is problematic because deployment of new technologies is dependent on an integration of technical, risk management, social, legal, and economic interactions. The current failure to develop a standardized platform for deployment undermines the ability of technology developers to consolidate and generalize successful efforts and learn from unsuccessful ones.

Based on interviews with technology developers, deployment experts, and site and program customers, levels of success achieved by different environmental technologies vary but are generally regarded as impaired and underperforming. Reviews and interviews also identified non-engineering activities such as definition of roles and responsibilities, communication, stakeholder engagement, development of strategies for regulatory compliance, budget cycles, and competition as important to success. Reviewed against components of the ISO 14001 standard, this range of issues was at least partially addressed. Interviewees also identified current programs which could be used in a more integrated and systematic approach but were currently fragmented and/or redundant. Site users and program managers viewed performance and cost data available as unreliable, regulatory acceptance and permitting as uncertain, and saw institutional, contractual, and professional barriers to use of new environmental technologies. Conversely, technology developers identified issues concerning management of the development process including funding, capturing of intellectual property, fear of failure, politics, and competition among developing organizations. While clearly important, analysis of these issues with the ISO 14001 standard showed a more modest level of application. However, there was broad consensus that a more effective management framework for the development and deployment of environmental technology was needed. A cross-walk of development and deployment-related issues was developed and series of recommendations prepared.

Presentations

J.E. Shorett. 1997. "Using ISO 14001 to Speed Deployment of New Environmental Technology." Waste Management '97 Conference, Tuscan, Arizona, March.

J.E. Shorett. 1997. "Expanding Roles for ISO 14001 in the Federal Sector." National Association of Environmental Professionals, Orlando, Florida, May. March 13, 1998.

Statistics and Applied Mathematics

Use of Wavelet Methods for the Homogenization of Dynamics

Mary E. Brewster (Theory, Modeling and Simulation)

Study Control Number: PN96072/1139

Project Description

The use of wavelets and the related theory of multiresolution analysis to represent and analyze solutions of systems with multiple length and/or time scales has shown considerable success in recent years. These methods have been applied to a range of partial differential equations, for example, equations describing transport and fluid flow and the time-dependent Schroedinger equation. The development of such methods provides a natural framework for extending molecular information (local interactions and chemistry) toward macroscopic scales (transport and diffusion). Initially, we considered systems containing high frequency, localized components that require a very small time step to resolve numerically such as intramolecular vibrations. These components in turn, have a collective effect on other lower-frequency and possibly delocalized components of the system. Multiresolution homogenization methods recently developed by the principal investigator were found to be appropriate for efficiently and accurately incorporating cumulative effects of high-frequency components while eliminating the need to solve the equation with very small time steps. We concentrated on developing mathematical and computational methods that can be applied to more complex systems. We initiated our studies on model, low-dimensional systems for the purpose of establishing the principles and numerical techniques.

Technical Accomplishments

Molecular dynamic simulations are important in a variety of fields, including environmental modeling, contaminant transport, and design of pharmaceuticals. The exact equations of molecular dynamic for large molecules contain high-frequency components which influence the long-time behavior of the system. Thus, numerical solution procedures require very fine time steps relative to the time intervals on which important behavior such as conformational changes typically occur. The size of the systems to be solved (number of dependent variables) can also be quite large. However, nearby atoms on, say, a polymer chain are expected to behave on the average as a unit. Standard techniques for addressing these problems are generally ad hoc and provide results whose errors are difficult to quantify. There is a need for new mathematical approaches to such multiscale problems.

A new approach to multiscale problems, multiresolution homogenization, was developed by the first author and collaborator Gregory Beylkin of the University of Colorado. This technique is based on the theory of multiresolution analysis, which includes wavelet analysis. The approach consists of two steps:

1. A so-called "multiresolution reduction" procedure that produces a large time step numerical method for obtaining the coarse-scale (average) behavior of the solution.

2. A multiresolution homogenization procedure that produces, from the results of the multiresolution reduction procedure of step 1, a generalized nonlinear system of ODEs whose solutions have the same coarse-scale behavior as the original system, but has minimal fine-scale behavior.

The methodology has been verified on a family of first-order time-dependent ODEs and has proved successful in providing a simple numerical method with a large time step, relative to that required by a standard numerical procedure, which accurately reproduces the coarse-scale behavior of solutions to the original problem. The proposed research will focus on extending and applying this technique to molecular dynamics models.

Significant contributions were made by visiting graduate student Anna Gilbert on extending the multiresolution homogenization methods to nonlinear ODEs. In particular, hybrid asymptotic/numerical methods were developed to ensure a robust and efficient reduction algorithm.

Several alternative formulations of the multiresolution homogenization procedure were also developed. These include an explicit transfer function form and an implicit form appropriate for boundary-value problems. Also, a fast algorithm for stochastic simulations has been proposed and tested.

Presentations

A. Gilbert. 1997. "Homogenization of Nonlinear ODE's." AMS National Meeting, January, San Diego.

A. Gilbert. 1997. "Multiresolution Homogenization Schemes for Differential Equations and Applications." Thesis, Princeton University, Princeton, New Jersey, June.

M. Brewster. 1997. "Multiresolution Homogenization." Sandia National Laboratory, Sandia, New Mexico, and Los Alamos National Laboratory, Los Alamos, New Mexico.

Thermal and Energy Systems

Flat Residential Commercial Light Architecture

Donald J. Hammerstrom (Thermal and Electric Systems Development and Analysis)

Study Control Number: PN96024/1091

Project Description

The purpose of this project was to develop a flat architecture for residential and commercial lighting. The lighting fixtures would fuse the functions of conventional room lighting and architectural structure. The distribution of light source over flat structures should greatly increase light quality and eliminate shadows. Less total light and light power are needed if one places light exactly where it is needed and distributes that light evenly. The flat light architecture might eventually serve the functions of ceiling and floor panels, desk tops, and moveable picture frame light panels. Flexible flat light structures might be molded around computer screen cabinets and safety equipment like children's bicycle helmets.

In FY 1997, a new plasma test stand was assembled, and a cathodoluminescent phosphor that had been developed at PNNL was qualitatively tested. In addition, information was collected to define what appears to be a fundamental phosphor criterion for anyone using a similar lighting approach. A laser design concept was tested, a flat dielectric wave-guide was designed, and a free-form lighting design to be constructed completely from sol-gel material was designed.

Background

The fluorescent tube has proven itself inexpensive, effective, and long-lived. However, the fluorescent primary lighting industry is still vulnerable to competition. First, fluorescent tubes achieve about 30% energy conversion efficiency. This efficiency is respectable, but it leaves room for revolutionary improvement. Second, the standard fluorescent tube contains mercury and is increasingly treated as a toxic waste. Manufacturers who reduce or eliminate mercury from their designs may profit. Third, one cannot deviate far from the geometry of the ubiquitous 40-watt fluorescent tube and still maintain efficiency. Finally, the human engineering of workplaces has become critical from the lighting perspective. The value of even small gains in worker productivity due to human engineering of lighting far exceeds the initial lighting capital costs.

Silent discharge plasmas were chosen as the flat light architecture technical path to investigate in FY 1996. In a silent discharge, at least one electrode is covered with a dielectric barrier, and the system can be excited only by an alternating-current electrical excitation. The silent discharge plasma is stable over a range of pressures from less than 10 kPa to about 300 kPa.

Technical Accomplishments

Several flat and annular silent discharge plasma test articles were designed, built, and tested in FY 1996. Both the flat and annular geometry supported noble gas plasmas equally well. Flat plasma regions of depth about 3 mm were the narrowest tested. High voltages created some problematic arcs from exposed edges of electrodes around the dielectric barrier. Typical excitation voltages were 1 kV, and alternating-current frequencies from 60 Hz to tens of kilohertz were successfully used.

Several gas combinations were observed to emit ultraviolet light near the important ultraviolet emission lines of mercury. However, our demonstrated efficiency of electrical to light energy conversion has not yet exceeded 1%.

A new, more compact plasma test stand was constructed in FY 1997. Using this test stand, a cathodoluminescent phosphor that had been synthesized at PNNL was exposed to the silent discharge argon plasma. The hypothesis behind this test was that the micro-streamers in the alternating-current discharge would excite the cathodo-luminescent phosphor. Phosphor emission was unfortunately minimal.

Calculations were performed to determine the design parameters for a thin dielectric light waveguide. The designed waveguide would conduct ultraviolet excitation but not visible (phosphor centers embedded in the dielectric would manufacture visible light that must exit the wave-guide in a diffuse manner). A possible limitation is posed by the need to introduce moderate optical powers into a dielectric layer about one-quarter of a micrometer thick. We also combined two published sol-gel processes whereby the sol-gel might both contain the excitation centers (mercury, perhaps) and act as the phosphor.

High Performance Micro Heat Engine Development

Perry A. Meyer (Fluid Dynamics)

Study Control Number: PN95039/1015

Project Description

Lightweight, portable, and modular power generation is a key technology for meeting a range of DOE missions including distributed and manportable power generation. There is a very strong and growing demand for small capacity (about 1 to 100 kW), compact, fixed, and portable, power generators that are efficient, have reduced emissions, and have fuel switching capabilities (including biomass fuels). This project explored a novel heat engine/power generator concept that has the potential for high efficiency, high reliability, and relatively low manufacturing cost compared with conventional engines. The engine is externally fired (multi-fuel), quiet, and promises to be much less expensive to manufacture than comparable engines.

The engine uses vapor (working fluid) bubble injection into a rotating heated liquid (base fluid) to impart kinetic energy to the liquid via centrifugal buoyant pumping (see Figure 1). The base fluid energy can be extracted mechanically via turbines (impact or reaction) or directly via magnetohydrodynamic generators. The magnetohydrodynamic mode requires the base fluid to be a liquid metal.

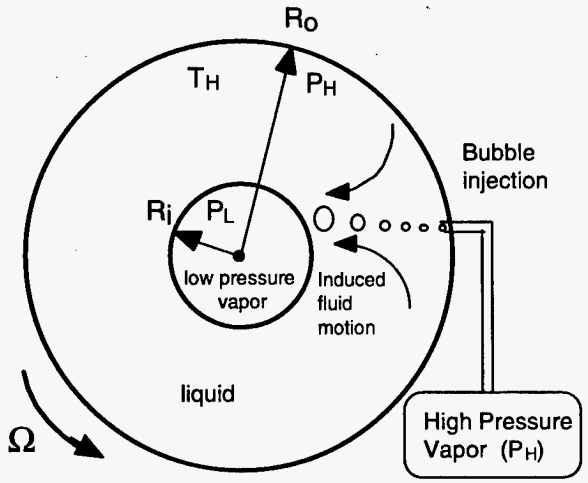

Figure 1. Bubbly flow energy conversion in a rotating liquid annulus.

The main objectives of this project were 1) demonstrate the bubble injection/base fluid motion energy conversion process which is the key principle of operation, and 2) develop theoretical models describing component processes and system performance.

Technical Accomplishments

Thermodynamic Cycle

The energy conversion process shown in Figure 1 can form the basis of a closed cycle heat engine with some very favorable features. After the vapor bubbles are separated from the base fluid, the vapor is collected, processed in a closed cycle thermodynamic cycle, and reintroduced as new injected bubbles. The optimum thermodynamic cycle for the engine is shown in Figure 2. Shown is an isothermal vapor compression cycle that approximates a Carnot cycle. Of particular importance is the isothermal expansion stage (4 to 5). Here, the saturated working fluid vapor is injected into the base fluid and expands as it moves toward the center of rotation. This is an isothermal process since the base fluid is maintained at constant temperature by the external heat source and the bubbles are very small. Work is extracted in this process and imparted to the base fluid in the form of kinetic energy. Since the process is isothermal, all losses (due to slip, turbulence, etc.) will be intrinsically recuperated since lost energy is made immediately available in the form of high-grade heat. Hence, the overall efficiency of the working cycle can be larger than the component efficiency of the expansion stage. The efficiency improvement is shown graphically in Figure 3.

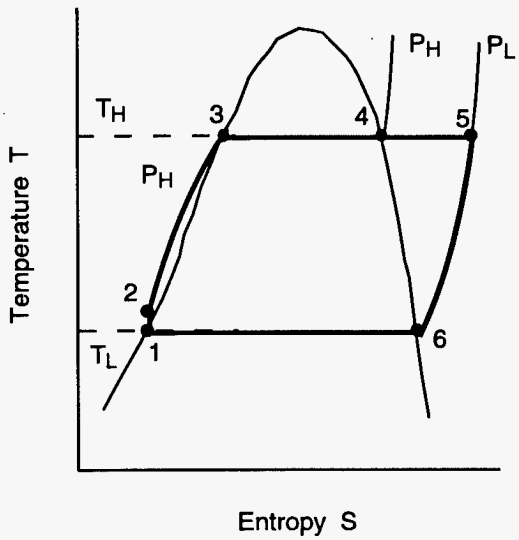

Figure 2. The ideal vapor compression cycle.

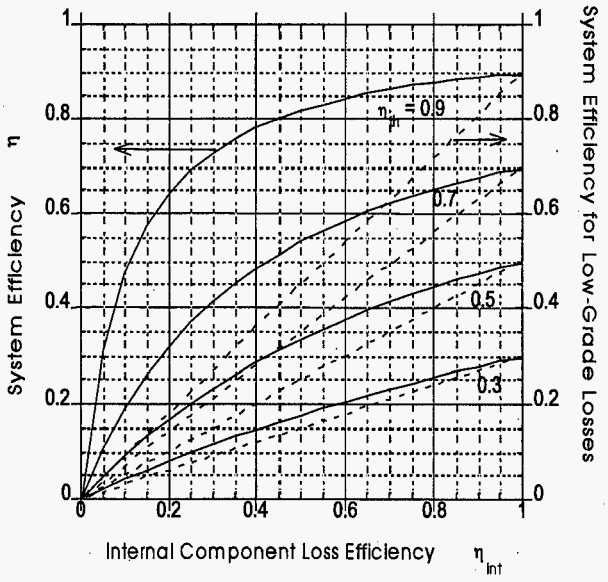

Figure 3. System efficiency for engine with adiabatic losses.

System Performance

Under the assumption of no slip between the bubbles and the working fluid, simplified equations governing the basic hydrodynamic system were formulated. These form an ideal set of performance equations that are approximately correct for a small amount of slip. The radial pressure distribution in the bubbly flow annulus of the engine is governed by

$$dp/dR=(1-\phi)\rho\Omega^2R \qquad (1)$$

In order to integrate Eq (1), the working fluid vapor void fraction $\phi(p)$ must be known. Using the fact that the bubble expansion process is isothermal, then applying continuity to the working fluid and the base fluid, respectively gives

$$\phi=\Pi\phi_o/(1+(\Pi-1)\phi_o) \qquad (2)$$

where $\Pi = p_o/p$ is the pressure ratio. Eq (1) can be integrated to obtain an implicit relation for the pressure ratio given by

$$\Pi+\Pi\phi_o/(1-\phi_o)\ln\Pi=\Pi_\Omega(1-r^2) \qquad (3)$$

where $r = R/R_o$. The quantity Π_Ω in Eq (3) is a dimensionless centrifugal pressure contribution given by

$$\Pi_\Omega=\rho\Omega^2R_o^2/2p \qquad (4)$$

The driving pressure differential created by the pressure imbalance between the upper, bubbly flow annulus and the lower, pure base fluid annulus is $p_L - p_o$ where $p_L=\rho\Omega^2R_o^2/2$.

The nondimensional differential driving pressure is given by

$$\Delta\Pi\equiv(p_L-p_o)/2=\Pi\phi_o\ln\Pi/(1-\phi_o) \qquad (5)$$

Equations (2) through (5) form a set of parametric design equations for engine performance.

Hydrodynamic Efficiency

The efficiency of centrifugal buoyant pumping energy exchange was found to depend primarily on the bubble slip velocity. The slip, or relative velocity of the bubbles will depend on a number of parameters including base fluid properties, bubble size, rotation rate, and radial position, assuming spherical bubbles limit expressions for the relative velocity where found. For low bubble Reynolds numbers, the Stokes flow limit applies and the slip velocity is

$$u_s=\Omega^2Rd^2/18\nu \qquad (6)$$

where d is the bubble diameter and ν is the kinematic viscosity of the base fluid. For bubble Reynolds numbers which are large, the relative velocity is given by

$$u_s=2\Omega\sqrt{Rd/3C_D} \qquad (7)$$

Example Design

Consider a two-stage engine operating between 60°C and 320°C and producing 100 kW output power. The low-temperature working fluid is R-11 and the high-temperature working fluid is Toluene. The base fluid specific gravity is assumed to be 10, corresponding to a liquid metal. Each cycle has a low pressure, p, of 45 psi and a high pressure of 600 psi corresponding to a pressure ratio, Π, of about 13. The theoretical efficiency for the engine is about 42%. The engine modules rotate at 1800 rpm. We assume an initial vapor bubble void fraction ϕ_o of 3%, corresponding to a maximum void fraction of about 30% at the inner radius. The driving pressure in the base fluid loop is about 45 psi. We also assume that the base fluid velocity, u_o is only 2 m/s, a very conservative assumption. From the design equations, we find that the outer radius, R_o, is about 50 cm and the inner radius is 39 cm. Therefore, the radial length of the bubble annular flow region is only about 5 cm. The channel height is determined to be 5 cm. Assuming a

90% conversion efficiency, a slip ratio of 0.1 is required. This requires the bubble diameter to be on the order of 10 mcrons.

Laboratory Testing

A proof-of-principle demonstration project was carried out at PNNL in FY 1997. The purpose of the project was to demonstrate the centrifugal buoyant pumping process which is fundamental to the engine. Tests were performed with compressed air (representing the working fluid) and water (representing the base fluid) at rotation rates up to 450 rpm. Buoyant pumping was confirmed. No measurements of efficiency were available due to difficulties with measuring the base fluid (water) flow rate in the rotating environment. The apparatus is shown in Figure 4. Several improvements to the design were performed. The initial apparatus did not use radial symmetry. The bubbly flow moved radially inward in a constricted channel. Strong swirl was observed via high-speed video as the flow moved radially inward. Later modifications provided symmetric radial flow. Bubble injection was carried out by using chemically etched stainless steel screens with hole diameters ranging from 75 microns to 175 microns. Very small bubbles were observed, confirming that efficient operation was possible.

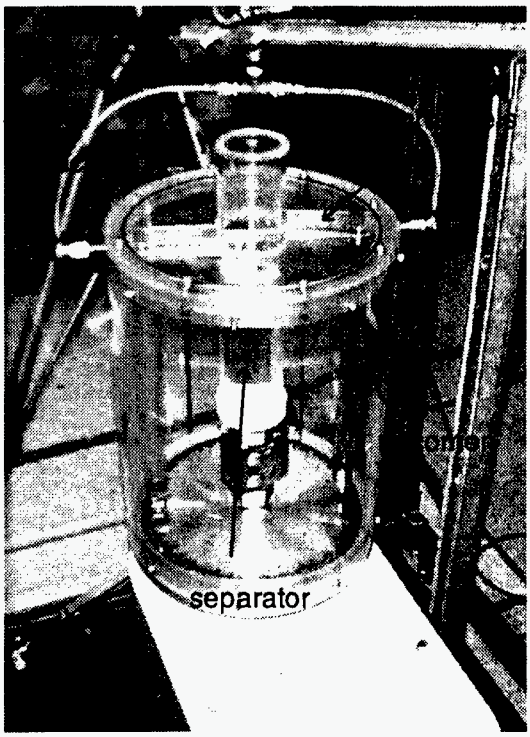

Figure 4. Test apparatus for demonstrating centrifugal buoyant pumping in air/water.

Integrated Mesoscopic Fuel Cell and Fuel Processor

M. Kevin Drost, Daryl R. Brown, Annalee Y. Tonkavich (Thermal and Electric Systems)

Study Control Number: PN97056/1197

Project Description

Using the high rates of heat and mass transfer attainable in microstructures, we will develop a mesoscopic integrated fuel cell and fuel processor that will allow for the efficient use of hydrocarbon fuels for small-scale power generation applications (1 We to 1000 We). Currently, we are planning to focus on issues related to removing CO from the exhaust of a microchannel partial oxidation reactor. The proposed device will be relevant to DOE needs in building and transportation energy efficiency and will have strong national security benefits.

Background

The key to obtaining high-energy storage density is the use of hydrocarbon fuels as the energy source. Hydrocarbon fuels typically store 13,000 Wt/kg (or 4,000 We assuming a 35% conversion efficiency of chemical energy to electric energy), while currently available batteries store 120 We/kg. The system will consist of liquid hydrocarbon fuel storage, a microchannel fuel processor, and a microchannel fuel proton exchange membrane (PEM) fuel cell.

The key element to the system is the fuel processor, which will produce hydrogen from a hydrocarbon fuel such as methanol or butane. We have demonstrated partial oxidation of hydrocarbon fuels in the 150 W size range, and we need to demonstrate our ability to scale this technology down to the 2 W size. In addition, we need to demonstrate our ability to remove CO and sulfur from the hydrogen stream. We will investigate two approaches for mitigating impurities in the hydrogen stream:

- Inclusion of a microchannel water shift and preferential oxidation reactor to remove CO and SO_2.
- Inclusion of microfluidic devices to allow regeneration of individual PEM fuel cells. The system would allow individual cells to be taken out of service and regenerated with air to remove CO thus reducing the need for a high degree of purity in the H_2 stream.

We will review a number of fuel cell technologies for small size applications; however, PEM fuel cells do appear to have significant advantages in this size range. The PEM fuel cell is well developed in larger sizes and the focus of our work will be on 1) developing a design that can take advantage of microfabrication techniques, 2) thermal management of a very small system and 3) on the development of miniature support equipment such as fans. We anticipate that the major technical challenge will be development of miniature support equipment.

This project platform will enable a number of products ranging from systems with a generating capacity of 1 to 2 We to systems with a generating capacity in the kWe size range.

- Portable Power Generation - There is a very large market for small (1 to 100 We) autonomous power sources for remote or portable power generation. Applications include commercial applications such as power supplies for portable electronics and Department of Defense applications such as man-portable cooling and remote or clandestine sensing. National Aeronautical and Space Administration (NASA) applications include space power. The key characteristics of systems for this class of application are small size, very long life, and reliability.
- Distributed Power Generation - In the 1-kWe range, the integrated mesoscopic fuel cell and fuel processor is a candidate for distributed power generation for utility, mobile, or remote applications. Users would include both utilities and DoD.
- Transportation Power - In still larger sizes, the integrated fuel cell/fuel processor may be a candidate for automotive applications.

If successful, this project will result in a product with high technical content and the potential for a very large market. In the small size range, we are proposing development of a chemical alternative to the battery with the potential for a factor of 10 to 100 increase in energy storage density without the use of dangerous materials such as lead or lithium.

Technical Accomplishments

FY 1997 activities focused on developing the road map, conducting system studies, and demonstrating the ammonia fuel cell. Specific accomplishments include

- System Studies - A variety of fuels (methanol, gasoline, light hydrocarbon, gasoline), fuel processor technology (steam reforming and partial oxidation) and fuel cells (PEM and solid oxide) are available. This task focuses on evaluating the various combinations of fuels, fuel cells, and fuel processors and fuel cells with the objective of identifying the most attractive options. Preliminary system studies were completed in FY 1997. Key results include the selection of the preferred fuel cell, the identification of two attractive fuel processor options, and the selection of the preferred hydrocarbon fuel. Based on a review of open literature and a number of personal contacts, we conclude that no current or projected technology is competitive with the integrated fuel cell/fuel processor for long-duration, small-size power generation. Typically competing systems are 4 to 6 times heavier. This includes a direct methanol fuel cell and advanced hydrogen storage.

- Ammonia Fuel Cell Demonstration - The ammonia fuel cell sensor developed in FY 1997 was tested as a power producer with higher concentrations of ammonia. The results showed the power density and efficiency of the ammonia fuel cell was far below that required for successful application in small distributed fuel cells. Based on these results, we will not pursue the ammonia fuel cell concept.

- 10-We Fuel Processor Demonstration Design - The design of a 10-We fuel processor demonstration was completed in FY 1997. This activity focused on identifying and resolving issues associated with operating very small high-temperature chemical reactors.

Mesoscopic Heat Actuated Heat Pump

Michele Friedrich, M. Kevin Drost (Engineering and Analytic Science)

Study Control Number: PN97070/1211

Project Description

This project's research is focused on assembly, demonstration, and performance characterization of a complete mesoscopic heat-actuated heat pump. This project will demonstrate our ability to integrate microtechnology-based components into complete systems.

Heat and mass transfer are immensely improved in microstructures and heat-actuated heat pumps rely primarily on heat and mass transfer to provide the "vapor compression" effect instead of using mechanical work. This makes heat-actuated heat pumps an attractive option for energy systems miniaturization.

Previously, researchers at PNNL have successfully demonstrated all of the microtechnology-based components of a mesoscopic absorption cycle heat pump except for the miniature liquid pump. Microtechnology-based evaporators and condensers were shown to have heat transfer coefficients that exceed 3.0 W/cm^2-K. In addition, a range of conceptual designs of the microchannel absorber and desorber have been tested. The results confirm analysis prediction of high absorption rates due to microstructure mass transfer enhancement. Using ammonia absorption in water, we have demonstrated the ability to absorb ammonia at a rate that generates 10 W/cm^2 of heating. We believe that we can ultimately reach a heat generation rate of 30 W/cm^2. And using desorption of water from lithium bromide, we have demonstrated a heat transfer rate of 0.1 W/cm^2-K. We believe we can achieve 1 W/cm^2-K with the right membrane.

Technical Accomplishments

FY 1997 mesoscopic heat-actuated heat pump demonstration focused on the following four activities:

1. Cycle Simulation - The ABSIM computer code developed at ORNL was used to simulate the performance of a bench-top LiBr absorption cycle heat pump. The results of this task were used to support the design of the components and the test apparatus.

2. Desorber Membrane and Pump Tests - A number of desorber membranes were tested in the desorber test apparatus developed in the FY 1996 thermochemical compressor project. The results showed that desorption rates of up to 0.3 g/min-cm^2 could be attained which is 18 times the rate of desorption in a macroscale falling-film desorber. A number of miniature, commercially available pumps were tested for use in the lithium bromide-water absorption heat pump. The pumps were tested for operation at test condition flow rates and under vacuum.

3. Heat Pump Component Design and Fabrication - The heat pump components were designed for the heat and flow rates obtained from the ABSIM simulation and for minimal pressure drop. The components were fabricated, assembled, and installed in the test apparatus. Pictures of the components are shown in Figure 1.

4. Design and Assembly of the Heat Pump Test Apparatus - The heat pump test apparatus was designed to minimize pressure drop while obtaining enough information to characterize and troubleshoot the performance of the heat pump. The test apparatus was assembled and commissioned.

Results of the FY 1997 LDRD mesoscopic heat pump project include ABSIM simulations of a test apparatus for a bench-top single-effect lithium bromide-water absorption cycle heat pump, and a completely assembled single-effect absorption cycle heat pump composed of microtechnology-based components.

Future work will focus on the completion of the heat pump demonstration and the design, development, and demonstration of an advanced heat-actuated heat pump.

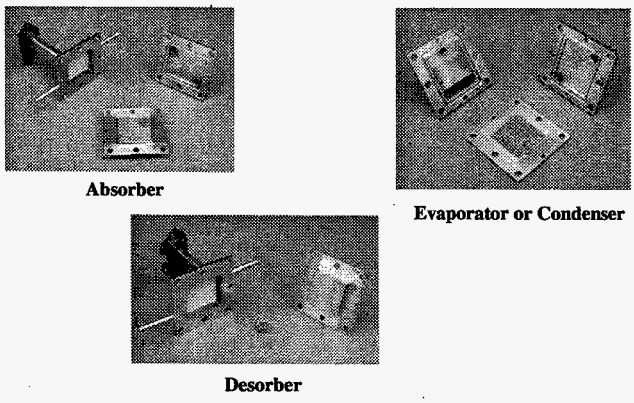

Figure 1. Absorption heat pump components.

Publications and Presentations

M.K. Drost and M. Friedrich. 1997. "Miniature Heat Pumps for Portable and Distributed Space Conditioning Applications." Proceedings of the Intersociety Energy Conversion Engineering Conference. Vol.2, pp. 1271-1274. Honolulu, Hawaii, July.

ASHRAE Forum "If A Wallet-sized Absorption Heat Pump Can Be Built, Does Anybody Care?". This forum produced three articles, written by editors, which were published in the following magazines: *Mechanical Engineering* (July), *Appliance Manufacturer* (May), and *Air Conditioning, Heating and Refrigeration News* (April 7).

Microscale Air-Side Heat Transfer Enhancement

M. Kevin Drost, Michele Friedrich (Energy Division)

Study Control Number: PN96048/11156

Project Description

Microchannel evaporators have been demonstrated to obtain heat flux rates up to 250 W/cm^2 on the refrigerant side of the heat exchanger. The use of microscale evaporators in air source heat pumps is limited by the air-side heat transfer resistance. To take advantage of the high performance of the microscale evaporators and condensers, a method to enhance the air-side heat transfer, using microtechnology, needs to be developed.

The research included in this project is focused on enhancing air-side heat transfer in microscale sheet heat exchangers. The air resistance is a bottleneck in obtaining high performance from the micromachined heat exchangers and the microscale sheet heat pump. This effort focused on evaluating current concepts and methodologies to enhance air-side heat transfer and a range of micromachining methods that could be used to produce microscale enhanced surfaces, and on designing and fabricating a proof-of-principle demonstration for one passive and one active concept.

Currently, we have identified at least three active microscale options for enhancing air-side heat transfer.

It is likely that any successful microscale heat transfer enhancement technique will also be applicable to mass transfer. This may allow the use of microscale mass transfer enhancements to further improve the performance of mass transfer in microstructures.

Success in demonstrating an attractive microscale enhancement technique for gas phase heat transfer would be relevant to the DOE's Office of Engineering Sciences and to DOE's Office of Industrial Technologies' heat exchanger development program. Other applications may exist in DOE's Office of Building Technologies (HVAC applications) and Office of Transportation Technologies (automotive radiator applications).

Specific objectives of the project include

- identify and assess options for microscale air-side heat transfer enhancement
- use simulation and experimental investigations to understand the impact of secondary flows within the laminar boundary layer on heat transfer
- design, fabricate, and test one active microscale air-side enhancement.

Technical Accomplishments

In FY 1997, this research effort involved four tasks primarily focused on understanding the impact of secondary flows within the laminar boundary layer on both natural and forced convection heat transfer. We relied on an array of microjets to entrain flow from the laminar boundary layer and consequently draw fluid into the laminar sublayer. The four tasks included 1) computer flow modeling, 2) design and fabrication of multiple samples of the active heat transfer enhancement, 3) modification of the exiting test apparatus to allow testing of forced convection enhancement schemes, and 4) testing of test articles fabricated in task 2.

Results to date suggest that the microtechnology-based enhancement scheme can enhance free convective heat transfer to air by up to 1000%, which approximately matched the level of enhancement predicted by computer simulation. Flow visualization showed that there was significant flow maldistribution and that up to one-half of the enhanced surface was not being effectively enhanced. This suggests that performance can be substantially improved.

Free and weakly forced convection heat transfer can be enhanced by a factor of at least four. Typically, finning will enhance heat transfer by a factor of 3 so the proposed system exceeds the performance of finning without the weight and volume of the fins. As we understand the impact of maldistribution, heat losses from the header region and the conduction to the surrounding material on relative enhancement, we expect the performance of the system to improve relative to the unenhanced surface.

Molecular Dynamics Simulation

Bruce J. Palmer (Theory, Modeling and Simulation)

Study Control Number: PN97076/1217

Project Description

Molecular dynamics simulations will be used to examine the hydrodynamic behavior of fluids in microchannels and to help in the development of appropriate constitutive relations and boundary conditions for simulating flow at the micron scale. While it is not possible to simulate micron-scale flows directly using molecular dynamics simulations, it should be possible to use the simulations to parameterize mezoscopic simulation techniques, such as lattice-Boltzmann simulations. Molecular dynamics can be used to examine the behavior of liquids near the hydrodynamic limit and to identify nonclassical effects that may influence fluid behavior at the micron scale. These might include the effect of Brownian fluctuations on the fluid flow and nonstick boundary conditions at small length scales, as well as a variety of surface phenomena. While these effects are usually negligible at macroscopic scales, they may dominate the behavior of microscale flows.

Modeling will use state-of-the-art molecular simulations to guide the development of appropriate mezoscopic simulation techniques. Simulations will be done using simplified models that allow calculations containing from 50,000 to 1,000,000 particles. These should be large enough to begin approaching the hydrodynamic limit from the microscopic side. The simulations will be used to examine the behavior of fluids in micropores and micro-channels, the relaxation behavior of fluids in confined geometries, the behavior of velocity fields near the solid-liquid interface, and surface tension between different phases.

Technical Accomplishments

A parallel code for molecular dynamics simulations was developed for use in molecular dynamics simulations of fluids in microchannels. The code used a spatial decomposition scheme to evenly distribute the data for all the particles to each of the available processors. Simulations performed with this code using four processors of an SGI Power Challenge computer have contained from 30,000 to 50,000 particles. A simulation of 20,000 steps on a system in this size range can usually be done overnight. Simulations were performed on a thin film of fluid confined between two flat parallel plates. For the periodically replicated configurations used in the simulation, this resulted in an infinite film of fluid. The simulations provided information on the density profile of the fluid throughout the system, the behavior of the stress tensor as a function of position, the relaxation behavior of fluid fluctuations as a function of position, and the relaxation of a parabolic velocity profile as a function of time. Two types of systems were examined, the only difference between the systems being the strength of the wall-fluid interaction. This was varied from a relatively strong interaction to a weak interaction. The main effect of changing the strength of this interaction appeared to be a change in the wetting properties of the fluid with respect to the solid.

Results were obtained from simulations on a thin film of fluid trapped between two solid walls for different values of the wall-fluid interaction strength. Density profiles of the fluid as a function of the coordinate perpendicular to the wall showed that the strong wall-fluid interaction case creates substantial structuring of the fluid near the wall while the weak interaction shows almost no structuring at all. The density variation occurs over a range of 5 or so particle diameters in both cases, suggesting that the influence of the wall on the fluid decreases rapidly with increasing distance from the wall. The behavior of the stress tensor also indicates that the influence of the wall on the fluid is relatively short-ranged and comparable to the range of oscillations in the density profile. There do not appear to be any correlations building up in the fluid near the wall that lead to long-ranged behavior in the stress tensor, which could in turn lead to nonhydrodynamic behavior in the liquid. Examination of the relaxation of short length scale spontaneous fluctuations in the micro-scopic velocity field show that the dynamical properties of the fluid are only weakly perturbed by the wall. The results showed that the fluctuations decay on approximately the same time scale throughout the fluid although right next to the wall the fluctuations decay with a slightly different time scale that appears. However, this effect appears to be very small.

The most interesting results from this study came from examining the relaxation of a parabolic velocity profile inside the microchannel. A parabolic velocity profile was created at the beginning of the simulation by adding a small incremental velocity to each of the fluid particles. The behavior of the transient for the case of the strong wall-fluid interaction is shown in Figure 1. The behavior of an

analytic calculation of the transient assuming stick boundary conditions is also included for comparison. The behavior of the transient seen in the simulation is very similar to the analytic solution, although it appears to decay on a faster time scale than the analytic result. This may point to some additional nonhydrodynamic effects, such as coupling to Brownian fluctuations, that cause the system relax more quickly.

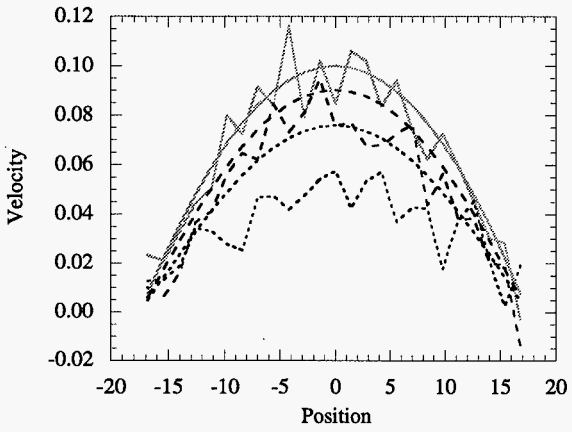

Figure 1. Comparison of decay for parabolic velocity profile from simulation with analytic solution calculated assuming stick boundary conditions. The solid line is for t=0, the dashed line is for t=15, and the dotted line is for t=37.5 (time is in reduced units). The smooth curves are the analytic solution, the noisy curves are the simulation results.

The behavior of the parabolic velocity transient for the weak wall-fluid interaction is very different from the strong wall-fluid interaction. For this case, there is very good agreement between the simulation and the analytic result with slip boundary conditions. These results demonstrate clearly that the boundary conditions on the hydrodynamic equations will depend on the wall-fluid interaction, at least at very small length scales. Whether this remains true at larger length scales will require more investigation.

These simulations provide some insight into the simulation of microscale flows using conventional hydrodynamic approaches as well as raising some issues that will require further investigation to resolve. They are

1. There does not appear to be any significant spatial dependence of the fluid properties created by the presence of the wall-fluid interface. The total volume of fluid with properties that are different from the bulk fluid is probable negligible for fluid channels with dimension on the scale of microns.

2. Simulations of the decay of the parabolic velocity profile suggest that the relaxation time in the micro-channel is slightly faster than predicted by a conventional hydrodynamic treatment. The reason for this is unclear, but indicates that something is renormalizing the effective viscosity for the microchannel.

3. Simulations of the decay of the parabolic velocity profile also show that there is a sensitive dependence on the choice of boundary condition to the properties of the wall-fluid interaction.

Publication

B.J. Palmer. "Direct Simulation of Hydrodynamic Relaxation in Microchannels." *J. Chem. Phys.* (to be submitted).

Acronyms and Abbreviations

Acronyms and Abbreviations

2D-PAGE	two-dimensional polyacrylamide gel electrophoresis
APL	Applied Physics Laboratory
APS	Advanced Photon Source
BW	biological warfare
CE-SDS	capillary electrophoresis-sodium dodecyl sulfate
CORE	collaboratory research environment
COTS	commercial off-the-shelf
CP	cross polarized
CTBT	Comprehensive Test Ban Treaty
CW	chemical warfare
DARPA	Defense Advanced Research Projects Agency
DCA	dichloroacetate
DMMP	dimethyl methylphosphonate
DMSO	dimethyl sulfoxide
DNAPL	dense nonaqueous phase liquids
EDTA	ethylenediaminetetraacetic acid
EMSL	Environmental Molecular Sciences Laboratory
EPR	electron paramagnetic resonance
ESD	electron-stimulated desorption
ESI	electrospray ionization
ESI-MS	electrospray ionization mass spectrometry
ESIX	electrically switched ion exchange
FEAST	Feature Extraction and Signature Tracking
FNR	ferredoxin-NADPH-reductose
FRAMES	Framework for Risk Analysis in Multimedia Environmental Systems
FTICR	Fourier transform ion cyclotron resonance
GCAM	Global Change Assessment Model
GChM	Global Chemistry Model
GC/MS	gas chromatography/mass spectrometry
GNP	glycine nitrate process
GPCR	gas-phase corona reactor
GSTs	glutathione S-transferases
HEPA	high efficienty particulate air
HERMES	Health and Ecological Risk Management and Evaluation System
HTLC	hydrotalcite-like compounds
ISRM	in situ redox manipulation
LBNL	Lawrence Berekeley National Laboratory
LEED	low energy electron diffraction
LLW	low-level waste
MALDI	matrix-assisted laser desorption ionization
MAPK	mitogen-activated protein kinase
MAS	magic angle spinning
MASS	magic angle sample spinning
MEC	microelectrochemical cell

MEPAS	Multimedia Environmental Pollutant Assessment System
MOs	molecular orbitals
MPI	Message-Passing Interface
MPR	micromachined plasma reactor
MS	mass spectrometry
NAPL	nonaqueous phase liquids
NARSTO	North American Research Strategy for Tropospheric Ozone
NASA	National Aeronatics and Space Administration
NIST	National Institute for Science and Technology
NMR	nuclear magnetic resonance
NNSF	near net shape forming
NTA	nitrilotriacetate
PAHs	polynuclear aromatic hydrocarbons
PBPK	physiologically based pharmacokinetic
PCB	polychlorinated biphenyls
PCE	perchloroethylene
PCR	polymerase chain reaction
PNC-CAT	Pacific Northwest Consortium Collaborative Access Team
RAMS	Regional Atmospheric Modeling System
RPA	Replication Protein A
RTDS	Rapid Thermal Decomposition of precursors in Solution
RTUIS	real-time ultrasonic imaging system
SAMMS	self-assembled monolayers on mesoporous supports
SARA	Superfund Amendments and Reauthorization Act
SEM	scanning electron microscope
STM	scanning tunneling microscope
TBP	TATA-box binding protein
TCA	trichloroacetate
TCE	trichloroethylene
TeCH-RD	tetrahydroquinone reductive dehalogenase (aka) tetrachloro-*p*-hydroquinone
TEM	transmission electron microscopy
TNT	trinitrotoluene
UXO	unexploded ordnance
VOAG	vibrating orifice aerosol generator
VOC	volatile organic compound
XAFS	x-ray absorption fine structure
XPAC	xeroderma pigmentosum A complementing
XPS	x-ray photoelectron spectroscopy
XRD	x-ray diffraction

Report Number (14) PNNL--11860

Publ. Date (11) 199803

Sponsor Code (18) DOE/ER , XF

UC Category (19) UC-400 , DOE/ER

ph